dc_46_10

Akadémiai doktori értekezés

HUMÁN ABC TRANSZPORTEREK FUNKCIONÁLIS VIZSGÁLATA

Homolya László

MTA-SE Membránbiológiai Kutatócsoport

Budapest, 2010.

"Az ember minden jel szerint arra van teremtve, hogy gondolkozzék; ebben rejlik minden méltósága; egyetlen kötelessége az, hogy helyesen gondolkozzék."
(Blaise Pascal: Gondolatok)

Tartalomjegyzék

Rövidítések jegyzéke

ABC	ATP-kötő kazetta
ALL	akut limfoid leukémia
ALLN	acetil-L-leucil-L-leucil-L-norleucinál
AM	acetoxi-metilészter
AMD	kor-függő makula degeneráció
AML	akut mieloid leukémia
apoA-I	apolipoprotein A-I
apoE	apolipoprotein E
BCRP	mellrák rezisztencia protein (ABCG2)
BFA	brefeldin A
BSA	marhaszérum albumin
BSEP	epesó efflux pumpa (ABCB11)
BSO	butionin-sulfoximin
CAM	calcein acetoxi-metilészter
CAR	konstitutív androsztán receptor
CCCP	klorokarboxi-cianid fenilhidrazon
CD	ciklodextrin
CD/Kol	koleszterinnel töltött ciklodextrin
CFTR	cisztikus fibrózis transzmembrán konduktancia regulátor
CYP	citokróm
CsA	ciklosporin A
DIC	differenciál interferencia kontraszt
DPBS	Dulbecco módosított foszfát puffer
ECL	erősített kemilumineszcens eljárás (enhanced chemiluminescence)
EGF	epidermális növekedési faktor
EGFR	epidermális növekedési faktor receptor
EKI	EKI-785 tirozinkináz inhibitor
EZ	ezetimib
FBS	borjúszérum
FTC	ABCG2-specifikus gátlószer
GFP	zöld fluoreszcens protein
GSH	glutation
GSSG	oxidált glutation
HA	hemagglutinin
HDL	nagy sűrűségű lipoprotein
IL-1β, IL-6	interleukin 1β, illetve interleukin 6
KM	lizin-metionin csere a Walker A motívumban
KO	Ko143, ABCG2-specifikus gátlószer
Ko143	ABCG2-specifikus gátlószer
LDL	alacsony sűrűségű lipoprotein
LDLR	LDL receptor
LTC_4	leukotrién C_4

LXR	máj X receptor
MAF	MDR aktivitásfaktor
MDR	multidrog rezisztencia
MDR1	multidrog rezisztencia protein 1 (P-glikoprotein)
MK571	MRP1 gátlószer (leukotrién D_4-receptor antagonista)
MRP1	multidrog rezisztencia-asszociált protein 1
MX	mitoxantron
MXR	mitoxantron-rezisztencia protein (ABCG2)
NBD	nukleotid-kötő domén
NEM	N-etil-maleimid
NPM	N-pirén-maleimid
OATP	organikus anion transzport protein
PAPS	3′-foszfoadenilszulfát
PC	foszfatidil-kolin
PE	foszfatidil-etanolamin
PFA	paraformadehid
PFIC	progresszív familiáris intrahepatikus kolesztázis
Pgp	P-glikoprotein (MDR1)
feoA	feoforbid A
PI	propidium-jodid
PM	plazmamembrán
PPARγ	peroxiszóma proliferátor-aktivált receptor γ
PS	foszfatidil-szerin
PXR	pregnán X receptor
RMSE	empirikus szórás (root mean square error)
ROI	kijelölt régió (region of interest)
RXR	retinoid X receptor
SEM	standard hiba
Sf9	*Spodoptera frugiperda* rovar sejt
SLC	multispecifikus solute carrier
STS	staurosporin
SUR1	szulfonurea receptor 1
TGF-β	transzformáló növekedési faktor β
TKRI	tirozinkináz-receptor inhibitor
TMD	transzmembrán domén
TMH	transzmembrán hélix
TNF-α	tumor nekrózis faktor α
UDPGlcUA	uridin 5′-difoszfo-glukoronsav
VBL	vinblasztin
Verap	verapamil
VLCFA	nagyon hosszú szénláncú zsírsav
WGA	búzacsíra agglutinin
VT	vad típus
YFP	sárga fluoreszcens protein

1. Bevezetés

1.1. Az ABC fehérjecsalád áttekintése

Az ATP-Binding Cassette (ABC) transzporterek a fehérjék egyik legnépesebb családját alkotják. Az ABC szuperfehérjecsalád tagjai a legtöbb élő szervezetben megtalálhatóak a baktériumoktól kezdve egészen az emberig [1]. Az egyes fajokban mintegy 30-100 ABC fehérje szekvenciát azonosítottak. Definíciójuk szerint három konzervatív szekvencia motívum megléte alapján soroljuk a fehérjéket ehhez a családhoz. Ezek az ATP-kötő fehérjékre jellemző Walker A (GXXGXGKS/T), Walker B (hhhhD), valamint az ABC transzportereket megkülönböztető „ABC signature" (LSGGQQ/R/KQR) motívum (1a ábra).

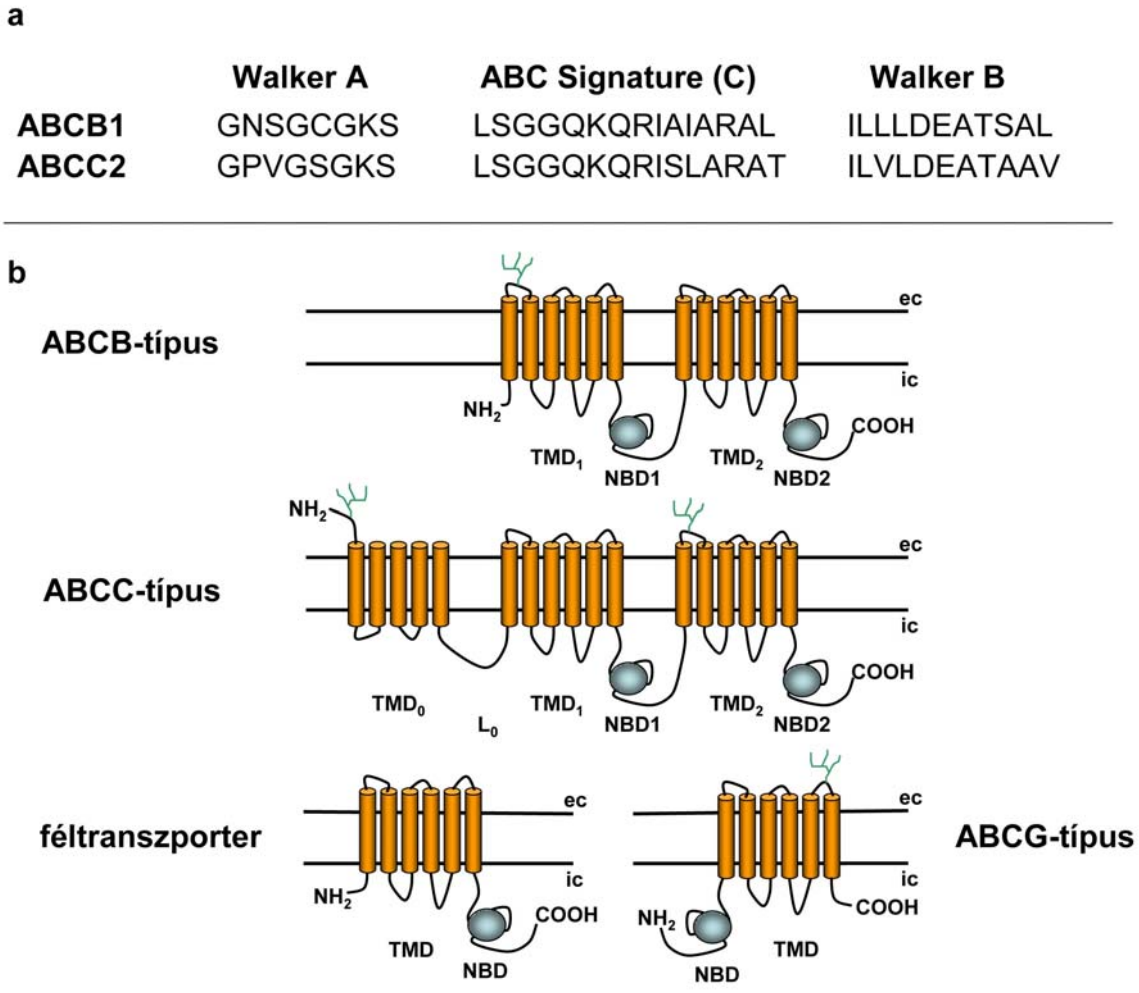

1. ábra: a) Az ABC transzportereket meghatározó konzervált szekvencia motívumok (az ABCB1 és ABCC2 példáján bemutatva): Walker A, Walker B és ABC signature szekvenciák. **b) Az ABC transzporterek jellegzetes doménszerkezete és membrántopológiája.** Az ABCB alcsalád tagjaira jellemző két transzmembrán doménből (TMD), valamint két nukleotid-kötő doménből (NBD) álló kanonikus szerkezet az ABCC alcsalád tagjainál kiegészül egy további transzmembrán doménnal (TMD_0) és egy linker (L_0) régióval. A féltranszporterek esetében a szekvenciában csak egy TMD és egy NBD található. [2]

A szekvencia homológián túl az ABC transzporterek nagyfokú szerkezeti hasonlóságot is mutatnak, jellemzően kétféle, funkcionálisan és szerkezetileg elkülönülő egységből épülnek fel. A fent említett konzervált szekvenciákat a citoplazmatikusan elhelyezkedő, 200-250 aminosavból álló globuláris szerkezet, az ún. ABC-egység vagy másképpen nukleotid-kötő domén (NBD) tartalmazza. A fehérjecsalád erről az „ATP-kötő kazettáról" nyerte az ABC nevet. Ez a domén képezi a fehérje katalitikus centrumát, itt történik a fehérje működéséhez szükséges ATP-kötés és hidrolízis.

Az ABC transzporterek másik jellegzetes szerkezeti egysége a transzmembrán domén (TMD), amely tipikusan 6 membránon átívelő hélixből áll. Általánosan elfogadottá vált, hogy egy működőképes ABC transzporter legalább 2 nukleotid-kötő doménből és 2 transzmembrán doménből áll. Számos bakteriális ABC transzporter szerkezeti egységeit egy operonon belül különálló gének kódolják, azonban arra is találunk példát, hogy egyetlen gén kódolja az összes domént. A humán ABC transzporterek esetében kizárólag az utóbbi a felépítéssel találkozunk.

A működéshez szükséges minimális (core) szerkezet jellemzi például a MDR1 (P-glikoprotein, Pgp, ABCB1) fehérjét, ahol TMD1-NBD1-TMD2-NBD2 sorrendben követik egymást a domének a polipeptidláncon belül (1b ábra). Ez a kanonikus szerkezet egészül ki sok esetben egy extra, N-terminálisan elhelyezkedő transzmembrán doménnal (TMD_0), amelyet tipikusan egy amfipatikus hélixet tartalmazó linker régió (L_0) köt össze a kanonikus szerkezettel. Ez a felépítés jellemző az ABCC alcsalád tagjaira (az alcsaládok felosztását ld. később). Több olyan humán ABC transzporterrel is találkozunk, amelyek molekulasúlyukat tekintve nagyjából fele akkorák, mint az eddig tárgyalt ún. „teljes transzporterek", és egyetlen NBD-ből, illetve egyetlen TMD-ből állnak (pl. TAP1/TAP2). Ezeknek a „féltranszportereknek" – a mai álláspont szerint – dimerizálódniuk kell ahhoz, hogy működőképes egységet alkossanak. A féltranszportereken belül egy érdekes csoportot képeznek az ABCG alcsalád tagjai, amelyek esetében a domén sorrend fordított a szokásoshoz képest, azaz az NBD N-termiálisan helyezkedik el a TMD-hez viszonyítva (1b ábra).

A 2 NBD és 2 TMD meglétének szükségességét indokolja az a mára már általánosan elfogadott nézet, miszerint a két L-alakú NBD fej-láb orientációban helyezkedik el, és a két ATP-kötőhelyet két külön NBD-ben lévő szekvenciák közösen alakítják ki. Azaz az egyik NBD-ben lévő Walker A motívum a másik NBD-ben lévő ABC signature szekvenciával együtt vesz részt a kompozit katalitikus centrum kialakításában. Hasonló szoros funkcionális együttműködést mutattak ki a transzmembrán domének között. Úgy tűnik minimálisan 12 hélix szükséges a transzportált szubsztráttal létrejövő komplex reakcióhoz.

Az emberi fajban 48 ABC fehérjét azonosítottak. Az egymás után felfedezett ABC transzportereket különféle, legtöbbször a funkcióra utaló névvel láttak el. Sokszor egyetlen fehérjét több névvel is illetnek. Hosszú évek zavaros nevezéktana után a közelmúltban bevezettek egy egységes, a szekvencia homológián alapuló szisztematikus nomenklatúrát, amely alapján a humán ABC fehérjéket hét alcsaládba soroljuk. Az alcsaládokat ABCA-tól ABCG-ig betűkóddal jelöljük, az egyes fehérjéket az alcsaládon belül pedig egy további számmal azonosítjuk (http://nutrigene.4t.com/humanabc.htm). A 2. ábrán látható a humán ABC transzporterek filogenetikai fája [12. sz. közlemény]. Sok ABC transzporter esetében továbbra is használatos a hagyományos elnevezés, ezért az MDR1 (ABCB1), az MRP1 (ABCC1), valamint a CFTR (ABCC7) megnevezésére az értekezésben a triviális nevet használom.

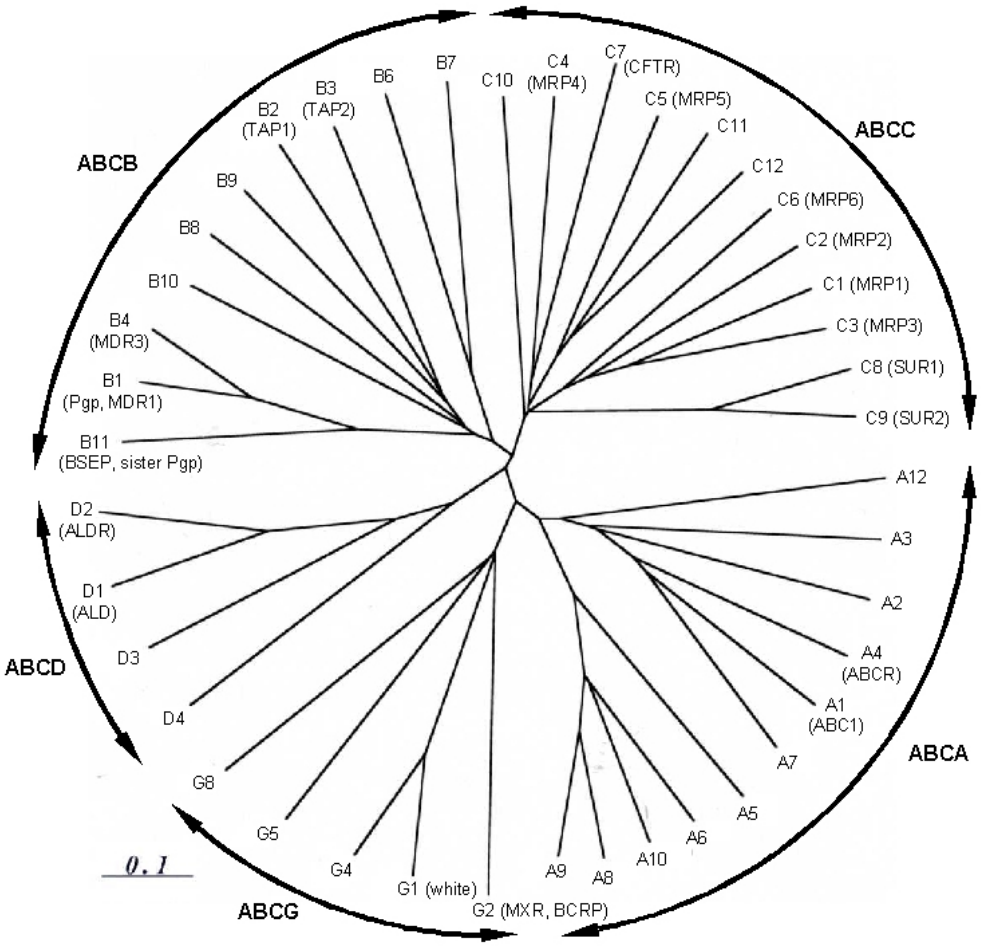

2. ábra: A humán ABC fehérjék rokonsági fája. A szekvencia homológia alapján készült a filogenetikai fa a 48 humán ABC fehérje közül annak a 42 fehérjének a rokonsági viszonyait mutatja be, amelyek transzporterként működnek. Így az ábrán csak az ABCA, ABCB, ABCC, ABCD, valamint az ABCG alcsalád szerepel. Az ABCE és ABCF alcsalád tagjaiként azonosított szekvenciák nem tartalmaznak transzmembrán domént. [12. sz. közlemény]

1.2. Az ABC fehérjék működése és élettani szerepe

Az ABC transzporterek integráns membránfehérjék, melyek az ATP kötés és hidrolízis energiáját hasznosítva látják el funkciójukat. A legtöbb humán ABC fehérje aktív transzporter, azaz az elektrokémiai hajtóerővel szemben végzi az anyagok transzlokációját. Találunk azonban arra is példát, amikor egy ABC transzporter ioncsatornaként funkcionál. A CFTR (ABCC7) - a cisztikus fibrózis kialakulásáért felelős transzporter - klorid csatornaként működik [3]. Hasonlóan a szulfonurea receptor 1 (SUR1/ABCC8) sem aktív transzporter, hanem más transzportereket – nevezetesen egy ATP-függő K^+-csatornát – szabályoz a hasnyálmirigyben, fontos szerepet töltve be az inzulin szekrécióban [4, 5]. Ez utóbbi esetekben az ATP kötése és hidrolízise nem energetikai szempontból fontos, hanem az ABC transzporter funkciójának szabályozásához szükséges.

A bakteriális ABC transzporterek körében uptake transzportereket és efflux pumpákat egyaránt találunk. A humán ABC transzporterek nukleotid-kötő doménja a citoplazmában helyezkedik el, a transzport legtöbbször a sejtből kifelé irányul, de számos esetben belső celluláris kompartmentek lumenjébe történik. Olyanra is találunk példát, ahol mind kifelé, mind az organellumokba irányuló transzport megtörténik, pl. magas expresszió esetén az ún. multidrog transzporterek nemcsak eltávolítják a drogot a sejtből, hanem belső kompartmentekbe szekvesztrálják [6, 7]. Uptake transzporterek az eukarióta ABC transzporterek körében ritka kivételnek számítanak.

Az aktív transzporterként működő ABC fehérjék sajátossága, hogy szemben a P-típusú ATPázokkal, esetükben a transzport ciklus során nem jön létre foszforilált komplex, a hidrolízis eredményeképpen egy feszült állapotú intermedier jön létre, ami kulcsszerepet játszik a transzportált szubsztrát transzlokációjában és a molekulán belüli affinitási viszonyok megváltozásában. Szintén fontos jellemzője ezeknek a transzportereknek, hogy mind az átmeneti komplex kialakulását, mind az ATP hidrolízis sebességét sok esetben fokozza a transzportált szubsztrátok jelenléte [8-10].

Az ABC transzporterek számos élettani folyamatban kulcsfontosságú szerepet játszanak. Sokan közülük részt vesznek a szervezet szintű detoxifikálásban (MDR1), az endo- és xenobiotikum elleni védelemben, az oxidatív stressz mérséklésében (MRP1), valamint különböző abszorpciós és szekréciós folyamatok szabályozásában (pl. SUR1/ABCC8). Más ABC fehérjék a lipidanyagcserében töltenek be fontos szerepet (ABCA1, ABCB4, ABCB11), de találunk példát arra is, hogy az MHC I-típusú antigénprezentációban (TAP1/TAP2) vagy a hámfelületek ionháztartásának szabályozásában (CFTR) játszanak meghatározó szerepet.

A számos fontos élettani funkcióból következően több ismert örökletes betegség köthető az ABC transzporterekben bekövetkező mutációkhoz. Példaként hozhatjuk a korábban említett CFTR-t a cisztikus fibrózissal összefüggésben, amely a kaukázusi populációban az egyik leggyakoribb öröklődő betegség. Ritkábban előforduló betegségek, mint a Stargardt-betegség kialakulásáért az ABCA4-ben, a Dubin-Johnson szindrómáért az ABCC2-ben, a pseudoxanthoma elasticum kórképért az ABCC6 transzporter génjében bekövetkező mutációk tehetők felelőssé. Az 1. táblázat foglalja össze az ABC transzporterek mutációja következtében kialakuló örökletes betegségeket. Fontos orvosi jelentőséggel bírnak ezeken kívül az ún. multidrog transzporterek, de mivel részben ehhez a csoporthoz tartoznak az értekezés tárgyát képező transzporterek, ezek részletesebb ismertetésével és a multidrog rezisztencia bemutatásával külön alfejezetben foglalkozom.

I. táblázat. ABC fehérjék szerepe különböző betegségekben

szisztematikus név	triviális név	feltételezett funkció	kapcsolódó betegség
ABCA1	ABC1	foszfolipid- és koleszterin-transzport	Tangier-betegség, familiáris HDL-hiányos kórképek
ABCA4	ABCR	N-retinil-PE transzportja a retinában	Stargardt-betegség, csap-pálcika disztrófia, makula degeneráció
ABCB2/ ABCB3	TAP1/ TAP2	MHC I-típusú antigénprezentáció	immundeficiencia, inzulin-függő diabétesz
ABCB4	MDR3	kanalikuláris foszfatidil-kolin szekréció	progresszív familiáris intra-hepatikus kolesztázis 3
ABCB6		mitokondriális porfirin transzport	letális újszülöttkori metabolikus szindróma (?)
ABCB7		mitokondriális porfirin transzport	X-kromoszómához kötött szideroblasztos anémia
ABCB11	BSEP, sister Pgp	kanalikuláris epesó szekréció	progresszív familiáris intra-hepatikus kolesztázis 2 (PFIC2)
ABCC2	MRP2	organikus anionok szekréciója az epébe	Dubin-Johnson szindróma
ABCC6	MRP6	ismeretlen	pseudoxanthoma elasticum
ABCC7	CFTR	kloridcsatorna (regulátor)	cisztikus fibrózis
ABCC8	SUR1	inzulin szekréció szabályozása	gyermekkori hiperinzulinémiás hipoglikémia
ABCD1	ALD	peroxiszómális zsírsav transzport	adrenoleukodisztrófia
ABCD2	ALDL1	peroxiszómális zsírsav transzport	adrenoleukodisztrófia, Zellweger-szindróma
ABCG5/ ABCG8		szterolok szelektív transzportja	szitoszterolémia

1.3. Multidrog ABC transzporterek

Az ABC transzporterek egyik legkülönösebb csoportját alkotják a korábban már említett multidrog transzporterek. Nevüket onnan nyerték, hogy ezek a transzporterek humán tumorokban és *in vitro* sejtes modellekben kereszt-, azaz multidrog-rezisztenciát (MDR) okoznak kémiailag és szerkezetileg a legkülönfélébb citotoxikus drogokkal szemben. Közös jellemzőjük, hogy nagyon széles szubsztrát-felismerő képességgel rendelkeznek, így a klasszikus értelemben vett szubsztrát-specifitásról nem is beszélhetünk ezen transzporterek esetében. Mára már általánosan elfogadottá vált, hogy a multidrog transzporterek a tumorsejtek plazmamembránjában elhelyezkedve a sejtekből kipumpálják a citotoxikus anyagokat, a hatásos „sejtölő" szint alatt tartva az intracelluláris drog koncentrációt [11]. A 48 humán ABC fehérje közül elsősorban az MDR1 (P-glikoprotein, ABCB1) transzportert, az ún. multidrog rezisztencia-asszociált fehérjét (MRP1, ABCC1), valamint az ABCG2 (MXR, BCRP) féltranszportert hozzák összefüggésbe a multidrog rezisztenciával. Érdemes azonban megemlíteni, hogy leírtak olyan eseteket is, ahol más ABC transzporterek, pl. az MRP2 (ABCC2), az MDR3 (ABCB4), vagy a BSEP (ABCB11) okoztak keresztrezisztenciát különböző citotoxikus szerekkel szemben [12].

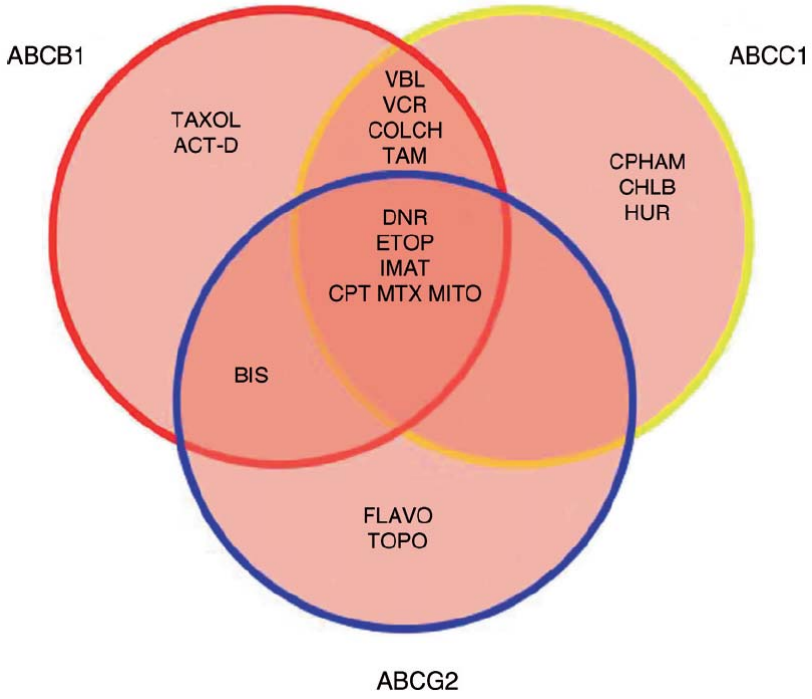

3. ábra: Az MDR-ABC transzporterek tumorellenes drog szubsztrátjai. Jelölések: ACT-D: aktinomicin D; VBL: vinblasztin, VCR: vinkrisztin, COLCH: kolhicin; TAM: tamoxifen, DNR: daunorubicin; ETOP: etopozid, IMAT: imatinib, CPT: kamptotecin, MTX: methotrexát, MITO: mitoxantrone, BIS: bizantrén, FLAVO: flavopiridol, TOPO: topotekán; CPHAM: ciklofoszfamid, CHLB: klorambucil; HUR, hidroxiurea. [2]

Az említett 3 fő MDR-ABC transzporter különböző, mégis sok esetben átfedő szubsztrát-felismerő képességgel rendelkezik. Az MDR1 elsősorban hidrofób karakterű, töltés nélküli vagy gyenge pozitív töltésű anyagok transzportját végzi. Az MRP1 fehérje a hidrofób anyagokon felül képes organikus anionokat, elsősorban glutation-, glukoronát- és szulfát-konjugátumokat is kipumpálni a sejtekből. Az eredetileg mitoxantron-rezisztencia proteinként azonosított ABCG2 szubsztrátjai közt szintén legkülönbözőbb szerkezetű és karakterű vegyületeket találunk: amfipatikus drogokat, szulfát-konjugátumokat, bioflavonidokat, porfirin-származékokat, stb. A 3 főbb MDR-ABC transzporter részben átfedő szubsztrát-felismerő képességét a 3. ábrán a különböző tumorellenes szerek példáján mutatom be [2].

Bár az *in vitro* modellek vitathatatlanul megmutatták, hogy a multidrog transzporterek védelmet nyújtanak a sejtek számára a citotoxikus drogokkal szemben, szerepük, jelentőségük a klinikai drog-rezisztenciában mégis vitatott. Egyedül az MDR1 esetében sikerült egyértelmű összefüggést kimutatni a klinikai kimenetel és a transzporter jelenléte között bizonyos tumoroknál (mellrák, szarkóma, bizonyos típusú leukémiák). Mind az MRP1, mind az ABCG2 esetében a klinikai drogrezisztenciában betöltött szerepük nem egyértelműen tisztázott. A vitatott eredmények hátterében legtöbbször a nem kielégítő módszerekkel és nem egységes módon végzett klinikai vizsgálatok állnak. Az MDR fehérjék diagnosztikája a mai napig nem megoldott a klinikumban. A problémát bonyolítja egyrészt, hogy potenciálisan többféle transzporter jöhet szóba, másrészt polimorfizmusok megváltoztathatják az egyes transzporterek szubsztrát-specifitását [13, 14].

Élettani szerepüket tekintve az eredetileg multidrog transzporterként azonosított ABC fehérjék a különböző fiziológiás barrierekben (pl. vér-agy gátban, placentában, bélhámban) expresszálódva szabályozzák az anyagok szelektív ki- és bejutását. Az MDR-ABC transzporterek fontos szerepet játszanak a szervezet szintű detoxifikálásban is. Egyrészt az első vonalban eleve megakadályozzák a toxikus anyagok bejutását, másrészt elősegítik a különböző oxidált és konjugált endo- és xenobiotikumok epébe történő kiválasztását.

Az abszorpciós és szekréciós folyamatokban betöltött szerepükön felül a multidrog transzporterek hatékony védelmet nyújtanak toxinok ellen bizonyos érzékeny, általában magas proliferatív állapotú sejtekben, szövetekben. Erre példa az ABCG2 magas expressziója az őssejtekben [15-17] vagy az MRP1 jelenléte a bélhám kripta (Paneth) sejtjeiben és a here Sertoli sejtjeiben [15, 16]. Az MRP1 sajátos szerepet tölt be ezen felül a leukotrién metabolizmusban, valamint az oxidatív stressz elleni védelemben, mivel az LTC_4 ennek a transzporternek az egyik legnagyobb affinitású szubsztrátja, a redukált glutationt (GSSG-t) pedig az MRP1 nagy transzportkapacitással képes a sejtekből eltávolítani [17, 18].

1.4. A multidrog transzporterek funkcionális detektálása (calcein assay)

A fluoreszcens indikátorok élő sejtekbe juttatásának egy szokásos, nem-invazív módja, hogy a festéket észteresítve, sejtpermeábilis formában adjuk a sejtekhez. A citoplazmatikus aspecifikus észteráz aktivitás következtében a sejten belül a festékészter hidrolízisére kerül sor. Mivel a szabad sav forma már nem permeábilis, így a festék becsapdázódik a sejtbe, és felhalmozódik a citoplazmában. A többféle észterforma közül a sejtek nem-invazív töltésére leginkább az acetoxi-metilészter (AM) használata terjedt el.

A korábbi évek kutatómunkája során kimutattuk, hogy az MDR1 fehérje szubsztrátként ismeri fel számos fluoreszcens indikátor AM formáját, és hatékonyan képes kipumpálni a sejtekből. Megfigyelésünk alapja, hogy az MDR1 fehérjét expresszáló sejtekben a festék citoplazmatikus felhalmozódása – a transzportert nem-expresszáló sejtekhez képest - csak csekély mértékben következik be. Amennyiben MDR1 gátlószert vagy nagy-affinitású szubsztrátot adunk feleslegben a sejtekhez, felfüggeszthetjük a transzporter festékeltávolító aktivitását, és a kontroll sejtekhez hasonló mértékű festékfelhalmozódást érhetünk el (4a ábra). A jelenséget részletesen tanulmányozva megmutattuk, hogy sokféle fluoreszcens indikátor AM formájával juthatunk hasonló eredményre (4b ábra) [19].

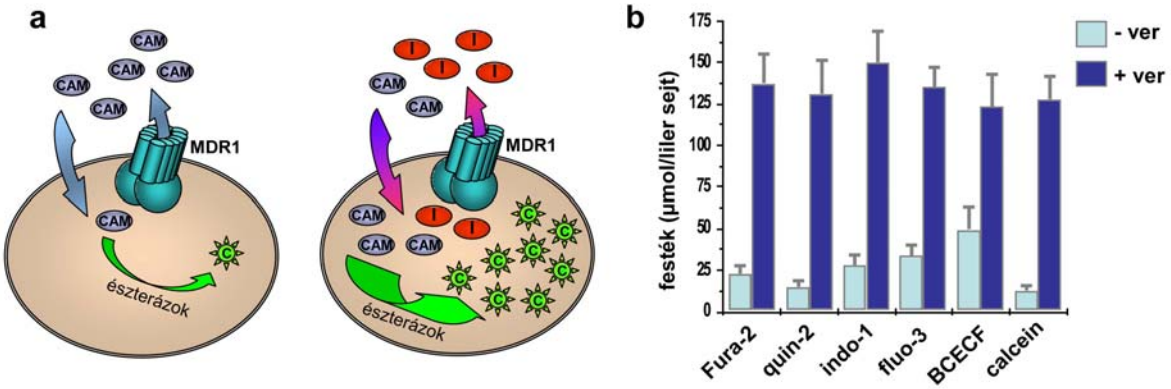

4. ábra: Az MDR1 fehérje transzportaktivitásának fluoreszcens-alapú detektálása. a) Az assay sémája. [11. sz. közlemény] Jelölések: CAM – a festék nem-fluoreszcens acetoxi-metilészter (AM) formája; C – a festék fluoreszcens, szabadsav formája; I – a festékeltávolítást gátló anyag (inhibitor vagy szubsztrátfelesleg). **b)** Különböző fluoreszcens indikátorok felhalmozódása 3T3 MDR sejtekben DMSO (oldószerkontroll, -ver) vagy 100 µM verapamil jelenlétében (+ver). A festékeket AM formában adtuk a sejtekhez. [19]

A fent leírt jelenség egy olyan fluoreszcens alapú módszer kidolgozását tette lehetővé, amely segítségével az MDR1 aktivitása könnyen, megbízhatóan és reprodukálható módon detektálható. Erre a célra legalkalmasabb fluoreszcens festéknek egy viabilitási indikátor, a calcein tűnt. Ez a festék azzal az előnnyel rendelkezik, hogy - szemben más fluoreszcens indikátorokkal – fluoreszcenciáját nem befolyásolják a sejten belüli különböző paraméterek

(pl. pH, Ca^{2+}-szint, stb.). Ráadásul a vizsgált fluoreszcens indikátorok közül az MDR1 egyik legnagyobb affinitású szubsztrátjának a calcein AM bizonyult [20].

Vizsgálataink során megmutattuk azt is, hogy az MDR1 expressziójának emelkedésével a fluoreszcencia felhalmozódása fokozatosan csökken a sejtekben (5a ábra) [21]. Ez lehetőséget ad arra, hogy módszerünkkel ne csak detektáljuk a fehérje funkcionális jelenlétét, hanem mennyiségileg is meghatározzuk az aktivitását. Mivel a festék felhalmozódása a sejtekben több olyan paramétertől függ, mint a sejtek mérete, citoplazmatikus észteráz aktivitása, stb., az MDR1 mennyiségi meghatározására egy olyan normalizált mérőszámot vezettünk be, amely egyrészt egyenes összefüggést mutat a transzporter aktivitással, másrészt független az említett paraméterektől. Ezt a mérőszámot MDR aktivitásfaktornak (MAF) neveztük el, és a következőképpen számoltuk:

$$MAF = \frac{F_v - F_0}{F_v} \qquad (1)$$

ahol F_v a transzporter teljes gátlása mellett mért festékfelvételi sebesség, F_0 pedig a gátlószer nélküli kapott érték [21]. Gyakorlati szempontból az előbbit leggyakrabban 50-100 μM verapamil jelenlétében határozzuk meg, és gyakran a festékfelvételi sebesség helyett az azonos inkubálási időkkel kapott fluoreszcencia értékekkel számolunk. Demonstráltuk, hogy a módszer alkalmas kevert követtás fluoriméterben, áramlási citométerben, vagy akár egy-sejtszintű, mikroszkópos képalkotórendszerben történő mérésekre is. Megmutattuk, hogy az MDR aktivitás faktor széles határok között független értéket ad az alkalmazott calcein AM koncentrációjától, az inkubálási időtől, a pH-tól és egyéb kísérleti paraméterektől.

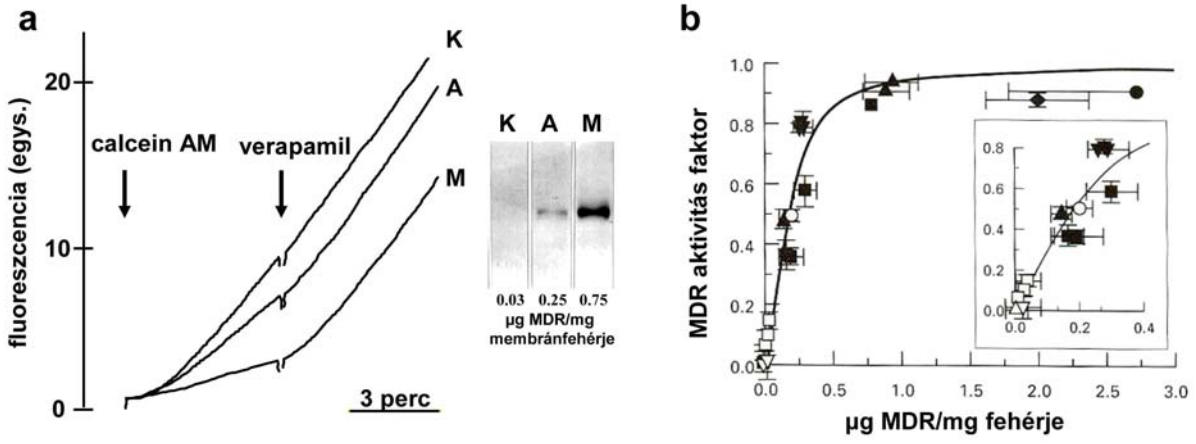

5. ábra: A calcein assay kvantitatív módszerré fejlesztése. a) A festék felhalmozódása a sejtekben az MDR1 expressziójával és aktivitásával fordított viszonyban áll. Jelölések: K – kontroll, drog-szenzitív, A – alacsony, M – magas expressziójú drog-rezisztens sejt **b)** A verapamil jelenlétében, illetve távollétében mért festékfelvételi sebességekből számolt MDR aktivitás faktor (ld. szöveg) érzékenyen tükrözi az MDR1 aktivitását, különösen az alacsony expressziós tartományban [21].

Mint azt az 5a ábrán bemutattuk, a sejteket calcein AM-mel inkubálva annál alacsonyabb festékfelhalmozódást tapasztalunk, minél magasabb az MDR1 expressziója. Az aktivitás faktor bevezetésének az volt az elsődleges célja, hogy olyan mérőszámot kapjunk, ami az MDR1 aktivitását nem fordított módon, hanem egyenes összefüggésben tükrözi. Annak igazolására, hogy a MAF teljesíti ezt a kívánalmat, különböző fajokból és szövetekből származó, drog-szenzitív és különböző mértékben drog-rezisztens sejteket analizáltunk calcein assay-vel. Az így kapott MAF értékeket korreláltattuk a kvantitatív immunoblottal meghatározott MDR1 expressziós szintekkel (5b ábra). A legkülönbözőbb sejtekben mért MAF értékek egyetlen görbe mentén helyezkedtek el, amin az is jól látszik, hogy az MDR1 mennyiségével az aktivitás faktor monoton emelkedik. Az alacsony expressziós szinteknél ráadásul arányosság áll fenn a két paraméter között (ld. mellékábra), míg a magasabbaknál a görbe telítésbe hajlik. Ennek oka valószínűleg az, hogy ebben a tartományban a transzporter már gyakorlatilag az összes festékészter molekulát eltávolítja a sejtből, így az F_0 érték közel 0-nak adódik, és ekkor már hiába növeljük tovább az MDR1 mennyiségét. Az alacsony expressziós tartományban a MAF és MDR1 mennyisége közötti arányosságot sejtkeveréses módszerrel is igazoltuk (ábrán nem mutatott eredmény).

A calcein assay-t, amely szabadalommal védett eljárás, széles körben használják az MDR1 és a MRP1 (ld. 4.1.1. fejezet) multidrog transzporterek vizsgálatára. A módszer egyrészt alkalmas arra, hogy segítségével meghatározzuk a multidrog transzporter aktivitást különböző sejtmintákban, ezért daganatos mintákon alkalmazva diagnosztikai jelentőséggel bír (ld. 4.1.3. fejezet). Másik oldalról farmakológiai tesztelésekre is fel lehet használni ezt a technikát, amennyiben ismert, stabil MDR1 (vagy MRP1) expressziót mutató sejteken különböző tesztanyagokat vizsgálunk a transzporterrel való kölcsönhatás szempontjából. A vizsgált anyag és a multidrog transzporter közötti interakciót a festékeltávolítás gátlása mutatja, melynek mértékét következőképpen fejezzük ki:

$$I(\%) = \frac{F_x - F_0}{F_v - F_0} \cdot 100 \qquad (2)$$

ahol F_x a tesztvegyület jelenlétében mért festékfelvételi sebességet jelenti [22]. Ugyan a módszer nagy érzékenységű és könnyen kivitelezhető, azonban hátrányként meg kell említeni, hogy a festéktranszport gátlása alapján nem tudjuk megkülönböztetni a szubsztrátokat (kompetitív gátlás) és a direkt inhibitorokat. A diagnosztikai és farmakológiai felhasználáson túl a módszer segítséget nyújthat a multidrog rezisztencia fehérjék működési mechanizmusára irányuló kutatásokhoz is (ld. 4.1.1. fejezet). Az MDR1 fehérje és hidrofób peptidek kölcsönhatását is ezzel a módszerrel sikerült korábban kimutatnunk [22].

1.5. A lipidanyagcserében szerepet játszó ABC transzporterek

Az ABC fehérjecsalád több tagja fontos szerepet játszik a sejtek, illetve a szervezet lipidháztartásában. Különleges és speciális funkciót látnak el a hepatociták kanalikuláris membránjában elhelyezkedő ABC transzporterek. Ezek közül az ABCB11 (BSEP, sister Pgp) fehérje végzi az epesók kanalikuláris kiválasztását [23, 24], míg az ABCB4 (MDR3) fehérje a foszfatidil-kolin (PC) szekréciójáért felelős [25, 26]. Általánosan elfogadott, hogy az ABCB4 transzporter floppázként működik, azaz a transzportált szubsztrátját a sejtmembrán belső rétegéből a külsőbe fordítja, ami végeredményben nettó kiáramláshoz vezet. A foszfatidil-kolinban feldúsult, feszült állapotú membránrészek egyrészt lefűződnek, PC-vezikulákat hozva létre, másrészt a foszfatidil-kolin az epekanalikulusba szekretált epesókkal vegyes micellákat képez [25, 26] (6. ábra).

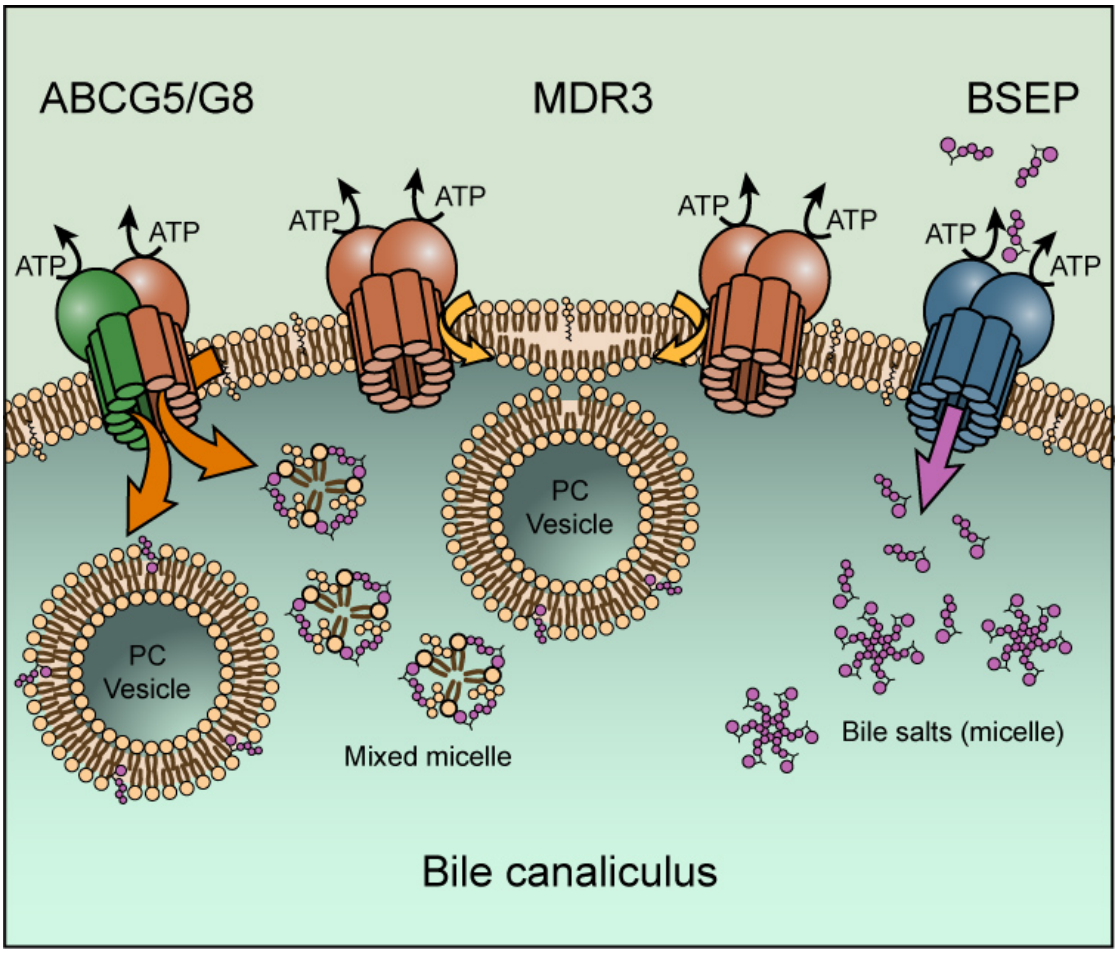

6. ábra: ABC transzporterek szerepe az epeszekrécióban. Az ABCB4 (BSEP) felelős az epesók kanalikuláris szekréciójáért, az ABCB4 (MDR3) a foszfatidil-kolint fordítja ki a membrán belső feléből a külsőbe, nettó kiáramlást idézve ezzel elő, az ABCG5/ABCG8 heterodimer pedig a koleszterin epébe juttatását végzi. Részletes magyarázatot lásd a szövegben. [11. sz. közlemény]

Némileg vitatott a jelenlegi szakirodalomban az ABCG5/ABCG8 transzporterpár szerepe az epekiválasztásban. Eredetileg a bélhámban a növényi eredetű szteroloknak a bél lumenjébe történő szelektív visszajutatásáért felelős obligát heterodimerként írták le az ABCG5/ABCG8 fehérjét [27-29]. Feltételezések szerint szintén ez a transzporterpár tehető felelőssé a koleszterin epébe történő kiválasztásáért [28, 29], azonban ezt az elképzelést újabban többen megkérdőjelezik [30, 31]. Kétféle transzportmechanizmust is javasoltak az ABCG5/ABCG8 kanalikuláris koleszterin transzport leírására: az egyik értelmében - az ABCB4 analógiájára alapozva - az ABCG5/ABCG8 heterodimer is floppázként működik [27]. A másik, ún. „aktiváció-ütközés" modell energetikai megfontolásokat is figyelembe véve azt javasolja, hogy a transzporterpár flip-flop transzlokáció nélkül csak kismértékben változtatja meg a koleszterin elhelyezkedését a membránban, de ezzel már elérhetővé válik a molekula az epekanalikulusban lévő lipidakceptorok, PC-vezikulák és vegyes micellák számára [32].

Az epeszekrécióban részt vevő ABC transzporterekben bekövetkező mutációkhoz szintén köthetők örökletes betegségek: az *ABCB4* gén mutációi a 3-as típusú progresszív familiáris intrahepatikus kolesztázisért (PFIC3) [33], míg az *ABCB11* génben lévő mutációk a 2-es típusú PFIC kialakulásáért tehetők felelőssé [34]. Akár az ABCG5-ben akár az ABCG8-ban bekövetkező mutációk a szitoszterolémia kórképhez vezetnek, melyet elsősorban a növényi eredetű szterolok felhalmozódása és korai ateroszklerózis jellemez.

A lipidháztartásában szerepet játszó ABC transzporterek között meg kell említeni a peroxiszómában expresszálódó ABCD féltranszportereket, melyek homodimereket és heterodimereket is képeznek. Az ABCD fehérjék a zsírsavak – elsősorban a nagyon hosszú szénláncú zsírsavak (VLCFA) – peroxiszómába történő felvételéért felelősek [34]. Az ABCD1 (ALD) és ABCD2 (ALDL1) transzporterek génjeiben lévő mutációk okozzák az adrenoleukodisztrófia betegséget, amely egy X-kromoszómához kötött öröklődésű, demielinizációval járó idegrendszeri kórkép [35].

Kiemelt szereppel bír a lipidanyagcserében az ABCA1 transzporter, amely a reverz koleszterin transzport egyik meghatározó eleme. Ez a transzporter felelős a koleszterinnek és a foszfolipideknek a lipid-szegény apolipoproteinekre (pl. apoA-I-re) történő transzportjáért mind a periférián, mind a májban és a vékonybélben, - fontos szerepet töltve be a felesleges celluláris koleszterin eltávolításában, illetve a nascens HDL partikulumok előállításában [36-38]. Bár az ABCA1 egy igen széles körben kutatott transzporter, működési mechanizmusa a mai napig vitatott. Egyrészt kétséges, hogy maga az ABCA1 fehérje transzporter-e vagy csak elősegíti a foszfolipidek és a koleszterin kiáramlását a sejtekből, másrészt megkérdőjelezik,

hogy a transzportfolyamathoz szükséges-e a közvetlen ABCA1-apoA-I kapcsolat, harmad-részt vitatják, hogy mindez a sejtfelszínen vagy endocitotikus vezikulákban zajlik [39].

Az ABCA1 fehérje mutációi húzódnak meg a Tangier-betegség hátterében, amelyet nagyon alacsony HDL-szint, a különböző szövetekben (pl. makrofágokban) történő nagyfokú koleszterin felhalmozódás és korai megjelenésű ateroszklerózis jellemez [40]. Újabban több más familiáris HDL-hiányos betegség, valamint egy igen ritka, öröklődő vérzékenység, a Scott betegség genetikai okaként írtak le az *ABCA1* génben lévő mutációkat [41].

Az ABCA alcsalád néhány további tagja is kapcsolatban áll a lipidanyagcserével. Az ABCA4 (RmP, ABCR) kizárólag a retinában expresszálódik, és a retinoid felvételben játszik kulcsszerepet. Szubsztrátját, az N-retinil-foszfatidil-etanolamint flippáz mechanizmussal transzportálja a fotoreceptor-sejtek külső lemezeibe. Több örökletes szembetegség hátterében az ABCA4 fehérje génjében lévő mutációk húzódnak meg. Ezek közé tartozik a fiatalkori makula degenerációval járó Stargardt-betegség, a csap-pálcika disztrófia, és a kor-függő makula degeneráció (AMD) [42, 43]. Az ABCA7 fehérje a mielo-limfatikus szövetekben expresszálódik, és a koleszterin, illetve a foszfolipidek transzportjával hozzák összefüggésbe. Funkciója nem teljesen tisztázott, de az immunsejtek lipidmetabolizmusában betöltött szerepét valószínűsítik az ABCA7-tel foglalkozó tanulmányok [45-47].

Egyre növekvő figyelem irányul az ABCG1 féltranszporterre, amely fehérjéről azt feltételezik, hogy a HDL partikulumok további lipidálásáért, koleszterinnel való feltöltéséért tehető felelőssé [44]. Az ABCG4, amely az ABCG1 legközelebbi rokona, az utóbbival - az egész fehérjét tekintve - 72 %-os szekvenciaazonosságot, bizonyos transzmembrán hélixek vonatkozásában (TMH2 és TMH5) pedig 100 %-os azonosságot mutat. Az ABCG1 alacsony szintű, ubikviter szöveti eloszlást mutat, azonban bizonyos szövetekben, mint az agy, a lép és a tüdő, viszonylag magas expressziót ér el [45]. Hepatikus kifejeződése a szöveti makrofágokra (Kupffer-sejtekre) korlátozódik [46]. Makrofágokban, dendritikus sejtekben, endotél sejtekben és a máj parenchima sejtjeiben expressziója jelentős mértékben fokozható a lipidanyagcseréhez köthető transzkripciós szabályozás révén (LXR, RXR, PPARγ útvonalakon) [47-51]. Az ABCG4 expressziója – az ABCG1-gyel szemben – csak bizonyos szövetekre korlátozódik, így az agyban és a szemben viszonylag magas ABCG4 szintet találtak, míg a makrofágokban kismértékű expressziót mutattak ki [52, 53]. Az ABCG1-hez hasonlóan az ABCG4 expressziója is indukálható oxiszterolokkal és retiniodokkal, LXR- és RXR-agonistákkal [52]. Mindezek megerősítik azt a feltételezést, hogy ezek a fehérjék funkciója a lipidanyagcseréhez köthető.

Mind az ABCG1, mind az ABCG4 féltranszporter, azaz - ahogy azt korábban kifejtettem - működésükhöz dimerizálódniuk kell. Az ABCG alcsalád egyéb tagjait tekintve az ABCG2-ről kimutatták, hogy homodimerként működik, míg az ABCG5 és ABCG8 esetében azt valószínűsítik, hogy heterodimerként működnek. A magas fokú szekvencia-azonosságuk, az ABCG alcsaládra jellemző fordított doménszerkezetük, illetve hasonló transzkripciós szabályozásuk alapján feltételezhető volt, hogy az ABCG1 és ABCG4 is heterodimert képez [54]. Megfelelő kísérleti eszközök hiánya miatt azonban ilyen irányú vizsgálatok munkánk megkezdéséig nem folytak, a dimerizáció kérdése nyitott maradt.

A humán ABCG1 fehérje a „White" nevű Drosophila ABC transzporter humán ortológjának tekinthető, amely fehérje egy triptofán transzporter. Erre az analógiára építve feltételezték, hogy az ABCG1 fehérje funkciója a triptofán-szerotonin anyagcseréhez köthető. Korábbi munkák összefüggésbe is hozták az *ABCG1* génben található mutációkat a pánik betegség, illetve az öngyilkos hajlam halmozódásával [55, 56], azonban ezeket az elméleteket későbbi tanulmányok nem erősítették meg. Jelenleg nem ismeretes olyan betegség, amely egyértelmű összefüggésbe hozható az ABCG1 vagy az ABCG4 génjében lévő mutációkkal.

Az ABCG1 és ABCG4 fiziológiás szubsztrátjait nem ismerjük, így élettani szerepük is egyelőre nyitott kérdés marad. Leginkább az az álláspont terjedt el, hogy az ABCG1 a makrofágokban az ABCA1-gyel együttműködve részt vesz a HDL partikulumok előállításában: míg az utóbbi a nascens HDL-t hozza létre az apoA-I és koleszterin kölcsönhatása révén, addig az ABCG1 szerepe a HDL részecske „hizlalása", azaz koleszterinnel való további töltése [57]. Ezt az elképzelést mind over-expressziós, mind knock-down kísérletekkel alátámasztják [46, 58, 59], azonban azt, hogy a transzporter közvetlenül részt venne a koleszterin transzportjában, a mai napig nem bizonyították. Érdemes megjegyezni, hogy ezekben a kísérletekben a sejtekből kikerülő koleszterin akceptoraként nemcsak HDL szerepel, hanem az apoA-I kivételével mindenféle más lipidakceptor: LDL, apoE-tartalmú lipoproteinek, BSA, ciklodextrin stb. Az ABCG1-deficiens egerekkel végzett tanulmányok sem támasztották alá teljesen az ABCG1 fent vázolt élettani szerepét, ugyanis a knockout és kontroll egerek makrofágjából a HDL-re történő koleszterin-kiáramlás alaphelyzetben nem különbözött [60]. Különbség csak akkor volt tapasztalható, ha a makrofágokat LXR-agonistával kezelték. Hasonlóképpen a knockout egerekkel végzett kísérletek sem igazolták vissza az ABCG1 ateroprotektív szerepét, hiszen a diétától függően egymásnak ellentmondó eredmények születtek [61-64]. Az ABCG4 élettani funkcióját illetően még kevesebb ismerettel rendelkezünk, azt feltételezik, hogy az idegsejtek lipidhomeosztázisában lehet szerepe [65, 66].

2. Célkitűzések

Munkánk alapvető célja az ABC transzporterek transzporttulajdonságainak megismerése, működési mechanizmusának, funkciójának és élettani szerepének megértése. Ezen belül ebben a disszertációban bemutatott munkában a következő konkrét célok megvalósítását tűztük ki feladatul:

1.) **Az MRP1 multidrog transzporter funkcionális detektálására** alkalmas fluoreszcens módszert kívántunk kidolgozni, hogy annak segítségével részletesen jellemezzük a fehérje transzporttulajdonságait. Célul tűztük ki azt is, hogy **az MDR1 és MRP1 fehérjék egymás melletti kimutatására** alkalmas módszert fejlesszünk ki.

2.) Igazolni kívántuk, hogy a korábban kidolgozott módszer, a calcein assay alkalmas **a multidrog transzporterek funkcionális jelenlétének mérésére klinikai mintákban**.

3.) Célul tűztük ki **az ABCG2 multidrog fehérje transzporttulajdonság**ainak vizsgálatát többféle szempontból. Egyrészt fel kívántuk tárni az ABCG2 kölcsönhatását az **Iressa (Gefitinib) nevű tumorellenes szerrel**, másrészt vizsgálni akartuk **a membrán koleszterintartalmának** az ABCG2 transzportaktivitására gyakorolt hatását.

4.) Megfelelő módszer kidolgozásával igazolni kívántuk azt a feltételezést, hogy **a multidrog transzporterek** nem a citoplazmából szállítják a transzportált szubsztrátot a külső térbe, hanem **közvetlenül a membránból pumpálják ki** ezeket a molekulákat.

5.) Célul tűztük ki a két kevéssé ismert ABC féltranszporter, **az ABCG1 és az ABCG4 alapvető karakterizálását:** szubsztrátjaiknak feltérképezését, dimerizációs partnerük, szubcelluláris lokalizációjuk és szerepük megismerését.

6.) Létre akartunk hozni egy olyan kísérleti eszközt, amely lehetővé teszi **az ABCA1 sejtfelszíni expressziójának szenzitív követését**, és vizsgálni kívántuk a különböző koleszterinszint-csökkentő szerek az ABCA1 plazmamembrán expressziójára gyakorolt hatását.

7.) Végül célul tűztük ki a multidrog transzporterek szerepének megértését a szervezet szintjén, az általuk alkotott **védelmi hálózat működésének megismerését**.

3. Alkalmazott módszerek

Mivel a disszertációnak a elsődleges célja a tudományos teljesítmény bemutatása, és nem a kísérleti munkának a reprodukálható közlése, ezért ebben a következő fejezetben csak a legalapvetőbb metodikák vázlatos leírását adom. A több év munkája során olyan sokféle és kisebb-nagyobb részletekben különböző módszert használtunk, hogy ezeknek a részletes leírása feleslegesen növelné a dolgozat terjedelmét. Az alkalmazott metodikák részletes leírását a csatolt közlemények ide vonatkozó fejezetei tartalmazzák.

Sejttenyésztés

Minden sejtkultúrát standard körülmények között az adott sejtnek megfelelő tenyésztő médiumban tartottuk az ajánlott kiegészítésekkel. Az Sf9 (*Spodoptera frugiperda*) rovar sejteket 27°C-on, 10% borjúszérummal (FCS) és penicillin/streptomicin keverékkel kiegészített TNM-FH (Sigma) médiumban tenyésztettük. Az emlős sejtek esetében legtöbbször 10% FCS-sel, 1% L-glutaminnal és penicillin/streptomicin keverékkel kiegészített RPMI vagy D-MEM médiumot (Gibco) alkalmaztunk. Az emlős sejtkultúrákat 5% CO_2 koncentráció mellett, 37°C-on tenyésztettük.

ABC fehérjék expressziója

Az Sf9 sejtekben a különböző ABC fehérjéket bakulovírus segítségével expresszáltuk, amihez a vírusfelülúszókat BaculoGold (Pharmingen) transzfekciós kit felhasználásával állítottuk elő általában pAcUW21-L bakulovektor használatával. Az Sf9 sejtekből az ABC transzportert tartalmazó membránok preparálására vonatkozó metodikai leírást a [8] sz. közlemény tartalmazza. Az emlős sejtekbe tranziens transzfekcióval vagy retrovírus transzdukcióval vittük be a vizsgálni kívánt ABC fehérjét. A transzfekcióhoz Fugene 6 (Roche) transzfekciós kittet és leggyakrabban pEGFP-N1 (Clontech) vektort használtunk. Az emlős sejtek transzdukciójához pedig két-lépéses retrovírus fertőzést alkalmaztunk, amihez a vírusfelülúszót Phoenix eco, illetve PG13 pakolósejtekkel állítottuk elő.

Western blot

A mintákban lévő ABC transzporterek kimutatására általában teljes sejtlizátumokkal SDS-PAGE gélelektroforézist végeztünk, majd a fehérjéket PVDF (Bio-Rad) membránra blottoltuk át. A membránokat megfelelő blokkolás után a vizsgálni kívánt ABC fehérjére specifikus elsődleges ellenanyaggal festettük, majd tormaperoxidáz-konjugált másodlagos antitesttel (Jackson Immunoresearch) hívtuk elő, végül „enhanced chemiluminescence" technikával (ECL, Amersham) tettük láthatóvá.

ATPáz mérés

Az Sf9 membránpreparátumok ATPáz aktivitását a felszabaduló inorganikus foszfát kolorimetriás detektálásával határoztuk meg 1 mM Na-ortovanadát jelenlétében, illetve távollétében [8] 2 mM DTT-t, 500 µM EGTA-Tris-t, 5 mM Na-azidot és 1 mM ouabaint tartalmazó 40 mM MOPS-Tris-ből és 50 mM KCl-ból álló reakcióelegyben (pH 7,0). A 20 µg fehérjét tartalmazó membránokat a vizsgálandó anyagokkal különböző koncentrációban 5 percig 37°C-on előinkubáltuk. A reakciót 3,3 mM MgATP hozzáadásával indítottuk el, és 20 perc elteltével 5% SDS hozzáadásával állítottunk le. ABC fehérjékre jellemző vanadát-szenzitív ATPáz aktivitást a vanadát jelenlétében mért aktivitás levonásával kaptuk meg.

Immunfluoreszcens jelölés

Az immunfluoreszcens festéshez a sejteket 8 lyukas LabTek II kamrán (Nunc Nalgene) vagy polarizált tenyésztés esetén Transwell Col (Corning) membránon növesztettük. A tenyészeteket általában először 4 % paraformaldehiddel, majd előhűtött metanollal fixáltuk. A blokkolást 2mg/ml BSA-t, 1% halzselatint, 0,1 % Triton X-100-t és 5% kecske szérumot tartalmazó Dulbecco módosított PBS (DPBS) oldattal végeztük. A megfelelő mosási lépések közbeiktatásával a vizsgálni kívánt ABC transzporterre specifikus elsődleges ellenanyaggal való inkubálást legtöbbször AlexaFluor fluorofórral konjugált másodlagos ellenanyaggal történő festés követte. A mintákat Olympus FV500-IX konfokális mikroszkóppal általában PLAPO 60× (1.4) olaj immerziós objektívvel vizsgáltuk.

A sejtfelszíni expresszió mérése

Az immunfestés előtt a sejteket tripszineztük, festettük 2 percig 10 mg/ml propidium-jodiddal (PI), majd kíméletesen fixáltuk 1% PFA-val. Az immunfestés további lépéseit 4 ºC-on végeztük. A mintákat 2 mg/ml BSA-t tartalmazó PBS oldatban 10 percig blokkoltuk. Ezután a megfelelő elsődleges, majd általában AlexaFluor fluorofórral konjugált másodlagos antitesttel inkubáltuk 30-30 percig. A jelölést áramlási citométerrel detektáltuk (Becton Dickinson FACS Calibur). Amennyiben valamilyen tesztanyag hatását vizsgáltuk, akkor a sejteket az egész eljárás előtt még a tenyésztőedényben 4 órán keresztül inkubáltuk a vizsgálandó anyaggal. A relatív sejtfelszíni expressziót a drog kezelt és az oldószer kezelt minták mértani átlag fluoreszcencia értékeinek a hányadosával fejeztük ki.

Fluoreszcens festékfelvétel mérése

A sejteket megfelelő festékkel (0,25 µM calcein AM-mel vagy 2 µM Hoechst 33342) inkubáltuk és kevert küvettás fluoriméterrel (Hitachi) vagy konfokális mikroszkóppal követtük a fluoreszcencia intenzitás változását. A multidrog ABC transzporter festékeltávolító

aktivitását 50-100 μM verapamil, 10 μM MK571, 50 μM benzbromaron vagy 1 μM Ko143 hozzáadásával függesztettük fel. Az MDR ABC transzporter festék-eltávolító tevékenységét az MDR aktivitás faktorral (MAF) jellemeztük, amelyet a festékfelvételi sebességekből a bevezetésben leírt módon számoltunk ki (1. egyenlet). A fluoreszcens festékfelvétel áramlási citometriás méréséhez a sejteket külön csövekben azonos ideig (általában 10 percig) inkubáltuk a festékkel (0,25 μM calcein AM-mel) a gátlószer jelenlétében és távollétében. Az aktivitás faktort ekkor az azonos idők alatt felhalmozódott fluoreszcenciák alapján számoltuk. Az áramlási citométeres méréseknél az elpusztult sejteket a PI festődés alapján kizártuk.

A festék kiáramlásának méréséhez (az efflux mérésekhez) a sejteket a festékkel inkubáltuk a megfelelő gátlószer (verapamil, Ko143) jelenlétében, majd alapos mosás után időben követtük a fluoreszcencia csökkenését a fent leírt módokon.

Némelyik vizsgálathoz módosítottuk a membránok koleszterintartalmát. A koleszterin deplécióhoz a sejteket 2,5-4 mM koncentrációjú ciklodextrinnel (CD) inkubáltuk 37 ˚C-on 20-30 percig. A koleszterinnel való feltöltéshez ugyanilyen körülmények között 4,4 % koleszterin-tartalmú CD-t használtunk.

Apoptotikus sejtek detektálása

A 8 lyukas LabTek II kamrán növesztett sejteket Alexa Fluor fluorofórral konjugált annexin V-tel (Invitrogen) inkubáltuk pár percig a megfelelő kötőpufferben (10 mM Hepes, 140 mM NaCl, 2,5 mM $CaCl_2$, pH: 7,4). Amennyiben szükséges volt, a sejteket különböző tesztanyagokkal (1 μM Iressa, 100 μM L-tiroxin, 50 μM benzamil) előkezeltük 24 órával a vizsgálat előtt. Kontroll kísérletekben az apoptózist 2 nM staurosporinnal indukáltuk 5 órával a vizsgálat előtt. A kaszpáz 3 aktivitás kimutatásához az annexin V festést megelőzően 10 μM PhiPhiLuxG_2D_2 (Calbiochem) + 10% FCS adtunk a sejtekhez 20 percen keresztül. A minták festődését a fent specifikált konfokális mikroszkóppal végeztük. A kvantitatív kiértékeléshez a látómezőben lévő összes sejt számát DIC felvétel vagy magfestés alapján határoztuk meg. Az eredményt az Annexin pozitív sejtek az össz-sejtszámhoz viszonyított arányában fejeztük ki legalább 6-8 látómezőt vizsgálva legalább 3 független kísérletben.

Statisztikai módszerek

Az eredményeket általában átlag ± standard hiba (SEM) formában tüntettük fel. A statisztikailag szignifikáns különbségek megítéléséhez Student t-tesztet használtunk, $p < 0,05$ küszöbértéket meghatározva. Az illesztéseket a legkisebb négyzetek módszerével végeztük.

4. Eredmények és diszkusszió

Az ABC transzporterekkel kapcsolatban a 90-es évek közepén felmerült annak lehetősége, hogy néhány közülük (pl. MDR1, CFTR) részt vehet a bizonyos sejtekből tapasztalható, nem vezikuláris úton történő ATP kiáramlásban. Ezért posztdoktori munkám során az extracelluláris nukleotidok jelátviteli szerepével és annak az ABC transzporterekkel való kapcsolatával foglalkoztam. Mivel a jelen disszertáció témájába ez a kutatási terület nem illeszthető be szervesen, itt csak röviden összefoglalom a purinerg jelátvitelben született eredményeimet.

Létrehoztunk egy olyan knockout egeret, amely az egyik legfontosabb purinerg receptor, a P2Y2 (P2U) tekintetében deficiens. Ezt az egeret, illetve annak légúti hámsejtjeit részletesen jellemeztük a Ca^{2+}-jelátvitel, illetve a Cl^--szekréció tekintetében [67, 68]. Kimutattuk, hogy a sejtekből mechanikai stimulus hatására – a sejtek sérülése nélkül - nemcsak ATP kerül ki az extracelluláris térbe, hanem UTP is [69]. Sikerült megmutatnunk, hogy a sejtek felszínén jelentős nukleozid-difoszfokináz aktivitás tapasztalható, amely alapvetően befolyásolja az extracelluláris nukleotidok féléletidejét és az általuk képviselt szignál hatótávolságát [70]. Végül kimutattuk, hogy a hámsejtekben leírt, mechanikai stimulus által kiváltott Ca^{2+}-hullám hátterében nem gap junction-okon keresztül történő kommunikáció áll, hanem mindkét epiteliális felszínen zajló (bilaterális) nukleotid jelátvitel [71]. Erőfeszítéseink ellenére sem sikerült azonban direkt összefüggést kimutatnunk több megvizsgált ABC transzporter (MDR1, MRP1, MRP2 és CFTR), valamint a nukleotid kiáramlás között (csak konferencia előadás formájában bemutatott eredmény).

4.1. A calcein assay kiterjesztése és alkalmazásai

4.1.1. Az MRP1 transzport tulajdonságainak vizsgálata

[1. sz. közlemény]

A bevezetőben részletesen szó esett arról, hogy korábbi munkánk során sikerült kimutatnunk, hogy az MDR1 transzporter hatékonyan képes kipumpálni a sejtekből különféle fluoreszcens indikátorok hidrofób karakterű, acetoxi-metilészter (AM) formáját. Ez a jelenség és a calcein kedvező tulajdonságai lehetőséget adtak egy olyan kvantitatív módszer kidolgozására, amellyel az MDR1 transzport aktivitását egyszerűen és megbízható módon detektálni tudjuk. Az MRP1 fehérje klónozását követően, az alapvető karakterizálások megmutatták, hogy az említett két multidrog transzporter részben átfedő szubsztrát felismeréssel rendelkezik, - leginkább a hidrofób karakterű drogokat tekintve (ld. 3. ábra).

Ez a megfigyelés volt az alapja annak a munkánknak, melynek elsődleges célja az volt, hogy feltérképezzük az újonnan azonosított multidrog transzporter, az MRP1 és a calcein AM kölcsönhatását. Vizsgálatainkhoz egy olyan tüdőkarcinóma sejtvonalat használtunk, amely transzfekciós, re-szelekciós és klónozási eljárás eredményeképpen stabilan expresszálja az MRP1 fehérjét (SW1573/S1/MRP). Összehasonlítva a kiindulási (parentális) sejtvonalat (S_1) az MRP-transzfekált sejtekkel (S_1MRP1), azt tapasztaltuk, hogy a calcein AM gyorsan bejut a parentális sejtekbe, és a szabad festék akkumulálódik azokban. Ezzel szemben az MRP1-t expresszáló sejtekben csak csekély mértékű festékfelhalmozódást lehetett megfigyelni (7a ábra). Vinblasztin, amelyről ismert volt, hogy az MRP1-nek is szubsztrátja, a fluoreszcencia gyors növekedését okozza a transzfektált sejtekben, de a kontroll sejtekben mérhető festék akkumulációt a VBL nem befolyásolta. Hasonlót tapasztaltunk verapamil hozzáadásával is. Mindez arra utalt, hogy az MRP1 transzporter, az MDR1-hez hasonlóan, a calcein AM-et kipumpálja a sejtekből. Az MRP1-transzfektált sejtek ATP-depléciójával megmutattuk, hogy az alacsony festékfelvétel ATP-függő, tovább erősítve azt a feltevést, hogy a jelenség hátterében az MRP1 transzportaktivitása húzódik meg.

Mivel az MRP1 feltérképezett szubsztrátjai között anionok is szerepeltek, megvizsgáltuk, hogy vajon ez a transzporter a szabad sav formájú calceint is képes-e kipumpálni a sejtekből. Calceinnel előre feltöltött sejtekből mértük a festék kiáramlását, és azt tapasztaltuk, hogy a transzfektált sejtekben valóban jelentős mértékű, vinblasztinnal vagy verapamillal gátolható calcein efflux tapasztalható (ábrán nem bemutatott eredmény). Ez a megfigyelés arra utalt, hogy szemben az MDR1-gyel, az MRP1 nemcsak a calcein AM formáját, hanem a szabad sav formáját is képes transzportálni. Érdemes megjegyezni, hogy a két szubsztrát transzportkinetikája jelentősen különbözik, az acetoxi-metilészter eltávolítása sokkal gyorsabb, mint a szabad sav transzportja. Figyelembe kell tehát venni, hogy az MRP1-et expresszáló sejtekben tapasztalható alacsony calcein akkumuláció a két jelenség eredője.

A fent ismertetett megfigyelések alapján a calcein assay az MRP1 vizsgálatára is kiterjeszthető. Ahogy korábban említettem, ez a módszer lehetőséget ad egyrészt a transzporter aktivitásának mérésére, diagnosztikájára, másrészt felhasználható a fehérje transzporttulajdonságainak vizsgálatára, szubsztrátjainak és gátlószereinek feltérképezésére. Ez utóbbi vonalat követve farmakológiailag aktív anyagokat vizsgáltunk, hogy vajon befolyásolják-e az MDR1-, illetve az MRP1-mediált festék eltávolítást. Ezzel a megközelítéssel számos olyan vegyületet azonosítottunk, amely mindkét multidrog transzporterrel kölcsönhatásba lép, de sikerült olyat is találnunk, amely csak az MRP1 fehérje hatott (ld. 1. közlemény 1. táblázat).

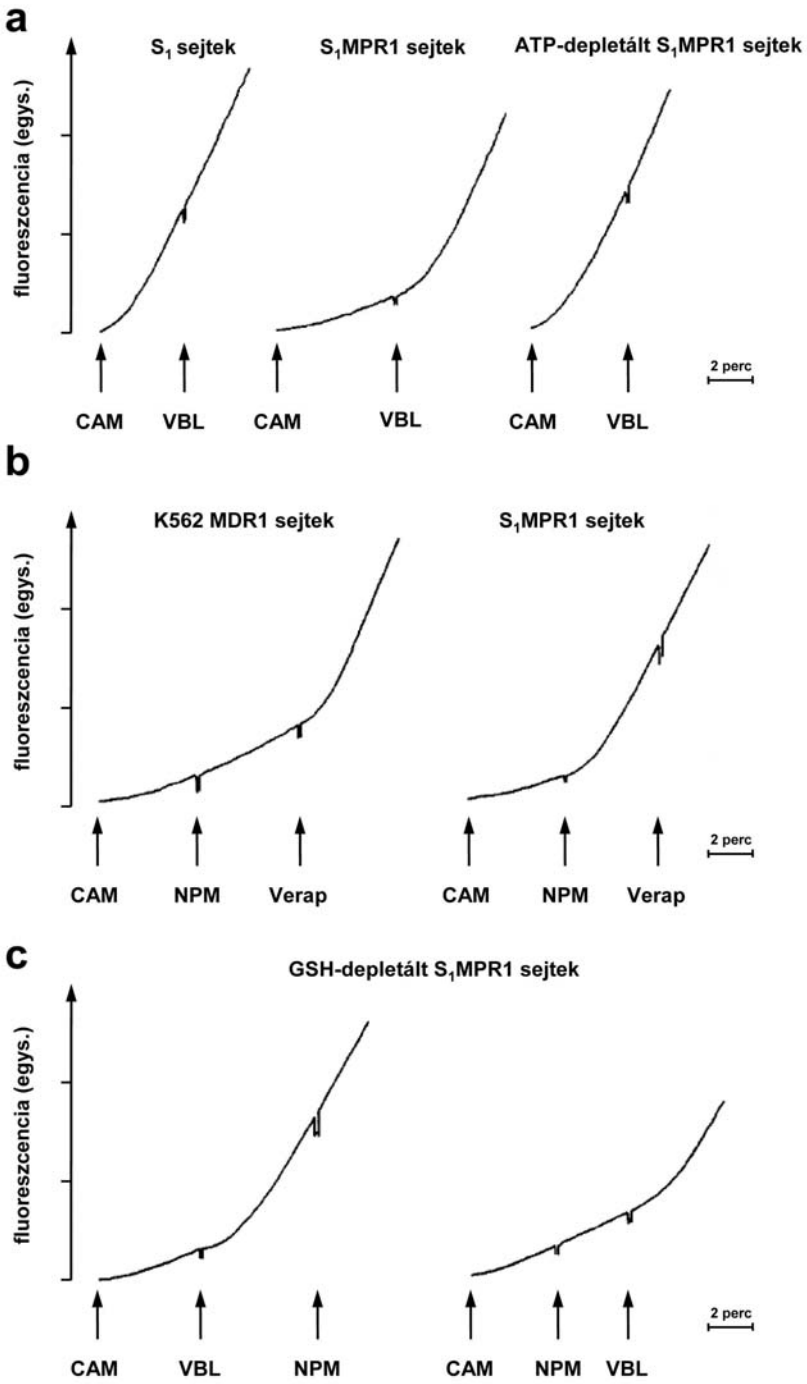

7. ábra: Az MPR1 transzporttulajdonságainak vizsgálata calcein assay-vel. Drog-szenzitív (S_1) és drog-rezisztens (S_1MRP1 és K562 MDR1) sejteket 0,25 μM calcein AM (CAM) festékkel inkubáltunk, majd a nyilakkal jelölt időpontban 10 μM vinblasztint (VBL), 1 μM N-pirén-maleimidet (NPM) vagy 100 μM Verapamilt (Verap) adtuk a médiumhoz. A sejtek fluoreszcenciáját fluoriméterben mértük. **a)** Gyors calcein felhalmozódást látunk S_1 kontroll sejtekben, amit nem befolyásol a VBL hozzáadása. Ezzel szemben S_1MRP1 sejtekben alacsony festék akkumulációt tapasztalunk, amit revertál a VBL. A folyamat ATP-függését ATP-depletált S_1MRP1 sejtekkel mutattuk meg. **b)** Az NPM nem volt hatással a calcein AM kipumpálásra K562 MDR1 sejtekben, viszont az MRP1-et expresszáló sejtekben meggátolta a CAM transzportját. **c)** A glutation (GSH) depléció VBL hatását nem befolyásolta, viszont az NPM gátlóhatását felfüggesztette S_1MRP1 sejtekben.

A mindkét transzporterre ható anyagok között leginkább hidrofób karakterű molekulák szerepelnek, mint a vinblasztin, verapamil, tamoxifen, ciklosporin A, kinin, stb. Kizárólag az MRP1-gyel kölcsönhatásba lépő szerek között azonban vannak hidrofób anionok (pl. CCCP), gyenge savak (pl. probenicid, benzbromaron, indometacin) is, de ugyanígy maleimid-származékok (pl. N-etil-maleimid - NEM, N-pirén-maleimid - NPM) vagy a prosztaglandin A_1. Példaként a 7b ábrán az NPM-mel kapott eredményeket mutatom be.

Mivel az MRP1 transzporterrel kapcsolatban felvetették, hogy a drogokat glutation (GSH) konjugátum formájában pumpálja ki a sejtekből, ezért megvizsgáltuk a GSH szerepét a calcein assay-ben, illetve az MRP1-mediált calcein eltávolítást gátló anyagok vonatkozásában. Az MRP1-et expresszáló sejteket többféle módszerrel (BSO, illetve diamin előkezeléssel) GSH-depletáltuk. Azt tapasztaltuk, hogy a GSH depléció érdemben nem befolyásolja a calcein AM eltávolítását, mivel ezekben a sejtekben is alacsony festékakkumulációt figyelhettünk meg (7c ábra). A vinblasztin ugyanúgy felfüggesztette a festék eltávolítását, mint a nem kezelt sejtekben (vö. 7a ábra középső panel). Mindez arra utal, hogy a glutation nem szükséges sem a calcein, sem a vinblasztin transzportjához. Ezzel szemben a hidrofób SH-reaktív ágensek (NEM vagy NPM) MRP1-gyel való kölcsönhatása glutation-függőnek bizonyult. A GSH-depletált sejtekben ezek a maleimid-származékok nem gátolták a festékeltávolítást (7c ábra jobb oldali panel, vö. 7b ábra jobb oldali panel). Ezek alapján az valószínűsíthető, hogy az MRP1 többféle mechanizmussal, GSH-függő és attól független utakon pumpálja ki a szubsztrátokat. A későbbiekben, itt nem bemutatott kísérletekben, kimutattuk az NPM-glutation-konjugátum kiáramlását is a sejtekből. Ez a folyamat egyrészt függött az MRP1 expressziójától, másrészt gátolható volt calcein AM-mel, illetve más MRP1-gyel kölcsönhatásba lépő szerekkel (1. közlemény 3 ábra).

Összefoglalva, ebben a munkában megmutattuk, hogy az MRP1 képes a calcein acetoxi-metilészter- és szabad sav formáját is kipumpálni a sejtekből. Ezek alapján a calcein assay megfelelő sejtek alkalmazásával az MRP1 transzporterre is alkalmazható. A farmakológiai tesztelés során azonosítottunk olyan vegyületeket, amelyek kizárólag az MRP1-gyel lépnek kölcsönhatásba, valamint olyanokat is, melyek mind az MDR1, mind az MRP1 fehérjékre hatnak. Demonstráltuk, hogy bizonyos anyagokat az MRP1 glutation-konjugátumként pumpál ki a sejtekből, míg vannak olyanok, melyek transzportja a glutationtól független.

4.1.2. Az MDR1 és MRP1 párhuzamos detektálása

[2. sz. közlemény]

Az a megfigyelés, hogy a calcein AM-et mind az MDR1, mind az MRP1 hatékonyan képes kipumpálni a sejtekből, azt a lehetőséget kínálta, hogy a calcein assay diagnosztikai célú alkalmazásánál képesek lehetünk mindkét multidrog transzporter funkcionális jelenlétét meghatározni. A módszer kidolgozásánál az alapvető elképzelés az volt, hogy szelektív gátlószer alkalmazásával először az egyik transzporter festékeltávolító aktivitását függesztjük fel, majd a másikét, így szétválasztva a két transzportaktivitást.

Mivel az MRP1 még az MDR1-nél is szélesebb szubsztrát-felismerő képességgel rendelkezik, elsősorban olyan inhibitort kerestünk, amely szelektíven az MRP1-et gátolja. Többféle vegyület is alkalmasnak bizonyult a két transzpert megkülönböztetésére, azonban kritikus volt a megfelelő inhibitor koncentráció meghatározása. Hármas kritérium rendszert állítottunk fel: egyrészt hogy az inhibitor teljes mértékben gátolja az MRP1-et, másrészt hogy legkevésbé se gátolja az MDR1-et, harmadrészt hogy ne befolyásolja a sejtek állapotát, illetve az észteráz aktivitást. Ezek a tulajdonságok és ennek következtében az ideális küszöb-koncentráció azonban némiképpen függött a mintáktól és az alkalmazott technikától (kevert követtás fluoriméter vagy áramlási citométer, stb.)

A módszer beállításához és finomhangolásához MRP1-et és MDR1-et expresszáló sejteket (HL60 MRP, 3T3 MDR) használtunk. Mivel a verapamil 50-100 μM tartományban - az észteráz aktivitás befolyása nélkül - teljes mértékben gátolja mindkét transzporter festékeltávolító aktivitását, pozitív kontrollként ezt a vegyületet használtuk. A 8. ábrán bemutatott áramlási citométerrel végzett kísérletben az MRP1 gátlására 10 μM MK571-et alkalmaztunk, amit eredetileg leukotrién D_4 receptor antagonistaként hoztak forgalomba, de az MRP1-nek is hatékony és szelektív gátlószerének bizonyult. A HL60 MRP sejtekben ez a gátlószer koncentráció teljes mértékben gátolta az MRP1 festékeltávolító aktivitását (8a ábra), az MDR1 aktivitására azonban csak csekély mértékben hatott (8b ábra). Érdemes felhívni a figyelmet arra, hogy az ábrán logaritmikus skála szerepel, ezért az MDR1 gátlása mindössze kb. 5 %-ra tehető.

Ezt követően különböző arányokban (50-50 %, illetve 5-95 %) összekevertük az MRP1-et és MDR1-et expresszáló két sejttípust, és megmutattuk, hogy az MK571 és a verapamil alkalmazásával a calcein assay segítségével a két multidrog transzporter aktivitása egymástól függetlenül is detektálható - még akár olyan kevert sejtkultúrákban is, ahol az egyik transzportert expresszáló sejtek aránya mindössze 5 %-ot tesz ki (8c-d ábra).

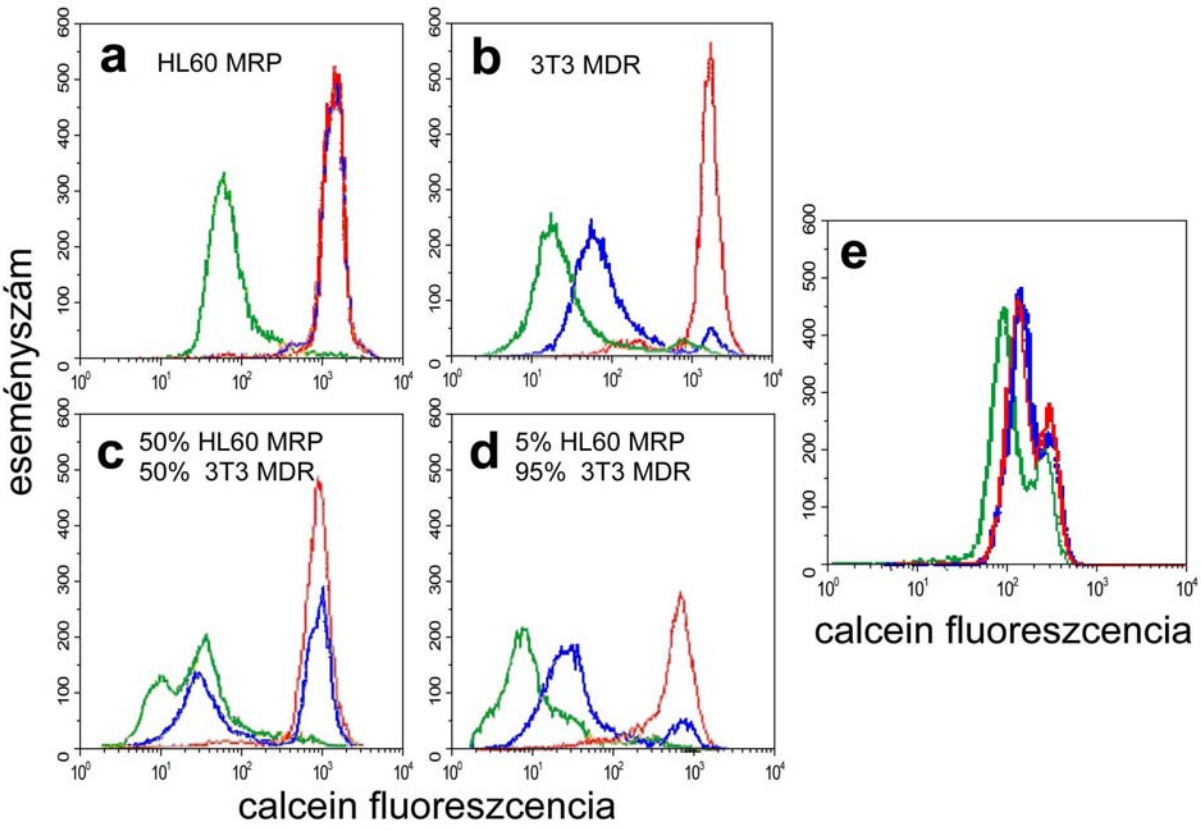

8. ábra: Az MDR1 és MRP1 funkcionális elkülönítése áramlási citométer használatával. a-d) HL60 MRP és 3T3 MDR sejteket különböző arányban kevertük és 0,25 µM calcein AM-mel inkubáltuk DMSO (oldószer-kontroll, zöld), 10 µM MK571 (MRP1 gátlószer, kék) vagy 60 µM verapamil (MDR1-MRP1 inhibitor, piros) jelenlétében, majd a mintákat áramlási citométerben vizsgáltuk. **a)** 100% HL60 MRP **b)** 100 % 3T3 MDR **c)** 50-50 % HL60 MRP és 3T3 MDR **d)** 5% HL60 MRP and 95 % 3T3 MDR sejt. **e)** MRP1 aktivitás detektálása akut mieloid leukémiában szenvedő beteg perifériális véréből izolált mononukleáris sejtekben. A kísérletet az előzőekhez hasonlóan végeztük annyival kiegészítve, hogy a betegmintát propidium-jodiddal (PI) is inkubáltuk, és az elpusztult sejteket a PI-festődés alapján kizártuk.

A calcein assay diagnosztikai célra történő alkalmazását a 4.1.3. fejezetben mutatom be részletesen leukémiás betegekből nyert mintákon. Azokat a vizsgálatokat még úgy indítottuk, hogy nem volt a kezünkben az MDR1 és az MRP1 aktivitását egymástól függetlenül meghatározó módszer, ezért az ott bemutatott adatok csak az általános (verapamil gátláson alapuló) MDR aktivitás faktor értékekre alapulnak. Viszont annak demonstrálására, hogy a módszer alkalmas arra, hogy akár klinikai mintákban is detektáljuk az MRP1 aktivitást, a 8e ábrán egy esettanulmányt mutatok be. Egy akut mieloid leukémiában szenvedő beteg perifériás véréből mononukleáris sejteket izoláltunk, majd a sejtmintán szelektív (MK571-t és verapamilt alkalmazó) calcein asssay-t végeztünk. Mivel ebben a bemutatott esetben az MK571 ugyanolyan mértékben gátolta a festékeltávolítást, mint a verapamil, az valószínűsíthető, hogy az adott beteg sejtjeiben MRP1 expresszálódik, de MDR1 nem.

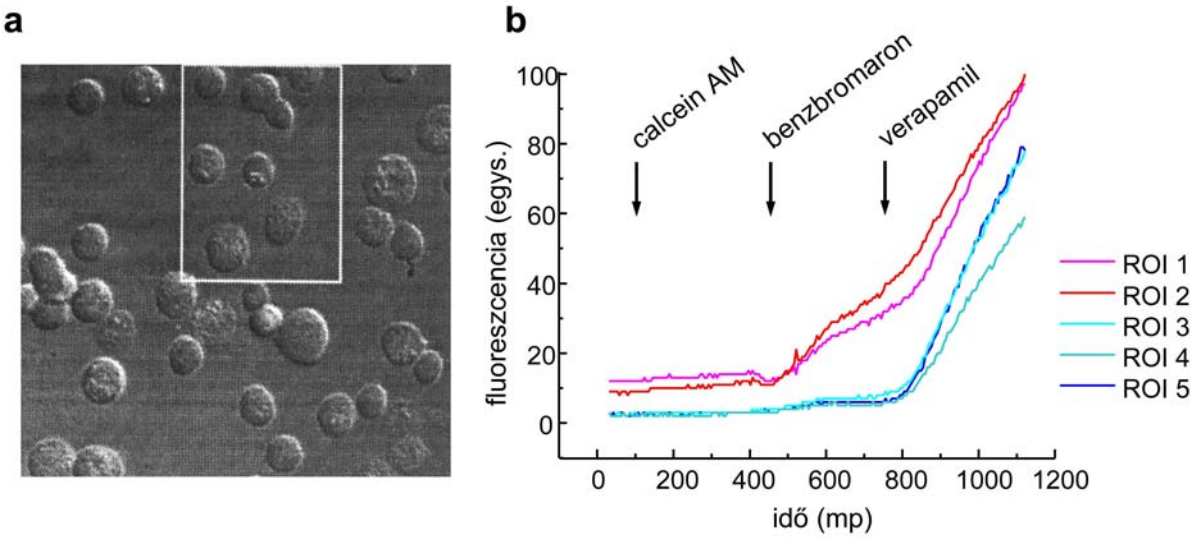

9. ábra: Az MDR1-et, illetve MRP1-et expresszáló sejtek elkülönítése egy-sejt szinten. HL60 MRP és 3T3 MDR sejteket tartalmazó kevert tenyészetet 0,25 µM calcein AM-mel inkubáltuk, majd a jelzett időpontban 50 µM benzbromaront, majd 50 µM verapamilt adtunk a médiumhoz. A sejtekben a calcein felhalmozódást fluoreszcens képalkotó rendszerrel vizsgáltuk. **a)** A DIC felvételen kiválasztottunk néhány sejtet. **b)** Az egyes sejtekre helyezett régiókkal (ROI: region of interest) meghatároztuk a festékfelvételi kinetikát. A benzbromaron gátlóhatása alapján az MRP1-et kifejező sejtek megkülönböztethetőek az MDR1-et expresszálóktól.

Az MDR1 és MRP1 aktivitásának az előzőekben bemutatott, calcein assay-vel történő megkülönböztetése nemcsak áramlási citométerrel lehetséges, hanem fluoreszcens mikroszkóp és ahhoz csatlakozó képalkotó rendszer segítségével akár az egyes sejtek szintjén is alkalmazható a módszer. Ennek bemutatására összekevertünk HL60 MRP és 3T3 MDR sejteket, és a calcein AM hozzáadását követően mikroszkópos rendszerrel követtük a fluoreszcencia felhalmozódását az egyes sejtekben (9. ábra). Ebben az esetben benzbromaront használtunk MRP1-szelektív gátlószerként. A 9b ábrán bemutatott festékfelvételi kinetikákból látható, hogy a tetszőlegesen kiválasztott 5 sejt közül kettőben növekedett meg a festék-felvétel sebessége, a másik háromban csak a verapamil hozzáadása után tapasztaltuk ezt, ami arra utal, hogy ezekben a sejtekben az MDR1 expresszálódik. A látómezőt rögzítve és a sejteket fixálva, immunfestéssel igazoltuk abban a három sejtben az MDR1 jelenlétét (ábrán nem bemutatott eredmény, 2. közlemény 4. ábra).

A fent ismertetett munkában megmutattuk, hogy a calcein assay alkalmas mind az MDR1, mind az MRP1 aktivitásának detektálására. Szelektív gátlószer alkalmazásával heterogén kultúrákban pedig megkülönböztethetők az egyik vagy másik multidrog transzportert expresszáló sejtpopulációk vagy akár egyes sejtek. Bár az itt bemutatott példákban ilyen eset nem fordult elő, de olyan is előfordulhat, hogy egy sejt expresszálja mindkét transzportert, módszerünk azonban alkalmas ennek detektálására is.

4.1.3. A calcein assay diagnosztikai alkalmazása

[3. sz. közlemény]

A calcein assay egyik alkalmazási területe a multidrog fehérjék (MDR1, MRP1) transzporttulajdonságainak vizsgálata. Ahogy ezt a 4.1.1. fejezetben az MRP1 példáján bemutattuk, a módszer segítségével fel lehet térképezni a transzporterekkel kölcsönhatásba lépő anyagokat. Az ilyen jellegű farmakológiai felhasználásán túl a calcein assay alkalmas arra is, hogy különböző mintákban kvantitatívan meghatározzuk a multidrog transzporterek (MDR1, MRP1) aktivitását. A technikának az ilyen irányú felhasználása szintén fontos lehet különböző kutatási területeken, azonban még jelentősebb szerepet kaphat a klinikai diagnosztikában. A következőkben azt a munkánkat foglalom össze, mely során a calcein assay segítségével rákos betegektől kapott mintákban határoztuk meg a multidrog transzporterek aktivitását, és összevetettük a klinikai paramétereikkel.

A multidrog rezisztencia diagnosztikájának elsősorban azokban a tumorokban van jelentősége, ahol az MDR fenotípus nem kötelező módon, de gyakorta megjelenik. Az akut leukémiák ehhez a csoporthoz tartoznak, ráadásul gyakorlati szempontból egy olyan előnnyel is bírnak a szolid tumorokkal szemben, hogy a minta könnyen hozzáférhető, és a rákos sejtek izolálása nem igényel különösebb előkészítést.

A bemutatott munkában 93 *de novo* akut leukémiával diagnosztizált beteg mintáit vizsgáltuk meg két nagy hematológiai központban, a Debreceni Egyetemen, illetve az Országos Hematológiai Intézetben, Budapesten. A betegek közül 65-nél akut mieloid leukémiát (AML), míg 28-nál akut limfoid leukémiát (ALL) diagnosztizáltak. A betegek perifériális véréből a mononukleáris sejteket izolálva, calcein assay-vel áramlási citométerben mértük a multidrog rezisztencia transzporterek aktivitását. A vizsgálatoknál csak az élő sejt-frakciót vettük figyelembe, amit propidium-jodid (PI) festéssel, és a PI-pozitív sejtek kizárásával hajtottunk végre. Az eredményeket a bevezetésben említett MDR aktivitás faktorral fejeztük ki az (1) képlet alapján. A budapesti centrumban vizsgált betegmintákban meghatározott MAF 17,6-nak adódott az AML-es esetekben ($n = 43$), míg 7,8-nak az ALL-es esetekben ($n = 14$) (10a ábra). Az utóbbi nem különbözött szignifikánsan a nem-beteg mononukleáris sejtekben mérhető MAF értéktől ($11,9 \pm 6,4$), míg az AML esetek szignifikáns eltérést mutattak ($p < 0,05$). A debreceni központban is hasonló különbséget mutattak ki az AML-es és ALL-es betegek mintái között (ábrán nem bemutatott eredmény, 3. közlemény 1a ábra). Ezek alapján a következőkben csak az AML-lel diagnosztizált betegcsoport elemzésével foglalkoztunk.

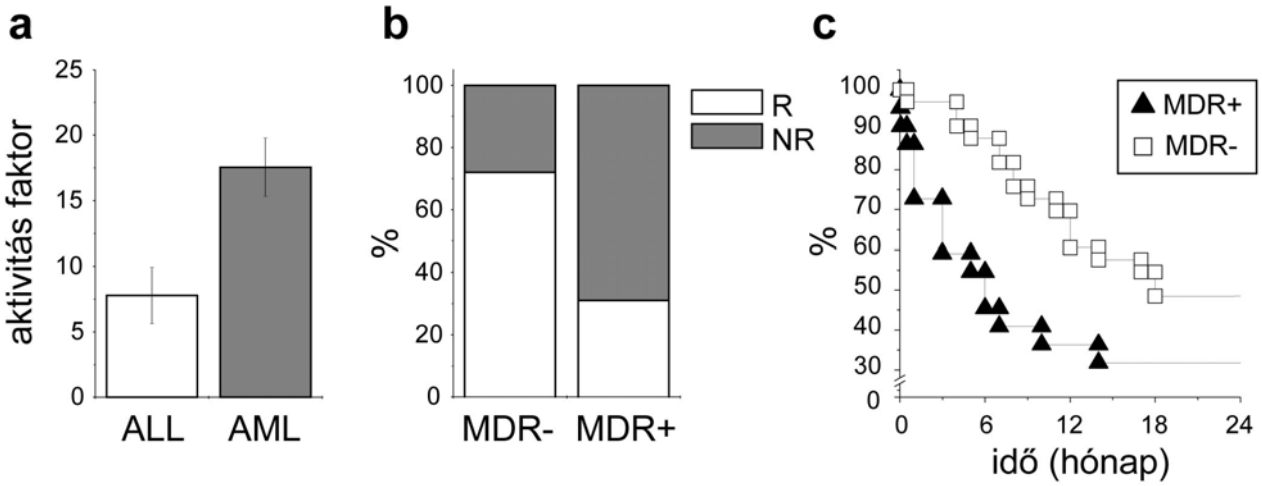

10. ábra: A calcein assay alkalmazása klinikai mintákon. a) Akut limfoid leukámiában (ALL) és akut mieloid leukémiában (AML) szenvedő betegek perifériális véréből izolált mononukleáris sejtekben calcein assay-vel (0,25 μM calcein AM, 100 μM verapamil) áramlási citométer segítségével meghatároztuk az MDR aktivitás faktort. Az oszlopokon az átlag ± SEM értékek szerepelnek (n = 14, illetve 43) **b)** A calcein assay prediktív értéke a terápiára adott válasz tekintetében 65 AML-es beteget vizsgálva. MDR+: aktivitás faktor > 20 (n = 26); MDR-: aktivitás faktor < 20/25 (n = 39); R (responder): az első vagy legalább a második kezelés hatására teljes remisszióba kerülő betegek; NR (non-responder): a terápiára nem válaszoló betegek. A calcein assay-vel meghatározott MDR fenotípus pozitív prediktív érték 69 %-nak adódott, ami szignifikáns összefüggést mutatott a terápiára adott válasszal ($p < 0,005$) **c)** Az MDR fenotípus alapján két csoportba sorolt 65 AML-es beteg Kaplan-Meier túlélési görbéje (n = 26, illetve 39). Csak a 8 hónapnál hosszabb túlélési időket vettük figyelembe. A két csoport között szignifikáns különbség mutatkozott a túlélés tekintetében is ($p < 0,05$).

Mindkét központban az AML-es betegeket standard, 7 + 3 remisszió indukciós kemoterápiás protokoll alapján kezelték a megfelelő kiegészítésekkel - egy vagy szükség esetén két ciklust alkalmazva. 4 hét elteltével a betegek kezelésre adott válaszát a csontvelői és perifériális vérminta morfológiája alapján értékelték. Teljes remissziónak – az ajánlások alapján - azt tekintették, ha a csontvelőben a blasztok aránya nem haladta meg az 5 %-ot, a periférián pedig egyáltalán nem volt blasztos sejt [72]. A kezelést követően meghatározva az MDR aktivitás faktort a betegek vérmintáiban, azt tapasztaltuk, hogy a terápiára reagálók (responder-ek) esetében szignifikánsan alacsonyabb értéket kaptunk, mint a nem-reagálók (non responder-ek) mintáiban. A kapott MAF értékek eloszlási görbéje alapján mindkét centrumban beállítottunk egy-egy küszöbértéket. A kisebb metodikai eltérések következtében ez az érték a budapesti központban 20-nak, míg a debreceni centrumban 25-nek adódott.

Ezek után a 65 betegmintát két csoportra (MDR-pozitív, illetve MDR-negatív) osztottuk az alapján, hogy az aktivitás faktor a megállapított küszöbértéket meghaladta vagy alatta maradt, és kiszámoltuk az egyes csoportokban a terápiára reagálók (R) és nem-reagálók (NR)

arányát. A calcein assay alapján meghatározott MDR-negativitás magas pozitív prediktív értéket adott a terápiára adott válasz tekintetében (72 %), míg az MDR-pozitív fenotípus 69 %-os eséllyel a kezelés negatív kimenetelét vetítette előre. Az esélyhányados az MDR-pozitivitás és a sikertelen terápia viszonylatában 5,7-nek adódott (95 %-os konfidencia intervallum: 1,7-19, p = 0,004). Érdekes módon a vizsgált betegcsoportban az MDR fenotípuson kívül csak a beteg kora bizonyult prognosztikai jelentőségű faktornak a kemoterápiára adott válasz tekintetében.

Megvizsgáltuk az említett két betegcsoportnál az MDR fenotípus és a hosszú távú klinikai kimenetel összefüggését. A 10c ábrán bemutatott Kaplan-Meier túlélési görbén csak azokat a betegeket vettük figyelembe, akik a diagnózist követően 8 hónapnál tovább éltek. Azt tapasztaltuk, hogy az MDR-negatív csoportba tartozó betegek 50 %-os túlélési iedeje kb. háromszorosa az MDR-pozitív betegekénél. Azonban statisztikailag ez a különbség nem bizonyult szignifikánsnak (p = 0,07).

Összefoglalva, ebben a munkában bemutattuk, hogy a calcein módszer alkalmas klinikai minták kvantitatív elemzésére is. Kimutattuk továbbá, hogy az ilyen módon meghatározott MDR fenotípus a *de novo* akut mieloid leukémiában szenvedő betegeknél prognosztikai értékkel bír a kemoterápiás kezelésre adott válasz tekintetében. A magas MDR aktivitás faktor kedvezőtlen terápiás válaszképességet vetít előre.

A jelen ismertetett munkában a calcein assay diagnosztikai célú felhasználását leukémiás mintákon mutattuk be. Érdemes azonban megemlíteni, hogy arra is erőfeszítéseket tettünk, hogy a módszert kiterjesszük a szolid tumorok MDR diagnosztikájára is. Ebből a munkából egy szabadalom született [73], azonban ennek ismertetésére ebben a disszertációban nem térek ki.

4.2. Az ABCG2 multidrog transzporter funkcionális vizsgálata

Az ABCG2 fehérje az ABCG alcsaládhoz tartozó féltranszporter. Az alcsalád mind az öt tagjára jellemző, hogy a nukleotid-kötő domén N-terminálisan helyezkedik el a polipeptid-láncon belül (ld. 1b ábra). Ahogy a bevezetőben arról szó esett, az ABCG1 és ABCG4 élettani szerepe nem teljesen tisztázott, de expressziós mintázatuk és transzkripciós szabályozásuk alapján leginkább a lipidanyagcserével hozhatók összefüggésbe. Az ABCG5 és ABCG8 fehérjékről viszont ismeretes, hogy heterodimert képezve az intesztinális és hepatikus szterol-transzportban töltenek be fontos szerepet. Bár az ABCG5/ABCG8 transzporterpár aktivitása révén növényi szterolokkal szembeni rezisztenciát biztosít a sejtek számára, az ABCG2 az ABCG alcsaládon belül az egyetlen klasszikus értelemben vett multidrog transzporter.

Az ABCG2 fehérjét eredetileg szelektált multidrog-rezisztens sejtvonalakból klónozták [74-76], később igazolták, hogy ez a fehérje atipikus multidrog rezisztenciát képes okozni [77]. Endogén expressziója számos szövetben kimutatható, ezek között meg kell említeni a petefészket, a vesét, az emlő hámsejtjeit, a vékonybelet, a vér-agy gátat és a placentát [78]. Ahogy az szintén szóba került, az ABCG2 több őssejt-típusban is megtalálható, és elsődlegesen felelős az ún. „side population" fenotípusért, melyet az őssejtek diagnosztikus markereként is szoktak használni [79]. Az ABCG2 szubsztrátjai között számos tumorellenes szer szerepel, mint például a mitoxantron, topotekán, flavopiridol, methotrexát. Bár fiziológiás szubsztrátjai a mai napig nincsenek feltérképezve, az Abcg2-deficiens egerekkel kapott eredmények arra utalnak, hogy ez a transzporter fontos szerepet játszhat a különböző toxikus anyagok elleni védelemben, valamint a sejt porfirin-háztartásában [80, 81].

A következő fejezetekben azokat a munkáinkat fogalom össze, amelyekben az ABCG2 multidrog fehérje transzport tulajdonságainak, működési mechanizmusának jobb megértéséhez vittek közelebb.

4.2.1. Az ABCG2 fehérje Iressával való kölcsönhatása

[4. sz. közlemény]

Számos rosszindulatú daganat esetében aktiválódik az EGFR (epidermális növekedési faktor receptor) szignálútvonal. E tumorok közé tartozik az egyik legsúlyosabb tüdőkarcinóma, a kissejtes tüdőrák is. A tumorellenes szerek egyik fejlesztési iránya, hogy az EGF-receptor gátlása révén próbálják a rákos sejtburjánzást megakadályozni. Ezen belül az egyik megközelítés monoklonális ellenanyagok alkalmazásával valósítja ezt meg, másrészt nagy erőkkel fejlesztenek olyan kis molekulákat is, amelyek az EGF-receptor tirozinkináz enzim-

aktivitását közvetlenül gátolják. Ezek közé a tirozinkináz-receptor inhibitor (TKRI) drogok közé tartozik az Iressa (Gefitinib, ZD1839) nevű tumorellenes szer is, amely szelektíven és reverzibilisen képes gátolni az EGF-receptort, és a hozzá kapcsolódó szignálutat [82, 83]. Az ígéretes eredmények után a kissejtes tüdőrák kezelésénél azonban az Iressa a klinikai vizsgálatok 3. fázisában elbukott [84, 85]. Valószínűleg ennek hátterében az áll, hogy az EGF-receptorban bekövetkező mutációk, melyek gyakoriak a kissejtes tüdőrákokban, nagymértékben befolyásolják a tumor Iressával szembeni érzékenységét [86, 87].

Rendkívül fontos kérdés azonban a tumorellenes szerek fejlesztésénél, hogy az adott molekula kölcsönhat-e a multidrog transzporterekkel, illetve, hogy milyen jellegű ez a kölcsönhatás. Azok a drogok, amelyeket az MDR-ABC fehérjék szubsztrátként ismernek fel, hatástalanok maradhatnak olyan tumorokban, melyekben a multidrog transzporterek expresszálódnak. Másrészt pedig a gátló hatású drogok elősegíthetik a terápiát, ha kombinációban alkalmazzák más tumorellenes szerrel. Ugyanakkor figyelembe kell venni, hogy az ilyen hatású szerek károsan befolyásolhatnak fontos élettani folyamatokat és nagymértékben megváltoztathatják más drogok biohasznosulását is. A kutatócsoportunkban zajló korábbi munkák során sikerült kimutatni számos tirozinkináz-receptor inhibitor és a multidrog transzporterek (MDR1, illetve ABCG2) közötti kölcsönhatást [88, 89]. Ezek közül figyelemre méltó volt az Iressa és az ABCG2 közötti nagy affinitású kapcsolat. Nyitva maradt azonban az a kérdés, hogy az ABCG2 valóban transzportálja-e ezt a drogot.

Az ABCG2 és az Iressa közötti funkcionális kölcsönhatást többféle megközelítéssel igazoltuk. Egyrészt közvetett módon, a korábban az MDR1, illetve az MRP1 esetében sikerrel alkalmazott módszer, a drog-stimulált ATPáz aktivitás mérés segítségével kimutattuk a drog és transzporter közötti kölcsönhatást (11. ábra). Az Iressa tizedmikromólos tartományban stimulálta az ABCG2-t tartalmazó membránpreparátumok vanadát-szenzitív ATPáz aktivitását, ami arra utal, hogy az Iressa az ABCG2-nek szubsztrátja. Magasabb koncentrációban a drog viszont gátolta az ABCG2-függő ATPáz aktivitást, amely más MDR-ABC transzperek, illetve más drogok esetében is gyakran tapasztalt jelenség. Ha ugyanezt a kísérletet az ABCG2 specifikus gátlószere, a Ko143 jelenlétében végeztük, az Iressa stimuláló hatása elmaradt, ami igazolja, hogy a jelenség az ABCG2 transzportaktivitásától függő folyamat. Hasonlóképpen nem tapasztaltunk ATPáz aktivitás fokozást olyan membrán-preparátumokon, melyek kontroll (ABCG2-t nem tartalmazó) sejtekből, illetve az inaktív mutáns variánst ($ABCG_{K86M}$-t) expresszáló sejtekből készültek (ábrán nem bemutatott eredmény). Ez utóbbi ABCG2 változat, amely a kritikus Walker A motívumban egy lizin-metionin cserét tartalmaz, szolgál kontrollként a legtöbb funkcionális vizsgálathoz.

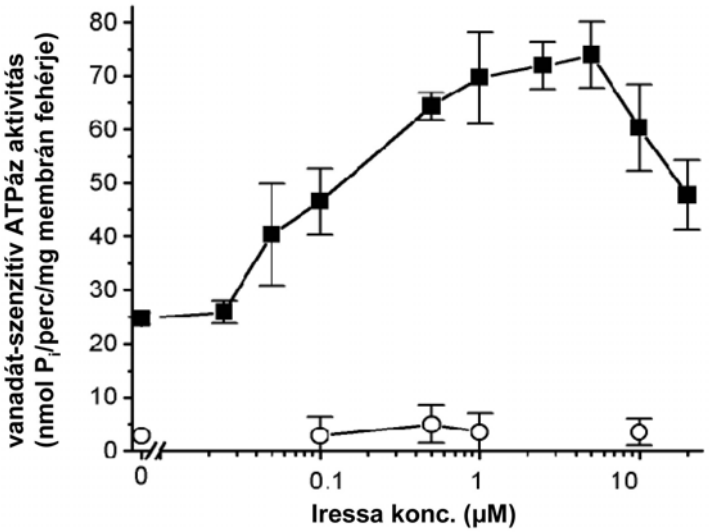

11. ábra: Az ABCG2 drog-stimulált, vanadát-szenzitív ATPáz aktivitása. Az ABCG2-t tartalmazó (MCF7/MX) membránpreparátumokban mérhető vanadát-szenzitív ATPáz aktivitást az Iressa koncentráció-függő módon fokozta (■). Magasabb koncentrációkban azonban gátló hatás volt tapasztalható. Az ABCG2 specifikus gátlószere (1 μM Ko143) jelenétében az Iressának ez a stimuláló hatása nem volt megfigyelhető (○). Az ábrán szereplő adatok átlag + SD értékeket mutatnak (n>3).

Az Iressa és a transzporter közötti funkcionális kölcsönhatás közvetlen kimutatására egy újszerű kísérleti megközelítést alkalmaztunk. Egy olyan pikkelysejtes karcinóma sejtvonalat használtunk (A431) kísérleteinkben, melynek a túlélése az EGFR-szignálúttól függ. Ezért az Iressa, amely specifikusan gátolja az EGF-receptort, ezekben a sejtekben sejtpusztulást okoz. Ebbe a sejtvonalba retrovírus segítségével expresszáltattuk a vad típusú ABCG2-t (G2), illetve az inaktív mutáns variánst ($G2_{K86M}$). Mitoxantronnal (MX) történt szelekciós eljárással a transzporter expresszióját fokoztuk a vad típusú ABCG2-vel transzdukált sejtekben ($G2_{Mx}$). Western analízissel igazoltuk, hogy az ABCG2 egyforma magas szinten expresszálódik a G2, illetve $G2_{K86M}$ jelű A431 sejtvonalakban. Ennél is magasabb expressziós szintet tapasztalunk az MX-szelekcióval létrehozott $G2_{Mx}$ sejtekben (12a ábra).

A calcein assay-hez hasonló, festék kipumpáláson alapuló módszer segítségével meghatároztuk a transzdukált A431-es sejtekben az ABCG2 transzportaktivitását is. Az alkalmazott fluoreszcens festék ebben az esetben a Hoechst 33342 volt, amely az ABCG2-nek nagy affinitású szubsztrátja, és a sejtben a DNS-hez kötődve válik fluoreszcenssé. Specifikus gátlószerként pedig itt is Ko143-at alkalmaztunk. Az eredményeket a korábban ismertetett aktivitás faktorral fejeztük ki. Jelentős ABCG2-függő transzportaktivitást tapasztaltunk a G2 jelű A431 sejtekben, amelyet felülmúlt a $G2_{Mx}$ sejtekben mért érték. Ezzel szemben a $G2_{K86M}$ mutáns variánst expresszáló sejtekben nem volt mérhető transzportaktivitás (12b ábra).

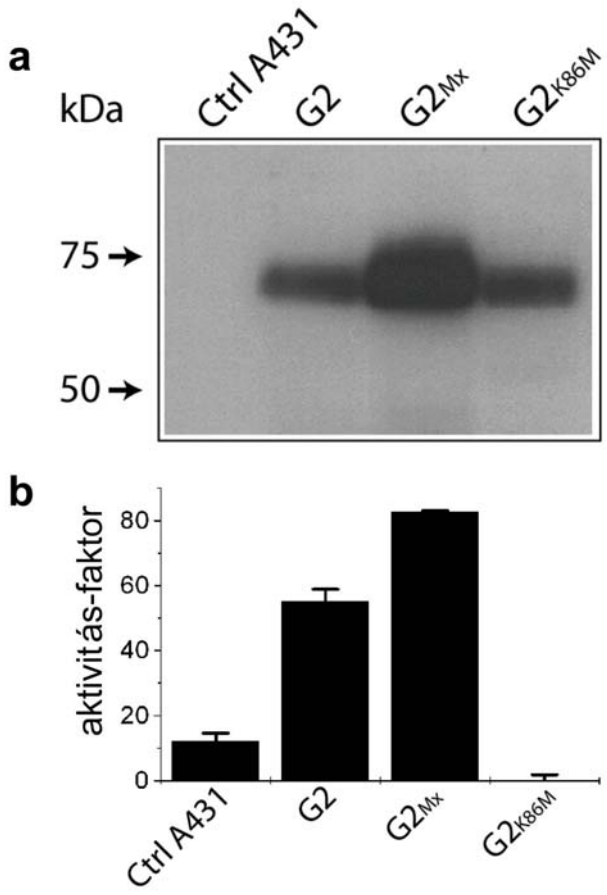

12. ábra: Az ABCG2 multidrog transzportert expresszáló A431 sejtek jellemzése. a) Az ABCG2 expresszióját a retrovírus transzdukcióval (G2, $G2_{K86M}$), illetve a G2-es sejtek további szelekciójával létrehozott ($G2_{Mx}$) A431 sejtek teljes sejtlizátumából (50 μg) Western blot technikával detektáltuk BXP-21, ABCG2-specifikus monoklonális ellenanyagot használva. Kontrollként a kiindulási sejtvonalat (Ctrl A431) használtuk. **b)** Az ABCG2 transzportaktivitását a Hoechst 33342 fluoreszcens festék kipumpálásán alapuló módszer segítségével határoztuk meg. Az ABCG2-függő festék eltávolítást 1 μM Ko143 gátlószerrel függesztettük fel, majd a kapott festékfelvételi sebességekből meghatároztuk az aktivitás faktor értékeket (részletesebb magyarázat az „Alkalmazott módszerek" fejezetben található). Az oszlopdiagramon átlag + SD értékek szerepelnek (n > 3).

Ezt követően citotoxicitási assay-vel meghatároztuk a létrehozott A431-es sejtvonalak Iressával szembeni rezisztenciáját. A sejteket az 50-500 nM koncentrációtartományba eső Iressával kezeltük 48 órán keresztül. Míg a kontroll sejtekben tapasztalt IC_{50} érték 26,7 nM-nak adódott, addig a vad típusú ABCG2-t expresszáló sejtekben (G2, $G2_{Mx}$) ez az érték 45,8 illetve 68,4 nM-nak bizonyult. Az inaktív mutánst kifejező sejtek ($G2_{K86M}$) esetében a kontroll sejtekhez hasonló 24,5 nM-os IC_{50} értéket kaptunk. Az ABCG2-gátlószer (1 μM Ko143) és az Iressa együttes alkalmazásakor mindegyik sejtvonalban - a kontroll sejtekkel kapott értékkel megegyező -, alacsony IC_{50} értékeket tapasztaltunk (ábrán nem bemutatott eredmény). Mindez egyértelműen megmutatja, hogy az ABCG2 transzporter képes megvédeni az őt expresszáló sejteket az Iressa sejtölő hatásával szemben. Az is kiderült, hogy ez a védőfunkció egyértelműen az ABCG2 transzportaktivitásához köthető, hiszen az inaktív mutáns esetében, illetve az ABCG2 gátlószer jelenlétében ez a védőhatás nem érvényesült.

Mivel az Iressa hatása az EGF-receptor gátlásán keresztül valósul meg, azt is kimutattuk, hogy a vad típusú ABCG2-t expresszáló sejtekben az Iressa kevésbé gátolta az EGFR foszforilációját, mint a parentális, illetve az inaktív mutánst expresszáló sejtvonalakban (ábrán nem bemutatott eredmény) [4. sz. közlemény 4. ábra].

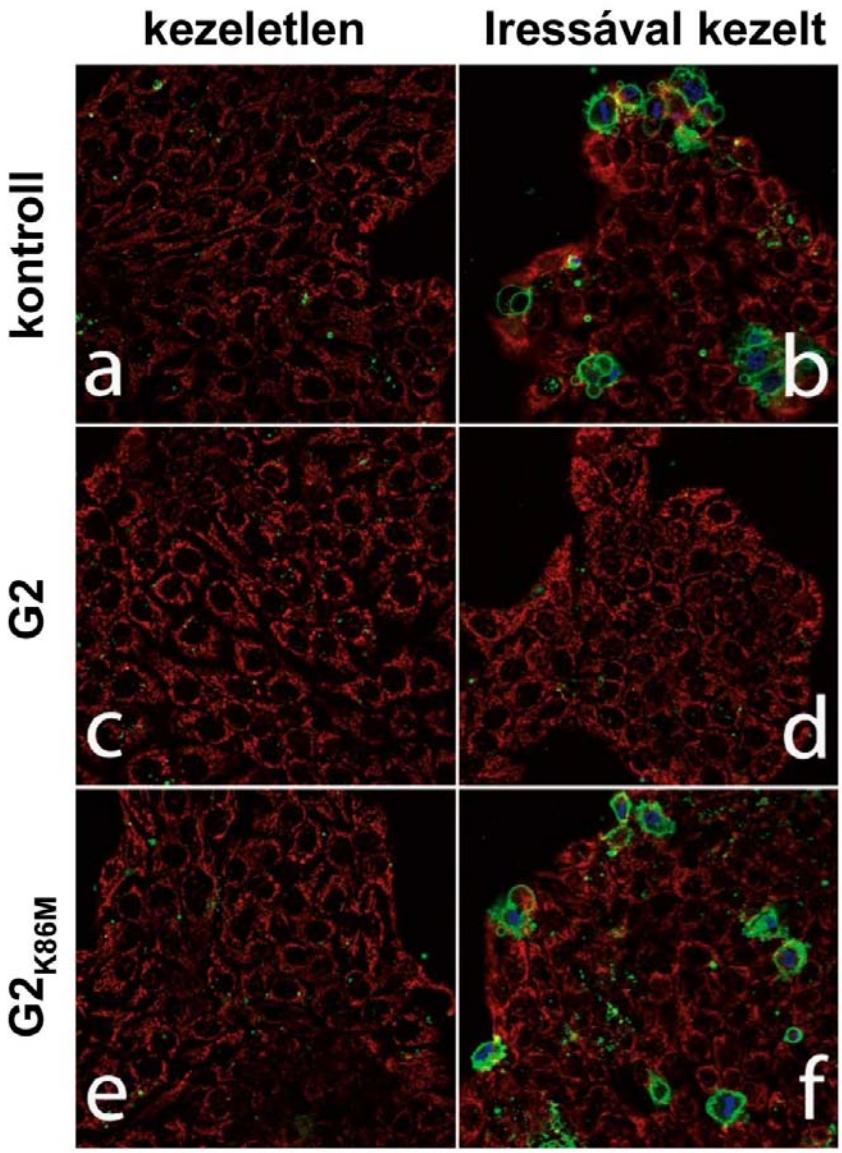

13. ábra: Iressával kiváltott sejthalál kontroll és ABCG2-t expresszáló A431 sejtekben. Kontroll sejteket (**a-b** panelek), valamint vad típusú (G2 – **c-d** panelek), illetve inaktív mutáns ($G2_{K86M}$ – **e-f** panelek) ABCG2-t expresszáló sejteket szérum mentes körülmények között tenyésztettünk 24 órán át. Míg az **a) c) e)** paneleken bemutatott kísérletekben a sejtek nem kaptak Iressa kezelést, addig a **b) d) f)** esetekben 1 μM Iressával egészítettük ki a tenyésztő médiumot. Konfokális mikroszkóp segítségével az apoptotizáló sejteket Annexin V kötés (zöld) alapján mutattuk ki, az elpusztult sejteket propidium-jodid festéssel (kék) jelöltük meg, míg a mitokondriális aktivitást MitoTracker Deep Red 633 festék (piros) alkalmazásával tettük láthatóvá.

Korábbi tanulmányok kimutatták, hogy az Iressa kezelés programozott sejthalált, apoptózist okoz a sejtekben [90]. Az ABCG2 Iressával szembeni védőhatását kimutattuk konfokális mikroszkópos elemzéssel is. Amennyiben kontroll A431 sejteket kezeltünk 1 μM Iressával 24 órán át, a tenyészetben jelentős mennyiségű apoptotikus sejtet figyelhettünk meg (13. ábra a, b), amit Annexin V kötéssel tettünk láthatóvá. Ez a fehérje specifikusan kötődik

foszfatidil-szerinhez, amely csak apoptotizáló sejtek külső membránfelszínén jelenik meg a programozott sejthalál korai szakaszában. Az Annexin V-tel festődő sejteken jól megfigyelhető az apoptotizáló sejtekre jellemző morfológiai változás is, a membrán „blebbing". A kísérlet során a látómezőben jelenlévő sejteket egy mitokondriális festék, a Mito Tracker Deep Red használatával tettük láthatóvá, valamint megfestettük a membrán-integritásukat elvesztett, gyakorlatilag elpusztult sejteket propidium-jodid segítségével. Az apoptotizáló sejtekben csökkent mitokondriális aktivitást tapasztaltunk, és sok sejt a propidium-jodidra permeábilissé vált. A kontroll sejtekkel ellentétben az ABCG2-t expresszáló sejtekben ilyen körülmények között az Iressa hatástalan maradt (13. ábra c, d). Az inaktív mutáns ABCG2 variánst expresszáló sejtekben az ABCG2-nek ez a protektív hatása nem érvénysült (13. ábra e, f), ami egyértelműen megmutatja, hogy a tapasztalt rezisztenciáért a fehérje transzportaktivitása a felelős.

Az itt bemutatott kísérleteink arra utalnak, hogy az ABCG2 Iressával szembeni védő hatása az EGF-receptor szintjén érvényesül. Mindez összhangban áll azzal az elképzeléssel, hogy a multidrog transzporterek a hidrofób szubsztrátokat azelőtt kipumpálják a sejtből, mielőtt azok a citoplazmát elérnék (hidrofób porszívó modell). Ezzel a modellel, illetve az ABCG2 transzportmechanizmusával részletesen foglalkozom a 4.3.4. fejezetben. Az A431 sejtekkel végzett kísérleteink egyértelműen megmutatták, hogy az ABCG2 aktívan kipumpálja az Iressát a sejtekből, így biztosítva számunkra a droggal szembeni védelmet. Két megközelítést alkalmaztunk ennek bemutatására: egyrészt használtunk egy - mind az ATPáz aktivitás, mind a transzport tekintetében - inaktív mutáns variánst ($G2_{K86M}$), másrészt alkalmaztunk egy specifikus ABCG2 inhibitort (Ko143). Mindkét módszerrel felfüggeszthető volt az ABCG2 védő hatása, bizonyítva a fehérje transzportaktivitásának szükségességét.

Érdekes megemlíteni, hogy egy másik fontos tirozinkináz-receptor inhibitor, a Glivec (Imatinib) az ABCG2 hatásos gátlószerének bizonyult, viszont ezt a drogot nem transzportálja a fehérje [91]. Megfigyelésünk, hogy az ABCG2 aktívan részt vesz egy tumoros sejt drog-rezisztenciájában, több fontos klinikai vonatkozással bír. Egyrészt az Iressa hatástalan maradhat olyan tumorokban, amelyekben ez a multidrog transzporter jelen van, másrészt az ABCG2 nagymértékben befolyásolhatja ennek a drognak az ADME-Tox tulajdonságait. Az ABCG2 polimorfizmusai és a polimorf változatok sokszor eltérő transzporttulajdonságai tovább bonyolíthatják az Iressa és az ABCG2-t kifejező tumorsejt kölcsönhatását. Megfigyeléseink tehát aara hívják fel a figyelmet, hogy mindezek a tényezők nagymértékben befolyásolhatják és bizonytalanná is tehetik az Iressával végzett klinikai vizsgálatok eredményét, ezért az ABCG2 figyelembevétele a következőkben elkerülhetetlen.

4.2.2. A membrán koleszterintartalmának hatása az ABCG2 aktivitására

[5. sz. közlemény]

Az ABCG2 funkcionális szabályozásáról ma még viszonylag keveset tudunk. Valamennyi ismerettel rendelkezünk az ABCG2 transzkripcióját befolyásoló tényezőkről. Ismeretes, hogy citotoxikus szerek, a hipoxia és bizonyos hormonok befolyásolják az ABCG2 átíródását [81, 92, 93]. Arról is beszámoltak már, hogy az ösztrogén poszt-transzlációs módosítás révén csökkenti az érett ABCG2 celluláris mennyiségét [94]. A membránok koleszterintartalma számos membránfehérje – többek között ABC transzporterek - funkcióját képes befolyásolni. Különös szereppel bírnak ebben a tekintetben a membránok magas koleszterin-tartalmú mikrodoménjei. Egy korábbi tanulmány beszámolt arról, hogy az ABCG2 ATPáz aktivitását stimulálja a koleszterin [95]. Mivel a transzportált szubsztrátok legtöbbször fokozzák az ABC transzporterek ATPáz aktivitását [8], a szerzők azt a következtetést vonták le, hogy az ABCG2 közvetlenül részt vehet a koleszterintranszportban. Ennek közvetlen igazolására azonban nem került sor. A következőkben bemutatott munkánkban a koleszterin ABCG2 aktivitására gyakorolt hatását vizsgáltuk meg.

A korábbiakban sikerrel alkalmazott Sf9 rovarsejtes heterológ expressziós rendszer segítségével az ABCG2 fehérjét tartalmazó membránpreparátumokon azt tapasztaltuk , hogy a drog-stimulált ATPáz aktivitást a membránok koleszterinnel való feltöltése jelentősen fokozza – még olyan vegyületek esetében is, amelyek máskülönben csak csekély mértékben stimulálják az ABCG2 ATPáz aktivitását (ábrán nem bemutatott eredmény). Fontos megjegyezni, hogy a rovarsejtek koleszterintartalma messze elmarad az emlős sejtek plazma-membránjának koleszterinszintjétől. Ezeknél a méréseknél a membránokhoz a koleszterin hozzáadását a preparálásnál alkalmazott koleszterinnel töltött random metilezett β-ciklodextrin (CD/Kol) segítségével végeztük. Érdemes megjegyezni azt is, hogy az alapaktivitást, azaz a kívülről hozzá adott szubsztrát nélkül tapasztalt aktivitást önmagában a koleszterin nem fokozta. Az ABCG2 viszonylag magas alap ATPáz aktivitással rendelkezik, amivel kapcsolatban két elképzelés él. Egyrészt szóba jöhet, hogy a fehérje ebben az expressziós rendszerben részben szétkapcsolt, azaz az ATPáz aktivitás és a transzport nincs teljesen összhangban, másrészt – többek által elfogadott nézet szerint – a preparátumban jelen lehet egy nem ismert endogén szubsztrát molekula. Ezért némileg meglepő, hogy a koleszterin nem fokozta az ABCG2 alap ATPáz aktivitását.

A következőkben arra kerestünk választ, hogy a koleszterin csak az ABCG2 által képviselt ATPáz aktvitást fokozza-e, vagy képes befolyásolni a transzportot is. Ennek a

kérdésnek a megválaszolásához első sorban emlős sejteket használtunk, és egy fordított megközelítést alkalmaztunk. Ebben az esetben nem növeltük a membránok koleszterin-tartalmát, hanem az emlős sejtek membránjának viszonylag magas koleszterinszintjét csökkentettük üres ciklodextrinnel (CD) történő előkezeléssel (depléció). Emellett persze koleszterin-tartalmú CD (CD/Kol) előkezeléssel megkíséreltük az emlős sejtekben tovább fokozni (töltés), illetve a koleszterin-depletált sejtekben helyreállítani a koleszterinszintet (repléció: CD+CD/Kol). Ezekhez a kísérletekhez az ABCG2-t stabilan expresszáló HEK293 sejteket (HEK/G2), illetve az előző fejezetben többször alkalmazott pikkelysejtes karcinóma sejteket (A431/G2) használtuk. Az ABCG2 transzportaktivitását a calcein assay-vel hasonló elvekre alapuló, a 12b ábra kapcsán már ismertetett Hoechst transzport méréssel határoztuk meg. Ennek lényege röviden, hogy a Hoechst 33342 fluoreszcens DNS festéket az ABCG2 hatékonyan kipumpálja a sejtekből, a transzportot specifikus ABCG2 gátlószerrel (Ko143-mal) felfüggesztve, a két kapott festékfelvételi sebességből meghatározhatjuk az ABCG2 transzportaktivitását (ld. 1. képlet). Vizsgálatainkat mind sejtszuszpenzióban (14. ábra), mind részletes konfokális mikroszkópos elemzéssel (15. ábra) elvégeztük.

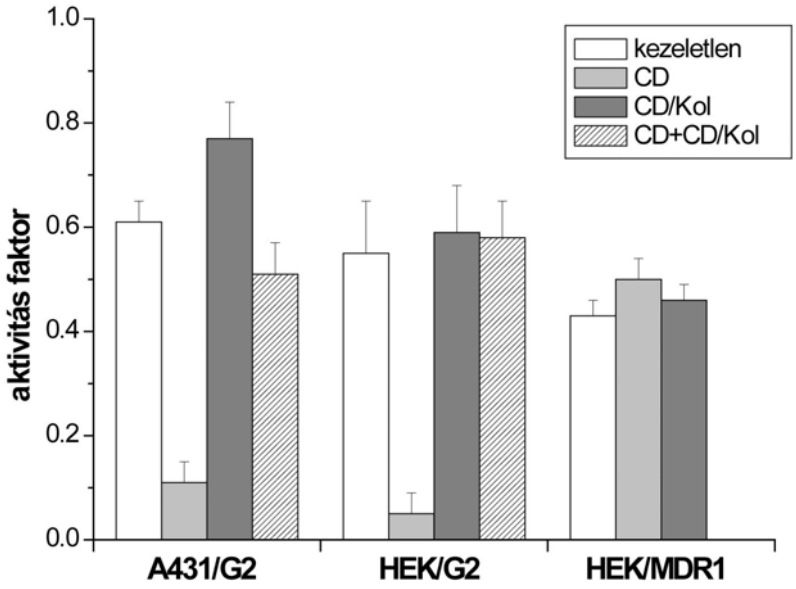

14. ábra: A koleszterin depléció és koleszterin töltés hatása az ABCG2 transzportaktivitására ép sejtekben. Az ABCG2-t expresszáló A431 (A431/G2) és HEK293 (HEK/G2) sejtekben, valamint az MDR1-et kifejező HEK293 sejtekben (HEK/MDR1) mértük a Hoechst 33342 fluoreszcens festék felvételét, majd az ABCG2-függő festék eltávolítást ABCG2-specifikus gátlószerrel (1 μM Ko143) függesztettük fel. Az eredményeket a festékfelvételi sebességekből számított aktivitás faktor értékkel (átlag + SD, n > 3) fejeztük ki (ld. „Alkalmazott módszerek"). A koleszterin depléciót közvetlenül a festékfelvételi kísérlet előtt végzett ciklodextrin (CD) kezeléssel (4 mM, 37 ˚C, 30 perc), míg a sejtek koleszterinnel való töltését ugyanilyen körülmények között végzett koleszterint tartalmazó CD (CD/Kol) előkezeléssel hajtottuk végre. A csíkozott oszlopok azt mutatják, amikor a CD-vel történt depléciót követően visszatöltöttük a sejteket koleszterinnel CD/Kol kezeléssel.

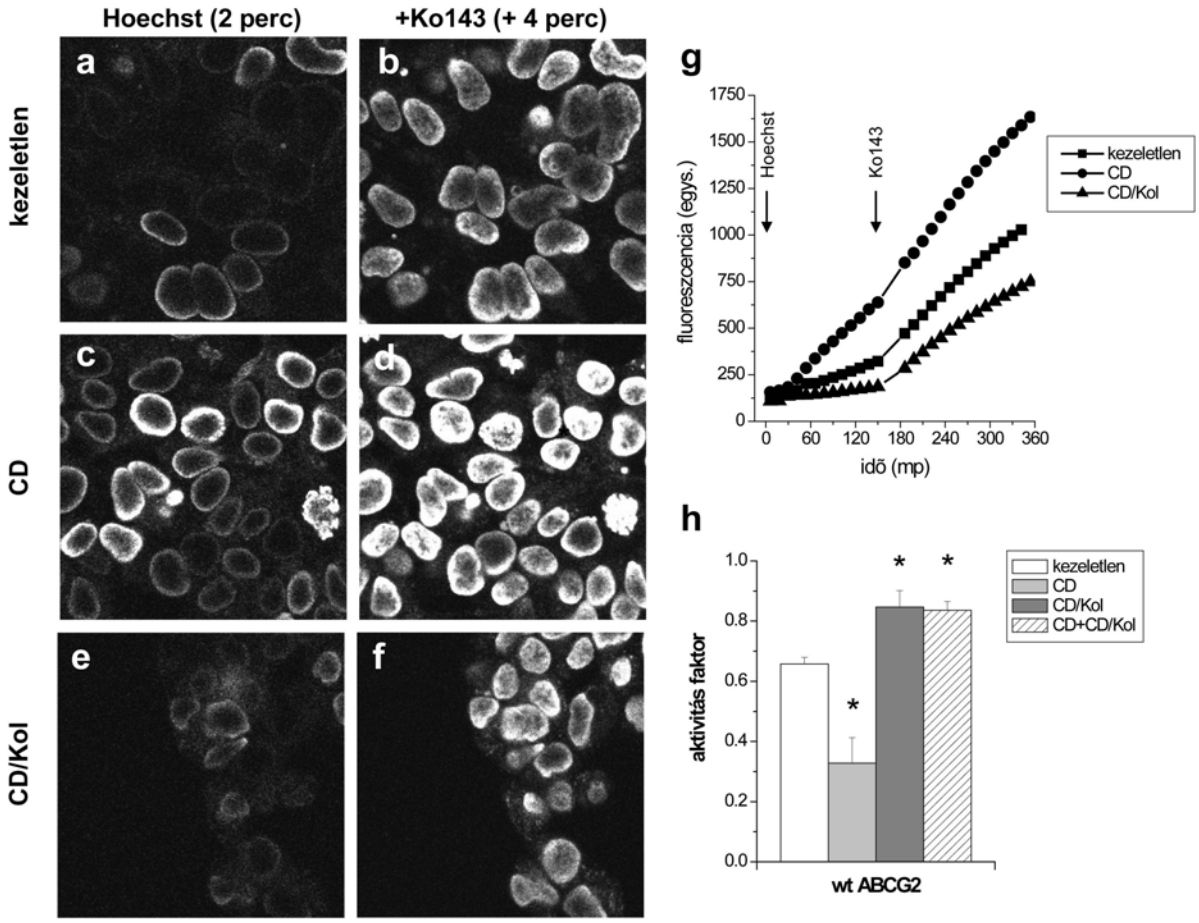

15. ábra: Az ABCG2-függő festéktranszport koleszterin-függésének konfokális mikroszkópos elemzése. ABCG2-t expresszáló HEK293 sejteket ciklodextrinnel (CD), illetve koleszterin-töltött ciklodextrinnel (CD/Kol) előkezeltünk (2,5 mM, 37 ˚C, 20 perc), majd követtük a Hoechst 33342 (2 μM) akkumulációt. A bal oldali (**a**, **c**, **e**) paneleken kb. 2 perccel a festék hozzáadása után készült, reprezentatív konfokális képek láthatók, míg a jobb oldaliak (**b**, **d**, **f**) az ABCG2-gátlószer (Ko143) addíciója után 4 perccel készült felvételeket mutatnak. **g)** A korábbi paneleken bemutatott kísérlet alapján készült, 12 sejt átlagából meghatározott festékfelvételi görbék. **h)** Az előzőekhez hasonló, több független kísérlet eredményeként kapott ABCG2-függő aktivitás faktor értékek (átlag + SD, n > 3). A csillagok a kezeletlen sejtekkel kapott értékhez viszonyított szignifikáns eltérést jelölik.

Azt tapasztaltuk, hogy az emlős sejtek koleszterin depléciója nagymértékben gátolta az ABCG2 transzportaktivitását mindkét ABCG2-t expresszáló sejtvonalban, a koleszterintöltés viszont csak az A431/G2 sejtekben volt képes tovább fokozni a festék kipumpálását. A jelenség reverzibilitását igazolta, hogy a koleszterin-depletált sejtekben a repléció helyre-állította az eredeti transzportaktivitást. Összehasonlításképpen MDR1-et expresszáló HEK293 sejtekben (HEK/MDR1) is mértük a koleszterin-tartalom transzportra gyakorolt hatását. Ezt az összehasonlítást az teszi lehetővé, hogy a Hoechst 33342 az MDR1-nek is jó szubsztrátja, ebben az esetben azonban inhibitorként verapamilt használtunk. Eredményeink azt mutatták, hogy a sejtek koleszterintartalma nem befolyásolja az MDR1 transzportaktivitását.

Fontos megjegyezni, hogy az ABCG2-t nem expresszáló kontroll (HEK293 és A431) sejtekben mért aktivitás faktort nem befolyásolta sem a koleszterin depléció, sem a koleszterinnel való töltés, valamint hogy hasonló eredményekre jutottunk más fluoreszcens szubsztrát molekulák (mitoxantron, feoforbid A) alkalmazásával is. Enzimatikus koleszterin méréssel megállapítottuk, hogy a HEK293 sejtekben lévő eredeti koleszterin szint 7,7 ± 1,1 μg/teljes fehérje értékről a CD kezelés hatására (4 mM, 37 ˚C, 30 perc) kb. 25 %-kal (5,7 ± 0,9 μg/teljes fehérje értékre) csökkent. A koleszterinnel való töltés (CD/Kol) kb. 50 %-os emelkedést okozott (12,0 ± 1,2 μg/teljes fehérje). A fenti körülmények között végrehajtott ciklodextrin-kezelések érdemben nem csökkentették a sejtek életképességét, amit propidium-jodid (PI) festéssel állapítottunk meg (a PI negatív sejtek aránya: > 85 %).

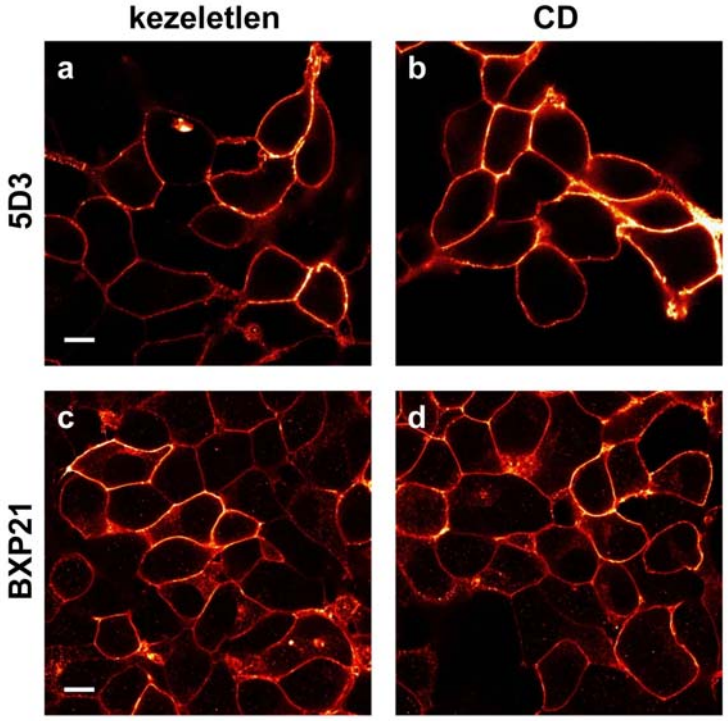

16. ábra: A koleszterin depléció hatása az ABCG2 sejten belüli elhelyezkedésére. ABCG2-t expresszáló HEK293 sejteket - a 15. ábrán bemutatott kísérlethez hasonló módon - ciklodextrinnel (CD) kezeltük, majd immunfluoreszcens festést végeztünk extracelluláris epitópot felismerő ellenanyag (5D3) segítségével nem-permeabilizált sejteken (**a**, **b**), illetve intracelluláris epitóp ellen készült ellenanyag (BXP21) felhasználásával permeabilizált sejteken (**c**, **d**). Az immunfluoreszcens festés eredményét konfokális mikroszkóppal vizsgáltuk.

Fontos volt tisztázni, hogy a koleszterin depléció következtében tapasztalt transzport-aktivitás csökkenés vajon a fehérje aktivitásának közvetlen modulálásából ered vagy pedig az ABCG2 sejtfelszíni expresszióját befolyásolja a membránok koleszterin tartalma. Ezért immunfluoreszcens festéssel ellenőriztük a CD-kezelés hatását az ABCG2 sejten belüli elhelyezkedésére HEK/G2 sejteken (16. ábra). A sejtfelszíni jelölést nem permeabilizált

sejteken végeztük extracelluláris epitópot felismerő, direkt jelölt ellenanyaggal (5D3), míg az ABCG2 lokalizációját az egész sejtben permeabilizált mintákon BXP21 ellenanyagot használva indirekt immunfestéssel vizsgáltuk. Megállapítottuk, hogy az ABCG2 elsődlegesen a sejtek plazmamembránjában helyezkedik el, és hogy ez a rövid idejű koleszterin depléció a fehérje lokalizációját sem a sejtfelszínen, sem a sejt egészét tekintve érdemben nem befolyásolja.

Az ép sejteken végzett kísérletek eredményét a későbbiekben megerősítettük közvetlen transzportmérésekkel is ABCG2-t tartalmazó Sf9 kifordított (inside out) membránvezikulákon. Mind a metotrexát, mind az ösztradiol-glükoronid ATP-függő felvételét jelentős mértékben (kb. 20-szorosára) fokozta a membránvezikulák előzetes feltöltése koleszterinnel (ábrán nem bemutatott eredmények). A transzport specifikusságát a Ko143 gátlószer alkalmazásával igazoltuk. Ezekben a mérésekben vizsgáltuk más szterolok hatását is, azonban sem az ergoszterol, sem a szitoszterol, sem a hidrokortizon nem fokozta az ABCG2-függő drog transzportot.

Összefoglalva, sikerült bemutatnunk, hogy a membrán koleszterin-tartalma jelentős mértékben, szelektíven és reverzibilisen képes modulálni az ABCG2 transzportaktivitását. Ez a megfigyelésünk felhívja a figyelmet a plazmamembrán magas koleszterintartalmú mikrodomén struktúráinak és az ABCG2 kölcsönhatásának jelentőségére, ugyanis ezek az interakciók az ABCG2 működésének finom szabályozását teszik lehetővé. Hasonlóképpen az intracelluláris kompartmentekben kifejeződő ABCG2 transzportaktivitását is befolyásolhatja a mikrokörnyezet koleszterin tartalma. Gyakorlati szempontból pedig eredményeink jelentős mértékben növelhetik az ABCG2 fiziológiai és farmakológiai szubsztrátjainak feltérképezését célzó vizsgálatok hatékonyságát, amennyiben az alkalmazott tesztrendszerek kihasználják a koleszterinnek ezt a moduláló hatását.

4.2.3. Az ABCG2 multidrog transzporter GFP-vel való címkézése

[6. sz. közlemény]

A fehérjék funkcionális tanulmányozására egyre szélesebb körben elterjedt módszer egy fluoreszcens protein (GFP, YFP, mCherry, stb.) kovalens kapcsolása a vizsgálandó objektumhoz. Ezek a fúziós fehérjék lehetőséget nyújtanak a sejtben zajló dinamikus folyamatok közvetlen tanulmányozására, mint például a sejten belüli trafficking vagy a szubcelluláris lokalizáció megváltozása. Az ABC transzporterek sejtbiológiai vizsgálatára is kiváló lehetőséget nyújtana egy ilyen konstrukció, azonban az ABC fehérjék speciális feltekeredése, a doménok szigorú elrendeződése és funkcionális együttműködése rendkívül érzékennyé teszi ezeket a transzportereket az ilyenfajta beavatkozásokra, amelyet sok más fehérjénél rutinszerűen alkalmaznak. Sokszor egy kisebb epitóp tag bevitele is jelentősen befolyásolja az ABC transzporter aktivitását, érését, sejten belüli elhelyezkedését. A következőkben arról a munkánkról számolok be, aminek eredményeképpen – számos sikertelen próbálkozás után – létrehoztunk egy olyan zöld fluoreszcens proteinnel (GFP-vel) fuzionáltatott ABCG2 fehérjét, amely teljes mértékben megőrizte minden fontos tulajdonságát, további lehetőségeket kínálva az ABCG2 részletes funkcionális vizsgálatára.

Az ABCG2 GFP-vel való címkézésére többféle konstrukciót készítettünk. Kritikusnak bizonyult, hogy a fehérje C-terminálisa érintetlen maradjon. Amennyiben a transzportert ezen a végén fuzionáltattuk a GFP-vel, akkor az instabil, intracelluláris kompartmentekben maradó és funkció-vesztett fehérjét eredményezett. Az N-terminálisan címkézett konstrukciók esetében is fontos volt a megfelelő linker régió közbeiktatása (17. ábra). A korábban használt inaktív mutáns ($ABCG2_{K86M}$) GFP-vel fuzionáltatott változatát is elkészítettük ($GFP\text{-}G2_{KM}$).

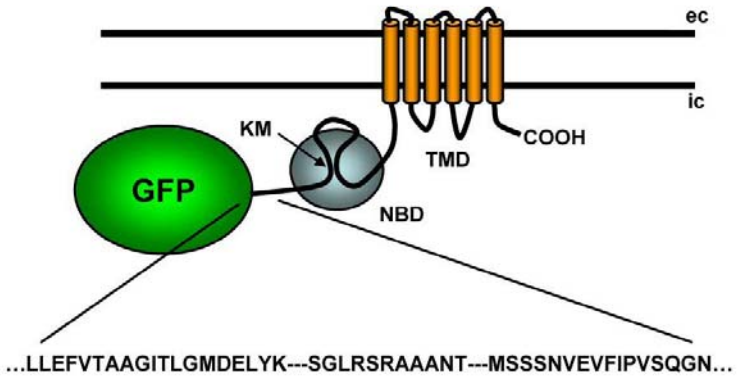

17. ábra: A GFP-vel címkézett ABCG2 szerkezete. NBD: nukleotid-kötő domén, TMD: transzmembrán domén. Az ábra alján a GFP és a fehérje közötti linker régió aminosav-sorrendje kiemelve látható. A KM és a nyíl a funkcionális vizsgálatok kontrolljaként használt mutáns változatban lévő lizin-metionin csere pozícióját jelöli.

Elvégeztük a GFP címkével ellátott ABCG2 (GFP-G2) részletes elemzését, a kapott eredményeket minden esetben a címke nélküli, vad típusú fehérjével (G2) hasonlítva össze. Western analízis egyértelműen megmutatta a két fehérje molekulatömege közötti különbséget, és demonstrálta a GFP-G2 fehérje stabilitását is (18a ábra). A vanadát-szenzitív ATPáz aktivitást mérve, a fúziós fehérje az eredeti transzporterrel egyenrangúnak bizonyult mind az alap-, mind drog-stimulált aktivitás tekintetében (18b ábra). A mérés specifikusságát a drog-szubsztrát mellé adott Ko143 inhibitor alkalmazásával igazoltuk.

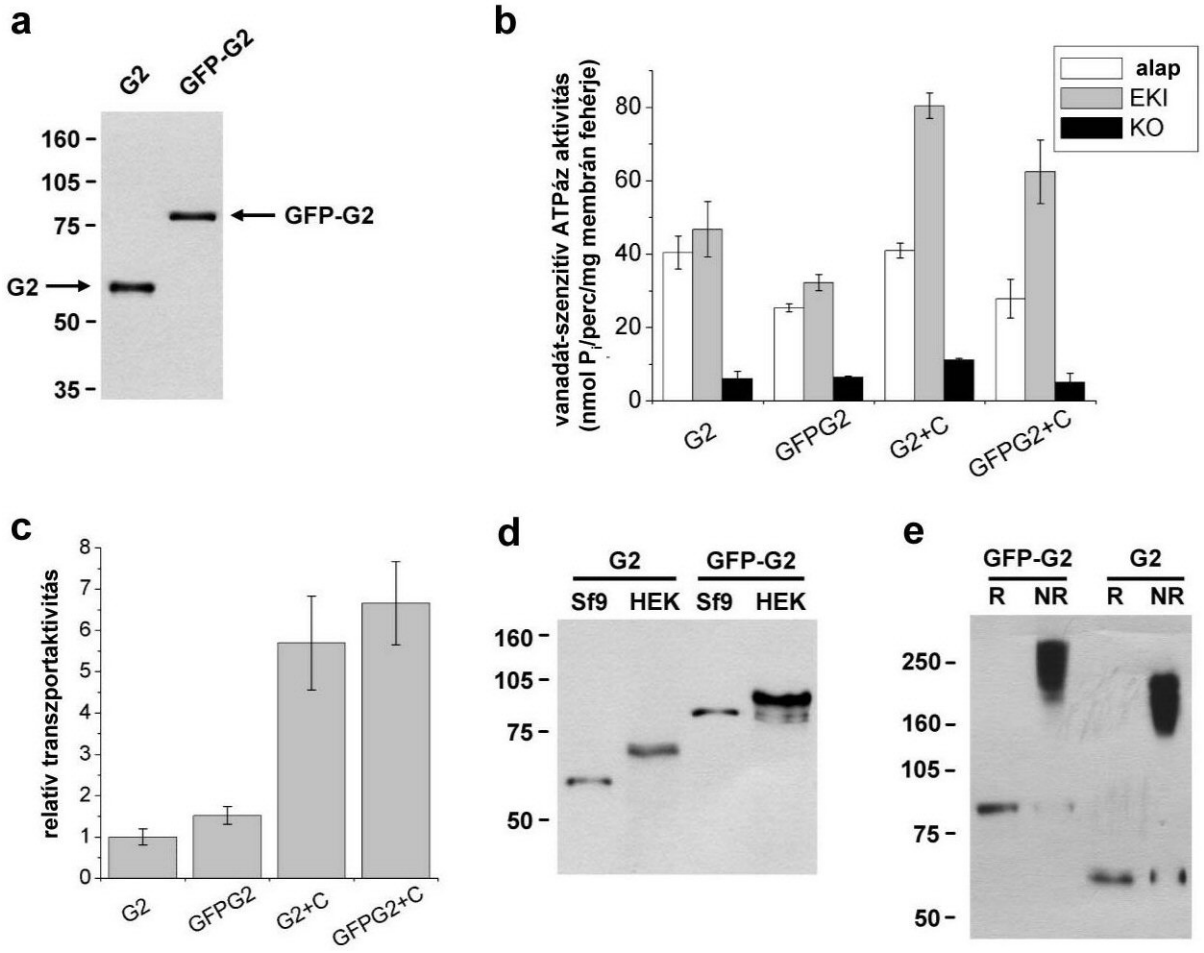

18. ábra: A GFP-G2 expressziója és funkcionális jellemzése. a) ABCG2-specifikus monoklonális ellen-anyaggal (BXP21) készült Western analízis vad típusú (G2), illetve GFP-vel címkézett (GFP-G2) ABCG2-t tartalmazó Sf9 membránpreparátumokon. **b-c)** Szubsztrát-stimulált APTáz aktivitás, illetve metotrexát vezikuláris transzport mérés ugyanezeken a mintákon. Jelölések: +C: koleszterintöltés, EKI: 1 μM EKI-785 (tirozinkináz inhibitor) KO: 1 μM EKI-785 + 1 μM Ko143 (ABCG2-specifikus gátlószer). Az oszlopdiagramok átlag ± SEM (n = 3) értékeket tüntetnek fel. A transzportmérésnél az eredményeket a vad típusú ABCG2-vel, koleszterintöltés nélkül kapott aktivitásra normalizáltuk. **d-e)** A glikoziláció és dimerképződés vizsgálata Western analízissel BXP21 ellenanyaggal G2-t, illetve GFPG2-t tartalmazó Sf9 membránokon, illetve HEK293 sejtlizátumokon. A dimerizáció vizsgálatához szintén HEK293 sejtekből preparáltunk mintákat redukáló (R), illetve nem-redukáló (NR) körülmények között.

Az előző fejezetben részletesen bemutattam, hogy az ABCG2 funkcióját jelentősen befolyásolja a membránok koleszterin tartalma. Azokat az eredményeket viszont a disszertációban nem ismertettem, amelyek azt demonstrálják, hogy az ABCG2 egy természetes előfordulású pontmutációt hordozó (R482G) változata nem mutat koleszterin-függést [5. sz. közlemény]. Ezek alapján indokolt volt a GFP-vel címkézett változat aktivitásának a koleszterintartalomtól való függését is megvizsgálni. Azt tapasztaltuk, hogy a koleszterin a vad típusú fehérjéhez teljesen hasonló módon fokozza GFP-címkézett ABCG2 aktivitását (18b ábra). Hasonlóképpen egyformának mutatkozott a címkézett és címkézetlen ABCG2 a kifordított vezikulákon mért drogtranszport (metotrexát felvétel) tekintetében is (18c ábra). A drogtranszportok koleszterin-függése is megegyezett.

Ismeretes, hogy az ABCG2 a legutolsó, a C-terminálisához legközelebb eső külső hurkon glikozilálódik [96]. Ha emlős glikoproteineket Sf9 rovarsejtes heterológ expressziós rendszerben termeltetünk, a fehérje glikozilációja csak részben megy végbe (ún. core glikoziláció). Ezért a glikoziláció ellenőrzésének egyik legegyszerűbb módja, ha a vizsgált fehérjét mind rovarsejtes, mind emlős expressziós rendszerben kifejeztetjük, és a két minta elektroforetikus migrációs tulajdonságait összehasonlítjuk. Eredményeink megmutatták, hogy a GFP-G2 a vad típusú fehérjéhez teljesen hasonlóan glikozilálódik (18d ábra). Bár ez a módosítás a fehérje normális lokalizációjához és funkciójához nem feltétlenül szükséges [97], de tükrözi a fehérje megfelelő érését és a plazmamembránba történő célbajuttatását (tageting-jét).

Korábban szó esett arról, hogy az ABCG2 homodimerként működik. Kritikus kérdés volt, hogy a GFP-vel való címkézés érinti-e a dimerképzést. Ezért redukáló és nem-redukáló körülmények között is preparáltunk mintákat GFP-G2-t, illetve vad típusú G2-t expresszáló HEK293 sejtekből. Western blot analízissel sikerült kimutatnunk, hogy a GFP-G2 a címkézetlen fehérjéhez hasonlóan dimerizálódik (18e ábra). Hasonlóképpen immun-fluoreszcens festéssel és konfokális mikroszkópos vizsgálattal ellenőriztük a GFP-G2, valamint a GFP-$G2_{KM}$ sejten belüli elhelyezkedését, és azt tapasztaltuk, hogy a címkézett változatok ugyanúgy, mint a címkézetlenek elsősorban a plazmamembránban helyezkednek el (ábrán nem bemutatott eredmény, 6. közlemény, 2. ábra). Az ABCG2-nek egy jellegzetessége, hogy konformáció-függő módon jelölhető az 5D3 felszíni antitesttel (5D3-shift) [98]. Szintén kimutattuk, hogy a GFP-vel ellátott ABCG2 az 5D3 ellenanyaggal történt jelölését- a címkézetlen fehérjéhez hasonló mértékben - fokozza az enyhe paraformaldehiddel történő fixálás vagy az ABCG2 inhibitorok (Ko143, FTC) alkalmazása [6. közlemény, 3. ábra].

A GFP-vel ellátott ABCG2 alkalmazásának legnagyobb előnyét az jelenti, hogy a GFP címke lehetővé teszi az ABCG2 expressziójának követését és funkciójának közvetlen vizsgálatát akár kevert sejtkultúrákban is. Ez különösen kedvező lehet nehezen transzfektálható, a klónozást nehezen toleráló vagy a drog-szelekcióra érzékeny sejttípusok tanulmányozásakor. További előnyt jelent az is, hogy a transzfekciót követő rövid időn belül, a hosszadalmas klónozási és szelekciós eljárások elhagyásával végezhetők el ezek a vizsgálatok. A következőkben a GFP-G2 ilyen irányú felhasználásának lehetőségét mutatom be.

Az előző két fejezetben már ismertettem a festék kipumpáláson alapuló fluoreszcens módszer, a transzport assay lényegét. A 19. ábrán bemutatott kísérletben is ezt a DNS festéket használtuk. Konfokális mikroszkóp segítségével követtük a Hoechst 33342 celluláris akkumulációját a GFP-címkézett ABCG2-vel tranziensen transzfektált HEK293 sejtekben 48 órával a transzfekciót követően. A festék ABCG2-függő kipumpálását - a szokásos módon -, ABCG2-specifikus gátlószer (1 μM Ko143) hozzáadásával függesztettük fel. A GFP fluoreszcenciája lehetőséget adott a sejtkultúrában a transzfektált sejtek azonosítására, így két külön csoportot képezve határoztuk meg a GFP-pozitív és a GFP-negatív sejtekben a festékfelvétel kinetikáját (19b ábra). A GFP-G2-t expresszáló sejtekben a transzporter hatékonyan megakadályozta a Hoechst bejutását, míg a kontroll (nem-transzfektált) sejtekben a festék gyors akkumulációját figyelhettük meg (19a ábra, felső, középső panel). A gátlószer hozzáadása után a transzfektált sejtekbe is bejutott a DNS-festék, fluoreszcenssé téve azok sejtmagját is (jobb panel). A 19b ábra mutatja a GFP-pozitív és -negatív sejtek nukleáris régiójában mért festékfelvétel kinetikáját. Hasonló kísérletet végeztünk a GFP-címkézett inaktív mutáns ABCG2 variánssal (GFP-$G2_{KM}$-mel) transzfektált sejtekkel is (19a-b ábra, alsó panelek). Ebben az esetben mind a transzfektált, mind a nem-transzfektált sejtekben hasonló kinetikájú, gyors festékakkumulációt figyelhettünk meg, megerősítve azt, hogy az ABCG2 transzportaktivitása felelős az előzőekben tapasztalt Hoechst-felvétel megakadályozásáért.

Ezt a kísérleti összeállítást használva, vad típusú GFP-G2-t expresszáló sejteken vizsgáltuk a koleszterin tartalom hatását az ABCG2 festékeltávolító aktivitására. Az előző fejezetben részletesen ismertetett, korábbi eredményeinkkel összhangban a ciklodextrin (CD) kezeléssel történt koleszterin depléció csökkentette, míg a koleszterinnel való töltés (CD/Kol) növelte a transzporter aktivitását (19c ábra). Érdekes megfigyelés, hogy a koleszterinszint emelkedésével a festék penetrációja is csökkent. Ahogy azt a calcein assay kapcsán részletesen tárgyaltuk, az aktivitás faktor képes kiküszöbölni ezeket az aspecifikus hatásokat. Így szoros összefüggést találtunk az enzimatikus úton meghatározott koleszterintartalom és a GFP-G2 aktivitás faktorral kifejezett transzportaktivitása között (19c ábra, jobb panel).

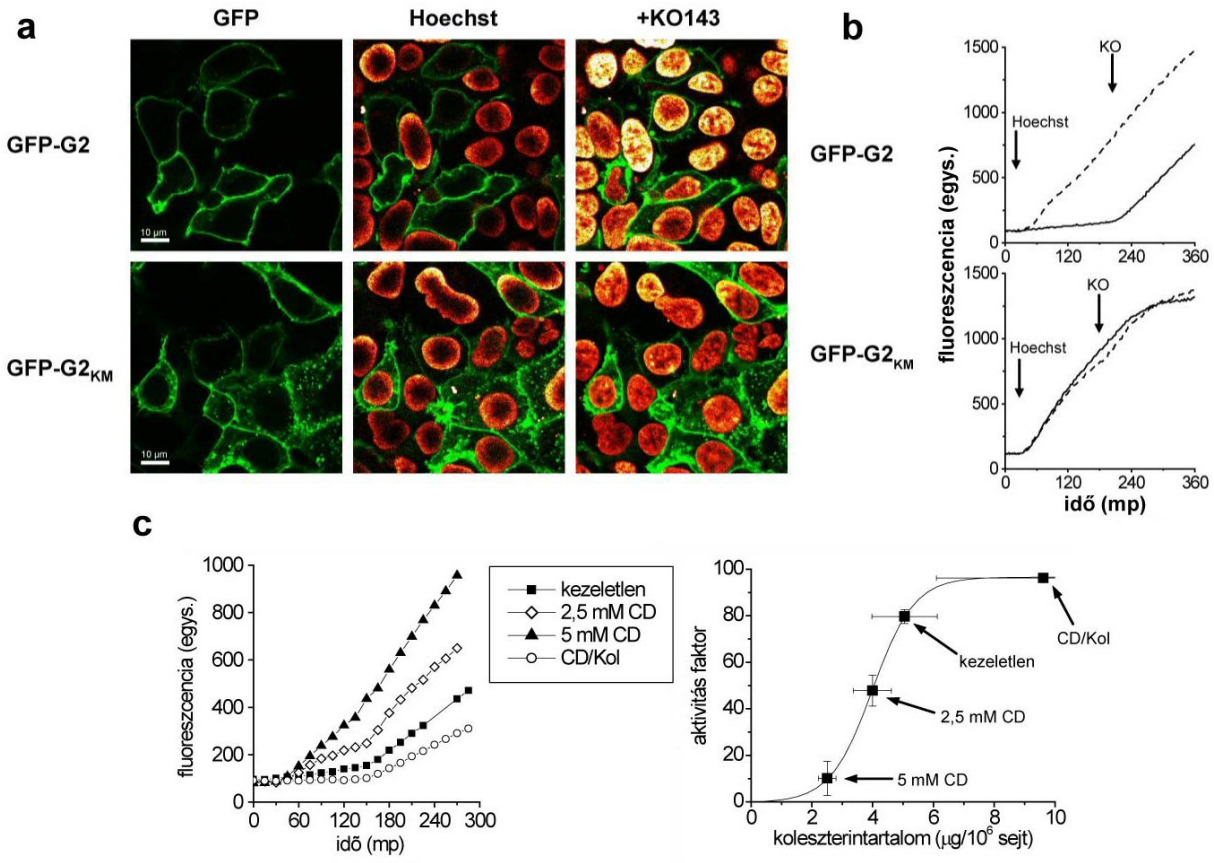

19. ábra: Fluoreszcens festékfelvétel mérése GFP-G2-t expresszáló ép sejteken. Tranziens transzfekcióval kapott HEK293 sejteken vizsgáltuk a GFP-G2, illetve annak mutáns változatának (GFP-$G2_{KM}$) transzport-aktivitását Hoechst 33342 festéket (2 µM) használva. Az ABCG2 aktivitását kb. 3 perccel a Hoechst hozzáadása után 1 µM Ko143 alkalmazásával függesztettük fel (KO). **a)** Konfokális felvételek, melyek a festék addíciója előtt (bal oldali), közvetlenül a KO hozzáadását megelőzően (középső), illetve 2-3 perccel azután (jobb oldali panelek) készültek. **b)** Festékfelvételi kinetikai görbék, melyeket az **a)** panelen bemutatott kísérletek alapján 6-6 transzfektált (nem szaggatott), illetve nem-transzfektált (szaggatott) sejtmagi régiójában mért fluoreszcencia értékek átlagából határoztuk meg. **c)** Hoechst akkumuláció mérése kezeletlen (■), 2,5 mM (◇), illetve 5 mM (▲) ciklodextrinnel (CD), valamint 2,5 mM koleszterin-töltött ciklodextrinnel (CD/Kol, ○) kezelt, GFP-G2-t expresszáló HEK293 sejtekben. A bal oldali panel a festékfelvételi görbéket mutatja, míg a jobb oldalon az azokból számolt aktivitás faktor és az enzimatikus úton meghatározott koleszterinszint korrelációja látható. Az ábrán feltüntetett eredmények átlag ± SEM értékeket tükröznek (n > 3).

Hasonló kísérletet végeztünk áramlási citométerrel is mitoxantron-transzportot mérve. Ebben az esetben a transzfektált sejteket a GFP fluoreszcencia alapján végzett kapuzással különítettük el a nem-transzfektálódott sejtektől, így ezzel a módszerrel is megbízhatóan tudtuk mérni az ABCG2-függő drogtranszportot [6. közlemény, 3. ábra].

Összefoglalva, ebben a fejezetben bemutattuk, hogy az ABCG2 multidrog transzporter GFP-vel való címkézésével a fehérje legfőbb jellemvonásai teljes mértékben megőrződtek, valamint demonstráltuk a GFP-címkézett ABCG2 alkalmazásában rejlő lehetőségeket.

4.2.4. Az ABCG2 transzportmechanizmusának vizsgálata

[7. sz. közlemény]

A membrántranszporterek többsége – az enzimekhez hasonlóan - egyfajta szubsztrát-specifitással rendelkezik, azaz egy vagy néhány molekulát képesek megkötni egy jól meghatározott szubsztrát-kötőhelyen. A szubsztrát-felismerést követően a transzporterek a megkötött vegyületet transzlokálják a membrán egyik oldaláról a másikra, amit egy elengedési lépés követ. Ez a klasszikus mechanizmus több tekintetben nehezen hozható összhangba a multidrog transzporterek aktivitásával. Ahogy arról korábban szó esett, az MDR-ABC fehérjék egyik legjellegzetesebb vonása a promiszkuitás, vagyis hogy rendkívül széles szubsztrát-felismerő képességgel rendelkeznek. A szubsztrátmolekulák sem kémiailag, sem szerkezetileg, de még méretben sem mutatnak hasonlóságot. Jellemző azonban, hogy sok hidrofób karakterű, illetve amfipatikus vegyületet találunk közöttük.

Mivel a hidrofób molekulák a lipid fázisban jól oldódnak, és megoszlás következtében magas koncentrációt érnek el a membránban, a fenti „klasszikus pumpa” mechanizmussal szemben az MDR-ABC fehérjék működésének magyarázatára alternatív modelleket javasoltak (20. ábra). Mindkettő lényege, hogy a szubsztrátfelismerés a lipid fázisban történik. A „hidrofób porszívó” modell értelmében a multidrog transzporter közvetlenül a membránból pumpálja ki a transzportált szubsztrátot az extracelluláris térbe [99, 100]. A másik elképzelés szerint a transzporter floppázként működik, azaz a transzportált szubsztrátot átfordítja a sejtmembrán belső lipid rétegéből a külsőbe [101, 102]. A membránban létrehozott és folyamatosan fenntartott egyenlőtlen eloszlás - a vizes fázisokkal történő megoszlásokkal együtt a molekula nettó kiáramlását eredményezi.

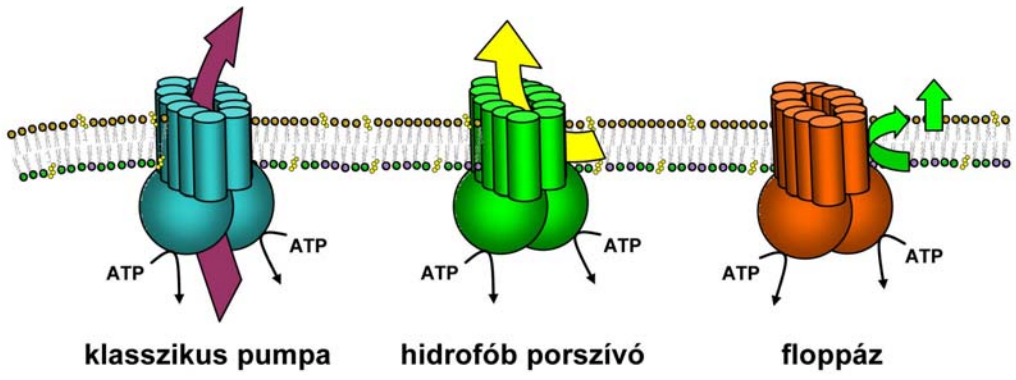

20. ábra: A multidrog transzporterek működési mechanizmusára javasolt modellek. A klasszikus pumpa a citoplazmából a külső térbe helyezi át a transzportált szubsztrátot, ezzel szemben a hidrofób porszívó mechanizmussal működő transzporter közvetlenül a lipid kettősrétegből pumpálja ki a hidrofób karakterű szubsztrátot. A floppáz a belső membránrétegből a külsőbe fordítja át a molekulákat, ezzel idézve elő azok nettó kiáramlását.

Ezek az alternatív modellek a multidrog transzporterek promiszkuitását is a lipid fázisban történő hidrofób kölcsönhatásra vezetik vissza, amely kevésbé specifikus, mint egy vizes fázisban létrejövő, hidrogénhidakon és egyéb erős molekuláris kölcsönhatásokon alapuló kapcsolat. Bár számos erőfeszítést tettek az alternatív transzportmodellek kísérletes igazolására, eddig csak közvetett eredmények születtek. A transzportált szubsztrátokkal történt affinitás-jelöléssel a transzporter membránba ágyazott felülete rajzolódik ki [103-106]. Jól definiált drog-kötőhely nem látszik ezekből az eredményekből, ami összhangban áll a gyenge hidrofób kölcsönhatásokra épülő transzporter-szubsztrát kapcsolat hipotézisével. Néhány, jelölt molekulákkal membránvezikulákon végzett funkcionális vizsgálat is arra utal, hogy a transzporter a lipid fázisból pumpálja ki a szubsztrát molekulát [107, 108].

Érdekes módon egy, a témával foglalkozó átfogó közlemény a calcein assay alapját képező korábbi felfedezésünket is az alternatív modelleket megerősítő kísérletes adatok közé sorolja [101]. A fluoreszcens acetoxi-metilészterekkel végzett munkánk megmutatta, hogy megfelelően magas MDR1 expresszió mellett csak minimális észterhasítás történik a sejtekben. Ez – az említett közlemény szerint – azt mutatja, hogy a transzporter kipumpálja a sejtből a szubsztrátot mielőtt az elérné a citoplazmát. Véleményem szerint eredményeinkből ez a következtetés nem vonható le, ugyanis ha a transzporter - az észterázok affinitásához és aktivitásához képest - kellően nagy affinitással és transzportkapacitással rendelkezik, akkor is tapasztalhatunk ilyen csekély festékfelhalmozódást a sejtekben.

A következőkben ismertetett munkánkban az ABCG2 multidrog transzporter működési mechanizmusát vizsgáltuk a fehérje GFP-vel címkézett változatát (GFP-G2) alkalmazva. Ezekben a tanulmányokban olyan ABCG2 szubsztrátokat használtunk, mint a mitoxantron (MX) vagy a feoforbid A (feoA), melyek azzal a különleges tulajdonsággal bírnak, hogy a lipid környezetben a fluoreszcenciájuk nagyságrendekkel megnő [109, 110]. Kimutattuk, hogy a 19. ábrán bemutatott kísérletekhez hasonlóan on-line konfokális elemzéssel az ABCG2 transzportaktivitása megbízhatóan meghatározható. A Hoechst transzport assay-vel ellentétben ezekben a tanulmányokban nem a sejtmagokban mértük a festék celluláris felhalmozódását, hanem az intracelluláris membránokban, ahol a MX és a feoA fluoreszcenssé válik (ábrán nem bemutatott eredmény, 7. közlemény 1. ábra). Azt is demonstráltuk, hogy a GFP-G2 drog-eltávolító aktivitása az expressziós szinttől függ. Hasonló összefüggést mutattunk ki a MX akkumulációval meghatározott aktivitás faktor és a GFP fluoreszcencia alapján becsült expressziós szint között, mint amit korábbi munkáinkban az MDR1 expressziója és a calcein assay-vel meghatározott aktivitásfaktorral kaptunk (ábrán nem bemutatott eredmény, 7. közlemény 2. ábra).

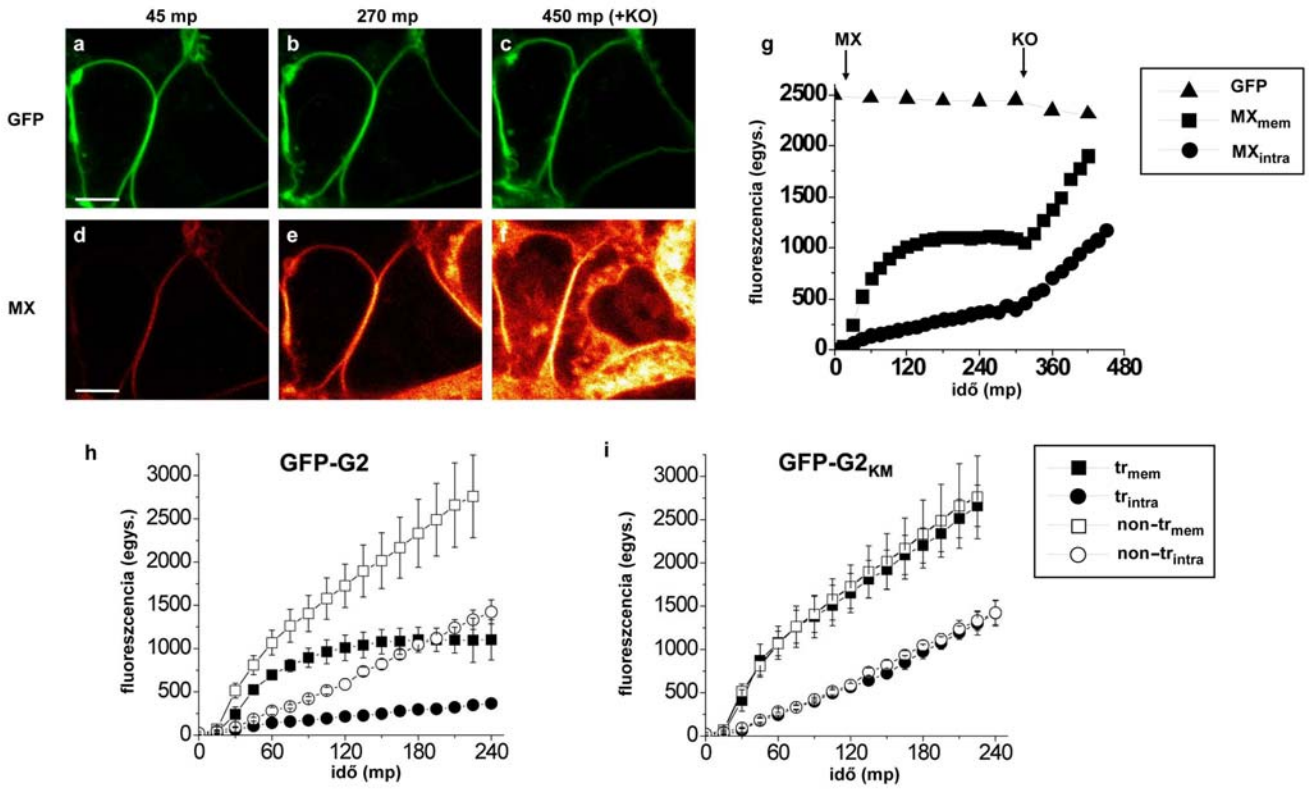

21. ábra: A mitoxantron plazmamembrán akkumulációjának mennyiségi meghatározása. a-f) A GFP-G2-t expresszáló HEK293 sejtekkel készült konfokális mikroszkópos felvételsorozaton a felső panelek a GFP fluoreszcenciát, míg az alsó panelek a mitoxantron (MX) távoli vörös fluoreszcenciáját mutatják. A képek fölötti számok a 2 μM MX addíciójától számított időt mutatják másodpercben kifejezve. A jobb oldali panelek az ABCG2-specifikus gátlószer (KO: 1 μM Ko143) hozzáadása után készültek. A skála 5 μm-t jelöl. **g)** A plazmamembrán pozícióját a GFP fluoreszcencia alapján követtük egy régióval (ROI-val) (▲, GFP). Ugyanazt a ROI-t használva meghatároztuk a mitoxantron fluoreszcenciáját a plazmamembránban (■, MX_{mem}), illetve közvetlenül a membrán alatti régióban (●, MX_{intra}). **h-i)** GFP-G2-t, illetve GFP-G2KM-et expresszáló sejtekben a mitoxantron akkumulációja a plazmamembránban (mem), illetve a membrán alatti régióban (intra). A teli szimbólumok a transzfektált sejteket (tr), míg az üresek a kontroll, azaz nem-transzfektált (non-tr) sejteket jelölik. Az utóbbi két panelen legalább 4 független kísérletből kapott átlag ± SEM értékek vannak feltüntetve.

Ezekben a kísérletekben megfigyeltük, hogy a MX-t vagy a feoA-t a sejtekhez adva, a fluoreszcencia növekedése nemcsak az intracelluláris membránokban tapasztalható, hanem a sejtmembránok is világosan kirajzolódnak (21a-f ábrák). Az ABCG2 fehérjéhez kapcsolt GFP-címke lehetőséget adott arra, hogy nyomon kövessük a plazmamembrán változó pozícióját, és így meghatározzuk a drog plazmamembránban történő akkumulációjának kinetikáját (21g ábra). Ezzel párhuzamosan közvetlenül a sejtmembrán alatti régióban követtük a drog intracelluláris felhalmozódását is. Azt tapasztaltuk, hogy a plazmamembránban a drog koncentráció hamar telítésbe hajlik, míg a sejten belül csak lassan, de fokozatosan emelkedik. Az ABCG2-specifikus gátlószer (Ko143) hozzáadása után mindkét

kompartmentben meredek fluoreszcencia emelkedést figyelhettünk meg (21f-g ábra), ami arra utal, hogy a tapasztalt jelenség az ABCG2 transzportaktivitásának következménye.

A tranziens transzfekciós rendszer, valamint a GFP-címkézett transzporter lehetőséget adott arra, hogy egy látómezőben párhuzamosan kövessük nyomon a drogfelvételt a transzgént expresszáló és a kontroll (nem-transzfektált) sejtekben. Összevetettük a drogfelvétel kinetikáját kontroll sejtekben, GFP-címkézett ABCG2 vad típusú (GFP-G2), illetve annak inaktív mutáns variánsát (GFP-$G2_{KM}$) expresszáló sejtekben - mind a plazmamembránt, mind a szubmembrán régiót tekintve. Azt tapasztaltuk, hogy a plazmamembrán drog koncentrációjának gyors telítésbe hajlása sem a kontroll, sem a GFP-$G2_{KM}$-t expresszáló sejtekre nem jellemző (21h-g ábra), tovább megerősítve azt a feltételezést, hogy a vad típusú sejteknél tapasztalt kinetika az ABCG2 aktivitásának következménye.

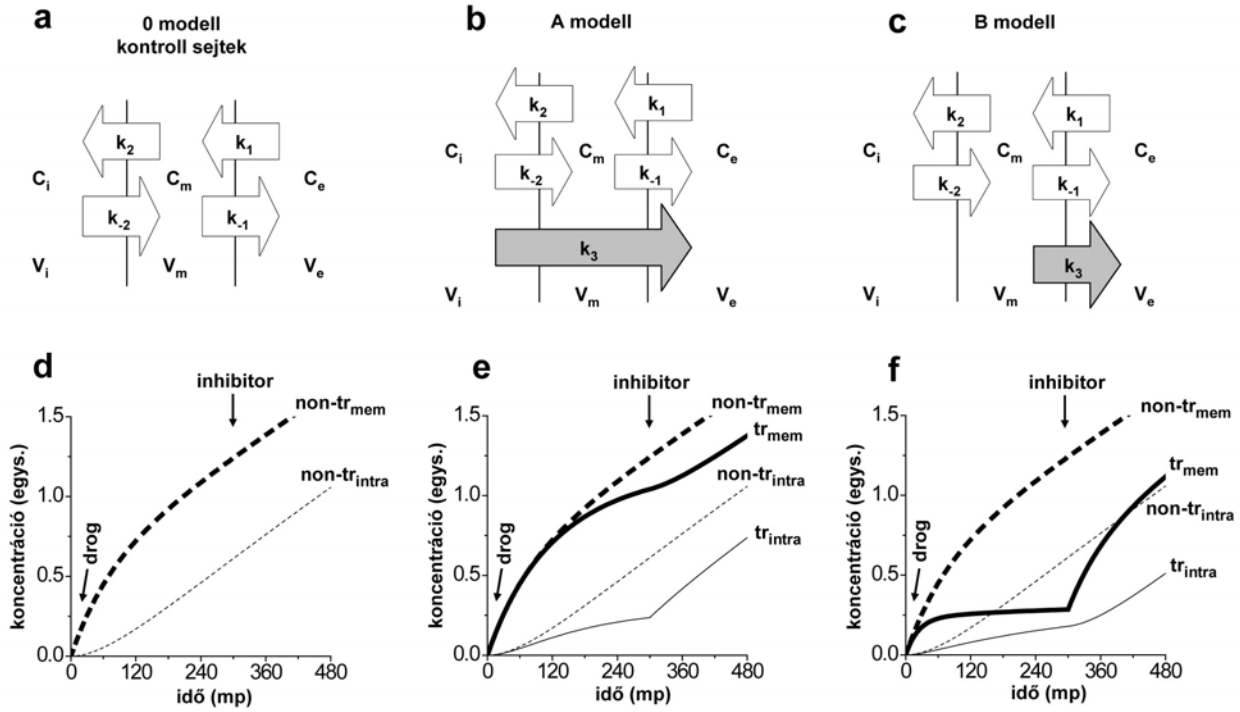

22. ábra: A drog celluláris felvételét és kipumpálást leíró különböző kinetikai modellek. a) A drogfelvétel nem-transzfektált, kontroll sejtekbe (0 modell) **b)** A klasszikus pumpa mechanizmusnak megfelelő séma (A modell), melyben a transzportált szubsztrát a citoplazmából a külső térbe transzlokálódik. **c)** Egy alternatív modell, melyben a szubsztrátot közvetlenül a plazmamembránból pumpálja ki a transzporter. Jelölések: *c* – koncentráció, *k* – sebességi állandó, *V* – térfogat; indexek: *e* – külső, *m* – plazmamembrán, *i* – intracelluláris. **d-f)** A kinetikai modellek zárt alakú parametrikus megoldásai. Szaggatott vonal: nem transzfektált (non-tr), folytonos vonal: transzfektált (tr) sejtek (tr); vastag vonal: plazmamembrán (mem); vékony vonal: intracelluláris (intra) koncentráció. Az inhibitor hozzáadását úgy modelleztük, hogy 300 másodpercnél a k_3 paramétert nullával tettük egyenlővé.

A drog celluláris felvételének, illetve kipumpálásának leírására különböző transzport-kinetikai modelleket alkottunk (22. ábra). A transzporter nélküli helyzetet, azaz a kontroll sejtekbe történő drog akkumulációt a „0 modell" segítségével, míg a transzportert expresszáló sejtekben a drog eloszlását két különböző, „A", illetve „B" modellel írtuk le. Az előbbi a „klasszikus pumpa" mechanizmusnak feleltethető meg, míg az utóbbiban a transzporter a szubsztrátot közvetlenül a membránból pumpálja ki, nem meghatározva a szubsztrát-felismerés pontos helyét. A „B" modell ezért tulajdonképpen egyesíti magában a „hidrofób porszívó" és a „floppáz" modelleket.

A transzportfolyamatok ilyenfajta leírása számos egyszerűsítést és feltételezést foglal magában. Egyrészt első közelítésben a membránt egy egységes kompartmentnek tekintettük, ezzel áttételesen feltételeztük azt, hogy a membránon belüli diffúzió és/vagy flip-flop mozgás nem sebesség-meghatározó lépés. Ezt a mitoxantron fizikai-kémiai tulajdonságai alapján tehettük meg, hiszen a lipid/víz megoszlási hányadosa 230 000. További egyszerűsítés, hogy a pumpa által képviselt transzportlépést – a többi lépéshez hasonlóan - elsőrendű kinetikával írtuk le, arra alapozva, hogy az adott drogkoncentráció a K_m alatti tartományba esik. A 22a-c ábrákon bemutatott sémákat egy-egy differenciál-egyenletrendszerrel írtuk le. Ezekben éltünk még egy feltételezéssel, nevezetesen, hogy a külső drog koncentráció az adott idő keretben állandó. Ezt az alapján tehettük meg, hogy a külső tér nagyságrendileg nagyobb a sejtek és a sejtmembránok térfogatánál. A differenciál-egyenletrendszerek zártalakú megoldásakor azt is feltételeztük, hogy $k_2 = k_{-2}$ azzal a megfontolással, hogy két lipid fázis közötti átmenetet írunk le ezekkel a lépésekkel, hiszen a kísérletekben a plazmamembránban és a belső membránok-ban határozzuk meg a drogkoncentrációt.

A differenciál-egyenletrendszerek parametrikus megoldása alapján több kvalitatív megállapítást tehettünk a modellek viselkedésére vonatkozóan. 1.) Az „A" modellben a drog plazmamembrán koncentrációja (c_m) csak kevéssé tér el a kontroll sejtekben mért értékektől, csak lassan éri el az egyensúlyi koncentrációt, ezzel szemben a „B" modell alapján c_m hamarosan egyensúlyba jut. 2.) A membrán (c_m) és az intracelluláris (c_i) drogkoncentráció az „A" modellben különböző értéket vesz fel egyensúlyban, míg a „B" modellben azonos érték felé tartanak. 3.) A gátlószer hozzáadása után az „A" modellben c_i növekedése indul meg gyorsan, amit a c_m emelkedése lassan követ, míg a „B" modellben éppen fordított a helyzet. 4.) Az is megállapítható – akár egyszerű logikai megfontolás alapján is -, hogy ha a droggal előzetesen megtöltött sejtekből a drogkiáramlást mérjük, akkor abból a kompartmentben csökken a koncentráció hamarább, ahonnan a transzporter kipumpálja a vegyületet. Ezeket a megállapításokat matematikailag is igazoltuk (7. sz. közlemény, függelék).

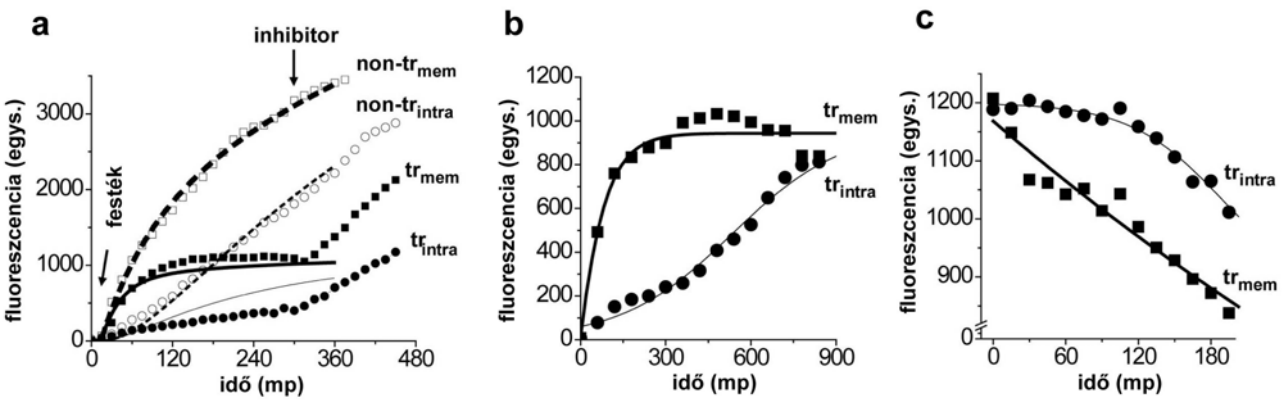

23. ábra: A drogfelvétel kísérleti adatainak és a modell predikciók összevetése. a) GFP-G2-t expresszáló (tr), illetve nem-transzfektált (non-tr) sejtekben a mitoxantron plazmamembránba (■, □, mem) és a membrán alatti régióba (●, ○, intra) történő akkumulációjának kísérletileg meghatározott kinetikája (n > 4). A szaggatott vonalak a kontroll sejtekben mért c_m és c_i értékeihez a „0 modell" alapján illesztett görbéket jelölik, míg a folytonos vonalak ugyanezt reprezentálják a GFP-G2-t expresszáló sejtekben a „B" modellt alapul véve. Vastag vonal: plazmamembrán (mem); vékony vonal: intracelluláris (intra) koncentráció. **b)** A drogfelvétel egyensúlyi értékeinek meghatározása GFP-G2-t expresszáló sejtek plazmamembránjában (■, tr_{mem}), illetve a szubmembrán régióban (●,tr_{intra}) mérve. **c)** A drogkiáramlás kinetikája mitoxantronnal előzetesen feltöltött sejtekből. A jelölések ugyanazok, mint az előző panelen.

Kísérleti adataink minden tekintetben a „B" modellt igazolták vissza, mivel c_m – mint ahogy azt korábban megállapítottuk - gyorsan telítődik (23a ábra), c_m és c_i azonos egyensúlyi érték felé konvergálnak (23b ábra), a Ko143 addícióját követően c_m növekedése indul meg gyorsan (23a ábra), és végül az efflux kísérletben a plazmamembránból indul meg a a drog kiáramlása először (23c ábra). Az is belátható, hogy a „B" modell esetében $1/c_m$ egyensúlyi értéke lineáris összefüggést mutat k_3-mal, ami arányos az expressziós szinttel. Kísérleti adataink visszaigazolták a lineáris kapcsolatot az egyensúlyi $1/c_m$ értékek és a GFP fluoreszcencia között (ábrán nem bemutatott eredmény, 7. közlemény 5f ábra).

Egy további megközelítésben a kísérleteinkben meghatározott c_m és c_i értékekre kinetikai görbéket illesztettük a különböző modellek alapján. Először a kontroll sejtekbe történő passzív drogfelvétel időgörbéjével végeztünk paraméterillesztést a legkisebb négyzetek módszerét használva (23a ábra, szaggatott vonalak). Érdemes megjegyezni, hogy ez a numerikus megközelítés is visszaigazolta a zártalakú megoldáskor tett feltételezésünket, miszerint $k_2 = k_{-2}$. Ezt követően a kontroll sejtek adataival kapott illesztés paramétereit rögzítve, a GFP-G2-t expresszáló sejtekkel kapott kísérleti értékekhez illesztettünk görbét k_3–mal, mint egyetlen szabad paraméterrel, mind az „A", mind a „B" modellt alapul véve. Az előbbi esetében nem kaptunk elfogadható illeszkedést (RMSE = 652,1), a „B" modellt használva viszont jó volt a kísérleti adatokhoz való illeszkedés (RMSE = 38,1) (23a ábra, folytonos vonalak).

Ezen felül alkottunk olyan transzportsémákat is, melyekben a membrán külső és belső rétege külön kompartmentet képez (7. közlemény 6. ábra). Ez a megközelítés egyrészt nem él azzal a feltételezéssel, hogy a membránon belüli tranzíció gyors folyamat, másrészt lehetőséget teremt a „hidrofób porszívó" és a „floppáz" modell megkülönböztetésére. Ezeket a sémákat leíró differenciál-egyenletrendszerek numerikus megoldása megmutatta, hogy az előbb említett feltételezés megalapozott volt. Másrészt szintén azt eredményezte, hogy a „klasszikus pumpa" modellhez való illesztés elfogadhatatlan. A másik két transzportmodellel viszonylag jó illeszkedést kaptunk, azonban azok közül a „floppáz" mechanizmust feltételező modell bizonyult jobbnak.

Összefoglalva, eredményeink megmutatták, hogy egy kulcsfontosságú multidrog transzporter, az ABCG2 az egyik legfontosabb drog-szubsztrátját, a mitoxantront nem a klasszikus mechanizmus révén transzportálja, hanem közvetlenül a membránból pumpálja ki a sejtből. Eredményeink ugyan valamelyest a „floppáz" modellt részesítik előnyben, azonban a kísérleteinkből nem vonható le olyan következtetés, amely a „hidrofób porszívó" modellt elvetné, viszont azt egyértelműen valószínűsítik, hogy a szubsztrátfelismerés a lipid fázisban történik. Meg kell jegyezni azonban azt is, hogy nem szabad általánosítani ezekből az eredményekből, hiszen ismeretes, hogy például az MRP1 többféle transzportmechanizmussal képes a különböző szubsztrátmolekulákat kezelni. Elképzelhető, hogy az ABCG2 is a kevésbé hidrofób szubsztrátjait (pl. a topotekánt) a klasszikus mechanizmussal transzportálja. Mindenestre a mostani eredményeink fontos adalékot jelenthetnek egy hosszú évekre visszanyúló tudományos vitához, és egyedülálló módon, ép sejteken végzett transzport-kísérletekkel igazolják az elméleti megfontolásokkal felállított alternatív transzportmodellek érvényességét.

4.3. A lipidanyagcserében szerepet játszó ABC transzporterek vizsgálata

4.3.1. Az ABCG1 fehérje funkcionális jellemzése

[8. sz. közlemény]

Ahogy a bevezetőben szó esett róla, az ABCG1 és különösen az ABCG4 két kevéssé ismert ABC transzporter. Mindkettő az ABCG alcsaládba tartozó féltranszporter, és rendkívül nagyfokú szekvencia-azonosságot mutatnak. Az ABCG1 és ABCG4 transzporterek tanulmányozásánál nemcsak a kevés rendelkezésre álló információ, hanem a megfelelő ellenanyag hiánya is nehézséget jelentett. Az ABCG1 és ABCG4 vizsgálatát tehát specifikus ellenanyagok előállításával kezdtük. A fehérjék N-terminális citoplazmatikus részével immunizáltunk állatokat, és differenciális szűréssel teszteltük a kapott szérumokat. A megfelelő érzékenységű és szelektivitású poliklonális ellenanyagot termelő állatokat felhasználva, később több lépésben specifikus monoklonális ellenanyagot állítottunk elő.

A legtöbb ABC fehérje az ATP kötéséből és hidrolíziséből biztosítja a transzport-funkciójához szükséges energiát. Több ABC transzporter biokémiai vizsgálatához használtuk korábban az Sf9 rovarsejtes heterológ expressziós rendszert, melyben a fehérje nagy mennyiségben előállítható. A transzporterek jellemzésére, szubsztrátjainak, illetve gátlószereinek feltérképezésére az Sf9 membránpreparátumokon végzett vanadát-szenzitív ATPáz aktivitás mérést használtuk, mivel jellemzően a transzportált szubsztrát fokozza, a transzportot gátló anyag pedig gátolja a transzporter ATPáz aktivitását is [8]. A korábban szerzett tapasztalatainkra építve, az ABCG1 és az ABCG4 fehérjéket is kifejeztettük Sf9 sejtekben. Összehasonlítás végett elkészítettük és kifejeztettük a transzporterek katalitikus hely mutáns variánsait, melyek a Walker A motívumban lévő kritikus pozícióban egy lizin-metionin cserét tartalmaznak (KM mutánsok: ABCG1K124M, ABCG4K108M). Kontrollként a β-galaktozidázt (βgal), valamint egy ABCG2 variánst, az ABCG2R482G-t, illetve annak inaktív mutáns változatát (ABCG2R482G;K86M) tartalmazó membránokat használtunk. Az ABCG2-nek azért ezt a variánsát választottuk, mert erről kimutatták, hogy a rodamin123 festékkel kölcsönhatásba lép, amit az ABCG1 esetében is megfigyeltünk (ld. később).

A membránokban mérve a vanadát-szenzitív ATPáz aktivitást, azt tapasztaltuk, hogy mind a vad típusú ABCG1, mind a vad típusú ABCG4 - a KM mutánsokkal kapott értékeknél szignifikánsan magasabb alapaktivitást mutat (24a ábra). A mutánsok ATPáz aktivitása nem különbözött a háttértől (βgal). A vad típusú ABCG1, de különösen az ABCG4 által képviselt alapaktivitás nem volt igazán magas, messze elmaradt az ABCG2-vel kapott értéktől.

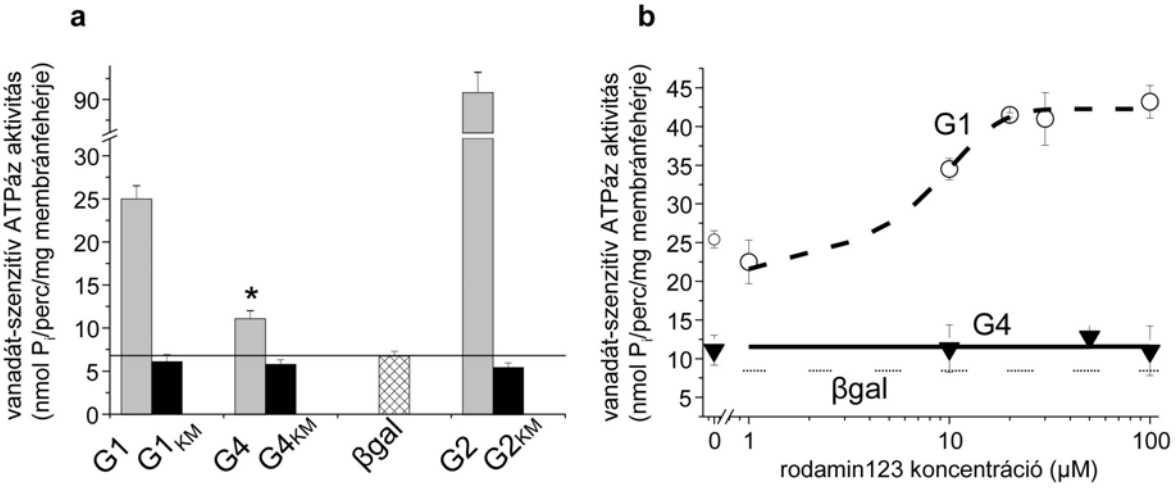

24. ábra: Az ABCG1 és ABCG4 ATPáz aktivitása. a) Az ABCG1 (G1), ABCG4 (G4), és ABCG2R482G (G2) transzportert tartalmazó Sf9 membránpreparátumokon mértük a vanadát-szenzitív ATPáz aktivitást (világos oszlopok). Negatív kontrollként egyrészt a katalitikus hely mutánsokat használtuk (KM indexek): ABCG1K124M, ABCG4K108M, és ABCG2R482G;K86M (sötét oszlopok), másrészt β-galaktozidázt (βgal). Ez utóbbi aktivitást vonallal is jelöltük az ábrán. Az ábrán átlag ± SEM értékek szerepelnek ($n > 3$). A csillag a βgal aktivitásához viszonyított szignifikáns eltérést jelez az ABCG4 esetében ($p < 0,001$). **b)** G1-t és G4-t tartalmazó membránok ATPáz aktivitása rodamin123 jelenlétében. A βgal által képviselt aktivitást szaggatott vonal jelöli.

Ahogy arról szó volt az ABCG2 kapcsán, a tapasztalt alapaktivitás lehet a transzporter szétkapcsoltságának következménye vagy utalhat arra, hogy endogén szubsztrát vagy szubsztrátok vannak jelen a preparátumban. Az ABCG1 és ABCG4 szubsztrátjainak és gátlószereinek feltérképezésére megvizsgáltunk egy kb. 100 vegyületből álló molekula-könyvtárat az ATPáz mérést használva. Ezek között szerepeltek tumorellenes szerek (pl. mitoxantron, doxorubicin), fluoreszcens vegyületek (pl. calcein AM, rodamin123), különböző ismert gátlószerek (pl. verapamil, Ko143), prosztaglandinok, hormonok, neurotranszmitterek, peptidek, konjugált molekulák, szterolok, stb.

Érdekes módon a nagyszámú vizsgálat ellenére csak két olyan vegyületet találtunk, amely az ABCG1 ATPáz aktivitását fokozta: a rodamin123 és a rodamin6G fluoreszcens molekulákat. Az előbbivel kapott koncentráció-függő stimuláló hatás látható a 24b ábrán, összehasonlítva az ABCG4 fehérjével kapott eredménnyel. Ez utóbbi esetében egyetlen vegyületet sem találtunk, amely fokozta volna az ATPáz aktivitását. Hasonló módon, ATPáz méréssel inhibitormolekulákat is próbáltunk azonosítani. Így az ABCG1-et tartalmazó membránokban a benzamil, a ciklosporin A és az L-tiroxin viszonylag alacsony koncentrációban gátolta mind az alap-, mind a rodamin123-stimulált ATPáz aktivitást (ábrán nem bemutatott eredmény, 8. közlemény 2d-f ábrák). Az ABCG4 esetében azonban gátló hatású vegyületeket sem sikerült azonosítanunk.

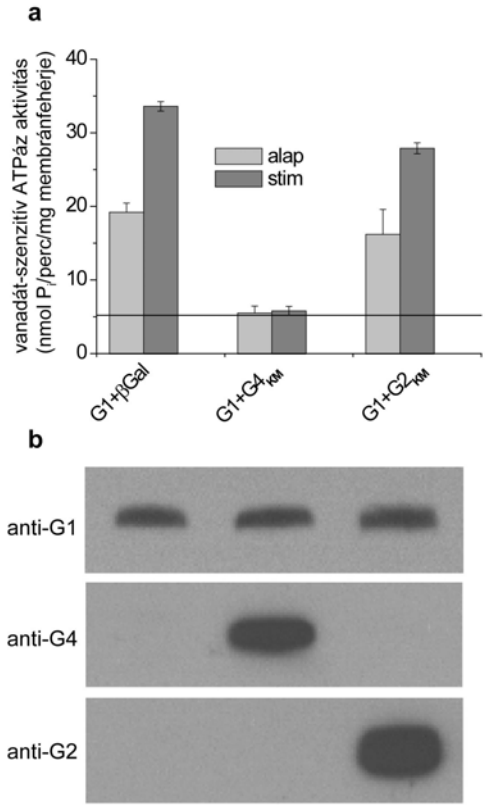

25. ábra: Ko-expresszált transzporterek ATPáz aktivitása. a) Sf9 rovarsejteket ko-infektáltunk ABCG1-gyel és azon felül β-galaktozidázzal (G1 + βgal), ABCG4K108M-mel (G1 + $G4_{KM}$), valamint ABCG2R482G;K86M-mel (G1 + $G2_{KM}$). Mértük a membránok vanadát-szenzitív alap- (világos oszlopok) és 100 μM rodamin123-mal stimulált (sötét oszlopok) ATPáz aktivitását. A háttéraktivitást (βgal) vonal jelöli az ábrán. Az értékek átlag ± SEM jelentenek (n > 3). **b)** A membránpreparátumokban lévő fehérjék jelenlétét és az egyenlő ABCG1 expressziós szintet Western blot analízissel specifikus ellenanyagokat használva mutattuk ki.

Ismeretes, hogy az ABC féltranszportereknek dimerizálódniuk kell ahhoz, hogy működőképes egységet alkossanak. Az ABCG1 esetében mért alap- és stimulálható ATPáz aktivitás arra utal, hogy az ABCG2 transzporterhez hasonlóan, ez a fehérje homodimerként funkcionál. Az ABCG4 esetében a csekély mértékű alapaktivitásból nem célszerű bármiféle következtetést levonni. Felmerült annak lehetősége, hogy az ABCG1 és ABCG4 dimerizációs partnerek lehetnek, hiszen nagyon nagyfokú közöttük a szekvencia-azonosság, és a Drosophila ortológoknál (White, Scarlet, Brow) leírták a heterodimerizációt [111]. Az ABCG1 által képviselt ATPáz aktivitás lehetőséget adott ennek a kérdésnek a megvizsgálására is. Ennek érdekében Sf9 membránokban együtt expresszáltunk vad típusú ABCG1-et és $ABCG4_{KM}$-et, és mértük mind az alap-, mind a rodamin123-stimulált ATPáz aktivitást. Azt tapasztaltuk, hogy az inaktív mutáns ABCG4 variáns gátolja az ABCG1 aktivitását (25a ábra), ami arra utal, hogy a két fehérje heterodimert képez. Kontrollként olyan membránokat használtunk, amelyben az ABCG1 mellett β-galaktozidázt (G1 + βgal), illetve az ABCG2 inaktív mutáns variánsát (G1 + $G2_{KM}$) expresszáltuk. Egyik esetben sem tapasztaltuk a $G4_{KM}$-mel látott domináns negatív hatást, bizonyítva a kölcsönhatás specifikusságát. Kritikus ezekben a kísérletekben, hogy azonos legyen az ABCG1 expressziós szintje a különböző membránpreparátumokban. Ezt Western analízissel igazoltuk (25b ábra).

Összefoglalva, sikeresen expresszáltuk a kevéssé jellemzett ABCG1 és ABCG4 féltranszportereket. Mindkét fehérje ellen sikerült specifikus monoklonális ellenanyagot előállítanunk, és mérhető ATPáz aktivitást mutattunk ki mindkettő esetében. Az ABCG1 ATPáz aktivitását a rodamin123 és a rodamin6G fluoreszcens molekulák stimulálták, ami arra utal, hogy ezek a vegyületek az ABCG1 szubsztrátjai. Ezt a későbbiekben közvetlen transzportmérésekkel nem sikerült igazolnunk. Továbbra is nyitott marad a kérdés, hogy ennek a transzporternek mi a fiziológiás szubsztrátja. A vizsgált vegyületek között szerepeltek bizonyos szterolok is, de ezeknél nem tapasztaltunk ATPáz aktivitást fokozó hatást. Legújabb, még nem publikált eredményeink megmutatták, hogy a koleszterin és a szitoszterin koncentráció-függő módon képes fokozni az ABCG1 ATPáz aktivitását. Annak megválaszolása, hogy vajon ez a stimuláció közvetlen transzportra utal, vagy hogy az ABCG2-nél tapasztalt moduláló hatást tükröz, további vizsgálatokat igényel.

Az ABCG1 és ABCG4 szöveti eloszlása csak részben fed át. A most ismertetett eredményeink arra utalnak, hogy ezek az ABC fehérjék mind homo-, mind heterodimerként képesek funkcionálni, ami összhangban áll a részben átfedő expressziós mintázattal. A legújabb eredményeinkben közvetlen módon, ko-immunprecipitációval is megmutattuk az ABCG1 és ABCG4 között létrejövő kölcsönhatást (publikálás alatt lévő, csak konferencián bemutatott eredmények). Ez a fajta felemás kapcsolat a két fehérje között fiziológiás szempontból finom szabályozásra ad lehetőséget, amennyiben a homodimer és a heterodimer szubsztrát-specifitása, affinitási és transzportkapacitási viszonyai eltérőek. Azonban ennek felderítése, különös tekintettel a heterodimer részletes jellemzésére, további vizsgálatokat igényel.

4.3.2. Az ABCG1 fehérje apoptotikus hatása

[9. sz. közlemény]

Az előző fejezetben bemutatott munkánkban az ABCG1 fehérjét heterológ, bakulovírus-Sf9 rendszer segítségével fejeztettük ki, és biokémiai szempontból jellemeztük. Ebben a tranziens expressziós rendszerben a vírusfertőzést követően a rovarsejtek egy idő után elpusztulnak. Az ABCG1 fehérjével végzett kísérleteinkben azonban azt tapasztaltuk, hogy a vad típusú fehérjét expresszáló kultúrákban sokkal gyorsabban következik be a sejtpusztulás, mint a kontrollként használt β-galaktozidáz, vagy az egyéb ABC fehérjével (pl. ABCG2-vel) vagy akár az ABCG1 inaktív mutáns változatával (ABCG1K124M-mel) transzdukált Sf9 tenyészetekben - annak ellenére, hogy a sejtek fertőzése teljesen azonos körülmények között történt, és hogy az expressziós szintek is egyformának bizonyultak (ábrán nem bemutatott eredmény, 9. sz. közlemény 1. ábra). A féléletidőket összevetve azt találtuk, hogy a vad típusú ABCG1 esetében ez a mutató 40,5± 1,2 óra, míg az összes többinél 60 óra körüli értékeket kaptunk.

Az ABCG1 fehérjével végzett tanulmányainkat kiterjesztettük emlős expressziós rendszerre is. Különféle emlős sejtvonalakat (HEK293, HepG2, COS-7 és MDCKII) használva azt figyeltük meg, hogy a vad típusú ABCG1 (G1) fehérjével transzfektált sejtek morfológiája jelentősen megváltozik. Ezekben a tenyészetekben sok lekerekedett és felúszott sejt figyelhető meg, valamint jelentős mennyiségű, immunfestéssel pozitívnak mutatkozó sejttörmeléket lehet találni. Ezzel szemben az ABCG1KM ($G1_{KM}$) variánst expresszáló sejtek a megszokott morfológiát mutatták (ábrán nem bemutatott eredmény, 9. sz. közlemény 2. ábra).

Mivel a megváltozott sejtmorfológia az apoptotikus sejtekre jellemző jegyeket mutatott, a következőkben megvizsgáltuk ezeket a sejttenyészeteket különböző apoptózis markerekkel. Fluoreszcensen jelölt annexin V kötődésével mutattuk ki a foszfatidil-szerin (PS) sejtfelszíni megjelenését, amely egy korai apoptotikus esemény. A kaszpáz 3 aktiválódását, ami az apoptotikus folyamatok egy központi szerepű enzime, hasonlóképpen fluoreszcens módszerrel, $PhiPhiLuxG_2D_2$ alkalmazásával detektáltuk. Ez a vegyület egy sejtpermeábilis kaszpáz 3 szubsztrát, ami a proteáz hasítása után válik fluoreszcenssé. Azt találtuk, hogy a vad típusú ABCG1-gyel transzfektált kultúrákban nagy számban lehetett látni annexin V-pozitív és magas kaszpáz 3 aktivitást mutató sejteket (26a-c ábra). Ezzel szemben a KM mutánssal transzfektált tenyészetben alig lehetett ilyen sejtet találni (26d-g ábra). Azt is kimutattuk, hogy a vad típusú G1-gyel transzfektált kultúrákban a transzgént expresszáló sejtekben lehet annexin V-pozitivitást látni (ábrán nem bemutatott eredmény, 9. sz. közlemény 4. ábra).

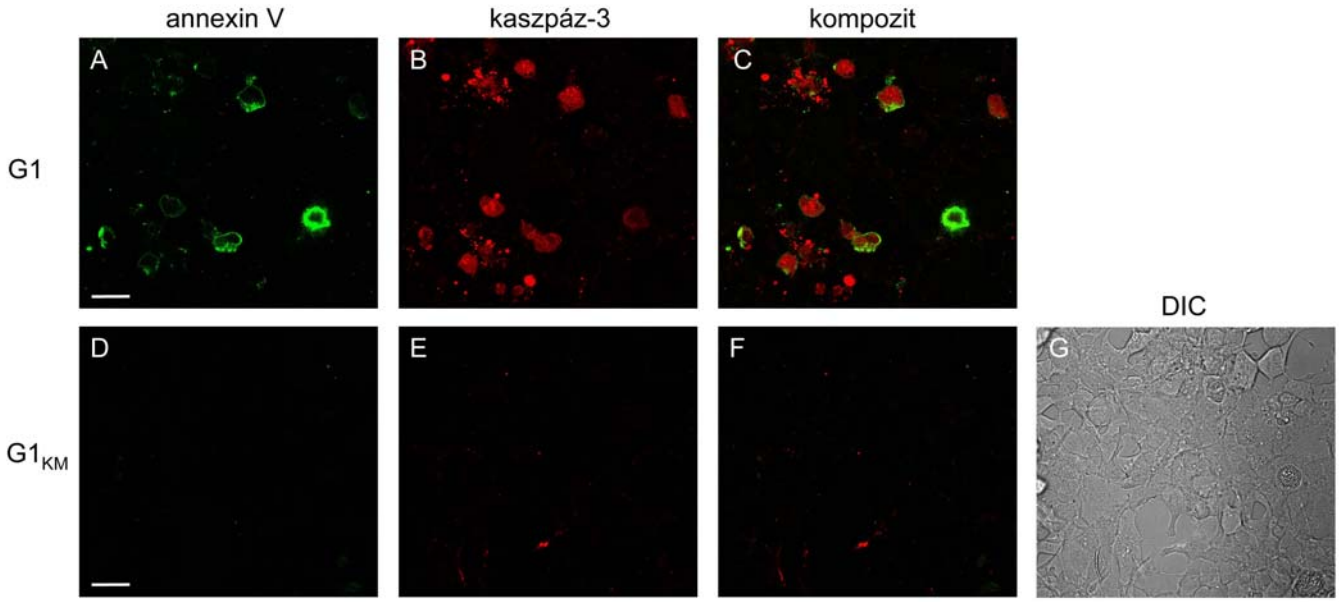

26. ábra: Apoptotikus markerek az ABCG1 és ABCG1KM fehérjékkel transzfektált sejtkultúrákban. (a-c) Annexin V kötéssel detektált foszfatidil-szerin transzlokáció (zöld), illetve PhiPhiLuxG_2D_2-vel láthatóvá tett kaszpáz 3 aktivitás (piros) az ABCG1-gyel (G1) transzfektált HEK293 tenyészetben. A jobb oldali panel az előző kettő kombinációja. **(d-g)** Hasonló kísérlet ABCG1K124M konstrukcióval ($G1_{KM}$) transzfektált sejtkultúrában. A jobb szélen lévő panel az előző paneleken feltüntetett látómezőről készült DIC felvétel, ami azt demonstrálja, hogy a negatív festődés ellenére vannak jelen sejtek a vizsgált területen. A skálák 30 μm-t jelölnek.

Az előbb ismertetett reprezentatív kísérleteket számszerűen is kiértékeltük. A kvantitatív analízis megmutatta, hogy az annexin V jelölést tekintve statisztikailag szignifikáns különbség adódik a vad típusú ABCG1-et expresszáló HEK293 sejtek és a vektor-kontroll között, mely utóbbitól az $ABCG1_{KM}$-et expresszáló sejtek nem különböztek (27a ábra). Mindezek a megfigyelések arra utalnak, hogy a tapasztalt apoptotikus események az ABCG1 fehérje aktivitásával állnak összefüggésben. Tovább vizsgálva ezt a kérdést, a sejteket előkezeltük olyan anyagokkal, melyekről korábbi vizsgálataink megmutatták, hogy gátolják az ABCG1 ATPáz aktivitását. Ezek a gátlószerek (L-tiroxin és benzamil) képesek voltak az ABCG1-által indukált PS-kifordulást is meggátolni. Hogy kizárjuk ezeknek a vegyületeknek az esetleges aspecifikus gátló hatását, kimutattuk, hogy egyikük sem befolyásolta a staurosporin által indukált PS-expozíciót (27ábra inzert). Mindezeket a kísérleteket nemcsak HEK293 sejteken, hanem HepG2 sejttenyészeteken is elvégeztük, és hasonló eredményre jutottunk (ábrán nem bemutatott eredmény).

Ezt követően megvizsgáltuk, hogy a tapasztalt jelenség, melyet transzfektált, a transzgént over-expresszáló sejtekben figyeltünk meg, reprodukálható-e endogén rendszerekben is. Az ABCG1 fehérjéről ismert, hogy expresszálódik makrofágokban, és hogy a transzkripciós szintje jelentősen megemelkedik az LXR magreceptor útvonal aktiválódása révén.

Ezért ezekhez a vizsgálatokhoz különböző makrofág modelleket használtunk: egyrészt forbol-észterrel előkezelt Thp-1 sejteket, másrészt primér monocita-eredetű makorfágokat. Mivel mindkét esetben hasonló eredményre jutottunk, értekezésemben csak az utóbbival kapott eredményeket mutatom be. Az LXR-agonista jelentős mértékben fokozta az ABCG1 expresszióját a makrofágokban, melyet sem a tiroxinnal, sem a benzamillal történő előkezelés nem befolyásolt (ábrán nem bemutatott eredmény, 9. sz. közlemény 7a ábra). Ezzel szemben a foszfatidil-szerin sejtfelszíni megjelenését jelentősen fokozta az LXR-agonista, mely hatást az ABCG1 inhibitorai, a tiroxin és a benzamil meggátolták (27b ábra). Itt szintén megmutattuk, hogy az említett két ABCG1 inhibitor nem gátolja a staurosporinnal kiváltott apoptózist, kizárva az aspecifikus hatás lehetőségét. Mindezek az eredmények azt támasztják alá, hogy az ABCG1 aktivitása révén képes apoptózist indukálni a különféle sejtekben.

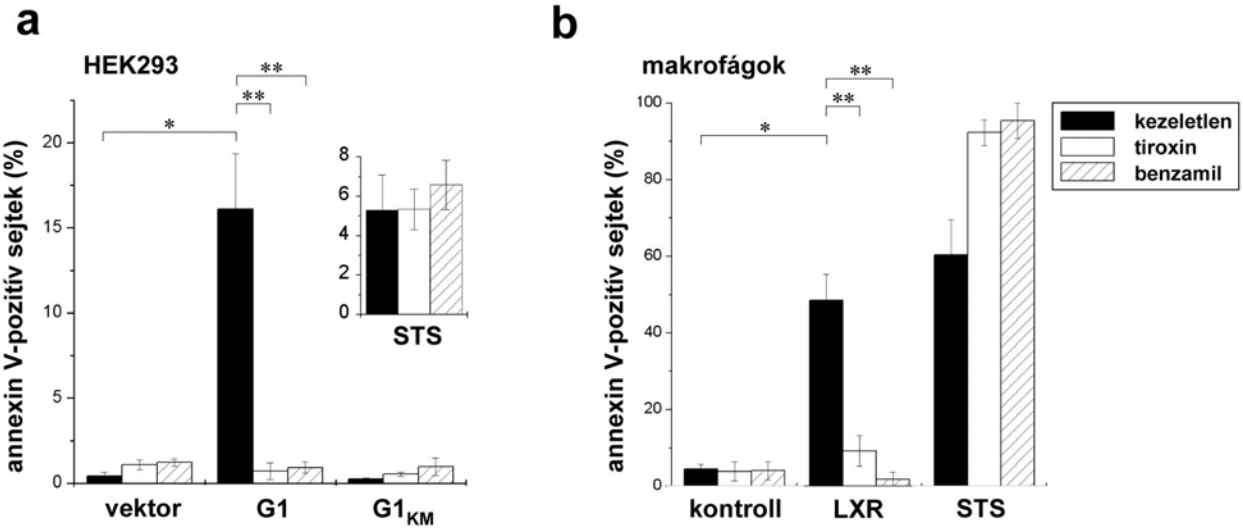

27. ábra: Az ABCG1 által indukált foszfatidil-szerin (PS) transzlokáció kvantitatív értékelése transzfektált HEK293 sejtekben és indukált makrofágokban. a) Annexin V-pozitív sejtek százalékos arányát határoztuk meg vad típusú ABCG1-et (G1) vagy inaktív mutáns ABCG1-et ($G1_{KM}$) tartalmazó konstrukcióval transzfektált HEK293 sejtekben (fekete oszlopok). Negatív kontrollként üres vektorral transzfektált sejteket használtunk. Az ABCG1-et expresszáló sejtekben tapasztalt PS-kifordulást teljes mértékben gátolták az ABCG1 ATPáz aktivitásának inhibitorai, az L-tiroxin (100 μM) és a benzamil (50 μM). A gátlás specifikus voltát azzal igazoltuk, hogy a staurosporin (STS) által indukált apoptózist ezek a vegyületek nem gátolták (mellékábra). Az oszlopok átlag ± SEM értékeket tüntetnek fel (1000-3000 sejt legalább 3 független kísérletben). A csillagok a szignifikáns különbségeket jelölik a vektor-kontrollhoz viszonyítva (*), illetve a vad típusú ABCG1-et expresszáló sejtekhez képest (**) ($p < 0{,}001$). **b)** Annexin V kötés humán monocita-eredetű makrofágokban. Az ABCG1 expressziót LXR-agonistával (1 μM T0901317) történt előkezeléssel indukáltuk (LXR). Negatív kontrollként a nem-indukált, csak az oldószerrel kezelt makrofágokat használtuk. A többi jelölés megegyezik az előző panelen feltüntetett jelölésekkel. A gátlószerek aspecifikus hatását a makrofágokon is STS-indukált annexin V méréssel zártuk ki.

Ezek a megfigyeléseink érdekes új kontextusba helyezik az ABCG1 fehérjét. Korábbi tanulmányok arról számoltak be, hogy ez a fehérje koleszterin kiáramlást okoz a sejtekből. Mivel kimutatták, hogy az ABCG1 jelenléte elősegíti a HDL partikulumok koleszterinnel való töltődését, ezért ennek a fehérjének érelmeszesedést gátló, ateroprotektív szerepet tulajdonítottak. A modell elképzelés szerint az ABCG1 - az ABCA1 által előállított nascens HDL-t alakítja tovább nagyobb koleszterintartalmú HDL partikulummá [57]. Az alaposabb vizsgálatok azonban arra is rávilágítottak, hogy a folyamat nem igazán specifikus, ugyanis az ABCG1 által kiváltott koleszterin kiáramlásban nemcsak a HDL szerepelhet lipid akceptorként, hanem az apoA-I-et kivéve sokféle más molekula, illetve molekula komplex is. Ezek között szerepel az LDL, apoE-tartalmú lipoproteinek, foszfatidil-kolin vezikulák, de még a BSA vagy a ciklodextrin is. A folyamat aspecifikus volta összhangban áll az általunk megfigyelt ABCG1-hez kapcsolható apoptózissal, mivel a programozott sejthalál könnyen magyarázhatja a sejtekből történő nem-specifikus koleszterin kiáramlást.

A knockout egerekkel végzett *in vivo* kísérletek sem erősítették meg egyértelműen az ABCG1 ateroprotektív szerepét. Ellentmondó eredményekre vezettek az Abcg1-deficiens egerekből származó csontvelővel átültetett ateroszklerózis modell egerekkel végzett tanulmányok, ugyanis hol az ateroszklerotikus lézió méretének növekedését, hol csökkenését figyelték meg [61-63]. Ldlr-deficiens egereket ABCG1 −/− csontvelővel transzplantálva a koleszterinszint csökkenését lehetett tapasztalni – meglepő módon - a nem-HDL lipoproteinekben [112]. Kimutatták, hogy az ABCG1 ateroszklerózist elősegítő, illetve gátló hatása erősen függött a diétától [63]. Ezeket az ellentmondásokat is fel tudja oldani az általunk megfigyelt ABCG1-hez kapcsolódó programozott sejthalál, hiszen ismeretes, hogy a makrofágok apoptózisa a korai léziókban ateroprotektív, míg az előrehaladott állapotban a folyamatok kedvezőtlen progresszióját segíti elő [113]. Feltételezésünket tovább erősíti az az *in vivo* megfigyelés, hogy az ABCG1 éppen a korai léziókban képes gátolni a plakk növekedését [64].

Ugyan kísérleteink egyelőre nem adnak magyarázatot az ABCG1 által kiváltott apoptózis mechanizmusára, de egy új megvilágításba helyezik ennek a fehérjének a szerepét. Megfigyeléseink alapján feloldható az ABCG1 - *in vivo* kísérletekben tapasztalt, az ateroszklerózis patomechanizmusában betöltött ellentmondásos szerepe. Az ABCG1 fehérjéhez kapcsolódó makrofág apoptózis magyarázatot adhat az ABCG1 hol aterogenikus, hol ateroprotektív szerepére.

4.3.3. Az ABCA1 fehérje sejtfelszíni expresszió változásainak vizsgálata

[10. sz. közlemény]

Az ABCA1 fehérje a koleszterin-anyagcsere egy kulcsfontosságú szereplője, mivel a reverz koleszterin transzport kezdeti lépésében, a koleszterin és az apoA-I kölcsönhatásában, a nascens HDL előállításában játszik meghatározó szerepet. A rendelkezésre álló adatok alapján nem teljesen világos, hogy maga az ABCA1 a koleszterin transzporter vagy más fehérjéket szabályozva segíti elő a transzportfolyamatot. Szintén vitatott kérdés, hogy az apoA-I koleszterinnel való feltöltése a sejtfelszínen történik vagy a sejten belül reciklizáló endoszómákban. Mindenesetre az apoA-I megkötése biztosan a sejtfelszínen zajlik, mely folyamatban az ABCA1 kulcsszerepet játszik, hiszen funkcióvesztéssel járó mutációi (pl. a Tangier betegségben) HDL-deficienciához és a koleszterin-anyagcsere zavaraihoz vezetnek.

Az ABC transzportereket általában tekintve, csak kevés olyan ellenanyag létezik, amely a fehérje külső felszínéhez köt. A legtöbb ezek közül ráadásul több epitópot keresztkötő, konformáció-szenzitív antitest (pl. 5D3 anti-ABCG2 ellenanyag). Még az olyan nagy külső hurkot tartalmazó ABC fehérjék ellen, mint az ABCA alcsalád tagjai, sem áll rendelkezésre megfelelően szenzitív és szelektív külső felismerésű ellenanyag. Mivel az ABCA1 működésének megértéséhez kulcsfontosságú a fehérje sejtfelszíni detektálása, a következőkben ismertetett munkánk célja az volt, hogy egy olyan kísérleti eszközt hozzunk létre, amely lehetővé teszi az ABCA1 funkcionális expressziójának szenzitív követését a sejtfelszínen.

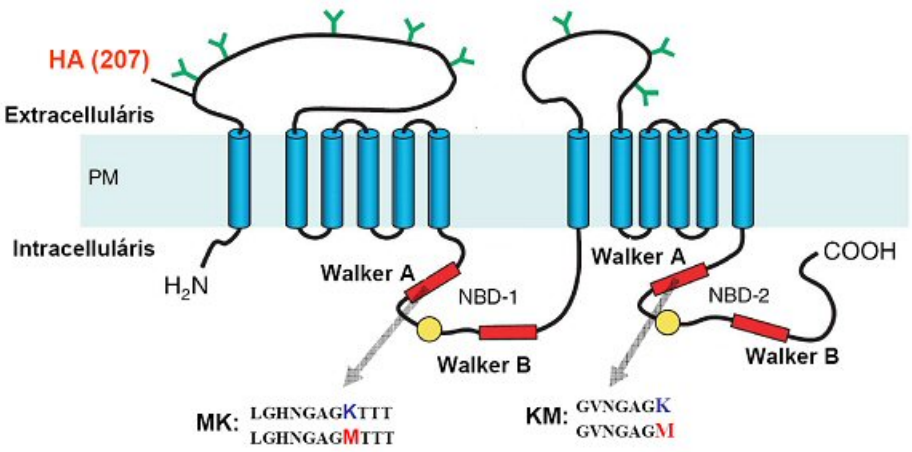

28. ábra: Az ABCA1 címkézése extracelluláris hemagglutinin (HA) epitóppal és a Walker A mutációk elhelyezkedése a polipeptidláncon belül. Az ABCA1 feltételezett membrántopológiáján feltüntettük a HA-epitóp pozícióját, amely az első külső hurok elején helyezkedik el (207-es pozíció). Mindkét nukleotid-kötő domén (NBD) Walker A motívumában kicseréltünk egy kritikus lizint metioninra: K939M, illetve K1952M. Jelölések: MK - a fehérje N-terminális felében egyetlen mutációt tartalmazó variáns; KM – az ABCA1 C-terminális felében mutáns változat; MM – dupla mutáns.

Ennek érdekében egy hemagglutinin (HA) epitópot helyeztünk be az ABCA1 fehérje első, külső hurkába, a 207-es pozícióba (28. ábra). A funkcionális vizsgálatokhoz létrehoztunk olyan mutáns variánsokat is, amelyeket korábbi munkáinkban sikeresen alkalmaztunk más ABC fehérjéknél. Így a nukleotid-kötő doménekben lévő Walker A motívumban a kritikus lizint metioninra cseréltük, létrehozva két egyes mutánst, a K939M (MK) és K1952M (KM) variánst, illetve egy dupla mutánst (MM). Ezeket a mutánsokat is HA-címkével láttuk el.

Retrovírus expressziós rendszer segítségével többféle emlős sejtvonalat (HEK293, MDCKII, HeLa) transzdukáltunk a különböző ABCA1 variánsokkal. Majd különböző szelekciós, szétválogatós (sorting) és klónozási eljárásokkal erőfeszítéseket tettünk arra, hogy a transzgént stabilan expresszáló sejtvonalakat hozzunk létre. Az irodalomból ismert volt, hogy az ABCA1 expresszió hamar lecseng a transzfektált/transzdukált sejtekben. Törekedtünk arra, hogy közepes, az endogén rendszerekkel összevethető expressziós szinteket állítsunk be az egyes sejtvonalaknál. Kvantitatív RT-PCR-rel ellenőriztük, hogy a HA-címkézett ABCA1 variánsok mRNS szintje hasonló az LXR-indukált makrofágokban tapasztalható értékekkel (ábrán nem bemutatott eredmény, 10. sz. közlemény 2a ábra).

Sikerült létrehoznunk olyan HEK293, illetve MDCKII sejtvonalakat, amelyek stabilan, 20, illetve 50 passzázson keresztül expresszálták a HA-címkézett ABCA1 variánsokat. A teljes fehérje expressziót Western blot analízissel követtük (29a ábra), az ABCA1 variánsok sejtfelszíni megjelenését pedig nem-permeabilizált sejteken végzett immunfestést követően áramlási citométerrel határoztuk meg (ábrán nem bemutatott eredmény, 10. sz. közlemény 3. ábra). Mindkét módszer esetében kereskedelmi forgalomban kapható, a HA-epitópot specifikusan felismerő, nagy érzékenységű ellenanyagot használtunk a bevitt fehérje-variánsok detektálására.

Megvizsgáltuk, szintén anti-HA ellenanyagot alkalmazva, a HA-címkézett ABCA1 variánsok sejten belüli elhelyezkedését. Különböző szubcelluláris markereket használva, HEK293 sejteken megmutattuk, hogy a bevitt fehérje mind a vad típusú, mind a mutáns változataiban elsősorban a plazmamembránban lokalizálódik (29b ábra). Valamennyi festődést láttunk a Golgi apparátusban és csekély mértékűt az endoszómákban (ábrán nem bemutatott eredmény, 10. sz. közlemény 4. ábra). MDCKII sejteken azt is demonstráltuk, hogy polarizáltan növesztve a sejteket, a HA-címkézett ABCA1 variánsok a bazolaterális membránban helyezkednek el (ábrán nem bemutatott eredmény, 10. sz. közlemény 5. ábra), ami megegyezik azzal, amit korábban leírtak a címke nélküli ABCA1 szubcelluláris lokalizációjáról. Összességében a fehérje expresszió és lokalizáció az általunk létrehozott sejtvonalakban minden tekintetben megfelelt az elvárásoknak.

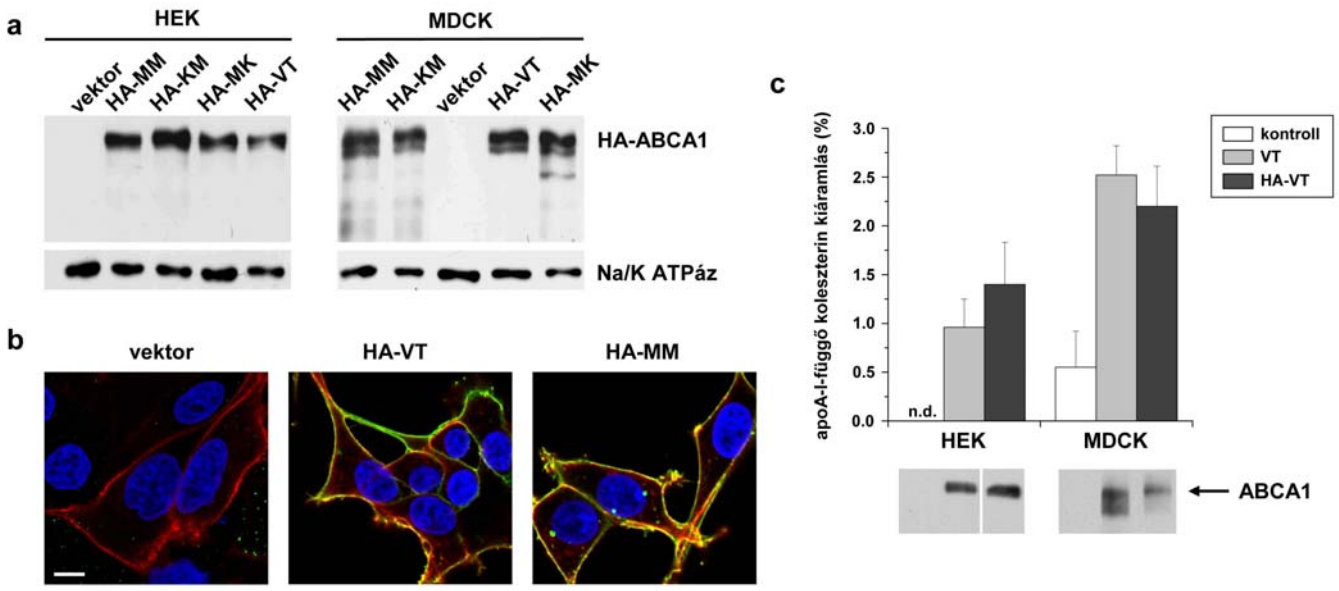

29. ábra: A HA-ABCA1 variánsok stabil expressziója és jellemzése. a) HA-címkézett vad típusú (HA-VT), K939M mutáns (HA-MK), K1952M mutáns (HA-KM), valamint dupla mutáns (HA-MM) ABCA1-gyel transzdukált HEK293 és MDCKII sejtek teljes sejtlizátumából készült mintákon Western blot analízissel ellenőriztük a fehérje expressziót 20-50 passzázson keresztül, anti-HA ellenanyagot használva. Az ábra az 5. passzázs utáni állapotot mutatja. Negatív kontrollként az üres vektorral transzdukált sejteket (vektor), felviteli kontrollként a Na^+/K^+-ATPázt használtuk. **b)** Anti-HA ellenanyaggal vizsgáltuk a címkézett fehérje sejten belüli lokalizációját transzdukált HEK293 sejteken, konfokális mikroszkópot használva (zöld). Plazmamembrán markerként jelölt búzacsíra agglutinint (WGA) használtunk a sejtek enyhe fixálása után, de a sejtek permeabilizálása nélkül (piros). **c)** ApoA-I-függő koleszterin kiáramlást mértünk a HA-címkézett, illetve címke nélküli, vad típusú ABCA1-et expresszáló HEK293 és MDCKII sejteken. Negatív kontrollként a kiindulási (parentális) sejtvonalakat használtuk. n.d. - nem detektálható. Az alsó panelek mutatják a fehérje expressziókat anti-ABCA1 ellenanyaggal készült Western blotokon.

A következő kérdés az volt, hogy vajon a bevitt HA-epitóp a fehérje funkcióját befolyásolja-e. Ennek felderítése érdekében megmértük az általunk létrehozott sejtvonalakban a sejtfelszíni apoA-I kötést (ábrán nem bemutatott eredmény, 10. sz. közlemény 6b ábra), valamint a sejtekből történő apoA-I-függő koleszterinkiáramlást (29c ábra), és összevetettük a címke nélküli ABCA1-gyel kapott értékekkel. Eredményeink azt mutatták, hogy az ABCA1 ezen funkcióit a HA-epitóp bevitele nem érintette.

Mivel munkánk célja az ABCA1 sejtfelszíni expressziójának detektálására alkalmas kísérleti eszköz létrehozása volt, a következőkben megmutattuk, hogy a létrehozott sejtvonalak – elsősorban a HA-ABCA1 variánsokat expresszáló HEK293 sejtek – alkalmasak az ilyen jellegű vizsgálatokra. Rendszerünk validálására olyan anyagokat használtunk, amelyek irodalmi adatok alapján mind pozitív, mind negatív irányba képesek befolyásolni az ABCA1 sejtfelszíni expresszióját.

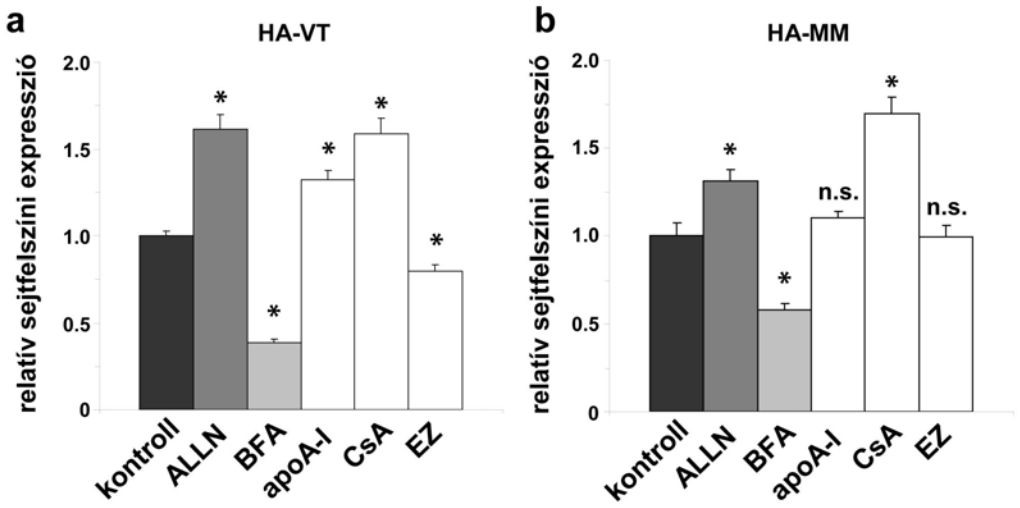

30. ábra: Különböző anyagok az ABCA1 sejtfelszíni expressziójára gyakorolt hatása. A HA-címkézett vad típusú ABCA1-gyel (HA-VT) **(a)**, illetve a K939M/K1952M dupla mutánssal (HA-MM) **(b)** transzdukált HEK293 sejteket különböző anyagokkal 4 órán át előkezeltünk, majd anti-HA ellenanyaggal, nem-permabilizált sejteken végzett immunfestést követően áramlási citométerrel határoztuk meg a sejtfelszíni expressziókat. Az elpusztult sejteket propidium-jodid festés alapján zártuk ki. A kapott eredményeket az oldószerrel előkezelt sejtekhez (kontroll) viszonyítottuk. Jelölések: ALLN – 50 μM acetil-L-leucil-L-leucil-L-norleucinál; BFA – 5 mg/ml brefeldin A; apoA-I - 10 μg/ml apoA-I; CsA – 10 μM ciklosporin A; EZ – 50 μM ezetimib. Az oszlopok átlag ± SEM értékeket mutatnak ($n > 3$), a csillagok a kontrollhoz viszonyított szignifikáns különbségeket jelölik ($p < 0{,}005$), n.s. – nem szignifikáns.

Mivel ismert, hogy az ABCA1 lebontásában közreműködik a kalpain cisztein-proteáz, ezért ennek gátlásával várhatóan növelni lehet a fehérje sejtfelszíni expresszióját. Ennek megfelelően az acetil-L-leucil-L-leucil-L-norleucinál (ALLN), ami egy kalpain inhibitor, a mi rendszerünkben is emelte a HA-ABCA1 szintet a plazmamembránban (30. ábra). A brefeldin A (BFA) pedig azáltal, hogy gátolja a membránfehérjék transz-Golgiból való továbbjutását, a várakozásnak megfelelően csökkentette az ABCA1 sejtfelszíni megjelenését. Ennek a két anyagnak a hatása az ABCA1 funkciójától független, és ezzel összhangban kísérleti rendszerünkben mind a vad típusú, mind a mutáns változat expresszióját megváltoztatta. Ezzel szemben az apoA-I csak a vad típusú ABCA1 sejtfelszíni expresszióját növelte, mivel a kölcsönhatásuk ismerten funkció-függő [114].

Miután ismert hatású anyagokkal meggyőződtünk tesztrendszerünk használhatóságáról, a továbbiakban megvizsgáltuk számos olyan anyag - az ABCA1 variánsok sejtfelszíni expressziójára gyakorolt hatását, melyekről azt tartják, hogy egymagukban vagy kombinációban alkalmazva *in vivo* csökkentik a koleszterinszintet. Ezek között szerepelt az atorvasztatin, ezetimib, niacin, a kálcium-csatorna blokkoló nifedipin és a verapamil.

Vizsgálatunk célja az volt, hogy kiderítsük, hogy esetleg ezek a szerek részben vagy teljesen az ABCA1 expressziójának módosítása révén fejtik-e ki hatásukat. Emellett tanulmányoztunk olyan anyagokat is, amelyekről más kísérleti rendszerekben kimutatták, hogy befolyásolják az ABCA1 fehérje plazmamembrán szintjét és működését. Ilyenek pl. a ciklosporin A (CsA), amelyről azt írták le, hogy „becsapdázza" a fehérjét a sejt felszínen [115], vagy a gliburid, amely több ABC fehérjével együtt képes gátolni az ABCA1 működést [116, 117]. Az ABCG2 koleszterin-függő működését látva (ld. 4.2.2. fejezet), megvizsgáltuk a koleszterin-depléciónak, illetve a membrán koleszterinnel való töltésének az ABCA1 sejtfelszíni megjelenésére gyakorolt hatását is.

Mivel a legtöbb vizsgált anyag érdemben nem befolyásolta az ABCA1 variánsok sejtfelszíni expresszióját, ezek részletes ismertetésére a jelen disszertációban nem térek ki (ld. 10. közlemény 1. táblázat). Két vegyületet azonban érdemes itt is megemlíteni. Azt tapasztaltuk, hogy a CsA mind a vad típusú, mind a mutáns HA-ABCA1 expressziós szintjét megemeli a plazmamembránban (30. ábra), ami egyrészt összhangban áll korábbi irodalmi adatokkal, másrészt újdonságként megmutatja, hogy ez az effektus nem a fehérje funkciójához kapcsolódik. A másik új és meglepő eredmény, hogy az ezetimib, a koleszterin bélből való felszívódását gátló gyógyszer, csökkentette a vad típusú HA-ABCA1 sejtfelszíni expresszióját, de nem befolyásolta a mutáns variáns plazmamembrán szintjét. Jelen vizsgálataink ugyan nem adnak magyarázatot az ABCA1 és az ezetimib kölcsönhatásának mechanizmusára, de felhívják a figyelmet arra, hogy ennek a farmakonnak az eredeti támadáspontján kívül más hatása is tapasztalható. Ráadásul a két effektus, a koleszterin-felszívódás gátlása és az ABCA1 szintjének csökkentése, a szervezet szintjén ellentétes hatást eredményez. Ezért ez a megfigyelésünk – és hasonló jövőbeli vizsgálatok eredménye - felhasználható lehet a tudatos gyógyszermolekula tervezéseknél.

Összefoglalva, a jelen bemutatott munkánk során sikerült létrehozni egy olyan kísérleti rendszert, amely segítségével érzékenyen, megbízhatóan és reprodukálható módon lehet vizsgálni az ABCA1 funkcionális jelenlétét a plazmamembránban. Vizsgálataink az ezetimib példáján keresztül arra is rávilágítottak, hogy bizonyos gyógyszermolekulák – esetleg az eredeti támadásponttól függetlenül – befolyásolhatják az ABCA1 sejtfelszíni megjelenését, és ezzel a koleszterinháztartásban betöltött szerepét.

4.4. Az ABC transzporterek védőhálója a szervezetben

[11-13. sz. közlemények]

Az élő szervezet egy olyan dinamikusan működő rendszer, aminek egyik legalapvetőbb funkciója integritásának biztosítása egy folyamatosan változó környezetben. A különböző mechanikai, kémiai és biológiai behatások állandó kihívást jelentenek az élő számára. A „hasznos" és „káros" anyagok, vagy másképpen a „saját" és idegen" alkotók megkülönböztetése és megfelelő kezelése a legfontosabb biológiai funkciók közé tartozik. A sejt szintjén ezt az integritást és a szelektív anyag-, energia- és információ-áramlást a sejtmembrán biztosítja a kettős lipidréteggel és a benne található membránfehérjékkel (transzporterekkel, receptorokkal, membrán-kötött enzimekkel, stb.). A szervezet szintjén a különböző védelmi vonalak (fiziológiai barrierek), a kiválasztó és detoxifikáló szervek és az immunrendszer látják el ezt az rendkívüli mértékben összetett feladatot. Különös kihívást jelent a szervezet számára a hidrofób karakterű anyagok kezelése, hiszen ezek szabadon átjutnak a lipid-alapú biológiai membránokon. Az MDR-ABC transzporterek ez utóbbi védekezésben kitüntetett szereppel bírnak mind a sejt, mind a szervezet szintjén.

A multidrog transzporterek a toxin metabolizmusban résztvevő enzimekkel és egyéb transzporterekkel együtt egy olyan összefüggő, koordinált működésű hálózatot alkotnak a szervezetben, amelynek feladata a különböző toxikus hatású anyagok: endo- és xenobiotikumok hatásának semlegesítése és azok eltávolítása a szervezetből. Mivel ez a védőhálózat számos tekintetben hasonlít a klasszikus immunrendszerre, egy nemrégiben megjelent átfogó közleményben javasoltuk a „kemoimmunitási hálózat" kifejezés bevezetését [11. sz. közlemény]. A következőkben azt fejtem ki, hogy mik a legfőbb jellemzői ennek a védőhálónak és milyen vonatkozásban állítható párhuzamba az immunrendszerrel.

Az endo- és xenobiotikumok elleni védekezésben mindhárom fő multidrog transzporter (MDR1, MRP1 és ABCG2) részt vesz, kiegészülve még az ABCC alcsalád számos tagjával (pl. MRP2/ABCC2, MRP4/ABCC4), illetve néhány további ABC transzporterrel (pl. ABCB4, ABCG5/ABCG8). Ezeknek a transzportereknek a legjellemzőbb tulajdonsága a promiszkuitás, vagyis hogy – szemben a klasszikus membrán transzporterekkel - ezek a fehérjék rendkívül széles szubsztrát-felismerő képességgel rendelkeznek. A sokféle szubsztrát molekula között nagyon sok hidrofób karakterű vegyületet találunk, de számos példa van amfipatikus vagy éppen töltéssel rendelkező szubsztrátmolekulákra is. Részben átfedő szubsztrát felismerésük és specifikus elhelyezkedésük a különböző védelmi vonalakban biztosítja a szervezet számára a széleskörű és hatékonyan működő védelmet.

Az MDR-ABC fehérjék szöveti eloszlását tekintve szembeötlő, hogy ezek a transzporterek magas expressziót mutatnak az említett védelmi vonalakban. A védekezés első helyszíne a bélhám, de legalább ilyen fontos a máj és a vese, ahol a toxikus anyagok kiválasztása zajlik. Mindezekben a szervekben, szövetekben az MDR-ABC transzporterek nemcsak jelen vannak, hanem jelentős mértékben hozzájárulnak az adott szerv/szövet élettani funkcióihoz [16, 78, 118, 119]. Hasonlóan magas expressziót és specifikus elhelyezkedést látunk az olyan fiziológiás barrierekben, amelyek különleges és érzékeny tereket választanak el a szervezetben. Ilyen határolók például a vér-agy gát, a vér-here gát vagy a placenta [78, 119-127]. Ezeken a határfelületeken a multidrog transzporterek a szorosan záró sejttípusokban expresszálódnak: az agyi kapillárisokban pl. az endotél, míg a choroid plexusban az epitél sejtekben, ráadásul úgy helyezkednek el ezekben a polarizált sejtekben, hogy a transzportjuk a védett térrész felől a kevésbé érzékeny szövet felé irányul (31. ábra). Sokszor megtaláljuk az MDR-ABC transzportereket olyan sejttípusokban is, amelyek különös védelmet igénylenek, így pl. az ABCG2 magas szinten expresszálódik az őssejtekben [79], az MRP1 a bélhám kriptasejtjeiben [16], vagy az MDR1 és MRP1 a here Leydig sejtjeiben [127].

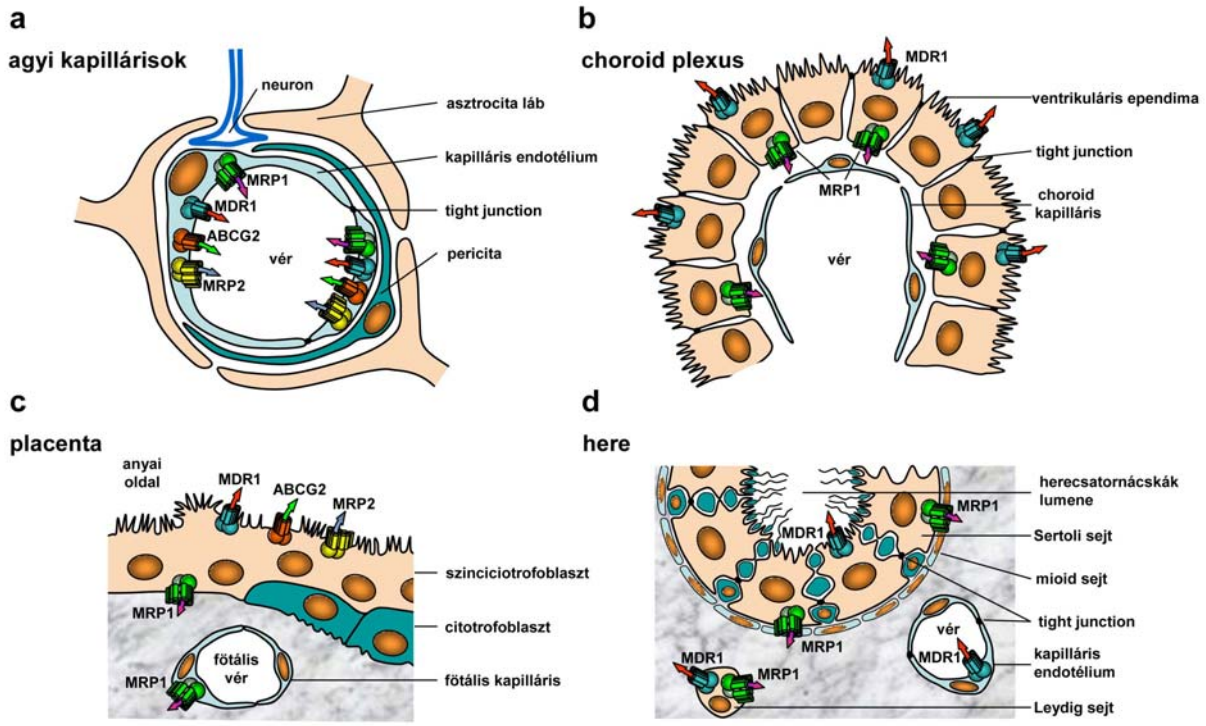

31. ábra: Multidrog transzporterek expressziója és elhelyezkedése néhány fiziológiai barrierben. a) Az agyi kapillárisokban az MDR1, MRP1, MRP2 és ABCG2 ipszilaterálisan helyezkedik el az endotél sejtek apikális oldalán. **(b-d)** A choroid plexus epitél sejtjeiben, a placenta szinciciotrofoblasztjaiban és a here Sertoli sejtjeiben az MDR1 apikálisan, míg az MRP1 bazolaterálisan lokalizálódik. Az ABCG2 és MRP2 a szinciciotrofoblasztokban szintén apikálisan helyezkedik el. A fötális kapillárisokban MRP1, míg a here kapillárisában MDR1 expresszálódik. [13. sz. közlemény]

A klasszikus immunrendszer elsődleges feladata az idegen anyagok: vízoldékony toxinok, mikroorganizmusok, és más nem kívánatos biológiai komponensek (pl. tumorsejtek) felismerése és eliminálása. Ennek a védekező mechanizmusnak az egyik kulcsfontosságú kezdeti lépése a hihetetlen nagyszámú ágens közül az „idegen" és a „saját" megkülönböztetése, vagyis az immunfelismerés. Az MDR-ABC transzporterek hasonló feladatot látnak el a kemoimmunitási hálózatban, hiszen transzportaktivitásuk és promiszkuitásuk révén szintén rendkívül nagyszámú vegyület közül válogatják szét a „hasznos" és „káros" anyagokat, és elősegítik a károsnak ítélt komponensek eltávolítását. Jellegzetes példaként lehet említeni az ABCG5/ABCG8 szerepét a bélhámban, – bár klasszikus értelemben ezt a transzporterpárt nem soroljuk a multidrog fehérjék közé. Az enterociták kefeszegély membránjában zajlik a szterolok felvétele – széles körben elfogadott nézet szerint - a Niemann-Pick C1 like 1 fehérje transzportaktivitása révén. Az ABCG5/ABCG8 heterodimer pedig ugyanitt elhelyezkedve szelektíven visszapumpálja a növényi eredetű szitoszterolokat a bél lumenébe, elvégezve a „hasznos" és „káros" anyagok leválogatását. Hasonlóan több más MDR-ABC transzporter (MDR1, MRP2, ABCG2) szintén alapvető befolyással van a különböző anyagok bélben történő szelektív felszívódására. Mivel a hasznos anyagok felvételre kerülnek és beépülnek a szervezetbe, a káros anyagok pedig kikerülnek a szervezetből, a szelektív transzport-folyamat teljes joggal tekinthető egyfajta „saját-idegen" megkülönböztetésnek.

A vesében és a májban az ABC transzporterek leválogató és elimináló szerepe kismértékben eltér az előbbiekben leírtaktól, mivel ez esetben az ABC fehérjék egy összetett detoxifikáló gépezet részeként töltik be funkciójukat. A tankönyvek a toxin metabolizmusban általában két fázist különböztetnek meg: a toxikus anyagok citokróm p-450 (CYP) enzimekkel történő oxidálását (1. fázis), valamint az oxidált toxinok konjugálását glutationnal, glukoroniddal vagy egyéb kisebb hidrofil molekulával (2. fázis). A detoxifikálás folyamata azonban kiegészíthető, illetve kiegészítendő két további lépéssel (32. ábra).

A toxin metabolizmus 0. fázisának lehet tekinteni azt a lépést, amikor a sejt szintjén döntés születik arról, hogy az anyag egyáltalán bejut-e a sejtbe vagy sem. Ebben a fázisban kulcsfontosságú szerepe van a multidrog transzportereknek – különösképpen hidrofób karakterű anyagok esetében. A 4.3.4. fejezetben ismertettem az MDR-ABC transzporterek működési mechanizmusára vonatkozó modelleket. Kísérleti eredményeink megerősítették azt az elképzelést, hogy a multidrog transzporterek a hidrofób karakterű szubsztrátokat közvetlenül a lipid fázisból pumpálják ki a sejtből [7. közlemény]. Tehát az MDR-ABC transzporterek képesek eleve megakadályozni bizonyos anyagok bejutását a sejtbe. A másik oldalon ehhez a folyamathoz hozzájárulnak az ún. „uptake transzporterek" vagy multi-

specifikus solute carrier-ek (SLC-k, pl. OATP-k), melyek számos olyan anyag celluláris felvételét segítik elő, amelyek további sorsát a toxin-metabolizáló rendszer határozza meg.

A detoxifikálás teljes folyamatát tekintve, a toxikus anyag oxidálását és konjugálását követően történik egy további fontos lépés: a konjugátumok eltávolítása a sejtekből (3. fázis). Ebben a lépésben is kulcsszerepet játszanak az MDR-ABC transzporterek. Elsősorban az ABCC alcsaládhoz tartozó MRP fehérjék felelősek a különféle konjugátumok sejtekből történő, ATP-függő kipumpálásáért, de hasonló szerephez jut az ABCG2 multidrog transzporter is. Különösképpen az MRP-típusú ABC transzporterek idomultak ehhez a speciális feladathoz. Bár a transzport kapacitásuk viszonylag kicsi – pl. az MDR1-hez mérve -, de a különböző membrán kompartmentekben való specifikus elhelyezkedésük, összehangolt működésük és a metabolikus kondíciók által szigorúan szabályozott aktivitásuk által gyorsan és hatékonyan képesek a konjugátumokat eltávolítani a sejtből. A konjugált endo- és xenobiotikumok ezáltal a transzportlépéssel kikerülnek a megfelelő extracelluláris térrészbe (az epekanalikulusokba, a vesetubulusokba), és végeredményben az epével, illetve a vizelettel ürülnek a szervezetből.

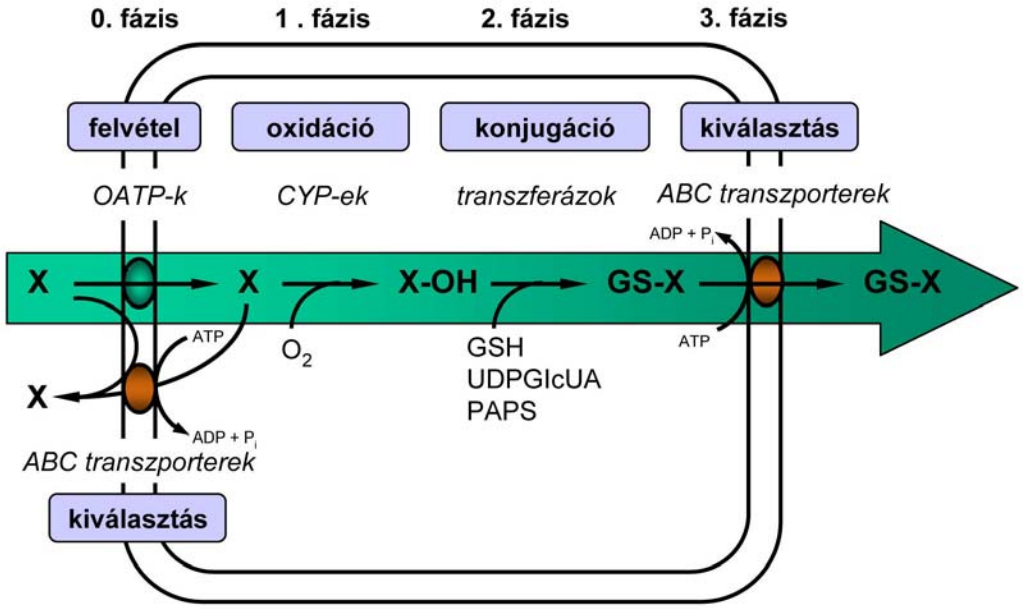

32. ábra: A multidrog-ABC transzporterek szerepe a detoxifikálás különböző fázisaiban. A toxin metabolizmus 0. fázisának tekinthető a toxikus anyag felvélte vagy ennek megakadályozása, mely utóbbiban az MDR-ABC transzporterek kulcsszerepet játszanak. A felvételt követően a toxint oxidálják (1. fázis), majd konjugálják (2. fázis) a megfelelő enzimek (citokrómok, transzferázok). A folyamat végén történik a konjugátumok sejtből történő, ATP-függő eltávolítása (3. fázis), melyet szintén MDR-ABC transzporterek végeznek. Jelölések: X: toxikus anyag, X-OH: oxidált toxikus anyag, GS-X: konjugált toxikus anyag, OATP-k: organikus anion transzporterek, CYP-ek: citokrómok, GSH: glutation, UDPGlcUA: uridin 5′-difoszfo-glukoronsav, PAPS : 3′-foszfoadenilszulfát. [12. sz. közlemény]

A klasszikus immunrendszert tekintve szokás megkülönböztetni a természetes és az adaptív immunitást. Az előző egy kevésbé specifikus, akut választ jelent az idegennel szemben, míg az utóbbi egy specifikus, hatékony és hosszú távú reakciót takar. Hasonló kettősség megfigyelhető a kemoimmunitási rendszerben is. A multidrog transzporterek – a természetes immunitás szereplőihez hasonlóan - képesek fellépni igen nagyszámú, olyan ágenssel szemben, amelyekkel a szervezet korábban nem találkozott. A gyógyszer fejlesztések állandó kihívása, hogy ezek a transzportrendszerek és a metabolikus utak hogyan reagálnak egy-egy új hatóanyag-molekulára. Az igen széles spektrumú, mégis szelektív, és azonnali reakciónak alapvető feltétele a korábban már említett promiszkuitás, amely a kemo-immunitási rendszer több szereplőjére is jellemző. A CYP fehérjéket tekintve szembeötlő, hogy az igen kiterjedt enzimcsalád nagyszámú tagja mind valamelyest eltérő feladattal és némileg különböző szubsztrát-specifitással rendelkezik [128, 129]. Emellett fontos jellemzőjük, hogy a CYP fehérjék egyenként is viszonylag kis specifitású enzimek, számos molekulát képesek szubsztrátként kezelni. Amennyire a mai ismereteink érteni engedik a konjugáló rendszer működését, a transzferázok a CYP enzimek által megjelölt molekulákat képesek módosítani, és szintén széles szubsztrát-felismerő képességgel rendelkeznek [130].

Ez utóbbi tulajdonság – ahogy már arról korábban szó volt - a multidrog transzporterekre is jellemző. Érdekesség azonban velük kapcsolatban, hogy esetükben viszonylag kevés számú fehérje látja el ezt a feladatot. Az MDR1, az MRP1 és az ABCG2 multidrog transzportereket tekintve, az emberi genom csak egy-egy gént tartalmaz. Sőt különböző izoformáik sem ismeretesek, amelyek alternatív splicing vagy más mechanizmus révén jönnének létre. Emiatt az egyes multidrog transzporterekkel szemben követelmény, hogy képesek legyenek akár több ezer molekulát szubsztrátként kezelni. Gyakran ezt a feladatot úgy biztosítják az MDR-ABC fehérjék, hogy többféle mechanizmussal képesek a transzportált szubsztrátmolekulát a külső térbe juttatni. Legjellemzőbb példaként lehet említeni az MRP1 transzportert [13. sz. közlemény], amely elsődlegesen glutation-, glukoronid- és szulfát-konjugátumokat szállít, de ismeretesek hidrofób, nem konjugált transzportált szubsztrátjai is, melyek kipumpálása - szemben az MDR1 fehérje hidrofób szubsztrátjainak transzportjával - glutation-függő [131-133]. Ráadásul sokszor kereszt-stimulációt mutat a drog a GSH-transzporttal (pl. vinkrisztin) [134]. Régebben ennek hátterében a GSH-val történő ko-transzportot sejtettek, a mai álláspont szerint kölcsönös heterotropikus kooperativitással magyarázható a jelenség [135]. Olyanra is találunk példát, amikor kereszt-stimuláció nélkül a GSH fokozza az MRP1 által mediált drog-transzportot (pl. daunorubicin) [132], vagy a drog stimulálja a GSH transzportot (pl. verapamil, bioflavonoidok) [136, 137].

Bár a multidrog transzporterek által nyújtott védelem jellegében leginkább a természetes immunitásra emlékeztet, de sok tekintetben adaptív jegyeket is felfedezhetünk az MDR-ABC transzporterekre épülő kemoimmunitási rendszerben. Számos adat bizonyítja, hogy multidrog transzporterek expressziója fokozódik a tumorokban a citotoxikus szerek hatására. Hasonló jelenség nemcsak patológiás esetekben, hanem fiziológiás körülmények között is bekövetkezhet. Számos transzkripciós és poszt-transzlációs szabályozó mechanizmus képes az MDR-ABC transzporterek expresszióját és aktivitását befolyásolni. Legfontosabb ezek közül megemlíteni a különböző stressz-faktorokat, mint a szteroid hormonok, a hősokk vagy a hipoxia [81, 138]. Leginkább azt feltételezik, hogy ennek a hátterében PXR (pregnán X receptor) és CAR (konstitutív androsztán receptor) szabályozás áll [139], így egy összehangolt, általános válasz részeként emelkedik meg az MDR-ABC transzporterek expressziója, számos más toxin-metabolizmushoz tartozó enzim, transzporter (pl. CYP-ek, SLC-k) szintjével együtt. Érdekes példaként lehet említeni, hogy az orbáncfű tartós alkalmazása megemeli mind az MDR1, mind a CYP3 expresszióját [140], alapvetően befolyásolva más anyagok, gyógyszerek felszívódását és metabolizmusát. Hasonlóan példázza az MDR-ABC fehérjék stresszre adott válaszkészségét az a megfigyelés, hogy az MDR1 expressziós szintje mérhetően megemelkedik limbikus görcsroham után [141].

Fontos megemlíteni, hogy az általános stresszválaszon kívül vagy éppen ahhoz kapcsolódóan, számos hormon is befolyásolja az MDR-ABC transzporterek expressziós szintjét. Ezek között találunk olyanokat, amelyek fokozzák (pl. tiroid hormonok, tesztoszteron, glutamát), illetve olyanokat, melyek csökkentik az expressziót (endotelin, ösztradiol, szerotonin) [94, 142-145]. A hormonokhoz hasonlóan az immunmediátorok között is vannak MDR-ABC transzporter szintet növelő anyagok (pl. IFγ, IL-6), illetve az expressziót csökkentő mediátorok (TGF-β, IL-1β, TNF-α) [146-149]. Érdekes további kapcsolódást jelent a klasszikus immunrendszer és az MDR-ABC fehérjék között az, hogy az MRP1 transzporter fontos szerepet tölt be a leukotrién-mediált gyulladásos válaszokban azáltal, hogy több gyulladásos citokint (LTC_4, LTD_4, LTE_4) képes szubsztrátként kezelni és kipumpálni a sejtekből. Knockout egereken végzett kísérletekkel bizonyították, hogy a különböző leukotrién-produkáló sejtekben (hízósejtekben, makrofágokban, dendritikus sejtekben) az MRP1 ténylegesen részt vesz a celluláris LTC_4 kiáramlásban [150, 151].

Érdekes módon az MDR-ABC fehérjék egy nem ismert szabályozó mechanizmus révén egymás expresszióját is képesek befolyásolni. Például a Dubin-Johnson betegségben, aminek molekuláris alapja az MRP2 diszfunkciója, illetve a betegség állatmodelljében (EHBR) megfigyelték az MRP3 expressziójának növekedését [152, 153], amely kompenzálja az

elégtelen kanalikuláris konjugátum-transzportot. Hasonlóképpen leírták az MDR1 expresszió növekedését az Abcg2-deficiens egerekben, különösképpen a vér-agy gátat tekintve [154].

Az MDR-ABC transzporterek, toxin-metabolizáló enzimek és uptake transzporterek fent leírt, koordinált és specifikus szabályozása egy olyan a környezeti behatásokra adott válasz, amely hosszabb távon hat és az adott körülményekhez igazítja a kemoimmunitási hálózat szereplőit, elősegítve ezzel a rendszer hatékonyabb működését. Ilyen tekintetben ez a fajta szabályozó mechanizmus az adaptív immunrendszer kézenfekvő analógiája.

A klasszikus immunrendszer és a kemoimmunitási hálózat párhuzamba állításakor érdemes szót ejteni arról, hogy túlműködéssel nemcsak az előbbi esetében találkozhatunk, hanem egyfajta hiperszenzitivitás a kemoimmunitási rendszerben is megfigyelhető. Számos tanulmány beszámol a „kollaterális szenzitivitás" jelenségről, vagyis, hogy az MDR-ABC transzporterek megnövekedett expressziója bizonyos drogokkal szembeni érzékenységet okoz. Példaként lehet említeni a gemcitabint, a citozin-arabinozidot, az arzenitet vagy az NSC73306 jelű vegyületet az MDR1 vonatkozásában [155-158], illetve a verapamilt és annak NMeOHI2 nevű derivátumát, a melfalánt, az apigenint, valamint a butionine-szulfoximint az MRP1 esetében [159-162]. Bár a jelenség mögött meghúzódó mechanizmusra még nem született magyarázat, legalább az MRP1 vonatkozásában létezik egy hipotézis. Ennek értelmében az MRP1 fehérjét magas szinten expresszáló sejtekben csökkent a glutation-szint, ami azzal a következménnyel jár, hogy a sejt érzékennyé válik azokra a drogokra, amelyek a GSH koncentráció további csökkenését okozzák. Elképzelhető, hogy a 4.4.2. fejezetben leírt jelenség, az ABCG1 által okozott apoptózis mögött is hasonló mechanizmus, azaz valamiféle endogén vegyülethez kapcsolódó kollaterális szenzitivitás húzódik meg [9. sz. közlemény].

A fentieket összefoglalva elmondható, hogy a kemoimmunitási hálózat számos tekintetben hasonlít a klasszikus immunrendszerre. Mindkét rendszer egy sok szereplőből felépülő, koordinált működésű, összefüggő hálózat, amelynek feladata a káros ágensek felismerése és eliminálása a szervezetből. Mindkettő kiindulópontja pontja az „idegen" felismerése és a „sajáttól" való megkülönböztetése. A kemoimmunitási rendszer is képes egy nagyon széleskörű, kevéssé specifikus akut válaszra, ami a természetes immunitásra jellemző. Ugyanakkor a körülmények hatására gyakran megtörténik a rendszer áthangolása, amely hosszabb távú hatással bír és hatékonyabb működést tesz lehetővé. Ez a sajátosság jellemzi az adaptív immunrendszert is. Ezen felül mindkét rendszer esetében találkozhatunk túlműködéssel, azaz a rendszer hiperszenzitivitásával. A szervezet védekezését tehát - a klasszikus immunrendszer vízoldékony világát kiegészítve - a kemoimmunitási rendszer teszi teljessé, biztosítva a hidrofób és amfipatikus toxikus anyagokkal szembeni védelmet.

5. Az új eredmények összefoglalása

A disszertációban bemutatott munkákban néhány kiválasztott ABC transzporter jellemzésével foglalkoztam. Ezek között szerepeltek olyanok, amelyek a tumorok multidrog-rezisztenciájáért tehetők felelőssé (MDR1, MRP1 és ABCG2), illetve olyanok, amelyek esetlegesen a lipidanyagcserében játszanak szerepet (ABCG1, ABCG4 és ABCA1). Alapvető célunk volt ezen fehérjék működésének megértése, ezért a vizsgálatok nagy részében vagy kidolgoztunk olyan módszert, vagy céljainknak megfelelően módosítottunk meglévő olyan mérési technikát, amellyel specifikusan és megfelelő érzékenységgel tudjuk az adott ABC transzporter aktivitását követni. Ezekkel a funkcionális mérésekkel erőfeszítéseket tettünk a felsorolt ABC fehérjék transzporttulajdonságainak, működési mechanizmusának és alapvető funkciójának megismerésére. Konkrétan a következő eredményeket sikerült vizsgálataink során elérni:

1.) Megmutattuk, hogy az MRP1 transzporter képes a calcein acetoxi-metilésztert kipumpálni a sejtekből, így a **calcein assay segítségével nemcsak az MDR1, hanem az MRP1 is vizsgálható**. Kifejlesztettünk egy olyan módszert, amely alkalmas a két multidrog transzporter egymás melletti funkcionális detektálására. A kiterjesztett calcein assay segítségével kimutattuk, hogy **bizonyos drogokat az MRP1 glutation-konjugátumként pumpál ki a sejtekből**, míg vannak olyanok, melyek transzportja a **glutationtól független**.

2.) Sikeresen alkalmaztuk a calcein módszert tumoros betegekből származó klinikai mintákon. Megmutattuk, hogy akut mieloid leukémiában a kemoterápiára adott válasz tekintetében **a calcein assay-vel meghatározott MDR fenotípus prognosztikai jelentőségű faktor**.

3.) Egyértelműen megmutattuk, hogy az ABCG2 multidrog transzportert expresszáló sejtekben tapasztalható **Iressa-val szembeni rezisztencia az ABCG2 transzport-aktivitásának a következménye.** Kimutattuk továbbá, hogy **a membrán koleszterin-tartalma** jelentős mértékben, szelektíven és reverzibilisen **modulálja az ABCG2 transzportaktivitását**.

4.) **Az ABCG2 multidrog transzportert GFP-címkével láttuk** el oly módon, hogy a fehérje funkciója és legfőbb jellemvonásai teljes mértékben megőrződtek. A GFP-címkézett variánsok felhasználásával kimutattuk, hogy az ABCG2 az egyik legfontosabb drog-szubsztrátját, a mitoxantront nem a klasszikus mechanizmus révén transzportálja, hanem **közvetlenül a membránból pumpálja ki a sejtekből**.

5.) Heterológ expressziós rendszerben sikeresen **kifejeztettük az ABCG1 és ABCG4 fehérjéket**, és mindkettő ellen **létrehoztunk megfelelően érzékeny, specifikus monoklonális ellenanyagot**. Megmutattuk, hogy mindkét fehérje **rendelkezik ATPáz aktivitással**, és **az ABCG1 esetében azonosítottunk 2 szubsztrátot** (rodamin123 és a rodamin6G) **és 3 gátlószert** (benzamil, ciklosporin A, L-tiroxin). Eredményeink arra is rávilágítottak, hogy ezek a féltranszporterek **mind homo-, mind heterodimerként képesek működni**.

6.) Az **ABCG1** szerepének vizsgálata során kimutattuk, hogy ez a fehérje **apoptózist indukál makrofágokban** és egyéb sejttípusokban, amely jelenség egyértelműen a fehérje aktivitásának a következménye. Mivel a makrofágok apoptózisa rendkívül fontos az ateroszklerotikus léziók fejlődésében, megfigyeléseink lényeges, új szerepkörbe helyezik az ABCG1 fehérjét.

7.) Az ABCA1 transzporterrel végzett munkánk eredményeképpen létrehoztunk egy olyan kísérleti eszközt, amely alkalmas **az ABCA1 sejtfelszíni expressziójának érzékeny és megbízható detektálására**. Ennek az assay-rendszernek a segítségével kimutattuk, hogy **az ezetimib** nevű gyógyszer **az ABCA1 sejtfelszíni megjelenését funkció-függő módon befolyásolja**.

8.) Végül megmutattuk, hogy **a multidrog transzporterek** a toxin metabolizmusban résztvevő enzimekkel és egyéb transzporterekkel együtt egy olyan **összefüggő, koordinált működésű hálózatot alkotnak a szervezetben**, amelynek feladata a különböző toxikus hatású anyagok: endo- és xenobiotikumok hatásának semlegesítése és azok eltávolítása a szervezetből.

6. Saját közlemények jegyzéke

6.1. Az értekezés alapjául szolgáló közlemények jegyzéke

1. Hollo, Z., Homolya, L., Hegedus, T., and Sarkadi, B.: Transport properties of the multidrug resistance-associated protein (MRP) in human tumour cells. *FEBS Lett*, 1996. **383**(1-2): 99-104.

2. Hollo, Z., Homolya, L., Hegedus, T., Muller, M., Szakacs, G., Jakab, K., Antal, F., and Sarkadi, B.: Parallel functional and immunological detection of human multidrug resistance proteins, P-glycoprotein and MRP1. *Anticancer Res*, 1998. **18**(4C): 2981-7.

3. Karaszi, E., Jakab, K., Homolya, L., Szakacs, G., Hollo, Z., Telek, B., Kiss, A., Rejto, L., Nahajevszky, S., Sarkadi, B., and Kappelmayer, J.: Calcein assay for multidrug resistance reliably predicts therapy response and survival rate in acute myeloid leukaemia. *Br J Haematol*, 2001. **112**(2): 308-14.

4. Elkind, N.B., Szentpetery, Z., Apati, A., Ozvegy-Laczka, C., Varady, G., Ujhelly, O., Szabo, K., Homolya, L., Varadi, A., Buday, L., Keri, G., Nemet, K., and Sarkadi, B.: Multidrug transporter ABCG2 prevents tumor cell death induced by the epidermal growth factor receptor inhibitor Iressa (ZD1839, Gefitinib). *Cancer Res*, 2005. **65**(5): 1770-7.

5. Telbisz, A., Muller, M., Ozvegy-Laczka, C., Homolya, L., Szente, L., Varadi, A., and Sarkadi, B.: Membrane cholesterol selectively modulates the activity of the human ABCG2 multidrug transporter. *Biochim Biophys Acta*, 2007. **1768**(11): 2698-713.

6. Orban, T.I., Seres, L., Ozvegy-Laczka, C., Elkind, N.B., Sarkadi, B., and Homolya, L.: Combined localization and real-time functional studies using a GFP-tagged ABCG2 multidrug transporter. *Biochem Biophys Res Commun*, 2008. **367**(3): 667-73.

7. Homolya, L., Orban, T.I., Csanady, L., and Sarkadi, B.: Mitoxantrone expelled by the ABCG2 multidrug transporter directly from the plasma membrane. *Biochim Biophys Acta*, 2010. in press.

8. Cserepes, J., Szentpetery, Z., Seres, L., Ozvegy-Laczka, C., Langmann, T., Schmitz, G., Glavinas, H., Klein, I., Homolya, L., Varadi, A., Sarkadi, B., and Elkind, N.B.: Functional expression and characterization of the human ABCG1 and ABCG4 proteins: indications for heterodimerization. *Biochem Biophys Res Commun*, 2004. **320**(3): 860-7.

9. Seres, L., Cserepes, J., Elkind, N.B., Torocsik, D., Nagy, L., Sarkadi, B., and Homolya, L.: Functional ABCG1 expression induces apoptosis in macrophages and other cell types. *Biochim Biophys Acta*, 2008. **1778**(10): 2378-87.

10. Kasza, I., Hegyi, Z., Szabo, K., Andrikovics, H., Nemet, K., Varadi, A., Sarkadi, B., and Homolya, L.: Model system for the analysis of cell surface expression of human ABCA1. *BMC Cell Biol*, 2009. **10**: 93.

11. Sarkadi, B., Homolya, L., Szakacs, G., and Varadi, A.: Human multidrug resistance ABCB and ABCG transporters: participation in a chemoimmunity defense system. *Physiol Rev*, 2006. **86**(4): 1179-236.

12. Homolya, L., Varadi, A., and Sarkadi, B.: Multidrug resistance-associated proteins: Export pumps for conjugates with glutathione, glucuronate or sulfate. *Biofactors*, 2003. **17**(1-4): 103-14.

13. Bakos, E., and Homolya, L.: Portrait of multifaceted transporter, the multidrug resistance-associated protein 1 (MRP1/ABCC1). *Pflugers Arch*, 2007. **453**(5): 621-41.

6.2. Egyéb saját közlemények jegyzéke

1. Sarkadi, B., Tordai, A., Homolya, L., Scharff, O., and Gardos, G.: Calcium influx and intracellular calcium release in anti-CD3 antibody-stimulated and thapsigargin-treated human T lymphoblasts. *J Membr Biol*, 1991. **123**(1): 9-21.
2. Homolya, L., Hollo, Z., Germann, U.A., Pastan, I., Gottesman, M.M., and Sarkadi, B.: Fluorescent cellular indicators are extruded by the multidrug resistance protein. *J Biol Chem*, 1993. **268**(29): 21493-6.
3. Hollo, Z., Homolya, L., Davis, C.W., and Sarkadi, B.: Calcein accumulation as a fluorometric functional assay of the multidrug transporter. *Biochim Biophys Acta*, 1994. **1191**(2): 384-8.
4. Sarkadi, B., Muller, M., Homolya, L., Hollo, Z., Seprodi, J., Germann, U.A., Gottesman, M.M., Price, E.M., and Boucher, R.C.: Interaction of bioactive hydrophobic peptides with the human multidrug transporter. *Faseb J*, 1994. **8**(10): 766-70.
5. Homolya, L., Hollo, M., Muller, M., Mechetner, E.B., and Sarkadi, B.: A new method for a quantitative assessment of P-glycoprotein-related multidrug resistance in tumour cells. *Br J Cancer*, 1996. **73**(7): 849-55.
6. Lazarowski, E.R., Homolya, L., Boucher, R.C., and Harden, T.K.: Direct demonstration of mechanically induced release of cellular UTP and its implication for uridine nucleotide receptor activation. *J Biol Chem*, 1997. **272**(39): 24348-54.
7. Lazarowski, E.R., Homolya, L., Boucher, R.C., and Harden, T.K.: Identification of an ecto-nucleoside diphosphokinase and its contribution to interconversion of P2 receptor agonists. *J Biol Chem*, 1997. **272**(33): 20402-7.
8. Cressman, V.L., Lazarowski, E., Homolya, L., Boucher, R.C., Koller, B.H., and Grubb, B.R.: Effect of loss of P2Y(2) receptor gene expression on nucleotide regulation of murine epithelial Cl(-) transport. *J Biol Chem*, 1999. **274**(37): 26461-8.
9. Homolya, L., Watt, W.C., Lazarowski, E.R., Koller, B.H., and Boucher, R.C.: Nucleotide-regulated calcium signaling in lung fibroblasts and epithelial cells from normal and P2Y(2) receptor (-/-) mice. *J Biol Chem*, 1999. **274**(37): 26454-60.

10. Homolya, L., Steinberg, T.H., and Boucher, R.C.: Cell to cell communication in response to mechanical stress via bilateral release of ATP and UTP in polarized epithelia. *J Cell Biol*, 2000. **150**(6): 1349-60.

11. Hegedus, T., Sessler, T., Scott, R., Thelin, W., Bakos, E., Varadi, A., Szabo, K., Homolya, L., Milgram, S.L., and Sarkadi, B.: C-terminal phosphorylation of MRP2 modulates its interaction with PDZ proteins. *Biochem Biophys Res Commun*, 2003. **302**(3): 454-61.

12. Sinko, E., Ilias, A., Ujhelly, O., Homolya, L., Scheffer, G.L., Bergen, A.A., Sarkadi, B., and Varadi, A.: Subcellular localization and N-glycosylation of human ABCC6, expressed in MDCKII cells. *Biochem Biophys Res Commun*, 2003. **308**(2): 263-9.

13. Ujhelly, O., Ozvegy, C., Varady, G., Cervenak, J., Homolya, L., Grez, M., Scheffer, G., Roos, D., Bates, S.E., Varadi, A., Sarkadi, B., and Nemet, K.: Application of a human multidrug transporter (ABCG2) variant as selectable marker in gene transfer to progenitor cells. *Hum Gene Ther*, 2003. **14**(4): 403-12.

14. Paszty, K., Antalffy, G., Penheiter, A.R., Homolya, L., Padanyi, R., Ilias, A., Filoteo, A.G., Penniston, J.T., and Enyedi, A.: The caspase-3 cleavage product of the plasma membrane Ca2+-ATPase 4b is activated and appropriately targeted. *Biochem J*, 2005. **391**(Pt 3): 687-92.

15. Apati, A., Orban, T.I., Varga, N., Nemeth, A., Schamberger, A., Krizsik, V., Erdelyi-Belle, B., Homolya, L., Varady, G., Padanyi, R., Karaszi, E., Kemna, E.W., Nemet, K., and Sarkadi, B.: High level functional expression of the ABCG2 multidrug transporter in undifferentiated human embryonic stem cells. *Biochim Biophys Acta*, 2008. **1778**(12): 2700-9.

16. Hegedus, C., Szakacs, G., Homolya, L., Orban, T.I., Telbisz, A., Jani, M., and Sarkadi, B.: Ins and outs of the ABCG2 multidrug transporter: an update on in vitro functional assays. *Adv Drug Deliv Rev*, 2009. **61**(1): 47-56.

17. Hou, Y.X., Li, C.Z., Palaniyandi, K., Magtibay, P.M., Homolya, L., Sarkadi, B., and Chang, X.B.: Effects of putative catalytic base mutation E211Q on ABCG2-mediated methotrexate transport. *Biochemistry*, 2009. **48**(38): 9122-31.

18. Orban, T.I., Apati, A., Nemeth, A., Varga, N., Krizsik, V., Schamberger, A., Szebenyi, K., Erdei, Z., Varady, G., Karaszi, E., Homolya, L., Nemet, K., Gocza, E., Miskey, C., Mates, L., Ivics, Z., Izsvak, Z., and Sarkadi, B.: Applying a "double-feature" promoter to identify cardiomyocytes differentiated from human embryonic stem cells following transposon-based gene delivery. *Stem Cells*, 2009. **27**(5): 1077-87.

19. Torocsik, D., Barath, M., Benko, S., Szeles, L., Dezso, B., Poliska, S., Hegyi, Z., Homolya, L., Szatmari, I., Lanyi, A., and Nagy, L.: Activation of liver X receptor sensitizes human dendritic cells to inflammatory stimuli. *J Immunol*, 2010. **184**(10): 5456-65.

20. Sarkadi, B., Orban, T.I., Szakacs, G., Varady, G., Schamberger, A., Erdei, Z., Szebenyi, K., Homolya, L., and Apati, A.: Evaluation of ABCG2 expression in human embryonic stem cells: crossing the same river twice? *Stem Cells*, 2010. **28**(1): 174-6.

7. Köszönetnyilvánítás

Mindenekelőtt köszönetet mondok mentoromnak, ***Prof. Sarkadi Balázsnak*** a tudományos gondolkodásom formálásáért, a folyamatos támogatásért és az önállóságra való biztatásáért. Meleg hálával emlékezem meg ***Prof. Gárdos Györgyről***, aki lehetővé tette számomra a tudományos pályán való elindulást.

Köszönettel tartozom közvetlen munkatársaimnak, ***dr. Hegedűs Tamásnak, dr. Cserepes Juditnak, dr. Kasza Ildikónak, Seres Lászlónak, Hegyi Zoltánnak, Erdélyi-Belle Boglárkának*** és ***Török Györgynek,*** hogy munkájukkal hozzásegítettek ahhoz, hogy a bemutatott eredmények megszülethessenek. Külön köszönet illeti ***Bézsenyi Gyöngyit***, aki mindig precíz és megbízható munkájával stabil hátteret biztosított a munkánkhoz.

Kiemelten köszönöm ***dr. Enyedi Ágnesnek*** és ***dr. Váradi Andrásnak***, hogy szakmai és emberi támogatásukkal folyamatosan segítettek munkámban. Megköszönöm ***Prof. Richard C. Boucher-nak***, hogy a kutatócsoportjában eltöltött évek alatt szélesíthettem látókörömet. Hálás vagyok szerzőtársaimnak, ***dr. Bakos Évának, dr. N. Barry Elkind-nek, dr. Holló Zsoltnak, dr. Karászi Évának, dr. Orbán Tamásnak, dr. Özvegy-Laczka Csillának, dr. Szabó Katalin-nak, dr. Szakács Gergelynek, dr. Szentpétery Zsófiának, dr. Telbisz Ágnesnek***, hogy együtt dolgozhattunk érdekes és izgalmas problémák megoldásán. Köszönöm ***dr. Német Katalinnak*** és ***dr. Tordai Attilának***, hogy tapasztalataikkal és tanácsaikkal támogatták munkámat, valamint osztályunk és kutatócsoportunk valamennyi munkatársának, hogy egymást segítve, támogató közösségként tudtunk előrehaladni a tudomány útján.

Köszönöm a különböző szponzoráló szervezeteknek, hogy anyagi támogatásukkal lehetővé tették a kutatómunkámat. Nagyra értékelem az Észak-amerikai Cisztikus Fibrózis Alapítvány (CFF), a Howard Hughes Medical Institute (HHMI), az European Molecular Biology Organization (EMBO), az Országos Tudományos Kutatási Alap (OTKA), a Nemzeti Kutatási és Technológia Hivatal (NKTH), Egészségügyi Minisztérium Egészségügyi Tudományos Tanácsa (ETT), a Felsőoktatási Kutatási és Fejlesztési Pályázat (FKFP), a Nemzeti Kutatási és Fejlesztési Program (NKFP) kutatási támogatását, valamint az Alapítvány a Magyar Felsőoktatásért és Kutatásért Magyary Zoltán posztdoktori ösztöndíját és az MTA Bolyai János kutatási ösztöndíját.

Végezetül köszönetet mondok családomnak, ***feleségemnek, Verának, szüleimnek*** és ***gyermekeimnek*** támogató szeretetükért, végtelen türelmükért és azért, hogy mindvégig biztosították számomra a stabil és harmonikus családi hátteret.

8. Irodalomjegyzék

1. Higgins, C.F.: ABC transporters: from microorganisms to man. Annu Rev Cell Biol, 1992. 8: 67-113.
2. Szakács, G., Homolya, L., Sarkadi, B., Váradi, A.: MDR-ABC Transporters. in Encyclopedia of Molecular Pharmacology, R. Offermanns S., W., Editor. 2008, Springer-Verlag: Berlin, Heidelberg, New York. ISBN: 978-3-540-38916-3 p. 749-52.
3. Kunzelmann, K., and Schreiber, R.: CFTR, a regulator of channels. J Membr Biol, 1999. 168(1): 1-8.
4. Aguilar-Bryan, L., Clement, J.P.t., Gonzalez, G., Kunjilwar, K., Babenko, A., and Bryan, J.: Toward understanding the assembly and structure of KATP channels. Physiol Rev, 1998. 78(1): 227-45.
5. Bryan, J., Munoz, A., Zhang, X., Dufer, M., Drews, G., Krippeit-Drews, P., and Aguilar-Bryan, L.: ABCC8 and ABCC9: ABC transporters that regulate K+ channels. Pflugers Arch, 2007. 453(5): 703-18.
6. Van Luyn, M.J., Muller, M., Renes, J., Meijer, C., Scheper, R.J., Nienhuis, E.F., Mulder, N.H., Jansen, P.L., and De Vries, E.G.: Transport of glutathione conjugates into secretory vesicles is mediated by the multidrug-resistance protein 1. Int J Cancer, 1998. 76(1): 55-62.
7. Rajagopal, A., and Simon, S.M.: Subcellular localization and activity of multidrug resistance proteins. Mol Biol Cell, 2003. 14(8): 3389-99.
8. Sarkadi, B., Price, E.M., Boucher, R.C., Germann, U.A., and Scarborough, G.A.: Expression of the human multidrug resistance cDNA in insect cells generates a high activity drug-stimulated membrane ATPase. J Biol Chem, 1992. 267(7): 4854-8.
9. Szabo, K., Welker, E., Bakos, Muller, M., Roninson, I., Varadi, A., and Sarkadi, B.: Drug-stimulated nucleotide trapping in the human multidrug transporter MDR1. Cooperation of the nucleotide binding domains. J Biol Chem, 1998. 273(17): 10132-8.
10. Ozvegy, C., Varadi, A., and Sarkadi, B.: Characterization of drug transport, ATP hydrolysis, and nucleotide trapping by the human ABCG2 multidrug transporter. Modulation of substrate specificity by a point mutation. J Biol Chem, 2002. 277(50): 47980-90.
11. Gottesman, M.M., Fojo, T., and Bates, S.E.: Multidrug resistance in cancer: role of ATP-dependent transporters. Nat Rev Cancer, 2002. 2(1): 48-58.
12. Borst, P., Evers, R., Kool, M., and Wijnholds, J.: A family of drug transporters: the multidrug resistance-associated proteins. J Natl Cancer Inst, 2000. 92(16): 1295-302.
13. Wada, M.: Single nucleotide polymorphisms in ABCC2 and ABCB1 genes and their clinical impact in physiology and drug response. Cancer Lett, 2006. 234(1): 40-50.

14. Yanase, K., Tsukahara, S., Mitsuhashi, J., and Sugimoto, Y.: Functional SNPs of the breast cancer resistance protein-therapeutic effects and inhibitor development. Cancer Lett, 2006. 234(1): 73-80.
15. Flens, M.J., Zaman, G.J., van der Valk, P., Izquierdo, M.A., Schroeijers, A.B., Scheffer, G.L., van der Groep, P., de Haas, M., Meijer, C.J., and Scheper, R.J.: Tissue distribution of the multidrug resistance protein. Am J Pathol, 1996. 148(4): 1237-47.
16. Peng, K.C., Cluzeaud, F., Bens, M., Duong Van Huyen, J.P., Wioland, M.A., Lacave, R., and Vandewalle, A.: Tissue and cell distribution of the multidrug resistance-associated protein (MRP) in mouse intestine and kidney. J Histochem Cytochem, 1999. 47(6): 757-68.
17. Leier, I., Jedlitschky, G., Buchholz, U., Center, M., Cole, S.P., Deeley, R.G., and Keppler, D.: ATP-dependent glutathione disulphide transport mediated by the MRP gene-encoded conjugate export pump. Biochem J, 1996. 314 (Pt 2): 433-7.
18. Leier, I., Jedlitschky, G., Buchholz, U., Cole, S.P., Deeley, R.G., and Keppler, D.: The MRP gene encodes an ATP-dependent export pump for leukotriene C4 and structurally related conjugates. J Biol Chem, 1994. 269(45): 27807-10.
19. Homolya, L., Hollo, Z., Germann, U.A., Pastan, I., Gottesman, M.M., and Sarkadi, B.: Fluorescent cellular indicators are extruded by the multidrug resistance protein. J Biol Chem, 1993. 268(29): 21493-6.
20. Hollo, Z., Homolya, L., Davis, C.W., and Sarkadi, B.: Calcein accumulation as a fluorometric functional assay of the multidrug transporter. Biochim Biophys Acta, 1994. 1191(2): 384-8.
21. Homolya, L., Hollo, M., Muller, M., Mechetner, E.B., and Sarkadi, B.: A new method for a quantitative assessment of P-glycoprotein-related multidrug resistance in tumour cells. Br J Cancer, 1996. 73(7): 849-55.
22. Sarkadi, B., Muller, M., Homolya, L., Hollo, Z., Seprodi, J., Germann, U.A., Gottesman, M.M., Price, E.M., and Boucher, R.C.: Interaction of bioactive hydrophobic peptides with the human multidrug transporter. Faseb J, 1994. 8(10): 766-70.
23. Arrese, M., and Ananthanarayanan, M.: The bile salt export pump: molecular properties, function and regulation. Pflugers Arch, 2004. 449(2): 123-31.
24. Trauner, M., and Boyer, J.L.: Bile salt transporters: molecular characterization, function, and regulation. Physiol Rev, 2003. 83(2): 633-71.
25. Elferink, R.P., Tytgat, G.N., and Groen, A.K.: Hepatic canalicular membrane 1: The role of mdr2 P-glycoprotein in hepatobiliary lipid transport. Faseb J, 1997. 11(1): 19-28.
26. Borst, P., Zelcer, N., and van Helvoort, A.: ABC transporters in lipid transport. Biochim Biophys Acta, 2000. 1486(1): 128-44.
27. Wittenburg, H., and Carey, M.C.: Biliary cholesterol secretion by the twinned sterol half-transporters ABCG5 and ABCG8. J Clin Invest, 2002. 110(5): 605-9.

28. Yu, L., Hammer, R.E., Li-Hawkins, J., Von Bergmann, K., Lutjohann, D., Cohen, J.C., and Hobbs, H.H.: Disruption of Abcg5 and Abcg8 in mice reveals their crucial role in biliary cholesterol secretion. Proc Natl Acad Sci U S A, 2002. 99(25): 16237-42.
29. Yu, L., Li-Hawkins, J., Hammer, R.E., Berge, K.E., Horton, J.D., Cohen, J.C., and Hobbs, H.H.: Overexpression of ABCG5 and ABCG8 promotes biliary cholesterol secretion and reduces fractional absorption of dietary cholesterol. J Clin Invest, 2002. 110(5): 671-80.
30. Klett, E.L., Lu, K., Kosters, A., Vink, E., Lee, M.H., Altenburg, M., Shefer, S., Batta, A.K., Yu, H., Chen, J., Klein, R., Looije, N., Oude-Elferink, R., Groen, A.K., Maeda, N., Salen, G., and Patel, S.B.: A mouse model of sitosterolemia: absence of Abcg8/sterolin-2 results in failure to secrete biliary cholesterol. BMC Med, 2004. 2: 5.
31. Paulusma, C.C., and Oude Elferink, R.P.: The type 4 subfamily of P-type ATPases, putative aminophospholipid translocases with a role in human disease. Biochim Biophys Acta, 2005. 1741(1-2): 11-24.
32. Small, D.M.: Role of ABC transporters in secretion of cholesterol from liver into bile. Proc Natl Acad Sci U S A, 2003. 100(1): 4-6.
33. de Vree, J.M., Jacquemin, E., Sturm, E., Cresteil, D., Bosma, P.J., Aten, J., Deleuze, J.F., Desrochers, M., Burdelski, M., Bernard, O., Oude Elferink, R.P., and Hadchouel, M.: Mutations in the MDR3 gene cause progressive familial intrahepatic cholestasis. Proc Natl Acad Sci U S A, 1998. 95(1): 282-7.
34. Wanders, R.J., Visser, W.F., van Roermund, C.W., Kemp, S., and Waterham, H.R.: The peroxisomal ABC transporter family. Pflugers Arch, 2007. 453(5): 719-34.
35. McGuinness, M.C., Zhang, H.P., and Smith, K.D.: Evaluation of pharmacological induction of fatty acid beta-oxidation in X-linked adrenoleukodystrophy. Mol Genet Metab, 2001. 74(1-2): 256-63.
36. Lee, J.Y., and Parks, J.S.: ATP-binding cassette transporter AI and its role in HDL formation. Curr Opin Lipidol, 2005. 16(1): 19-25.
37. Yokoyama, S.: Assembly of high density lipoprotein by the ABCA1/apolipoprotein pathway. Curr Opin Lipidol, 2005. 16(3): 269-79.
38. Brunham, L.R., Kruit, J.K., Iqbal, J., Fievet, C., Timmins, J.M., Pape, T.D., Coburn, B.A., Bissada, N., Staels, B., Groen, A.K., Hussain, M.M., Parks, J.S., Kuipers, F., and Hayden, M.R.: Intestinal ABCA1 directly contributes to HDL biogenesis in vivo. J Clin Invest, 2006. 116(4): 1052-62.
39. Zarubica, A., Trompier, D., and Chimini, G.: ABCA1, from pathology to membrane function. Pflugers Arch, 2007. 453(5): 569-79.

40. Rust, S., Rosier, M., Funke, H., Real, J., Amoura, Z., Piette, J.C., Deleuze, J.F., Brewer, H.B., Duverger, N., Denefle, P., and Assmann, G.: Tangier disease is caused by mutations in the gene encoding ATP-binding cassette transporter 1. Nat Genet, 1999. 22(4): 352-5.
41. Albrecht, C., McVey, J.H., Elliott, J.I., Sardini, A., Kasza, I., Mumford, A.D., Naoumova, R.P., Tuddenham, E.G., Szabo, K., and Higgins, C.F.: A novel missense mutation in ABCA1 results in altered protein trafficking and reduced phosphatidylserine translocation in a patient with Scott syndrome. Blood, 2005. 106(2): 542-9.
42. Sun, H., Molday, R.S., and Nathans, J.: Retinal stimulates ATP hydrolysis by purified and reconstituted ABCR, the photoreceptor-specific ATP-binding cassette transporter responsible for Stargardt disease. J Biol Chem, 1999. 274(12): 8269-81.
43. Mata, N.L., Weng, J., and Travis, G.H.: Biosynthesis of a major lipofuscin fluorophore in mice and humans with ABCR-mediated retinal and macular degeneration. Proc Natl Acad Sci U S A, 2000. 97(13): 7154-9.
44. Nicholls, S.J., Rye, K.A., and Barter, P.J.: High-density lipoproteins as therapeutic targets. Curr Opin Lipidol, 2005. 16(3): 345-9.
45. Chen, H., Rossier, C., Lalioti, M.D., Lynn, A., Chakravarti, A., Perrin, G., and Antonarakis, S.E.: Cloning of the cDNA for a human homologue of the Drosophila white gene and mapping to chromosome 21q22.3. Am J Hum Genet, 1996. 59(1): 66-75.
46. Hoekstra, M., Kruijt, J.K., Van Eck, M., and Van Berkel, T.J.: Specific gene expression of ATP-binding cassette transporters and nuclear hormone receptors in rat liver parenchymal, endothelial, and Kupffer cells. J Biol Chem, 2003. 278(28): 25448-53.
47. Laffitte, B.A., Repa, J.J., Joseph, S.B., Wilpitz, D.C., Kast, H.R., Mangelsdorf, D.J., and Tontonoz, P.: LXRs control lipid-inducible expression of the apolipoprotein E gene in macrophages and adipocytes. Proc Natl Acad Sci U S A, 2001. 98(2): 507-12.
48. Venkateswaran, A., Repa, J.J., Lobaccaro, J.M., Bronson, A., Mangelsdorf, D.J., and Edwards, P.A.: Human white/murine ABC8 mRNA levels are highly induced in lipid-loaded macrophages. A transcriptional role for specific oxysterols. J Biol Chem, 2000. 275(19): 14700-7.
49. Tangirala, R.K., Bischoff, E.D., Joseph, S.B., Wagner, B.L., Walczak, R., Laffitte, B.A., Daige, C.L., Thomas, D., Heyman, R.A., Mangelsdorf, D.J., Wang, X., Lusis, A.J., Tontonoz, P., and Schulman, I.G.: Identification of macrophage liver X receptors as inhibitors of atherosclerosis. Proc Natl Acad Sci U S A, 2002. 99(18): 11896-901.
50. Li, A.C., Binder, C.J., Gutierrez, A., Brown, K.K., Plotkin, C.R., Pattison, J.W., Valledor, A.F., Davis, R.A., Willson, T.M., Witztum, J.L., Palinski, W., and Glass, C.K.: Differential inhibition of macrophage foam-cell formation and atherosclerosis in mice by PPARalpha, beta/delta, and gamma. J Clin Invest, 2004. 114(11): 1564-76.

51. Torocsik, D., Barath, M., Benko, S., Szeles, L., Dezso, B., Poliska, S., Hegyi, Z., Homolya, L., Szatmari, I., Lanyi, A., and Nagy, L.: Activation of liver X receptor sensitizes human dendritic cells to inflammatory stimuli. J Immunol, 2010. 184(10): 5456-65.
52. Engel, T., Lorkowski, S., Lueken, A., Rust, S., Schluter, B., Berger, G., Cullen, P., and Assmann, G.: The human ABCG4 gene is regulated by oxysterols and retinoids in monocyte-derived macrophages. Biochem Biophys Res Commun, 2001. 288(2): 483-8.
53. Lorkowski, S., Rust, S., Engel, T., Jung, E., Tegelkamp, K., Galinski, E.A., Assmann, G., and Cullen, P.: Genomic sequence and structure of the human ABCG1 (ABC8) gene. Biochem Biophys Res Commun, 2001. 280(1): 121-31.
54. Annilo, T., Tammur, J., Hutchinson, A., Rzhetsky, A., Dean, M., and Allikmets, R.: Human and mouse orthologs of a new ATP-binding cassette gene, ABCG4. Cytogenet Cell Genet, 2001. 94(3-4): 196-201.
55. Nakamura, M., Ueno, S., Sano, A., and Tanabe, H.: Polymorphisms of the human homologue of the Drosophila white gene are associated with mood and panic disorders. Mol Psychiatry, 1999. 4(2): 155-62.
56. Rujescu, D., Giegling, I., Dahmen, N., Szegedi, A., Anghelescu, I., Gietl, A., Schafer, M., Muller-Siecheneder, F., Bondy, B., and Moller, H.J.: Association study of suicidal behavior and affective disorders with a genetic polymorphism in ABCG1, a positional candidate on chromosome 21q22.3. Neuropsychobiology, 2000. 42 Suppl 1: 22-5.
57. Vaughan, A.M., and Oram, J.F.: ABCA1 and ABCG1 or ABCG4 act sequentially to remove cellular cholesterol and generate cholesterol-rich HDL. J Lipid Res, 2006. 47(11): 2433-43.
58. Klucken, J., Buchler, C., Orso, E., Kaminski, W.E., Porsch-Ozcurumez, M., Liebisch, G., Kapinsky, M., Diederich, W., Drobnik, W., Dean, M., Allikmets, R., and Schmitz, G.: ABCG1 (ABC8), the human homolog of the Drosophila white gene, is a regulator of macrophage cholesterol and phospholipid transport. Proc Natl Acad Sci U S A, 2000. 97(2): 817-22.
59. Wang, N., Lan, D., Chen, W., Matsuura, F., and Tall, A.R.: ATP-binding cassette transporters G1 and G4 mediate cellular cholesterol efflux to high-density lipoproteins. Proc Natl Acad Sci U S A, 2004. 101(26): 9774-9.
60. Kennedy, M.A., Barrera, G.C., Nakamura, K., Baldan, A., Tarr, P., Fishbein, M.C., Frank, J., Francone, O.L., and Edwards, P.A.: ABCG1 has a critical role in mediating cholesterol efflux to HDL and preventing cellular lipid accumulation. Cell Metab, 2005. 1(2): 121-31.

61. Baldan, A., Pei, L., Lee, R., Tarr, P., Tangirala, R.K., Weinstein, M.M., Frank, J., Li, A.C., Tontonoz, P., and Edwards, P.A.: Impaired development of atherosclerosis in hyperlipidemic Ldlr-/- and ApoE-/- mice transplanted with Abcg1-/- bone marrow. Arterioscler Thromb Vasc Biol, 2006. 26(10): 2301-7.
62. Ranalletta, M., Wang, N., Han, S., Yvan-Charvet, L., Welch, C., and Tall, A.R.: Decreased atherosclerosis in low-density lipoprotein receptor knockout mice transplanted with Abcg1-/- bone marrow. Arterioscler Thromb Vasc Biol, 2006. 26(10): 2308-15.
63. Out, R., Hoekstra, M., Hildebrand, R.B., Kruit, J.K., Meurs, I., Li, Z., Kuipers, F., Van Berkel, T.J., and Van Eck, M.: Macrophage ABCG1 deletion disrupts lipid homeostasis in alveolar macrophages and moderately influences atherosclerotic lesion development in LDL receptor-deficient mice. Arterioscler Thromb Vasc Biol, 2006. 26(10): 2295-300.
64. Out, R., Hoekstra, M., Meurs, I., de Vos, P., Kuiper, J., Van Eck, M., and Van Berkel, T.J.: Total body ABCG1 expression protects against early atherosclerotic lesion development in mice. Arterioscler Thromb Vasc Biol, 2007. 27(3): 594-9.
65. Wang, N., Yvan-Charvet, L., Lutjohann, D., Mulder, M., Vanmierlo, T., Kim, T.W., and Tall, A.R.: ATP-binding cassette transporters G1 and G4 mediate cholesterol and desmosterol efflux to HDL and regulate sterol accumulation in the brain. Faseb J, 2008. 22(4): 1073-82.
66. Uehara, Y., Yamada, T., Baba, Y., Miura, S., Abe, S., Kitajima, K., Higuchi, M.A., Iwamoto, T., and Saku, K.: ATP-binding cassette transporter G4 is highly expressed in microglia in Alzheimer's brain. Brain Res, 2008. 1217: 239-46.
67. Cressman, V.L., Lazarowski, E., Homolya, L., Boucher, R.C., Koller, B.H., and Grubb, B.R.: Effect of loss of P2Y(2) receptor gene expression on nucleotide regulation of murine epithelial Cl(-) transport. J Biol Chem, 1999. 274(37): 26461-8.
68. Homolya, L., Watt, W.C., Lazarowski, E.R., Koller, B.H., and Boucher, R.C.: Nucleotide-regulated calcium signaling in lung fibroblasts and epithelial cells from normal and P2Y(2) receptor (-/-) mice. J Biol Chem, 1999. 274(37): 26454-60.
69. Lazarowski, E.R., Homolya, L., Boucher, R.C., and Harden, T.K.: Direct demonstration of mechanically induced release of cellular UTP and its implication for uridine nucleotide receptor activation. J Biol Chem, 1997. 272(39): 24348-54.
70. Lazarowski, E.R., Homolya, L., Boucher, R.C., and Harden, T.K.: Identification of an ecto-nucleoside diphosphokinase and its contribution to interconversion of P2 receptor agonists. J Biol Chem, 1997. 272(33): 20402-7.
71. Homolya, L., Steinberg, T.H., and Boucher, R.C.: Cell to cell communication in response to mechanical stress via bilateral release of ATP and UTP in polarized epithelia. J Cell Biol, 2000. 150(6): 1349-60.

72. Cheson, B.D., Cassileth, P.A., Head, D.R., Schiffer, C.A., Bennett, J.M., Bloomfield, C.D., Brunning, R., Gale, R.P., Grever, M.R., Keating, M.J., and et al.: Report of the National Cancer Institute-sponsored workshop on definitions of diagnosis and response in acute myeloid leukemia. J Clin Oncol, 1990. 8(5): 813-9.
73. Schwab, R., Petak, I., Sarkadi, B., Kopper, L., Pap, A., Szakacs, G., Homolya, L., Jakab, F., Moldvay, J., Feher, A.: Method and Reagent Kit For Evaluation of Multidrug-Resistance Activity. Patent num.: WO2005116648, 2005.
74. Allikmets, R., Schriml, L.M., Hutchinson, A., Romano-Spica, V., and Dean, M.: A human placenta-specific ATP-binding cassette gene (ABCP) on chromosome 4q22 that is involved in multidrug resistance. Cancer Res, 1998. 58(23): 5337-9.
75. Doyle, L.A., Yang, W., Abruzzo, L.V., Krogmann, T., Gao, Y., Rishi, A.K., and Ross, D.D.: A multidrug resistance transporter from human MCF-7 breast cancer cells. Proc Natl Acad Sci U S A, 1998. 95(26): 15665-70.
76. Lage, H., and Dietel, M.: Effect of the breast-cancer resistance protein on atypical multidrug resistance. Lancet Oncol, 2000. 1: 169-75.
77. Miyake, K., Mickley, L., Litman, T., Zhan, Z., Robey, R., Cristensen, B., Brangi, M., Greenberger, L., Dean, M., Fojo, T., and Bates, S.E.: Molecular cloning of cDNAs which are highly overexpressed in mitoxantrone-resistant cells: demonstration of homology to ABC transport genes. Cancer Res, 1999. 59(1): 8-13.
78. Maliepaard, M., Scheffer, G.L., Faneyte, I.F., van Gastelen, M.A., Pijnenborg, A.C., Schinkel, A.H., van De Vijver, M.J., Scheper, R.J., and Schellens, J.H.: Subcellular localization and distribution of the breast cancer resistance protein transporter in normal human tissues. Cancer Res, 2001. 61(8): 3458-64.
79. Zhou, S., Schuetz, J.D., Bunting, K.D., Colapietro, A.M., Sampath, J., Morris, J.J., Lagutina, I., Grosveld, G.C., Osawa, M., Nakauchi, H., and Sorrentino, B.P.: The ABC transporter Bcrp1/ABCG2 is expressed in a wide variety of stem cells and is a molecular determinant of the side-population phenotype. Nat Med, 2001. 7(9): 1028-34.
80. Jonker, J.W., Buitelaar, M., Wagenaar, E., Van Der Valk, M.A., Scheffer, G.L., Scheper, R.J., Plosch, T., Kuipers, F., Elferink, R.P., Rosing, H., Beijnen, J.H., and Schinkel, A.H.: The breast cancer resistance protein protects against a major chlorophyll-derived dietary phototoxin and protoporphyria. Proc Natl Acad Sci U S A, 2002. 99(24): 15649-54.
81. Krishnamurthy, P., Ross, D.D., Nakanishi, T., Bailey-Dell, K., Zhou, S., Mercer, K.E., Sarkadi, B., Sorrentino, B.P., and Schuetz, J.D.: The stem cell marker Bcrp/ABCG2 enhances hypoxic cell survival through interactions with heme. J Biol Chem, 2004. 279(23): 24218-25.
82. Arteaga, C.L., and Johnson, D.H.: Tyrosine kinase inhibitors-ZD1839 (Iressa). Curr Opin Oncol, 2001. 13(6): 491-8.

83. Barker, A.J., Gibson, K.H., Grundy, W., Godfrey, A.A., Barlow, J.J., Healy, M.P., Woodburn, J.R., Ashton, S.E., Curry, B.J., Scarlett, L., Henthorn, L., and Richards, L.: Studies leading to the identification of ZD1839 (IRESSA): an orally active, selective epidermal growth factor receptor tyrosine kinase inhibitor targeted to the treatment of cancer. Bioorg Med Chem Lett, 2001. 11(14): 1911-4.
84. Cohen, M.H., Williams, G.A., Sridhara, R., Chen, G., McGuinn, W.D., Jr., Morse, D., Abraham, S., Rahman, A., Liang, C., Lostritto, R., Baird, A., and Pazdur, R.: United States Food and Drug Administration Drug Approval summary: Gefitinib (ZD1839; Iressa) tablets. Clin Cancer Res, 2004. 10(4): 1212-8.
85. Giaccone, G., Herbst, R.S., Manegold, C., Scagliotti, G., Rosell, R., Miller, V., Natale, R.B., Schiller, J.H., Von Pawel, J., Pluzanska, A., Gatzemeier, U., Grous, J., Ochs, J.S., Averbuch, S.D., Wolf, M.K., Rennie, P., Fandi, A., and Johnson, D.H.: Gefitinib in combination with gemcitabine and cisplatin in advanced non-small-cell lung cancer: a phase III trial--INTACT 1. J Clin Oncol, 2004. 22(5): 777-84.
86. Lynch, T.J., Bell, D.W., Sordella, R., Gurubhagavatula, S., Okimoto, R.A., Brannigan, B.W., Harris, P.L., Haserlat, S.M., Supko, J.G., Haluska, F.G., Louis, D.N., Christiani, D.C., Settleman, J., and Haber, D.A.: Activating mutations in the epidermal growth factor receptor underlying responsiveness of non-small-cell lung cancer to gefitinib. N Engl J Med, 2004. 350(21): 2129-39.
87. Paez, J.G., Janne, P.A., Lee, J.C., Tracy, S., Greulich, H., Gabriel, S., Herman, P., Kaye, F.J., Lindeman, N., Boggon, T.J., Naoki, K., Sasaki, H., Fujii, Y., Eck, M.J., Sellers, W.R., Johnson, B.E., and Meyerson, M.: EGFR mutations in lung cancer: correlation with clinical response to gefitinib therapy. Science, 2004. 304(5676): 1497-500.
88. Hegedus, T., Orfi, L., Seprodi, A., Varadi, A., Sarkadi, B., and Keri, G.: Interaction of tyrosine kinase inhibitors with the human multidrug transporter proteins, MDR1 and MRP1. Biochim Biophys Acta, 2002. 1587(2-3): 318-25.
89. Ozvegy-Laczka, C., Cserepes, J., Elkind, N.B., and Sarkadi, B.: Tyrosine kinase inhibitor resistance in cancer: role of ABC multidrug transporters. Drug Resist Updat, 2005. 8(1-2): 15-26.
90. Janmaat, M.L., and Giaccone, G.: The epidermal growth factor receptor pathway and its inhibition as anticancer therapy. Drugs Today (Barc), 2003. 39 Suppl C: 61-80.
91. Houghton, P.J., Germain, G.S., Harwood, F.C., Schuetz, J.D., Stewart, C.F., Buchdunger, E., and Traxler, P.: Imatinib mesylate is a potent inhibitor of the ABCG2 (BCRP) transporter and reverses resistance to topotecan and SN-38 in vitro. Cancer Res, 2004. 64(7): 2333-7.
92. Ee, P.L., Kamalakaran, S., Tonetti, D., He, X., Ross, D.D., and Beck, W.T.: Identification of a novel estrogen response element in the breast cancer resistance protein (ABCG2) gene. Cancer Res, 2004. 64(4): 1247-51.

93. Szatmari, I., Vamosi, G., Brazda, P., Balint, B.L., Benko, S., Szeles, L., Jeney, V., Ozvegy-Laczka, C., Szanto, A., Barta, E., Balla, J., Sarkadi, B., and Nagy, L.: Peroxisome proliferator-activated receptor gamma-regulated ABCG2 expression confers cytoprotection to human dendritic cells. J Biol Chem, 2006. 281(33): 23812-23.
94. Imai, Y., Ishikawa, E., Asada, S., and Sugimoto, Y.: Estrogen-mediated post transcriptional down-regulation of breast cancer resistance protein/ABCG2. Cancer Res, 2005. 65(2): 596-604.
95. Janvilisri, T., Venter, H., Shahi, S., Reuter, G., Balakrishnan, L., and van Veen, H.W.: Sterol transport by the human breast cancer resistance protein (ABCG2) expressed in Lactococcus lactis. J Biol Chem, 2003. 278(23): 20645-51.
96. Diop, N.K., and Hrycyna, C.A.: N-Linked glycosylation of the human ABC transporter ABCG2 on asparagine 596 is not essential for expression, transport activity, or trafficking to the plasma membrane. Biochemistry, 2005. 44(14): 5420-9.
97. Takada, T., Suzuki, H., and Sugiyama, Y.: Characterization of polarized expression of point- or deletion-mutated human BCRP/ABCG2 in LLC-PK1 cells. Pharm Res, 2005. 22(3): 458-64.
98. Ozvegy-Laczka, C., Varady, G., Koblos, G., Ujhelly, O., Cervenak, J., Schuetz, J.D., Sorrentino, B.P., Koomen, G.J., Varadi, A., Nemet, K., and Sarkadi, B.: Function-dependent conformational changes of the ABCG2 multidrug transporter modify its interaction with a monoclonal antibody on the cell surface. J Biol Chem, 2005. 280(6): 4219-27.
99. Gottesman, M.M., and Pastan, I.: Biochemistry of multidrug resistance mediated by the multidrug transporter. Annu Rev Biochem, 1993. 62: 385-427.
100. Raviv, Y., Pollard, H.B., Bruggemann, E.P., Pastan, I., and Gottesman, M.M.: Photosensitized labeling of a functional multidrug transporter in living drug-resistant tumor cells. J Biol Chem, 1990. 265(7): 3975-80.
101. Higgins, C.F.: Flip-flop: the transmembrane translocation of lipids. Cell, 1994. 79(3): 393-5.
102. Higgins, C.F., and Gottesman, M.M.: Is the multidrug transporter a flippase? Trends Biochem Sci, 1992. 17(1): 18-21.
103. Shapiro, A.B., and Ling, V.: Extraction of Hoechst 33342 from the cytoplasmic leaflet of the plasma membrane by P-glycoprotein. Eur J Biochem, 1997. 250(1): 122-9.
104. Shapiro, A.B., and Ling, V.: Stoichiometry of coupling of rhodamine 123 transport to ATP hydrolysis by P-glycoprotein. Eur J Biochem, 1998. 254(1): 189-93.
105. Lugo, M.R., and Sharom, F.J.: Interaction of LDS-751 with P-glycoprotein and mapping of the location of the R drug binding site. Biochemistry, 2005. 44(2): 643-55.

106. Qu, Q., and Sharom, F.J.: Proximity of bound Hoechst 33342 to the ATPase catalytic sites places the drug binding site of P-glycoprotein within the cytoplasmic membrane leaflet. Biochemistry, 2002. 41(14): 4744-52.
107. Omote, H., and Al-Shawi, M.K.: A novel electron paramagnetic resonance approach to determine the mechanism of drug transport by P-glycoprotein. J Biol Chem, 2002. 277(47): 45688-94.
108. Shapiro, A.B., Corder, A.B., and Ling, V.: P-glycoprotein-mediated Hoechst 33342 transport out of the lipid bilayer. Eur J Biochem, 1997. 250(1): 115-21.
109. Feofanov, A., Sharonov, S., Kudelina, I., Fleury, F., and Nabiev, I.: Localization and molecular interactions of mitoxantrone within living K562 cells as probed by confocal spectral imaging analysis. Biophys J, 1997. 73(6): 3317-27.
110. Kaestner, L.: Red blood cell ghosts and intact red blood cells as complementary models in photodynamic cell research. Bioelectrochemistry, 2004. 62(2): 123-6.
111. Ewart, G.D., Cannell, D., Cox, G.B., and Howells, A.J.: Mutational analysis of the traffic ATPase (ABC) transporters involved in uptake of eye pigment precursors in Drosophila melanogaster. Implications for structure-function relationships. J Biol Chem, 1994. 269(14): 10370-7.
112. Terasaka, N., Wang, N., Yvan-Charvet, L., and Tall, A.R.: High-density lipoprotein protects macrophages from oxidized low-density lipoprotein-induced apoptosis by promoting efflux of 7-ketocholesterol via ABCG1. Proc Natl Acad Sci U S A, 2007. 104(38): 15093-8.
113. Tabas, I.: Consequences and therapeutic implications of macrophage apoptosis in atherosclerosis: the importance of lesion stage and phagocytic efficiency. Arterioscler Thromb Vasc Biol, 2005. 25(11): 2255-64.
114. Chambenoit, O., Hamon, Y., Marguet, D., Rigneault, H., Rosseneu, M., and Chimini, G.: Specific docking of apolipoprotein A-I at the cell surface requires a functional ABCA1 transporter. J Biol Chem, 2001. 276(13): 9955-60.
115. Le Goff, W., Peng, D.Q., Settle, M., Brubaker, G., Morton, R.E., and Smith, J.D.: Cyclosporin A traps ABCA1 at the plasma membrane and inhibits ABCA1-mediated lipid efflux to apolipoprotein A-I. Arterioscler Thromb Vasc Biol, 2004. 24(11): 2155-61.
116. Le Goff, W., Zheng, P., Brubaker, G., and Smith, J.D.: Identification of the cAMP-responsive enhancer of the murine ABCA1 gene: requirement for CREB1 and STAT3/4 elements. Arterioscler Thromb Vasc Biol, 2006. 26(3): 527-33.
117. Gedeon, C., Behravan, J., Koren, G., and Piquette-Miller, M.: Transport of glyburide by placental ABC transporters: implications in fetal drug exposure. Placenta, 2006. 27(11-12): 1096-102.

118. Chandra, P., and Brouwer, K.L.: The complexities of hepatic drug transport: current knowledge and emerging concepts. Pharm Res, 2004. 21(5): 719-35.
119. Thiebaut, F., Tsuruo, T., Hamada, H., Gottesman, M.M., Pastan, I., and Willingham, M.C.: Cellular localization of the multidrug-resistance gene product P-glycoprotein in normal human tissues. Proc Natl Acad Sci U S A, 1987. 84(21): 7735-8.
120. Atkinson, D.E., Greenwood, S.L., Sibley, C.P., Glazier, J.D., and Fairbairn, L.J.: Role of MDR1 and MRP1 in trophoblast cells, elucidated using retroviral gene transfer. Am J Physiol Cell Physiol, 2003. 285(3): C584-91.
121. Tribull, T.E., Bruner, R.H., and Bain, L.J.: The multidrug resistance-associated protein 1 transports methoxychlor and protects the seminiferous epithelium from injury. Toxicol Lett, 2003. 142(1-2): 61-70.
122. Melaine, N., Lienard, M.O., Dorval, I., Le Goascogne, C., Lejeune, H., and Jegou, B.: Multidrug resistance genes and p-glycoprotein in the testis of the rat, mouse, Guinea pig, and human. Biol Reprod, 2002. 67(6): 1699-707.
123. Cooray, H.C., Blackmore, C.G., Maskell, L., and Barrand, M.A.: Localisation of breast cancer resistance protein in microvessel endothelium of human brain. Neuroreport, 2002. 13(16): 2059-63.
124. Rao, V.V., Dahlheimer, J.L., Bardgett, M.E., Snyder, A.Z., Finch, R.A., Sartorelli, A.C., and Piwnica-Worms, D.: Choroid plexus epithelial expression of MDR1 P glycoprotein and multidrug resistance-associated protein contribute to the blood-cerebrospinal-fluid drug-permeability barrier. Proc Natl Acad Sci U S A, 1999. 96(7): 3900-5.
125. Sugiyama, D., Kusuhara, H., Lee, Y.J., and Sugiyama, Y.: Involvement of multidrug resistance associated protein 1 (Mrp1) in the efflux transport of 17beta estradiol-D-17beta-glucuronide (E217betaG) across the blood-brain barrier. Pharm Res, 2003. 20(9): 1394-400.
126. Zhang, Y., Schuetz, J.D., Elmquist, W.F., and Miller, D.W.: Plasma membrane localization of multidrug resistance-associated protein homologs in brain capillary endothelial cells. J Pharmacol Exp Ther, 2004. 311(2): 449-55.
127. Bart, J., Hollema, H., Groen, H.J., de Vries, E.G., Hendrikse, N.H., Sleijfer, D.T., Wegman, T.D., Vaalburg, W., and van der Graaf, W.T.: The distribution of drug-efflux pumps, P-gp, BCRP, MRP1 and MRP2, in the normal blood-testis barrier and in primary testicular tumours. Eur J Cancer, 2004. 40(14): 2064-70.
128. Choudhary, D., Jansson, I., Stoilov, I., Sarfarazi, M., and Schenkman, J.B.: Metabolism of retinoids and arachidonic acid by human and mouse cytochrome P450 1b1. Drug Metab Dispos, 2004. 32(8): 840-7.
129. Lewis, D.F.: 57 varieties: the human cytochromes P450. Pharmacogenomics, 2004. 5(3): 305-18.

130. Xu, C., Li, C.Y., and Kong, A.N.: Induction of phase I, II and III drug metabolism/transport by xenobiotics. Arch Pharm Res, 2005. 28(3): 249-68.
131. Cole, S.P., Sparks, K.E., Fraser, K., Loe, D.W., Grant, C.E., Wilson, G.M., and Deeley, R.G.: Pharmacological characterization of multidrug resistant MRP-transfected human tumor cells. Cancer Res, 1994. 54(22): 5902-10.
132. Renes, J., de Vries, E.G., Nienhuis, E.F., Jansen, P.L., and Muller, M.: ATP- and glutathione-dependent transport of chemotherapeutic drugs by the multidrug resistance protein MRP1. Br J Pharmacol, 1999. 126(3): 681-8.
133. Qian, Y.M., Song, W.C., Cui, H., Cole, S.P., and Deeley, R.G.: Glutathione stimulates sulfated estrogen transport by multidrug resistance protein 1. J Biol Chem, 2001. 276(9): 6404-11.
134. Loe, D.W., Deeley, R.G., and Cole, S.P.: Characterization of vincristine transport by the M(r) 190,000 multidrug resistance protein (MRP): evidence for cotransport with reduced glutathione. Cancer Res, 1998. 58(22): 5130-6.
135. Borst, P., Zelcer, N., van de Wetering, K., and Poolman, B.: On the putative co-transport of drugs by multidrug resistance proteins. FEBS Lett, 2006. 580(4): 1085-93.
136. Leslie, E.M., Deeley, R.G., and Cole, S.P.: Bioflavonoid stimulation of glutathione transport by the 190-kDa multidrug resistance protein 1 (MRP1). Drug Metab Dispos, 2003. 31(1): 11-5.
137. Loe, D.W., Deeley, R.G., and Cole, S.P.: Verapamil stimulates glutathione transport by the 190-kDa multidrug resistance protein 1 (MRP1). J Pharmacol Exp Ther, 2000. 293(2): 530-8.
138. Comerford, K.M., Cummins, E.P., and Taylor, C.T.: c-Jun NH2-terminal kinase activation contributes to hypoxia-inducible factor 1alpha-dependent P-glycoprotein expression in hypoxia. Cancer Res, 2004. 64(24): 9057-61.
139. Staudinger, J.L., Madan, A., Carol, K.M., and Parkinson, A.: Regulation of drug transporter gene expression by nuclear receptors. Drug Metab Dispos, 2003. 31(5): 523-7.
140. Perloff, M.D., von Moltke, L.L., Stormer, E., Shader, R.I., and Greenblatt, D.J.: Saint John's wort: an in vitro analysis of P-glycoprotein induction due to extended exposure. Br J Pharmacol, 2001. 134(8): 1601-8.
141. Volk, H.A., Potschka, H., and Loscher, W.: Increased expression of the multidrug transporter P-glycoprotein in limbic brain regions after amygdala-kindled seizures in rats. Epilepsy Res, 2004. 58(1): 67-79.
142. Hiraoka, H., Kimura, N., Furukawa, Y., Ogawara, K., Kimura, T., and Higaki, K.: Up-regulation of P-glycoprotein expression in small intestine under chronic serotonin-depleted conditions in rats. J Pharmacol Exp Ther, 2005. 312(1): 248-55.

143. Mitin, T., Von Moltke, L.L., Court, M.H., and Greenblatt, D.J.: Levothyroxine up-regulates P-glycoprotein independent of the pregnane X receptor. Drug Metab Dispos, 2004. 32(8): 779-82.
144. Tanaka, Y., Slitt, A.L., Leazer, T.M., Maher, J.M., and Klaassen, C.D.: Tissue distribution and hormonal regulation of the breast cancer resistance protein (Bcrp/Abcg2) in rats and mice. Biochem Biophys Res Commun, 2005. 326(1): 181-7.
145. Zhu, H.J., and Liu, G.Q.: Glutamate up-regulates P-glycoprotein expression in rat brain microvessel endothelial cells by an NMDA receptor-mediated mechanism. Life Sci, 2004. 75(11): 1313-22.
146. Belliard, A.M., Lacour, B., Farinotti, R., and Leroy, C.: Effect of tumor necrosis factor-alpha and interferon-gamma on intestinal P-glycoprotein expression, activity, and localization in Caco-2 cells. J Pharm Sci, 2004. 93(6): 1524-36.
147. Dreuw, A., Hermanns, H.M., Heise, R., Joussen, S., Rodriguez, F., Marquardt, Y., Jugert, F., Merk, H.F., Heinrich, P.C., and Baron, J.M.: Interleukin-6-type cytokines upregulate expression of multidrug resistance-associated proteins in NHEK and dermal fibroblasts. J Invest Dermatol, 2005. 124(1): 28-37.
148. Dohgu, S., Yamauchi, A., Takata, F., Naito, M., Tsuruo, T., Higuchi, S., Sawada, Y., and Kataoka, Y.: Transforming growth factor-beta1 upregulates the tight junction and P-glycoprotein of brain microvascular endothelial cells. Cell Mol Neurobiol, 2004. 24(3): 491-7.
149. Hisaeda, K., Inokuchi, A., Nakamura, T., Iwamoto, Y., Kohno, K., Kuwano, M., and Uchiumi, T.: Interleukin-1beta represses MRP2 gene expression through inactivation of interferon regulatory factor 3 in HepG2 cells. Hepatology, 2004. 39(6): 1574-82.
150. Robbiani, D.F., Finch, R.A., Jager, D., Muller, W.A., Sartorelli, A.C., and Randolph, G.J.: The leukotriene C(4) transporter MRP1 regulates CCL19 (MIP-3beta, ELC)-dependent mobilization of dendritic cells to lymph nodes. Cell, 2000. 103(5): 757-68.
151. Wijnholds, J., Evers, R., van Leusden, M.R., Mol, C.A., Zaman, G.J., Mayer, U., Beijnen, J.H., van der Valk, M., Krimpenfort, P., and Borst, P.: Increased sensitivity to anticancer drugs and decreased inflammatory response in mice lacking the multidrug resistance-associated protein. Nat Med, 1997. 3(11): 1275-9.
152. Corpechot, C., Ping, C., Wendum, D., Matsuda, F., Barbu, V., and Poupon, R.: Identification of a novel 974C-->G nonsense mutation of the MRP2/ABCC2 gene in a patient with Dubin-Johnson syndrome and analysis of the effects of rifampicin and ursodeoxycholic acid on serum bilirubin and bile acids. Am J Gastroenterol, 2006. 101(10): 2427-32.
153. Kuroda, M., Kobayashi, Y., Tanaka, Y., Itani, T., Mifuji, R., Araki, J., Kaito, M., and Adachi, Y.: Increased hepatic and renal expressions of multidrug resistance-associated protein 3 in Eisai hyperbilirubinuria rats. J Gastroenterol Hepatol, 2004. 19(2): 146-53.

154. Cisternino, S., Mercier, C., Bourasset, F., Roux, F., and Scherrmann, J.M.: Expression, up-regulation, and transport activity of the multidrug-resistance protein Abcg2 at the mouse blood-brain barrier. Cancer Res, 2004. 64(9): 3296-301.
155. Bergman, A.M., Munch-Petersen, B., Jensen, P.B., Sehested, M., Veerman, G., Voorn, D.A., Smid, K., Pinedo, H.M., and Peters, G.J.: Collateral sensitivity to gemcitabine (2',2'-difluorodeoxycytidine) and cytosine arabinoside of daunorubicin- and VM-26-resistant variants of human small cell lung cancer cell lines. Biochem Pharmacol, 2001. 61(11): 1401-8.
156. Martin-Aragon, S., Mukherjee, S.K., Taylor, B.J., Ivy, S.P., Fu, C.H., Ardi, V.C., and Avramis, V.I.: Cytosine arabinoside (ara-C) resistance confers cross-resistance or collateral sensitivity to other classes of anti-leukemic drugs. Anticancer Res, 2000. 20(1A): 139-50.
157. Seo, T., Urasaki, Y., Takemura, H., and Ueda, T.: Arsenic trioxide circumvents multidrug resistance based on different mechanisms in human leukemia cell lines. Anticancer Res, 2005. 25(2A): 991-8.
158. Szakacs, G., Annereau, J.P., Lababidi, S., Shankavaram, U., Arciello, A., Bussey, K.J., Reinhold, W., Guo, Y., Kruh, G.D., Reimers, M., Weinstein, J.N., and Gottesman, M.M.: Predicting drug sensitivity and resistance: profiling ABC transporter genes in cancer cells. Cancer Cell, 2004. 6(2): 129-37.
159. Bergman, A.M., Pinedo, H.M., Talianidis, I., Veerman, G., Loves, W.J., van der Wilt, C.L., and Peters, G.J.: Increased sensitivity to gemcitabine of P-glycoprotein and multidrug resistance-associated protein-overexpressing human cancer cell lines. Br J Cancer, 2003. 88(12): 1963-70.
160. Jonsson-Videsater, K., Andersson, G., Bergh, J., and Paul, C.: Doxorubicin-resistant, MRP1-expressing U-1285 cells are sensitive to idarubicin. Ther Drug Monit, 2003. 25(3): 331-9.
161. Laberge, R.M., Karwatsky, J., Lincoln, M.C., Leimanis, M.L., and Georges, E.: Modulation of GSH levels in ABCC1 expressing tumor cells triggers apoptosis through oxidative stress. Biochem Pharmacol, 2007. 73(11): 1727-37.
162. Trompier, D., Chang, X.B., Barattin, R., du Moulinet D'Hardemare, A., Di Pietro, A., and Baubichon-Cortay, H.: Verapamil and its derivative trigger apoptosis through glutathione extrusion by multidrug resistance protein MRP1. Cancer Res, 2004. 64(14): 4950-6.

9. Függelék

A dolgozat alapjául szolgáló 13 közlemény teljes terjedelemben.

1. sz. közlemény

dc_46_10

FEBS 16851

dc_46_10

FEBS Letters 383 (1996) 99–104

Transport properties of the multidrug resistance-associated protein (MRP) in human tumour cells

Zsolt Holló, László Homolya, Tamás Hegedüs, Balázs Sarkadi*

National Institute of Haematology and Immunology, Daróczi u. 24, H-1113 Budapest, Hungary

Received 3 November 1995; revised version received 19 February 1996

Abstract In this paper we demonstrate that the expression of the multidrug resistance-associated protein (MRP) in a variety of intact human tumour cells results in the ATP-dependent, mutually exclusive extrusion of both the acetoxymethyl ester and the free anion forms of the fluorescent dye calcein, as well as that of a fluorescent pyrenemaleimide–glutathione conjugate. The MRP-dependent transport of all these three model compounds closely correlates with the expression level of MRP and is cross-inhibited by hydrophobic anticancer drugs, by reversing agents for MDR1, and also by compounds not influencing MDR1, such as hydrophobic anions, alkylating agents, and inhibitors of organic anion transporters. Cellular glutathione depletion affects neither the MRP-dependent extrusion of calcein AM or free calcein, nor its modulation by most hydrophobic or anionic compounds, although eliminating the cross-inhibitory effect of glutathione conjugates. These results suggest that the outward pumping of both hydrophobic uncharged and water-soluble anionic compounds, including glutathione conjugates, is an inherent property of MRP, and offer sensitive methods for the functional diagnostics of this transport protein as well as for the rapid screening of drug-resistance modulating agents.

Key words: Multidrug resistance-associated protein; Multidrug-resistance protein; P-glycoprotein; Drug resistance; Calcein; Fluorometry; Immunoblotting; Transport assay

1. Introduction

A large number of clinically observed resistance of cancers to chemically unrelated cytotoxic compounds is caused by the overexpression of multidrug transporter proteins in the tumour cell membranes. The two major multidrug transporter gene products identified are MDR1 (P-glycoprotein, P-170), and MRP (multidrug resistance-associated protein, P-190), which are both members of the ATP binding cassette (ABC) transporter family, and perform an ATP-dependent extrusion of various cytotoxic agents. Many of the transported compounds are of natural origin, and in the case of MDR1 they are relatively large, hydrophobic, either uncharged or weakly basic molecules [1–4].

MRP has recently been cloned [4] and its function as a drug-extrusion pump established [5,6], but the nature of the transported drugs and other chemicals is still controversial. According to several reports, MRP effectively pumps out most substrates of MDR1, but may also interact with a wider range of chemicals, and seems to be specifically modulated by genistein and probenecid [6–14]. MRP was shown to bind and transport glutathione S (GS) conjugates, such as leukotriene C_4 [8–10], and other large anionic substances ([15]; P. Twentyman, personal communication), thus raising the possible similarity or identity of MRP and the multispecific organic anion transporter (MOAT; [16]). Moreover, a recent communication [17] suggested that the key mechanism of the cytotoxic drug resistance induced by MRP is the extrusion of intracellularly formed drug–GS conjugates.

Earlier we have shown [18] that hydrophobic acetoxymethyl ester (AM) derivatives, but not the free acid forms of various fluorescent indicators, are actively extruded by the P-glycoprotein (MDR1), and that the measurement of the cellular accumulation of such an indicator, e.g. calcein, can be effectively utilised for the diagnostics and the transport characterization of MDR1 [19,20]. Moreover, the rapid extrusion of calcein AM before its cleavage by cellular esterases suggested a drug-transport mechanism by MDR1 directly from the membrane phase. The experiments described in this paper demonstrate that calcein AM is also extruded by the human MRP, although in this case the hydrophilic free calcein anion, and an intracellularly formed fluorescent GS-pyrenemaleimide complex can also be exported. The studies presented here on the cross-inhibition of the transported compounds, as well as the effects of different drugs and of cellular glutathione depletion on the MRP-dependent transport, may significantly help our understanding of the molecular mechanism of this clinically important transport pathway.

2. Materials and methods

2.1. Cell culturing

Cell culturing was performed under standard conditions in RPMI or DMEM media, containing 10% fetal calf serum, 5 mM glutamine, 100 U/ml penicillin, and 100 μg/ml streptomycin. S1 (SW1573 cells), and S1MRP (MRP-transfected S1 cells re-selected and cloned in ADR-containing media), were originally prepared as described in [6]. GLC4, and GLC4 ADR (GLC4 cells selected in ADR and regularly re-selected with 1 μM ADR containing media) were described in [21]. These cell lines were kind gifts of Drs. P. Borst, A. Schinkel and G. Zaman, while HL60 ADR (ADR-selected HL60 cells) were gifts of Dr. M. Center (see [22]). K562 MDR1 (selected in ADR and regularly re-selected in 50 ng/ml ADR), were prepared in our laboratory. KB3 and KB-V1 (containing MDR1 and grown in media containing 50–500 ng/ml vincristine) human epidermoid carcinoma cells, NIH 3T3 fibroblasts and their human MDR1-transfected counterpart (NIH 3T3 MDR1 G185, see [23]) were kind gifts of Dr. M. M. Gottesman. Drug resistance was determined by cell counting after a

*Corresponding author. Fax: (36) (1) 185 2234.

Abbreviations: ADR, adriamycin (doxorubicin); AM, acetoxymethylester; CCCP, chlorocarbonyl cyanide phenylhydrazone; 2,4-DNP, 2,4-dinitrophenol; DMEM, Dulbecco's modified Eagle's medium; FCS, fetal calf serum; GSH, reduced glutathione; MDR1, multidrug-resistance protein; MRP, multidrug resistance-associated protein; NEM, *N*-ethylmaleimide; NPM, *N*-pyrenemaleimide; PGA1, prostaglandin A_1; PVDF, polyvinylidene difluoride; VBL, vinblastine.

SSDI S0014-5793(96)00237-2

72 h incubation of the cells in 24-well plates in the respective culture media, supplemented with various concentrations of adriamycin. Adherent cells (NIH 3T3, S1, GLC4, KB, and KBV1 control and drug-resistant counterparts) were detached by mild trypsinization (5 min, 1 mg/ml trypsin), then washed and resuspended in HPMI medium.

2.2. Calcein fluorescence

Calcein fluorescence was measured by incubating $2–5 \times 10^5$ cells/ml in HPMI medium [18,24] containing 0.25 μM calcein AM (Molecular Probes, Eugene, OR, USA), at 37°C with gentle stirring in a Hitachi F-4000 fluorescence spectrophotometer (excitation and emission wavelengths for calcein were 493 and 515 nm, respectively, with a band width of 5 nm). No self-quenching of free calcein was observed under the experimental conditions used in the present experiments (short incubation periods and low concentrations of calcein AM in the incubation medium). The multidrug-resistance activity factor (MAF, see [20]) was calculated according to the equation:

$$MAF = (F^* - F)/F^* \quad (1)$$

where F^* and F designate the dye accumulation rate in the presence and absence of an inhibitor of the multidrug transporter, respectively.

2.3. Inhibition of MRP-, or MDR1-dependent calcein AM extrusion

Inhibition of MRP-, or MDR1-dependent calcein AM extrusion by various compounds was determined by measuring the rate of increase in fluorescence of free calcein for 5 min periods, and the IC_{50} values were obtained by estimating the drug concentrations resulting in 50% of the maximum transport inhibition. Maximum inhibition was achieved in each experiment by the addition of 100 μM verapamil or 100 μM vinblastine, and the 100% range was calculated by subtracting the rate of fluorescence increase without any inhibitor from that at maximum inhibition. In each case the values represent the range obtained in at least 3 independent experiments with each cell line.

2.4. ATP depletion

ATP depletion was achieved by 1 h incubation of the cells at 37°C in HPMI media containing no glucose but 5 mM 2-deoxyglucose and 5 mM NaN_3, producing cellular ATP levels below 10% of the original [15].

2.5. GSH depletion

GSH depletion was achieved by 24 h preincubation of the cells in the culture media supplemented with 50 μM butathione sulfoximine (BSO), or with a 5 min preincubation with 50 μM diamide, followed by a washing in HPMI medium. Cellular GSH levels were examined by NPM fluorescence measurements (see below), and in both methods the non-protein SH levels were reduced to less than 10% of the original (see also [12–14]).

2.6. Quantitative immunoblotting

Quantitative immunoblotting was performed by washing the cultured cells twice in a protein-free (HPMI) medium followed by dissolution and sonication in a disaggregation buffer [24]. Detection of human MRP with the R1 (rat) monoclonal anti-MRP antibody, kindly provided by Dr. R. Schaper, was carried out as described in [25], while detection of MDR1 was performed with the 4077 anti-MDR1 polyclonal antibody on the same blots [18]. The second antibodies were obtained from Boehringer (anti-rat, peroxidase conjugated IgG, 1000× dilution), and from Jackson Immunoresearch (anti-rabbit, peroxidase conjugated goat IgG, 20000× dilution). HRP-dependent luminescence on the blots (ECL, Amersham) was determined by autoradiography and by excising the respective bands from the PVDF membrane and measuring their luminescence in a liquid scintillation counter (Beckman LS 6000, Single Photon Monitor mode).

2.7. NPM labelling

NPM labelling of the cells was performed by incubating 5×10^6 cells in 1 ml HPMI medium in the presence of 0.5 μM NPM for 5 min at 4°C. The cell suspension was spun in an Eppendorf microcentrifuge (20 s, 10000×*g*) and the pellet rapidly diluted in 5 ml of HPMI, prewarmed to 37°C. The concentration of unconjugated NPM (the fluorescence of which is less than 10% of the S-conjugated molecule) after the loading procedure was determined by the addition of free glutathione to the loading medium, and was found to be negligible. Non-protein SH was determined by NPM titration of the supernatant of trichloroacetic acid-precipitated cells.

2.8. NPM-S conjugate efflux measurements

In the NPM-S conjugate efflux measurements, samples of the cell suspension, taken at the times indicated, were rapidly spun as above, and the supernatants were collected. The amount of total releasable NPM-S conjugate was determined by the addition of 1 mg/ml digitonin to the cell suspension and by preparing a cell-free supernatant by rapid centrifugation, as described above (this was not significantly different from the amount of non-protein NPM-S conjugate, determined after trichloroacetic acid precipitation of the cells). The fluorescence of NPM-S conjugate was determined at excitation and emission wavelengths of 337 and 375 nm, respectively, with a band width of 20 nm, in samples diluted 5 times with distilled water. The above fluorescence measurement procedure minimised the possible effects of energy transfer due to the changing environment of the fluorophore.

3. Results and discussion

Calcein AM is non-fluorescent, and the fluorescence of free calcein, which is produced by esterases and then trapped in the cytoplasm of most living cells, is essentially insensitive to changes of pH, calcium, or magnesium concentrations [26]. As shown in Fig. 1A, when tumour cells were incubated in the presence of low concentrations (e.g. 0.25 μM) of calcein AM, and the increase of free calcein concentration was followed by fluorometry in a stirred cuvette at 37°C, this increase was much slower in MRP-transfected SW1573/S1 lung cancer cells

Table 1
Inhibitors of the MRP-and/or MDR1-mediated calcein AM extrusion

Compound	IC_{50} (μM)	
	MRP	MDR1
Vinblastine	2–5	2–3
Tamoxifen	3–6	2–5
Cyclosporine A	2–4	0.5–1
Verapamil	4–8	2–5
Econazole	3–10	1–3
Quinine	50–100	20–30
Oligomycin	1–2	1–2
CCCP	10–30	>200[a]
2,4-DNP	30–50	>200[a]
Probenecid	500–800	>2000[a]
Sulfinpyrazone	300–500	>2000[a]
Benzbromarone	5–10	>500[a,b]
Indomethacin	10–20	>800[a,b]
Na-cholate	200–300	>1000[b]
Bromosulfophthalein	100–150	>1000[b]
Ethacrynic acid	20–30	>800[b]
Merthiolate	10–20	>200[b]
NEM	0.2–0.5	>50[b]
NPM	0.1–0.2	>20[b]
Genistein	150–200[b]	>1000[a,b]
Chlorambucil	30–50	>500[b]
Prostaglandin A_1	3–5	>100[a]

Drug effects on MRP were estimated from calcein accumulation measurements in S1MRP and in HL60 ADR cells, while the effects on MDR1 were deduced from similar measurements in 3T3 MDR and K562 MDR cells. In each case the values represent the range obtained in at least 3 independent experiments with each cell line. > indicates that 50% inhibition could not be achieved in the measurable concentration range, and either a solubility problem ([a]), or a strong esterase inhibition ([b]) was experienced at higher concentrations.

than in untransfected control cells. Since in the MRP-transfected cells the rate of calcein production was greatly increased (up to the rates seen in the control cells) by ATP depletion, or by the addition of vinblastine or verapamil, the slower calcein production was not due to reduced cellular esterase activity, but to active, MRP-dependent elimination of calcein AM from tumour cells. A similar strong reduction of free calcein production, and its reversal by ATP depletion, verapamil or vinblastine was observed in HL60 ADR and in GLC4 ADR multidrug-resistant tumour cells, all of which express MRP but not MDR1 (see below).

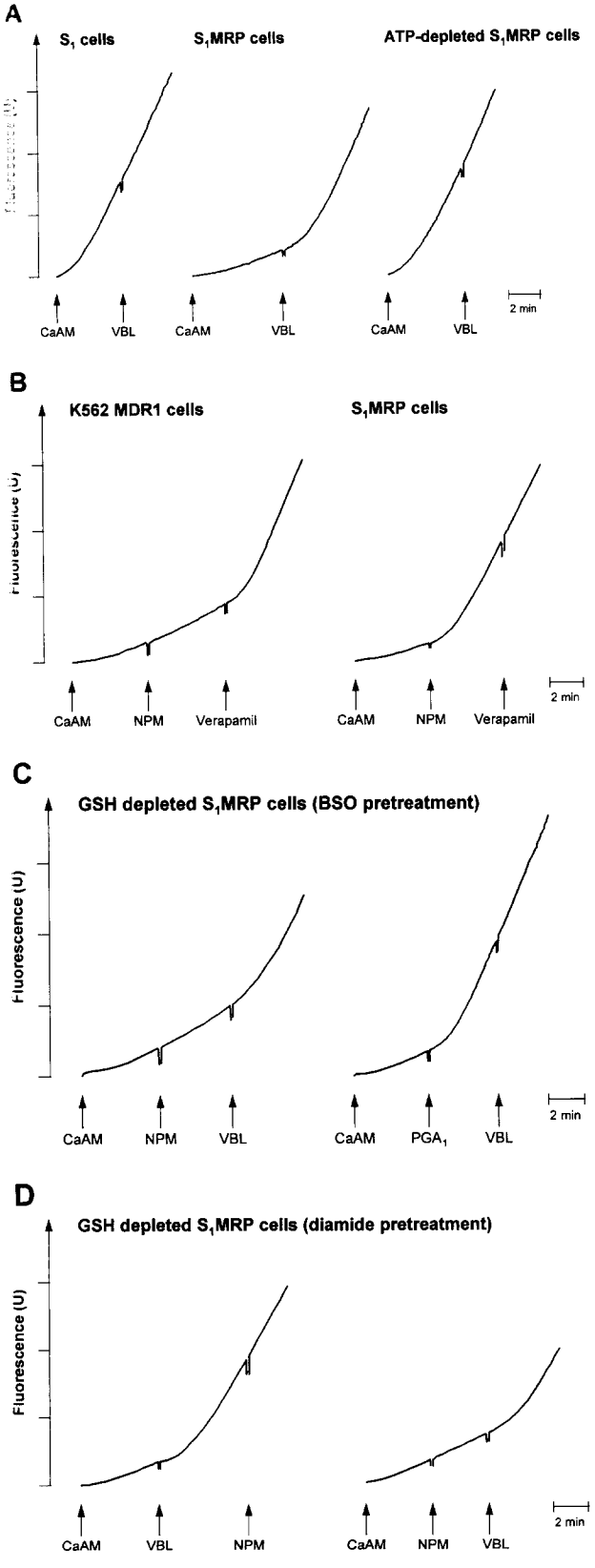

In these fluorometry experiments the conversion of calcein AM to free calcein was measured, thus MRP most probably extrudes the hydrophobic calcein AM before its esterase cleavage. These findings indicate a similar drug transport mechanism to that seen in the case of MDR1 [18]. In order to clarify the possible role of MDR1 in the observed phenomena, the cell extracts were subjected to immunoblotting with specific monoclonal antibodies. As shown in Fig. 2, MRP-expressing cell lines had no detectable levels of MDR1, and MDR1-expressing cells did not show increased MRP expression (a very low level of MRP could be detected even in most of the parental cell lines as well). Moreover, the differences in calcein accumulation rates in the absence and presence of vinblastine, respectively (shown as the multidrug-resistance activity factor, MAF), as well as the drug resistance of these different cell lines, closely correlated with the relative amounts of the respective multidrug-resistance proteins (Fig. 2).

In the following experiments we have compared the modulation of the MRP-dependent and MDR1-dependent calcein AM extrusion, respectively, by several pharmacologically active compounds. Acceleration of cellular calcein production to the control level, i.e. inhibition of calcein AM extrusion, was produced in the S1MRP and HL60 ADR cells by several unrelated compounds, acting with the respective apparent IC_{50} values as listed in Table 1. The inhibitory effects of all these compounds on calcein extrusion were found to be similar in GLC4 ADR cells as well, although in this case the respective IC_{50} values were generally about 50% higher than in the two other MRP-expressing cell types. As shown in Table 1, some of these compounds (e.g. vinblastine, tamoxifen, verapamil, cyclosporin A, quinine, or econazole) inhibited calcein AM extrusion from MRP or MDR1-expressing cells with almost the same efficiency. However, several molecules, such as the hydrophobic anions CCCP, 2,4-DNP; weak acids modulating uric acid or bile acid transport (e.g. probenecid, sulfinpyrazone, benzbromarone, bromosulfophthalein, ethacrynic acid, indomethacin, cholic acid); alkylating agents (e.g. chlorambucil), cell-permeant mercury or maleimide derivatives (e.g. merthiolate, NEM and NPM; see Fig. 1B), as well as prostaglandin A_1, but not E_1 or $F_{2\alpha}$, selectively inhibited MRP-dependent dye extrusion. Although some of these compounds during longer incubations may induce cellular ATP depletion or a non-specific increase in membrane permeability, during the measurement periods of 10–15 min the applied concentrations had no such effects, as shown by

←

Fig. 1. Production of free calcein in drug-sensitive and drug-resistant cells: effects of glutathione depletion. Drug-sensitive (S1) and drug-resistant (S1MRP and K562 MDR1) cells were incubated in the presence of 0.25 μM calcein-AM, and at the times indicated by the arrows the respective agents were added to the media. The plots show calcein fluorescence (in arbitrary units) against time. (A) S1, S1MRP and ATP-depleted S1MRP cells; (B) K562 MDR1 and S1MRP cells; (C) S1MRP cells depleted from GSH by 24 h BSO pretreatment; (D) S1MRP cells depleted from GSH by pretreatment with diamide. Additions: CaAM = 0.25 μM calcein AM; VBL = 10 μM vinblastine, verapamil = 100 μM; NPM = 1 μM *N*-pyrenemaleimide.

dc_46_10

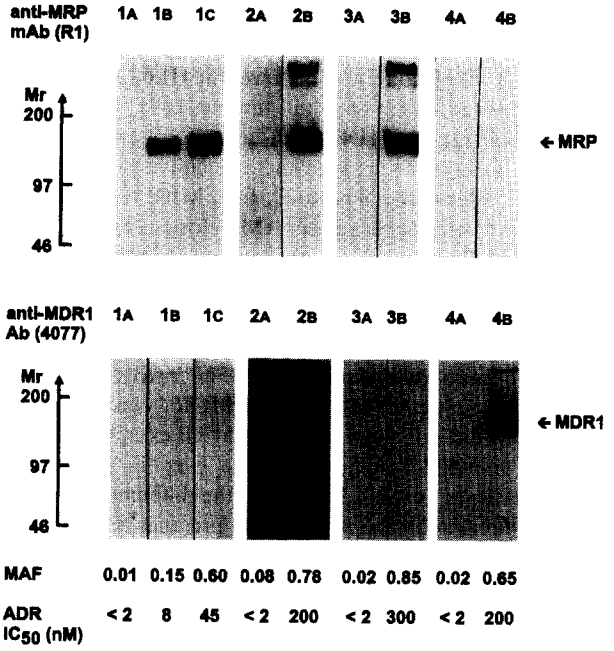

Fig. 2. Estimation of MRP and MDR1 expression by immunoblotting in various cell lines, and characteristics of their calcein extrusion rate and ADR resistance. (A) Immunoblot detection of human MRP by the R1 anti-MRP monoclonal antibody; (B) detection of MDR1 protein by the polyclonal antibody, 4077. Each lane contained 20 μg cellular protein. Lanes: 1A, S1 control cells; 1B, S1MRP cells; 1C, S1MRP cells with ADR selection; 2A, HL60 control cells; 2B, HL60 ADR cells; 3A, GLC4 control cells; 3B, GLC4 ADR cells; 4A, K562 control cells; 4B, K562 MDR1 cells. For the calculation of the multidrug-transporter activity factor (MAF), and the measurement of adriamycin resistance see section 2.

the lack of modulation of calcein AM extrusion in MDR1-expressing cells (Fig. 1B).

Since the formation of drug-GS conjugates was suggested as the key mechanism for MRP-dependent drug extrusion [11–15,27], in the following experiments we have examined the effects of cellular glutathione (GSH) depletion on MRP-dependent calcein AM efflux. In S1MRP or HL60 ADR cells GSH depletion, achieved either in a 24 h preincubation with 50 μM BSO (a specific inhibitor of glutathione synthetase, see [11–15,27]), as shown in Fig. 1C, or in a 5 min preincubation with 50 μM diamide (a selective glutathione oxidising agent; see [28]), followed by washing of the cells in a medium without amino acids (Fig. 1D), did not significantly affect calcein AM extrusion, or its inhibition by vinblastine. This was true for many other agents, e.g. verapamil, cyclosporine A, PGA1 (see Fig. 1C), or probenecid. In contrast, the inhibition of the MRP-dependent calcein AM extrusion by micromolar concentrations of the hydrophobic SH-reactive agents, *N*-ethylmaleimide (NEM) and *N*-pyrenemaleimide (NPM; see Table 1) was eliminated by GSH depletion (Fig. 1C,D). It should be mentioned that the addition of 50 μM BSO or diamide to the calcein AM uptake assay induced a slight increase in free calcein production, thus these compounds may (partially) directly inhibit MRP-dependent drug transport.

In the calcein AM transport experiments we noted that NEM or NPM inhibition of free calcein formation was fully reversible upon 5–10 min incubation of the cells at 37°C, in spite of the irreversible reaction of these agents with SH groups. The S-conjugates of NPM show a characteristic fluorescence emission, thus the complex formation and transport of this molecule in the tumour cells could be directly examined. The NPM fluorescence measurements (see section 2) showed that this maleimide derivative, when added in submicromolar concentrations to the medium, rapidly diffused into the cells and formed predominantly non-protein S-, thus mostly GS-conjugates. As shown in Fig. 3 for HL60 cells, in contrast to the parental non-resistant cells, MRP-containing tumour cells exhibited rapid extrusion of the intracellularly formed, water-soluble GS-NPM complex, and this extrusion was inhibited by low concentrations of calcein AM, vinblastine, or PGA1. The same results were obtained with S1 and S1MRP cells, respectively, i.e. rapid GS-NPM efflux was only observed in the MRP-expressing cell, while the MDR1-expressing K562 cells did not show such GS-NPM extrusion. In both HL60 MRP and S1MRP cells the rapid phase of GS-NPM efflux was inhibited by verapamil, quinine, or probenecid, and also eliminated by ATP depletion (data not shown).

The above experiments indicate that intracellular GS conjugates are transported substrates of MRP, although, as shown above, the interaction of MRP with several transported molecules does not seem to involve GS-conjugate formation. Still, GS conjugates inhibit calcein AM extrusion and calcein AM inhibits GS-NPM conjugate transport, while both of these transports are similarly affected by all the different MRP-modulating compounds.

In most living cells, including MDR1-expressing tumour cells, free calcein is trapped and is not significantly released [18,26]. However, a recent report indicated relatively rapid, ATP-dependent efflux of the accumulated free calcein from MRP-expressing cells [15]. Indeed, when measuring the efflux of free calcein from the S1 MRP and HL60 ADR cells, in contrast to that seen in the MDR1-expressing fibroblasts or K562 tumour cells, we also observed increased calcein efflux, blocked by low concentrations of verapamil, vinblastine, prostaglandin A_1, NEM, NPM, and by all the agents inhibiting calcein AM extrusion (as listed in Table 1). In accordance with the results in [15], in our experiments GSH depletion by BSO did not modify the MRP-dependent free calcein efflux either. The rates of free calcein extrusion in the different cell types correlated well with the expressed amounts of MRP: the time required for a 50% decrease of cellular free calcein (at an

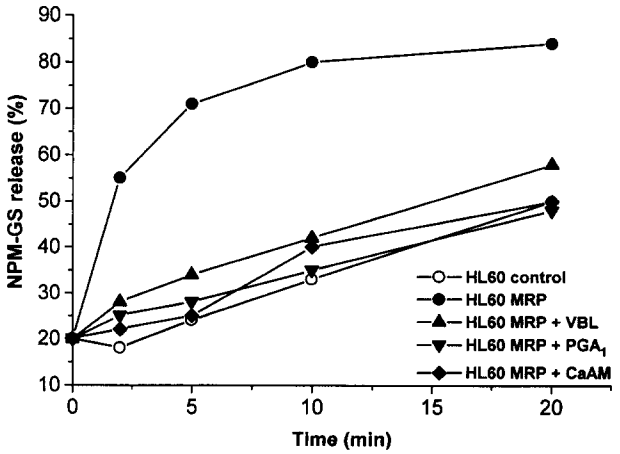

Fig. 3. Efflux of water-soluble NPM-S conjugate from HL60 tumour cells. (○) HL60 control cells; (●) HL60 ADR cells; (▲) HL60 ADR cells+100 μM vinblastine; (▼) HL60 ADR cells + 10 μM PGA1; (◆) HL60 ADR cells + 0.5 μM calcein AM.

initial value of about 1 mM) was more than 60 min in S1MRP cells, 25 min in ADR-selected S1MRP cells and 20 min in HL 60 ADR cells. An important point in these experiments is that relatively high intracellular free calcein concentrations (0.5–2 mM, achieved by preincubating the cells for 10 min in media containing 1–5 μM calcein AM) were required for a full stimulation of the free dye efflux by MRP, while submicromolar concentrations of calcein AM already produced efficient MRP-dependent extrusion (see Fig. 1). These observations render it unlikely that the MRP-dependent transport of any non-fluorescent, partially hydrolysed (thus negatively charged) form of calcein AM may significantly contribute to the observed calcein AM extrusion.

Based on the above experimental data, we suggest that MRP has an inherent transport activity for a variety of chemically and pharmacologically unrelated compounds, e.g. uncharged hydrophobic molecules, lipid-soluble anions, and hydrophilic anions, including glutathione conjugates with multiple and fully dissociating negative charges. The hydrophobic substrates most probably do not have to be converted into GS conjugates, but seem to be recognised by MRP near to or in the hydrophobic membrane phase, as suggested for MDR1. This versatility makes MRP a highly efficient xenobiotic efflux pump, although the large differences in the apparent IC_{50} values for the different chemicals still indicate a limited substrate acceptance. The specificity of the transporter is clearly shown by the relatively small transport effect of the intracellularly formed GS-SG complex (obtained in millimolar levels during GSH depletion by diamide), or the selective inhibition of the MRP-dependent calcein movements by PGA1, and not by several other closely related prostaglandins. An earlier report [29], by studying multidrug resistance in L1210 mouse leukaemia cell line, demonstrated a pattern of shared substrates and inhibitors closely resembling that shown in the present paper (including verapamil, quinidine, cholate, and prostaglandin A_1).

An interesting observation in these experiments is the close correlation of the MRP-inhibitory effects with the pharmacological effectivity of several agents (probenecid, sulfinpyrazone and benzbromarone) in blocking the active reabsorption of uric acid in the human kidney [30]. This finding and the effects of other agents, e.g. indomethacin and bromosulfophthalein, on the MRP-dependent drug transport further support the possible molecular similarity or identity of MRP with the multispecific organic anion transporter (MOAT; see [16]), present in various secretory epithelia.

In this report we demonstrate that the measurement of the formation of free calcein from calcein AM in the tumour cells is especially suitable for characterizing the transport activity of MRP (in flow cytometry the additive effects of calcein AM and free calcein extrusion may occur), and by using appropriate inhibitors, the function of MDR1 and MRP can be differentiated. This method has several advantages over other fluorescent dye (e.g. rhodamine 123 [31], or free calcein [15]) efflux measurements, due to the steady-state conditions for calcein AM transport, and the high-level accumulation of free calcein (see [20]). Both the calcein accumulation and fluorescent GS-NPM conjugate transport measurements are also applicable for screening the MRP-inhibitory effects of various compounds, as well as for determining the involvement of intracellular glutathione conjugation in the MRP-dependent transport of a given molecule.

Acknowledgements: This work has been supported by research grants from COST, ACCORD, OMFB, OTKA (F13178, T17602) and ETT Hungary. B.S. is a recipient of a Howard Hughes International Fellowship. We thank Drs. G.J.R. Zaman, A. Schinkel and P. Borst for helpful discussions and for providing the S1 and S1MRP cells, and Dr. E.G. de Vries for providing the GLC4 and GLC4/ADR cells. We are grateful to Drs. G. Gárdos, András Váradi, and J. Mandl for consultations, to Dr. R.J. Scheper for providing the anti-MRP antibodies, to Dr. M.M. Gottesman for providing the NIH 3T3 MDR1 G185 cell line and the anti-MDR1 antibodies, and to Dr. Melvin S. Center for the HL60 ADR cell line. The technical help of Andrea Siposs and Ilona Zombori is gratefully acknowledged.

References

[1] Endicott, J.A. and Ling, V. (1989) Annu. Rev. Biochem. 58, 137–171.
[2] Higgins, C.F. (1992) Annu. Rev. Cell Biol. 8, 67–113.
[3] Gottesman, M.M. and Pastan, I. (1993) Annu. Rev. Biochem 62, 385–427.
[4] Cole, S.P.C., Bhardway, G., Gerlach, J.H., Mackie, J.E., Grant, C.E., Almquist, K.C., Stewart, A.J., Kurtz, E.U., Duncan, A.M.V. and Deeley, R.G. (1992) Science 258, 1650–1654.
[5] Cole, S.P.C., Sparks, K.E., Fraser, K., Loe, D.W., Grant, C.E., Wilson, G.M. and Deeley, R.G. (1994) Cancer Res. 54, 5902–5910.
[6] Zaman, G.J.R., Flens, M.J., Van Leusden, M.R., De Haas, M., Mülder, H.S., Lankelma, J., Pinedo, H.M., Scheper, R.J., Baas, F., Broxterman, H.J. and Borst, P. (1994) Proc. Natl. Acad. Sci. USA 91, 8822–8826.
[7] Almquist, K.C., Loe, D.W., Hipfner, D.R., Mackie, J.E., Cole, S.P.C. and Deeley, R.G. (1995) Cancer Res. 55, 102–110.
[8] Jedlitschky, G., Leier, I., Buchholz, U., Center, M.S. and Keppler, D. (1994) Cancer Res. 54, 4833–4836.
[9] Leier, I., Jedlitschky, G., Buchholz, U., Cole, S.P.C., Deeley, R.G. and Keppler, D. (1994) J. Biol. Chem. 269, 27807–27810.
[10] Gekeler, V., Ise., W., Sanders, K.H., Ulrich, W.R. and Beck, J. (1995) Biochem. Biophys. Res. Commun. 208, 345–352.
[11] Barrand, M.A., Rhodes, T., Center, M.S. and Twentyman P.R. (1993) Eur. J. Cancer 29A, 408–415.
[12] Versantvoort, C.H.M., Broxterman, H.J., Pinedo, H.M., De Vries E.G., Feller, N., Kuiper, C.M. and Lankelma, J. (1992) Cancer Res. 52, 17–23.
[13] Versantvort, C.H.M., Schuurhuis, G.J., Pinedo, H.M., Eekman, C.A., Kuiper, C.M., Lankelma, J. and Broxterman, H.J. (1993) Br. J. Cancer 68, 939–946.
[14] Versantvoort, C.H.M., Broxterman, H.J., Lankelma, J., Feller, N. and Oiendo, H.M. (1994) Biochem. Pharmacol. 48, 1129–1136.
[15] Feller, N., Broxterman, H.J., Währer, D.C.R. and Pinedo, H.M. (1995) FEBS Lett. 368, 385–388.
[16] Oude-Elferink, R.P. and Jansen, P.L.M. (1994) Pharmacol. Ther. 64, 77–97.
[17] Zaman, G.J.R., Lankelma, J., Van Tellingen, O., Beijnen, J., Dekker, H., Paulusma, C., Oude-Elferink, R.P.J., Baas, F. and Borst, P. (1995) Proc. Natl. Acad. Sci. USA 92, 7690–7694.
[18] Homolya, L., Holló, Zs., Germann, U.A., Pastan, I., Gottesman, M.M. and Sarkadi, B. (1993) J. Biol. Chem. 268, 21493–21496.
[19] Holló, Zs., Homolya, L., Davis, C.W. and Sarkadi, B. (1994) Biochim. Biophys. Acta 1191, 384–388.
[20] Homolya L., Holló, Zs., Müller, M., Mechetner, E.B., Sarkadi, B. (1996) Br. J. Cancer (in press).
[21] Zaman, G.J.R., Versantvoort, C.H.M., Smit, J.J.M., Eijdems, E.W.H.M., De Haas, M., Smith, A.J., Broxterman, H.J., Mulder, N.H., De Vries, E.G.E., Baas, F. and Borst, P. (1993) Cancer Res. 53, 1747–1750.
[22] McGrath, T., Latoud, C., Arnold, S.T., Safa, A.R., Felsted, E.R. and Center, M.S. (1990) Biochem. Pharmacol. 38, 3611–3619.
[23] Bruggemann, E.P., Currier, S.J., Gottesman, M.M. and Pastan, I. (1992) J. Biol. Chem. 267, 21020–21026.
[24] Sarkadi, B., Price, E.M., Boucher, R.C., Germann, U.A. and Scarborough, G.A. (1992) J. Biol. Chem. 267, 4854–4858.
[25] Flens, M.J., Izquierido, M.A., Scheffer, G.L., Fritz, J.M., Meijer, C.J.L.M., Scheper, R.J. and Zaman, G.J.R. (1994) Cancer Res. 54, 4557–4563.

dc_46_10

[26] Haughland, R.P. and Larison K.D. (1992) Handbook of Fluorescent Probes and Research Chemicals, Molecular Probes, Inc., Eugene, OR.
[27] Versantvoort, C.H.M., Broxterman, H.J., Bagjir, T., Scheper, R.J. and Twentyman, P.R. (1995) Br. J. Cancer 72, 82–89.
[28] Plummer, J.L., Smith, B.R., Sies, H. and Bend, J.R. (1981) Methods. Enzymol. 77, 50–63.
[29] Henderson, G.B. and Tsuji, J.M. (1990) Biochim. Biophys. Acta 1051, 60–70.
[30] Ullrich, K.J. and Rumrich, G. (1993) Clin. Invest. 71, 843–848.
[31] Twentyman, P.R., Rhodes, T. and Rayner, S. (1994) Eur. J. Cancer 30A, 1360–1369.

2. sz. közlemény

dc_46_10

Parallel Functional and Immunological Detection of Human Multidrug Resistance Proteins, P-Glycoprotein and MRP1

ZSOLT HOLLÓ, LASZLÓ HOMOLYA, TAMÁS HEGEDÛS, MARIANNA MÜLLER, GERGELY SZAKÁCS, KATALIN JAKAB, FERENC ANTAL and BALÁZS SARKADI

National Institute of Haematology and Immunology, Membrane Research Group of the Hungarian Academy of Sciences, Budapest, Hungary

Abstract. *The proper assessment of the expression and drug extrusion activity of multidrug resistance proteins in various tumor cells is a challenging clinical laboratory problem. Recently, we have introduced a fluorescent dye (calcein) accumulation assay for the estimation of the functional expression of both P-glycoprotein (MDR1) and the multidrug resistance-associated protein (MRP1). Since both MDR1 and MRP1 decrease the intracellular accumulation of the fluorescent free calcein, by applying appropriate inhibitors of MDR1 and MRP1, the transport activity of these proteins could be quantitatively and selectively estimated in fluorometry or flow-cytometry assays. In the present work single-cell fluorescence digital imaging has been applied to characterize the kinetics and inhibitor-sensitivity of calcein accumulation in a mixture of HL60 MRP1 and NIH 3T3 MDR1 cells. Subsequent immunofluorescence labeling was performed by the anti-MDR1 monoclonal antibody (mAb) UIC2 in the same cell population. We report that the double labeling approach, based on the single cell calcein accumulation assay and an immunofluorescence detection, provides good sensitivity and selectivity for the simultaneous functional and immunological detection of cellular MDR1 and MRP1.*

Abbreviations used: AM, acetoxymethyl ester; BSA, bovine serum albumin; CCD, charge-coupled device (video camera); CD, cluster of differentiation; cMOAT, canalicular multispecific organic anion transporter; DIC, differential interference contrast; ICCD, intensified CCD video camera; mAb, monoclonal antibody; MDR1, P-glycoprotein, multidrug resistance protein; MAF, multidrug resistance activity factor; MRP1, multidrug resistance associated protein; TRITC, tetramethylrhodamine B isothiocyanate; ROI, region of interest.

Correspondence to: Balázs Sarkadi, MD, Ph.D., National Institute of Haematology and Immunology, H-11 13 Budapest, Daroczi u. 24, Hungary. Phone/FAX: (36-1) 372-4353, e-mail: Sarkadi@ohvi.hu

Key Words: Multiple drug resistance, P-glycoprotein, multidrug resistance-associated protein, ABC transporters, fluorometry, digital imaging, neoplasms, immunofluorescence, calcein.

The human multidrug resistance protein MDR1, and the multidrug resistance-associated protein (MRP1) are expressed in several human malignancies (for reviews see 1, 2, 3). However, the relevance of these proteins in clinical multidrug resistance is still a matter of debate. Clinicians are especially interested in learning the drug resistance profile, and the substrate specificity and drug extrusion activity of the various multidrug resistance proteins in a given tumor sample. The demonstration of the transport activity of various multidrug resistance proteins (*e.g.* MDR1, MRP1, cMOAT) in the plasma membrane would require sensitive and reproducible *in vitro* multidrug resistance assays. Currently, a wide range of different approaches are used for functional MDR diagnostics, but the lack of standardization makes the comparison of literature data rather difficult (4).

The major requirements concerning current methods are the following: a) high sensitivity for the detection of relatively low levels of various MDR proteins; b) standardization, which is suitable for inter-laboratory comparison; c) functional characterization of the actual transport activity and substrate specificity of a given tumor sample; d) possible combination of different approaches for the simultaneous detection of several aspects of the MDR phenotype e) selective detection of various MDR proteins in order to elucidate the contribution of a single mechanism to the overall MDR phenotype.

Over the past few years a series of fluorescent dyes have been applied for MDR activity testing, the most common examples include fluorescent drugs like daunorubicin (5), the mitochondrial dye rhodamine 123 (6) and some of the acetoxy-methylester dyes like Fluo-3 AM (7) , BCECF AM and calcein AM (8, 9). New compounds have been developed with the hope of providing more sensitive P-glycoprotein testing (10, 11).

Recently we have demonstrated that the transport activity of both MDR1 and MRP1 can be quantitatively characterized by the measurement of the accumulation of the cell viability indicator, calcein in tumor cells. The sensitivity and MDR protein selectivity of the calcein assay has been established by using specific inhibitors of the MDR proteins (26). The

present single cell digital imaging study for the calcein accumulation assay of MDR1 and MRP1 expressing cells shows the simultaneous functional detection of two major human MDR proteins. The specificity of the assay was further enhanced by the combination of this functional assay with the immunofluorescence detection of MDR1. We propose that the high sensitivity, the selectivity between MDR1 and MRP1, and the compatibility with two-color immunofluorescence makes the quantitative calcein accumulation the assay of choice for complex functional and immunological testing of plasma membrane associated MDR.

Materials and Methods

Cell culturing. NIH 3T3 murine fibroblast cell line and its human MDR1-transfected counterpart (NIH 3T3 MDR1 G185, (12)) were obtained from Dr. M. M. Gottesman (National Institute of Cancer/National Institute of Health, Bethesda, MD) and were cultured in DMEM under standard conditions. Drug-selected HL60 MRP1 cells, kindly provided by Dr. Melvin Center, were cultured in RPMI medium as described in (13). Experiments with intact living cells were carried out in HPMI medium (14).

Calcein accumulation. A 1:1 mixture of $2.5x10^5$ HL60 MRP1 and $2.5x10^5$ NIH 3T3 MDR cells was attached to poly-L-lysin (Sigma) treated glass coverslips in a thermostatted sample chamber. Calcein accumulation was initiated by the addition of calcein acetoxy-methylester (AM) (Molecular Probes, Eugene, OR) in a final concentration of 0.25 μM to the incubation medium at 37°C. Inhibitors of MDR proteins, benzbromarone (40 μM) and verapamil (50 BM) were added as indicated. All experiments were repeated at least 3 times, and representative data and images were selected from a single experiment. Data are given as mean±SD.

Immunofluorescence labeling. For immunofluorescence staining the cells were fixed with 1% formaldehyde in HPMI medium for 20 minutes. Non-specific binding was prevented by 10% (w/v) BSA/HPMI blocking. After a short washing step the cells were labeled with the UIC2 monoclonal antibody (5 μg/ml), which reacts with extracellular epitope(s) of the MDR1 protein (15). Labeling was performed on the microscope stage at 20°C for 30 minutes, then the cells were washed twice with 1% BSA/HPMI medium, and once with HPMI. Thereafter, an anti-mouse tetramethylrhodamine B isothiocyanate (TRITC) conjugated second antibody (1:50 dilution) was applied, similarly to the first antibody. Finally the cells were washed twice with HPMI.

Imaging system. Cellular fluorescence was detected by the Photon Technology International (PTI, NJ) fluorescence digital imaging system. The imaging system consists of a Zeiss Axiovert 135 inverted microscope equipped with dichroic mirror sets (Chroma, OR); 40x oil immersion Neofluar lens; and two camera ports for the ICCD (Photonic Science. UK) and the silicon tube CCD (Hamamatsu) video cameras. Cells were incubated in a thermostatted sample chamber (Life Sciences, UK) on the microscope stage. Epifluorescence illumination was provided by a Deltascan (PTI) illuminator unit containing a 75W xenon lamp and Czerny-type monochromators. For the calcein accumulation measurements the sample was excited at 488 nm (2 nm bandwidth) for the UIC2/TRITC labeling experiment at 552 nm (5 nm bandwidth). Emitted fluorescence was detected between 515-545 nm for calcein, and at ≥590 nm for TRITC, respectively. 8 video images were collected and averaged at 5 second intervals and analyzed by the Imagemaster 1.31 software (PTI) on a DELL Optiplex PC workstation equipped with a DIPIX P360F Power Grabber video imaging board.

Calculation of the inhibitory efficiency of reversing agents. For the quantitative evaluation of the inhibitory potential of benzbromarone, the relative inhibitory potential was calculated according to equation (1). F0 designates the rate of calcein accumulation in the absence of MDR protein inhibitors, F_b indicates the rate of calcein accumulation in the presence of benzbromarone, and F_v is the rate of calcein accumulation after the addition of verapamil.

$$\text{inhibition (\%)} = \frac{F_b - F_{0*}}{F_v - F_0} 100 \qquad (1)$$

Results

The effect of benzbromarone and verapamil on calcein accumulation in HL60 MRP1 NIH 3T3 MDR1 cells. Differential interference contrast enhanced (DIC) images of the cells studied were obtained prior to the calcein accumulation measurements. Figure 1 demonstrates the attachment of living HL60 MRP1 and NIH 3T3 MDR1 cells to the poly-L-lysin treated glass coverslip in a DIC image. The cells keep their round shape for extended periods (more than 2 hours), *i.e.* at this stage complete attachment to the glass surface with full contacts and interaction with extracellular matrix still does not take place. It is not possible to differentiate between HL60 MRP1 and NIH 3T3 MDR1 cells on the basis of cellular morphology. The presented field of view contains a mixture of about 50 HL60 MRP1 and NIH 3T3 MDR1 cells.

Calcein accumulation in HL60 MRP1 and NIH 3T3 MDR1 cells was measured by fluorescence digital imaging techniques during an approximately 16 minute dye loading period. Calcein AM is a cell viability indicator which rapidly penetrates the cell membrane, thereafter, it is cleaved by non-specific cytoplasmic esterases, and the free acid calcein accumulates in the cell. Loading was started by the addition of 0.25 μM calcein AM to the incubation medium. Fluorescence images were taken at 5 second intervals. 32 individual cells were selected (region of interest, ROI 1-32) and the mean fluorescence in each ROI was analyzed as a function of time. For demonstration purposes we have selected a small region (Figure 1, rectangular area with white border) of the entire image with 7 individual cells. The kinetics of calcein accumulation, the effects of the MDR protein inhibitors benzbromarone and verapamil, and labeling with UIC2 anti-MDR1 antibody are demonstrated in Figure 2-4 in this representative area.

In order to analyze calcein fluorescence images, regions of interests were defined over individual cells, and in Figure 2 the mean values of fluorescence in the ROI are depicted as a function of time. As a consequence of the MDR1- and MRP1-mediated pumping out of calcein AM the initial rate of calcein accumulation is very low in these multidrug resistant cells. After the addition of benzbromarone, there was an initial higher rate of increase of fluorescence in the case of ROI 1 and 2 (Figure 3), and after approximately 600 seconds, the slope of calcein accumulation was stabilized again. In contrast to ROIs 1 and 2, the cells defined by ROIs

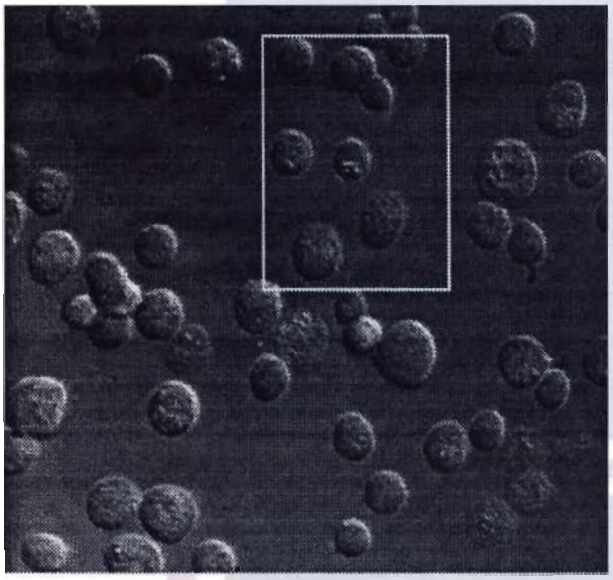

Figure 1. Differential interference contrast enhanced image of a mixture of living NIH 3T3 MDR1 and HL60 MRP1 cells. Cells were attached to a poly-L-lysin treated coverslip and DIC images were collected as described in Materials and Methods. A representative region containing 7 cells (see also Figure 2-4) from this field of view, selected for detailed analysis, is outlined here with a rectangular white border.

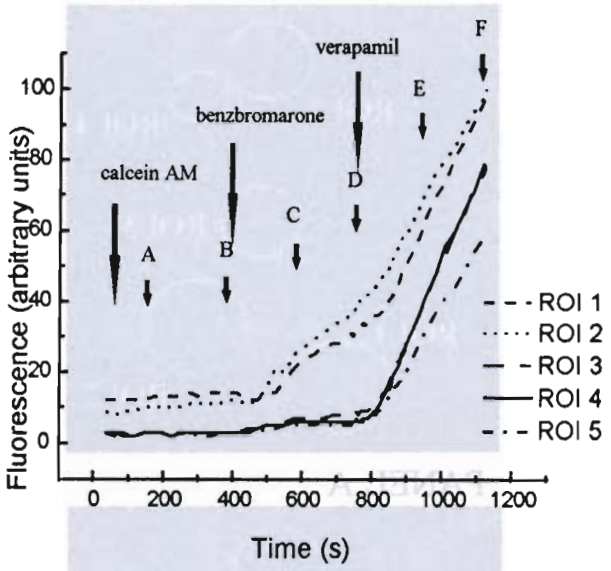

Figure 2. *Calcein accumulation kinetics of individual multidrug resistant cells defined by ROIs 1-5. After the addition of calcein AM to the incubation chamber, fluorescence images were collected at 5 second intervals for approximately 20 minutes. Afterwards the images were analysed by defining regions of interests (ROIs) over individual cells, and the time course of calcein accumulation is depicted here for 5 representative cells (ROI 1-5, see also Figure 3) in the rectangular area depicted in Figure 1. Each plot represents the sum of pixel values (in arbitrary units of fluorescence) in the specific ROI. The addition of calcein AM (0.25 μM), benzbromarone (40 μM) and verapamil (50 μM) is indicated by arrows. Representative images (Figure 3) were selected at different time points (indicated by arrowheads A-F) during the experiment.*

3-5 displayed a slight and short-lived increase, afterwards the rate of calcein accumulation remained almost identical to the initial dye uptake rate.

The addition of verapamil had a dual effect on these multidrug resistant cells. The benzbromarone-responsive cells, defined by ROI 1-2, still exhibited some calcein AM pumping activity after the benzbromarone treatment, since verapamil could further increase the rate of calcein accumulation in these cells. On the other hand, the calcein fluorescence in benzbromarone-insensitive cells (defined by ROI 3-5) dramatically increased after the addition of verapamil. After the addition of verapamil, the rate of calcein accumulation in ROI 1-2 and ROI 3-5 cells became almost identical. We assumed that after the addition of 50 μM verapamil the full inhibiton of the transport activity of both MDR proteins was achieved. The calcein transport activity of both MRP1 and MDR1 could be completely inhibited by 50 μM verapamil in spectrofluorometry and flow cytometry measurements as well (16, 17). No effects of benzbromarone and verapamil have been observed on the rate of calcein accumulation in drug-sensitive HL60 control and NIH 3T3 control cells in fluorescence digital imaging experiments (data not shown).

Fluorescence images at different intervals were selected from the entire time course of the experiment (Figure 3). At 151 and 396 seconds (Panel A and B, respectively) very low fluorescence could be observed in the cells, the initial fluorescence values did not exceed 20 arbitrary units. After the addition of benzbromarone (Panel C and D) a uniform increase in cellular fluorescence was clearly demonstrated over ROIs 1 and 2, while there was hardly any change in calcein fluorescence of ROIs 3-5 at 580 and 745 seconds. Images taken after the addition of verapamil at 946 and 1126 seconds (Panel E and F, respectively) demonstrate the abrupt increase of calcein fluorescence in ROIs 3-5, and also the benzbromarone responsive ROIs 1-2 achieved higher fluorescence intensities.

Quantitative analysis of the calcein accumulation of MDR1 and MRP1 expressing cells. For the quantitative characterization of the transport-inhibitory potential of benzbromarone and verapamil, we have calculated the relative inhibitory efficiency for each cell. 100% inhibition was achieved by verapamil treatment, and the inhibitory potential of benzbromarone was compared to that of verapamil. The slope of calcein accumulation was determined in phases A to B (initial rate), C to D (benzbromarone addition) and E to F (verapamil addition) as indicated in Figure 2, and normalized for the rate of fluorescence increase after verapamil inhibition. The inhibitory potential was calculated according to equation (1).

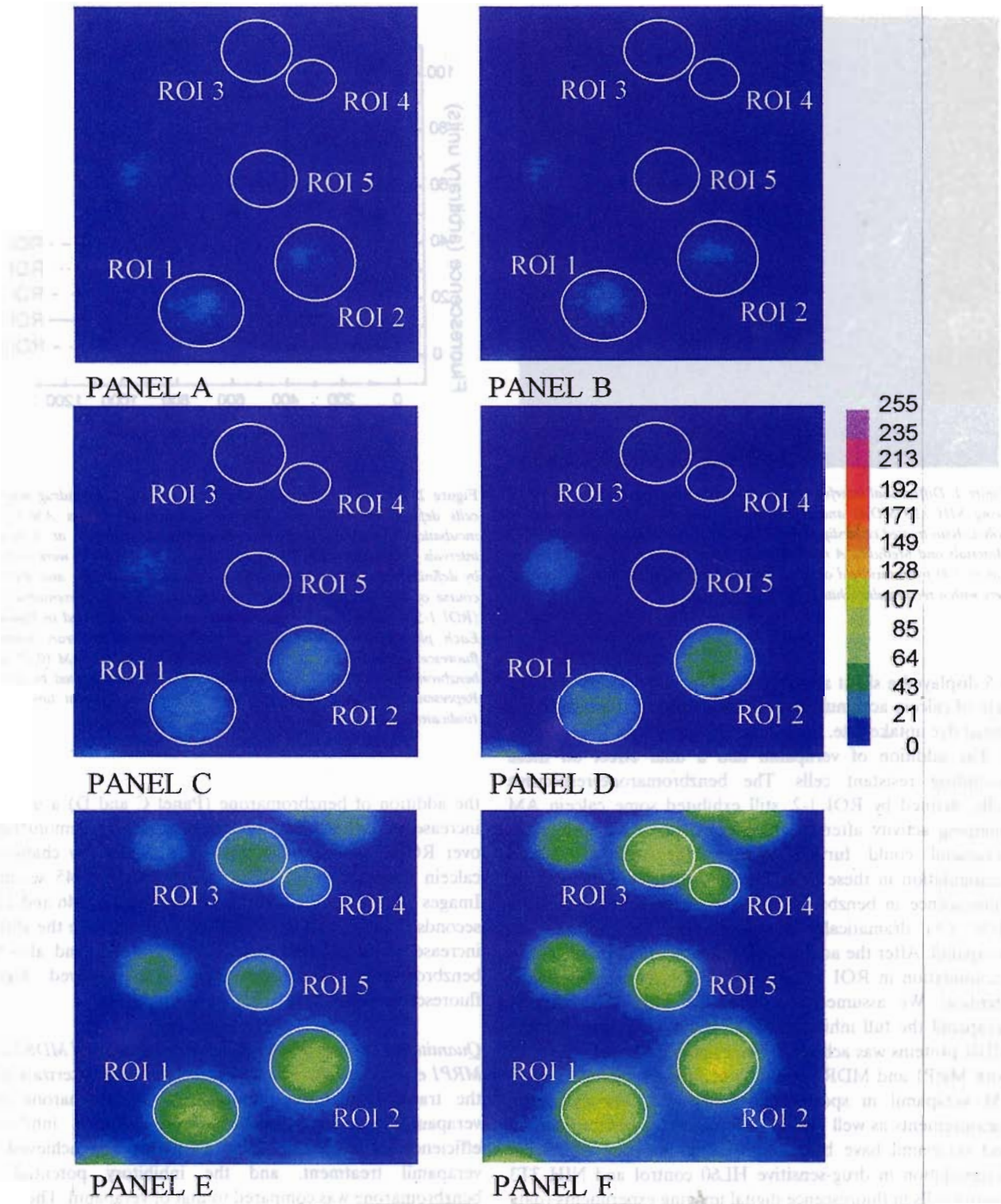

Figure 3. *Representative images selected from the 20 minute time course of calcein accumulation in MDR cells. MDR cells were loaded with calcein AM, and representative images taken at the time points according to Figure 2 are presented here. The ROIs No. 1-5 were defined within the selected area of Figure 1. Images are displayed in pseudocolor encoding. the different intensities of fluorescence (i.e. pixel values between 0-255) were artificially color-encoded according to the scale bar. Images of Panel A and B were collected after the addition of calcein AM/HPMI (0.25 μM) solution, for Panel C and D after the addition of benzbromarone (40 μM) and for Panel E and F after the addition of verapamil (50 μM).*

Benzbromarone exhibited high inhibitory potential in the case of ROIs 1-2 (Table I), with 29.1% and 46.5%, respectively, while the maximum inhibition for ROI 3-5 did not exceed 5% in any case. The complete analysis of 32 cells showed two populations: a benzbromarone responsive population of 15 cells where the average inhibitory efficiency of benzbromarone was 47±20%, and an exclusively verapamil sensitive population of 17 cells with an average benzbromarone inhibitory efficiency of 8±3%. These quantitative data support the view that individual multidrug resistant cells can be separated into two distinct populations by analyzing the inhibitory potential of the MRP1-specific benzbromarone and the nonspecific MDR protein inhibitor, verapamil.

UIC2/TRITC labeling of multidrug resistant cells. We have applied a human MDR1 external epitope-specific monoclonal antibody, UIC2, in order to visualize the expression of MDR1 in the plasma membrane of multidrug resistant cells. The immunostaining was performed as described in Materials and Methods and fluorescent images were collected with the imaging system. A strong UIC2/TRITC fluorescence was detected in ROI 3-5 cells, while ROI 1-2 cells exhibited practically no staining (Figure 4). The mean fluorescence value of UIC2/TRITC labeling was also measured in ROIs 1-5 (Table I) for the semi-quantitative evaluation of cell surface MDR1 expression, and the corresponding mean fluorescence was 65, 70, 61 for ROI 3, 4 and 5, respectively. In spite of the heterogeneous staining (intense staining of plasma membrane, low staining in the middle of the cell) and the differences in cell size, the measured and calculated mean fluorescence values gave a good indication about the level of staining. The very low mean fluorescence value (less than 36 arbitrary units) for ROI 1-2 cells also indicates the lack of specific staining. The visual picture and the mean fluorescence values conclusively indicate high expression of human MDR1 in ROI 3-5 cells, on the other hand, ROI 1-2 cells do not express this multidrug resistance protein in spite of their high efficiency calcein AM transport activity. Out of the total 32 cells analyzed in this experiment, the mean fluorescence of the 17 UIC2/TRITC positive cells was 64±20, while a 23±8 mean fluorescence value was measured in the UIC2/TRITC negative population (15 cells).

The quantitative data of the calcein accumulation assays were compared with those obtained by UIC2/TRITC labeling. Cells were divided into two groups during the analysis. If the inhibitory potential of benzbromarone was more than 10% and verapamil was also efficient in increasing calcein accumulation, we considered the cell functionally MRP1 positive. The criteria of functional MDR1 positivity were less than 10% inhibitory potential of benzbromarone, and concurrent inhibitory potential by verapamil. Functionally MRP1 positive cells exhibited no UIC2/TRITC staining (Table I, Figure 2 and 3), while functionally MDR1 positive cells appeared as strongly UIC2/TRITC positive cells (Figure 2 and 4). We observed a discrepancy between functional data and the cell surface staining in case of one cell out of the 32 cells analyzed in this experiment.

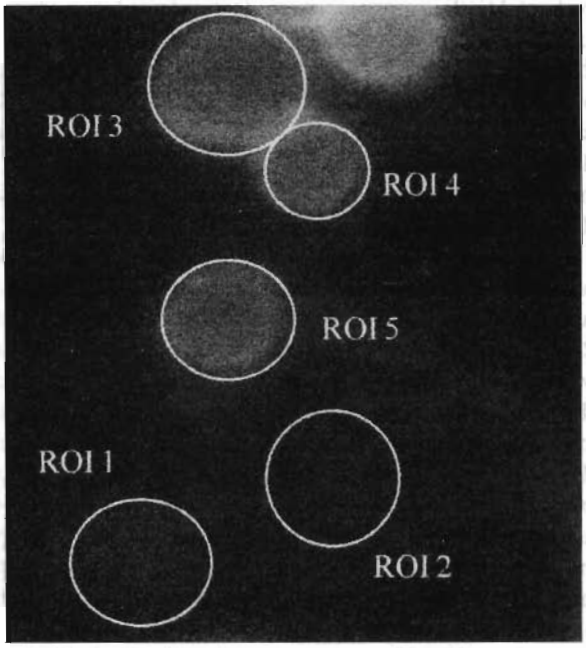

Figure 4. *The mixture of NIH 3T3 MDR1 and HL60 MRP1 cells were fixed by formaldehyde and stained with the UIC2 mAb (1 st antibody) and a TRITC conjugated anti-mouse IgG antibody, as described in Materials and Methods. Red fluorescence images were taken of the stained sample and the same ROIs as in Figure 3 were used for the analysis of UIC2/TRITC labeling. The sum of pixel values for ROIs 1-5 are given in Table I.*

Discussion

In the past few years several attempts have been made to improve MDR protein detection. One of the main purposes was the development of specific and sensitive assay systems which are also suitable for clinical diagnostic testing. Although studying the pumping activity of these proteins provided the biochemical background for these developments, several difficulties have been recognized in clinical MDR testing.

It has been demonstrated that the external epitope specific anti-MDR monoclonal antibodies (UIC2, MRK 16) were superior in sensitivity over antibodies recognizing internal epitopes (C219, JSB-1) (18, 19). The two commercially available anti-MRP1 monoclonal antibodies (R1 and M6), recognize internal epitopes (19, 20). The requirement of the permeabilization of the plasma membrane (21) and the possibility of increased non-specific intracellular staining might complicate detection of low level MRP1 expression by flow cytometry. There is a low, but almost ubiquitous expression of MRP1 in most human tissues tested so far, including liver, pancreas and lung epithelium; and also high

levels of MRP1 expression were demonstrated in a series of human malignancies, including non-small cell lung cancers (22). In comparison to MDR1, it might be even more difficult to assess the significance of various levels of MRP1 expression and to define the level of clinically significant MRP1 expression. Moreover, the expression of both MDR1 and MRP1 in the same cells has been reported in a series of MDR cell lines (23).

A discrepancy between high MDR1 expression levels and rhodamine 123 efflux capacity in acute myeloid cell lines with various stages of differentiation has also been demonstrated (24). Concerning clinical cases, only limited data are available about the significance and frequency of mutations which may render the MDR proteins inactive, but this possibility underlines the importance of multiparameter MDR testing. There are two major possibilities (among several other combinations) for developing functional multiprotein MDR assays: a) application of selective dyes and non-selective inhibitors of transport activity, b) the combination of non-selective fluorescent dyes with selective inhibitors of the different MDR proteins. The combination of rhodamine 123 efflux measurement with the cyclosporine analogue PSC 833 was proposed as a selective MDR1 assay (25). However, rhodamine 123 is effluxed by MRP1 too, and cyclosporine A (at relatively higher concentrations) was not selective between MDR1 and MRP1 in the calcein accumulation assay (26). Other disadvantages of the rhodamine efflux assay are discussed elsewhere (17).

MRP1-selective fluorescent dyes include the glutathione conjugate-forming N-pyrenemaleimide, but alterations of glutathione conjugation and changes in glutathione levels are common in multidrug resistant cells. Dual parameter detection (immunofluorescence detection and functional assessment) of MDR proteins should provide relevant data about the relative contribution of the different MDR proteins to overall drug resistance.

The current study focuses on the application of a functional MDR protein assay, the calcein accumulation method, for the simultaneous detection and characterization of multiple MDR protein activity in tumor cell lines and clinical samples. Recently, we have suggested a novel quantitative parameter of MDR protein function (17). We have compared the sensitivity and reproducibility of the quantitative calcein accumulation assay (for spectrofluorometry and flow cytometry) with Western-blotting and flow cytometry immunophenotyping of MDR1 in a series of mammalian multidrug resistant cell lines. An excellent correlation has been found between the multidrug resistance activity factor, MAF (calculated from the calcein AM transport activity of MDR1) and protein expression levels in mammalian multidrug resistant cell lines. We have also demonstrated that new groups of potential reversing agents of MRP1, including the uric acid transport inhibitor (benzbromarone) the antitumor prostaglandin (PGA1) and the maleimide derivative (N-ethyl-maleimide) at low concentrations

Table I. *The inhibitory potential of benzbromarone in the calcein accumulation assay (a functional marker for MRP1 activity) and the UIC2 labeling of MDR cells. The efficiency of the inhibition of calcein AM transport by benzbromarone was compared to that of verapamil for individual cells according to equation (1) of Materials and Methods. UIC2/TRITC labeling was measured in ROIs 1-5 and the sum of pixel values are given for individual cells.*

	% inhibition by benz-bromarone	UIC2 labeling (arb. unit)*
ROI 1	29.1	35
ROI 2	46.5	30
ROI 3	4.9	65
ROI 4	0.8	70
ROI 5	2.2	61

*UIC2 background values varied between 0-30 arb. unit.

selectively modulate the MRP1-mediated calcein AM extrusion activity, while these compounds have no effect on the transport activity of MDR1. However, most of the substrates/modulators of MDR1 (*e.g.* cyclosporine A, verapamil, vinblastine) were excellent inhibitors of the calcein AM transport activity of MRP1 as we!l (25). At present, the only specific inhibitor of MDR1 transport activity is the inhibitory mAb UIC2; however, we were unable to fully inhibit calcein AM transport activity even at high concentrations of UIC2, where saturation of cell surface staining takes place (14).

The present results confirmed the effectiveness and high sensitivity of the calcein accumulation assay for both MDR and MRP1 expressing cells. Since both MDR1 and MRP1 expel calcein AM, the selectivity of such a functional assay could solely be based on the selectivity of the applied modulators. Benzbromarone selectively modulated the UIC2-negative population of MDR cells (compare Figure 3 with Figure 4), while verapamil was an efficient inhibitor of both MDR1 and MRP1 mediated calcein AM transport in our system (Figure 3) (26). We have found an excellent correlation between MDR1/MRP1 discrimination based on the calcein accumulation assay and anti-MDR1 UIC2 labeling. Although single cell fluorescence imaging is time consuming, and therefore only low capacity screening of MDR protein expression and function is possible, it might be a useful alternative in selected cases. The heterogeneous expression and function of MDR proteins could be studied in, *e.g.* a) bone marrow samples prior to autologous bone marrow transplantation in order to assess the efficiency of the elimination of the drug resistant tumor cell population, b) in

transfected cells for testing MDR protein constructs at the single cell level, c) in biopsy samples with a usually very low number of cells. The feasibility of dual labeling as demonstrated in this single cell model system provides the possibility of flexible combination of a quantitative calcein accumulation assay with immunostaining of *e.g.* cluster of differentiaton (CD) markers also in flow cytometry based clinical studies.

Acknowledgements

This work has been supported by research grants from OTKA (F13187 and 17602), FIRCA-NIH, FKFP 1006, ETT and OMFB. Balázs Sarkadi is a Howard Hughes International Scholar. The technical help of Andrea Siposs is grateffully acknowledged.

References

1 Loe DW, Deeley RG and Cole SP: Biology of the multidrug resistance-associated protein, MRP. Eur J Cancer *32A:* 945-957, 1996.
2 Germann UA: P-glycoprotein - a mediator of multidrug resistance in tumour cells. Eur J Cancer *32A:* 927-944, 1996.
3 Gottesman MM and Pastan I: Biochemistry of multidrug resistance mediated by the multidrug transporter. Annu Rev Biochem *62:* 385-427 1993.
4 Beck WT, Grogan TM, Willman CL, Cordon-Cardo C, Parham DM, Kuttesch JF, Andreeff M, Bates SE, Berard CW, Boyett JM, Brophy NA, Broxterman HJ, Chan HS, Dalton WS, Dietel M, Fojo AT, Gascoyne RD, Head D, Houghton PJ, Srivastava DK, Lehnert M, Leith CP, Paietta E, Pavelic ZP, Weinstein R: Methods to detect P-glycoprotein-associated multidrug resistance in patients' tumors: consensus recommendations. Cancer Res *56:* 3010-3020, 1996.
5 Gheuens EE, van der Heyden SA, Elst HE, Van Oosterom AT and De Bruijn EA: Comparison of daunorubicin and Fluo-3 for detection of multidrug resistance in human tumor cells. Cancer Detect Prev *21:* 78-82, 1997.
6 Weaver JL, Pine PS, Aszalos A, Schoenlein PV, Currier SJ, Padmanabhan R and Gottesman MM: Laser scanning and confocal microscopy of daunorubicin, doxorubicin, and rhodamine 123 in multidrug-resistant cells. Exp Cell Res *196:* 323-329, 1991.
7 Wall DM, Hu XF, Zalcberg JR and Parkin JD: Rapid functional assay for multidrug resistance in human tumor cell lines using the fluorescent indicator fluo-3. J Natl Cancer Inst *83:* 206-207, 1991.
9 Versantvoort CH, Bagrij T, Wright KA and Twentyman PR: On the relationship between the probenecid-sensitive transport of daunorubicin or calcein and the glutathione status of cells overexpressing the multidrug resistance associated protein (MRP). Int J Cancer *63:* 855-862, 1995.
10 Lelong IH, Guzikowski AP, Haughland RP, Pastan 1, Gottesman MM and Willingham MC: Fluorescent verapamil derivative for monitoring activity of the multidrug transporter. Mol Pharmacol *40:* 490-494, 1991.
11 Frey T, Yue S and Haugland RP: Dyes providing increased sensitivity in flow-cytometric dye-efflux assays for multidrug resistance. Cytometry *20:* 218-227, 1995.
12 Bruggemann EP, Currier SJ, Gottesman MM and Pastan I: Characterization of the azidopine and vinblastine binding site of P-glycoprotein. J Biol Chem *267:* 21020-21026, 1992.
14 Homolya L, Hollo Z, Germann UA, Pastan 1, Gottesman MM and Sarkadi B: Fluorescent cellular indicators are exdruded by the multidrug resistance protein. J Biol Chem *268:* 21493-21496, 1993.
15 Mechetner EB and Roninson IB: Efficient inhibition of P-glycoprotein-mediated multidrug resistance with a monoclonal antibody. Proc Natl Acad Sci USA *89:* 5824-5828, 1992.
16 Hollo Z, Homolya L, Davis CW and Sarkadi B: Calcein accumulation as a fluorometric functional assay of the multidrug transporter. Biochim Biophys Acta *1191:* 384-388, 1994.
17 Homolya L, Hollo Z, Muller M, Mechetner EB and Sarkadi B: A new method for the quantitative assessment of P-glycoprotein-related multidrug resistance in tumor cells, British J Cancer *73:* 849-855, 1996.
18 Lehne G, De Angelis P, Calusen OPF, Egeland T, Tsuruo T and Rugstad HE: Binding diversity of antibodies against external and internal epitopes of the multidrug resistance gene product P-glycoprotein. Cytometry *20:* 228-237, 1995.
19 Van Acker KL, Van Hove LM and Bogaerts MA: Evaluation of flow cytometry for multidrug resistance detection in low resistance K562 cells using daunorubicin and monoclonal antibodies. Cytometry *14:* 736-746, 1993.
20 Flens MJ, Izquerido MA, Scheffer GL, Frik JM, Meijer CJLM, Scheper RJ and Zaman GJR: Immunochemical detection of the multidrug resistance-associated protein MRP in human multidrug-resistant tumor cells by monoclonal antibodies. Cancer Res *54:* 4557-4563, 1994.
21 Bakos E, Hegedus T, Hollo Z, Welker E, Tusnady GE, Zaman GJR, Flens MJ, Varadi A and Sarkadi B: Membrane topology and glycosylation of the human multidrug resistance-associated protein (MRP). J Biol Chem *271:* 12322-12326, 1996.
22 Giaccone G, van ARk-Otte J, Rubio GJ, Gazdar AF, Broxterman HJ, Dingenmans AM, Flens MJ, Scheper RJ and Pinedo HM: MRP is frequently overexpressed in human lung cancer cell lines, in non-small -cell lung cancer and in normal lungs. Int J Cacner *66:* 760-767, 1996.
23 Izquierdo MA, Shoemaker RH, Flens MJ, Scheffer GL, Wu L, Prather TR, Scheper RJ: Overlapping phenotypes of multidrug resistance among panels of human cancer-cell lines. Int J Cancer *65:* 230-237, 1996.
24 Bailly JD, Muller C, Jaffrezou JP, Demur C, Cassar G, Bordier C, Laurent G: Lack of correlation between expression and function of P-glycoprotein in acute myeloid leukemia cells. Leukemia *9:* 799-807, 1995.
25 Feller N, Kuiper CM, Lankelma J, Ruhdal JK, Scheper RJ, Pinedo HM, Broxterman HJ: Functional detection of MDR1/P170 and MRP/P190-mediated multidrug resistance in tumour cells by flow cytometry. Br J Cancer *72:* 543-549, 1995.
26 Holló Z, Homolya L, Hegedus T and Sarkadi B: Transport properties of the multidrug resistance associated protein (MRP) in human tumour cells. FEBS Letters *363:* 99-104, 1996.

Received January 13, 1998
Accepted January 27, 1998

dc_46_10

3. sz. közlemény

dc_46_10

British Journal of Haematology, 2001, **112**, 308–314

Calcein assay for multidrug resistance reliably predicts therapy response and survival rate in acute myeloid leukaemia

Éva Karászi,[1] Katalin Jakab,[2] László Homolya,[3] Gergely Szakács,[3] Zsolt Holló,[2] Béla Telek,[4] Attila Kiss,[4] László Rejtô,[4] Sarolta Nahajevszky,[2] Balázs Sarkadi,[2,3] and János Kappelmayer[1] [1]*Department of Clinical Biochemistry and Molecular Pathology, Medical and Health Sciences Centre, University of Debrecen,* [2]*National Institute of Haematology and Immunology, Budapest,* [3]*Membrane Research Group of the Hungarian Academy of Sciences, Budapest, and* [4]*Second Department of Medicine, Medical and Health Sciences Centre, University of Debrecen, Hungary*

Received 24 July 2000; accepted for publication 2 October 2000

Summary. In this study, we evaluated the suitability of the calcein assay as a routine clinical laboratory method for the identification of multidrug-resistant phenotype in acute leukaemia. This study presents the results of the calcein tests obtained in two large haematological centres in Hungary. Assays were performed with blast cells of 93 *de novo* acute leukaemia patients, including 65 patients with acute myeloid leukaemia (AML). Results were expressed as multidrug resistance activity factor (MAF) values. AML patients were divided into responders and non-responders and MAF values were calculated for each group. In both centres, responder patients displayed significantly lower MAF values than non-responders ($P = 0{\cdot}0045$ and $P = 0{\cdot}0454$). Cut-off values were established between the MAF_R + SEM and MAF_{NR} − SEM values. On the basis of these cut-off levels, multidrug resistance (MDR) negativity showed a 72% predictive value for the response to chemotherapy, whereas MDR positivity was found to have an average predictive value of 69% for therapy failure. MDR activity was a prognostic factor for survival rate and the test was suitable for detecting patients at relapse. The calcein assay can be used as a quantitative, standardized, inexpensive screening test in a routine clinical laboratory setting. The assay detects both P-glycoprotein and multidrug resistance-associated protein activities, and identifies AML patients with unfavourable therapy responses.

Keywords: P-glycoprotein, calcein-AM, acute myeloid leukaemia, verapamil.

Several types of drug resistance mechanisms have been identified in acute leukaemias, including the presence of the multidrug resistance proteins; MDR1 or P-glycoprotein (MDR1-Pgp) and multidrug resistance-associated protein (MRP1) seem to be the most frequent and best-characterized causes of therapy failure (Marie *et al*, 1996; Nussler *et al*, 1996; Dalton, 1997; Hunault *et al*, 1997; Bradshaw & Arceci, 1998). Both MDR1-Pgp and MRP1 are transmembrane glycoproteins and work as ATP-dependent efflux pumps that are able to remove hydrophobic molecules, including cytotoxic drugs and dyes, from cells. The expression of the multidrug resistance (MDR) proteins confers resistance by maintaining the level of a wide range of currently used anti-neoplastic drugs below a cell-killing threshold in the tumour cells. Proper evaluation of clinical MDR should lead to a more efficient treatment of malignant diseases. However, the routine laboratory assessment of the level of such a resistance in clinical samples awaits standardization.

There are at least three different approaches to detect clinical MDR: (i) functional tests measuring drug or dye efflux/accumulation; (ii) detection of the expression level by monoclonal antibodies; and (iii) detection of the mRNA level by Northern blot analysis or quantitative reverse transcription polymerase chain reaction (RT-PCR). Several investigations have compared and evaluated these approaches (Legrand *et al*, 1998). Some studies found a good correlation between the results of the functional test and antigen or mRNA detection (Leith *et al*, 1995; Broxterman *et al*, 1996; Homolya *et al*, 1996), whereas others failed to confirm these data (Brophy *et al*, 1994). The inconsistency and variability are largely the result of technical differences and the absence of a standardized methodology. Another possible

Correspondence: János Kappelmayer MD PhD, Department of Clinical Biochemistry and Molecular Pathology, Medical and Health Sciences Centre, University of Debrecen, PO Box 40, H-4012, Hungary. E-mail:kappelmayer@jaguar.dote.hu

explanation is that functional tests measure transport activity maintained by different drug transporters. Recent studies indicated a significant contribution of MRP1 to the multidrug resistance phenotype observed in leukaemia (Nooter *et al*, 1995, 1996; Hollo *et al*, 1996; Bradshaw & Arceci, 1998; Legrand *et al*, 1998). However, the immunological detection of MRP1 imposes a special problem as no antibodies against external epitopes of MRP1 are currently available (Den Boer *et al*, 1997; Boutonnat *et al*, 1998). Furthermore, MDR positivity may depend on differences in sample preparation, the type and binding site of antibody used, possible cross-reactions between MDR1 and MDR3 proteins, and on the probes used for reporting MDR activity. In addition, the results of molecular biological methods may be compromised by the presence of normal cells, as molecular genetic methods can not distinguish normal and tumour cells (Hegewisch-Becker & Hossfeld, 1996).

From the clinical laboratory point of view, the important question is how effectively the proteins function as drug transporters and, indeed, the clinical outcome shows the strongest correlation with functional measurements, as opposed to antigen or mRNA detection (Lamy *et al*, 1995; Del Poeta *et al*, 1996; Martinez *et al*, 1997).

Many types of functional MDR tests have been described: some use drugs (daunorubicin, doxorubicin) and others use dyes (rhodamin 123, calcein, $DiOC_2$) as fluorescent probes (Maslak *et al*, 1994; Feller *et al*, 1995; Minderman *et al*, 1996; Tiberghien & Loor, 1996; Szakacs *et al*, 1998; Sievers *et al*, 1999). A multiparameter analysis – by simultaneously applying two independent tests – can be helpful in defining MDR-positive phenotype, as recommended in a previous consensus document (Beck *et al*, 1996). However, as with all other types of laboratory diagnostics, a single quantitative functional assay, if performed in a standardized form with appropriate sensitivity and specificity, may serve as a front-line test for the identification of drug resistance.

Members of our group have previously shown that calcein-acetoxymethyl ester (calcein-AM), the hydrophobic derivative of calcein, is actively extruded from resistant cells by both MDR1-Pgp and MRP1 (Hollo *et al*, 1998). The consequent reduction in the cellular accumulation of the fluorescence-free calcein, relative to that seen when the transport is blocked by an inhibitor, e.g. verapamil, provides a quantitative measure of transport activity (Hollo *et al*, 1994, 1998; Homolya *et al*, 1996; Szakacs *et al*, 1998). Here, we demonstrate that the use of the calcein assay can be assembled to provide sufficient precision, accuracy and stability of the components as a routine diagnostic procedure. We show that MDR1-P-gp- and/or MRP1-mediated drug resistance, as determined using this assay, predicts therapy response and survival rate in AML patients.

PATIENTS AND METHODS

Patients and samples. The study was performed in two large haematological centres in Hungary, at the University of Debrecen and at the National Institute of Haematology, Budapest, between December 1997 and December 1999. The results of calcein assays performed with the samples from 93 untreated *de novo* acute leukaemia patients are presented [65 acute myeloid leukaemia (AML) and 28 acute lymphoblastic leukaemia (ALL) patients]. The mean age of the 65 AML patients was 50·5 years and the sex distribution was 40 male and 25 female patients. Classification of AML patients was established using FAB criteria, and immunophenotyping was carried out in all cases using three-colour analysis to confirm diagnosis. Distribution of AML subtypes was as follows: M1:9, M2:11, M3:6, M4:25, M5:7, M6:1, M7:3 and biphenotypic:3. In Debrecen, the patients were uniformly treated with the 7 + 3 remission induction protocol, consisting of cytosine arabinoside 200 mg/m^2 for 7 d and anthracycline for 3 d (adriamycin 45 mg/m^2 or idarubicin 12 mg/m^2), supplemented with 100 mg/m^2 etoposide in the case of AML M4 and M5. In Budapest, the patients were treated with the 7 + 3 remission induction protocol, consisting of cytosine arabinoside 200 mg/m^2 for 7 d and anthracycline for 3 d (idarubicin 12 mg/m^2 or daunoblastin 60 mg/m^2), supplemented with 100 mg/m^2 etoposide for 4 d in the case of AML M4 and M5. Patients were given one or two cycles of the above protocol depending on the response to therapy. To evaluate treatment efficiency, bone marrow and peripheral blood were examined morphologically at 4 weeks. Complete remission was defined as less than 5% blasts in the bone marrow and no blasts in the peripheral blood (Cheson *et al*, 1990).

Clinical laboratory procedures. Immunophenotypic analysis of surface and intracellular markers was performed using standard three-colour methodology as described previously (Rothe *et al*, 1996). Prognostic factors such as leucocyte count, percentage of CD34-positive cells and lactate dehydrogenase activity were determined using standard laboratory procedures.

Calcein assay. Measurements were performed at the time of diagnosis as described previously (Homolya *et al*, 1993; Hollo *et al*, 1994), with slight modification and small differences in the two centres. Briefly, mononuclear cells from peripheral blood and bone marrow samples were separated on Ficoll gradient (Histopaque-1077, Sigma, St Louis, MO, USA) and washed twice in phosphate-buffered saline (PBS). In Debrecen, 5×10^5 cells were preincubated for 5 min at room temperature in Hanks' balanced salt solution (HBSS, Sigma) containing 50 μmol/l verapamil (Sigma) or its solvent HBSS. In Budapest, 5×10^5 cells solely from bone marrow samples were preincubated for 5 min at room temperature in HPMI medium (pH 7·4) containing 100 μmol/l verapamil or 0·5% dimethyl sulphoxide (DMSO). The cells were then incubated with 0·25 μmol/l calcein-AM (Molecular Probes, Eugene, OR, USA) for 10 min at 37°C in both centres. After a fast centrifugation (15 s, 14 000 r.p.m.), the cells were resuspended and 5 μg/ml propidium-iodide (PI) was added to investigate cell viability. Samples were stored at 4°C and measured within 4 h on a FACScan or FacsCalibur flow cytometer (Becton Dickinson Biosciences, San Jose, CA, USA) in Debrecen and Budapest respectively. During analysis, three regions (from R1 to R3) were defined. Blast

cells were selected on forward scatter-side scatter (FS-SS) dot plot (R1), cells with low fluorescence intensity were excluded on FL1 histogram (R2), and dead cells were excluded on the basis of their high PI fluorescence (R3). A gate was defined as R1 + R2 + R3 for the green fluorescence; thus, only live, leukaemic blast cells were examined. List mode data of 10 000 PI-negative cells were collected using either CELLQUEST or LYSIS II software. The activity of the multidrug transporters was expressed as a dimensionless value using the mean fluorescence intensity (MFI) values measured in the presence and absence of verapamil (MFI_V and MFI_0 respectively). The MDR activity factor (MAF) was determined using the formula: $MAF = 100 \times (MFI_V - MFI_0)/MFI_V$ as previously described (Hollo *et al*, 1994).

Quality control measurements for calcein assay. Human epidermoid carcinoma cell line and peripheral blood samples from normal subjects and patients with AML were used as quality control for this method. KBV1 (human MDR1-positive) cell line was cultured in Dulbecco's modified Eagle medium supplemented with 10% fetal bovine serum and 0·2 μg/ml vinblastine at 37°C and 5% CO_2 content. MAF values were determined for accuracy.

The stability of assay components (stock solutions of verapamil in HBSS and calcein-AM in DMSO) stored at 4°C and −20°C was monitored for up to 12 months. MAF values of the resistant cell line were determined using the stored reagents at 0, 1, 3, 6 and 12 months. At the same time, points fluorescence intensity of stored calcein-AM was measured using a Perkin Elmer fluorescence spectrophotometer at an excitation wavelength of 488 nm and an emission wavelength of 525 nm, with a 12-nm slit to monitor potential hydrolysis. We found that the stock solution of modulator verapamil (8 mmol/l in HBSS) could be stored for up to 1 year at both 4°C and −20°C without any effect on its inhibitory activity. The stock solution of calcein-AM (100 μmol/l in DMSO) stored at 4°C showed considerable hydrolysis after 12 months of storage, but can reliably be used for up to 12 months when stored at −20°C. The procedure was patented as 'Assay and reagent kit for the quantitative *in vitro* determination in biological specimens of the activity of proteins causing multidrug resistance in tumors' United States Patent no. 5 872 014, European Patent no. PCT/Hu95/0042.

Statistical analysis. Differences for significance between groups were analysed using the unpaired Student's *t*-test. Multiple logistic regression models were used for evaluating therapy response and Cox regression was used for analysis of survival data. Kaplan–Meier survival curves were evaluated statistically using the log-rank test. *P*-values below 0·05 were reported as significant.

RESULTS

Reproducibility of the test

The calcein assay was studied for precision in an MDR-positive cell line, as well as in peripheral blood samples from normal subjects and patients with AML. Although the test was found to be the most reproducible in the cell line, which demonstrated extremely high levels of drug resistance, it was also reproducible in a wide range of MAF values in clinical samples (Table I).

Table I. Reproducibility of the calcein assay.

Sample	Mean MAF	CV (%)
KBV1 cell line	97·9	0·3
AML sample	45·8	11
Normal sample	16	13

To examine the reproducibility of the test, we checked within-run precision with different samples in a wide range of MAF: (1) KBV1 (human MDR-positive) cell line; (2) peripheral blood sample from an AML patient; (3) peripheral blood from a healthy individual. With each sample, 10 consecutive measurements were carried out using 50 μmol/l verapamil as the modulator. Mean MAF values and the coefficient of variation (CV) are shown. These results also confirm the accuracy of the test, showing high MAF values with the P-gp-expressing cell line and low values with the normal peripheral blood sample.

Comparison of MDR activity of AML and ALL cases

We have investigated the MAF values in 93 *de novo* acute leukaemia cases (65 AML and 28 ALL). The results obtained are presented separately for each centre because, in Debrecen, mostly peripheral blood samples were assayed with 50 μmol/l verapamil as a transport inhibitor, whereas the samples in Budapest, were obtained from bone marrow and the final concentration of verapamil was 100 μmol/l. Otherwise, all steps of the assay and the data analysis were the same.

In both centres, the mean MAF values in ALL were not different from that found in normal mononuclear cells ($n = 40$, mean $\pm$ SEM $= 11{\cdot}9 \pm 6{\cdot}4$). In contrast, the

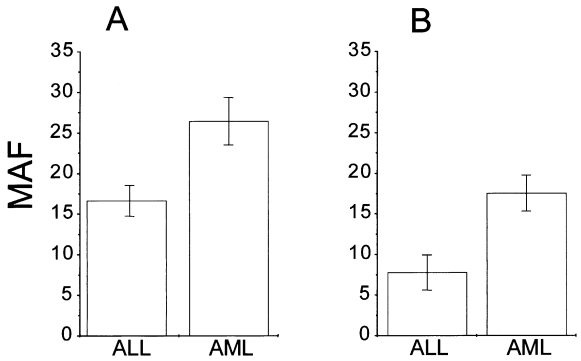

Fig 1. Comparison of MAF values obtained in AML and ALL cases in both centres. The mean MAF ± SEM values obtained in the Department of Clinical Biochemistry and Molecular Pathology at the University of Debrecen (A), and the National Institute of Haematology and Immunology in Budapest (B) are plotted. The mean MAF values in AML patients were found to be significantly higher than those in ALL cases in both centres. A. The values were 26·5 and 16·6 in AML ($n = 22$), and ALL ($n = 14$) respectively ($P = 0{\cdot}029$). B. The values were 17·6 and 7·8 in AML ($n = 43$) and ALL ($n = 14$) respectively ($P = 0{\cdot}021$).

AML cases gave significantly higher MAF values than ALL cases (Fig 1). The differences in the absolute MAF values in the Debrecen and Budapest centres can be explained, either by the different origin of the samples or by the small variance in methodology, i.e. by the difference in verapamil concentration.

Determination of the predictive value of the test for induction therapy

In order to analyse the clinical relevance of the MAF values determined, the 65 patients with AML were divided into two groups on the basis of their response to remission induction chemotherapy. In the group of responders (R), complete remission was achieved during the first or second course of chemotherapy, whereas in non-responders (NR), blast counts remained above 5% in bone marrow and/or blasts were still detectable in the peripheral blood. Mean values of MAF and SEM for the two centres were calculated in both groups. MAF values of 17·1 and 14·1 were obtained for responders, whereas non-responder patients displayed significantly higher values of MDR activity (MAF values were 32·9 and 23·3 respectively).

Based on the distribution of MAF values in responders and non-responders we established cut-off values between the (MAF_R + SEM) and (MAF_{NR} − SEM) values. These cut-off limits were 25 and 20 in the Debrecen and Budapest centres respectively. The validity of these values was confirmed statistically by area under the curve (AUC) analysis of receiver operator characteristic (ROC) curves and we found the highest sensitivity and specificity of the test at these cut-off limits. By using the respective cut-off values, patients were divided into MDR-positive and MDR-negative groups, and the percentage of responders and non-responders in both groups was calculated by pooling AML samples from both centres to determine the positive and negative predictive value of the test (Fig 2). As documented, MDR negativity showed a high predictive value for therapy response (72%), whereas the predictivity of MDR positivity for therapy failure was 69%. If the terms MDR+ and MDR− patients are defined as binary variables, the presence of MDR positivity resulted in a 5·7 odds ratio for therapy failure (95% confidence interval 1·7–19, $P = 0·004$). In addition to MDR activity, in this study, only patient age proved to be significant as a prognostic factor. Each 10-year increment in patient age resulted in an odds ratio of 1·8 (95% confidence interval 1·2–2·6, $P = 0·005$).

Relationship between test results and survival rates

In order to assess the effect of the presence or absence of MDR-positive phenotype on the long-term clinical outcome – as expressed by the MAF values – survival times were investigated in both MDR-positive and MDR-negative cases. Only patients with 8 months or longer follow-up periods were included. As shown on Kaplan–Meier curves in Fig 3, MDR-negative cases displayed a threefold increase in 50% survival rate compared to MDR-positive cases; however, the difference between curves did not reach a statistically significant level in the log rank test ($P = 0·07$).

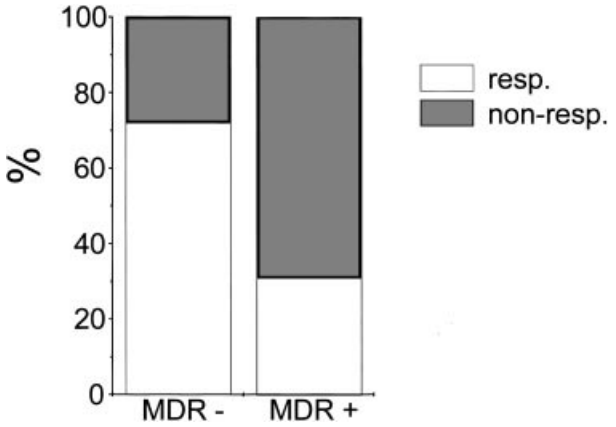

Fig 2. Positive- and negative-predictive value of the test. Using the cut-off limits determined previously, patients were divided into MDR-positive and MDR-negative groups in both centres. This figure shows the pooled data of both centres. The percentage of responder patients (resp.) in the MDR-negative group ($n = 39$) was 72% (negative predictive value), whereas the percentage of non-responder (non-resp.) patients in the MDR-positive group ($n = 26$) was 69% (positive predictive value). The relationship between the MDR phenotype determined by calcein assay and the response to the induction therapy (responder/non-responder type) was highly significant ($P = 0·004$).

Results of follow-up examinations

In selected cases, repeated measurements were also performed, i.e. the MAF values were determined with the calcein assay at the onset of disease and later, at the time of relapse or in the refractory state. Two different patterns were seen. Either the previously MDR-negative cases were found to turn to MDR-positive or the relatively high MAF values remained basically unchanged. No case of an MDR-positive to an MDR-negative switch was detected upon relapse (Fig 4).

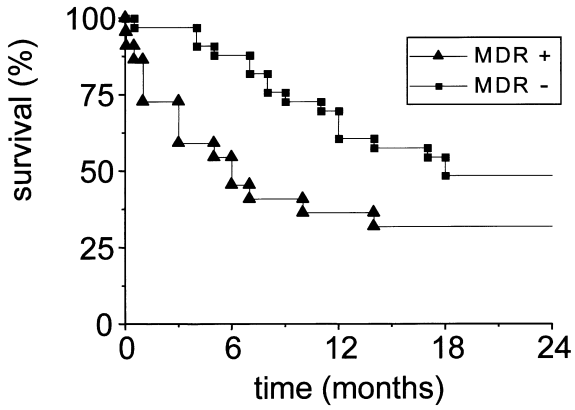

Fig 3. Kaplan–Meier overall survival curves of 26 MDR-positive and 39 MDR-negative patients. The mean follow-up period was 11·7±11·1 months and only patients with 8 months or longer follow-up periods were included. We found a remarkable difference between the survival function of MDR-positive and MDR-negative cases established by long-term follow-up, but using the previously determined cut-off limits, the difference between the two groups was not statistically significant ($P = 0·07$).

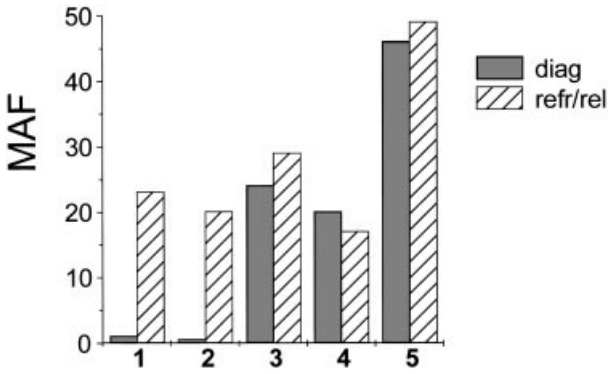

Fig 4. Follow-up examinations in selected cases. Determination of MDR activity was accomplished at the time of the diagnosis (diag) and was repeated later in the course of the disease in relapsed patients or in refractory state (refr/rel). Two different patterns were found: MDR-negative cases turned to MDR-positive at the time of relapse/refractory state (cases 1 and 2), indicating the possibility of drug induced resistance mechanism, or MDR status remained unchanged (cases 3–5). In relapse, no MDR-positive →MDR-negative switch was found.

DISCUSSION

There is a definite clinical need for accurate detection of MDR-positive cells in haematological malignancies. Chemotherapy is the key choice of treatment in these diseases and therapy outcome is significantly affected by primary or secondary drug resistance, observed in many cases. Moreover, the recent clinical trials, involving the co-application of drug resistance-modulating agents (Kaye, 1998; Merlin *et al*, 1998; Advani *et al*, 1999), should be planned and performed on the basis of a proper diagnosis of the actual presence and form of MDR.

Laboratory methods detecting MDR comprise molecular biology- (Marie *et al*, 1991) and immunology-based assays (Filipits *et al*, 1997; Huet *et al*, 1998) or various functional tests (Feller *et al*, 1995; Leith *et al*, 1995; Den Boer *et al*, 1997; Legrand *et al*, 1998). In this paper, we present the results of a two-centre study that was performed with samples derived from 95 *de novo* acute leukaemia patients by using a quantitative functional MDR assay, the calcein test.

Calcein-AM was chosen as the efflux indicator because this compound is an excellent substrate for both MDR1-Pgp and MRP1, and can therefore ideally screen for the functional presence of the two major proteins causing drug resistance. In contrast to other MDR substrate dyes, e.g. Rhodamin 123 or Fluo-3, the fluorescence of calcein is independent of intracellular environment or binding, and the assay provides a quantitative estimation of the drug pumping function. It has also been established (Hollo *et al*, 1994, 1998; Homolya *et al*, 1996) that results of the calcein assay, expressed as multidrug resistance activity factor, i.e. MAF values, reliably and quantitatively differentiate MDR-positive and MDR-negative cells. As a further advantage, the use of selective inhibitors in the calcein assay system enables discrimination between drug resistance caused by the MDR1-Pgp or the MRP1 efflux pumps (Feller *et al*, 1995; Hollo *et al*, 1998; Legrand *et al*, 1998).

In the current study, we focused on establishing the efficient clinical laboratory application of the basic calcein assay, that is, a combined determination of MDR1-Pgp and MRP1 activities. By using cell lines and clinical samples, both the accuracy and the reproducibility of the method has been examined, and the applicability of the stored chemical components has also been monitored. This allowed us to assemble a 'calcein assay kit', which proved to be stable for up to 1 year. To minimize preanalytical variables, all cellular samples were assayed within 4 h after sample preparation.

In the present study, by using the calcein test, we could confirm previous results when MDR activity was found to be significantly higher in AML patients than in ALL patients. In fact, the MAF values determined in mononuclear cells from 40 normal donors were not significantly different from those observed in ALL patients.

Because no 'normal control' values could be established for AML cases with normal myeloblast cells, we determined cut-off values for clinical relevance. To achieve this goal, the mean MAF values in the chemotherapy responder and non-responder AML patients were calculated, and a cut-off value between the (MAF_R + SEM) and (MAF_{NR} − SEM) values was established. Using this cut-off value to classify the patients into MDR-negative and MDR-positive groups, we found that MDR negativity was highly predictive for a successful clinical response to chemotherapy and had a prognostic value for better survival in AML patients (see Figs 3 and 4). It should be noted, however, that MAF values in *de novo* AML patients have to be interpreted in relation to the patient's age. Older patients, even those with low MAF values, may exhibit an unfavourable therapy response, as has been described previously.

The data obtained in the current study using the calcein test are in agreement with some other clinical studies (Martinez *et al*, 1997; Legrand *et al*, 1998), but contradict several results obtained using immunological assays (Ino *et al*, 1994; Wattel *et al*, 1995). It should be noted that, in immunophenotyping studies, the methods used for the estimation of MDR1-Pgp expression are not uniform; the established reference ranges are variable and there is no generally used method for MRP1 detection. The only previous report on a large cohort of AML patients using calcein-AM (Legrand *et al*, 1998) found that functional testing by selective inhibitors for MDR1-Pgp and MRP1 is of prognostic value. This study investigated MRP1 activity on the basis of calcein efflux. As verapamil blocks both efflux pumps, our test screens for both MDR1-Pgp and MRP1 activities, and the measured values correlate with survival and clinical response. This approach permits a reliable identification of patients prone to resist chemotherapy or relapse during treatment. Therefore, clinically relevant multidrug resistance is measured better by this functional assay than by antigenic tests. In fact, in our own studies, several MDR1-Pgp negative cases – determined by UIC2 monoclonal antibody staining – were identified as drug resistant, both by the calcein assay and by their clinical response (data not shown). It should be noted that other drug resistance mechanisms, such as the expression of breast cancer resistance protein (BCRP), may have an

influence on disease outcome in AML (Ross *et al,* 2000). However, in our AML samples, the presence of BCRP probably did not influence the results, as recently it has been described that neither calcein-AM nor calcein is a substrate for BCRP (Litman *et al,* 2000).

The overall percentage of the MDR-positive cases reported in this study was in a similar range to that found previously using a functional assay (Lamy *et al*, 1995). The highest MAF values were found in cases transformed to AML from preleukaemic states such as myelodysplasia, myelofibrosis or chronic granulocytic leukaemia.

Our data present a standardized form of the calcein assay: that is, a reproducible, inexpensive, feasible and quantitative functional test for MDR detection that can be easily used in routine clinical laboratories. These investigations verified the correlation between the clinical outcome and the test results and estimated a high predictive value of the assay for therapy response. Therefore, it should be considered a clinically relevant method for examining MDR activity.

ACKNOWLEDGMENTS

The technical assistance of Valéria Kiss and Katalin Petrovics is gratefully acknowledged. We would like to thank Dr László Kardos for statistical evaluation of the data, and the Department of Biophysics and Cell Biology at the Medical and Health Sciences Centre in Debrecen for providing the KBV1 cell line. This study was supported in part by a grant from the Hungarian National Science Foundation OTKA-T030389. Gergely Szakács was supported by Soros predoctoral fellowship. B. Sarkadi is a recipient of a Howard Hughes International Scholarship.

REFERENCES

Advani, R., Visani, G., Milligan, D., Saba, H., Tallman, M., Rowe, J.M., Wiernik, P.H., Ramek, J., Dugan, K., Lum, B., Villena, J., Davis, E., Paietta, E., Lichtman, M., Covelli, A., Sikic, B. & Greenberg, P. (1999) Treatment of poor prognosis AML patients using PSC833 (valspodar) plus mitoxantron, etoposide, and cytarabine (PSC-MEC). *Advances in Experimental Medicine and Biology*, **456**, 47–56.

Beck, W.T., Grogan, T.M., Willman, C.L., Cordon-cardo, C., Parham, D.M., Kuttesh, J.F., Andreff, M., Bates, S.E., Berard, C.W., Boyett, J.M., Brophy, N.A., Broxterman, H.J., Chan, H.S.L., Dalton, W.S., Dietel, M., Fojo, A.T., Gascoyne, R.D., Head, D., Houghton, P.J., Srivastava, D.K., Lehnert, M., Leith, C.P., Paietta, E., Pavelic, Z.P., Rimsza, L., Roninson, I.B., Sikic, B.I., Twentyman, P.R., Warnke, R. & Weinstein, R. (1996) Methods to detect P-glycoprotein-associated multidrug resistance in patients' tumors: consensus recommendations. *Cancer Research*, **56**, 3010–3020.

Boutonnat, J., Bonnefoix, M., Seigneurin, D. & Ronot, X. (1998) Coexpression of multidrug resistance involve proteins: a flow cytometric analysis. *Anticancer Research*, **18**, 2993–2999.

Bradshaw, D.M. & Arceci, R.J. (1998) Clinical relevance of transmembrane drug efflux as mechanism of multidrug resistance. *Journal of Clinical Oncology*, **16**, 3674–3690.

Brophy, N.A., Marie, J.P., Rojas, V.A., Warnke, R.A., McFall, P.J., Smith, S.D. & Sikic, B.I. (1994) Mdr1 gene expression in childhood acute lymphoblastic leukemias and lymphomas: a critical evaluation by four techniques. *Leukemia*, **8**, 327–335.

Broxterman, H.J., Sonneveld, P., Feller, N., Ossenkoppele, G.J., Wahrer, D.C.R., Eekman, C.A., Schoester, M., Lankelma, J., Pineda, H.M., Lowenberg, B. & Schuurhuis, G.J. (1996) Quality control of multidrug resistance assays in adult acute leukemia: correlation between assays for P-glycoprotein expression and activity. *Blood*, **87**, 4809–4816.

Cheson, B.D., Cassileth, P.A., Head, D.R., Schiffer, C.A., Bennett, J.M., Bloomfield, C.D., Brunning, R., Gale, R.P., Grever, M.R., Keating, M.J., Sawitsky, A., Stass, S., Weinstein, H. & Woods, W.G. (1990) Report of the National Cancer Institute-sponsored workshop on definitions of diagnosis and response in acute myeloid leukaemia. *Journal of Clinical Oncology*, **8**, 813–819.

Dalton, W.S. (1997) Mechanism of drug resistance in hematologic malignancies. *Seminars in Hematology*, **34**, 3–8.

Del Poeta, G., Stasi, R., Aronica, G., Venditti, A., Cox, M.C., Bruno, A., Buccisano, F., Masi, M., Tribalto, M., Amadori, S. & Papa, G. (1996) Clinical relevance of P-glycoprotein expression in *de novo* acute myeloid leukaemia. *Blood*, **87**, 1997–2004.

Den Boer, M.L., Zwaan, C.M., Pieters, R., Kazemier, K.M., Rottier, M.M., Flens, M.J., Scheper, R.J. & Veerman, A.J. (1997) Optimal immunocytochemical and flow cytometric detection of P-gp, MRP and LRP in childhood acute lymphoblastic leukemia. *Leukemia*, **11**, 1078–1085.

Feller, N., Kuiper, C.M., Lankelma, J., Ruhdal, J.K., Scheper, R.J., Pinedo, H.M. & Broxterman, H.J. (1995) Functional detection of MDR1/P170 and MRP/P190-mediated multidrug resistance in tumour cells by flow cytometry. *British Journal of Cancer*, **72**, 543–549.

Filipits, M., Suchomel, R.W., Lechner, K. & Pirker, R. (1997) Immunocytochemical detection of the multidrug resistance-associated protein and P-glycoprotein in acute myeloid leukaemia: impact of antibodies, sample source and disease status. *Leukemia*, **11**, 1073–1077.

Hegewisch-Becker, S. & Hossfeld, D.K. (1996) The MDR phenotype in hematologic malignancies: prognostic relevance and future perspectives. *Annals of Hematology*, **72**, 105–117.

Hollo, Z., Homolya, L., Davis, C.W. & Sarkadi, B. (1994) Calcein accumulation as a fluorometric functional assay of the multidrug transporter. *Biochimica et Biophysica Acta*, **1191**, 384–388.

Hollo, Z., Homolya, L., Hegedus, T. & Sarkadi, B. (1996) Transport properties of the multidrug resistance-associated protein (MRP) in human tumour cells. *FEBS Lettters*, **383**, 99–104.

Hollo, Z., Homolya, L., Hegedus, T., Muller, M., Szakacs, G., Jakab, K., Antal, F. & Sarkadi, B. (1998) Parallel functional and immunological detection of human multidrug resistance proteins, P-glycoprotein and MRP1. *Anticancer Research*, **18**, 2981–2987.

Homolya, L., Hollo, Z., Germann, U.A., Pastan, I., Gottesman, M.M. & Sarkadi, B. (1993) Fluorescent cellular indicators are extruded by the multidrug resistance protein. *Journal of Biological Chemistry*, **268**, 21493–21496.

Homolya, L., Hollo, Zs., Muller, M., Mechetner, E.B. & Sarkadi, B. (1996) A new method for a quantitative assessment of P-glycoprotein-related multidrug resistance in tumour cells. *British Journal of Cancer*, **73**, 849–855.

Huet, S., Marie, J.P., Gualde, N. & Robert, J. (1998) Reference method for detection of Pgp mediated multidrug resistance in human hematological malignancies: a method validated by the laboratories of the French drug resistance network. *Cytometry*, **34**, 248–256.

Hunault, M., Zhou, D., Delmer, A., Ramond, S., Viguie, F., Cadiou, M., Perrot, J.Y., Levy, V., Rio, B., Cymbalista, F., Zittoun, R. & Marie, J.P. (1997) Multidrug resistance gene expression in acute myeloid leukemia: major prognosis significance for *in vivo*

drug resistance to induction treatment. *Annals of Hematology*, **74**, 65–71.

Ino, T., Miyazaki, H., Isogai, M., Nomura, T., Tsuzuki, M., Tsuruo, T., Ezaki, K. & Hirano, M. (1994) Expression of P-glycoprotein in *de novo* acute myelogenous leukemia at initial diagnosis: results of molecular and functional assays, and correlation with treatment outcome. *Leukemia*, **8**, 1492–1497.

Kaye, S.B. (1998) Multidrug resistance: clinical relevance in solid tumours and strategies for circumvention. *Current Opinion in Oncology*, **10**, 15–19.

Lamy, T., Drenou, B., Grulois, I., Fardel, O., Jacquelinet, C., Goasguen, J., Dauriac, C., Amiot, I., Bernard, M., Fauchet, R. & Le Prise, P.-Y. (1995) Multi-drug resistance (MDR) activity in acute leukemia determined by rhodamin 123 efflux assay. *Leukemia*, **9**, 1549–1555.

Legrand, O., Simonin, G., Perrot, J.Y., Zittoun, R. & Marie, J.P. (1998) Pgp and MRP activities using calcein-AM are prognostic factors in adult acute myeloid leukemia patients. *Blood*, **91**, 4480–4488.

Leith, C.P., Chen, I.M., Kopecky, K.J., Appelbaum, F.R., Head, D.R., Godwin, J.E., Weick, J.K. & Willman, C.L. (1995) Correlation of multidrug resistance (MDR1) protein expression with functional dye/drug efflux in acute myeloid leukemia by multiparameter flow cytometry: identification of discordant MDR-/efflux+ and MDR1+/efflux– cases. *Blood*, **86**, 2329–2342.

Litman, T., Brangi, M., Hudson, E., Fetsch, P., Abati, A., Ross, D.D., Miyake, K., Resau, J.H. & Bates, S.E. (2000) The multidrug-resistant phenotype associated with overexpression of the new ABC half-transporter, MXR. *Journal of Cell Science*, **113**, 2011–2021.

Marie, J.P., Zittoun, R. & Sikic, B.I. (1991) Multidrug resistance (mdr1) gene expression in adult acute leukemias: correlations with treatment outcome and *in vitro* drug sensitivity. *Blood*, **78**, 586–592.

Marie, J.P., Zhou, D.C., Gurbuxani, S., Legrand, O. & Zittoun, R. (1996) MDR/P-glycoprotein in hematological neoplasms. *European Journal of Cancer*, **32**, 1034–1038.

Martinez, A., San Miguel, J.F., Valverde, B., Barez, A., Moro, M.J., Garcia-Marcos, M.A., Perez-Simon, J.A., Vidriales, B. & Orfao, A. (1997) Functional expression of MDR-1 in acute myeloid leukemia: correlation with clinical-biological, immunophenotypical and prognostic disease characteristic. *Annals of Hematology*, **75**, 81–86.

Maslak, P., Hegewish-Becker, S., Godfrey, L. & Andreeff, M. (1994) Flow cytometric determination of the multidrug-resistant phenotype in acute leukemia. *Cytometry*, **17**, 84–93.

Merlin, J.L., Guerci, A.P., Marchal, S., Bour, C., Colosetti, P., Kataki, A. & Guerci, O. (1998) Influence of SDZ-PSC833 on daunorubicin intracellular accumulation in bone marrow specimens from patients with acute myeloid leukaemia. *British Journal of Haematology*, **103**, 480–487.

Minderman, H., Vanhoefer, U., Toth, K., Yin, M.B., Minderman, M.D., Wrzosek, C., Slovak, M.L. & Rustum, Y.M. (1996) $DiOC_2$ is not a substrate for multidrug resistance protein (MRP)-mediated drug efflux. *Cytometry*, **25**, 14–20.

Nooter, K., Westerman, A.M., Flens, M.J., Zaman, G.J., Scheper, R.J., van Windenger, K.E., Burger, H., Oostrum, R., Boersma, T., Sonneveld, P., Gratama, J.W., Kok, T., Eggermont, A.M.M., Bosman, F.T. & Stoter, G. (1995) Expression of the multidrug resistance-associated protein (MRP) gene in human cancers. *Clinical Cancer Research*, **1**, 1301–1310.

Nooter, K., Burger, H. & Stoter, G. (1996) Multidrug resistance-associated protein (MRP) in hematological malignancies. *Leukemia and Lymphoma*, **20**, 381–387.

Nussler, V., Pelka-Fleischer, R., Zwierzina, H., Nerl, C., Beckert, F., Diem, H., Ledderose, G., Gullis, E., Sauer, H. & Willmans, W. (1996) P-glycoprotein expression in patients with acute leukemia – clinical relevance. *Leukemia*, **10**, S23–S31.

Ross, D.D., Karp, J.E., Chen, T.T. & Doyle, L.A. (2000) Expression of breast cancer resistance protein in blast cells from patients with acute leukemia. *Blood*, **96**, 365–368.

Rothe, G., Schmitz, G., Adorf, D., Barlage, S., Gramatzki, M., Hanenberg, H., Höffkes, H.G., Janossy, G., Knüchel, R., Ludwig, W.D., Nebe, T., Nerl, C., Orfao, A., Serke, S., Sonnen, R., Tichelli, A. & Wörmann, B. (1996) Consensus protocol for the flow cytometric immunophenotyping of hemopoietic malignancies. *Leukemia*, **10**, 877–895.

Sievers, E.L., Appelbaum, F.R., Spielberger, R.T., Forman, S.J., Flowers, D., Smith, F.O., Shannon-Dorcy, K., Berger, M.S. & Bernstein, I.D. (1999) Selective ablation of acute myeloid leukemia using antibody–targeted chemotherapy: a phase I study of an anti-CD33 calicheamicin immunoconjugate. *Blood*, **93**, 3678–3684.

Szakacs, G., Jakab, K., Antal, F. & Sarkadi, B. (1998) Diagnostics of multidrug resistance in cancer. *Pathology Oncology Research*, **4**, 251–257.

Tiberghien, F. & Loor, F. (1996) Ranking of P-glycoprotein substrates and inhibitors by a calcein-AM fluorometry screening assay. *Anticancer Drugs*, **7**, 568–578.

Wattel, E., Lepelley, P., Merlat, A., Sartiaux, F., Jouet, J.P. & Fenaux, P. (1995) Expression of multidrug resistance P glycoprotein in newly diagnosed adult acute lymphoblastic leukaemia: absence of correlation with response to treatment. *Leukemia*, **9**, 1870–1874.

dc_46_10

4. sz. közlemény

dc_46_10

Multidrug Transporter ABCG2 Prevents Tumor Cell Death Induced by the Epidermal Growth Factor Receptor Inhibitor Iressa (ZD1839, Gefitinib)

N. Barry Elkind,[1] Zsófia Szentpétery,[2] Ágota Apáti,[1] Csilla Özvegy-Laczka,[1,2] György Várady,[1] Olga Ujhelly,[1] Katalin Szabó,[2] László Homolya,[1] András Váradi,[2] László Buday,[3] György Kéri,[4] Katalin Német,[1] and Balázs Sarkadi[1]

[1]National Medical Center, Institute of Haematology and Immunology, Membrane Research Group of the Hungarian Academy of Sciences; [2]Institute of Enzymology, Biological Research Center of the Hungarian Academy of Sciences; and Departments of [3]Medical Chemistry, Pathobiochemistry, and Molecular Biology and [4]Medical Chemistry, Peptide Biochemistry Research Group of the Hungarian Academy of Sciences, Semmelweis University, Budapest, Hungary

Abstract

Iressa (ZD1839, Gefitinib), used in clinics to treat non–small cell lung cancer patients, is a tyrosine kinase receptor inhibitor that leads to specific decoupling of epidermal growth factor receptor (EGFR) signaling. Recent data indicate that Iressa is especially effective in tumors with certain EGFR mutations; however, a subset of these tumors does not respond to Iressa. In addition, certain populations have an elevated risk of side effects during Iressa treatment. The human ABCG2 (BCRP/MXR/ABCP) transporter causes cancer drug resistance by actively extruding a variety of cytotoxic drugs, and it functions physiologically to protect our tissues from xenobiotics. Importantly, ABCG2 modifies absorption, distribution, and toxicity of several pharmacologic agents. Previously, we showed that ABCG2 displays a high-affinity interaction with several tyrosine kinase receptor inhibitors, including Iressa. Here, we show that the expression of ABCG2, but not its nonfunctional mutant, protects the EGFR signaling-dependent A431 tumor cells from death on exposure to Iressa. This protection is reversed by the ABCG2-specific inhibitor, Ko143. These data, reinforced with cell biology and biochemical experiments, strongly suggest that ABCG2 can actively pump Iressa. Therefore, variable expression and polymorphisms of ABCG2 may significantly modify the antitumor effect as well as the absorption and tissue distribution of Iressa. (Cancer Res 2005; 65(5): 1770-7)

Introduction

The epidermal growth factor receptor (EGFR) signaling pathway regulates diverse physiologic responses, including proliferation, differentiation, cell motility, and survival (1). However, this pathway is also used to promote tumor growth in a variety of epithelial tumors, including the most malignant form of lung carcinoma, non–small cell lung cancer (2, 3). EGFR belongs to the ErbB/HER family of tyrosine kinase receptors, which homodimerize or heterodimerize on ligand activation, resulting in transphosphorylation on tyrosine residues in the tyrosine kinase receptor cytoplasmic domain. The subsequent recruitment and activation of signaling effectors transmit the EGFR signal within the cell.

Much effort has been taken to develop specific methods of inhibiting EGFR to prevent cancerous processes. The two most promising therapeutic approaches make use of monoclonal antibodies and small molecule inhibitors that specifically target the EGFR tyrosine kinase enzymatic activity. Iressa (ZD1839, Gefitinib, AstraZeneca Pharmaceuticals, London, United Kingdom) is a small, orally active molecule that is a selective and reversible inhibitor of the EGFR tyrosine kinase activity, blocking EGFR signal transduction pathways (4, 5). As an antitumor agent, after passing phase I and II of clinical trials, Iressa failed phase III trials for the treatment of non–small cell lung cancer patients (6–8). Despite phase III failure, Iressa was the first drug of its kind to receive approval in Japan, the United States, and in Australia, and Iressa has shown promising efficacy in other solid tumors that rely on EGFR-related mechanisms for growth and survival (9).

Data explaining why Iressa works well in some cancer patients and not in others were discovered recently (10, 11). Somatic mutations clustered around the active site of the kinase domain of EGFR, present in the majority of non–small cell lung cancer tumors, correlate with hypersensitivity to Iressa. This important observation will allow enhanced success in the treatment of patients in the future. However, there is a subset of cancer patients with EGFR mutations that do not respond well to Iressa treatment. This could be explained by inadequate dosing and delivery of drug to the tumor, which may have resulted in suboptimal receptor modulation.

In addition, inappropriate dosing could also be the cause for the elevated risk of toxicity (compared with worldwide statistics) experienced by Japanese patients (12, 13). In fact, the search for factors that may cause severe side effects from Iressa treatment are now under way in Japan, where hundreds of patients have died from treatment (14). Factors affecting the absorption, distribution, metabolism, excretion, and toxicity of Iressa are of interest for study in order that a phase III clinical trial might appropriately choose patients whose tumors are likely to respond to treatment.

A group of ATP binding cassette proteins, including P-glycoprotein, several multidrug resistance proteins, and the ABCG2 protein (also known as BCRP/MXR/ABCP), cause multidrug resistance in tumors, as they actively extrude a wide variety of anticancer drugs (for reviews, see refs. 15–17). These proteins are regarded as potential clinical targets for regulation to inhibit cancer multidrug resistance as well as to alter the

Note: N.B. Elkind, Z. Szentpétery, and Á. Apáti contributed equally to this work.
Requests for reprints: Balázs Sarkadi, National Medical Center, Institute of Haematology and Immunology, Membrane Research Group of the Hungarian Academy of Sciences, Diószegi u 64, H-1113 Budapest, Hungary. Phone: 36-1-372-4316; Fax: 36-1-372-4353; E-mail: sarkadi@biomembrane.hu.

absorption, distribution, metabolism, excretion, and toxicity variables for various chemotherapeutic drugs (18, 19). One of the key multidrug transporters, ABCG2, is a primary active transporter for mitoxantrone, topotecan, or flavopiridol, and its overexpression was documented in several drug-resistant cell lines and tumors (15, 20–23). ABCG2 is present in the plasma membrane in stem cells, placenta, liver, small intestine, colon, lung, and kidney, suggesting its role in the protection/detoxification of xenobiotics (15, 24–26). Importantly, single polymorphisms, which result in amino acid substitutions, have been identified in relatively large percentage of populations (e.g., in Japan; refs. 27, 28). These naturally occurring mutations could alter drug absorption and metabolism as well as render some cancer patients differently susceptible to chemotherapy (29).

Recent work in our laboratory showed that ABCG2 has a high-affinity (nanomolar range) interaction with several tyrosine kinase receptor inhibitors (TKRI), including Iressa. Although ABCG2 possesses a partially overlapping substrate profile with both P-glycoprotein and multidrug resistance protein-1 (15–17, 26, 30), and although all three interacted with Iressa, only ABCG2 had a high affinity to the drug (31).

In the present study, we used the A431 squamous cell carcinoma line as a model system for studying the functional interaction of ABCG2 and Iressa. This tumor cell line is dependent on EGFR signaling for survival. In fact, EGFR is amplified in these cells, allowing them to grow in serum-free medium (32–35). In contrast, drug-induced inactivation of the EGFR tyrosine kinase enzyme by Iressa or other EGFR inhibitors causes the cessation of growth and induction of mostly apoptotic cell death in A431 cells (2, 36, 37).

For our studies, we have generated retrovirally transduced A431 cells, expressing various levels of the wild-type ABCG2, or a functionally inactive mutant (K86M) ABCG2 variant. We analyzed if functional ABCG2 provided a selective growth advantage during Iressa treatment and followed the changes in the phosphorylation state of the EGFR in these cells. We also examined if the Iressa-induced cell death was modulated by ABCG2 by using Annexin V binding and confocal microscopy to detect apoptosis. Our cell biology experiments were extended by direct biochemical studies for studying the effect of Iressa on the ABCG2-ATPase activity in isolated mammalian cell membranes. The results obtained strongly suggest that the function of ABCG2 results in an active extrusion of Iressa, preventing the apoptotic effect of this molecule at the level of receptor tyrosine kinase inhibition in tumor cells.

Materials and Methods

Materials. Ko143 was a generous gift from Drs. J. Allen and G. Koomen (University of Amsterdam, Amsterdam, the Netherlands). Mitoxantrone and propidium iodide (PI) were purchased from Sigma-Aldrich (St. Louis, MO). Hoechst 33342, Alexa Fluor 488 Annexin V, and MitoTracker Deep Red 633 were purchased from Molecular Probes (Eugene, OR).

Retroviral DNA Expression Construction. The retroviral vector, SPsLdS (38), was modified previously by us to contain a neomycin resistance cassette (39). cDNA encoding wild-type (R482) ABCG2 or $ABCG2_{K86M}$ was inserted by blunt-end ligation into the *Eco*RI sites of the retroviral vector, thus removing the original gp91 cDNA. Expression plasmids were purified from endotoxins with Endo-free Qiagen (Hilden, Germany) kits and used to transfect Phoenix-Eco packaging cells.

Cell Growth and Propagation. The human skin–derived, epidermoid carcinoma cells, A431, were maintained in α-MEM (Life Technologies, Grand Island, NY) supplemented with 10% FCS, 50 units/mL penicillin, 50 units/mL streptomycin, and 5 mmol/L glutamine at 37°C in 5% CO_2.

MCF-7/MX cells (40) were a generous gift from Dr. Susan Bates (NIH, Bethesda, MD). These were maintained in DMEM supplemented with 10% FCS, 50 units/mL penicillin, 50 units/mL streptomycin, and 5 mmol/L glutamine at 37°C in 5% CO_2.

Retroviral Transduction of A431 Cells with ABCG2 Constructs. The expression of ABCG2, its nonfunctional mutant variant, $ABCG2_{K86M}$, and vector control in A431 cells was achieved by a method described previously by us (41). Briefly, Phoenix-Eco packaging cells were transiently transfected with retroviral DNA (see above). Viral supernatants were collected and used to transduce A431 cells. Cells expressing retroviral DNA were then selected with 10 mg/mL G418. Mitoxantrone selection of the transduced A431 cells was achieved by culturing the cells in 500 nmol/L drug.

Detection of ABCG2 and Its Variant in A431 Cells by Western Analysis and Hoechst 33342 Dye Accumulation Assay. ABCG2 and its catalytically inactive variant, $ABCG2_{K86M}$, were detected in A431 lysates by Western analysis as described previously (42) using the BXP-21 anti-ABCG2 monoclonal antibody. BXP-21 was a kind gift from Drs. George Scheffer and Rik Scheper (Department of Pathology, VU University Medical Center, Amsterdam, the Netherlands).

Accumulation of Hoechst 33342 dye was done by using intact A431 cells without (control) or with the overexpression of wild-type ABCG2 or its inactive K86M mutant in a fluorescence spectrophotometer (Perkin-Elmer LS 50B, Perkin-Elmer/Applied Biosystems, Foster City, CA) at 350 nm (excitation)/460 nm (emission) as described (31). The increase in cellular fluorescence due to Hoechst 33342 accumulation was determined in the absence (F_0) or presence of 1 μmol/L Ko143 (F_{100}, giving 100% inhibition of ABCG2 transport activity). The value reflecting the transport activity was calculated as $[(F_{100} - F_0) / F_{100}] \times 100$.

A431/Iressa Cytotoxicity Assay. Parental A431 cells and those expressing ABCG2, $ABCG2_{MX}$, and $ABCG2_{K86M}$ were grown to subconfluency, trypsinized, and diluted in an Eppendorf tube to 10^5 cells/mL serum-free medium. Cells were treated for 15 minutes at room temperature in the absence or presence of different concentrations of Ko143 and Iressa. Cells (4×10^4 per 0.4 mL) were then dispersed into a well of a 24-well plate in triplicates and incubated for 48 hours in the same Iressa- and/or Ko143-containing medium at 37°C, 5% CO_2. Cells were then harvested with trypsin and collected in complete medium. Subsequently, PI (2 μg/mL) was added and the samples were counted in a FACSCalibur cytometer (Becton Dickinson, San Jose, CA) for live cells.

Iressa-Mediated EGFR Dephosphorylation. Parental A431 cells and those expressing ABCG2, $ABCG2_{MX}$, and $ABCG2_{K86M}$ were stimulated with epidermal growth factor (20 ng/mL) for 15 minutes and subsequently incubated for an additional 15 minutes in the presence or absence of Iressa as described in A431/Iressa Cytotoxicity Assay. Cell lysates were produced as described previously (43), and proteins (30 μg) were separated by SDS-PAGE and transferred to polyvinylidene difluoride membrane using the Mini-Protean II System (Bio-Rad, Hertfordshire, United Kingdom). Western blots were probed with mouse anti-phosphotyrosine (clone 4G-10) monoclonal antibody, which was used to detect the phosphorylation state of the EGFR. Subsequently, membranes stained with the primary antibody were incubated in TBS/0.5% Tween 20 containing 0.5% H_2O_2 at room temperature for 30 minutes and then washed thrice with TBS/0.5% Tween 20 to deactivate residual horseradish peroxidase activity. Then, detection by anti-EGFR rabbit polyclonal IgG (Upstate, Lake Placid, NY) was used to ensure that equal levels of EGFR were present in the lysates. Secondary antibodies were mouse and rabbit IgG horseradish peroxidase conjugate (Jackson Immunoresearch, West Grove, PA). The enhanced chemiluminescence system was used for chemiluminescence detection (Amersham, Little Chalfont, United Kingdom). For quantitative analysis of Western blots, image analysis of X-ray films was done by Bioscan version 1.0 software following digitalization with Hewlett Packard (Palo Alto, CA) 5100 C scanner.

Annexin V Binding and Confocal Microscopy. The cells (4×10^4 per well) were seeded onto eight-well Nunc Lab-Tek Chambered Coverglass

(Nalge Nunc International, Rochester, NY) coated previously with 0.03 mg/mL Vitrogene (Cohesion Technology, Palo Alto, CA) and grown overnight in α-MEM containing 10% FCS. The cells were then cultured in serum free α-MEM for an additional 24 hours. The medium contained 1 μmol/L Iressa where indicated. For microscopy studies, the cultures were subjected to Annexin V binding buffer containing 10 mmol/L HEPES (pH 7.4), 140 mmol/L NaCl, 2.5 mmol/L $CaCl_2$, Alexa Fluor 488 Annexin V (in 1:80 dilution), 10 μg/mL PI, and 100 nmol/L MitoTracker Deep Red 633 and studied after 5 minutes of incubation time. The samples were observed using an Olympus FV500-IX confocal laser scanning microscope using an Olympus PLAPO 60× (1.4) oil immersion objective (Olympus Europa GmbH, Hamburg, Germany). For green, red, and deep red fluorescence acquisitions, the samples were illuminated with 488, 543, and 633 nm laser lines, respectively, and confocal images were taken at 505 to 545, 560 to 600, and >660 nm, respectively.

Membrane ATPase Measurements. To produce human ABCG2-containing membranes, MCF-7/MX (ABCG2/R482) and A431 cells were harvested and their membranes were isolated and stored at −80°C (44). ATPase activity was measured basically as described previously by determining the liberation of inorganic phosphate from ATP with a colorimetric reaction (44). The incubation medium contained 40 mmol/L MOPS-Tris (pH 7.0), 50 mmol/L KCl, 2 mmol/L DTT, 0.5 mmol/L EDTA, 5 mmol/L sodium azide, 1 mmol/L ouabain, 10 μg membrane, and 3.3 mmol/L Mg ATP. Data represent means of at least three independent experiments with duplicates.

Results

Recently, we documented (31) that ABCG2 displays a high-affinity, submicromolar interaction with the tyrosine kinase inhibitor Iressa. To extend these results and show that ABCG2-mediated transport activity can protect cells from the toxic effects of Iressa in cells, we generated an appropriate cellular model system. Because Iressa efficiently acts as an anticancer agent in EGFR-dependent tumor cells, we used the human skin–derived, epidermoid carcinoma cells, A431, for studying ABCG2-Iressa interactions. This cell line, which is dependent on EGFR signaling for survival, was retrovirally transduced by ABCG2 and also by an inactive, catalytic site mutant, $ABCG2_{K86M.}$ We obtained several clones of these cells, expressing variable levels of ABCG2, and for comparative experiments, we further selected some of the ABCG2-transduced A431 cells in mitoxantrone, resulting in high levels of the ABCG2 protein expression ($ABCG2_{MX}$).

In Fig. 1, we show the steady-state ABCG2 protein expression levels in the cells used in this study by Western analysis (Fig. 1*A*). Western blot analysis, using the specific anti-ABCG2 monoclonal antibody, BXP-21, revealed well measurable levels of ABCG2 protein in the transduced A431 cells overexpressing ABCG2 (G2) and considerably higher levels in cells further selected with the ABCG2 substrate, mitoxantrone ($G2_{MX}$; ref. 42). $ABCG2_{K86M}$ ($G2_{K86M}$) represents cells expressing the inactive, catalytic site mutant of ABCG2 at comparable levels with the cells transduced with the active, wild-type ABCG2 (G2). As a negative control, parental A431 cells were also used (control A431). As we will present below, A431 cells express low levels of endogenous ABCG2, which was not detected by Western analysis.

To detect functionality of the expressed ABCG2 protein in the transduced A431 cell lines, we used the Hoechst 33342 dye accumulation assay (Fig. 1*B*). Hoechst 33342 is a cell-permeable hydrophobic dye, which is a characterized substrate of ABCG2 (26, 45). Whereas drug-sensitive cells rapidly take up this dye, which becomes fluorescent on binding to DNA, cells expressing functional ABCG2 show only a low rate of increase in fluorescence. By applying the specific ABCG2 inhibitor, Ko143, the Hoechst 33342 dye extrusion activity of ABCG2 can be quantified (46).

This assay is very sensitive and allowed the detection of functional endogenous ABCG2 even in control A431 cells (Fig. 1*B*, *Ctrl A431*). However, in the ABCG2 (G2)–expressing cells, a much greater Hoechst 33342 extrusion activity was seen, which was further augmented after mitoxantrone selection of the transduced A431 ($G2_{MX}$) cells. In contrast, the catalytic site mutant, $ABCG2_{K86M}$, possessed even less Hoechst 33342 transport activity than the A431 control cells. This is likely due to the overexpressed mutant protein, which may form a dominant-negative heterodimeric complex with endogenous ABCG2. In conclusion, we have created A431 cell lines expressing differing levels of transport-competent ABCG2 as well as its inactive mutant form, $ABCG2_{K86M}$.

In the following experiments, we studied if the overexpression of ABCG2 conferred a survival advantage to A431 cells exposed to Iressa. As shown in Fig. 2*A*, we compared the effects of Iressa on cell survival of A431 cells over a 48-hour period of exposure to various concentrations of Iressa (50-500 nmol/L). Cells were treated with Iressa and then plated for following cell growth in the surface-attached cell populations. As shown, low concentrations

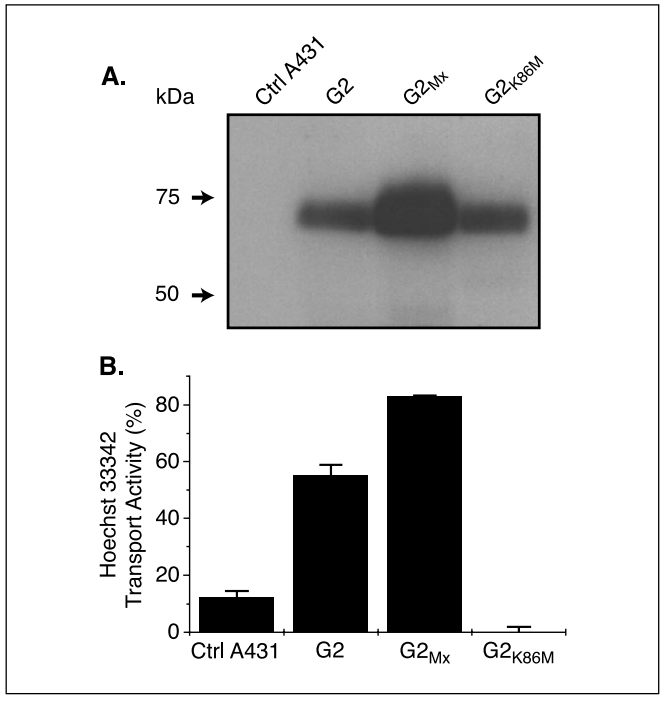

Figure 1. Expression and function of ABCG2 in A431 cells. *A,* detection of expression of ABCG2 in A431 cells. Total cell lysates (50 μg) of A431 cells stably expressing ABCG2 (G2) or $ABCG2_{K86M}$ ($G2_{K86M}$) by retroviral transduction were detected in Western analysis using the anti-ABCG2 monoclonal antibody, BXP-21. $G2_{MX}$ are G2 cells that were selected for high ABCG2 expression with 500 nmol/L mitoxantrone. Parental A431 cells (*Ctrl A431*) were used as a control. kDa represents the protein size markers and show that ABCG2 in its glycosylated form is ~70 kDa. *B,* ABCG2 function detected by Hoechst 33342 dye accumulation assay. A431 cells expressing ABCG2 (as described above) had a significantly slower Hoechst 33342 fluorescent dye accumulation (and higher dye extrusion) than the control cells. The increase in cellular fluorescence due to Hoechst 33342 accumulation was determined in the absence or presence of 1 μmol/L Ko143 as described in Materials and Methods. *Columns,* mean of four different experiments; *bars,* SD.

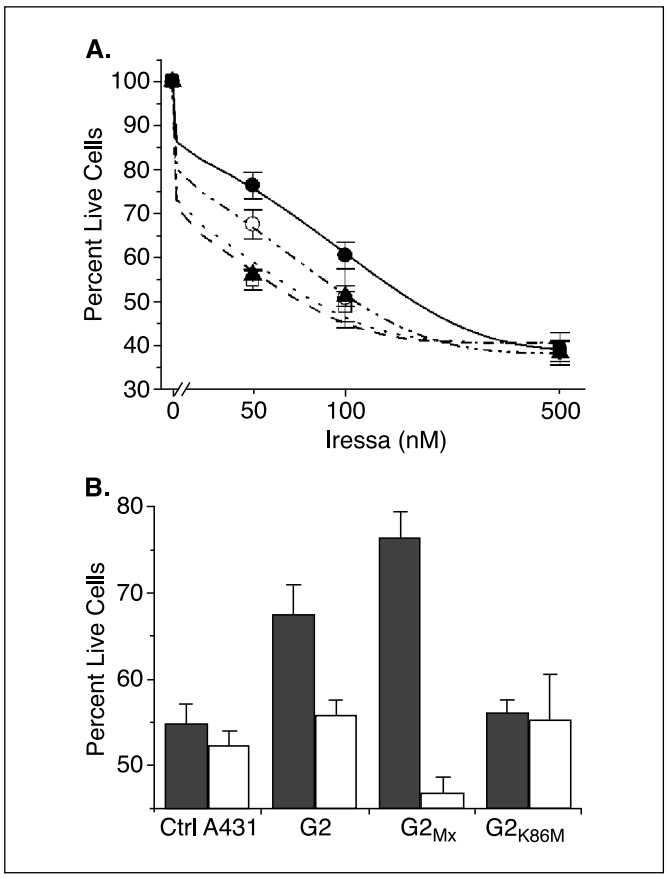

Figure 2. ABCG2-mediated protection of A431 cytotoxicity caused by exposure to Iressa. *A,* A431 cells expressing ABCG2 are protected from the cytotoxic effects mediated by exposure to Iressa. Cells expressing ABCG2 (○, *double dot-dash line*), $ABCG2_{MX}$ (●, *solid line*), $ABCG2_{K86M}$ (▲, *dotted line*), and parental A431 cells (□, *dashed line*) were exposed to 0, 50, 100, and 500 nmol/L Iressa in serum-free medium for 48 hours on which cells were collected, stained with PI, and counted by fluorescence-activated cell sorting. Mean percentage of live cells (seven independent experiments, each done in triplicate) is plotted against the log of Iressa concentration, and exponential fit was applied. *Bars,* SE. *B,* A431 cell protection from Iressa cytotoxicity is ABCG2 specific. Experiments were done as in *A*, except that cells were incubated with 50 nmol/L Iressa (*solid columns*) or 50 nmol/L Iressa plus 100 nmol/L of the specific ABCG2 inhibitor, Ko143 (*white columns*). *Columns,* mean percentage of ABCG2 (G2), $ABCG2_{MX}$ ($G2_{MX}$), $ABCG2_{K86M}$ ($G2_{K86M}$), and parental A431 (control A431) live cells from three independent experiments each done in triplicate; *bars*, SE. These data were found to be statistically significant using Student's *t* test ($P = 0.05$). Parental A431 cell (control A431) survival data are significantly different from ABCG2 (G2) and $ABCG2_{MX}$ ($G2_{MX}$) ($P = 0.00329$ and 0.00003, respectively). In contrast, parental A431 cell (control A431) survival data are the same as for the nonfunctional ABCG2-expressing cells ($P = 0.30764$).

(50-200 nmol/L) of Iressa caused significant cell death in the control A431 cells, although there was statistically significant protection against these concentrations of Iressa in the ABCG2-expressing A431 cells. This inhibition of Iressa effect was even stronger in the mitoxantrone-selected, ABCG2-overexpressing cells ($ABCG2_{MX}$), whereas the expression of the inactive mutant of ABCG2 ($ABCG2_{K86M}$) did not provide such a protection. The calculated IC_{50} values are 26.7 μmol/L for control A431 cells, 45.8 nmol/L for ABCG2-expressing cells, 68.4 nmol/L for $ABCG2_{MX}$ cells, and 24.5 nmol/L Iressa for $ABCG2_{K86M}$-expressing A431 cells. Under these experimental conditions, at higher Iressa concentrations (500 nmol/L-1 μmol/L), cell death was maximal, and ABCG2 expression could no longer protect A431 cells from Iressa-mediated death.

To further characterize this protective effect in terms of its specific dependence on the activity of the ABCG2 protein, we carried out a detailed study using 50 nmol/L exposure of Iressa in A431 cells expressing various levels of ABCG2 protein or its nonfunctional mutant with and without the addition of the specific, high-affinity ABCG2 inhibitor, Ko143 (47). As documented in Fig. 2*A* and *B*, ABCG2 expression protected A431 cells from Iressa-induced death, observed in the parental A431 cells or those expressing $ABCG2_{K86M}$. In contrast, when the ABCG2 inhibitor Ko143 was included in the Iressa treatment (Fig. 2*B*, *white columns*), the protective effect of ABCG2 expression was removed (i.e., cell death was not significantly different from that found in the parental or $ABCG2_{K86M}$-expressing A431 cells). We also observed a small increase in death rate in the parental A431 cells when Iressa was combined with Ko143, but this effect was not statistically significant. Ko143 applied alone did not cause any cell death (data not shown).

To analyze the molecular basis of these cellular effects, we did direct ABCG2-ATPase measurements in isolated membranes of ABCG2-expressing mammalian MCF-7/MX and A431 cells. We measured the vanadate-sensitive ATPase activity (44), reflecting the ABCG2 transport activity in these membranes, and studied the effects of various concentrations of Iressa as well as that of Ko143 on this ABCG2-ATPase activity.

As shown in Fig. 3, both MCF-7-ABCG2 and A431-ABCG2 membranes had a significant basal ATPase activity, which was absent in the control, MCF-7, or A431 cell membranes (data not shown) and strongly inhibited by the addition of Ko143. Low concentrations of Iressa significantly activated the ABCG2-ATPase in these membrane preparations, whereas higher Iressa concentrations (>1 μmol/L) had a decreasing stimulatory effect. The same tendency was observed in ABCG2-expressing A431 cells, although

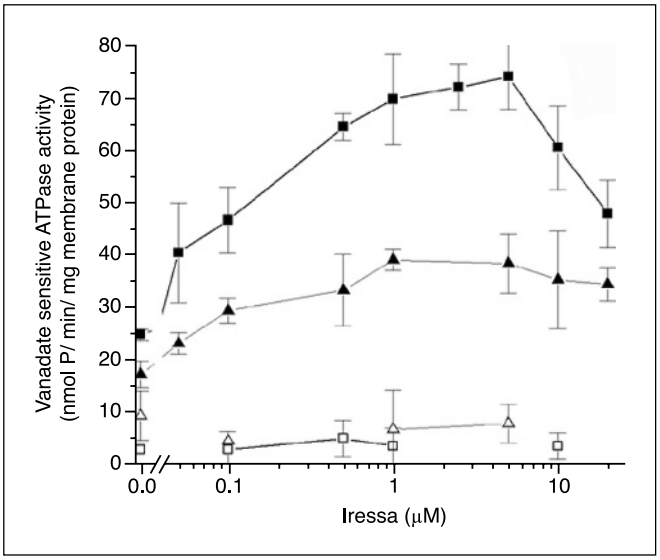

Figure 3. Iressa stimulates ABCG2-ATPase activity in isolated mammalian cell membranes ABCG2-containing MCF-7/MX and A431-ABCG2 membranes (10 μg) were assayed for vanadate-sensitive ATPase activity (nmol P_i/min/mg membrane protein) in the presence of Iressa and with or without the ABCG2 inhibitor, Ko143. Various Iressa concentrations in MCF-7/MX membranes with (■) or without (□) Ko143. Various Iressa concentrations used in A431-ABCG2 membranes with (▲) or without (△) Ko143. Membranes of MCF-7 and A431 control cells had a low level of vanadate-sensitive ATPase activity comparable with that in the ABCG2-containing membranes in the presence of Ko143 (data not shown). *Points,* means of at least three independent experiments with duplicates; *bars, SD.*

the lower expression levels of ABCG2 in these membranes yielded lower maximum ATPase activities. The maximum stimulation obtained by Iressa was ~2.6 to 3 in both membranes, and the K_m for ATPase activation was also similar (~100 nmol/L in both cases). The V_{max} of the vanadate-sensitive ATPase activity was 73.97 ± 6.0 nmol P_i/mg membrane protein/min in the MCF-7/MX membranes and 38.9 ± 2.0 nmol P_i/mg membrane protein/min in the A431-ABCG2 membranes. When we compared the effect of Iressa on this ATPase activity with that by other drug substrates, we found that in the A431-ABCG2 membranes prazosin gave a similar (2.5-fold) activation, whereas mitoxantrone activated the ATPase with somewhat lower effectivity (1.9-fold stimulation; data not shown).

The present data are in line with our earlier experiments carried out using ABCG2-expressing isolated Sf9 cell membranes (31) but, due to the lower basal ABCG2-ATPase activity in the mammalian cell membranes, the stimulatory effect of Iressa is much better appreciated here. It should be noted that because we used relatively high membrane concentrations in these ATPase experiments, most probably due to the high lipid absorption of this compound, the effective Iressa concentrations were shifted to somewhat higher levels than found in the whole cell studies.

In the following experiments, we analyzed the cellular mode of action of ABCG2 in protecting A431 tumor cells from Iressa. According to unequivocal evidence presented in the literature, Iressa exposure leads to rapid dephosphorylation of the EGFR, and this loss of specific phosphorylated tyrosine in the membrane-bound receptor is the basis of cell death induction in the EGFR-dependent A431 cells. We were interested in exploring if the presence of the functional ABCG2 transporter could protect the cells from this Iressa effect directly at the membrane receptor level.

To this end, parental A431 cells and those expressing ABCG2 (G2), $ABCG2_{MX}$ ($G2_{MX}$), and $ABCG2_{K86M}$ ($G2_{K86M}$) were exposed to Iressa concentrations between 25 and 100 nmol/L, and the phosphorylation status of the EGFR was directly assayed by Western blotting using anti-phosphotyrosine antibodies. As documented in Fig. 4*A*, EGFR in parental A431 cells (control A431) became ~80% dephosphorylated on treatment with 25 nmol/L Iressa. In $ABCG2_{K86M}$ ($G2_{K86M}$) cells, the receptor was dephosphorylated to a greater extent (i.e., less ABCG2 protection) than the parental cells, probably owing to the dominant-negative effect of $ABCG2_{K86M}$ ($G2_{K86M}$) on endogenous ABCG2 in A431 cells as discussed above. In contrast, ABCG2, and to a greater extent ABCG2 mitoxantrone-selected cells ($ABCG2_{MX}$; $G2_{MX}$), were protected significantly, and phosphorylated EGFR was still observed at 25 and 50 nmol/L Iressa treatment levels (Fig. 4*A*). As in the cytotoxicity experiments, ABCG2 could not protect from higher levels of Iressa treatment (Fig. 4*B*, 100 nmol/L Iressa). Figure 4*B* shows the quantitation of the Western data shown in Fig. 4*A*.

These data suggest that ABCG2 acts at the EGFR level by preventing the action of Iressa on tyrosine kinase activity. This action is significantly inhibited by a functional ABCG2, most likely acting through the active transport of Iressa from the plasma membrane before it reaches the plasma membrane resident EGFR.

It has been established that Iressa leads to cell death partly through apoptosis in A431 cells (2, 36, 37). To examine if ABCG2 protected against the early apoptotic steps of cell death, we used an Annexin V binding assay in conjunction with confocal microscopy. We followed the apoptotic process by staining the cells with

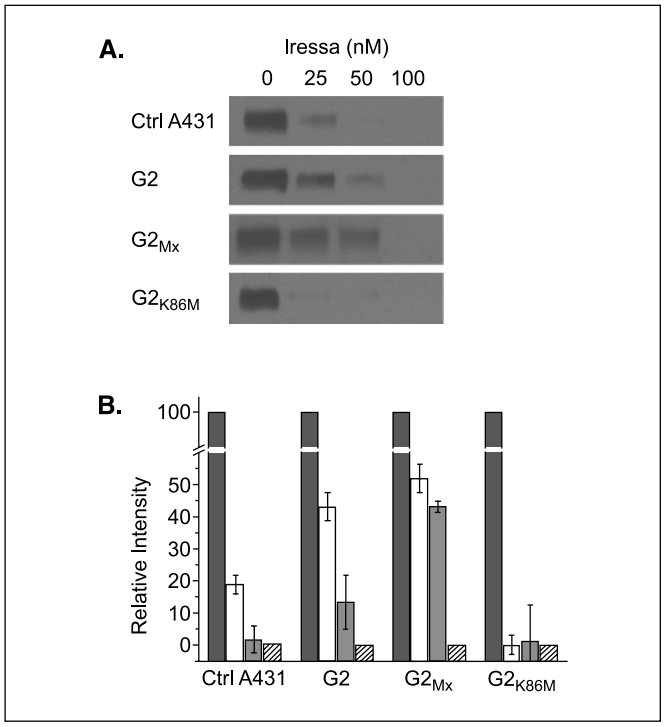

Figure 4. ABCG2 protects cells from Iressa-mediated EGFR dephosphorylation. *A,* parental A431 cells (control A431) and those expressing ABCG2 (G2), $ABCG2_{MX}$ ($G2_{MX}$), and $ABCG2_{K86M}$ ($G2_{K86M}$) were incubated first in epidermal growth factor and subsequently in the absence or presence of 25, 50, and 100 nmol/L Iressa as described in Materials and Methods. EGFR phosphorylation status in cell lysates (30 μg) was probed by Western analysis using the anti-phosphotyrosine monoclonal antibodies. *B,* quantitation of EGFR dephosphorylation study. Experiments conducted above (*A*) were repeated and quantified using Bioscan version 1.0 software following digitalization with a Hewlett Packard 5100C scanner. *Black columns,* nontreated cells; *white, gray,* and *hatched columns,* cells treated with increasing concentrations of Iressa. *Columns,* normalized mean ratio of band signal (n = 2 independent experiments); *bars,* SE.

fluorescent Annexin V, which reports the appearance of extracellular phosphatidylserine in the early apoptotic phase. Cell membrane destruction, leading to the influx and nuclear staining by PI, was also followed in the same cell samples. These experiments were carried out directly in tissue culture well–plated A431 cells, and under these conditions, cell death was prevented by ABCG2 up to Iressa concentrations of 1 μmol/L (see below). According to our experience with similar, hydrophobic drugs, due to drug absorption, higher drug concentrations are required in tissue culture plates than in cell suspensions to obtain similar cellular effects (see Materials and Methods).

As shown in Fig. 5, in the parental control A431 cells, the addition of 1 μmol/L Iressa (Fig. 5*B*, *D*, and *F*) produced an early appearance of significant Annexin V staining (Fig. 5*B*) compared with the nontreated parental A431 cells. In apoptotic cell membranes, blebbing was observed as Annexin V–stained (green) membrane vesicles coming off the plasma membrane. Mitochondrial activity of the cells (red) was visualized by MitoTracker Deep Red 633 to demarcate cells present in the field. In apoptotic cells, mitochondria typically lose the ability to bind MitoTracker Deep Red 633 as was the case here (48).

As documented in Fig. 5, on exposure to Iressa, in the control A431 cells, both Annexin V–positive/PI-negative (apoptotic) cells

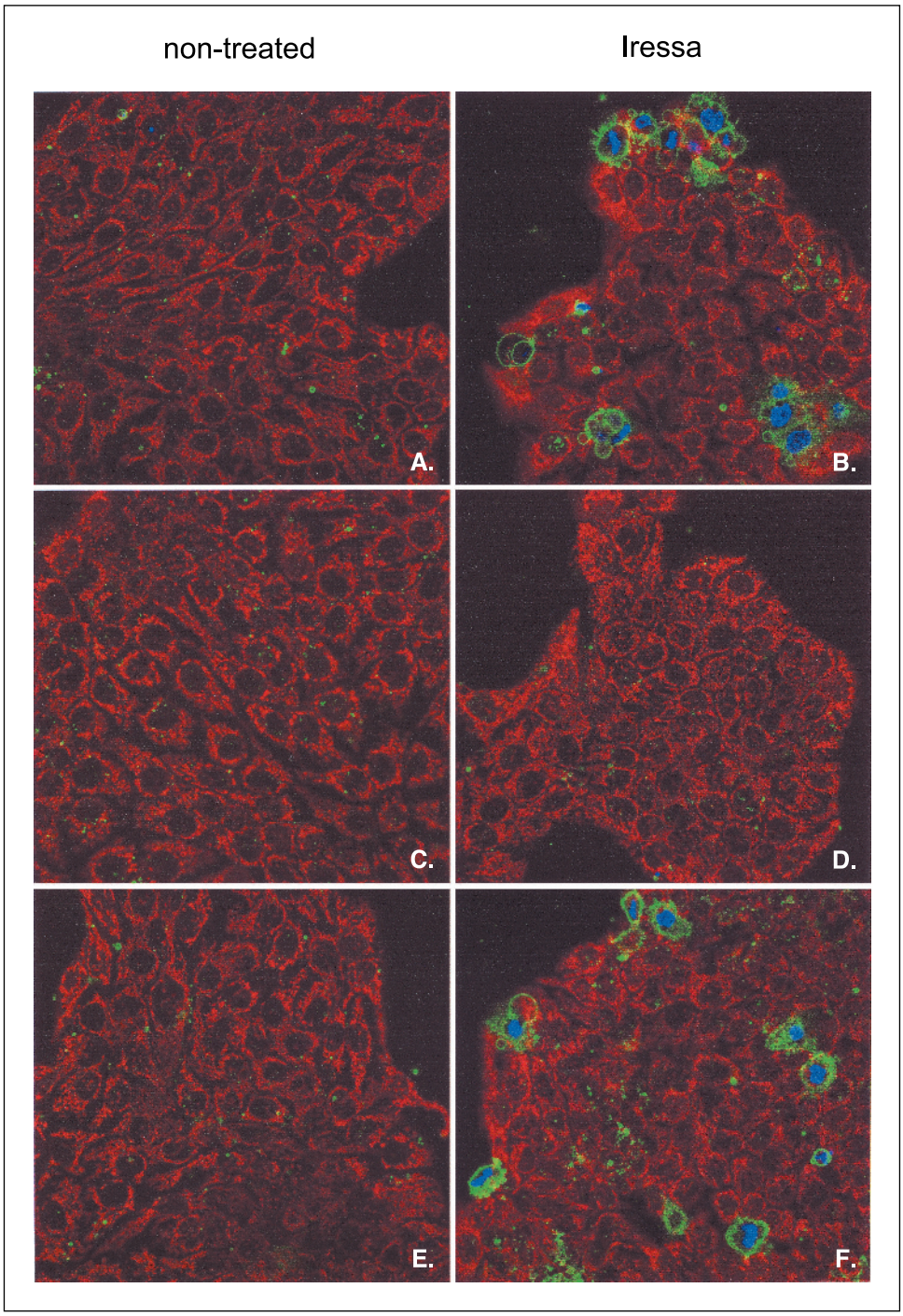

Figure 5. Morphology of Iressa-induced cell death in control and ABCG2-expressing A431 cells. Control (*A* and *B*), ABCG2 (*C* and *D*), and $ABCG2_{K86M}$ (*E* and *F*) transduced A431 cells were cultured in serum-free medium for 24 hours in the absence (*A*, *C*, and *E*) and presence (*B*, *D*, and *F*) of 1 μmol/L Iressa. Confocal images show Annexin V binding (*green*), nuclear DNA of dead cells stained with PI (*blue*), and mitochondrial activity of cells (*red*) visualized by MitoTracker Deep Red 633.

and Annexin V–positive/PI-positive (in late phase of death) cells could be observed. Both of these phases were absent in the ABCG2-expressing A431 cells (Fig. 5*D*), whereas cells expressing $ABCG2_{K86M}$ displayed a similar cell death pattern as the control A431 cells (Fig. 5*F*). These microscopic data indicate that the protective effect of ABCG2 against Iressa at the EGFR level indeed removes all the following steps of the apoptotic and cell destruction process.

In conclusion, the data presented here strongly suggest that the expression of functional ABCG2 provides significant protection against low, therapeutically relevant concentrations of Iressa in causing apoptosis-related tumor cell death. This protection correlates with the active transport capacity of ABCG2 and is directly correlated with the prevention of Iressa effect at the EGFR level.

Discussion

In this study we have examined the protective effects of the human multidrug resistance transporter, ABCG2, on A431 tumor cells when exposed to the TKRI, Iressa. Iressa is a potent inhibitor of the EGFR, and when cells, such as A431, which depend on

epidermal growth factor signaling for survival, are exposed to Iressa, they die due to disruption of the essential epidermal growth factor signal. ABCG2 is an active transporter of small hydrophobic drugs and was found recently to interact with several TKRIs with high affinity (31).

Our results presented here strongly suggest that ABCG2 actively transports Iressa from A431 cells and thus protects the cells by a transport-based mechanism. ABCG2 expressed in A431 cells by retroviral transduction (Fig. 1*A*) was functional for Hoechst 33342 transport (Fig. 1*B*), which is a well-established method for determining ABCG2 transport function (31). In experiments not shown in detail, we found that 1 μmol/L Iressa interfered with Hoechst 33342 transport in A431-ABCG2 cells, inhibiting this transport by >95%. Although this effect shows only an interaction between Iressa and ABCG2, the ABCG2-associated ATPase activity in isolated membranes was significantly stimulated by Iressa, indicating a direct transport activity for this compound (Fig. 3). Most importantly, abolishment of ABCG2-mediated protection of A431 cells to Iressa was shown in two ways: (*a*) using an ATPase- and transport-defective catalytic center mutant ($ABCG2_{K86M}$) expressed at similar levels as wild-type ABCG2 (see Fig. 1) and (*b*) using a well-established, specific, potent inhibitor of ABCG2 activity, Ko143.

Using the above-mentioned controls, we have shown ABCG2-mediated protection at several levels. In cytotoxicity experiments (Fig. 2*A*), we found that parental A431 cells or those expressing catalytically inactive ABCG2 ($G2_{K86M}$) die when exposed to low nanomolar concentrations, whereas cells expressing lower (G2) or higher ($G2_{MX}$) amounts of transporter are protected. The greatest level of protection was seen at 50 nmol/L Iressa treatment. At this concentration, we show that the ABCG2 inhibitor, Ko143, can completely reverse ABCG2-mediated protection from Iressa in these cells (Fig. 2*B*). An important point to note is that ABCG2 prevented the cytotoxic effects at Iressa concentrations likely to be present in tumor tissues after the oral administration of this TKRI (the pharmacologically relevant maximum plasma Iressa concentrations are between 500 nmol/L and 1 μmol/L; see ref. 8). In addition, the ABCG2 expression level in the transduced cells, especially without mitoxantrone selection, is in the range of that observed in drug-resistant tumor samples. Interestingly, at higher Iressa concentrations, a decreasing protection was seen by ABCG2. One explanation for the difficulty of ABCG2 in overcoming these excessive Iressa concentrations (>500 nmol/L) could be that the drug off-rate from the transporter is becoming slower, thus leading to a decreased transport rate. This phenomenon most probably does not affect the pharmacologic function of ABCG2 in the tumor cells with respect to Iressa because, as mentioned, there may be rather low local concentrations of Iressa during cancer therapy.

We have also explored the biochemical mechanism of the ABCG2-mediated cytotoxic protection by probing the EGFR phosphorylation state. On epidermal growth factor treatment, the EGFR was found highly phosphorylated (see Fig. 4*A*). Low concentrations of Iressa caused the rapid dephosphorylation of the receptor, which was reversed by functional ABCG2 (G2, $G2_{MX}$) but not by a nonfunctional transporter ($G2_{K86M}$). These data suggest that ABCG2 acts at the EGFR level, preventing the action of Iressa. ABCG2 most likely acts through the active transport of Iressa from the plasma membrane before it reaches plasma membrane resident EGFR. This finding is in line with earlier results showing that the multidrug transporters (e.g., P-glycoprotein) remove their drug substrates from the lipid phase or from the vicinity of the plasma membrane, thus preventing the cellular entry of cytotoxic agents (49).

We also did direct ABCG2-ATPase measurements in isolated membranes of ABCG2-expressing mammalian MCF-7/MX and A431 cells at various concentrations of Iressa and Ko143 concentrations (Fig. 3). We found that the ABCG2 ATPase activity was activated by low concentrations of Iressa and strongly inhibited by Ko143. These direct enzymatic studies indicate that Iressa is a transported substrate of ABCG2. In addition, higher Iressa concentrations were inhibitory for the maximum ATPase (and transport) activity of this protein. The data are also in accordance with the less effective protective effect of ABCG2 in the A431 cells at higher Iressa concentrations.

Collectively, based on all these cellular and biochemical data, we suggest that ABCG2 is actively transporting Iressa out from the cells, and this is the basis of ABCG2 protecting the tumor cells from the cytotoxic effects of this TKRI.

These results, indicating direct extrusion of Iressa by ABCG2 are somewhat unexpected based on recent studies indicating that another TKRI, STI-571 (Imatinib, Glivec), showing high-affinity interaction with ABCG2 (31), was found to be only an inhibitor and not a transported substrate of this multidrug resistance protein (50). In another study, however, the specific cytotoxic effect of STI-571 was also shown to be inhibited by ABCG2 expression (51). A possible source of this controversy is that STI-571 may have an even narrower window in the low concentration ranges, where its active transport by ABCG2 is efficient, although higher concentrations are inhibitory (31).

The findings that ABCG2 can actively protect the relevant tumor cells from Iressa have important implications regarding the clinical use of this tyrosine kinase inhibitor. First, a subset of tumors, bearing a sensitizing EGFR mutation but still unresponsive to Iressa, may be protected by an elevated level ABCG2. Second, because ABCG2 is expressed in many tissues, it could play an important role in the absorption, distribution, metabolism, excretion, and toxicity of Iressa in the patients. This would certainly affect the local concentrations of Iressa in the tumors as well as other, potentially sensitive tissues. Further, detailed clinical studies are required to examine the functional expression and the direct *in vivo* relevance of ABCG2 in this regard.

Importantly, inappropriate dosing could also be the cause of overall elevated risk of toxicity to Japanese patients and the hundreds of deaths that have occurred (12, 13). In fact, naturally occurring single nucleotide polymorphisms of ABCG2 in the Japanese population significantly alter the expression and/or the activity of this protein (27, 28), and these polymorphisms may be important modulators of individual therapeutic potential and toxicity (29).

In conclusion, our data strongly suggest that ABCG2 can actively extrude the clinically effective TKRI, Iressa, at low, therapeutically relevant concentrations of this compound. Our results also indicate that specific ABCG2 transporter modulation (such shown here by Ko143) may greatly increase the antitumor efficacy of Iressa.

Acknowledgments

Received 9/13/2004; revised 11/22/2004; accepted 12/15/2004.

Grant support: Országos Tudományos Kutatási Alapprogramok and Oktatási Minisztérium grants T31952, T35926, T038337, T38337, D45957, ETT, F034247, and NKFP; Hungarian Academy of Sciences Young Investigator Fellowship (N.B. Elkind); János Bolyai Scholarship (C. Özvegy-Laczka); and Howard Hughes International Scholarship (B. Sarkadi).

The costs of publication of this article were defrayed in part by the payment of page charges. This article must therefore be hereby marked advertisement in accordance with 18 U.S.C. Section 1734 solely to indicate this fact.

We thank Sui Li, Zsuzsanna Andrási, Judit Kis, and Györgyi Demeter for technical help.

References

1. Marmor MD, Kochupurakkal BS, Yarden Y. Signal transduction and oncogenesis by ErbB/HER receptors. Int J Radiat Oncol Biol Phys 2004;58:903–13.
2. Salomon DS, Brandt R, Ciardiello F, Normanno N. Epidermal growth factor-related peptides and their receptors in human malignancies. Crit Rev Oncol Hematol 1995;19:183–232.
3. Bunn PA Jr, Franklin W. Epidermal growth factor receptor expression, signal pathway, and inhibitors in non-small cell lung cancer. Semin Oncol 2002;29:38–44.
4. Arteaga CL, Johnson DH. Tyrosine kinase inhibitors—ZD1839 (Iressa). Curr Opin Oncol 2001;13:491–8.
5. Barker AJ, Gibson KH, Grundy W, et al. Studies leading to the identification of ZD1839 (IRESSA): an orally active, selective epidermal growth factor receptor tyrosine kinase inhibitor targeted to the treatment of cancer. Bioorg Med Chem Lett 2001;11:1911–4.
6. Herbst RS, Giaccone G, Schiller JH, et al. Gefitinib in combination with paclitaxel and carboplatin in advanced non-small-cell lung cancer: a phase III trial–INTACT 2. J Clin Oncol 2004;22:785–94.
7. Giaccone G, Herbst RS, Manegold C, et al. Gefitinib in combination with gemcitabine and cisplatin in advanced non-small-cell lung cancer: a phase III trial–INTACT 1. J Clin Oncol 2004;22:777–84.
8. Cohen MH, Williams GA, Sridhara R, et al. United States Food and Drug Administration drug approval summary: gefitinib (ZD1839; Iressa) tablets. Clin Cancer Res 2004;10:1212–8.
9. Vansteenkiste J. Gefitinib (Iressa(R)): a novel treatment for non-small cell lung cancer. Expert Rev Anticancer Ther 2004;4:5–17.
10. Lynch TJ, Bell DW, Sordella R, et al. Activating mutations in the epidermal growth factor receptor underlying responsiveness of non-small-cell lung cancer to gefitinib. N Engl J Med 2004;350:2129–39.
11. Paez JG, Janne PA, Lee JC, et al. EGFR mutations in lung cancer: correlation with clinical response to gefitinib therapy. Science 2004;304:1497–500.
12. Inoue A, Saijo Y, Maemondo M, et al. Severe acute interstitial pneumonia and gefitinib. Lancet 2003; 361:137–9.
13. Dancey JE, Freidlin B. Targeting epidermal growth factor receptor—are we missing the mark? Lancet 2003;362:62–4.
14. Cyranoski D. Biologists take tentative steps towards bespoke cancer drugs. Nature 2003;423:209.
15. Litman T, Druley TE, Stein WD, Bates SE. From MDR to MXR: new understanding of multidrug resistance systems, their properties and clinical significance. Cell Mol Life Sci 2001;58:931–59.
16. Haimeur A, Conseil G, Deeley RG, Cole SP. The MRP-related and BCRP/ABCG2 multidrug resistance proteins: biology, substrate specificity and regulation. Curr Drug Metab 2004;5:21–53.
17. Sarkadi B, Ozvegy-Laczka C, Nemet K, Varadi A. ABCG2—a transporter for all seasons. FEBS Lett 2004; 567:116–20.
18. Fisher GA, Lum BL, Hausdorff J, Sikic BI. Pharmacological considerations in the modulation of multidrug resistance. Eur J Cancer 1996;32A:1082–8.
19. Bakos E, Evers R, Sinko E, et al. Interactions of the human multidrug resistance proteins MRP1 and MRP2 with organic anions. Mol Pharmacol 2000;57:760–8.
20. Ross DD, Karp JE, Chen TT, Doyle LA. Expression of breast cancer resistance protein in blast cells from patients with acute leukemia. Blood 2000;96:365–8.
21. Brangi M, Litman T, Ciotti M, et al. Camptothecin resistance: role of the ATP-binding cassette (ABC), mitoxantrone-resistance half-transporter (MXR), and potential for glucuronidation in MXR-expressing cells. Cancer Res 1999;59:5938–46.
22. Diestra JE, Scheffer GL, Catala I, et al. Frequent expression of the multi-drug resistance-associated protein BCRP/MXR/ABCP/ABCG2 in human tumours detected by the BXP-21 monoclonal antibody in paraffin-embedded material. J Pathol 2002;198:213–9.
23. Doyle LA, Yang W, Abruzzo LV, et al. A multidrug resistance transporter from human MCF-7 breast cancer cells. Proc Natl Acad Sci U S A 1998;95:15665–70.
24. Cooray HC, Blackmore CG, Maskell L, Barrand MA. Localisation of breast cancer resistance protein in microvessel endothelium of human brain. Neuroreport 2002;13:2059–63.
25. Maliepaard M, van Gastelen MA, Tohgo A, et al. Circumvention of breast cancer resistance protein (BCRP)-mediated resistance to camptothecins *in vitro* using non-substrate drugs or the BCRP inhibitor GF120918. Clin Cancer Res 2001;7:935–41.
26. Zhou S, Schuetz JD, Bunting KD, et al. The ABC transporter Bcrp1/ABCG2 is expressed in a wide variety of stem cells and is a molecular determinant of the side-population phenotype. Nat Med 2001;7: 1028–34.
27. Mizuarai S, Aozasa N, Kotani H. Single nucleotide polymorphisms result in impaired membrane localization and reduced ATPase activity in multidrug transporter ABCG2. Int J Cancer 2004;109:238–46.
28. Imai Y, Nakane M, Kage K, et al. C421A polymorphism in the human breast cancer resistance protein gene is associated with low expression of Q141K protein and low-level drug resistance. Mol Cancer Ther 2002;1:611–6.
29. Sparreboom A, Gelderblom H, Marsh S, et al. Diflomotecan pharmacokinetics in relation to ABCG2 421C>A genotype. Clin Pharmacol Ther 2004;76:38–44.
30. Volk EL, Farley KM, Wu Y, et al. Overexpression of wild-type breast cancer resistance protein mediates methotrexate resistance. Cancer Res 2002;62:5035–40.
31. Ozvegy-Laczka C, Hegedus T, Varady G, et al. High-affinity interaction of tyrosine kinase inhibitors with the ABCG2 multidrug transporter. Mol Pharmacol 2004;65:1485–95.
32. Merlino GT, Xu YH, Ishii S, et al. Amplification and enhanced expression of the epidermal growth factor receptor gene in A431 human carcinoma cells. Science 1984;224:417–9.
33. Ullrich A, Coussens L, Hayflick JS, et al. Human epidermal growth factor receptor cDNA sequence and aberrant expression of the amplified gene in A431 epidermoid carcinoma cells. Nature 1984;309:418–25.
34. Lin CR, Chen WS, Kruiger W, et al. Expression cloning of human EGF receptor complementary DNA: gene amplification and three related messenger RNA products in A431 cells. Science 1984;224:843–8.
35. Barnes DW. Epidermal growth factor inhibits growth of A431 human epidermoid carcinoma in serum-free cell culture. J Cell Biol 1982;93:1–4.
36. Bianco R, Shin I, Ritter CA, et al. Loss of PTEN/MMAC1/TEP in EGF receptor-expressing tumor cells counteracts the antitumor action of EGFR tyrosine kinase inhibitors. Oncogene 2003;22:2812–22.
37. Janmaat ML, Giaccone G. The epidermal growth factor receptor pathway and its inhibition as anticancer therapy. Drugs Today (Barc) 2003;39 Suppl C:61–80.
38. Becker S, Wasser S, Hauses M, et al. Correction of respiratory burst activity in X-linked chronic granulomatous cells to therapeutically relevant levels after gene transfer into bone marrow $CD34^+$ cells. Hum Gene Ther 1998;9:1561–70.
39. Sinko E, Ilias A, Ujhelly O, et al. Subcellular localization and *N*-glycosylation of human ABCC6, expressed in MDCKII cells. Biochem Biophys Res Commun 2003;308:263–9.
40. Ross DD, Yang W, Abruzzo LV, et al. Atypical multidrug resistance: breast cancer resistance protein messenger RNA expression in mitoxantrone-selected cell lines. J Natl Cancer Inst 1999;91:429–33.
41. Ujhelly O, Ozvegy C, Varady G, et al. Application of a human multidrug transporter (ABCG2) variant as selectable marker in gene transfer to progenitor cells. Hum Gene Ther 2003;14:403–12.
42. Ozvegy C, Litman T, Szakacs G, et al. Functional characterization of the human multidrug transporter, ABCG2, expressed in insect cells. Biochem Biophys Res Commun 2001;285:111–7.
43. Apati A, Janossy J, Brozik A, Bauer PI, Magocsi M. Calcium induces cell survival and proliferation through the activation of the MAPK pathway in a human hormone-dependent leukemia cell line, TF-1. J Biol Chem 2003;278:9235–43.
44. Sarkadi B, Price EM, Boucher RC, Germann UA, Scarborough GA. Expression of the human multidrug resistance cDNA in insect cells generates a high activity drug-stimulated membrane ATPase. J Biol Chem 1992;267:4854–8.
45. Kim M, Turnquist H, Jackson J, et al. The multidrug resistance transporter ABCG2 (breast cancer resistance protein 1) effluxes Hoechst 33342 and is overexpressed in hematopoietic stem cells. Clin Cancer Res 2002; 8:22–8.
46. Ozvegy C, Varadi A, Sarkadi B. Characterization of drug transport, ATP hydrolysis, and nucleotide trapping by the human ABCG2 multidrug transporter. Modulation of substrate specificity by a point mutation. J Biol Chem 2002;277:47980–90.
47. Allen JD, van Loevezijn A, Lakhai JM, et al. Potent and specific inhibition of the breast cancer resistance protein multidrug transporter *in vitro* and in mouse intestine by a novel analogue of fumitremorgin C. Mol Cancer Ther 2002;1:417–25.
48. Poot M, Gibson LL, Singer VL. Detection of apoptosis in live cells by MitoTracker Red CMXRos and SYTO dye flow cytometry. Cytometry 1997;27:358–64.
49. Higgins CF, Gottesman MM. Is the multidrug transporter a flippase? Trends Biochem Sci 1992;17: 18–21.
50. Houghton PJ, Germain GS, Harwood FC, et al. Imatinib mesylate is a potent inhibitor of the ABCG2 (BCRP) transporter and reverses resistance to topotecan and SN-38 *in vitro*. Cancer Res 2004;64: 2333–7.
51. Burger H, Van Tol H, Boersma AW, et al. Imatinib mesylate (STI571) is a substrate for the breast cancer resistance protein (BCRP)/ABCG2 drug pump. Blood 2004;104:2940–2.

5. sz. közlemény

dc_46_10

dc_46_10
Available online at www.sciencedirect.com
ScienceDirect
Biochimica et Biophysica Acta 1768 (2007) 2698–2713
Biochimica et Biophysica Acta
BBA
www.elsevier.com/locate/bbamem

Membrane cholesterol selectively modulates the activity of the human ABCG2 multidrug transporter

Ágnes Telbisz [a], Marianna Müller [a], Csilla Özvegy-Laczka [a], László Homolya [a], Lajos Szente [b], András Váradi [c], Balázs Sarkadi [a,*]

[a] National Medical Center, Institute of Hematology and Immunology, Membrane Research Group of Hung. Acad. Sci, 1113 Budapest, Diószegi u. 64, Hungary
[b] CycloLab Ltd. H-1525 Budapest, P.O. Box 435, Hungary
[c] Institute of Enzymology, Hungarian Academy of Sciences, 1113 Budapest, Hungary

Received 17 April 2007; received in revised form 13 June 2007; accepted 25 June 2007
Available online 10 July 2007

Abstract

The human ABCG2 multidrug transporter provides protection against numerous toxic compounds and causes multidrug resistance in cancer. Here we examined the effects of changes in membrane cholesterol on the function of this protein. Human ABCG2 was expressed in mammalian and in Sf9 insect cells, and membrane cholesterol depletion or enrichment was achieved by preincubation with beta cyclodextrin or its cholesterol-loaded form. We found that mild cholesterol depletion of intact mammalian cells inhibited ABCG2-dependent dye and drug extrusion in a reversible fashion, while the membrane localization of the transporter protein was unchanged. Cholesterol enrichment of cholesterol-poor Sf9 cell membrane vesicles greatly increased ABCG2-driven substrate uptake, substrate-stimulated ATPase activity, as well as the formation of a catalytic cycle intermediate (nucleotide trapping). Interestingly, modulation of membrane cholesterol did not significantly affect the function of the R482G or R482T substrate mutant ABCG2 variants, or that of the MDR1 transporter. The selective, major effect of membrane cholesterol on the wild-type ABCG2 suggests a regulation of the activity of this multidrug transporter during processing or in membrane micro-domain interactions. The experimental recognition of physiological and pharmacological substrates of ABCG2, as well as the fight against cancer multidrug resistance may be facilitated by demonstrating the key role of membrane cholesterol in this transport activity.

Keywords: ABC transporters; ABCG2 transport activity; Multidrug resistance; Membrane cholesterol; ATPase activity

1. Introduction

ABCG2 is a member of the ABC multidrug resistance protein family, a plasma membrane glycoprotein, present in many human tissues, including the placenta, liver, kidney, and intestine. The tissue distribution of ABCG2 suggests that its main physiological role is the regulation of intestinal absorption and biliary secretion of potentially toxic xenobiotics. ABCG2 may also be a protective element in the maternal–fetus and in the blood–brain barrier, and the protein is present at high levels in stem cells, currently with an unknown physiological function [1–5].

ABCG2 is also used by tumor cells to fight anticancer medicines, as ABCG2 overexpression provides an active protection against a number of chemotherapeutic drugs. ABCG2 expression was found in various leukemias, in the tumors of the ovary, lung, breast, colon and gastric cancer. The anticancer cytotoxic compounds extruded by ABCG2 include mitoxantrone, topotecan, camptothecin, irinotecan, flavopiridol, as well as methotrexate and its polyglutamated metabolites [1,3,6–8].

ABCG2 is an ABC "half-transporter", which requires homodimerization for its transport function [9]. Similarly to all ABC multidrug transporters, drug extrusion by ABCG2 is closely coupled to a drug-stimulated, vanadate-sensitive ATPase activity, which requires the presence of Mg^{2+} ions [9,10]. During its substrate transport and ATP hydrolytic cycle ABCG2 occludes

Abbreviations: ABC transporters, ATP binding cassette transporters; CD, cyclodextrin; C-CD, cyclodextrin loaded with cholesterol; S-CD, cyclodextrin loaded with sitosterol; EKI, EKI-785 tyrosine kinase inhibitor; ESG, estradiol 17-beta glucuronide; E3S, estrone 3-sulfate; MDR1, multidrug resistance protein 1; MRP1, multidrug resistance associated protein 1; MTX, methotrexate; PheA, Pheophorbide A; R123, Rhodamine 123

* Corresponding author. Tel./fax: +36 1 372 4353.
E-mail address: sarkadi@biomembrane.hu (B. Sarkadi).

0005-2736/$ - see front matter © 2007 Elsevier B.V. All rights reserved.
doi:10.1016/j.bbamem.2007.06.026

ADP, and this catalytic intermediate can be "trapped" in the presence of vanadate. The direct, ATP-dependent transport of several substrates of ABCG2, including methotrexate, glucuronidated or sulfated estrogens and xenobiotics, has been demonstrated [11–14].

The R482G and R482T mutant variants of ABCG2, found only in drug-selected tumor cells, show a significantly altered drug resistance pattern, as compared to the wild-type protein. These mutants efficiently transport various anthracycline derivatives or Rhodamine 123, while the wild-type ABCG2 shows very little transport activity for these compounds. In contrast, the R482G and R482T variants practically do not transport methotrexate or drug conjugates [14–17]. There are several polymorphic variants of ABCG2 present in large percentage in the human population (e.g. V12M, Q141K), and the possible alterations in the transport capacity and substrate handling of these variants have been examined in numerous experimental systems [18–24].

The functional regulation of the ABCG2 transport activity is relatively unexplored as yet. There are several data for the modulation of ABCG2 transcription during cell differentiation, cytotoxic exposure, or hypoxia, as well as after exposure to hormones or hormone derivatives [25–27]. It has also been proposed that estrogen may have a post-translational regulatory effect by altering the biosynthesis and maturation of ABCG2 [28]. Membrane cholesterol has been implicated in the regulation of many membrane proteins, including several ABC transporters, and membrane micro-domains with increased cholesterol content have been suggested to play a role in such a regulation [29,30]. In the case of ABCG2 one study found a significant cholesterol stimulation of its ATPase activity, when the protein was expressed in *Lactococcus* bacteria [31]. The authors suggested that ABCG2 may be directly involved in cholesterol transport. However, no detailed studies are available as yet for the transport and ATPase modulation of ABCG2 activity by cholesterol in eukaryote model systems.

In the present experiments we have examined the effects of membrane cholesterol modulation on the function of the human ABCG2 protein. We followed the function and localization of this transporter in intact mammalian cells, depleted from, or loaded with cholesterol. We also studied the direct transport and ATPase activity, as well as the formation of a catalytic intermediate of the human ABCG2, expressed in recombinant baculovirus-infected Sf9 cells. Sf9 cell membranes contain significantly lower cholesterol than mammalian cell membranes [32] and proteins sensitive to membrane cholesterol have different activities when expressed in this system [33,34]. Thus Sf9 cell membrane preparations provide an excellent opportunity to directly explore the effects of increasing membrane cholesterol on the characteristics of a given mammalian membrane protein.

Our experiments show a major effect of membrane cholesterol on the activity of ABCG2. We found that cholesterol depletion strongly inhibited ABCG2-dependent drug/dye extrusion in intact mammalian cells in a reversible fashion, while cellular cholesterol loading increased this transport activity. There was no effect of cholesterol loading or depletion on the general membrane localization of ABCG2 in these short-term experiments. In isolated Sf9 cell membranes cholesterol loading greatly and specifically increased the maximum transport capacity and ATPase activity of ABCG2, and increased the rate of the formation of a catalytic intermediate. Interestingly, membrane cholesterol modulation under the same conditions had only a negligible effect on the activity of ABCG2–R482G and ABCG2–R482T mutant variants, or that of the MDR1 multidrug transporter. These data indicate a significant, selective, and reversible modulation of ABCG2 activity by membrane cholesterol.

2. Materials and methods

2.1. Cell and membrane preparations

Mammalian HEK and A431 cells, selectively overexpressing the human ABCG2 or its mutant variants, were prepared either by transfection and selection as described in [23], or by retroviral transduction as described in [35]. For Sf9 cell expression, cDNAs of human ABCG2 and its mutant variants were cloned into recombinant baculovirus transfer vectors, the insect cells were cultured, and infected with the baculoviruses as described in [14]. Virus-infected Sf9 cells were harvested, cell membranes were isolated, and membrane protein concentrations were determined as described previously [9,14,36]. The membrane preparation was optimized to yield high amount of inside-out vesicles in these preparations, and the constant amount of these vesicles was assured by measuring endogenous calcium transport activity, as described in refs. [14,17].

The level of ABCG2 expression was detected by immunoblotting, using the BXP-21 monoclonal antibody and the enhanced chemiluminescence technique (ECL, Amersham Biosciences). Quantitation of ABCG2 expression was achieved by densitometry of the immunoblots.

2.2. Cholesterol loading and depletion

For the modulation of membrane cholesterol content in mammalian cells, we used cyclodextrin pretreatments. In case of intact cells (see Figure legends) 10^6–10^7 suspended cells were preincubated at 37 °C for 20–30 min in 1 ml serum-free media, containing 2–4 mM of random methylated beta (RAMEB) cyclodextrin (CD, CycloLab), either without lipids or loaded with cholesterol (C-CD, cholesterol content 4.4%). The cells were washed to remove CD or free cholesterol and used for further transport experiments within 1 h. Cell viability was tested by trypan-blue exclusion or propidium-iodide staining, indicating that CD or C-CD treatments did not significantly increase the number of dead cells. Cholesterol content of the cells was measured by the enzymatic (Molecular Probes, Amplex Red) cholesterol assay kit.

For cholesterol loading of Sf9 cell membranes, we used two different techniques. In experiments shown in Fig. 3A, isolated membranes were prepared as described in [17], and then preincubated for 10 min at 4 °C with the indicated concentrations of CD–lipid complexes, including cholesterol-CD (cholesterol content 4.4%), sitosterol-CD (sitosterol content 1.9%), ergosterol-CD (ergosterol content 2%), or hydrocortisone–CD (hydrocortisone content 10.2%), prepared by CycloLab technology. The following transport or ATPase experiments were then performed by directly using these membrane preparations. In most experiments, during the course of the membrane preparation, before the final centrifugation step, the isolated membranes were incubated for 20 min at 4 °C with 2–4 mM of various RAMEB cyclodextrin preparations, and then cyclodextrin complexes were eliminated by a 20× dilution and a following high speed (100,000×*g*) centrifugation. Membrane preparations were stored at −80 °C in aliquots and cholesterol content was estimated by the Amplex red kit, described above.

2.3. ABCG2 activity measurements

In intact mammalian cells ABCG2 activity was measured in various assay systems. Hoechst 33342 dye uptake in a fluorescence spectrophotometer was

followed as described in [17]. Dye transport activity factor was calculated as described [17,37], that is the initial uptake rate (without inhibitor) was subtracted from the rate measured in the presence of a specific inhibitor, and divided by the uptake rate measured with the inhibitor. Mitoxantrone (MX) or Pheophorbide A (PheA) uptake was measured by flow cytometry, essentially as described in [38]. PheA uptake was followed for 12 min after the addition of 0.5 μM PheA, either in the absence or in the presence of 1 μM Ko143. Cellular PheA fluorescence was determined at excitation and emission wavelengths of 635 and 661 nm, respectively, in a FACSCalibur cytometer. Dead cells were excluded on the basis of propidium iodide staining.

In isolated Sf9 cell membranes *vanadate-sensitive ATPase activity* was measured as described in [39], using 20 min incubation times at 37 °C. MgATP-dependent uptake of ^{3}H-labeled methotrexate (MTX) and ^{3}H-labeled estradiol-17-beta glucuronide (ESG) in inside-out membrane vesicles was measured by a rapid filtration method as described [14,40], using 5-min incubations at 37 °C. We ensured that during this time period the rate of vesicular substrate uptake was linear, allowing to estimate the kinetic values. ATP-dependent transport activity of ABCG2 was determined by subtracting the uptake measured in the presence of MgAMP. MgATP-dependent transport by ABCG2 was fully inhibited by Ko143 (see Figures). MgATP-dependent Rhodamine 123 uptake by Sf9 membrane vesicles was measured by flow cytometry, by using the parameters described for Rhodamine fluorescence [14], and selecting the vesicle population based on FSC/SSC parameters. R123 uptake was followed in the presence of 1 μM R123, by taking 30 second time points for 5 min either at 37 °C or 22 °C. Again, the addition of MgAMP and Ko143 served as negative controls.

Formation of the *catalytic intermediate* ("nucleotide trapping") by the ABCG2 protein was measured as described in [17]. In brief, control or cholesterol-loaded Sf9 membranes (150 μg/assay) were incubated with 2.5 μM Co-8-azido-ATP (containing alpha-^{32}P-8-azido-ATP) for 2 or 5 min, then washed with ATP-containing media and UV-irradiated on ice. After gel-electrophoresis and electroblotting the labeled bands were visualized by Phospho-Imager and identified by immunoblotting, using the BXP-21 anti-ABCG2 antibody, as well as by Coomassie staining.

2.4. Confocal microscopy

HEK cells stably transfected with ABCG2 (wt) or ABCG2–R482G were seeded onto eight-well Nunc Lab-Tek II Chambered Coverglass (Nalge Nunc International, Rochester, NY) at 3×10^4 per well cell density, and grown for 48 h in D-MEM containing 10% FCS. Prior to the microscopy studies, the cultures were incubated with serum-free D-MEM containing 2.5 mM CD or 2.5 mM cholesterol-CD, for 20 min at 37 °C. For cholesterol repletion, the cells were first subjected to 2.5 mM CD for 20 min, then to 2.5 mM C-CD for an additional 20 min at 37 °C. Following the preincubation, the cells were gently washed, placed into serum free D-MEM, and studied by an Olympus FV500-IX confocal laser scanning microscope using an Olympus PLAPO 60× (1.4) oil immersion objective (Olympus Europa GmbH, Hamburg, Germany) at room temperature. The blue fluorescence was acquired at 405 nm excitation. The samples were subjected to 2 μM Hoechst dye, and after a 120 sec incubation time, 1 μM Ko143 was added to the medium. The activity factor was determined from the steady state fluorescence accumulation rates before and after Ko143 addition (see Fig. 1B).

For *immunofluorescence* studies the cells were seeded, cultured and preincubated with CD or C-CD as described above. For cell surface labeling, the cells were gently washed with Dulbecco's modified PBS (DPBS), and fixed with 1% paraformaldehyde in DPBS for 15 min at room temperature, and then blocked for 1 hr at room temperature in DPBS containing 0.5% bovine serum albumin. The samples were then incubated for 1 h at room temperature with the monoclonal anti-ABCG2 antibody, 5D3, conjugated with allophycocyanin (APC), diluted 5× in DPBS containing 0.5% BSA, finally washed with DPBS. For immunostaining of permeabilized cells, the CD- or C-CD pretreated samples were gently washed, and fixed with 4% paraformaldehyde in DPBS for 15 min at room temperature. After few washes with DPBS, the cells were further fixed and permeabilized in pre-chilled methanol for 5 min at −20 °C. Following further washing steps, the cells were blocked for 1 hr at room temperature in DPBS containing 2% bovine serum albumin, 1% fish gelatin, 0.1% Triton-X 100, and 5% goat serum (blocking buffer). The samples were then incubated for 1 hr at room temperature with the monoclonal anti-ABCG2, BXP-21 diluted 100× in blocking buffer. After washing with DPBS, the cells were incubated for 1 hr at room temperature with Alexa Fluor 488-conjugated goat anti-mouse IgG (H+L) diluted 250× in blocking buffer. As isotype controls, APC-conjugated mouse IgG2b (5 μg/ml) and mouse IgG2a (2.5 μg/ml) plus Alexa Fluor 488-conjugated goat anti-mouse IgG (1:250) were used. The APC-conjugated 5D3, the BXP-21, and the anti-mouse secondary antibodies were obtained from R&D

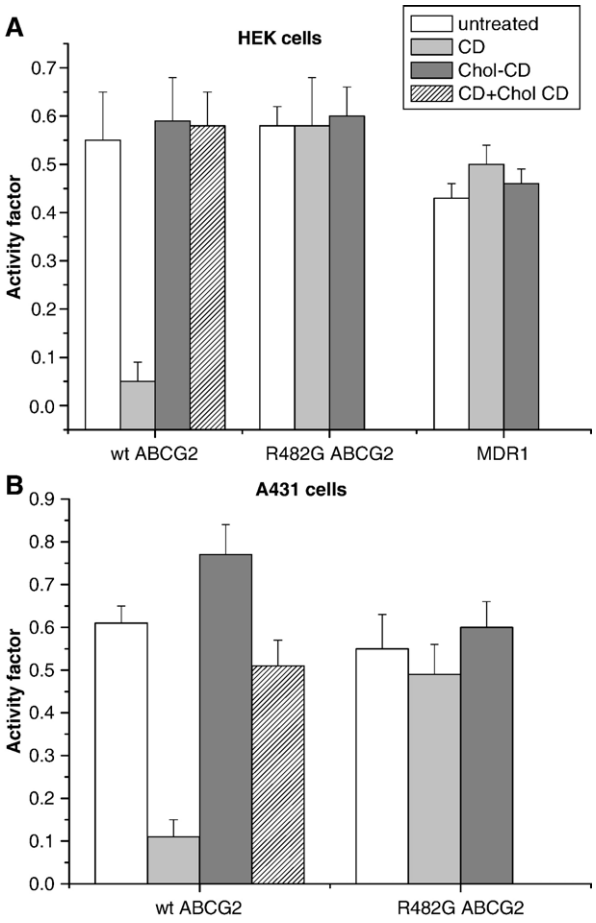

Fig. 1. Effect of cholesterol depletion or cholesterol loading on the activity of ABCG2 in intact HEK and A431 cells. Panel A. Effect of cyclodextrin (CD) or cholesterol-cyclodextrin (Chol-CD) pre-treatment on the Hoechst dye uptake activity factor in HEK cells, as measured in a fluorescence spectrophotometry assay. HEK cells, expressing the human wild-type ABCG2, the ABCG2–R482G variant, or the MDR1 protein, were pretreated in HPMI medium by 4 mM CD or 4 mM C-CD for 30 min at 37 °C, then washed twice to eliminate cyclodextrin. Hoechst dye (2 μM) accumulation was continuously measured at 37 °C in HPMI medium in a fluorescence spectrophotometer for 8 min, then 1 μM Ko143 (to the ABCG2 expressing cells) or 30 μM verapamil (to the MDR1 expressing cells) was added, and Hoechst fluorescence was measured for another 8 min. Dye extrusion activity factor was calculated based on the difference between the control uptake rate and that in the presence of inhibitor, as described in Materials and methods. The mean values±SD are presented. Empty columns: untreated cells, light gray columns: cyclodextrin (CD) pretreated cells, dark gray columns: cholesterol-cyclodextrin (C-CD) pretreated cells, striped columns: cyclodextrin (CD) pretreated, and then cholesterol repleated cells by cholesterol-cyclodextrin (C-CD) treatment. Panel B. Effect of cyclodextrin (CD) or cholesterol-cyclodextrin (Chol-CD) pre-treatment on the Hoechst dye uptake activity factor in A431 cells, as measured in a fluorescence spectrophotometry assay. The A431 cells were treated and dye accumulation measured as described for panel A. Empty columns: untreated cells, light gray columns: cyclodextrin (CD) pretreated cells, dark gray columns: cholesterol-cyclodextrin (C-CD) pretreated cells, striped columns: cyclodextrin (CD) pretreated, and then cholesterol repleated cells by cholesterol-cyclodextrin (C-CD) treatment.

Systems (Minneapolis, USA), Axxora/Alexis (Lausen, Switzerland), and Molecular Probes (Eugene, USA), respectively. The APC-conjugated mouse IgG2b, and the mouse IgG2a isotype controls were purchased from eBioscience (San Diego, USA) and DAKO Cytomation (Glostrup, Denmark), respectively. The stained samples were studied with confocal microscope specified above. The green and deep red fluorescence were acquired above 505 nm and 650 nm, using 488 nm and 633 nm excitations, respectively.

All documented measurements were carried out in at least two independent membrane preparations, at least in triplicates.

3. Results

3.1. Experiments with intact mammalian cells

For modulation of membrane cholesterol in intact mammalian cells, we applied mild treatments with beta cyclodextrin (CD), or with its cholesterol-loaded form (C-CD). Cyclodextrin complexes have been shown to be rapidly and effectively transferring cholesterol to and from cells and biological membranes [41,42].

In the experiments documented in Fig. 1A, we examined the effect of cholesterol depletion or cholesterol loading, respectively, on fluorescent dye extrusion from ABCG2-expressing intact HEK cells. The Hoechst 33342 dye is a good substrate of both the wild-type and the R482G or R482T mutant variants of ABCG2 [1,3], as well as of the MDR1 transporter [4]. This dye becomes fluorescent only inside the cells, when bound to DNA, thus increase in fluorescence directly reflects dye accumulation. In control cells this uptake is fast and not influenced by the addition of transporter inhibitors. The expression of ABCG2, its R482G mutant form, as well as MDR1 strongly decrease Hoechst dye accumulation. In the case of the addition of a specific inhibitor there is a major increase in rate of dye accumulation, reaching the level seen without transporter overexpression. As specific inhibitors, in the case of ABCG2 we used 1 μM Ko143, while in the case of MDR1 we applied 30 μM verapamil. The activity factor calculations (see Methods and 17) provide a quantitative estimate of the transporter activity in intact cells. As shown below in the isolated membrane experiments (see Fig. 3), the applied Ko143 concentration resulted in a full inhibition of ABCG2, independent of the membrane cholesterol concentrations.

Fig. 1 shows the effect of cholesterol depletion or loading on the activity factors calculated for Hoechst 33342 dye extrusion at 37 °C in ABCG2-expressing HEK (Panel A) and A431 cells (Panel B), respectively, measured in a fluorescence spectrophotometer. For demonstrating the effect of cholesterol we chose here cells expressing medium levels of the transporters, thus having a Hoechst transport activity factor between 0.4 and 0.7.

As documented in Fig. 1A, cholesterol depletion of HEK cells by 4 mM CD for 30 min at 37 °C practically eliminated Hoechst dye extrusion by the wild-type ABCG2 (the activity factor decreased from 0.54 to 0.05), while this treatment had no effect on dye extrusion in ABCG2–R482G expressing, or MDR1 expressing HEK cells. The effect of additional cholesterol loading by C-CD was not significant in these experiments in any of the above cell types.

It is also important to note, that the applied cholesterol depletion or cholesterol loading did not significantly affect the rate of Hoechst 33342 dye accumulation in the control HEK or A431 (see below) cells. Also, as measured by trypan-blue or propidium iodide exclusion, this mild pre-treatment did not increase the number of dead cells in the preparation (cell viability was over 85% in each experiment), and preserved the function of the ABCG2 mutant variants or other ABC-multidrug transporters (see also below).

Based on the enzymatic cholesterol measurements (see Methods), the original total cholesterol content in the HEK cells used in this study was 7.71 ± 1.1 μg/mg total protein, and this cholesterol content could be decreased by about 25%, to 5.71 ± 0.9 μg/mg total protein by 4 mM CD preincubation, or increased to 12 ± 1.2 μg/mg total protein, that is to about 150%, by 4 mM C-CD incubation.

When examining the possible reversibility of cholesterol depletion, we depleted HEK-ABCG2 cells from cholesterol for 30 min, as described above, and then after one washing step further incubated these cells for 20 min in a serum-free medium, or in a medium containing 4 mM Cholesterol-CD. When measuring Hoechst dye uptake in these cells we found that the original activity factor of 0.54 ± 0.06 decreased to 0.05 ± 0.04 during CD treatment, and the activity factor was increased to 0.58 ± 0.07 after cholesterol reloading. Thus, the modulation of ABCG2 transport activity by cholesterol was fully reversible.

As shown in Fig 1B, we have also performed Hoechst dye uptake experiments in ABCG2-expressing A431 tumor cells, overexpressing ABCG2 after a retroviral transduction [35]. In these cells the results were essentially similar to those obtained in HEK cells. The activity factor in the ABCG2 expressing A431 cells decreased to very low levels after 30 min cholesterol depletion, and increased to slightly above the control values after cholesterol loading. Cholesterol repletion of cholesterol-depleted cells restored the activity factor to the level of the control cells. Thus cholesterol modulation of ABCG2 transport activity in both HEK and A431 cells was also fully reversible and selective for the wild-type protein.

In experiments not documented here in detail, we have repeated these cellular transport experiments by measuring the uptake of mitoxantrone (MX) and Pheophorbide A (PheA), both transported compounds for both ABCG2 and its R482G variant, by using flow cytometry. We found that after cholesterol depletion the HEK cells expressing the wild-type ABCG2 had a significantly lower extrusion capacity, while cholesterol depletion had no effect on MX or PheA extrusion in HEK cells expressing the R482 mutant variant.

In order to demonstrate the major effect of membrane cholesterol on the ABCG2-dependent Hoechst dye transport in intact cells, we performed similar experiments in a real-time microscopic transport assay system, by using confocal microscopy. Cellular Hoechst dye uptake was directly, *in situ* followed under the microscope, and the changes in the rate of dye uptake were analyzed by determining the mean fluorescence in a selected number [10–12] of cell nuclei.

As shown in Fig. 2A, left panel, after the Hoechst dye addition, ABCG2-expressing HEK cells showed a low level of

nuclear staining, which was greatly increased upon the addition of the ABCG2 inhibitor, Ko143. CD-pretreatment of the attached HEK cells significantly increased Hoechst dye uptake, while C-CD pretreatment rather decreased this accumulation. The actual dye accumulation rate was determined in a 60- to 120-s steady state uptake period, before and after the addition of Ko143 (see Fig. 2A, upper right panel), and the activity factors were calculated. The lower right panel shows that the activity factor was significantly decreased in the CD-treated, while increased in the C-CD treated cells. Moreover, the decrease in activity factor caused by CD treatment was fully reversible upon a following C-CD incubation. Again, dye extrusion activity by the ABCG2–R482G variant was practically unaffected by CD or C-CD treatment. These experiments confirm that Hoechst 33342 dye extrusion in HEK cells, expressing the wild-type ABCG2, is strongly modulated by membrane cholesterol, while Hoechst transport by the ABCG2–R482G variant is not affected by this membrane lipid. Cell viability was unchanged in these studies—when measured by propidium iodide exclusion, viability was above 85% in all samples examined.

In order to examine the possible changes in ABCG2 localization during cholesterol depletion, we have performed immunostaining of the HEK cells by using confocal microscopy. We used both a cell-surface reactive anti-ABCG2 monoclonal antibody (5D3) [43], and another monoclonal antibody (BXP21) [44], recognizing an intracellular epitope of ABCG2. As documented in Fig. 2B, both antibodies detected exclusive plasma membrane staining, both in the control, and in the CD-treated, cholesterol-depleted cells. A similar picture was observed in the cholesterol repleted HEK cells as well (not shown).

These experiments strongly suggested that in intact cells membrane cholesterol has a major effect on the wild-type ABCG2 protein, while the morphology or the basic functions of the cells were unaltered under the mild cholesterol depletion applied. Moreover, the ATP-dependent transport by ABCG2-R482G or MDR1 was also not significantly affected under these conditions.

3.2. Experiments with isolated Sf9 cell membranes

In order to explore the molecular details of the cholesterol effects observed in intact cells, ABCG2 and its R482G, R482T mutant variants were expressed in Sf9 cells. Sf9 cells, as compared to mammalian cells, contain low level of endogenous membrane cholesterol, thus in this system a direct effect of cholesterol loading can be better examined [32–34]. Sf9 cells were engineered to express high amounts of the human ABCG2 variants, at about equal transporter protein levels [14]. Moreover, in isolated membranes of Sf9 cells both direct vesicular transport, drug-stimulated ATPase activity and catalytic intermediate formation (nucleotide trapping) could be examined [17].

For cholesterol loading of Sf9 cell membranes we applied a preincubation of the membranes at 4 °C with sterol-containing beta cyclodextrin, followed by a removal of this agent during the further centrifugation steps. The original membrane cholesterol content in our Sf9 cell membrane preparations was between 5 and 8 μg/mg membrane protein, and with 1–5 mM cholesterol-cyclodextrin (C-CD) preincubation this cholesterol content could be gradually increased up to 60–80 μg cholesterol/mg membrane protein. As a comparison, we found that the cholesterol content of the HEK or MCF7 human cell membrane preparations was between 30 and 40 μg/mg membrane protein, irrespective of the presence or absence of ABCG2 expression, while isolated red cell membranes contain up to 100 μg cholesterol/mg protein [45].

3.3. Vesicular transport studies

We carried out direct, ATP-dependent substrate transport measurements by using isolated inside-out membrane vesicles of ABCG2-expressing Sf9 cells [14,17]. In the first set of experiments we studied the effects of various sterol–CD complexes directly added to the membrane vesicles in a short preincubation period at 4 °C (see Materials and methods). Methotrexate (MTX) transport activity of the wild-type ABCG2 was measured at 100 μM MTX concentration, by the addition of 5 mM ATP in a 5 min incubation period at 37 °C. To correct for any endogenous MTX transport activity, ABCG2-dependent active MTX uptake was calculated by subtracting MTX uptake measured in the presence of 1 μM Ko143, fully inhibiting ABCG2.

As documented in Fig. 3A, the addition of 1–4 mM CD did not have any significant effect of MTX transport activity. However, Cholesterol-CD greatly increased ABCG2-dependent MTX uptake in a concentration-dependent manner (we found a maximum effect at 4 mM C-CD, data not shown in detail). There was no such transport increase in the presence of 1-4 mM sitosterol-CD or hydrocortisone-CD, while ergosterol-CD actually slightly decreased ABCG2-dependent MTX uptake. It has been shown earlier that all these sterol-CD complexes allow a rapid exchange of sterol molecules with hydrophobic binding materials [41].

In order to further investigate the effect of cholesterol loading of Sf9 cell membranes, the following experiments were performed by C-CD pretreated, cholesterol preloaded isolated membrane preparations. In these experiments the preloaded membranes, with stable membrane sterol content, could be characterized in detail. As shown in Fig. 3B, preloading of the membranes with cholesterol (C-CD) greatly increased the MTX transport activity of the wild-type ABCG2, to yield a 15–20 fold increase, when the initial membrane cholesterol was elevated to 65 μg cholesterol/mg membrane protein. We found a similar large increase in the ABCG2-dependent uptake of estradiol beta-17-glucuronide (ESG—see below), and of estrone 3-sulfate (E3S—not shown) in the Sf9 membrane vesicles after cholesterol loading. We found that pretreatment with free cyclodextrin (CD) did not significantly affect either the MTX (see Fig. 3), ESG or E3G transport activity of the human ABCG2 protein. Also, when we applied sitosterol (S) loaded CD (Fig. 3B—part 4) we found no effect on the ABCG2-dependent transport activity. Ko143, a specific inhibitor of ABCG2, abolished substrate transport both in the control and cholesterol-loaded membrane vesicles.

The R482G or R482T variants of ABCG2 have significantly different substrate handling properties than the wild-type protein. These mutant variants transport certain negatively charged compounds, e.g. MTX, ESG or E3S only with a very low activity [17–21]. As shown in Fig. 3B, MTX transport by the ABCG2–R482G variant was very low both in the control

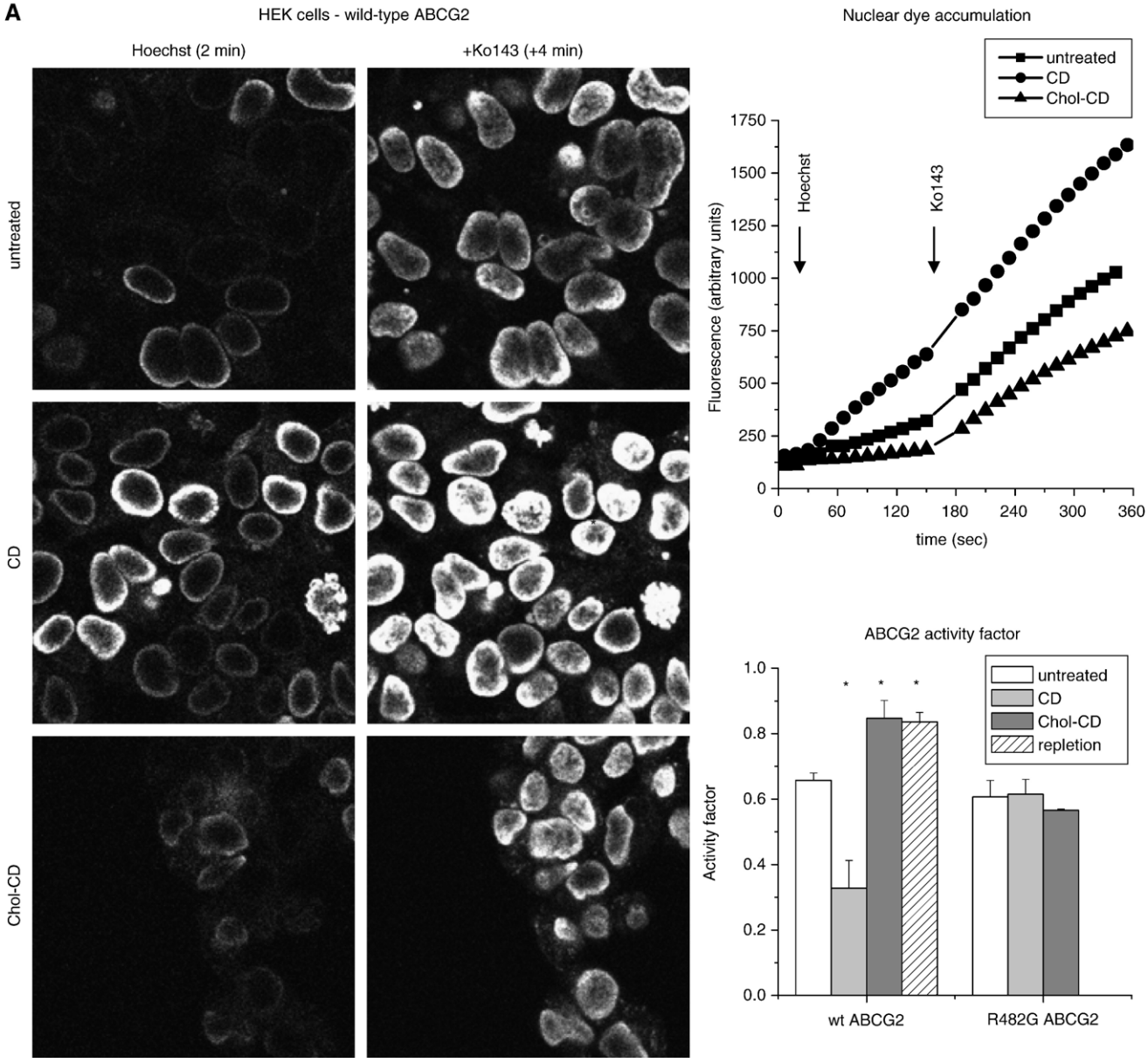

Fig. 2. Confocal microscopy studies on the effect of membrane cholesterol on Hoechst dye uptake and ABCG2 localization in ABCG2-expressing HEK cells. (A) Effect of cyclodextrin (CD) or cholesterol-cyclodextrin (Chol-CD) pre-treatment on the Hoechst dye uptake in HEK cells, as followed in a confocal microscopy assay. Cholesterol depletion or repletion by CD or C-CD was carried out in the surface attached HEK cells by 2.5 mM CD or 2.5 mM C-CD for 20 min at 37 °C, in serum free D-MEM medium, as described in Materials and methods. Hoechst dye accumulation was measured in cells expressing the human wild-type ABCG2 or the ABCG2–R482G variant at 37 °C, and cellular dye content was estimated based on the fluorescence in selected regions of interests. Activity factor, based on the difference between the control uptake rate and that in the presence of 1 μM Ko143, was calculated as described in Materials and methods. Left panel: confocal microscopy picture of HEK cells after 2 min of the Hoechst dye addition, and after an additional 4 min, following the addition of the ABCG2 inhibitor, Ko143. Upper right panel: nuclear Hoechst dye accumulation averaged in 12 cells during the experiment described above. ■—Hoechst dye uptake in the control, untreated HEK cells, expressing the wild-type ABCG2 transporter, ●—Hoechst dye uptake in cyclodextrin (CD) pretreated HEK cells, expressing the wild-type ABCG2 transporter, ▲—Hoechst dye uptake in cholesterol-cyclodextrin (C-CD) pretreated HEK cells, expressing the wild-type ABCG2 transporter. Lower right panel: the calculated ABCG2 activity factors based on the average values obtained in at least 3 independent experiments. Empty columns: untreated HEK cells, light gray columns: cyclodextrin (CD) pretreated HEK cells, dark gray columns: cholesterol-cyclodextrin (C-CD) pretreated HEK cells, striped columns: cyclodextrin (CD) pretreated HEK cells, after a second treatment with cholesterol-cyclodextrin (C-CD—see Materials and methods). The mean values ± SD are presented, the stars indicate significant differences. (B) Effect of cyclodextrin (CD) pre-treatment on the immunolocalization of ABCG2 protein in HEK cells, followed by confocal microscopy. Cholesterol depletion by CD was carried out as described for panel A. Untreated control, or cholesterol-depleted (CD) ABCG2-expressing HEK cells were fixed and immunostained as described in Materials and methods, by the 5D3 monoclonal antibody, reacting with an extracellular epitope, or by BXP21, reacting with an intracellular epitope of ABCG2.

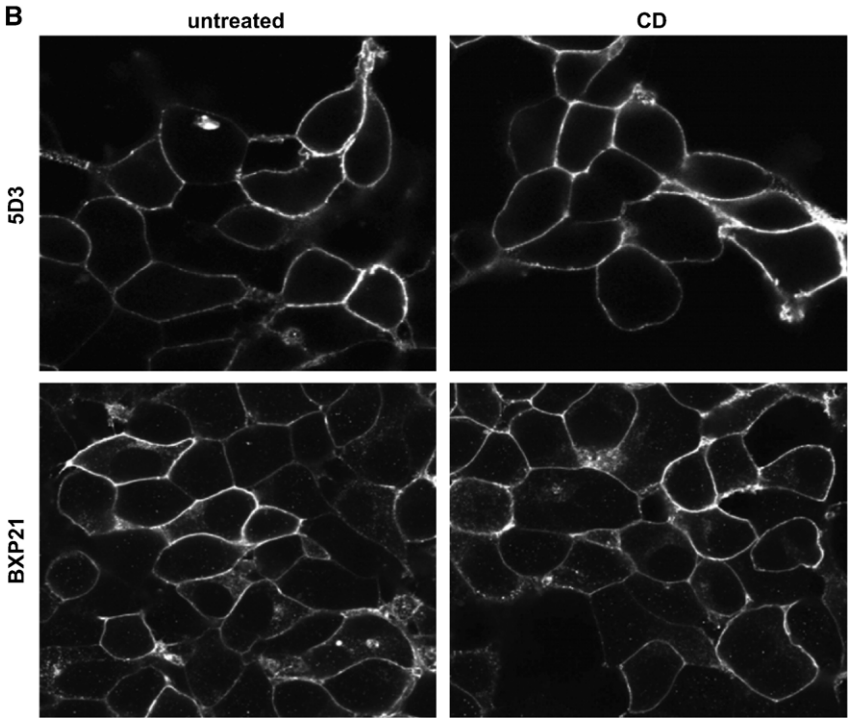

Fig. 2 (*continued*).

and in the cholesterol-loaded Sf9 membrane vesicles. Similarly, the MTX transport rate by the ABCG2–R482T variant was below 50 pmol/mg membrane protein/min, irrespective of the membrane cholesterol content. We found a similar lack of significant ESG and E3S transport by the R482G and R482T variants, irrespective of the cholesterol content of the membrane vesicles (not shown).

It is important to note that we found little effect of sterol loading or CD treatment on the endogenous ATP-dependent calcium transport activity, used to estimate the vesicle content of the Sf9 membrane preparations [17,40]. In the transport experiments documented in this manuscript, CD or sterol-CD treatment of the vesicles before the actual transport experiment did not affect, while preloading with CD-cholesterol during membrane preparation decreased the relative membrane vesicular content by 20–30%, as measured by endogenous calcium transport activity. Thus in these experiments the increase in the ABCG2 transport activity is probably underestimated, as we did not perform a correction of the data based on the calcium transport activity.

All these experiments suggest that the cholesterol effect was specific for the wild-type ABCG2, and depletion of other lipid constituents of the Sf9 cell membrane (e.g. by unloaded CD), an increase in other related membrane sterols, or non-specific permeability changes caused by various CD complexes could not be accounted for the observed effects.

In the following experiments we examined how cholesterol loading affected the kinetic parameters of MTX and ESG transport by ABCG2. Fig. 4A shows the MTX concentration dependence of the ABCG2-dependent MTX uptake in control, and cholesterol-loaded Sf9 membrane vesicles, respectively. In the original, untreated Sf9 cell membrane vesicles (containing 6–8 μg cholesterol/mg membrane protein) the rate of MTX uptake was low, with an apparent Vmax of about 0.5 nmol MTX/mg membrane protein/min. In contrast, in the C-CD pretreated vesicles (in this experiment containing 55 μg cholesterol/mg membrane protein), MTX uptake had an estimated Vmax of about 10 nmol MTX/mg membrane protein/min. The apparent Km of MTX uptake was about 0.5 mM in both cases, but the proper determination of the Km and Vmax values in these experiments was hindered by the low solubility of MTX at higher than 3 mM concentrations. Fig. 4A also documents that the R482G variant of ABCG2 had a very low MTX transport activity, irrespective of the MTX concentrations examined.

When we examined the effect of membrane cholesterol on the ATP concentration dependence of the MTX uptake in the ABCG2-containing Sf9 membrane vesicles we found that, irrespective of the membrane cholesterol content, MTX transport had a saturable ATP-dependence, with an apparent Km of 0.6–0.8 mM ATP and a maximum transport rate at about 5 mM ATP. These values are in agreement with the data in the literature for the ATP-dependence of vesicular transport by ABCG2 [17,21–23]. Again, neither the R482G, nor the R482T variants showed any MTX transport activity, irrespective of the ATP concentration or the cholesterol content of the Sf9 cell membrane vesicles.

In the following experiments we examined the ESG concentration dependence of ATP-dependent ESG uptake in Sf9 membrane vesicles (Fig. 4B). Similarly to that seen for MTX, in the cholesterol-loaded vesicles this transport showed simple saturation kinetics, with an apparent Vmax of 700 pmol

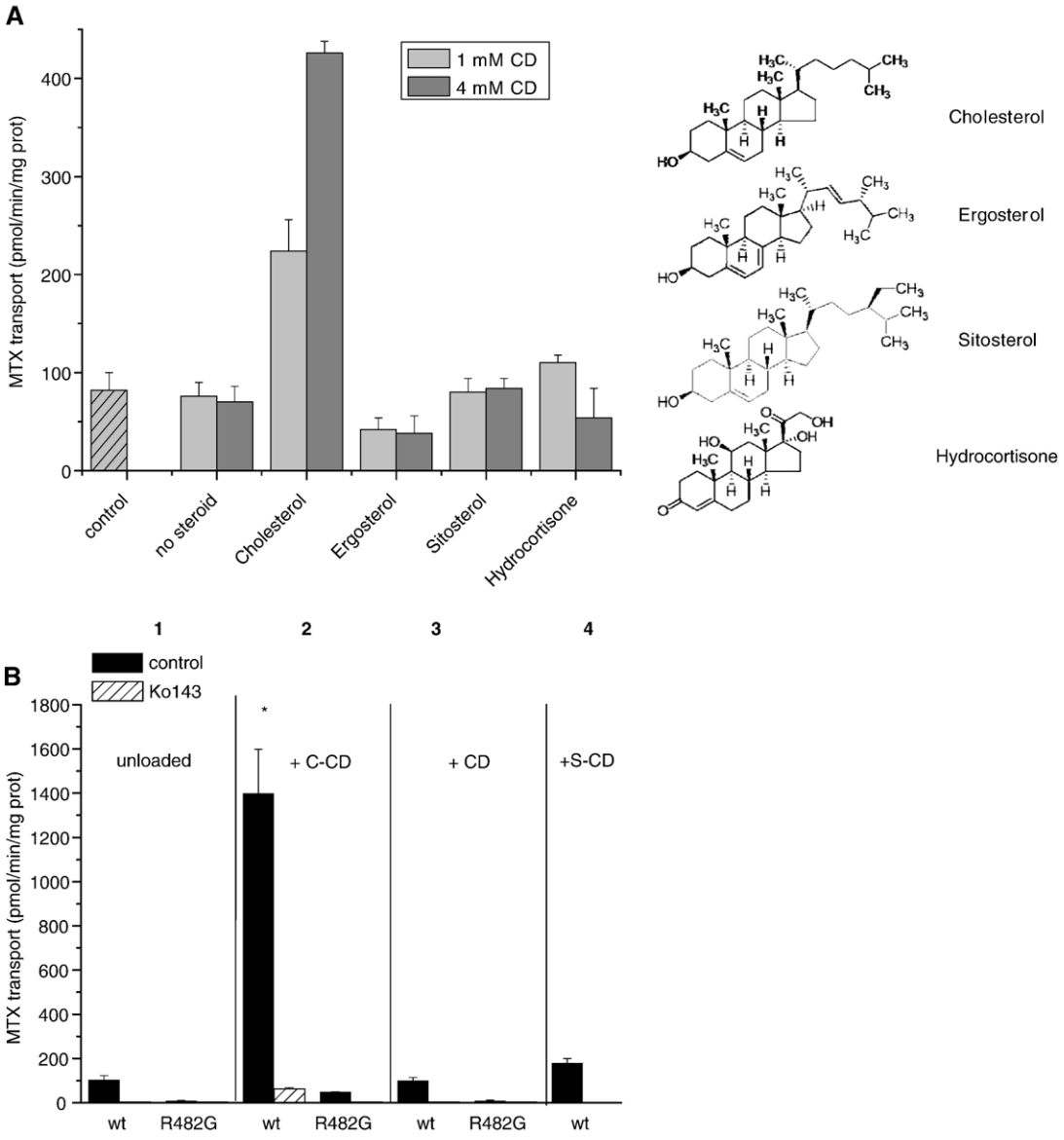

Fig. 3. (A) Effect of CD and sterol-CD complexes on the ATP-dependent transport of MTX in inside-out Sf9 membrane vesicles. Isolated membranes were preincubated for 10 min at 4 °C with CD or with the indicated concentrations of CD–lipid complexes, including cholesterol-CD, sitosterol-CD, ergosterol-CD, or hydrocortisone-CD. MTX uptake was measured at 100 μM MTX concentration for 5 min at 37 °C in membrane vesicles containing the human wild-type ABCG2 (WT), or R482G–ABCG2 (G) transporter. ABCG2-dependent transport was calculated by subtracting MTX uptake measured in the presence of 1 μM Ko143. Light gray columns: 1 mM CD or sterol-CD, dark gray columns: 4 mM CD or sterol-CD. The respective structures of the sterols applied are shown in the right panel. (B) Effect of cholesterol and sitosterol loading on ATP-dependent MTX uptake in Sf9 membrane vesicles preloaded with sterol-CD complexes. MTX uptake was measured at 100 μM MTX concentration for 5 min at 37 °C in membrane vesicles containing the human wild-type ABCG2 (WT), or R482G–ABCG2 (G) transporter. Dark columns: vesicular MTX transport without inhibitor, striped columns: MTX transport in the presence of the specific ABCG2 inhibitor, Ko143 (1 μM). Part 1 demonstrates MTX uptake in the unloaded, control vesicles (containing 8 μg cholesterol/mg membrane protein), Part 2 shows MTX uptake in cholesterol-cyclodextrin (C-CD) pre-treated vesicles (containing 56 μg cholesterol/mg membrane protein), and Part 3 shows MTX uptake in empty cyclodextrin (CD) pre-treated vesicles (containing 5 μg cholesterol/mg membrane protein). Part 4 shows the effect of sitosterol loading on ATP-dependent MTX uptake in Sf9 membrane vesicles, when the vesicles were pre-treated with sitosterol-beta-cyclodextrin (S-CD), similarly to the CD or C-CD pre-treatments. The mean values±SD are presented. Significant differences are indicated by stars.

ESG/mg membrane protein/min, while the apparent Km for ESG was about 45 μM. In the control Sf9 membrane vesicles ESG uptake was too low for a proper estimation of Km. An apparent saturation of this uptake was also achieved above 100 μM ESG, with an apparent Vmax of less than 50 pmol ESG/mg membrane protein/min.

These experiments suggest that modulation of the MTX and ESG transport by membrane cholesterol has a predominant effect on the Vmax, that is increasing the substrate transport capacity of this active transporter. Cholesterol may also slightly modulate the substrate affinity and the transporter/substrate interactions, but we need further studies in this respect.

Fig. 4C demonstrates the stimulation of the MTX and ESG transport in inside-out Sf9 cell membrane vesicles by different membrane cholesterol levels. The effect of cholesterol on the vesicular transport was measured at MTX and ESG concentrations (50 μM MTX and 25 μM ESG, respectively) below saturating values. In these experiments pooled membrane preparations, containing the same amount of human ABCG2, but loaded to different cholesterol levels, were applied. Although a slight difference in these activation curves may be observed, the effect of cholesterol on both ABCG2-dependent MTX and ESG transport was maximum above 55 μg cholesterol/mg membrane protein. Thus cholesterol modulation of ABCG2 transport activity was the most pronounced in the range of physiological cholesterol levels in various mammalian cellular membranes (see Discussion).

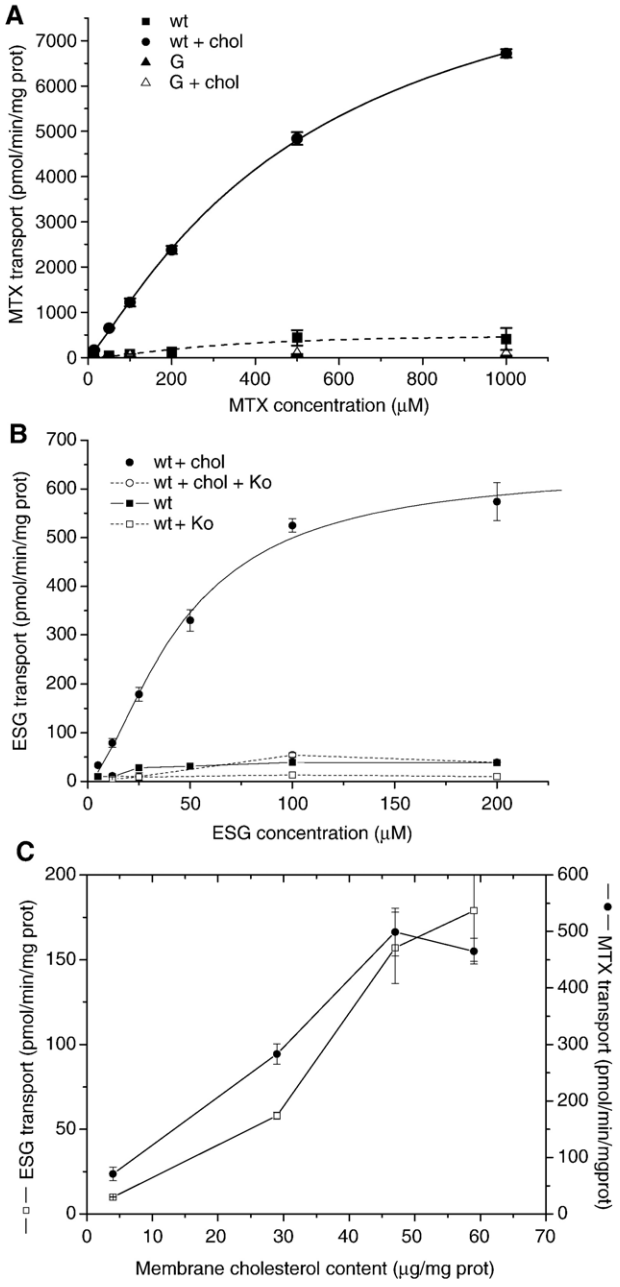

The experiments shown in Fig. 4 demonstrate that increased membrane cholesterol did not convert the ABCG2–R482G mutant into an efficient MTX or ESG transporter. However, in order to further explore the effect of cholesterol on the substrate specificity of the mutant and wild-type ABCG2, we have also examined Rhodamine 123 (R123) uptake by the Sf9 membrane vesicles. R123 is a transported substrate of the ABCG2–R482G variant, while this compound is practically not transported by the wild-type protein. As shown in Fig. 5, MgATP-dependent, rapid vesicular R123 uptake was well measurable by flow cytometry in Sf9 membrane vesicles, expressing the human R482G–ABCG2 protein. This transport was fully inhibited by 1 μM Ko143. Under the same conditions membrane vesicles containing the wild-type ABCG2 showed no measurable R123 uptake. Also, no such ATP-dependent Rhodamine uptake was observed in the control, beta-galactosidase expressing Sf9 membrane vesicles.

These data indicate that cholesterol loading of the vesicles (in these experiments to 55–62 μg cholesterol/mg membrane protein) did not evoke R123 uptake in the vesicles containing the wild-type ABCG2, while slightly increased (as an average by 25–30%) both the initial rate and the maximum level of the R123 uptake in the R482G–ABCG2 vesicles. This effect was negligible as compared to the cholesterol effect seen on the MTX or ESG transport activity of the wild-type ABCG2 transporter. We have performed these experiments with similar results with three independent membrane preparations, both at 22 °C and 37 °C, and in Fig. 5 we show a representative experiment, performed in triplicates, at 22 °C.

Fig. 4. Effect of cholesterol loading on ATP-dependent MTX and ESG uptake in Sf9 membrane vesicles. MTX and ESG uptake was measured for 5 min at 37 °C at 5 mM ATP in membrane vesicles containing the human wild-type ABCG2 (WT), or R482G–ABCG2 (G) transporter. During this time period drug uptake was linear. The mean values±SD are presented. Panel A MTX concentration dependence of MTX uptake. ABCG2-specific uptake at each substrate concentration was calculated by subtracting the rate obtained in the presence of 1 μM Ko143 ABCG2 inhibitor. ■—MTX uptake in the control vesicles (8 μg cholesterol/mg membrane protein), containing the human wild-type ABCG2 (WT) transporter, ●—MTX uptake in cholesterol-loaded vesicles (56 μg cholesterol/mg membrane protein), containing the human wild-type ABCG2 (WT) transporter, ▲—MTX uptake in the control vesicles (8 μg cholesterol/mg membrane protein), containing the human R482G ABCG2 (G) transporter, △—MTX uptake in cholesterol-loaded vesicles (62 μg cholesterol/mg membrane protein), containing the human R482G ABCG2 (G) transporter. Panel B ESG concentration dependence of ESG uptake. ■—ESG uptake in the control vesicles (8 μg cholesterol/mg membrane protein), containing the human wild-type ABCG2 (WT) transporter, □—ESG uptake in the control vesicles (8 μg cholesterol/mg membrane protein), containing the human wild-type ABCG2 (WT) transporter, in the presence of 1 μM Ko143, ●—ESG uptake in cholesterol-loaded vesicles (56 μg cholesterol/mg membrane protein), containing the human wild-type ABCG2 (WT) transporter, ○—ESG uptake in cholesterol-loaded vesicles (56 μg cholesterol/mg membrane protein), containing the human wild-type ABCG2 (WT) transporter, in the presence of 1 μM Ko143. Panel C Relative stimulation of MTX and ESG transport by cholesterol loading in Sf9 membrane vesicles. MTX uptake (●) was measured at 50 μM MTX concentration, while ESG transport (□) was measured at 25 μM ESG, for 5 min at 37 °C, in Sf9 membrane vesicles containing the human wild-type ABCG2. Membranes from the same cell preparation, containing identical amount of ABCG2, were pre-loaded by variable C-CD concentrations to contain different levels of cholesterol. On the figure for each data point the mean values±SD are presented.

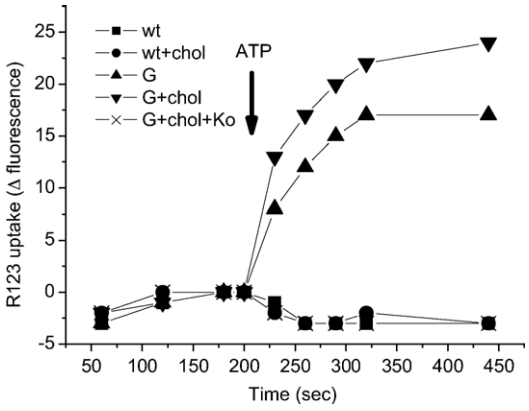

Fig. 5. Effect of cholesterol loading on ATP-dependent Rhodamine 123 (R123) uptake in Sf9 membrane vesicles. R123 uptake was measured by flow cytometry (see Materials and methods) at 1 μM R123 concentration, by taking 30-s time points for 5 min at 22 °C in membrane vesicles containing the human wild-type ABCG2 (WT), or R482G–ABCG2 (G) transporter. The figure shows a representative experiment, depicting the mean values of a triplicate measurement. The SD values for these data points were within the size of the symbols. ■—R123 uptake in the control vesicles (8 μg cholesterol/mg membrane protein), containing the human wild-type ABCG2 (WT) transporter, ●—R123 uptake in cholesterol-loaded vesicles (56 μg cholesterol/mg membrane protein), containing the human wild-type ABCG2 (WT) transporter, ▲—R123 uptake in the control vesicles (8 μg cholesterol/mg membrane protein), containing the human R482G ABCG2 (G) transporter, ▼—R123 uptake in cholesterol-loaded vesicles (62 μg cholesterol/mg membrane protein), containing the human R482G ABCG2 (G) transporter. ×—R123 uptake in cholesterol-loaded vesicles (62 μg cholesterol/mg membrane protein), containing the human R482G ABCG2 (G) transporter, in the presence of 1 μM Ko143.

As a summary, membrane cholesterol greatly and selectively increased substrate transport by the wild-type ABCG2, while we found no major changes by cholesterol in the substrate handling properties of the mutant ABCG2 protein variants.

3.4. Membrane ATPase measurements

In the following experiments we examined the effect of cholesterol loading on the membrane ATPase activity of the ABCG2 and the MDR1 proteins. Vanadate-sensitive membrane ATPase activity, selectively blocked by a specific inhibitor, reflects the transport activity of a number of the ABC multidrug transporters [1,5,39]. As reported earlier, the ABCG2-ATPase activity can be specifically inhibited by Fumitremorgin C or its analog, Ko143. This "basal" ABCG2-ATPase activity is relatively high in isolated Sf9 cell membrane vesicles, but a significant substrate-activation could not be detected in the case of the wild-type protein in the Sf9 cell membrane preparations. In contrast, many substrates caused a strong activation for the ABCG2-ATPase of the R482G or R482T variants [9,14]. The significant substrate-stimulation of the human MDR1-ATPase activity in Sf9 membranes has also been extensively documented [4,39].

Fig. 6A shows the vanadate-sensitive ATPase activity of the wild-type ABCG2 as well as the R482G and the R482T variants, both in the absence and presence of two potential transported substrates. In these studies we selected prazosin, and the EKI-785 tyrosine kinase inhibitor (EKI), as these compounds were shown to be substrates both for the wild-type, as well as the R482G or R482T variants of ABCG2 [14,35].

In Fig. 6A we document the respective ATPase activities measured at two different membrane cholesterol levels, that is in the control (6–8 μg cholesterol/mg membrane protein) and cholesterol-loaded (50–65 μg cholesterol/mg membrane protein) Sf9 cell membranes, respectively. Ko143 was shown to fully and selectively inhibit the transport activities in all these ABCG2 variants [14], and the level of the endogenous vanadate-sensitive ATPase activity in the control Sf9 cell membranes was in the range of that measured in the presence of Ko143 in the ABCG2 expressing membranes (about 8–10 nmol/mg membrane protein/min). These data indicate that the Ko143 sensitive fraction of the membrane ATPase activity closely correlates with the activity of the ABCG2 protein.

As documented in Fig. 6A, cholesterol loading of the Sf9 cell membranes did not significantly affect, or only slightly increased the basal ATPase activity of all the three ABCG2 variants, and did not affect the low background ATPase activity measured in the presence of Ko143. However, cholesterol loading greatly increased the drug-stimulated ATPase activity of the wild-type ABCG2 in the presence of both substrates, while it had no such effect in the case of the R482G or R482T mutant variants. Thus, the effect of cholesterol on the drug-stimulated ATPase activity is in close correlation with the observed alterations in the direct vesicular substrate transport, while the basal ATPase activity may not be directly related to this transport.

In the following experiments we have examined the effects of several transported substrates on the ABCG2-ATPase activity (the Ko143-sensitive fraction) in isolated Sf9 cell membranes in a concentration range of 0.1–50 micromolar. According to our earlier studies [14,35], in this system we did not observe, or obtained only a minor stimulation of the ABCG2-ATPase activity by the compounds examined. As shown in Fig. 6B, the compounds already indicated to be transported substrates of ABCG2, that is the tyrosine kinase inhibitor Iressa (Gefitinib), the widely applied topotecan, the irinotecan metabolite SN38, the experimental anticancer agent flavopiridol, and the flavonoid compound quercetin, all produced a major stimulation of the ABCG2-ATPase activity in the cholesterol-loaded Sf9 cell membranes (Panel II), while there was only a small stimulation in the control membranes (Panel I). In the case of quercetin and some tyrosine kinase inhibitors this stimulation was observed already in sub-micromolar concentrations and produced very high maximum ATPase activity levels. These data show that in cholesterol-loaded Sf9 membranes ABCG2 substrate screening, based on measuring Ko143-sensitive ATPase activity, can be efficiently and reliably performed. This is an important practical point in drug development studies, as the Sf9 membrane system is a powerful method for measuring substrate modulation or inhibition of ABC transporter ATPase activity, due to the much higher and well-controlled expression level of membrane proteins than achievable in mammalian cell membranes.

Fig. 6C shows the membrane cholesterol content dependence of the percent drug-stimulation of the ABCG2-ATPase activity by prazosin and EKI. In the case of the wild-type ABCG2, drug-

stimulation was greatly increased by increasing membrane cholesterol levels. Although the cholesterol dependence of this modulation was somewhat different for the two substrate molecules applied, a maximum effect of membrane cholesterol above 40 μg cholesterol/mg membrane protein was observed in both cases. Fig. 6C also depicts the effect of membrane

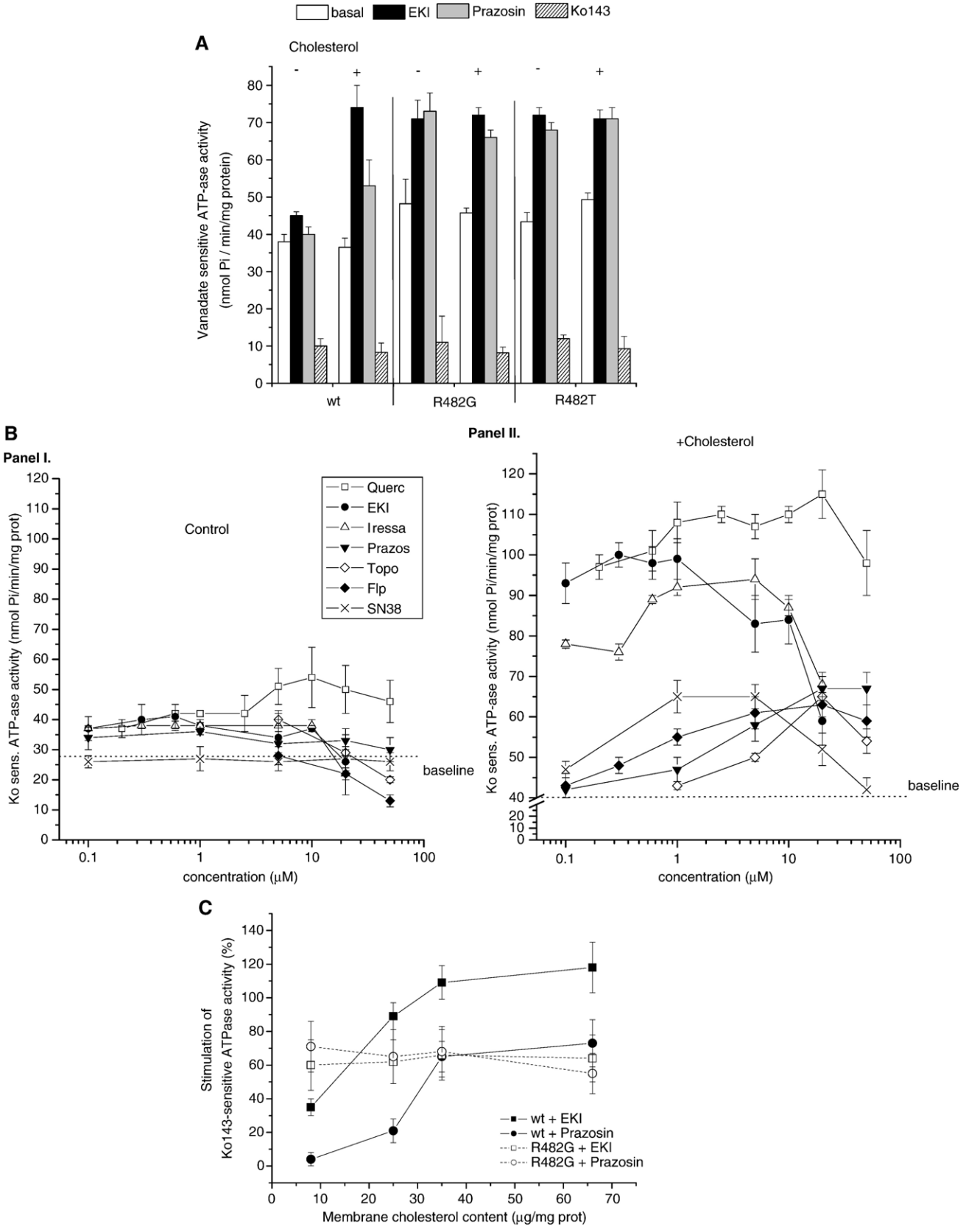

cholesterol on the prazosin and EKI stimulation of the ATPase activity of the ABCG2–R482G variant. In the case of this mutant transporter, increasing membrane cholesterol levels caused only a slight decrease in the relative substrate stimulation.

In experiments not documented here in detail, we have repeated these experiments with human MDR1-containing Sf9 membrane vesicles, and analyzed the verapamil-stimulation of the MDR1-ATPase under various cholesterol loading conditions. We found that the basal activity of the MDR1-ATPase was slightly increased, while the verapamil-stimulated maximum ATPase activity, measured at 50 μM verapamil, was practically unchanged in cholesterol-loaded Sf9 membranes. A detailed study on the cholesterol modulation of MDR1 and MRP1 activities is underway in our laboratory.

3.5. Nucleotide trapping measurements

In order to explore the molecular mechanism of the cholesterol effect on human ABCG2, we examined the vanadate-sensitive nucleotide trapping in the control and the cholesterol-loaded isolated Sf9 cell membranes, respectively. Most active ABC transporters form a catalytic intermediate, stabilized by the presence of vanadate, which can be visualized through UV-dependent photo-cross-linking and covalent labeling by alpha ^{32}P-8-azido-ATP [1,3,4]. As we documented earlier [17], in the case of ABCG2 this experiment requires the use of Co-alpha ^{32}P-8-azido-ATP, and nucleotide trapping is entirely vanadate-dependent.

In our earlier nucleotide trapping experiments, carried out in human ABCG2-containing Sf9 cell membranes, we found that in the case of wild-type ABCG2 the addition of drugs, e.g. prazosin, did not increase, but rather slightly decreased the formation of this intermediate (see 17). In contrast, nucleotide trapping in the ABCG2–R482G variant was significantly increased by transported substrates.

In the current study we repeated these experiments in Sf9 cell membranes, expressing ABCG2, either without or with cholesterol preloading. As shown in Fig. 7, in the control Sf9 cell membranes vanadate-dependent nucleotide trapping was well measurable, but the addition of prazosin or EKI only slightly decreased the formation of this intermediate. When calculating the average values in three independent experiments, corrected by the immunoblot loading control of ABCG2, the relative ABCG2 labeling was decreased to 45% by prazosin and to 55% by EKI. Cholesterol loading did not alter the basic level of ABCG2-nucleotide trapping (the mean relative value of ABCG2 labeling was 105%). However, the addition of prazosin (a relative increase to 125%), or even more significantly, of EKI (an increase to 180%), stimulated nucleotide trapping in the cholesterol-loaded membranes, in contrast to the strong

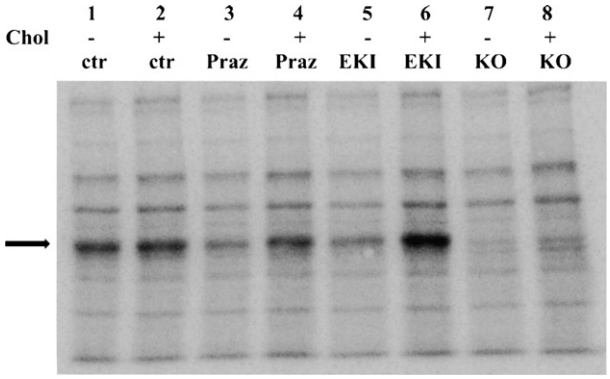

Fig. 7. Effect of cholesterol loading on the formation of the catalytic intermediate (nucleotide trapping) of human ABCG2 in isolated Sf9 membrane preparations. 8-azido-nucleotide trapping by the human, wild-type ABCG2 protein, expressed in Sf9 cell membranes, was measured as described in Materials and methods, in the presence of 2.5 μM Co-8-azido-ATP (containing alpha-^{32}P-8-azido-ATP) at 37 °C for 2 min. Following UV-irradiation, gel-electrophoresis and electroblotting, the labeled bands were visualized by Phospho-Imager. The arrow indicates the position of the ABCG2 protein identified by immunoblotting. Isolated Sf9 cell membranes, containing the same amount of wild-type ABCG2 protein were loaded with cholesterol by preincubation with 4 mM C-CD, as described in the Materials and methods. Cholesterol-loaded membrane vesicles contained 50 μg cholesterol/mg membrane protein, while the control membranes contained 8 μg cholesterol/mg membrane protein. The concentration of EKI or Ko143 was 1 μM, the concentration of prazosin was 20 μM in the assay. The figure shows a representative experiment.

Fig. 6. Effect of cholesterol loading on the ATPase activity of ABCG2 in isolated Sf9 membrane preparations. Panel A Effect of cholesterol loading on the vanadate-sensitive ATPase activity in isolated Sf9 membrane preparations. ATPase activity in the vesicles was measured for 20 min at 37 °C in membranes containing the human wild-type ABCG2 (WT), the R482G–ABCG2 (R482G), or the R482T–ABCG2 (R482T) transporter. The basal ATPase activity and the effects of two potential substrates of the ABCG2 transporter were examined. Prazosin was applied in 20 μM concentration, EKI was used in 1 μM concentration. The effect of Ko143, a specific ABCG2 inhibitor was measured at 1 μM concentration. The mean values±SD are presented. Control membranes contained 8 μg cholesterol/mg membrane protein, while cholesterol-loaded membranes contained 56 μg cholesterol/mg membrane protein in the case of the wt ABCG2, 62 μg cholesterol/mg membrane protein in the case of the ABCG2–R482G, and 65 μg cholesterol/mg membrane protein in the case of the ABCG2–R482 T variant. Empty columns: basal ATPase activity, black columns: 1 μM EKI, light gray columns: 20 μM prazosin, striped columns: 1 μM Ko143. Panel B Concentration dependence of the stimulatory effect of different drugs on the ABCG2 ATPase activity in control (Panel I) and in cholesterol loaded (Panel II) Sf9 cell membrane preparations. ATPase activity was measured for 20 min at 37 °C in membranes containing the human wild-type ABCG2, either without cholesterol-loading (left panel) or loaded with cholesterol (right panel). The ABCG2-specific ATPase activity was determined as the Ko143-sensitive fraction of the activity. Cholesterol loading by C-CD was achieved as described in the Materials and methods. Each drug was tested in at least two independent membrane preparations, the mean±SD values are presented in a representative experiment with triplicate measurements. The control membranes contained 8 μg cholesterol/mg membrane protein, while cholesterol-loaded membrane vesicles contained 42 μg cholesterol/mg membrane protein. □—Quercetin, ●—EKI-785, △—Iressa, ▼—Prazosin, ◇—Topotecan, ◆ Flavopiridol, ×—SN-38. Panel C Effect of membrane cholesterol content on the substrate stimulation of the ABCG2 ATPase activity in Sf9 membranes. ATPase activity was measured for 20 min at 37 °C in membranes containing the human wild-type ABCG2 (WT), or the R482G–ABCG2 (R482G) transporter. The specific ATPase activity for ABCG2 was calculated as the Ko143-sensitive fraction. Cholesterol loading by C-CD was achieved as described in Materials and methods. The mean values obtained in three independent experiments±SD are presented. ●—Per cent stimulation of the Ko143-sensitive ATPase activity by 20 μM Prazosin in membranes containing the human wild-type ABCG2 (WT) transporter, ■—Per cent stimulation of the Ko143-sensitive ATPase activity by 1 μM EKI in membranes containing the human wild-type ABCG2 (WT) transporter, ○—Per cent stimulation of the Ko143-sensitive ATPase activity by 20 μM Prazosin in membranes containing the human R482G ABCG2 (G) transporter, □—Per cent stimulation of the Ko143-sensitive ATPase activity by 1 μM EKI in membranes containing the human R482G ABCG2 (G) transporter.

decrease produced by these drugs in the unloaded control membranes. Similar results were obtained at two different time-points (2 min and 5 min) in these nucleotide trapping studies. In all cases the addition of Ko143 eliminated ABCG2-dependent nucleotide trapping.

In the case of the ABCG2–R482G mutant variant, prazosin and EKI stimulation of nucleotide trapping was already present in the control membranes [17], and in this case we did not find any significant difference by cholesterol enrichment of the Sf9 cell membranes in the present study (data not shown).

These experiments indicate a significant effect of membrane cholesterol on the rate of nucleotide trapping by the human ABCG2 protein. In correlation with the observed acceleration of direct vesicular substrate transport, and the appearance of drug-stimulated ATPase activity, cholesterol loading was found to promote the drug stimulation of the formation of the catalytic intermediate, indicating a cholesterol stimulation of the turnover of the wild-type transporter.

4. Discussion

Our present experiments document a major effect of membrane cholesterol on the activity of the human ABCG2 protein. We found that in intact mammalian cells a rapid and mild cholesterol depletion, without causing a significant cellular damage, strongly reduced ABCG2-dependent transport activity. This effect was fully reversible, and selective for the wild-type ABCG2, while the function of the highly active mutant variant ABCG2–R482G, found in drug-selected tumor cells, was not influenced by a similar cholesterol depletion. It is important to note that cell viability or membrane localization of ABCG2 was unchanged in the course of these cholesterol modulating experiments. Moreover, under similar conditions we found no measurable effect of cholesterol depletion or cholesterol loading on the activity of another ABC multidrug transporter, the MDR1 (ABCB1) protein.

In intact cells several non-specific effects may occur, including the removal of various hydrophobic membrane components by cyclodextrin. Moreover, long-term cholesterol depletion significantly reduces survival, thus drug-resistance experiments could not be performed under these conditions. Therefore, the molecular details of cholesterol effects could be much better examined in isolated membrane preparations. In order to perform such studies we used Sf9 cell membrane vesicles, obtained from insect cells expressing high levels of the human ABCG2 or its variants. Sf9 cell membranes contain relatively low levels of endogenous cholesterol, thus variable levels of increased membrane cholesterol, approaching or even exceeding those in mammalian cell membranes, could be achieved.

Direct vesicular transport studies performed in such preparations indicated that the maximum transport rate of ABCG2 can be increased up to 20 fold by increasing membrane cholesterol levels. By using various sterol-cyclodextrin complexes we found that this effect on ABCG2 was selective for alterations in membrane cholesterol. Although the structurally similar ergosterol or sitosterol also have the capacity to increase membrane order in artificial membranes, and they have a stabilizing role in drosophila (ergosterol) or plant (sitosterol) membranes [see refs. [34,42,50], none of them were able to mimic the effect of cholesterol in our experiments. Similarly to that seen in intact cells, this effect of membrane cholesterol was absent in the case of the R482G mutant variant of the transporter.

Vanadate- and inhibitor-sensitive membrane ATPase activity in ABC transporter expressing cell membrane preparations has been shown to correlate with the transport activity of these proteins [5]. However, according to our earlier experiments, in the case of the wild-type ABCG2 transporter, in spite of a pronounced basal ATPase activity, the substrate drug stimulation in the Sf9 cell membranes was relatively small [14]. In contrast, in isolated mammalian cell (e.g. MCF7) membranes, ABCG2-ATPase activity could be significantly stimulated by various drug substrates. It has been suggested for MDR1 and for ABCG2 as well, that the basal ATPase activity, measured in the absence of added substrates, may be due to activation by endogenous substrates, or may reflect a partially uncoupled ATPase activity of the transporter [1,4]. Interestingly, the ATPase activity of the R482G or R482T mutant variants of ABCG2 could be significantly enhanced by the respective substrate drugs both in the Sf9 and the mammalian cell membrane preparations [10,14].

Since membrane proteins, when expressed in Sf9 cells, are underglycosylated, we first speculated that the loss of glycosylation may result in these alterations of the ABCG2-ATPase activity. However, it has been demonstrated that glycosylation of ABCG2 has no effect either on its activity, processing, or membrane localization [46–48]. The present experiments strongly suggest that alterations in ABCG2-ATPase are mostly due to the different membrane cholesterol levels, that is cholesterol enrichment of the Sf9 cell membranes enables a substrate-stimulation of the wild-type ABCG2-ATPase activity. An important result of these experiments is that by using cholesterol preloaded Sf9 cell membranes this technology allows the screening of a wide variety of ABCG2-specific substrate molecules by measuring ABCG2-ATPase activity. This is clearly shown by the large effects of submicromolar concentrations of e.g. Gefitinib (Iressa), or quercetin in this system (see Fig. 6B-II).

Earlier we examined the vanadate-dependent formation of a trapped nucleotide by ABCG2, reflecting the catalytic intermediate in ABC transporters in isolated Sf9 cell membrane preparations [17]. In these experiments we found that in the case of the wild-type ABCG2 protein, the transported substrates did not increase, rather slightly decreased the formation of this intermediate. In contrast, transported substrates significantly increased nucleotide trapping by the ABCG2-R482G variant [17]. In our present experiments we found that in cholesterol enriched Sf9 cell membranes transported substrates produced an increased rate of catalytic intermediate formation also in the wild-type ABCG2. This finding indicates that cholesterol enhances the drug substrate-dependent turnover of ABCG2.

In this study we observed that the effect of membrane cholesterol was specific for the wild-type ABCG2 protein, containing an Arg (R) at the proposed intracellular membrane region of the third transmembrane loop of the protein. Replacement of this

Arg by Gly or Thr significantly alters the substrate specificity of ABCG2, and seems to removes its cholesterol modulation. This finding excludes a non-specific stabilization or modulation of this protein by cholesterol, and suggests a special role of this protein region both in the substrate recognition and cholesterol modulation of ABCG2. A recent study [48,49] concluded that mutations at position 482 in ABCG2, while alter the transport and ATPase profile of this protein, do not affect drug binding. Thus cholesterol may interact with a region involved in the catalytic/transport region of ABCG2. An exploration of the exact molecular or conformational specificity of this cholesterol effect needs further experiments.

Based on Sf9 membrane ATPase measurements, earlier we proposed that the R482G and R482T variants of ABCG2 may have "gain-of-function" properties [14]. Our present experiments indicate that these mutant ABCG2 variants may show a higher ATPase and transport activity only in the cholesterol-poor membranes, and at increasing membrane cholesterol levels in the Sf9 cell membranes the wild-type protein may achieve an ATPase and transport capacity approaching that in the mutant variants. We speculate that in spite of the reduced xenobiotic recognition profile of the wild-type ABCG2, its cholesterol-modulation may explain the evolutionary conservation of Arg at position 482.

In these experiments we observed gradual effects of the Sf9 cell membrane cholesterol on the transport and ATPase activity of ABCG2. The range where membrane cholesterol had the most significant effect, in mammalian cells corresponds to the values observed between the low-cholesterol intracellular (e.g. ER) membranes, and the high-cholesterol plasma membranes [50]. Certain plasma membrane microdomains (e.g. "membrane rafts") were shown to have especially high cholesterol levels [34,50]. Thus in mammalian cells a complex, reversible cholesterol modulation of the ABCG2-dependent xenobiotic extrusion or cancer drug resistance may be expected. The routing of the ABCG2 protein to specific plasma membrane regions, or the internalization of the protein to intracellular membrane compartments, may alter ABCG2 transport activity by more than an order of magnitude.

Several members of the ABCG family are involved in active cholesterol transport [51–53], and this may be true for ABCG2 as well. However, direct vesicular cholesterol transport measurements could not be performed in our system. Still, the present study does not suggest that cholesterol itself is a transported substrate for ABCG2. We did not observe any cholesterol competition in the transport assays, and found no major stimulation of the ABCG2-ATPase activity or nucleotide trapping by cholesterol in the absence of added substrates. However, a possible co-transport of cholesterol with specific ABCG2 substrates cannot be excluded at present.

Cholesterol modulation of multidrug transporters, especially that of MDR1 (ABCB1) has been reported in the literature [29,30]. In our present study, under similar conditions as examined for ABCG2, we found no major effect of the mild cholesterol depletion of mammalian cell membranes on the MDR1 transport activity (see Fig. 1A). In experiments to be reported in detail elsewhere, we have examined the effects of membrane cholesterol both on the human MDR1 and the MRP1 proteins, expressed in Sf9 cell membrane preparations. However, under conditions used in the present study, the effect of membrane cholesterol on these transporters was almost negligible, as compared to the wild-type human ABCG2. In earlier studies with isolated MDR1 protein it has been shown [54] that cholesterol increased the basal ATPase activity but did not significantly modulate the drug-stimulated MDR1-ATPase in proteoliposomes. In a similar system, recent experiments documented that cholesterol directly and variably modulated the drug-affinity of the isolated MDR1 protein, while did not affect its maximum turnover rate in the case of most substrates, having high stimulatory activity. Paclitaxel, a substrate with a low stimulatory effect, was found to be an exception [55].

As a summary, here we found that membrane cholesterol depletion inhibits, while cholesterol enrichment greatly augments the active transport and ATPase activity, as well as the catalytic intermediate formation of the ABCG2 protein. Detailed studies on these cholesterol effects, regarding various toxin and drug substrates, as well as the polymorphic variants of ABCG2, are underway in our laboratory. These combined studies may allow the exploration of a functional, complex regulation of this medically important ABC transporter protein.

5. Note added in proof

While this manuscript was under reviewing, a communication (Ref. [56]) described a stimulating effect of cholesterol loading on the ABCG2 ATPase and transport activity in isolated membrane preparations.

Acknowledgments

This work has been supported by OTKA (AT48986, AT48729), and NKFP. Csilla Özvegy-Laczka is a Postdoctoral Fellow (OTKA D45957), and recipient of the János Bolyai Scholarship. We thank for the valuable advice of Peter Krajcsi, György Báthori and Gergely Szakács. The experimental help by Dr. Attila Iliás, Judit Kis, Éva Krizsán, Zsuzsanna Andrási and Györgyi Demeter is greatly appreciated.

References

[1] M.M. Gottesman, T. Fojo, S.E. Bates, Multidrug resistance in cancer: role of ATP-dependent transporters, Nat. Rev., Cancer 2 (2002) 48–58.
[2] B. Sarkadi, C. Ozvegy-Laczka, K. Nemet, A. Varadi, ABCG2—A transporter for all seasons, FEBS Lett. 567 (2004) 116–120.
[3] P. Krishnamurthy, J.D. Schuetz, Role of ABCG2/BCRP in biology and medicine, Annu. Rev. Pharmacol. Toxicol. 46 (2006) 381–410.
[4] G. Szakacs, J.K. Paterson, J.A. Ludwig, C. Booth-Genthe, M.M. Gottesman, Targeting multidrug resistance in cancer, Nat. Rev., Drug Discov. 5 (2006) 219–234.
[5] B. Sarkadi, L. Homolya, G. Szakacs, A. Varadi, Human multidrug resistance ABCB and ABCG transporters: participation in a chemoimmunity defense system, Physiol. Rev. 86 (2006) 1179–1236.
[6] B.L. Abbott, ABCG2 (BCRP): a cytoprotectant in normal and malignant stem cells, Clin. Adv. Hematol. Oncol. 4 (2006) 63–72.
[7] S. Choudhuri, C.D. Klaassen, Structure, function, expression, genomic organization, and single nucleotide polymorphisms of human ABCB1

(MDR1), ABCC (MRP), and ABCG2 (BCRP) efflux transporters, Int. J. Toxicol. 25 (2006) 231–259.
[8] A.E. van Herwaarden, A.H. Schinkel, The function of breast cancer resistance protein in epithelial barriers, stem cells and milk secretion of drugs and xenotoxins, Trends Pharmacol. Sci. 27 (2006) 10–16.
[9] C. Ozvegy, T. Litman, G. Szakacs, Z. Nagy, S. Bates, A. Varadi, B. Sarkadi, Functional characterization of the human multidrug transporter, ABCG2, expressed in insect cells, Biochem. Biophys. Res. Commun. 285 (2001) 111–117.
[10] T. Litman, M. Brangi, E. Hudson, P. Fetsch, A. Abati, D.D. Ross, K. Miyake, J.H. Resau, S.E. Bates, The multidrug-resistant phenotype associated with overexpression of the new ABC half-transporter, MXR (ABCG2), J. Cell. Sci. 113 (Pt 11) (2000) 2011–2021.
[11] E.L. Volk, K.M. Farley, Y. Wu, F. Li, R.W. Robey, E. Schneider, Overexpression of wild-type breast cancer resistance protein mediates methotrexate resistance, Cancer Res. 62 (2002) 5035–5040.
[12] Z.S. Chen, R.W. Robey, M.G. Belinsky, I. Shchaveleva, X.Q. Ren, Y. Sugimoto, D.D. Ross, S.E. Bates, G.D. Kruh, Transport of methotrexate, methotrexate polyglutamates, and 17beta-estradiol 17-(beta-D-glucuronide) by ABCG2: effects of acquired mutations at R482 on methotrexate transport, Cancer Res. 63 (2003) 4048–4054.
[13] Y. Imai, S. Asada, S. Tsukahara, E. Ishikawa, T. Tsuruo, Y. Sugimoto, Breast cancer resistance protein exports sulfated estrogens but not free estrogens, Mol. Pharmacol. 64 (2003) 610–618.
[14] C. Ozvegy-Laczka, G. Koblos, B. Sarkadi, A. Varadi, Single amino acid (482) variants of the ABCG2 multidrug transporter: major differences in transport capacity and substrate recognition, Biochim. Biophys. Acta 1668 (2005) 53–63.
[15] Y. Honjo, C.A. Hrycyna, Q.W. Yan, W.Y. Medina-Perez, R.W. Robey, A. van de Laar, T. Litman, M. Dean, S.E. Bates, Acquired mutations in the MXR/BCRP/ABCP gene alter substrate specificity in MXR/BCRP/ABCP-overexpressing cells, Cancer Res. 61 (2001) 6635–6639.
[16] E.L. Volk, E. Schneider, Wild-type breast cancer resistance protein (BCRP/ABCG2) is a methotrexate polyglutamate transporter, Cancer Res. 63 (2003) 5538–5543.
[17] C. Ozvegy, A. Varadi, B. Sarkadi, Characterization of drug transport, ATP hydrolysis, and nucleotide trapping by the human ABCG2 multidrug transporter. Modulation of substrate specificity by a point mutation, J. Biol. Chem. 277 (2002) 47980–47990.
[18] Y. Honjo, K. Morisaki, L.M. Huff, R.W. Robey, J. Hung, M. Dean, S.E. Bates, Single-nucleotide polymorphism (SNP) analysis in the ABC half-transporter ABCG2 (MXR/BCRP/ABCP1), Cancer Biol. Ther. 1 (2002) 696–702.
[19] H. Mitomo, R. Kato, A. Ito, S. Kasamatsu, Y. Ikegami, I. Kii, A. Kudo, E. Kobatake, Y. Sumino, T. Ishikawa, A functional study on polymorphism of the ATP-binding cassette transporter ABCG2: critical role of arginine-482 in methotrexate transport, Biochem. J. 373 (2003) 767–774.
[20] C.P. Zamber, J.K. Lamba, K. Yasuda, J. Farnum, K. Thummel, J.D. Schuetz, E.G. Schuetz, Natural allelic variants of breast cancer resistance protein (BCRP) and their relationship to BCRP expression in human intestine, Pharmacogenetics 13 (2003) 19–28.
[21] M. Miwa, S. Tsukahara, E. Ishikawa, S. Asada, Y. Imai, Y. Sugimoto, Single amino acid substitutions in the transmembrane domains of breast cancer resistance protein (BCRP) alter cross resistance patterns in transfectants, Int. J. Cancer 107 (2003) 757–763.
[22] C. Kondo, H. Suzuki, M. Itoda, S. Ozawa, J. Sawada, D. Kobayashi, I. Ieiri, K. Mine, K. Ohtsubo, Y. Sugiyama, Functional analysis of SNPs variants of BCRP/ABCG2, Pharm. Res. 21 (2004) 1895–1903.
[23] K. Morisaki, R.W. Robey, C. Ozvegy-Laczka, Y. Honjo, O. Polgar, K. Steadman, B. Sarkadi, S.E. Bates, Single nucleotide polymorphisms modify the transporter activity of ABCG2, Cancer Chemother. Pharmacol. 56 (2005) 161–172.
[24] J. Cervenak, H. Andrikovics, C. Ozvegy-Laczka, A. Tordai, K. Nemet, A. Varadi, B. Sarkadi, The role of the human ABCG2 multidrug transporter and its variants in cancer therapy and toxicology, Cancer Lett. 234 (2006) 62–72.
[25] P.L. Ee, S. Kamalakaran, D. Tonetti, X. He, D.D. Ross, W.T. Beck, Identification of a novel estrogen response element in the breast cancer resistance protein (ABCG2) gene, Cancer Res. 64 (2004) 1247–1251.
[26] P. Krishnamurthy, D.D. Ross, T. Nakanishi, K. Bailey-Dell, S. Zhou, K.E. Mercer, B. Sarkadi, B.P. Sorrentino, J.D. Schuetz, The stem cell marker Bcrp/ABCG2 enhances hypoxic cell survival through interactions with heme, J. Biol. Chem. 279 (2004) 24218–24225.
[27] I. Szatmari, G. Vamosi, P. Brazda, B.L. Balint, S. Benko, L. Szeles, V. Jeney, C. Ozvegy-Laczka, A. Szanto, E. Barta, J. Balla, B. Sarkadi, L. Nagy, Peroxisome proliferator-activated receptor gamma-regulated ABCG2 expression confers cytoprotection to human dendritic cells, J. Biol. Chem. 281 (2006) 23812–23823.
[28] Y. Imai, E. Ishikawa, S. Asada, Y. Sugimoto, Estrogen-mediated post transcriptional down-regulation of breast cancer resistance protein/ABCG2, Cancer Res. 65 (2005) 596–604.
[29] Z. Bacso, H. Nagy, K. Goda, L. Bene, F. Fenyvesi, J. Matko, G. Szabo, Raft and cytoskeleton associations of an ABC transporter: P-glycoprotein, Cytometry, Part A 61 (2004) 105–116.
[30] S. Orlowski, S. Martin, A. Escargueil, P-glycoprotein and 'lipid rafts': some ambiguous mutual relationships (floating on them, building them or meeting them by chance?), Cell. Mol. Life Sci. 63 (2006) 1038–1059.
[31] T. Janvilisri, H. Venter, S. Shahi, G. Reuter, L. Balakrishnan, H.W. van Veen, Sterol transport by the human breast cancer resistance protein (ABCG2) expressed in *Lactococcus lactis*, J. Biol. Chem. 278 (2003) 20645–20651.
[32] K. Marheineke, S. Grunewald, W. Christie, H. Reilander, Lipid composition of *Spodoptera frugiperda* (Sf9) and Trichoplusia in (Tn) insect cells used for baculovirus infection, FEBS Lett. 441 (1998) 49–52.
[33] G. Gimpl, U. Klein, H. Reilander, F. Fahrenholz, Expression of the human oxytocin receptor in baculovirus-infected insect cells: high-affinity binding is induced by a cholesterol-cyclodextrin complex, Biochemistry 34 (1995) 13794–13801.
[34] K. Burger, G. Gimpl, F. Fahrenholz, Regulation of receptor function by cholesterol, Cell Mol. Life Sci. 57 (2000) 1577–1592.
[35] N.B. Elkind, Z. Szentpetery, A. Apati, C. Ozvegy-Laczka, G. Varady, O. Ujhelly, K. Szabo, L. Homolya, A. Varadi, L. Buday, G. Keri, K. Nemet, B. Sarkadi, Multidrug transporter ABCG2 prevents tumor cell death induced by the epidermal growth factor receptor inhibitor Iressa (ZD1839, Gefitinib), Cancer Res. 65 (2005) 1770–1777.
[36] M. Muller, E. Bakos, E. Welker, A. Varadi, U.A. Germann, M.M. Gottesman, B.S. Morse, I.B. Roninson, B. Sarkadi, Altered drug-stimulated ATPase activity in mutants of the human multidrug resistance protein, J. Biol. Chem. 271 (1996) 1877–1883.
[37] L. Homolya, M. Hollo, M. Muller, E.B. Mechetner, B. Sarkadi, A new method for a quantitative assessment of P-glycoprotein-related multidrug resistance in tumour cells, Br. J. Cancer 73 (1996) 849–855.
[38] R.W. Robey, K. Steadman, O. Polgar, K. Morisaki, M. Blayney, P. Mistry, S.E. Bates, Pheophorbide a is a specific probe for ABCG2 function and inhibition, Cancer Res. 64 (2004) 1242–1246.
[39] B. Sarkadi, E.M. Price, R.C. Boucher, U.A. Germann, G.A. Scarborough, Expression of the human multidrug resistance cDNA in insect cells generates a high activity drug-stimulated membrane ATPase, J. Biol. Chem. 267 (1992) 4854–4858.
[40] A. Bodo, E. Bakos, F. Szeri, A. Varadi, B. Sarkadi, Differential modulation of the human liver conjugate transporters MRP2 and MRP3 by bile acids and organic anions, J. Biol. Chem. 278 (2003) 23529–23537.
[41] L. Szente, J. Szejtli, Highly soluble cyclodextrin derivatives: chemistry, properties, and trends in development, Adv. Drug Deliv. Rev. 36 (1999) 17–28.
[42] G.H. Rothblat, M. de la Llera-Moya, V. Atger, G. Kellner-Weibel, D.L. Williams, M.C. Phillips, Cell cholesterol efflux: integration of old and new observations provides new insights, J. Lipid Res. 40 (1999) 781–796.
[43] S. Zhou, J.D. Schuetz, K.D. Bunting, A.M. Colapietro, J. Sampath, J.J. Morris, I. Lagutina, G.C. Grosveld, M. Osawa, H. Nakauchi, B.P. Sorrentino, The ABC transporter Bcrp1/ABCG2 is expressed in a wide variety of stem cells and is a molecular determinant of the side-population phenotype, Nat. Med. 7 (2001) 1028–1034.
[44] M. Maliepaard, G.L. Scheffer, I.F. Faneyte, M.A. van Gastelen, A.C. Pijnenborg, A.H. Schinkel, M.J. van De Vijver, R.J. Scheper, J.H.

Schellens, Subcellular localization and distribution of the breast cancer resistance protein transporter in normal human tissues, Cancer Res. 61 (2001) 3458–3464.
[45] M. Parmahamsa, K.R. Reddy, N. Varadacharyulu, Changes in composition and properties of erythrocyte membrane in chronic alcoholics, Alcohol Alcohol. 39 (2004) 110–112.
[46] K. Mohrmann, M.A. van Eijndhoven, A.H. Schinkel, J.H. Schellens, Absence of N-linked glycosylation does not affect plasma membrane localization of breast cancer resistance protein (BCRP/ABCG2), Cancer Chemother. Pharmacol. 56 (2005) 344–350.
[47] T. Takada, H. Suzuki, Y. Sugiyama, Characterization of polarized expression of point- or deletion-mutated human BCRP/ABCG2 in LLC-PK1 cells, Pharm. Res. 22 (2005) 458–464.
[48] N.K. Diop, C.A. Hrycyna, N-Linked glycosylation of the human ABC transporter ABCG2 on asparagine 596 is not essential for expression, transport activity, or trafficking to the plasma membrane, Biochemistry 44 (2005) 5420–5429.
[49] K.F. Ejendal, N.K. Diop, L.C. Schweiger, C.A. Hrycyna, The nature of amino acid 482 of human ABCG2 affects substrate transport and ATP hydrolysis but not substrate binding, Protein Sci. 15 (2006) 1597–1607.
[50] G. van Meer, D. Halter, H. Sprong, P. Somerharju, M.R. Egmond, ABC lipid transporters: extruders, flippases, or flopless activators? FEBS Lett. 580 (2006) 1171–1177.
[51] M. Dean, The genetics of ATP-binding cassette transporters, Methods Enzymol. 400 (2005) 409–429.
[52] G. Schmitz, T. Langmann, High-density lipoproteins and ATP-binding cassette transporters as targets for cardiovascular drug therapy, Curr. Opin. Investig. Drugs 6 (2005) 907–919.
[53] K. Takahashi, Y. Kimura, K. Nagata, A. Yamamoto, M. Matsuo, K. Ueda, ABC proteins: key molecules for lipid homeostasis, Med. Mol. Morphol. 38 (2005) 2–12.
[54] A. Rothnie, D. Theron, L. Soceneantu, C. Martin, M. Traikia, G. Berridge, C.F. Higgins, P.F. Devaux, R. Callaghan, The importance of cholesterol in maintenance of P-glycoprotein activity and its membrane perturbing influence, Eur. Biophys. J. 30 (2001) 430–442.
[55] Y. Kimura, N. Kioka, H. Kato, M. Matsuo, K. Ueda, Modulation of drug-stimulated ATPase activity of human MDR1/P-glycoprotein by cholesterol, Biochem. J. 401 (2007) 597–605.
[56] A. Pal, D. Mehn, E. Molnar, S. Gedey, P. Meszaros, T. Nagy, H. Glavinas, T. Janaky, O. von Richter, G. Bathori, L. Szente, P. Krajcsi, Cholesterol potentiates ABCG2 activity in a heterologous expression system: improved in vitro model to study function of human ABCG2, J. Pharmacol. Exp. Ther. 321 (2007) 1085–1094.

6. sz. közlemény

dc_46_10

dc_46_10
Available online at www.sciencedirect.com
ScienceDirect
Biochemical and Biophysical Research Communications 367 (2008) 667–673
BBRC
www.elsevier.com/locate/ybbrc

Combined localization and real-time functional studies using a GFP-tagged ABCG2 multidrug transporter

Tamás I. Orbán, László Seres, Csilla Özvegy-Laczka, N. Barry Elkind, Balázs Sarkadi, László Homolya *

Research Group for Membrane Biology, Hungarian Academy of Sciences, Diószegi u. 64, 1113 Budapest, Hungary

Received 23 December 2007
Available online 7 January 2008

Abstract

ABCG2 is a half-transporter which causes multidrug resistance when overexpressed in tumor cells. Availability of combined localization and functional assays would greatly improve cell biology and drug modulation studies for this transporter. Here we demonstrate that an N-terminally GFP-tagged version of the protein (GFP-G2) can be used to directly monitor ABCG2 expression, dimerization, localization and function in living cells. GFP-G2 is fully functional when tested for drug-stimulated ATPase activity, vesicular transport assay, subcellular localization or cell surface epitope conformational changes. By measuring both GFP and Hoechst 33342 dye fluorescence in HEK-293 cells, we provide evidence that a real-time transport assay can be reliably applied to identify ABCG2 substrates, transport modulators, as well as to monitor the cellular functions of this multidrug transporter protein. This approach also avoids the need of cloning, drug selection or other further separation or characterization of the transgene-expressing cells.

Keywords: Multidrug resistance; ABCG2; Green fluorescent protein; Hoechst 33342; Dye transport; Functional assay

The ABCG2 protein is a key multidrug transporter in the human body. Originally cloned from cells selected for multidrug resistance [1–3], it was later confirmed to elicit an "atypical" multidrug resistance phenotype [4]. This 655 amino acid long half-transporter is endogenously expressed in various tissues, including the ovary, the kidney, breast epithelial cells, the small intestine, the blood–brain barrier, and the placenta [5,6]. It is also present in a variety of stem cells, conferring a "side population" phenotype determined by dye efflux properties [7]. ABCG2 participates in protecting the cells from endogenous and environmental toxins but its physiological substrates have still not been identified [5,6]. Molecular tools improving studies on its function would unambiguously facilitate our understanding of the exact role of ABCG2 in the human body, as well as to identify its *bona fide* cellular substrate(s).

To study the cellular function of a protein, it is widely accepted to generate a fusion species with a fluorescent tag, since it provides an opportunity to directly monitor dynamic processes in living cells such as subcellular trafficking or change in localization. The most convenient of such molecules is GFP because it represents an independent folding unit operating without cofactors, it is active in a variety of organisms, and its detection is easy and rapid [8]. Such a fusion protein for an ABC transporter opens up new opportunities for cell-based, fluorescence transport assay systems applicable for studying transporter function, drug-transporter interactions, as well as substrate or inhibitor identification [9]. GFP-tagging of an ABC-transporter makes possible to carry out these assays rapidly without the usual laboratory practice of establishing a transporter-expressing cell line with laborious cloning and selection procedures, even in short-term transient transfec-

* Corresponding author. Fax: +36 1 372 4353.
E-mail address: homolya@biomembrane.hu (L. Homolya).

0006-291X/$ - see front matter © 2008 Elsevier Inc. All rights reserved.
doi:10.1016/j.bbrc.2007.12.172

tion systems. In addition, such a system is well-suited for kinetic analysis of a given drug transport or study the cellular function of ABCG2 by the use of fluorescent substrate molecules.

However, the tagged versions of membrane transporter proteins often become inactive or mislocalized, which greatly inhibits their use in further functional or localization studies. Due to these technical difficulties, up to now very limited number of studies demonstrated functional ABC transporters tagged with a fluorescent protein. Such tagging of the ABCG2 half-transporter has not been reported yet. Therefore, in order to generate a useful tool for the elucidation of ABCG2 function, in the present work we examined in detail both N- and C-terminally GFP-tagged ABCG2 fusion proteins. We demonstrated the applicability and practical advantage of an N-terminally GFP-tagged ABCG2 transporter in functional assays using both membrane-based and whole-cell assay systems, including flow cytometry and confocal microscopy.

Materials and methods

Expression vectors and cell lines. For expression in mammalian cells, N- or C-terminally tagged ABCG2 proteins were generated using pEGFP-C1 or pEGFP-N1 vectors (Clontech), respectively. As a control, K86M catalytic site mutant was also created for the tagged proteins [10]. HEK-293, HepG2, N2a and COS-7 cells were transfected using the FuGENE® 6 (Roche). For Sf9 expression system, the tagged proteins were cloned into a pAcUW21-L vector; Sf9 cells were cultured and infected as previously described [11].

ABCG2 activity measurements. Sf9 membrane fractions were isolated as described earlier [11,12]. For cholesterol loading, the membranes were preincubated with 1–2.5 mM randomly methylated-β-cyclodextrin (CD, CycloLab) containing 4.4% cholesterol [13]. Western analysis was carried out by standard methodology using BXP-21 monoclonal antibody. Vanadate-sensitive ATPase activity was measured as described earlier [12,14]. MgATP-dependent uptake of ^{3}H-methotrexate in inside-out vesicles was determined by a rapid filtration after 5 min incubation at 37 °C; Ca^{2+}-transport was used for vesicle integrity control as described previously [11].

Flow cytometry. Cell surface expression was measured by the ABCG2-specific, conformation-sensitive 5D3 antibody directly labeled with AlexaFluor-647 dye. For 5D3-shift detection, cells were treated with ABCG2-specific inhibitors (Ko143, FTC), or fixed with 0.5% paraformaldehyde (PFA) [15]. The ABCG2-mediated drug extrusion was evaluated by the modified mitoxantrone (MX) uptake assay as previously described [15]. Fluorescence was detected by a FACSCalibur flow cytometer (BD Biosciences).

Confocal microscopy. For immunofluorescence staining, GFP-G2-transfected cells were permeabilized, then labeled with BXP-21 and AlexaFluor-647-conjugated secondary antibody as detailed in [13]. For real-time fluorescent dye transport studies, GFP-G2-transfected cells were subjected to 2 μM Hoechst 33342 (Hst), whilst the blue and green fluorescence was simultaneously acquired by a confocal microscope specified in [13]. After a certain time 1 μM Ko143 was added to the medium. For cholesterol loading or depletion, the cells were preincubated with 2.5 mM cholesterol-CD, 2.5 or 5 mM bare CD as previously described [13]. For kinetic analysis, the cells were classified into two groups (non-transfected and transfected cells) on basis of the green fluorescence, and time course of nuclear Hst accumulation was determined for both. The activity factors were calculated from the steady state uptake rates before and after Ko143 addition [16]. Cholesterol content of the cells was determined by Amplex Red assay kit (Invitrogen) [13].

Results and discussion

Examination of GFP-tagged ABCG2 proteins in isolated membrane preparations

As a pre-screening approach, we tested the N- and C-terminally GFP-fused ABCG2 proteins in Sf9 insect cells by using the baculovirus expression system, and in HEK-293 mammalian cells using a lipid-based transfection method. Although the C-terminally tagged ABCG2 was expressed at high level in Sf9 cells, it showed no transport or ATPase activity in isolated membrane vesicle preparations. Also, this fusion protein was not stable in mammalian cells and could not be detected in the plasma membrane, but was retained in intracellular compartments (data not shown). These data are consistent with the finding of another group [17] and thus we carried out our further experiments with the N-terminally tagged ABCG2 protein (GFP-G2, see Supplementary Fig. 1).

To test and compare the function of GFP-G2 to that of the wild-type transporter, we first expressed the corresponding protein variants in Sf9 insect cells. In isolated Sf9 cell membranes, the vanadate-sensitive ATPase assay is a reliable method for testing the function of ABC transporters [14]. Measurements were carried out in Sf9 membrane preparations where the normal and the GFP-tagged ABCG2 proteins were expressed at comparable levels (Fig. 1A and B). As described earlier, the ATPase activity of ABCG2 can be slightly stimulated by a known substrate, EKI-785, and specifically inhibited by the compound Ko143 [11,18]. GFP-G2 shows a comparable basal ATPase activity to the wild-type protein. In addition, the stimulatory or the specific inhibitory compounds resulted in similar effects on the activity of the fusion protein to that of the wild-type transporter.

It has recently been demonstrated that membrane cholesterol acts as an activator of the wild-type ABCG2, and cholesterol loading of isolated Sf9 cell membranes significantly increases its drug-stimulated ATPase activity [13,19]. We therefore measured the ATPase activity of ABCG2 in cholesterol loaded Sf9 membranes (Fig. 1B), and observed a similar increase in the EKI-stimulated activity both in the wild-type and the GFP-tagged proteins. In addition, we examined the direct, ATP-dependent methotrexate transport of GFP-G2, which was not different from that of the wild-type ABCG2 (Fig. 1C). The effect of cholesterol loading of the membranes was also found to increase the methotrexate transport activity of the wild-type and the GFP-G2 in a similar manner (Fig. 1C). These results support the notion that the function of GFP-G2 is comparable to the wild-type counterpart.

The ABCG2 protein was shown to undergo glycosylation and to appear in the plasma membrane as an S–S bridge stabilized homodimer [5,6], thus we tested the glycosylation and the dimerization of the GFP-G2 protein. Western blot analysis was carried out on total cell lysates of HEK-293 cells transiently transfected with ABCG2 or

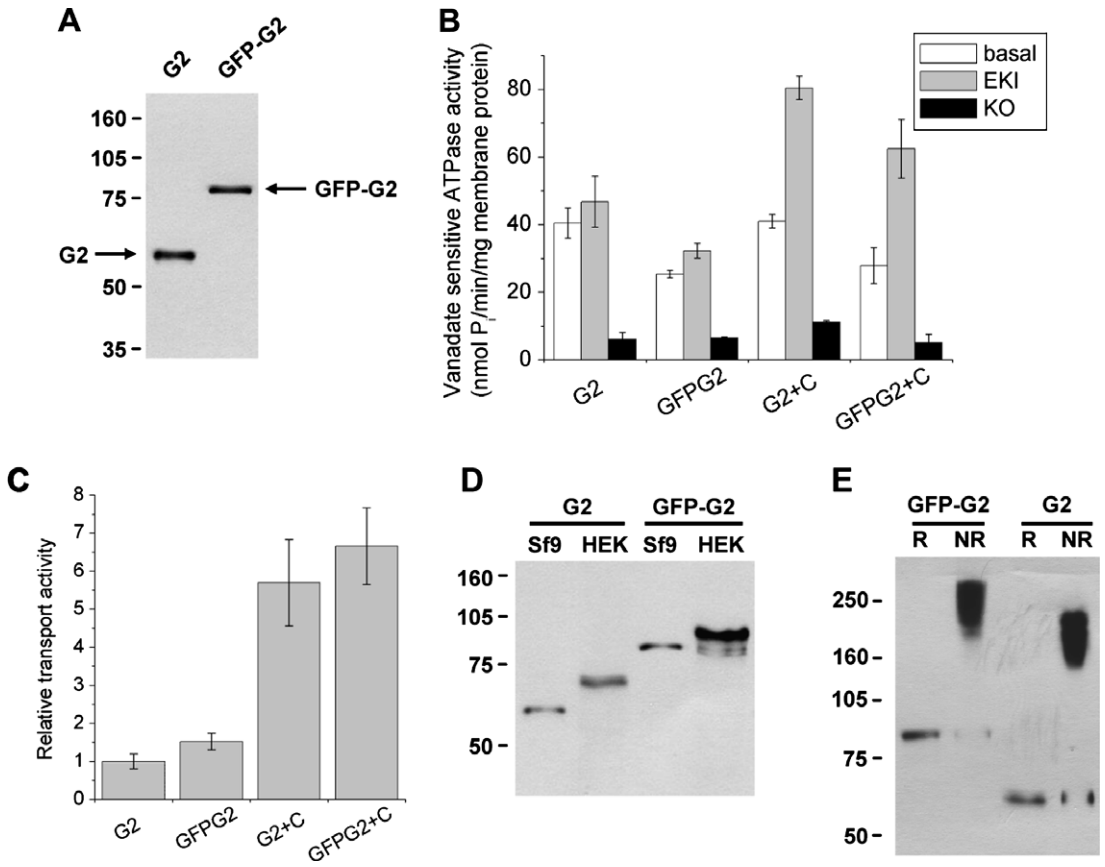

Fig. 1. Expression and functional examination of GFP-G2. Western analysis using the BXP-21 antibody (A), ATPase activity measurements (B), and methotrexate transport studies (C) were performed with Sf9 membranes containing wild-type or GFP-tagged ABCG2. The basal ATPase activity (empty columns) was stimulated by 1 μM EKI-785 (gray columns) or blocked by 1 μM Ko143 (black columns). Cholesterol loading (+C) elevated the EKI-stimulated ATPase activity and methotrexate transport of both variants. Results are given as mean ± S.E.M. ($n = 3$). Glycosylation (D) and dimer formation (E) of ABCG2 and GFP-G2 was investigated by Western analysis using BXP-21. A difference in the apparent molecular weights of the proteins expressed in Sf9 or HEK-293 is indicative for glycosylation. Monomeric ABCG2 and the dimers are visualized by using total HEK-293 cell lysates prepared under reducing (R) or non-reducing (NR) conditions, respectively.

GFP-G2, as well as on isolated Sf9 cell membranes containing the same protein species. In insect cells, the expressed membrane proteins undergo only core glycosylation, therefore glycosylated proteins appear with a lower molecular weight as compared to those expressed in mammalian cells. Fig. 1D shows that both ABCG2 variants expressed in Sf9 cells result in a faster migrating protein than those expressed in mammalian cells. Although glycosylation does not seem to be crucial for ABCG2 function [10,12,20], the finding that this characteristic remained unchanged further suggests a proper folding of GFP-G2 and is indicative for plasma membrane targeting.

Due to the presence of extracellular S–S bridges, ABCG2 homodimers are covalently cross-linked when present in the cell surface membranes. This dimer formation can be assessed by SDS gel-electrophoresis carried out under non-reducing conditions. As shown in Fig. 1E, when ABCG2 or GFP-G2 was expressed in HEK-293 cells, and the cell lysates were prepared under non-reducing conditions, the immunoblot indicated dimer formation in the case of both variants.

Taken together, all the above data indicate that N-terminal GFP-tagging did not disturb the expression, glycosylation, dimerization, or the ATPase activity and transport characteristics of the ABCG2 protein.

Localization and function of GFP-G2 in mammalian cells

The mature ABCG2 protein has been shown to localize to the plasma membrane [21]. To determine the subcellular localization of GFP-G2, we studied transiently transfected HEK-293, HepG2, N2a and COS-7 cells by using confocal microscopy. By detecting both GFP fluorescence and immunostaining with an anti-ABCG2 monoclonal antibody, we observed co-localization of GFP and the antibody, and both signals were predominantly found in the plasma membrane (Fig. 2). Similar experiments with the GFP-tagged ABCG2 catalytic site mutant (GFP-G2$_{K86M}$) also showed predominant plasma membrane localization (Fig. 2, lower panels). As proven earlier, this mutant is nonfunctional in terms of transport activity, though still properly localized in mammalian cells [15]. These studies indicate that processing of the N-terminally tagged protein

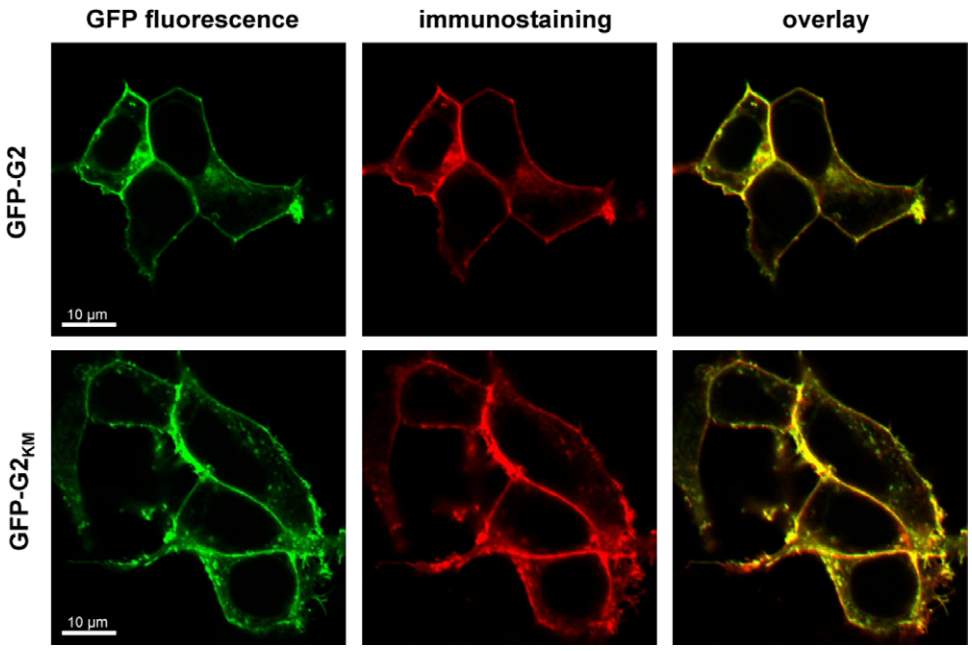

Fig. 2. Subcellular localization of GFP-tagged ABCG2. GFP-G2 and GFP-$G2_{K86M}$-transfected HEK-293 cells were immunostained with BXP21, and studied by confocal microscopy. See text for details. Bars: 10 µm.

is not disturbed, and GFP-G2 localizes properly in mammalian cells.

The monoclonal antibody 5D3 recognizes the ABCG2 protein on the cell surface [7,21]. However, the interaction of this antibody with an extracellular ABCG2 epitope is sensitive to the actual conformation of the transporter protein. As shown earlier, 5D3 antibody labeling of plasma membrane ABCG2 is greatly increased by the addition of the ABCG2 inhibitors Ko143 or FTC, as well as by mild fixation with PFA [15]. Based on these results, we performed cell surface labeling with 5D3 antibody on HEK-293 cells transiently expressing the GFP-G2 protein, assessed by flow cytometry in the GFP-positive cell population. As a positive control, HEK-293 cells stably and uniformly expressing ABCG2 were used [15]. As documented in Fig. 3, a significant cell surface expression of ABCG2 was detected in both cell types. Moreover, increased 5D3 labeling (5D3-shift) was seen both in the wild-type ABCG2 and the GFP-G2-expressing cells upon fixation with PFA (Fig. 3A, lower panels). We observed a similar 5D3-shift after the addition of Ko143 or FTC (data not shown). These experiments further document the cell surface expression of the GFP-G2 protein and indicate the typical conformational changes in this N-terminally tagged ABCG2.

The most prominent advantage deriving from the GFP-tagged ABCG2 is its application in functional assays within 48 h after transfection. As shown in Fig. 3B, MX uptake could be determined selectively in the GFP-positive cells by flow cytometry in the presence or absence of the ABCG2-specific inhibitor Ko143. The reduced MX uptake in the absence of Ko143 reflects the transporter dye extrusion activity (lower left panel). Similar transport activity was seen in cells expressing the wild-type protein [15]. The lack of transport activity of the inactive GFP-$G2_{K86M}$ mutant (lower right panel) provided evidence that the MX extrusion is fully attributed to GFP-G2 function. This experiment exemplifies that the GFP-tagged multidrug transporter can be easily applied in functional assays.

The major advantage of this assay system is that the drug transport characteristics can be rapidly assessed on the cell population gated for GFP-positivity, without the need of the laborious establishment of a cell line stably expressing the transporter. It also becomes very practical for applications on hard-to-transfect or difficult-to-clone cell lines. The system allows to identify compounds interacting with the transporter (either substrates or inhibitors), or modulators of the transporter protein in a short period of time. Such experiments are especially informative together with the use of the inactive mutant version of the GFP-tagged transporter (see Fig. 3B).

Real-time direct Hoechst 33342 transport assay in cells expressing GFP-G2

As the above described experiments indicate the fully functional expression of GFP-G2, we attempted to monitor fluorescent dye uptake in cells transiently expressing this fusion protein by microscopy analysis, and tested the effects of transport activators and inhibitors. After 48 h of transfection, HEK-293 cells were subjected to Hoechst 33342 (Hst) fluorescent dye, a known transported substrate of ABCG2 [7,22,23]. The Hst becomes fluorescent only after interaction with cellular DNA, thus a fluorescence increase reflects the intracellular, nuclear accumulation of

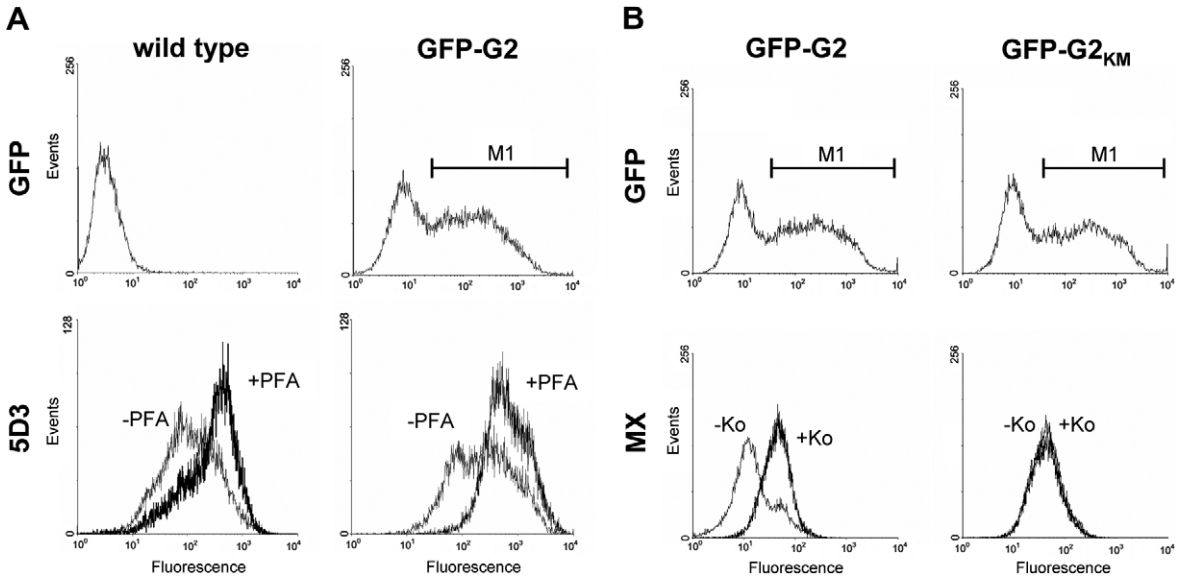

Fig. 3. Conformational changes (5D3-shift) and drug extrusion of GFP-G2. (A) 5D3 antibody labeling of GFP-G2-transfected HEK-293 cells pretreated with or without 0.5% paraformaldehyde (+PFA/−PFA) were studied by flow cytometry. Transfectants were gated by the indicated marker (M1). For comparison, HEK-293 cells stably expressing wild-type ABCG2 were used (left panels); no gating for green fluorescence was applied. (B) MX uptake was determined in GFP-G2- or GFP-G2$_{K86M}$-expressing HEK-293 cells in the presence and absence of Ko143. M1 gate was applied to identify the transfectants.

Hst, which was monitored in parallel with GFP fluorescence by confocal microscopy.

As shown in Fig. 4, non-transfected (GFP-negative) HEK cells showed a rapid accumulation of Hst, while in the cells expressing GFP-G2, hardly any dye uptake was observed (Fig. 4A, upper panels). After a certain time period, the ABCG2 inhibitor Ko143 was added to the cells, resulting in a rapid accumulation of the Hst in the GFP-G2-expressing cells, while the Ko143 addition had no detectable effect in the non-transfected cells (see Supplementary Movie 1).

In order to demonstrate the specificity of Hst dye extrusion, similar experiments were carried out in cells transfected with the non-functional GFP-G2$_{K86M}$. In this case, Hst accumulation was similar in both the control and GFP-positive cells, indicating that the mutant transporter could not protect the cells from dye accumulation (Fig. 4A, lower panels). Also, no noticeable effect of Ko143 was observed on dye uptake in either GFP-G2$_{K86M}$-transfected or non-transfected cells (Supplementary Movie 2).

The kinetics of cellular accumulation of Hst can easily be derived from acquired image sequences (Fig. 4B). It is important to note that in the case of GFP-G2-transfected cells, dye uptake rate after Ko143 addition became similar to that in the non-transfected cells, indicating that the ABCG2 transporter function was rapidly and completely blocked by this inhibitor. The previously defined activity factors [16] were calculated and found to be 0.905 and 0.0 for GFP-G2-expressing and non-transfected cells, respectively. On the other hand, no differences between the dye uptake rate of transfected and non-transfected cells could be observed in ABCG2$_{K86M}$-transfected cultures (activity factors were 0.0 for both).

In mammalian cells, plasma membrane cholesterol is abundant, but cholesterol depletion strongly reduces ABCG2 activity [13]. In order to further analyze the applicability of the GFP-G2 monitoring system, we tested the effect of membrane cholesterol content on the transporter activity. HEK-293 cells transfected with GFP-G2 were treated with CD or with cholesterol-CD complex (to reduce or increase membrane cholesterol content, respectively). ABCG2 function was monitored by the Hst extrusion assay described above. Time courses of the dye accumulation were plotted and activity factors of the transporter after CD or cholesterol-CD treatments were calculated. As shown in Fig. 4C, cholesterol-depletion strongly decreased, while cholesterol loading increased the activity of the GFP-G2 in the Hst extrusion assay as previously shown with non-tagged ABCG2 [13].

We have provided evidence that using a fluorescent substrate, the transport properties and kinetics, as well as the effects of modulators of a transporter protein, ABCG2, can be reliably investigated when applying a GFP-tagged version of the transporter. ABCG2-negative (non-transfected) and ABCG2-expressing (transfected) cells can be examined "real-time" next to each other, thereby providing juxtaposed controls for the measurement. Graphical representation of the data allows the investigator to carefully evaluate the effect of an inhibitor or an enhancer on the transport reaction and potentially fine tune the applicable concentration of a specific modulator. A proof of concept for such experiments is provided by the use of cholesterol, a known stimulator of the ABCG2 transport activity. In addition, this method can be further refined to provide high-throughput assays.

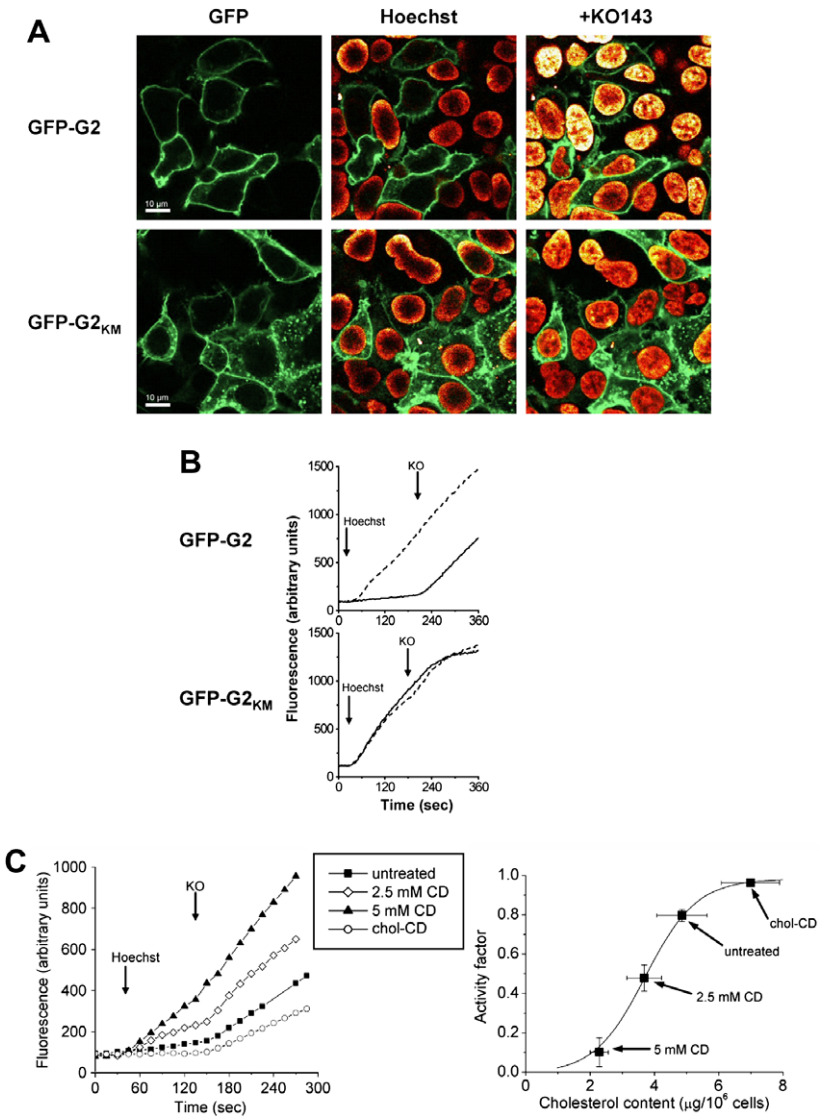

Fig. 4. Fluorescent dye uptake in cells expressing GFP-G2. (A) The intracellular accumulation of Hst in HEK-293 cells transfected with GFP-G2 (upper panels) or GFP-$G2_{K86M}$ (lower panels) was monitored by confocal microscopy. Approx. 3 min after Hst addition, ABCG2-mediated dye extrusion was blocked by 1 μm Ko143. Left panels depict the cells before Hst addition; the middle and right panels show the same filed right before and 2–3 min after Ko143 addition, respectively. The blue fluorescence is pseudo-colored; bars: 10 μm. (B) Kinetics of nuclear accumulation of Hst in transfected (solid lines) and non-transfected cells (dashed lines). The upper panels: GFP-G2-transfectants; lower panels: GFP-$G2_{K86M}$-transfectants. (C) The effect of membrane cholesterol content on the GFP-G2-mediated dye extrusion. Hst accumulation was followed in GFP-G2-expressing cells pretreated with 2.5 or 5 mM CD, or 2.5 mM chol-CD (left panel). The activity factors calculated from the kinetic curves were correlated with the cholesterol content (right panel). Results are presented as mean ± SEM ($n > 3$).

The availability of modern microtiter plate-based fluorescence image devices, e.g., FLIPR makes such cell-based kinetic assays feasible for automated, fast version of functional drug testing in various multi-well formats.

In summary, we demonstrated the applicability and practical advantages of a GFP-tagged ABC transporter, in this case GFP-G2, in functional assays using flow cytometry and confocal microscopy.

Acknowledgments

We appreciate the technical help from Gyöngyi Bézsenyi, Zsuzsanna Sebestyén and Krisztina Lór, and the grant supports from OTKA-K68936, OTKA-T48986, OTKA-D45957, ETT-557/2006, and NKFP-1A/005/2004. L.H. was an EMBO-HHMI Young Scientist; Cs.Ö.L. is a recipient of the János Bolyai Scholarship. CD-derivatives obtained from Lajos Szente, and the directly labeled 5D3 antibody obtained from Katalin Goda are greatly appreciated.

Appendix A. Supplementary data

Supplementary data associated with this article can be found, in the online version, at doi:10.1016/j.bbrc.2007.12.172.

References

[1] R. Allikmets, L.M. Schriml, A. Hutchinson, V. Romano-Spica, M. Dean, A human placenta-specific ATP-binding cassette gene (ABCP) on chromosome 4q22 that is involved in multidrug resistance, Cancer Res. 58 (1998) 5337–5339.
[2] L.A. Doyle, W. Yang, L.V. Abruzzo, T. Krogmann, Y. Gao, A.K. Rishi, D.D. Ross, A multidrug resistance transporter from human MCF-7 breast cancer cells, Proc. Natl. Acad. Sci. USA 95 (1998) 15665–15670.
[3] K. Miyake, L. Mickley, T. Litman, Z. Zhan, R. Robey, B. Cristensen, M. Brangi, L. Greenberger, M. Dean, T. Fojo, S.E. Bates, Molecular cloning of cDNAs which are highly overexpressed in mitoxantrone-resistant cells: demonstration of homology to ABC transport genes, Cancer Res. 59 (1999) 8–13.
[4] H. Lage, M. Dietel, Effect of the breast-cancer resistance protein on atypical multidrug resistance, Lancet. Oncol. 1 (2000) 169–175.
[5] P. Krishnamurthy, J.D. Schuetz, Role of ABCG2/BCRP in biology and medicine, Annu. Rev. Pharmacol. Toxicol. 46 (2006) 381–410.
[6] B. Sarkadi, L. Homolya, G. Szakacs, A. Varadi, Human multidrug resistance ABCB and ABCG transporters: participation in a chemoimmunity defense system, Physiol. Rev. 86 (2006) 1179–1236.
[7] S. Zhou, J.D. Schuetz, K.D. Bunting, A.M. Colapietro, J. Sampath, J.J. Morris, I. Lagutina, G.C. Grosveld, M. Osawa, H. Nakauchi, B.P. Sorrentino, The ABC transporter Bcrp1/ABCG2 is expressed in a wide variety of stem cells and is a molecular determinant of the side-population phenotype, Nat. Med. 7 (2001) 1028–1034.
[8] R.H. Stauber, K. Horie, P. Carney, E.A. Hudson, N.I. Tarasova, G.A. Gaitanaris, G.N. Pavlakis, Development and applications of enhanced green fluorescent protein mutants, Biotechniques 24 (1998) 462–466, 468-471.
[9] C.Q. Xia, M.N. Milton, L.S. Gan, Evaluation of drug-transporter interactions using in vitro and in vivo models, Curr. Drug Metab. 8 (2007) 341–363.
[10] C. Ozvegy, A. Varadi, B. Sarkadi, Characterization of drug transport, ATP hydrolysis, and nucleotide trapping by the human ABCG2 multidrug transporter. Modulation of substrate specificity by a point mutation, J. Biol. Chem. 277 (2002) 47980–47990.
[11] C. Ozvegy-Laczka, G. Koblos, B. Sarkadi, A. Varadi, Single amino acid (482) variants of the ABCG2 multidrug transporter: major differences in transport capacity and substrate recognition, Biochim. Biophys. Acta. 1668 (2005) 53–63.
[12] C. Ozvegy, T. Litman, G. Szakacs, Z. Nagy, S. Bates, A. Varadi, B. Sarkadi, Functional characterization of the human multidrug transporter, ABCG2, expressed in insect cells, Biochem. Biophys. Res. Commun. 285 (2001) 111–117.
[13] A. Telbisz, M. Muller, C. Ozvegy-Laczka, L. Homolya, L. Szente, A. Varadi, B. Sarkadi, Membrane cholesterol selectively modulates the activity of the human ABCG2 multidrug transporter, Biochim. Biophys. Acta. 1768 (2007) 2698–2713.
[14] B. Sarkadi, E.M. Price, R.C. Boucher, U.A. Germann, G.A. Scarborough, Expression of the human multidrug resistance cDNA in insect cells generates a high activity drug-stimulated membrane ATPase, J. Biol. Chem. 267 (1992) 4854–4858.
[15] C. Ozvegy-Laczka, G. Varady, G. Koblos, O. Ujhelly, J. Cervenak, J.D. Schuetz, B.P. Sorrentino, G.J. Koomen, A. Varadi, K. Nemet, B. Sarkadi, Function-dependent conformational changes of the ABCG2 multidrug transporter modify its interaction with a monoclonal antibody on the cell surface, J. Biol. Chem. 280 (2005) 4219–4227.
[16] L. Homolya, M. Hollo, M. Muller, E.B. Mechetner, B. Sarkadi, A new method for a quantitative assessment of P-glycoprotein-related multidrug resistance in tumour cells, Br. J. Cancer 73 (1996) 849–855.
[17] T. Takada, H. Suzuki, Y. Sugiyama, Characterization of polarized expression of point- or deletion-mutated human BCRP/ABCG2 in LLC-PK1 cells, Pharm. Res. 22 (2005) 458–464.
[18] J.D. Allen, A. van Loevezijn, J.M. Lakhai, M. van der Valk, O. van Tellingen, G. Reid, J.H. Schellens, G.J. Koomen, A.H. Schinkel, Potent and specific inhibition of the breast cancer resistance protein multidrug transporter in vitro and in mouse intestine by a novel analogue of fumitremorgin C, Mol. Cancer Ther. 1 (2002) 417–425.
[19] A. Pal, D. Mehn, E. Molnar, S. Gedey, P. Meszaros, T. Nagy, H. Glavinas, T. Janaky, O. von Richter, G. Bathori, L. Szente, P. Krajcsi, Cholesterol potentiates ABCG2 activity in a heterologous expression system: improved in vitro model to study function of human ABCG2, J. Pharmacol. Exp. Ther. 321 (2007) 1085–1094.
[20] T. Janvilisri, H. Venter, S. Shahi, G. Reuter, L. Balakrishnan, H.W. van Veen, Sterol transport by the human breast cancer resistance protein (ABCG2) expressed in Lactococcus lactis, J. Biol. Chem. 278 (2003) 20645–20651.
[21] B.L. Abbott, A.M. Colapietro, Y. Barnes, F. Marini, M. Andreeff, B.P. Sorrentino, Low levels of ABCG2 expression in adult AML blast samples, Blood 100 (2002) 4594–4601.
[22] C.W. Scharenberg, M.A. Harkey, B. Torok-Storb, The ABCG2 transporter is an efficient Hoechst 33342 efflux pump and is preferentially expressed by immature human hematopoietic progenitors, Blood 99 (2002) 507–512.
[23] M. Kim, H. Turnquist, J. Jackson, M. Sgagias, Y. Yan, M. Gong, M. Dean, J.G. Sharp, K. Cowan, The multidrug resistance transporter ABCG2 (breast cancer resistance protein 1) effluxes Hoechst 33342 and is overexpressed in hematopoietic stem cells, Clin. Cancer Res. 8 (2002) 22–28.

dc_46_10

7. sz. közlemény

dc_46_10

Biochimica et Biophysica Acta xxx (2010) xxx–xxx
dc_46_10

Contents lists available at ScienceDirect

Biochimica et Biophysica Acta

journal homepage: www.elsevier.com/locate/bbamem

Mitoxantrone is expelled by the ABCG2 multidrug transporter directly from the plasma membrane

László Homolya [a,*], Tamás I. Orbán [a], László Csanády [b], Balázs Sarkadi [a]

[a] Membrane Biology Research Group, Semmelweis University, Hungarian Academy of Sciences, Diószegi u. 64, H-1113 Budapest, Hungary
[b] Department of Medical Biochemistry, Semmelweis University, Tűzoltó utca 37-47, H-1094 Budapest, Hungary

ARTICLE INFO

Article history:
Received 28 April 2010
Received in revised form 24 July 2010
Accepted 27 July 2010
Available online xxxx

Keywords:
ABCG2
mitoxantrone
ABC transporter
multidrug resistance
transport kinetic model
hydrophobic vacuum cleaner

ABSTRACT

ABC multidrug transporter proteins expel a wide variety of structurally unrelated, mostly hydrophobic compounds from cells. The special role of these transporters both at the physiological barriers and in cancer cells is based on their extremely broad substrate recognition. Since hydrophobic compounds are known to partition into the lipid bilayer and accumulate in membranes, the "classical pump" model for the mechanism of multidrug transporter proteins has been challenged, and alternative models suggesting substrate recognition within the lipid bilayer have been proposed. Although much effort has been made to validate this concept, unambiguous evidence for direct drug extrusion from the plasma membrane has not been provided yet. Here we show a detailed on-line microscopic analysis of cellular extrusion of fluorescent anti-cancer drugs, mitoxantrone and pheophorbide A, by a key human multidrug transporter, ABCG2. Using the fully active GFP-tagged ABCG2 and exploiting the special character of mitoxantrone that gains fluorescence in the lipid environment, we were able to determine transporter-modulated drug concentrations separately in the plasma membrane and the intracellular compartments. Different kinetic models describing the various transport mechanisms were generated and the experimental data were analyzed using these models. On the basis of the kinetic analysis, drug extrusion from the cytoplasm can be excluded, thus, our results indicate that ABCG2 extrudes mitoxantrone directly from the plasma membrane.

1. Introduction

Human multidrug transporters, including MDR1, MRP1, and ABCG2, play crucial role in absorption, distribution, metabolism, excretion and toxicity of pharmacologically relevant drugs [1–5]. The medical importance of these transporters is even more evident in cancer therapy, since they significantly contribute to the clinical drug resistance, hindering the effectivity of chemotherapeutical regimens [6–10]. Both the physiological and pathophysiological roles of these transporters are based on their ability to expel an astonishingly wide variety of drugs from cells. Explaining this extremely broad substrate recognition remained a major challenge to the scientists for decades, even though a better understanding of the molecular mechanism of these transporters is crucial for the generation of structure-based specific drugs and modulators.

Similar to enzymes, most membrane transporter proteins specifically bind one or a limited number of substrates in a well-defined binding pocket. Following substrate recognition, transporter proteins translocate the transported substrate from one side to the other side of the membrane. However, this classical mechanism cannot be directly applied to the so-called multidrug transporters, which recognize an exceptionally large number of chemically unrelated compounds as substrates. In the early 1990s, special transport mechanisms were proposed to explain the "promiscuity" of these transporters. Since the transported substrates of the multidrug transporters are mostly lipophilic, the hypothetical models suggested less specific, hydrophobic substrate-transporter interaction within the lipid bilayer of the membrane. The "hydrophobic vacuum cleaner" model suggested direct extrusion of the drugs from the membrane lipid bilayer [11,12], whereas the "floppase" model proposed translocation of the substrate from the inner leaflet to the outer leaflet of the membrane resulting in a net cellular efflux [13]. Although the concept of hydrophobic substrate recognition seems to be rational, these proposals launched a long-lasting scientific debate, since only indirect experimental evidences supported the alternative models. Some experimental data indicated that ABC pumps are capable of extruding their substrates before they reach

Abbreviations: ABC transporter, ATP-binding cassette transporter; ABCG2, G2 multidrug transporter (breast cancer resistance protein, MXR/BCRP/ABCP); GFP, green fluorescent protein; GFP-G2, ABCG2 protein tagged with GFP; Ko143 or KO, specific inhibitor of ABCG2; MDR1, multidrug resistance transporter 1 (ABCB1, Pgp, P-glycoprotein); MRP1, multidrug resistance-associated protein (ABCC1); MX, Mitoxantrone; Pheo, Pheophorbide A; RMSE, Root Mean Square Error; ROI, Region of Interest

* Corresponding author. Tel.: +36 1 372 4317; fax: +36 1 372 4353.
E-mail addresses: homolya@biomembrane.hu (L. Homolya), orbant@biomembrane.hu (T.I. Orbán), laszlo.csanady@eok.sote.hu (L. Csanády), sarkadi@biomembrane.hu (B. Sarkadi).

0005-2736/$ – see front matter © 2010 Elsevier B.V. All rights reserved.
doi:10.1016/j.bbamem.2010.07.031

the cytosole [14–16]. Also, mapping the drug-binding sites to membrane-embedded part of the transporter [17–21] and a limited number of functional studies using reconstituted MDR1/Pgp [17,22,23] supported the idea of substrate recognition within the membrane.

Recently, we generated and expressed an N-terminally GFP-tagged version of ABCG2 (GFP-G2), and proved that this fusion protein is fully functional [24]. The transport activity of GFP-tagged ABCG2 has been demonstrated in various transport assays using radiolabeled drug substrate, methotrexate and the fluorescent dye, Hoechst 33342. The spectral separation in fluorescence techniques allows identifying subpopulation of cells expressing the transporter, and in parallel, monitoring cellular dye accumulation. This combined fluorescence transport assay was proven to be particularly useful in inhomogeneous cultures, such as transiently transfected cells [24].

In the present work, we employed the GFP-tagged ABCG2 in confocal microscopy studies to determine the kinetics of drug distribution in the plasma membrane and other cellular compartments using the fluorescent anti-cancer agent, mitoxantrone. To investigate whether ABCG2 acts as a classical pump or extrudes its transported substrate directly from the plasma membrane, we generated kinetic models describing the transport processes according to both the classical pump model and the alternative models, and compared the characteristic features of these models with our experimental observations. We found full agreement between experimental data and the models, which indicates substrate recognition by the pump within the plasma membrane.

2. Materials and methods

2.1. Fluorescent drug uptake studies

Cell culturing and expression of GFP-tagged ABCG2 variants in HEK-293 cells was performed as described in [24]. Briefly, the cells were maintained in D-MEM containing 10 % FCS, seeded onto eight-well Lab-Tek II Chambered Coverglass (Thermo Scientific Nunc) at 5×10^4 per well cell density. 24 h after seeding the cells were transfected with GFP-ABCG2 plasmid using the FuGENE® 6 (Roche) in accordance with the manufacturer's instruction. The medium was changed 24 h after transfection. Fluorescent drug transport studies were carried out usually 48 h after transfection, but when cells with various GFP-G2 expression levels were examined, the cultures were studied 24 h after transfection.

To study drug uptake kinetics, the transfected cultures were subjected to 5 μM mitoxantrone (MX) (Sigma-Aldrich) or 2 μm pheophorbide A (Pheo) (Frontier Scientific) in serum free culturing medium (pH 7.4) at room temperature. To block the dye extrusion activity of the transporter, 1 μM Ko143 (gift of Dr. G.J. Kooman) was used approximately 5 min after the addition of the drug. The green (505–525 nm) and far red (> 650 nm) fluorescence were monitored by an Olympus FV500-IX confocal laser scanning microscope using a PLAPO 60× (1.4) oil immersion objective (Olympus) at 488 and 633 nm excitations, respectively. For acquisition and image analysis FluoView (Olympus) software was used.

For efflux studies, transfected cells were incubated with 5 μM MX in the presence of 1 μm Ko143 for 15 min, and washed twice with medium prior to the experiment. Thereafter the fluorescence was monitored as described for the drug uptake experiments.

2.2. Analysis of cellular drug uptake

For kinetic analysis, the cells were classified into two groups (non-transfected and transfected cells) on the basis of green fluorescence. To determine the kinetics of intracellular drug accumulation, the mean far red fluorescence was monitored in various regions of interest (ROIs) positioned in the cell interior apart from the nuclear region. The drug extrusion activity of ABCG2 was expressed by the activity factor calculated from the steady state uptake rates before (F_o) and after (F_i) Ko143 addition by using the formula $(F_i-F_o)/F_i$ as described previously [25]. To correlate activity factor with protein expression at a single cell level, the mean GFP fluorescence was determined in the plasma membrane of the individual cells by placing ROIs over their cell membrane, and the activity factors were plotted against the corresponding GFP fluorescence values.

To study the kinetics of MX accumulation within the plasma membrane, the mean far red fluorescence was monitored in ROIs positioned at the plasma membrane of the cells (c_m). The exact location of the plasma membrane was determined on the basis of GFP fluorescence. Whenever the plasma membrane changed position, the ROI was moved accordingly. The proper tracking of the plasma membrane was verified by the steady green fluorescence values over time (see Fig. 3G). In parallel with monitoring GFP and MX fluorescence in this ROI, the mean far red fluorescence was followed in another ROI with the exact same shape and size, positioned in the cell interior adjacent to the ROI at the plasma membrane. The GFP fluorescence in the second ROI was not different from the background level. The mean far red fluorescence in this ROI was designated as internal or submembrane MX fluorescence (c_i).

2.3. Transport kinetic models

To describe cellular drug uptake and extrusion, various transport kinetic models have been generated. In the first set of models the membrane leaflets are not distinguished, the plasma membrane is considered as a “black box.” In these models the drug distribution has been analyzed in three compartments, i.e., the extracellular space, the plasma membrane, and the intracellular submembrane region (see Fig. 4). Model 0 represents the non-transfected (control) cells, in which no ABCG2 is expressed. Model A corresponds to the ”classical pump” mechanism, in which the transported substrate is expelled from cell interior, whereas model B describes a situation, where the substrate is recognized within the plasma membrane and exported from this compartment. The latter model includes both the “hydrophobic vacuum cleaner” and “floppase” models. To make our models manageable, some reasonable assumptions have been introduced. (i) All transport steps, including ABCG2-mediated transport, are taken as first order kinetic reactions, assuming that the transport capacity of ABCG2 is much larger than the actual transport rate under the given conditions ($c<K_m$). (ii) We have considered the external drug concentration as a constant parameter, based on the fact that the external volume is orders of magnitude larger than the cell membrane volume. Thus, in these three-compartment models there are only two variables: the drug concentration in the membrane (c_m) and in the submembrane region (c_i). The differential equations for the three above mentioned models are as follows.

model 0:

$$\frac{dc_m}{dt} = \frac{1}{V_m}(k_1c_e - k_2c_m - k_{-1}c_m + k_{-2}c_i) \quad (1)$$

$$\frac{dc_i}{dt} = \frac{1}{V_i}(k_2c_m - k_{-2}c_i) \quad (2)$$

model A:

$$\frac{dc_m}{dt} = \frac{1}{V_m}(k_1c_e - k_2c_m - k_{-1}c_m + k_{-2}c_i) \quad (3)$$

$$\frac{dc_i}{dt} = \frac{1}{V_i}(k_2c_m - k_{-2}c_i - k_3c_i) \quad (4)$$

Please cite this article as: L. Homolya, et al., Mitoxantrone is expelled by the ABCG2 multidrug transporter directly from the plasma membrane, Biochim. Biophys. Acta (2010), doi:10.1016/j.bbamem.2010.07.031

model B:

$$\frac{dc_m}{dt} = \frac{1}{V_m}(k_1 c_e - k_2 c_m - k_{-1} c_m - k_3 c_m + k_{-2} c_i) \quad (5)$$

$$\frac{dc_i}{dt} = \frac{1}{V_i}(k_2 c_m - k_{-2} c_i) \quad (6)$$

where the designations are as follows: c—concentration, k—rate constant, V—volume; indexes: e—external, m—membrane, i—intracellular (submembrane).

Although our experimental approach is not suitable for distinguishing the individual membrane leaflets, to attempt to discriminate between the "hydrophobic vacuum cleaner" and the "floppase" models, we have generated another set of transport kinetic models, which comprise four compartments (see Fig. 6). In these models, the plasma membrane is divided into two separate compartments, and three variables are considered: the drug concentration in the outer leaflet ($c_{m,e}$), in the inner leaflet ($c_{m,i}$), and in the submembrane region (c_i). There are additional assumptions in these models: (i) the volumes of the inner and outer leaflets are taken as equal; (ii) the rate constants for the passive translocation from the outer leaflet to the inner leaflet ("flip") and for the reverse process ("flop") are considered as an identical parameter (k_m). The differential equations for the four-compartment models are as follows

model 0:

$$\frac{dc_{me}}{dt} = \frac{1}{V_{me}}(k_1 c_e - k_m c_{me} - k_{-1} c_{me} + k_m c_{mi}) \quad (7)$$

$$\frac{dc_{mi}}{dt} = \frac{1}{V_{mi}}(k_m c_{me} - k_m c_{mi} - k_2 c_{mi} + k_{-2} c_i) \quad (8)$$

$$\frac{dc_i}{dt} = \frac{1}{V_i}(k_2 c_{mi} - k_{-2} c_i) \quad (9)$$

In model A, the differential equations are the same as in model 0, with the exception of Eq. (9), which has been modified as follows:

$$\frac{dc_i}{dt} = \frac{1}{V_i}(k_2 c_{mi} - k_{-2} c_i - k_3 c_i) \quad (10)$$

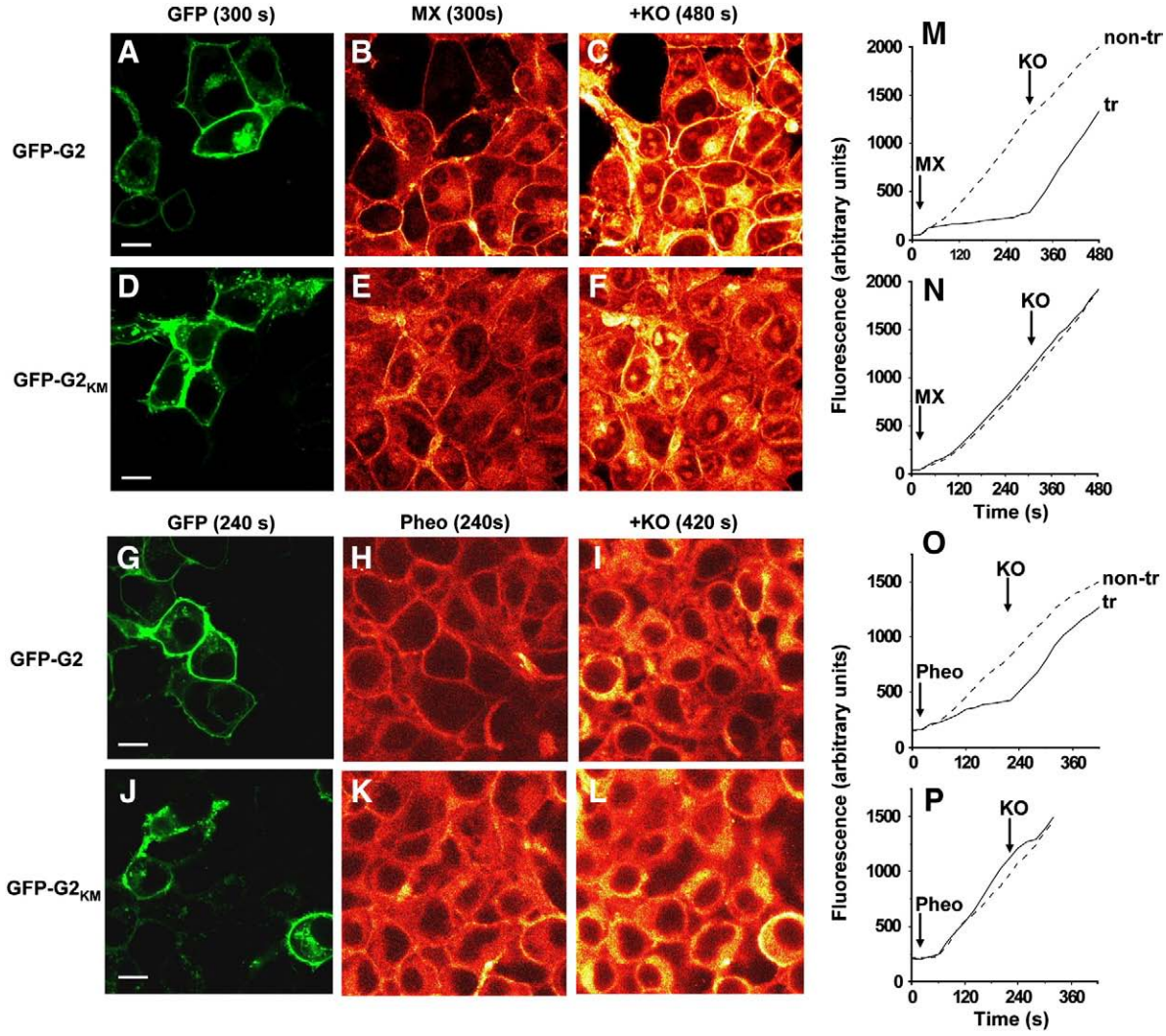

Fig. 1. GFP-tagged ABCG2 prevents cells from intracellular accumulation of fluorescent drugs. HEK-293 cells transfected with GFP-G2 or its inactive mutant variant, GFP-G2$_{KM}$ were subjected to mitoxantrone (MX) (A–F) or pheophorbide A (Pheo) (G–L). Confocal images of GFP fluorescence (A, D, G, J) identify transfected cells, whereas far red fluorescence (pseudo-colored) images depict cellular accumulation of the drugs before (B, E, H, K) and 3 min after the addition of Ko143 (KO), a specific inhibitor of ABCG2 (C, F, I, L). Bars represent 10 μm. The elapsed times are shown in brackets above the images. Time course of drug uptake in cells transfected with GFP-G2 (M, O) or GFP-G2$_{KM}$ (N, P) were also determined and shown by solid lines (tr). Non-transfected cells are represented by dashed lines (non-tr).

Please cite this article as: L. Homolya, et al., Mitoxantrone is expelled by the ABCG2 multidrug transporter directly from the plasma membrane, Biochim. Biophys. Acta (2010), doi:10.1016/j.bbamem.2010.07.031

In model B, both Eqs. (7) and (8) are altered, but Eq. (9) remains the same as it is in model 0:

$$\frac{dc_{me}}{dt} = \frac{1}{V_{me}}(k_1 c_e - k_m c_{me} - k_{-1} c_{me} - k_3 c_{me} + k_m c_{mi}) \quad (11)$$

$$\frac{dc_{mi}}{dt} = \frac{1}{V_{mi}}(k_m c_{me} - k_m c_{mi} - k_2 c_{mi} - k_3 c_{mi} + k_{-2} c_i) \quad (12)$$

Similarly, in model C, Eq. (9) remains the same, but Eqs. (7) and (8) are modified as follows:

$$\frac{dc_{me}}{dt} = \frac{1}{V_{me}}(k_1 c_e - k_m c_{me} - k_{-1} c_{me} + k_m c_{mi} + k_3 c_{mi}) \quad (13)$$

$$\frac{dc_{mi}}{dt} = \frac{1}{V_{mi}}(k_m c_{me} - k_m c_{mi} - k_2 c_{mi} - k_3 c_{mi} + k_{-2} c_i) \quad (14)$$

For numerical analysis of the kinetic models, first the kinetic parameters of passive drug uptake were determined in both the three-compartment or the four-compartment models. Kinetic curves, based on model 0, were fitted to the pairs of experimental time courses of c_m and c_i values measured in non-transfected (control) cells using the least squares method. For fitting the four-compartment model to the experimental values, c_m was considered as the mean of $c_{m,e}$ and $c_{m,i}$. Once the parameters of passive drug uptake had been determined, predicted kinetic curves based on either model A, model B, or model C were fitted to the pair of experimental time courses of c_m and c_i values of GFP-G2-expressing cells, with k_3 as a single free parameter.

3. Results

3.1. Cellular drug uptake in GFP-G2-transfected cells

In our previous work, the applicability of GFP-G2 in fluorescence transport assay system was demonstrated by using Hoechst 33342, which becomes fluorescent after interaction with cellular DNA [24]. To study the transport mechanism of the ABCG2 multidrug transporter, we chose such known ABCG2 substrates for the transport assay, which gain fluorescence in the lipid environment. The uptake of mitoxantrone (MX) and pheophorbide A (Pheo) were measured in GFP-G2-expressing HEK-293 cells by confocal microscopy, 48 h after transfection (Fig. 1). Transfected and non-transfected cells were identified on the basis of GFP fluorescence, whereas cellular drug uptake was monitored by far red fluorescence. As documented in Fig. 1B, intracellular accumulation of MX was completely prevented in GFP-G2-expressing cells, while rapid drug uptake was observed in non-transfected cells. The addition of Ko143, a specific inhibitor of ABCG2 [26], resulted in a fast accumulation of MX even in the GFP-G2-transfectants without affecting drug uptake in the non-transfected cells (Fig. 1C), demonstrating that the protection from drug uptake is due to the transport activity of GFP-G2. The specificity of drug extrusion was further supported by the observation that a catalytic site mutant variant of GFP-G2 (GFP-$G2_{K86M}$) did not prevent MX uptake (Fig. 1D–F). Accordingly, for this construct Ko143 addition had no effect on intracellular drug uptake in either transfected or non-transfected cells. Similar results were obtained when Pheo uptake was measured in GFP-G2- and GFP-$G2_{KM}$-transfected cells (Fig. 1G–L). The kinetic curves of intracellular drug accumulation were also obtained from the image sequences (Fig. 1M–P). Activity factors were calculated from the drug uptake rates before (F_o) and after (F_i) inhibitor addition by the formula $(F_i - F_o)/F_i$ as described previously [25]. In GFP-G2-expressing cells these activity factors were 0.89 and 0.86 for MX and Pheo, respectively, whereas these values were 0 for both dyes in either non-transfected or GFP-$G2_{KM}$-expressing cells.

24 h after transfection, the expression levels vary from cell to cell. When dye uptake kinetics and activity factors were determined in individual cells with different expression levels of GFP-G2 (Fig. 2A–C), a close correlation between the activity factor and plasma membrane GFP-fluorescence was found (Fig. 2D). The characteristics of this relationship are similar to those reported previously for MDR1-expressing cells [25].

3.2. Determination of drug uptake kinetics in the plasma membrane

As mentioned above, in contrast to Hoechst 33342, MX and Pheo become fluorescent in non-polar environment [27,28]. We observed that some accumulation of MX also takes place in the plasma membrane of GFP-G2-expressing cells (Fig. 3D–E), whereas drug uptake into the internal membranes can be seen only after the inhibition of the transporter (Fig. 3F). Tracking the position of the plasma membrane in the GFP image allows determining the kinetics of MX accumulation separately in the plasma membrane and in the submembrane regions (Fig. 3G). Drug concentration in the plasma membrane rapidly saturates in GFP-G2-expressing cells, whereas in non-transfected cells it shows a continuous increase within the studied time frame (Fig. 3H). Uptake into the internal membranes monotonically increased in both cell types, although the uptake rate was much higher in control cells than in transfectants. GFP-$G2_{KM}$-expressing cells exhibited drug accumulation kinetics similar to that seen in control cells (Fig. 3I), demonstrating that the observed

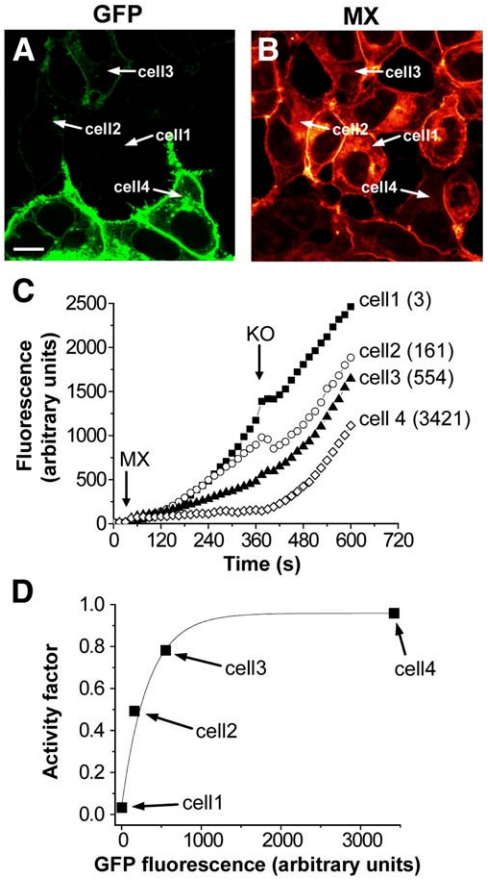

Fig. 2. Analysis of mitoxantrone uptake in cells expressing different levels of GFP-G2. Confocal images of green (A) and far red fluorescence (B) are shown 5 min after MX addition. Bar represents 10 μm. (C) Kinetic curves of intracellular accumulation of MX in four selected cells indicated by arrows in the images. The numbers represent the mean fluorescence intensities of GFP in the plasma membrane. (D) Correlation of the expression level with the ABCG2-mediated drug extrusion activity factor calculated as described previously [25]. (For interpretation of the references to colour in this figure legend, the reader is referred to the web version of this article.)

Please cite this article as: L. Homolya, et al., Mitoxantrone is expelled by the ABCG2 multidrug transporter directly from the plasma membrane, Biochim. Biophys. Acta (2010), doi:10.1016/j.bbamem.2010.07.031

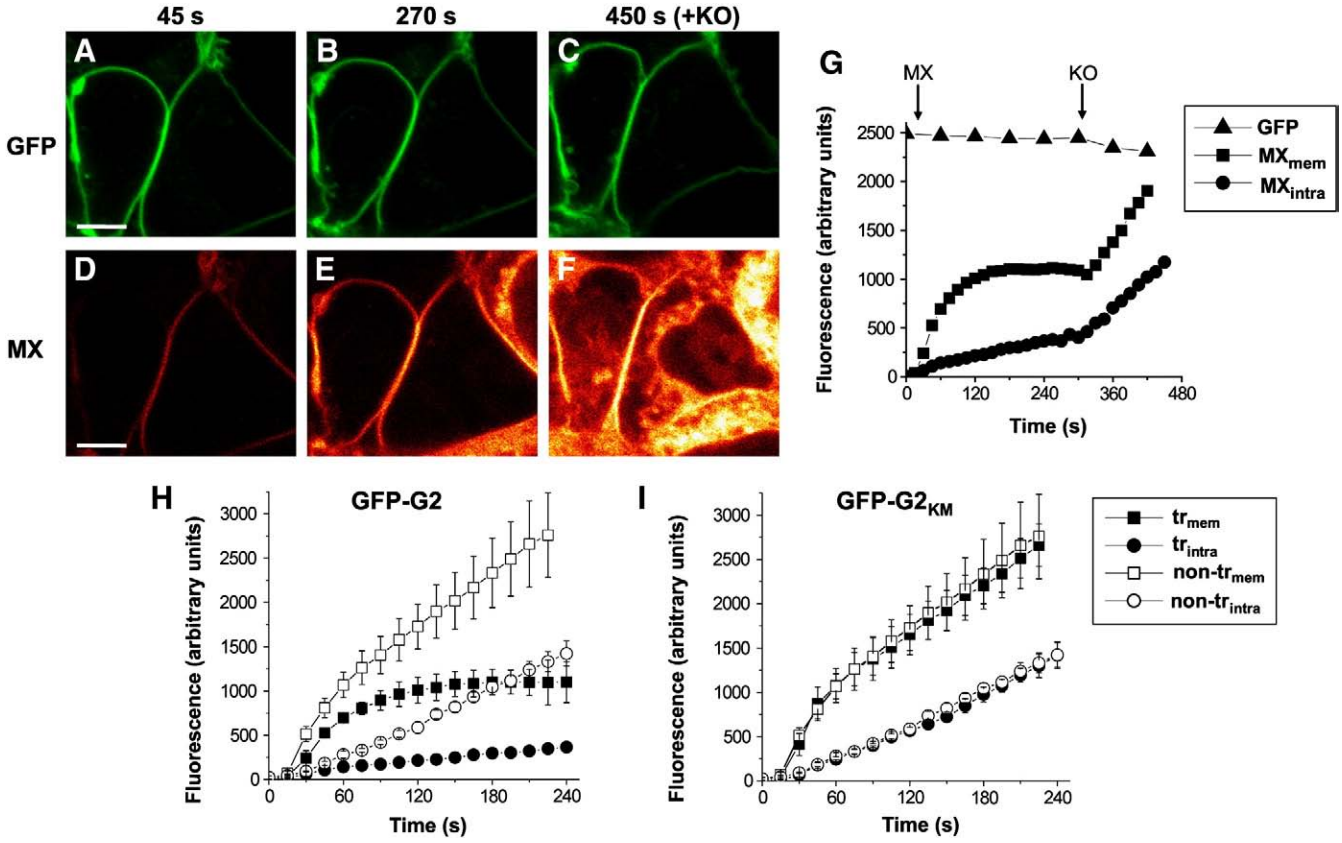

Fig. 3. Quantitative determination of mitoxantrone accumulation in the plasma membrane. (A–F) Image sequence of a representative mitoxantrone uptake experiment performed with GFP-G2-transfected HEK-293 cells (for details see the legend of Fig. 1). (A–C) GFP fluorescence; (D–F) far red fluorescence; numbers on the top indicate the elapsed time in seconds; bars represent 5 μm. The ABCG2 inhibitor KO was added at around 300 s. (G) Kinetic analysis of mitoxantrone uptake experiment shown in Panels A–F. The plasma membrane was tracked by a region of interest (ROI) on the basis of GFP fluorescence (GFP, triangles). MX accumulation into the plasma membrane was determined by using the same ROI in the far red fluorescence images (MX_{mem}, squares) while the submembrane dye concentration was measured by another ROI situated next to the first one, inside the cell (MX_{intra}, circles). (H, I) Comparison of mitoxantrone uptake into the plasma membrane (mem, squares) and the submembrane region (intra, circles) of GFP-G2- and GFP-$G2_{KM}$-transfected cells (tr, filled symbols) to that of non-transfected (non-tr, empty symbols) cells. Values are means ± S.E.M. of at least four independent experiments. (For interpretation of the references to colour in this figure legend, the reader is referred to the web version of this article.)

saturation of the drug level in the plasma membrane of GFP-G2-expressing cells is due to the activity of the transporter. This notion is further supported by the observation that addition of Ko143 to GFP-G2-expressing cells resulted in rapid and continuous elevation in the plasma membrane drug concentration (Fig. 3G).

3.3. Transport kinetic models of cellular drug uptake

To evaluate the kinetics of drug accumulation in the plasma membrane and the internal membranes, we generated various transport kinetic models, which describe cellular drug uptake and extrusion. Since the experimentally measured parameter is the integral average of MX fluorescence across the entire plasma membrane, as a first approach a three-compartment model was used, in which the plasma membrane was considered as a "black box", the membrane leaflets are not distinguished. Using the three-compartment scheme, three different models were generated: model 0 describes the drug movement in the non-transfected (control) cells, whereas model A and model B illustrate the situation with the GFP-G2-transfected cells. Model A corresponds to the "classical pump" mechanism, in which the transported substrate is expelled from cell interior. In model B the substrate is recognized within the plasma membrane, thus, this model combines the "hydrophobic vacuum cleaner" and the "floppase" models (see Fig. 4A–C).

These three-compartment models implicitly suggest that the passive transition rate between the membrane leaflets is not a rate limiting step, thus, it is larger than the diffusion rates to any other compartments. This assumption is reasonable, considering the chemical properties of mitoxantrone at pH 7.4, the pH value of the experiments. This drug is a very weak base, has four amines with two different dissociation constants (pKa 5.99 and 8.13 in pairs), thus, it is slightly positively charged at physiological pH. Mitoxantrone is a hydrophobic molecule, sparingly soluble in water even in its hydrochloride form [29]. It is more soluble in octanol, but its solubility is extremely good in lipids as demonstrated in Ref. [30]. The lipid/water partitioning coefficient for mitoxantrone was found to be 230,000. Taking together these characteristics of mitoxantrone, it is reasonable to assume that it crosses the plasma membrane at a high rate. This notion is in accordance with our experimental observation that MX rapidly accumulates within the non-transfected cells.

To describe our models mathematically, we employed some other assumptions. The transport activity of ABCG2 was described with a first order kinetics, on the basis of the fact that the transport capacity substantially exceeds the particular transport rate under the given conditions ($c < K_m$). Similarly, we assumed that the external drug concentration (c_e) is constant. Although the lipid/water partitioning coefficient for mitoxantrone is relatively high (230,000) [30] as mentioned earlier, the several orders of magnitude difference between the volume of the external space and the cell membranes along with the short time frame of the study makes this assumption reasonable. The differential equations for the three different models are given in Section 2.3 (Eqs. (1)–(6)).

For closed-form solution of the differential equations, we also assumed that the rate constants for spontaneous drug equilibration

Please cite this article as: L. Homolya, et al., Mitoxantrone is expelled by the ABCG2 multidrug transporter directly from the plasma membrane, Biochim. Biophys. Acta (2010), doi:10.1016/j.bbamem.2010.07.031

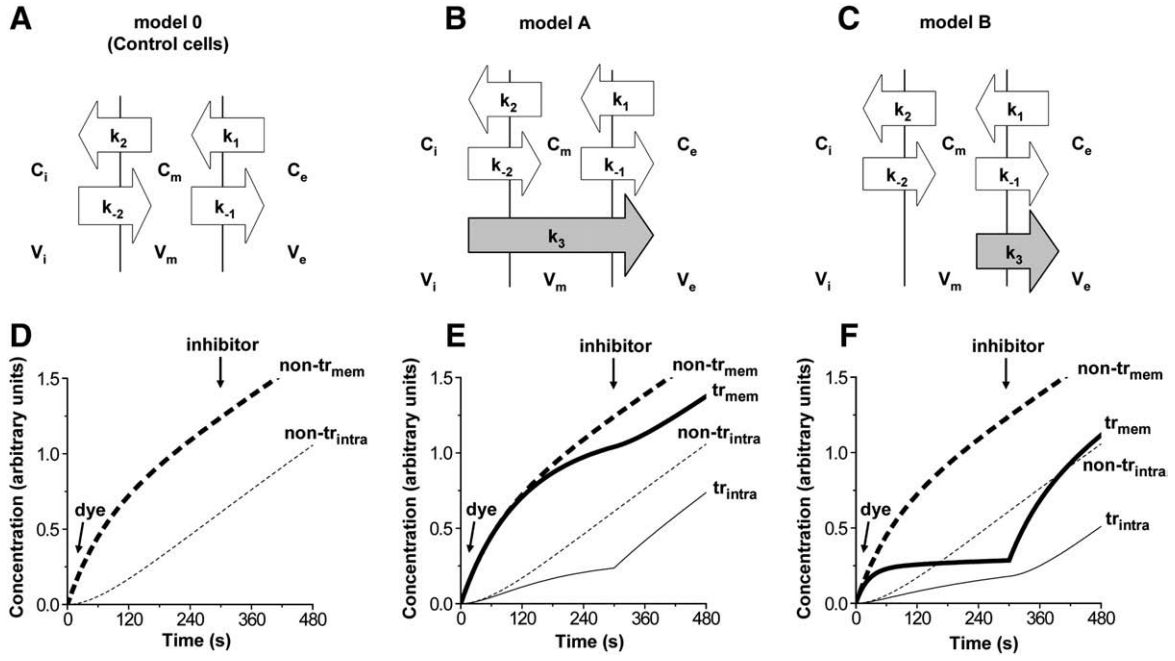

Fig. 4. Kinetic models describing drug uptake and extrusion by a multidrug transporter. (A) Drug uptake into non-transfected, control cells (model 0); (B) Classical pump mechanism, where the substrate transported from the cytosole (model A); (C) an alternative model, in which the transporter expels its substrate directly from the membrane (model B). The variables are as follows: *c*—concentration, *k*—rate constant, *V*—volume; indexes: *e*—external, *m*—membrane, *i*—intracellular. The differential equations for these models are given in Section 2.3 (Eqs. (1)–(6)). (D–E) Closed-form solutions of the kinetic models. Dashed lines: non-transfected cells (non-tr), solid lines: transfected cells (tr); thick lines: plasma membrane concentrations (mem); thin lines: intracellular concentrations (intra). At the time point 300 s k_3 is made equal to 0, mimicking the addition of the inhibitor.

between the plasma membrane and intracellular compartments are identical both ways ($k_2 = k_{-2}$), based on the consideration that the measured intracellular drug concentration (c_i) reflects the mitoxantrone level in internal membranes, thus, in another lipid environment.

Parametric solution of the differential equations elucidated various qualitative distinguishing features of the different models. (i) In model A, the plasma membrane concentration of the drug (c_m) in transfectants differs only slightly from the c_m value in control cells, whereas in model B, c_m rapidly saturates at a greatly reduced level (Fig. 4E–F). (ii) It is also easy to show that the equilibrium values for c_m and c_i are different in model A, whereas they approach the same equilibrium value in model B. For mathematical verification see Statement 1 in the Appendix. iii) Upon addition of an inhibitor to the system, i.e., when k_3 is suddenly made 0, model A predicts a prompt increase in c_i, followed with a delay by an elevation in c_m. In contrast, in model B c_m elevates first and c_i lags behind. In other words, if an inhibitor is added when the system has already reached equilibrium, then model A predicts a positive value for the initial slope of c_i and a zero value for that of c_m, whereas for model B the initial slope of c_m is positive and that of c_i is zero. The detailed mathematical demonstrations of this statement (Statement 2) can be found in the Appendix.

3.4. Comparison of experimental data with the kinetic models

The experimental time courses shown in Fig. 5A are congruent with the features of model B, i.e. (i) c_m in transfected cells rapidly saturates, (ii) c_m and c_i seem to tend towards the same equilibrium (see below), and (iii) c_m promptly increases after the addition of the inhibitor (Fig. 5A). To study the equilibrium of c_m and c_i values further, we performed an extended uptake experiment without adding inhibitor to the cells. This experiment also confirmed the validity of model B, since c_m and c_i approach the same equilibrium value (Fig. 5B).

To determine the kinetic parameters of passive drug uptake (k_1, k_{-1}, k_2, k_{-2}) in our system, we fitted kinetic curves based on model 0 to the pairs of experimental c_m and c_i time courses of non-transfected cells, using the least squares method (Fig. 5A, dashed lines, RMSE = 75.3). Interestingly, the fitting returned k_2 equal to k_{-2}, as was previously assumed based on theoretical considerations for obtaining closed-form solutions (see above). Using these parameters we then fitted kinetic curves, based on either model A or model B, to the pairs of experimental c_m and c_i time courses of transfected cells, with k_3 as the single free parameter. While the fit was unacceptable when model A was used (RMSE = 655.7, not shown), we obtained a reasonable fit using model B (Fig. 5A, solid lines, RMSE = 158.7). It is noteworthy that the obtained value for k_3 was 10^8-fold larger than k_2 or k_{-2} when model A was fitted, whereas this ratio proved to be only 35 when model B was used. In other words, overcoming drug influx would require extremely high transport rates if the drug were extruded from the cytoplasm, whereas a reasonable transport rate can efficiently compensate for the influx if the drug is expelled directly from the membrane.

3.5. Kinetics of drug efflux and equilibrium drug concentrations

In addition to drug uptake, we also studied efflux of mitoxantrone from preloaded cells. It is easily conceivable that the drug concentration should decrease first in the intracellular compartment, and its plasma membrane concentration should fall with a delay, if the drug were extruded from the cell's interior (model A). However, the efflux experiment shown in Fig. 5C demonstrates the reverse situation, i.e. the drug concentration drops first in the membrane followed with a delay by a decrease in c_i,—a scenario which is in accordance with model B.

Finally, we determined the equilibrium concentrations of mitoxantrone in the plasma membrane ($c_{m,eq}$) in cells expressing different amounts of GFP-G2 as demonstrated in Fig. 5D–E. The inverses of these values were correlated with GFP-fluorescence, which is

Please cite this article as: L. Homolya, et al., Mitoxantrone is expelled by the ABCG2 multidrug transporter directly from the plasma membrane, Biochim. Biophys. Acta (2010), doi:10.1016/j.bbamem.2010.07.031

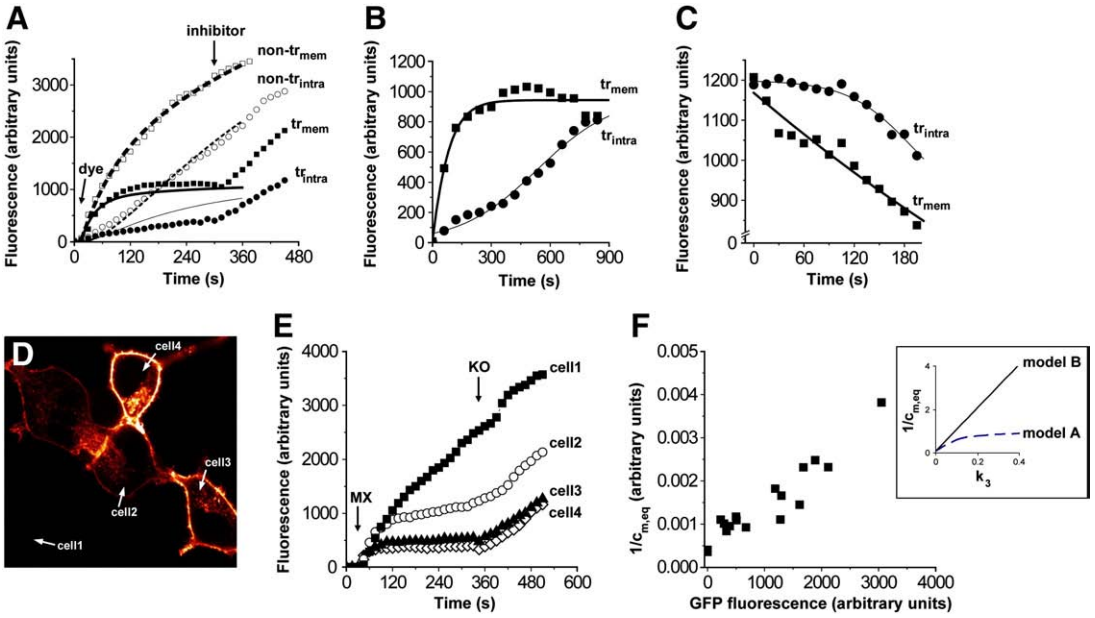

Fig. 5. Experimental evaluations of model predictions on cellular drug accumulation. (A) Experimental values of mitoxantrone uptake into the plasma membrane (mem, squares) and the submembrane region (intra, circles) of GFP-G2-transfected (tr, filled symbols) and non-transfected cells (non-tr, empty symbols). Values are means of at least four independent experiments, error bars are not shown to avoid confusion. Dashed lines represent fitted kinetic curves based on model 0 to the pairs of experimental c_m and c_i time courses of non-transfected cells. Similar fitted curves based on model B to the experimental values of GFP-G2-expressing cells are shown by solid lines. Thick lines: plasma membrane concentrations; thin lines: intracellular concentrations. (B) Determination of equilibrium values of mitoxantrone uptake in GFP-G2-transfected cells. Kinetics of drug uptake into the plasma membrane (tr_{mem}, squares) and the intracellular space (tr_{intra}, circles) are shown in a representative extended experiment. Symbols: squares—plasma membrane; circles—intracellular concentrations. (C) Time course of drug efflux from cells preloaded with mitoxantrone. Symbols are the same as in Panel B. (D) Representative experiment demonstrating mitoxantrone uptake in cells expressing various levels of GFP-G2. (E) Kinetics of mitoxantrone uptake into the plasma membrane of the cells shown in Panel D. (F) Correlation of the inverses of the equilibrium concentrations of mitoxantrone in the plasma membrane ($1/c_{m,eq}$) in different GFP-G2-expressing cells with the corresponding GFP fluorescence. Each symbol represents a value pair ($1/c_{m,eq}$–GFP fluorescence) for an individual cell; data derived from four independent experiments. Inset shows model predictions: dependency of $1/c_{m,eq}$ value on k_3 is indicated for both model A and B (for detailed mathematical explanation see Statement 3 in the Appendix).

proportional to the expression level of the transporter, i.e., to the rate constant k_3. Model A suggests a saturating curve when $1/c_{m,eq}$ is plotted against k_3, whereas model B predicts a linear relationship (inset in Fig. 5F) (for explanation see Statement 3 in the Appendix). The experimental values exhibit a linear correlation between $1/c_{m,eq}$ and GFP fluorescence, providing further support for the validity of model B (Fig. 5F).

3.6. Four-compartment kinetic models

As discussed above, the three-compartment models imply that the passive transition across the membrane is not a rate limiting step. Although this assumption seemed reasonable on the basis of the chemical properties of mitoxantrone, we considered the possibility that the membrane translocation rate is comparable with the rates of the other steps, and generated another set of models, in which the membrane leaflets were considered as separate compartments (Fig. 6A–D). Similar to the designation used earlier, model 0 describes the drug movement in the control cells; model A illustrates the "classical pump" mechanism. Nevertheless, this four-compartment model scheme allowed us to distinguish between the "hydrophobic vacuum cleaner" (model B) and the "floppase" mechanisms (model C). To keep the number of parameters at a reasonable level, equal volumes for the inner and outer leaflets were assumed, as well as the rate constants for passive inward and outward translocation in the membrane were described with a single parameter (k_m). The differential equations for the four-compartment models are given in Section 2.3 (Eqs. (7)–(14)).

Due to resolution limits, our experimental approach does not allow discriminating between the individual membrane leaflets. Therefore, only two experimental parameters were measured: the mean MX fluorescence across the entire plasma membrane (c_m) and in the submembrane region (c_i). When fitting the four-compartment models, this measured c_m value was compared with the arithmetic mean of the predicted $c_{m,i}$ and $c_{m,e}$ values. Similar to the method used for the three-compartment models, first the kinetic parameters of passive drug uptake (k_1, k_{-1}, k_2, k_{-2}, k_m) were determined by fitting the four-compartment model 0 to the pair of the kinetic curves (c_m and c_i) measured in the non-transfected cells (Fig. 6A). This resulted in a reasonable fit (RMSE = 75.7, Fig. 6E), and again returned k_2 equal to k_{-2}. In addition, the membrane translocation rate (k_m) was obtained to be 16-fold larger than k_{-1} and 60-fold larger than k_2 or k_{-2}, supporting our previous assumption that the passive transition across the membrane is not a rate limiting step.

Using the parameters obtained for the control cells and model 0, the experimental c_m and c_i time courses of GFP-G2-expressing cells were fitted either with model A, model B, or model C, with k_3 as a single free parameter (Fig. 6F–H). Similar to that seen in the case of the three-compartment models, the fit was unacceptable when model A was used (Fig. 6F, RMSE = 652.1). A substantially better fit was obtained on the basis of model B (Fig. 6G, RMSE = 155.2), nevertheless, the best fit was obtained when model C, corresponding to the "floppase" mechanism, was used (Fig. 6H, RMSE = 38.1).

In addition to separately fitting the time courses of control and GFP-G2-expressing cells, we also performed ensemble fits of all 8 free parameters to all four kinetic curves using either model A, model B, or model C. A reasonable fit was obtained only when model C was used (RMSE = 63.4), returning the same kinetic parameters obtained by the separate fitting approach. In contrast, 8-parametric fitting with models A and B resulted in unacceptable fits and meaningless parameters, e.g., negative rate constants.

In the four-compartment models, we assumed that the passive "flip" and "flop" rate constants are identical (k_m). To examine whether this assumption is acceptable, we also analyzed a model in which

Please cite this article as: L. Homolya, et al., Mitoxantrone is expelled by the ABCG2 multidrug transporter directly from the plasma membrane, Biochim. Biophys. Acta (2010), doi:10.1016/j.bbamem.2010.07.031

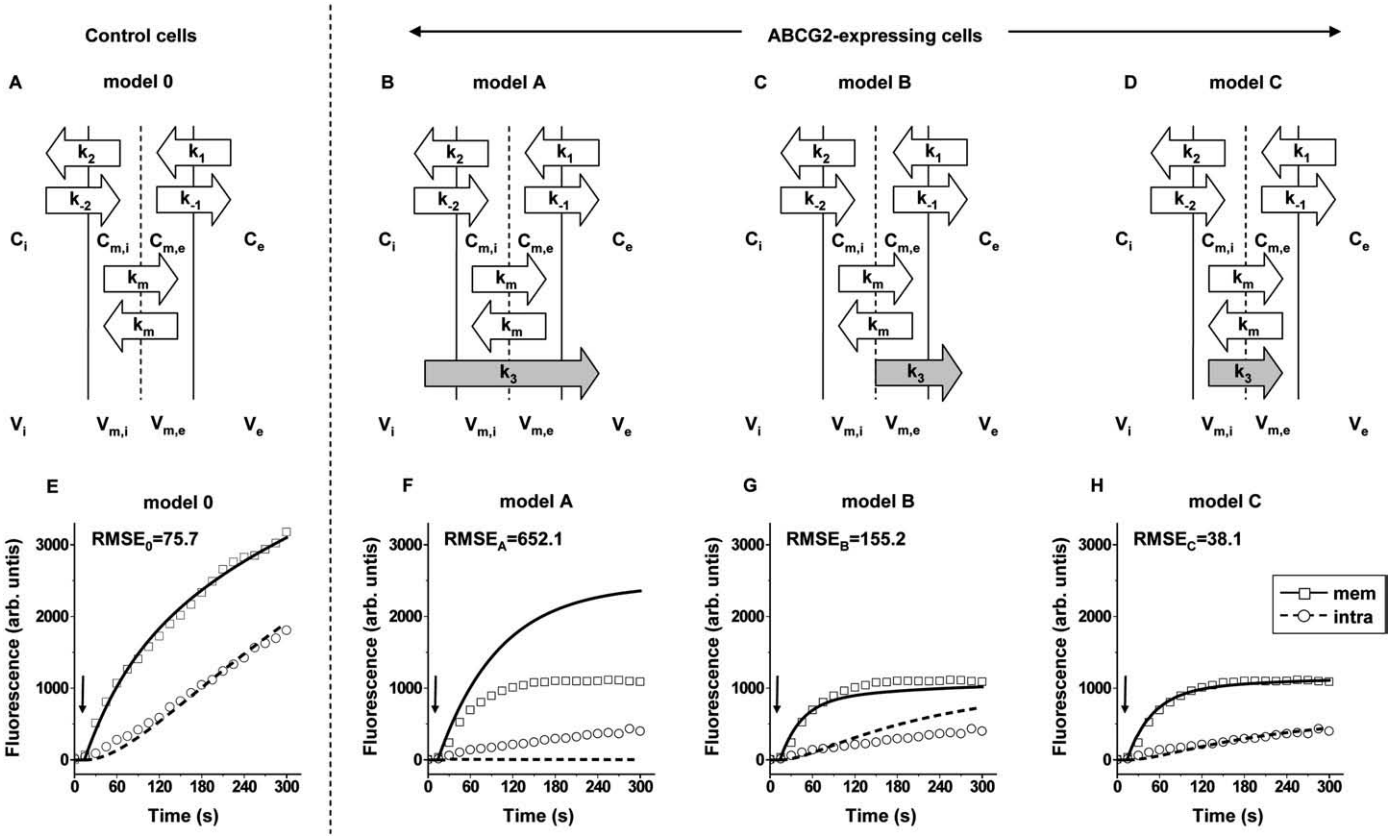

Fig. 6. Numerical analysis of kinetic models comprising four compartments. In these model schemes the membrane leaflets are considered as separate compartments. (A) Model 0 describes drug distribution in non-transfected (control cells); (B–D) drug movement in GFP-G2-espressing cells is shown in accordance with different transport models: the "classical pump" (model A), the "hydrophobic vacuum cleaner" (model B) and the "floppase" (model C) mechanisms. Designations are similar used in Fig. 4: *c*—concentration, *k*—rate constant, *V*—volume; indexes: *e*—external, *m*—membrane, *i*—intracellular; *m,i*—inner membrane leaflet; *m,e*—outer membrane leaflet. The differential equations for these models are given in Section 2.3 (Eqs. (7)–(14)). (E–H) The four-compartment models were fitted to the experimental time courses of mitoxantrone uptake into the plasma membrane (mem, squares) and the submembrane region (intra, circles). The solid lines represent the fitted kinetic curves to membrane MX fluorescence time course, whereas the dashed lines indicate the intracellular (submembrane) values. The fittings were based on the corresponding models shown above. The experimental values of control cells were fitted with 7 free parameter using model 0. These parameters were then used for fitting the other models to the time courses of GFP-G2-expressing cells, with k_3 as a single free parameter. The quality of the fits is represented by the root mean square error (RMSE) values. Arrows mark the addition of the drug.

these rate constants were independent variables ($k_{m,i}$ and $k_{m,e}$). Interestingly, the fit using this model scheme returned a $k_{m,i}/k_{m,e}$ ratio close to 1, verifying the applicability of our original assumption. Finally, we also examined a modified model B. In our "hydrophobic vacuum cleaner" model, drug extrusion was allowed from both leaflets (see Fig. 6C). We analyzed a model scheme in which the transported substrate is exported exclusively from the inner leaflet. This modification of model B had little effect on the fit (data not shown, RMSE = 152.1).

Taken together, the four compartment models provide further support to the notion that the drug is transported by ABCG2 from the plasma membrane, rather than from the cell interior. Moreover, this approach prefers the "floppase" mechanisms over the "hydrophobic vacuum cleaner" model.

4. Discussion

To investigate the substrate-transporter interaction, we employed the fully functional fluorescently labeled multidrug transporter, GFP-tagged ABCG2 [24] in an on-line confocal microscopic assay system. The GFP-tag allowed us to identify the ABCG2-expressing cells and to track down the position of the plasma membrane in living cells. We studied the cellular uptake of well-known fluorescent substrates of ABCG2, mitoxantrone and pheophorbide A. The peculiarity of this experimental setup is that these compounds become fluorescent in the lipid environment, which feature made possible to determine the drug concentration in the plasma membrane. We performed a detailed kinetic analysis of drug uptake and efflux, and found that (i) the plasma membrane drug concentration (c_m) rapidly saturates in the AGCG2-expressing cells as compared to control cells; (ii) the plasma membrane and intracellular drug concentrations approach to the same equilibrium value ($c_{m,eq} = c_{i,eq}$); (iii) the drug concentration increases first in the plasma membrane, when ABCG2 is inhibited; (iv) the drug concentration drops first in the plasma membrane in the efflux experiment; (v) there is a linear relationship between $1/c_{m,eq}$ values and GFP fluorescence. Numerical analysis of both the three-compartment and four-compartment models resulted in reasonable fits only when transport from plasma membrane was assumed (model B and model C). Acceptable fit was never obtained with model A.

Taken together, all observed characteristics of mitoxantrone uptake and efflux experiments in concert disprove model A, which corresponds to the "classical pump" mechanism. Classical pumps translocate the transported substrate from the cytosole to the external space through a pore. In contrast, in the "hydrophobic vacuum cleaner" model, drugs partition into the membrane and are expelled by the transporter directly from the lipid bilayer. In the "floppase model", drugs are translocated by the transporter from the cytoplasmic leaflet to the external leaflet of the lipid bilayer. This redistribution of the drug along with the portioning between the membrane leaflets and the aqueous phases results in a net flux of the drug. Both the hydrophobic vacuum cleaner and floppase models suggest

Please cite this article as: L. Homolya, et al., Mitoxantrone is expelled by the ABCG2 multidrug transporter directly from the plasma membrane, Biochim. Biophys. Acta (2010), doi:10.1016/j.bbamem.2010.07.031

substrate recognition within the lipid bilayer. Our three-compartment model B, considering the membrane as a "black box", also based on substrate recognition within the membrane, and combines these two mechanisms. The four compartment model scheme, however, where the membrane leaflets are distinguished, may allow discriminating between the "hydrophobic vacuum cleaner" and the "floppase" models. Numerical analysis of these models showed a slight preference for the "floppase" mechanism, although we do not feel confident to exclude the "hydrophobic vacuum cleaner" model on the basis of our results. Nevertheless, all approaches clearly invalidated the "classical pump" mechanism.

As mentioned earlier, c_i is in fact not the cytoplasmic concentration of MX, but reflects the drug level in the internal membranes adjacent to the plasma membrane. Thus, disapproval of model A at first excludes only the mechanism that the drug is expelled directly from the internal membrane. Nevertheless, if we assume drug extrusion from an aqueous layer (quasi cytoplasm) located between the plasma membrane and the internal membrane compartments, at least a mixed behavior should be observed, since the drug diffuses equally to both neighboring compartments. It is easy to see, for instance, that there would always be a difference in the equilibrium c_m and c_i values ($c_{m,eq}$, $c_{i,eq}$), or that c_m and c_i would decrease with the same delay in the efflux experiment, or that there would be no linear relationship between $1/c_{m,eq}$ and the expression level, if the changes in the membrane drug concentrations are indirect consequence of drug extrusion from the "cytoplasmic" compartment and redistribution of drug by passive diffusion. Since all the arguments, listed here and above, unambiguously support the validity of model B in the three-compartment model, we can excluded drug extrusion from the aqueous phase.

Some ABC transporters, e.g. MRP1, are known to transport their substrates by multiple transport mechanisms [4]. Thus, it is plausible to raise the question whether ABCG2 might extrude drugs from both the cytoplasm and the plasma membrane. Our observations exclude the possibility of such a mixed transport mechanism, since c_m and c_i approach the same equilibrium (Fig. 5B), and $1/c_{m,eq}$ exhibited clear linear relationship with k_3 (Fig. 5F). However, it should be mentioned that our studies were limited to the transport mechanism of one particular drug, mitoxantrone. It is still possible that other, less hydrophobic substrates of ABCG2 are transported via the classical mechanism. It is especially plausible to assume this for water soluble ABCG2 substrates, such as topotecan, although most ABCG2 substrates, such as flavopiridol, methotrexate, Imatinib mesylate, or pheophorbide A are strongly hydrophobic.

5. Conclusions

Our study clearly indicates that the anti-cancer drug, mitoxantrone is expelled by ABCG2 directly from the plasma membrane, providing unambiguous experimental evidence for the non-canonical way of action of a multidrug protein. In general, this mechanism can explain the extremely broad substrate recognition of the multidrug transporters, which feature is indispensable for fulfilling their special physiological role. In addition, our novel experimental approach, using substrate molecules, which are fluorescent in the lipid environment, combined with transport kinetic analysis, offers a new tool for studying the mechanism of membrane transporters.

Acknowledgements

This work has been supported by research grants from OTKA (K68936, CK80283, T48986), ETT (211-09), NKFP-1A-060/2004, and KMOP-1.1.2-07/1-2008-0003. T. I. Orbán and L. Csanády have been recipients of the János Bolyai Scholarship of the Hungarian Academy of Sciences. We appreciate the technical help of Gyöngyi Bézsenyi. We thank for the valuable advice of Zoltán Noszticiusz.

Appendix

For comparison of the kinetic models with experimental data, various features of the models were used. These features, given as statements, can be mathematically verified as follows.

Statement 1: the equilibrium values for c_m and c_i are different in model A, whereas they approach the same equilibrium value in model B. In equilibrium dc_i/dt is equal to 0, the relation between the equilibrium values of c_m and c_i can be expressed from Eqs. (4) and (6) as follows

model A:

$$c_{m,eq} = \frac{k_{-2} + k_3}{k_2} c_{i,eq} \tag{A.1}$$

model B:

$$c_{m,eq} = \frac{k_{-2}}{k_2} c_{i,eq} \tag{A.2}$$

With the assumption that $k_2 = k_{-2}$ (for explanation see Section 3.3),

model A:

$$c_{m,eq} = \left(1 + \frac{k_3}{k_2}\right) c_{i,eq} \tag{A.3}$$

model B:

$$c_{m,eq} = c_{i,eq} \tag{A.4}$$

Since k_3 and k_2 are positive values, $c_{m,eq}$ is always greater than $c_{i,eq}$ in model A, whereas they are equal in model B.

Statement 2: if an inhibitor is added when the system has already reached equilibrium, then model A predicts a positive value for the initial slope of c_i and a zero value for that of c_m, whereas for model B the initial slope of c_m is positive and that of c_i is zero. To prove this statement Eqs. (3)–(6) were made equal to zero, and the equilibrium values of c_m and c_i were expressed as follows

model A:

$$c_{m,eq} = \frac{k_1(k_{-2} + k_3)}{k_2 k_3 + k_{-1}(k_{-2} + k_3)} c_e \tag{A.5}$$

$$c_{i,eq} = \frac{k_1 k_2}{k_2 k_3 + k_{-1}(k_{-2} + k_3)} c_e \tag{A.6}$$

model B:

$$c_{m,eq} = \frac{k_1}{k_{-1} + k_3} c_e \tag{A.7}$$

$$c_{i,eq} = \frac{k_1 k_2}{k_{-2}(k_{-1} + k_3)} c_e \tag{A.8}$$

Eqs. (A.5) and (A.6) were introduced into Eq. (1) or Eq. (2), mimicking complete inhibition by the inhibitor by model 0

model A:

$$\frac{dc_m}{dt} = 0 \tag{A.9}$$

$$\frac{dc_i}{dt} = \frac{k_3 c_{i,eq}}{V_i} \tag{A.10}$$

Please cite this article as: L. Homolya, et al., Mitoxantrone is expelled by the ABCG2 multidrug transporter directly from the plasma membrane, Biochim. Biophys. Acta (2010), doi:10.1016/j.bbamem.2010.07.031

The latter is always greater then zero, since k_3, $c_{i,eq}$ and V_i are positive values. Similarly, introducing Eqs. (A.7) and (A.8) into Eq. (1) or Eq. (2) yields

model B:

$$\frac{dc_m}{dt} = \frac{k_3 c_{m,eq}}{V_m} \tag{A.11}$$

$$\frac{dc_i}{dt} = 0 \tag{A.12}$$

The former is always greater then zero, since k_3, $c_{m,eq}$ and V_m are positive values.

Statement 3: model A suggests a saturating curve when $1/c_{m,eq}$ is plotted against k_3, whereas model B predicts a linear relationship. Rearrangement of Eqs. (A.5) and (A.7) yields

model A:

$$\frac{1}{c_{m,eq}} = \frac{k_{-1}}{k_1 c_e} + \frac{1}{k_1 c_e} \cdot \frac{k_2 k_3}{k_{-2} + k_3} \tag{A.13}$$

model B:

$$\frac{1}{c_{m,eq}} = \frac{k_{-1}}{k_1 c_e} + \frac{k_3}{k_1 c_e} \tag{A.14}$$

Since the volume of the external space is several orders of magnitude larger than that of the cells, c_e is considered as constant, thus, Eq. (A.14) shows linear relationship between $1/c_{m,eq}$ and k_3. In contrast, on the basis of Eq. (A.13), $1/c_{m,eq}$ approaches $(k_{-1}+k_2)/(k_1 c_e)$ as k_3 becomes extremely large.

References

[1] M.M. Gottesman, T. Fojo, S.E. Bates, Multidrug resistance in cancer: role of ATP-dependent transporters, Nat. Rev. Cancer 2 (2002) 48–58.
[2] B. Sarkadi, L. Homolya, G. Szakacs, A. Varadi, Human multidrug resistance ABCB and ABCG transporters: participation in a chemoimmunity defense system, Physiol. Rev. 86 (2006) 1179–1236.
[3] R.G. Deeley, C. Westlake, S.P. Cole, Transmembrane transport of endo- and xenobiotics by mammalian ATP-binding cassette multidrug resistance proteins, Physiol. Rev. 86 (2006) 849–899.
[4] E. Bakos, L. Homolya, Portrait of multifaceted transporter, the multidrug resistance-associated protein 1 (MRP1/ABCC1), Pflugers Arch. 453 (2007) 621–641.
[5] G. Szakacs, A. Varadi, C. Ozvegy-Laczka, B. Sarkadi, The role of ABC transporters in drug absorption, distribution, metabolism, excretion and toxicity (ADME-Tox), Drug Discov. Today 13 (2008) 379–393.
[6] P. Borst, J. Jonkers, S. Rottenberg, What makes tumors multidrug resistant? Cell Cycle 6 (2007) 2782–2787.
[7] G. Szakacs, J.K. Paterson, J.A. Ludwig, C. Booth-Genthe, M.M. Gottesman, Targeting multidrug resistance in cancer, Nat. Rev. Drug Discov. 5 (2006) 219–234.
[8] R.W. Robey, O. Polgar, J. Deeken, K.W. To, S.E. Bates, ABCG2: determining its relevance in clinical drug resistance, Cancer Metastasis Rev. 26 (2007) 39–57.
[9] F.J. Sharom, ABC multidrug transporters: structure, function and role in chemoresistance, Pharmacogenomics 9 (2008) 105–127.
[10] O. Polgar, S.E. Bates, ABC transporters in the balance: is there a role in multidrug resistance? Biochem. Soc. Trans. 33 (2005) 241–245.
[11] Y. Raviv, H.B. Pollard, E.P. Bruggemann, I. Pastan, M.M. Gottesman, Photosensitized labeling of a functional multidrug transporter in living drug-resistant tumor cells, J. Biol. Chem. 265 (1990) 3975–3980.
[12] M.M. Gottesman, I. Pastan, Biochemistry of multidrug resistance mediated by the multidrug transporter, Annu. Rev. Biochem. 62 (1993) 385–427.
[13] C.F. Higgins, M.M. Gottesman, Is the multidrug transporter a flippase? Trends Biochem. Sci. 17 (1992) 18–21.
[14] L. Homolya, Z. Hollo, U.A. Germann, I. Pastan, M.M. Gottesman, B. Sarkadi, Fluorescent cellular indicators are extruded by the multidrug resistance protein, J. Biol. Chem. 268 (1993) 21493–21496.
[15] H. Bolhuis, H.W. van Veen, D. Molenaar, B. Poolman, A.J. Driessen, W.N. Konings, Multidrug resistance in *Lactococcus lactis*: evidence for ATP-dependent drug extrusion from the inner leaflet of the cytoplasmic membrane, EMBO J. 15 (1996) 4239–4245.
[16] W.D. Stein, Kinetics of the P-glycoprotein, the multidrug transporter, Exp. Physiol. 83 (1998) 221–232.
[17] A.B. Shapiro, V. Ling, Extraction of Hoechst 33342 from the cytoplasmic leaflet of the plasma membrane by P-glycoprotein, Eur. J. Biochem. 250 (1997) 122–129.
[18] A.B. Shapiro, V. Ling, Stoichiometry of coupling of rhodamine 123 transport to ATP hydrolysis by P-glycoprotein, Eur. J. Biochem. 254 (1998) 189–193.
[19] D. Ferry, R. Boer, R. Callaghan, W.R. Ulrich, Localization of the 1, 4-dihydropyridine drug acceptor of P-glycoprotein to a cytoplasmic domain using a permanently charged derivative N-methyl dexniguldipine, Int. J. Clin. Pharmacol. Ther. 38 (2000) 130–140.
[20] Q. Qu, F.J. Sharom, Proximity of bound Hoechst 33342 to the ATPase catalytic sites places the drug binding site of P-glycoprotein within the cytoplasmic membrane leaflet, Biochemistry 41 (2002) 4744–4752.
[21] M.R. Lugo, F.J. Sharom, Interaction of LDS-751 with P-glycoprotein and mapping of the location of the R drug binding site, Biochemistry 44 (2005) 643–655.
[22] A.B. Shapiro, A.B. Corder, V. Ling, P-glycoprotein-mediated Hoechst 33342 transport out of the lipid bilayer, Eur. J. Biochem. 250 (1997) 115–121.
[23] H. Omote, M.K. Al-Shawi, A novel electron paramagnetic resonance approach to determine the mechanism of drug transport by P-glycoprotein, J. Biol. Chem. 277 (2002) 45688–45694.
[24] T.I. Orban, L. Seres, C. Ozvegy-Laczka, N.B. Elkind, B. Sarkadi, L. Homolya, Combined localization and real-time functional studies using a GFP-tagged ABCG2 multidrug transporter, Biochem. Biophys. Res. Commun. 367 (2008) 667–673.
[25] L. Homolya, Z. Hollo, M. Muller, E.B. Mechetner, B. Sarkadi, A new method for a quantitative assessment of P-glycoprotein-related multidrug resistance in tumour cells, Br. J. Cancer 73 (1996) 849–855.
[26] J.D. Allen, A. van Loevezijn, J.M. Lakhai, M. van der Valk, O. van Tellingen, G. Reid, J.H. Schellens, G.J. Koomen, A.H. Schinkel, Potent and specific inhibition of the breast cancer resistance protein multidrug transporter in vitro and in mouse intestine by a novel analogue of fumitremorgin C, Mol. Cancer Ther. 1 (2002) 417–425.
[27] A. Feofanov, S. Sharonov, I. Kudelina, F. Fleury, I. Nabiev, Localization and molecular interactions of mitoxantrone within living K562 cells as probed by confocal spectral imaging analysis, Biophys. J. 73 (1997) 3317–3327.
[28] L. Kaestner, Red blood cell ghosts and intact red blood cells as complementary models in photodynamic cell research, Bioelectrochemistry 62 (2004) 123–126.
[29] The Merck Index: an encyclopedia of chemicals, drugs, and biologicals, 14th edMerck & Co., Inc, Whitehouse Station, 2006.
[30] R. Regev, D. Yeheskely-Hayon, H. Katzir, G.D. Eytan, Transport of anthracyclines and mitoxantrone across membranes by a flip-flop mechanism, Biochem. Pharmacol. 70 (2005) 161–169.

Please cite this article as: L. Homolya, et al., Mitoxantrone is expelled by the ABCG2 multidrug transporter directly from the plasma membrane, Biochim. Biophys. Acta (2010), doi:10.1016/j.bbamem.2010.07.031

8. sz. közlemény

dc_46_10

dc_46_10
Available online at www.sciencedirect.com
SCIENCE DIRECT®
Biochemical and Biophysical Research Communications 320 (2004) 860–867
BBRC
www.elsevier.com/locate/ybbrc

Functional expression and characterization of the human ABCG1 and ABCG4 proteins: indications for heterodimerization☆

Judit Cserepes,[a,d,1] Zsófia Szentpétery,[a,1] László Seres,[d] Csilla Özvegy-Laczka,[a,d] Thomas Langmann,[b] Gerd Schmitz,[b] Hristos Glavinas,[c] Izabella Klein,[a] László Homolya,[d] András Váradi,[a] Balázs Sarkadi,[d,*] and N. Barry Elkind[d]

[a] *Institute of Enzymology, Biological Research Center, Hungarian Academy of Sciences, Hungary*
[b] *Institute of Clinical Chemistry and Laboratory Medicine, University of Regensburg, Regensburg, Germany*
[c] *Solvo Biotechnology, Béke u. 5/a, H-6721 Szeged, Hungary*
[d] *National Medical Center, Institute of Haematology and Immunology, Membrane Research Group of the Hungarian Academy of Sciences, H-1113 Budapest, Hungary*

Received 5 June 2004

Abstract

The closely related human ABC half-transporters, ABCG1 and ABCG4, have been suggested to play an important role in cellular lipid/sterol regulation but no experimental data for their expression or function are available. We expressed ABCG1 and ABCG4 and their catalytic site mutant variants in insect cells, generated specific antibodies, and analyzed their function in isolated membrane preparations. ABCG1 had a high basal ATPase activity, further stimulated by lipophilic cations and significantly inhibited by cyclosporin A, thyroxine or benzamil. ABCG4 had a lower basal ATPase activity which was not modulated by any of the tested compounds. The catalytic site (K–M) mutants had no ATPase activity. Since dimerization is a requirement for half-transporters, we suggest that both ABCG1 and ABCG4 function as homodimers. Importantly, we also found that co-expression of the ABCG4-KM mutant selectively abolished the ATPase activity of the ABCG1 and therefore they most probably also heterodimerize. The heterologous expression, specific recognition, and functional characterization of these transporters should help to delineate their physiological role and mechanism of action.

Keywords: ABC half-transporter; ABCG1; ABCG4; Heterodimer; Sf9 cells; Drug-stimulated ATPase activity; Dominant negative

The five members of the human ATP-binding cassette (ABC) G subfamily of transporters (ABCG1, ABCG2, ABCG4, ABCG5, and ABCG8) have a unique domain structure consisting of one single nucleotide-binding domain (NBD) located N-terminally of the six pass transmembrane domain (TMD) (for review [1], Fig. 1). These half-transporters have to homo- or heterodimerize in order to form functionally active transporters. ABCG2 is thought to act as homodimer [2,3] while ABCG5 and G8 function as an obligatory heterodimeric complex [4].

Human ABCG2 (BCRP/MXR/ABCP) is a well-characterized member of the ABCG family. The overexpression of ABCG2 in drug-resistant cell lines and tumors, as well as its demonstrated transport activity for a number of clinically applied antitumor agents, suggests an important role for this protein in cancer multidrug resistance. In addition, ABCG2 is expressed in stem cells, placenta, liver, small intestine, colon, lung, kidney, adrenal and sweat glands, and in the endothelia, suggesting its important role in protection against xenobiotics. Homodimerization, the ATP-dependent active transport function and the molecular mechanism of ABCG2, as well as of its mutant and polymorphic variants have been analyzed in

☆ *Abbreviations:* ABC, ATP-binding cassette; wt, wildtype; Sf9, *Spodoptera frugiperda*.

* Corresponding author. Fax: +36-1-372-4353.
E-mail address: sarkadi@biomembrane.hu (B. Sarkadi).

[1] These authors contributed equally.

0006-291X/$ - see front matter © 2004 Elsevier Inc. All rights reserved.
doi:10.1016/j.bbrc.2004.06.037

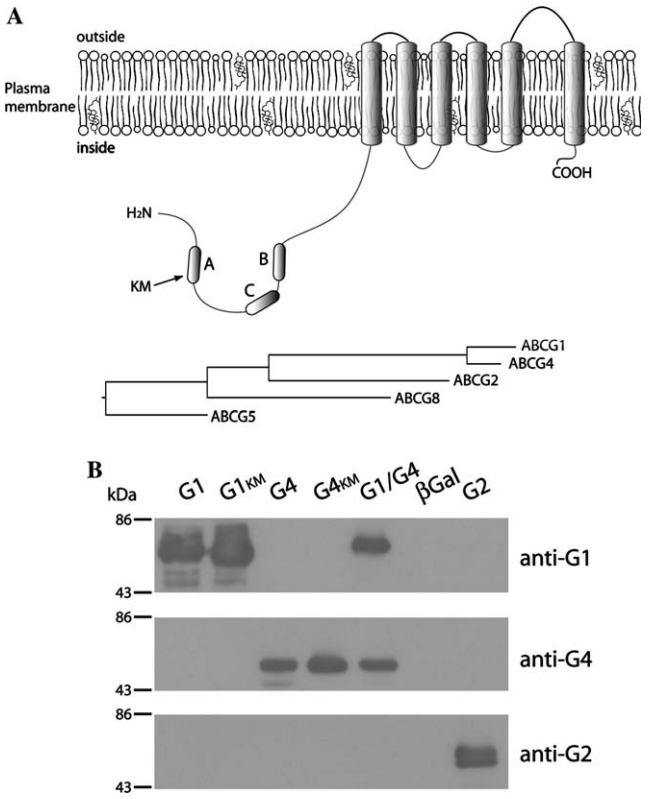

Fig. 1. (A) Membrane topology and phylogenetic tree model for the half-transporter ABCG family. The NBD is located N-terminally (H_2N) to the TMD (proximal to the COOH end). The six membrane-spanning helices (grey gradient) of the TMD are shown as cylinders passing through the lipid bilayer. (A,B,C) The ATPase catalytic Walker A, Walker B, and the signature motifs, respectively. The KM arrow marks the catalytic site mutation (KM) engineered into the Walker A motif. The phylogenetic tree (bottom), comparing human ABCG family members, shows that ABCG1 and ABCG4 are more closely related to each other than to ABCG2, the next most related member. (B) Western blot analysis of Sf9 expressed ABCG family members used in this study. Membrane fractions (20 μg membrane protein), dissolved in disaggregation buffer, were separated on a 7.5% Laemmli-type gel and blotted onto PVDF. Filters were probed with anti-G1, anti-G4 polyclonal antisera or anti-G2 monoclonal antibody. ABCG1 (G1), $ABCG1_{K124M}$ ($G1_{KM}$), ABCG4 (G4), $ABCG4_{K108M}$ ($G4_{KM}$), co-expressed ABCG1 and ABCG4 (G1/G4), ABCG2 (G2), and control membranes from β-Gal virus-infected cells.

several experimental studies in various expression systems (for review see [5,6]).

It is well documented that ABCG5 and ABCG8 function as heterodimeric active transporters for sitosterols and probably also for cholesterol and cholesterol derivatives. The inherited disease, sitosterolemia, is caused by a mutation in either one of these proteins, and the proper plasma membrane localization and function of ABCG5 and ABCG8 is only achieved when they form heterodimers and co-processed by the cellular expression machinery [4].

There is much less information known as yet about the function, localization, and the mechanism of action of ABCG1 and ABCG4. The ABCG1 gene and its putative gene product were independently recognized by two groups as the *Drosophila white* gene homologue [7,8]. The human ABCG1 mRNA was found to be expressed primarily in the heart, spleen, brain, liver, lung, skeletal muscle, kidney, and placenta [7–10]. In human macrophages elevated expression of ABCG1 mRNA was identified subsequent to cholesterol loading [9,11,12], oxidized LDL treatment, or upon the addition of LXR and RXR agonists [13]. Thus, a growing body of evidence indicates ABCG1 involvement in lipid/sterol regulation (for review see [14]). According to initial studies in human cells, endogenous ABCG1 was found to localize to both plasma membrane and to internal membranes [9,15].

Human ABCG4 was identified independently in two laboratories based on its homology and close similarity to ABCG1, and its cDNA was cloned from testes libraries [10,16]. ABCG4 gene expression was also found to be regulated by oxysterols and retinoids in a similar manner to ABCG1 [13]. There are no protein expression and localization data available for ABCG4 as yet.

ABCG1 and ABCG4 share 72% identity at the amino acid level. Based on high sequence similarity (refer to Fig. 1A phylogenetic tree) and the observation that both transporter mRNAs are upregulated upon stimulation of sterol pathways, ABCG1 and ABCG4 make good candidates for heterodimer partners, as was proposed [16].

In the present study we expressed ABCG1, ABCG4, and their catalytic site mutants alone, and in various combinations, utilizing the Sf9 insect cell expression system. We prepared specific polyclonal antibodies that distinguish ABCG1 and ABCG4 in Western blot analysis; these antibodies allowed us to monitor the expression levels of both transporters in Sf9 membranes. In isolated membrane preparations we studied the vanadate-sensitive ATPase activity and screened over 100 compounds to stimulate or inhibit their ATPase activity. By using the catalytic site mutants we could analyze the specificity of the observed ATPase activities and their stimulation by putative transported substrate compounds. Moreover, by combined expression of the ABCG1, ABCG4, and their mutant variants we analyzed the possible effects of the co-expressed proteins. Our data suggest that both ABCG1 and ABCG4 are active and they may function both as homo- and heterodimers in membranes. This first functional expression and characterization of ABCG1 and ABCG4 as interacting proteins may "fuel the fire" in the hunt for the physiological function of these proteins.

Materials and methods

Material. Rhodamine123, Rhodamine6G, Na-orthovanadate, 3-OH-kynurenine, cyclosporin A, benzamil, L-thyroxin, and ATP were

from Sigma. Ko143 was a generous gift from Drs. J. Allen and G. Koomen (University of Amsterdam, Amsterdam, The Netherlands).

Generation of baculovirus vectors expressing the cDNAs of human ABCG1 and ABCG4. To construct a human ABCG1 expression vector, a 2038 nucleotide cDNA fragment of the long isoform of ABCG1 was amplified with primers ABCG1F (5′-caccatggcctgtctgatggccgc-3′) and ABCG1R (5′-tcctctctgcccggattttgtac-3′) by RT-PCR from macrophage cDNA and inserted into the pcDNA3.1/CT-GFP-TOPO vector (Invitrogen) by TA-cloning. Subsequent PCR subcloning placed the cDNA in the baculovirus expression vector, pAcUW21-L, and added a stop coding. ABCG4 cDNA was purchased from the I.M.A.G.E. consortium (clone ID 1537140). It was PCR cloned to add an A to the Start ATG at the 5′-end of the gene and cloned into pAcUW21-L as described elsewhere [17]. ABCG1 and ABCG4 cDNAs were sequenced to confirm no errors existed. Catalytic site mutants were prepared using PCR mutagenic primers and subcloning as described above.

Generation of polyclonal antibodies against ABCG1 and ABCG4 and Western blot analysis. Polyclonal antibodies were prepared by fusing the N-terminal soluble domain of each transporter, which contain the ATP-binding domains (amino acids 1–418 for ABCG1 and 1–386 for ABCG4), to the C-terminus of GST. We expressed these proteins in bacteria, inclusion bodies were purified, and proteins were resolved on 7.5% protein gels. Protein bands were cut from the gel, pulverized, dried, mixed with adjuvant, and injected into mice. Mice were boosted and small amounts of sera were recovered for use in this study.

Western blot analysis was performed as previously described [18]. Secondary antibody was anti-mouse, peroxidase-conjugated, goat IgG (Jackson Labs), used in 10,000× dilutions.

Generation of recombinant baculoviruses, expression in Sf9 cells, and ATPase activity measurements. Recombinant baculoviruses carrying transporter cDNA were generated with BaculoGold Transfection Kit (Pharmingen), in accordance with the manufacturer's protocol. The infection and culturing of Sf9 (*Spodoptera frugiperda* ovarian) cells as well as the membrane preparations were carried out as described [18]. Membrane ATPase activity was measured by colorimetric detection of inorganic phosphate liberation as described [17,18].

Results

Expression and detection of ABCG1 and ABCG4

Human ABCG1 and ABCG4 are ABC half-transporters with similar length (ABCG1 and ABCG4 contain 678 and 646 amino acids, respectively) and share 72% amino acid sequence identity. The membrane topology of ABCG family transporters is assumed to be similar (the phylogenetic tree and the ABCG family structure are shown schematically in Fig. 1A). We modeled this structure using the online software program HMMTOP (http://www.enzim.hu/hmmtop/ [19]). The NBD (or ABC) is N-terminal to the TMD (Fig. 1A). Based on the topology model and computer predictions, neither ABCG1 nor ABCG4 has N-glycosylation receptor sites.

In order to biochemically characterize ABCG1 and ABCG4, we utilized the baculovirus-infected Sf9 cell system which had been used to successfully express biologically active ABCG2 at high levels in Sf9 cell membranes [17]. We also generated specific antisera that distinguished ABCG1 and ABCG4 in Western blot analysis. We generated recombinant baculoviruses containing the cDNAs of the ABCG family members. Viruses were propagated in Sf9 cells and high-titer viruses were produced and used to infect new cultures of Sf9 cells. Two days after transfection, the cells were harvested and membranes containing the transporter of interest were prepared.

As a control of activity, we generated catalytic site mutants by replacing the conserved lysine residue in the Walker A region of ABCG1 and ABCG4 with methionine in both transporters ($ABCG1_{K124M}$ and $ABCG4_{K108M}$—see Fig. 1A, KM and arrow pointing to the Walker A motif mutation) which we expected would abrogate ATPase activity as we also observed for ABCG2 [2]. To determine the background ATPase activity in the Sf9 cell membranes we produced β-galactosidase (β-Gal) virus-infected Sf9 membranes. For comparison, we chose to express the glycine variant, $ABCG2_{R482G}$ (and its catalytic site mutant $ABCG2_{R482G, K86M}$), which is well characterized and its ATPase activity is stimulated by Rhodamine123 [17] as we found for ABCG1 (see below [2]). All transporters were expressed at high, similar, levels as observed by Coomassie staining (data not shown).

In order to follow the expression of ABCG1 and ABCG4 and to distinguish these two closely related transporters, we produced polyclonal antibodies against the N-terminal soluble domain of each transporter (see Materials and methods). These antibodies proved to be specific in distinguishing ABCG1 and ABCG4 in Western blots (Fig. 1B) while, due to the high sequence similarity of the two proteins, several earlier attempts failed to produce specific antibodies (data not shown).

We used these antibodies to follow the expression of ABCG1, $ABCG1_{K124M}$, ABCG4, $ABCG4_{K108M}$, ABCG2, β-Gal, and the co-expressed ABCG1 and ABCG4, in isolated Sf9 cell membranes, by Western blot analysis. As documented in Fig. 1B, the anti-G1 antibody specifically recognized ABCG1 and $ABCG1_{K124M}$ but not ABCG4, $ABCG4_{K108M}$, ABCG2 or any other Sf9 protein bands (anti-G1 panel). ABCG1 and $ABCG1_{K124M}$ were expressed at high levels in the membrane; when ABCG1 was co-expressed with ABCG4, the ABCG1 level was reduced but still observed as a single band migrating at approximately 60 kDa. ABCG4 and $ABCG4_{K108M}$ were specifically recognized migrating slightly faster than ABCG1, also at approximately 60 kDa, by the anti-G4 antibody (Fig. 1B, anti-G4 panel). Neither antisera recognized ABCG2 or other nonspecific bands in the control β-Gal lane. The anti-G2 monoclonal antibody, BXP-21, was specific for ABCG2 (Fig. 1B, anti-G2 panel). Two bands for ABCG2 were observed; the higher one may be the core glycosylated form of ABCG2 [17]. These specific antisera allowed us to fine-tune the levels of transporter expression in Sf9 cells.

ATPase activity of ABCG1 and ABCG4 and its modulation in Sf9 cell membranes

Most ABC transporters bind and hydrolyze ATP, which provides the energy for transport. When expressed in Sf9 membranes, the function of several ABC transporters has been successfully examined by investigating the sodium orthovanadate-sensitive and substrate-modified phosphate liberation in isolated membranes [2,17,18].

In order to characterize the function of ABCG1 and ABCG4 we subjected isolated Sf9 cell membranes containing these transporters to ATPase activity measurements. Fig. 2A shows that ABCG1 has a relatively high vanadate-sensitive basal ATPase activity of 25 ± 1.57 (SEM, $n = 15$) nmol Pi/mg membrane protein/min (defined as units), compared to background activity. The background ATPase activity for Sf9 membranes not expressing a heterologous transporter is low, as found in membranes of Sf9 cells expressing the β-Gal protein (6.8 ± 0.56, SEM, $n = 15$, units). The $ABCG1_{K124M}$ catalytic site mutant has an activity of 6.1 ± 0.83 (SEM, $n = 8$) units which is similar to that of the background and therefore is considered inactive.

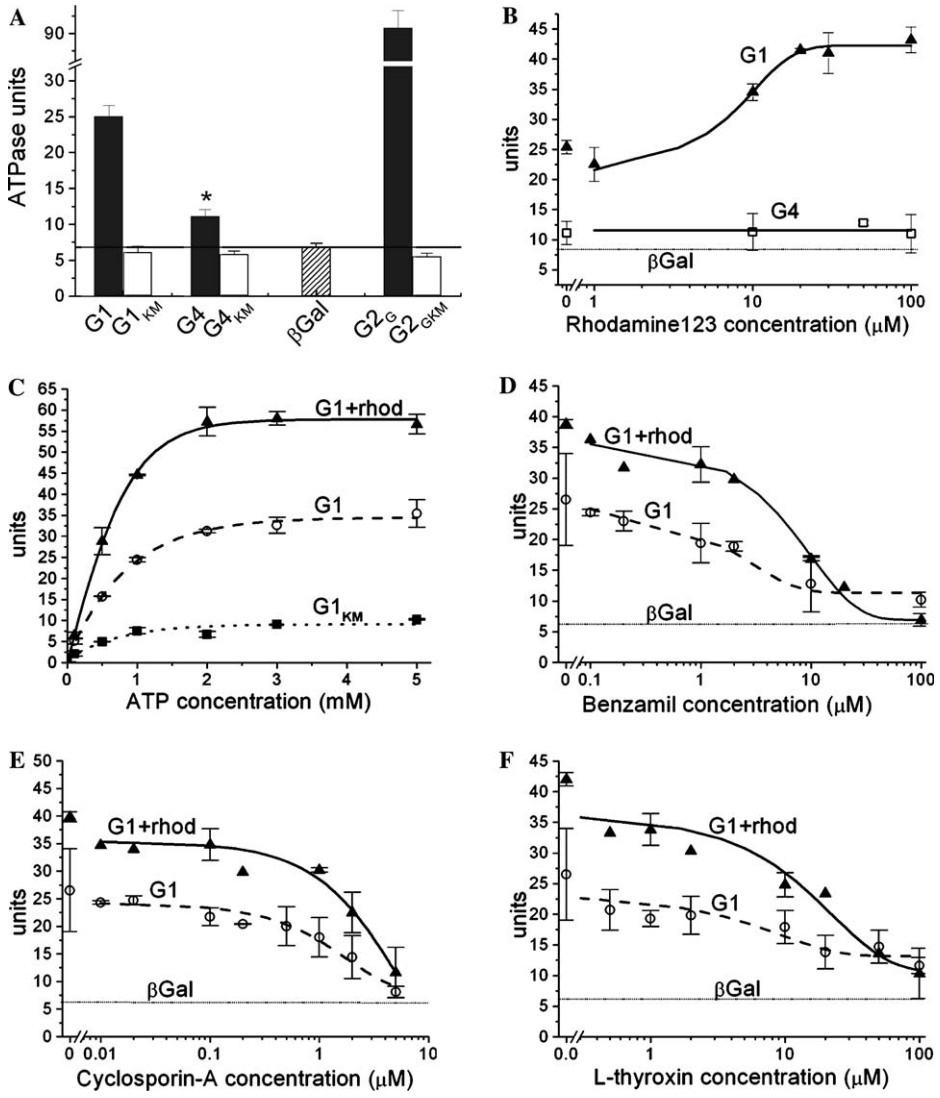

Fig. 2. ATPase activities measured for ABCG1 and ABCG4 in Sf9 membranes. ATPase activity of isolated Sf9 membranes was determined by measuring vanadate-sensitive inorganic phosphate liberation, using 3.3 mM MgATP. All measurements represent means ± SEM of the vanadate-sensitive ATPase activity in nmol Pi/min/mg membrane protein and are referred to as units. (A) ATPase activities of membranes containing ABCG1 (G1), ABCG4 (G4), and $ABCG2_{R482G}$ ($G2_G$) are shown as black bars, the corresponding KM mutants, $ABCG1_{K124M}$ ($G1_{KM}$), $ABCG4_{K108M}$ ($G4_{KM}$), and $ABCG2_{R482G,\ K86M}$ ($G2_{GKM}$) are represented by white bars, whereas the background ATPase activity of β-Gal is shown as hatched bar and corresponding horizontal line. The asterisks denote ATPase activities statistically different from β-Gal activity ($p < 0.001$). (B–F) Rhodamine123 stimulation Sf9 membranes containing ABCG1 and ABCG4 (B) ATP-dependence (C) and inhibition of ABCG1 activity by benzamil (D), cyclosporin A (E), and L-thyroxin (F). The ATPase activity of ABCG1 in the presence and absence of rhodamine123 is plotted as black up-triangles/solid lines and open circles/dashed lines. Open squares and solid line are ABCG4, solid squares and dotted line represent $ABCG1_{K124M}$ whereas straight, dotted, line is β-Gal.

We measured the basal ATPase activity for ABCG4 and observed 11.1 ± 0.95 (SEM, $n = 15$) unit activity. This ABCG4 activity was shown to be statistically different from that of the background ($p < 0.001$, Fig. 2A, labeled by an asterisk). Although this basal activity is relatively small, it is similar to that found for some functional, transport competent ABC transporters, e.g., MRP6 and MRP3 [20,21]. As expected, the $ABCG4_{K108M}$ catalytic site mutant is inactive (5.8 ± 0.51, SEM, $n = 3$, units).

For comparison, we plotted $ABCG2_{R482G}$ ($G2_G$; 90.84 ± 2.49, SD, units). $ABCG2_{R482G,\ K86M}$ activity was similar to the background ATPase activity. These results are consistent with those published for ABCG2 and small differences could result from varying amounts of protein expressed in the Sf9 cells [2].

The ATPase activity measurements for ABCG1 and ABCG4 in isolated Sf9 cell membranes allowed us to search for substrates and inhibitors which could stimulate or inhibit this ATPase activity. To this end, we screened about 100 compounds for their ability to alter the ATPase activity of these transporters. These compounds fell into several categories: anticancer agents (e.g., mitoxantrone, doxorubicin), receptor/channel modifiers (e.g., benzamil), prostaglandins, kynurenine (e.g., 3-OH-kynurenine), hormones and neurotransmitters (e.g., L-thyroxine), conjugated bile-acids, glutathione conjugates, ionophores, peptides, sterols, fluorescent (e.g., Rhodamine123, calcein-AM), and other small molecules (e.g., cyclosporin A, Ko134, and verapamil). Surprisingly, we found that Rhodamine123 (and to a lesser extent Rhodamine6G, data not shown) could substantially stimulate the ATPase activity of ABCG1 in a concentration-dependent manner (Fig. 2). In the presence of 20 μM Rhodamine123, the ATPase activity of ABCG1 was increased almost twofold and we calculated a K_{act} for Rhodamine123 of about 10 μM. The compound had no effect on ABCG4 ATPase activity (Fig. 2B). The effect of Rhodamine123 on $ABCG1_{K124M}$ was negligible (data not shown). It should be mentioned that Rhodamine123 also stimulates the $ABCG2_{R482G}$ mutant ATPase activity about 1.4-fold [17].

Basal ATPase activity could reflect a partial uncoupling of the ATPase function in unfolded transporter. To explore this, and to determine the correct working concentration of ATP in experiments, we measured the MgATP dependence on ABCG1 in the presence and absence of substrate. Fig. 2C shows the ABCG1 ATPase dependence on ATP with or without 100 μM Rhodamine123, over a range of ATP concentrations. The calculated K_m for ATP was found to be approximately 0.5 mM in both cases. The ATP dependence of the $ABCG1_{K124M}$ ATPase activity is also shown (dotted line). These data are consistent with those published for $ABCG2_{R482G}$, showing a K_m for ATP of about 0.6 mM [17]. Since the K_m ATP for ABCG1 in the presence or absence of the stimulating compound, Rhodamine123, are similar, we conclude that the majority of ABCG1 in Sf9 membranes is intact and that the high vanadate-sensitive basal ATPase activity observed for ABCG1 is brought about by molecules, possibly lipid or lipid derivatives, present in the membrane as previously proposed for ABCG2 [17]. ABCG4 activity was maximal at the ATP concentrations used in these experiments (data not shown).

The search for compounds that interact with ABCG1 led to the identification of several inhibitors of ABCG1 function (Figs. 2D–F). These drugs inhibited both the basal and the Rhodamine123 activated ATPase activity of ABCG1 but not the KM mutant (data not shown). Benzamil, a substrate of ABCG2, decreased the ABCG1 ATPase activity to the control level with a K_i about 0.5 μM. Cyclosporin A, an inhibitor of ABCG2, also inhibited ABCG1 ATPase activity at low concentrations. Additionally, the thyroid hormone L-thyroxine also inhibited ABCG1. It is worth mentioning that the specific ABCG2 inhibitor, Ko143, had no effect on the activity of ABCG1 (data not shown).

ABCG1 and ABCG4 may act as a heterodimer when co-expressed in Sf9 membranes

ABCG half-transporters function either as homodimers (ABCG2) [3,17] or heterodimers (ABCG5 and ABCG8) [4]. Since *Drosophila* homologues of ABCG1 and ABCG4 appear to function as a heterodimer [22] it has been proposed their human counterparts may do the same [16]. In order to investigate this question we co-expressed ABCG1 in various combinations and assayed the basal- and Rhodamine123-stimulated ATPase activity in these membranes. We reasoned that the co-expression of ABCG1 with the non-functional catalytic site mutant, $ABCG4_{K108M}$, could result in lowered ATPase activity if the two proteins interacted.

In order to study the interaction between ABCG1 and ABCG4, ABCG1 was co-expressed with different viral quantities of β-Gal baculovirus, which allowed the normalization of ABCG1 expression per milligram membrane protein. ATPase activity was measured for membranes expressing certain levels of ABCG1, as assayed by using the anti-G1 specific antibody. In similar experiments, ABCG1 was also co-expressed with ABCG4 or the $ABCG4_{K108M}$ mutant protein, and the same enzymatic assays were performed, in membranes containing the same levels of ABCG1, as detected by Western blotting and subsequent signal densitometry analysis (Fig. 3B).

As shown in Fig. 3A, when co-expressed with β-Gal, ABCG1 had a basal- and Rhodamine123-stimulated activity of 19.2 ± 1.24 (SEM, $n = 3$) and 33.6 ± 0.65 (SEM, $n = 3$) units (Fig. 3A, G1 + β-Gal). The non-

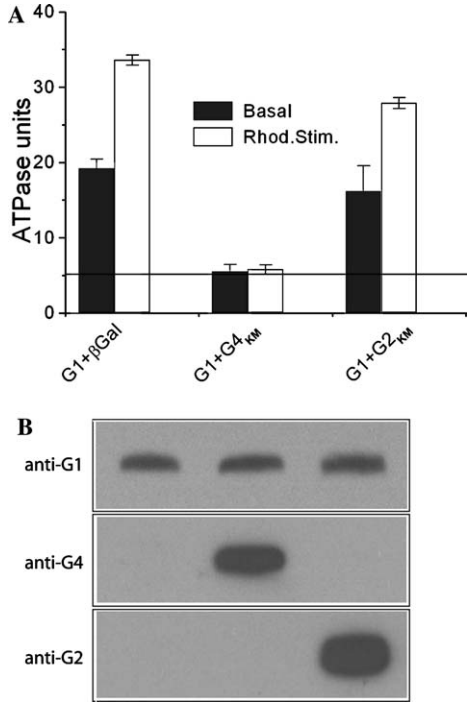

Fig. 3. ABCG1/ABCG4 co-expression ATPase activity in Sf9 membranes. Sf9 cells were co-infected with ABCG1 plus β-Gal (G1 + β-Gal), ABCG1 plus $ABCG4_{K108M}$ (G1 + $G4_{KM}$), and ABCG1 plus $ABCG2_{R482G,\ K86M}$ (G1+$G2_{KM}$) viruses. Membranes were isolated and ATPase assays were performed (A). Expression levels of ABCG1, ABCG4, and ABCG2 were determined with specific antibodies (B). (A) Membranes for each group, expressing similar levels of ABCG1, were used in ATPase assays. Black bars show basal activity and white bars show the Rhodamine123-stimulated (100 μM) activities. The solid, horizontal, line represents the β-Gal basal activity. Units are defined in Fig. 2A legend. Values are means ± SEM for one experiment done in triplicate. (B) To ensure that a similar level of ABCG1 was expressed in each co-expression experiment, equal amounts of membranes (5 μg) were loaded onto 10% SDS–PA gels, electro-blotted, and analyzed as described for Fig. 1B, using the same antibodies.

functional $ABCG4_{K108M}$ mutant, when co-expressed in several fold excess over ABCG1, severely abrogated the ABCG1 activity over background (Fig. 3A, G1 + $G4_{KM}$). The horizontal line through the bar graph represents the background (β-Gal) ATPase activity level observed for the experiment. This experiment, performed with similar levels of ABCG1 expression (see Fig. 3B), strongly suggests that $ABCG4_{K108M}$ can interact with ABCG1 in membranes and the mutant ABCG4 induces a dominant-negative effect on ABCG1 ATPase activity.

In order to examine the specificity of the ABCG1–ABCG4 interaction, the catalytic site mutant $ABCG2_{R482G,K86M}$ was also co-expressed with ABCG1. As documented, the $ABCG2_{R482G,\ K86M}$ mutant did not interfere with ABCG1 activity (Fig. 3A, G1 + $G2_{KM}$). As a further control, the $ABCG4_{K108M}$ mutant was co-expressed with the functional $ABCG2_{R482G}$; however, no dominant-negative effect of $ABCG4_{K108M}$ on the ATPase activity was observed (data not shown). Western blot analysis confirmed the presence of $ABCG4_{K108M}$ and $ABCG2_{R482G,\ K86M}$ in these membrane preparations (Fig. 3B, anti-G4 and anti-G2).

In similar experiments, various ratios of ABCG1 and ABCG4 were also co-expressed but no appreciable differences in the ABCG1 ATPase activity (as compared to β-Gal controls) were detected (data not shown). It will be important to test the effects of co-expression of ABCG1 and ABCG4 in other systems and using (still unknown) physiological substrates of these proteins.

Discussion

In this study we utilized a baculovirus Sf9 insect cell system to express and biochemically characterize the human ABCG1 and ABCG4 transporters. Heterologous baculovirus expression allows high level and "fine-tuning" of the transporter protein(s) expressed, without the possible interference of endogenous mammalian type ABC transporters. This methodology has been used earlier in our laboratory to characterize several transporters of the MDR, MRP, and ABCG family. For this work we also developed specific polyclonal antisera that recognize and distinguish the highly similar (72% identity at the amino acid level) ABCG1 and ABCG4 proteins, allowing detection of their expression in Sf9 membranes.

We found that these closely related human ABC half-transporters functioned as vanadate-sensitive membrane ATPases. Since dimerization is a requirement for the function of the G type ABC half-transporters, we suggest that both ABCG1 and ABCG4 can work as homodimers. Moreover, as we found a functional interaction between the two proteins, they most probably can also form heterodimeric complexes.

The vanadate-sensitive basal ATPase activity of ABCG1 was relatively high and, similar to ABCG2 [17], it appears that a yet unidentified compound in Sf9 membranes can stimulate ABCG1 activity. In fact, ABCG2 has been found to transport sterols in bacteria [23] and overexpression leads to the extracellular exposure of phosphatidylserine in cancer cells [24]. Also, ABCG1 has been implicated in sterol transport (see Introduction).

We also identified Rhodamine123 as an ATPase activator and thus potential substrate for ABCG1. Moreover, by screening a large compound library, we found several agents which strongly inhibited ABCG1 ATPase activity at relatively low concentrations.

ABCG4 had a low, but statistically significant, level of ATPase activity, which could not be stimulated or inhibited by more than 100 potential substrate compounds tested. It is possible that no drugs affect the basal activity of ABCG4 because the protein is not

properly folded in Sf9 cells and therefore can bind and turn over ATP at a low rate and cannot be stimulated by substrate. Another possibility is that ABCG4 is fully functional but we did not find a substrate that can further stimulate its ATPase activity above its basal level. In fact, the relatively low ABCG4 basal activity observed here is reminiscent of the activity found for functional, transport competent, MRP6 and MRP3 [20,21].

When co-expressing the catalytic site mutant $ABCG4_{K108M}$ with functional ABCG1, we observed a dominant-negative effect of the mutant ABCG4 on ABCG1 activity (Fig. 3). In contrast, the ABCG2 catalytic site mutant, when co-expressed with ABCG1, had no effect. We conclude that this is due to a specific interaction of ABCG4 with ABCG1 in a heterodimeric complex. Catalytic site mutations (KM) in the Walker A motif of ABCG1, ABCG4 or ABCG2 rendered the homodimeric transporters inactive. We previously reported that mutating just one Walker A motif in a full transporter, like MDR1, is enough to inactivate the transporter [25]. In line with this, we now show that one functional ABCG1 subunit interacting with a catalytically inactive $ABCG4_{K108M}$ subunit is not active as a whole. In summary, our data indicate that ABCG1 and ABCG4 can form both homo- and heterodimers.

The suggestion that human ABCG1 and ABCG4 may function both as homodimers and heterodimers is consistent with the mRNA expression data from several laboratories, which show that this transporter expression overlaps in some but not all tissues assayed [7–10,16,26]. Our newly developed specific antibodies can specifically recognize ABCG1 and ABCG4 protein expression, thus these reagents should help establish tissue expression, cellular localization, and distribution for these proteins.

The physiological functions of mammalian ABCG1 and ABCG4 are not known, yet there is a growing body of evidence that they are involved in lipid/sterol regulation (for review see [14]). Elevated expression of ABCG1 [9,11,12] and ABCG4 mRNAs [13] was identified subsequent to cholesterol loading of macrophages. Acetylated or oxidized LDL strongly induced ABCG1 expression as does their treatment with LXR and RXR agonists, oxysterols and retinoids [13]. Also, cholesterol efflux mediated by the cholesterol acceptor HDL_3 completely suppressed ABCG1 expression [9,12,15]. Inhibition of ABCG1 expression by antisense oligonucleotides decreased HDL_3 cholesterol efflux from cells [9]. The physiological substrates for ABCG1, ABCG4, and the potential heterodimer are unknown. We are currently investigating whether these transporters act individually or in complex as lipid and/or sterol transporters, as previously proposed. The *Drosophila* homologues (White, Scarlet, and Brown) of the human ABCG1 and ABCG4 were proposed to work as heterodimers in various combinations: the White and Scarlet heterodimers are thought to transport 3-OH kynurenine from the cytoplasm into the pigment granules in the eye of the fly [27]. Since ABCG4 is expressed in the human eye [10], we tested if this compound could stimulate the ATPase activity of ABCG1, ABCG4, and ABCG1–ABCG4, co-expressed in Sf9 membranes. However, we could not detect a change in activity when 3-OH kynurenine was added at various concentrations (data not shown).

Based on the present data, future ABCG1 or ABCG4 expression studies in mammalian cells should take note of the endogenous levels of both transporters. The overexpression of one transporter or the other may dramatically influence the dimeric state of the transporters and thus influence function. We generated specific mouse polyclonal antisera that can recognize ABCG1 and ABCG4 on Western blot. Monoclonal antibody production is well underway and the encouraging specificity of the polyclonal antisera suggests that we will be able to perform studies that consider endogenous transporter levels.

Acknowledgments

The technical help by Zsuzsanna Andrási, Judit Kis, and Györgyi Demeter is gratefully acknowledged. The authors are also grateful for Gábor E. Tusnády for useful discussion on the topology/structure of ABCG. We appreciate the kind gift of the BXP-21 antibody obtained from Drs. George Scheffer and Rik Scheper. This work has been supported by research grants from OTKA and OM, Hungary (T-31952, T35926, T38337, D 45957, ETT, F034247, and NKFP). N. Barry Elkind was a recipient of a young investigator fellowship of the Hung. Acad. Sci., Balázs Sarkadi is a recipient of a Howard Hughes International Scholarship. László Homolya is an HHMI/EMBO scientist.

References

[1] I. Klein, B. Sarkadi, A. Varadi, An inventory of the human ABC proteins, Biochim. Biophys. Acta 1461 (1999) 237–262.
[2] C. Ozvegy, A. Varadi, B. Sarkadi, Characterization of drug transport, ATP hydrolysis, and nucleotide trapping by the human ABCG2 multidrug transporter. Modulation of substrate specificity by a point mutation, J. Biol. Chem. 277 (2002) 47980–47990.
[3] H. Mitomo, R. Kato, A. Ito, S. Kasamatsu, Y. Ikegami, I. Kii, A. Kudo, E. Kobatake, Y. Sumino, T. Ishikawa, A functional study on polymorphism of the ATP-binding cassette transporter ABCG2: critical role of arginine-482 in methotrexate transport, Biochem. J. 373 (2003) 767–774.
[4] G.A. Graf, L. Yu, W.P. Li, R. Gerard, P.L. Tuma, J.C. Cohen, H.H. Hobbs, ABCG5 and ABCG8 are obligate heterodimers for protein trafficking and biliary cholesterol excretion, J. Biol. Chem. 278 (2003) 48275–48282.
[5] A. Haimeur, G. Conseil, R.G. Deeley, S.P. Cole, The MRP-related and BCRP/ABCG2 multidrug resistance proteins: biology, substrate specificity and regulation, Curr. Drug Metab. 5 (2004) 21–53.

[6] B. Sarkadi, C. Özvegy-Laczka, K. Német, A. Váradi, ABCG2—a transporter for all seasons, FEBS Lett. 567 (2004) 116–120.
[7] J.M. Croop, G.E. Tiller, J.A. Fletcher, M.L. Lux, E. Raab, D. Goldenson, D. Son, S. Arciniegas, R.L. Wu, Isolation and characterization of a mammalian homolog of the *Drosophila* white gene, Gene 185 (1997) 77–85.
[8] H. Chen, C. Rossier, M.D. Lalioti, A. Lynn, A. Chakravarti, G. Perrin, S.E. Antonarakis, Cloning of the cDNA for a human homologue of the *Drosophila* white gene and mapping to chromosome 21q22.3, Am. J. Hum. Genet. 59 (1996) 66–75.
[9] J. Klucken, C. Buchler, E. Orso, W.E. Kaminski, M. Porsch-Ozcurumez, G. Liebisch, M. Kapinsky, W. Diederich, W. Drobnik, M. Dean, R. Allikmets, G. Schmitz, ABCG1 (ABC8), the human homolog of the *Drosophila* white gene, is a regulator of macrophage cholesterol and phospholipid transport, Proc. Natl. Acad. Sci. USA 97 (2000) 817–822.
[10] S. Oldfield, C. Lowry, J. Ruddick, S. Lightman, ABCG4: a novel human white family ABC-transporter expressed in the brain and eye, Biochim. Biophys. Acta 1591 (2002) 175–179.
[11] A. Venkateswaran, J.J. Repa, J.M. Lobaccaro, A. Bronson, D.J. Mangelsdorf, P.A. Edwards, Human white/murine ABC8 mRNA levels are highly induced in lipid-loaded macrophages. A transcriptional role for specific oxysterols, J. Biol. Chem. 275 (2000) 14700–14707.
[12] B.A. Laffitte, J.J. Repa, S.B. Joseph, D.C. Wilpitz, H.R. Kast, D.J. Mangelsdorf, P. Tontonoz, LXRs control lipid-inducible expression of the apolipoprotein E gene in macrophages and adipocytes, Proc. Natl. Acad. Sci. USA 98 (2001) 507–512.
[13] T. Engel, S. Lorkowski, A. Lueken, S. Rust, B. Schluter, G. Berger, P. Cullen, G. Assmann, The human ABCG4 gene is regulated by oxysterols and retinoids in monocyte-derived macrophages, Biochem. Biophys. Res. Commun. 288 (2001) 483–488.
[14] G. Schmitz, T. Langmann, S. Heimerl, Role of ABCG1 and other ABCG family members in lipid metabolism, J. Lipid Res. 42 (2001) 1513–1520.
[15] S. Lorkowski, M. Kratz, C. Wenner, R. Schmidt, B. Weitkamp, M. Fobker, J. Reinhardt, J. Rauterberg, E.A. Galinski, P. Cullen, Expression of the ATP-binding cassette transporter gene ABCG1 (ABC8) in Tangier disease, Biochem. Biophys. Res. Commun. 283 (2001) 821–830.
[16] T. Annilo, J. Tammur, A. Hutchinson, A. Rzhetsky, M. Dean, R. Allikmets, Human and mouse orthologs of a new ATP-binding cassette gene, ABCG4, Cytogenet. Cell. Genet. 94 (2001) 196–201.
[17] C. Ozvegy, T. Litman, G. Szakacs, Z. Nagy, S. Bates, A. Varadi, B. Sarkadi, Functional characterization of the human multidrug transporter, ABCG2, expressed in insect cells, Biochem. Biophys. Res. Commun. 285 (2001) 111–117.
[18] B. Sarkadi, E.M. Price, R.C. Boucher, U.A. Germann, G.A. Scarborough, Expression of the human multidrug resistance cDNA in insect cells generates a high activity drug-stimulated membrane ATPase, J. Biol. Chem. 267 (1992) 4854–4858.
[19] G.E. Tusnady, I. Simon, Principles governing amino acid composition of integral membrane proteins: application to topology prediction, J. Mol. Biol. 283 (1998) 489–506.
[20] A. Ilias, Z. Urban, T.L. Seidl, O. Le Saux, E. Sinko, C.D. Boyd, B. Sarkadi, A. Varadi, Loss of ATP-dependent transport activity in pseudoxanthoma elasticum- associated mutants of human ABCC6 (MRP6), J. Biol. Chem. 277 (2002) 16860–16867.
[21] A. Bodo, E. Bakos, F. Szeri, A. Varadi, B. Sarkadi, Differential modulation of the human liver conjugate transporters MRP2 and MRP3 by bile acids and organic anions, J. Biol. Chem. 278 (2003) 23529–23537.
[22] G.D. Ewart, D. Cannell, G.B. Cox, A.J. Howells, Mutational analysis of the traffic ATPase (ABC) transporters involved in uptake of eye pigment precursors in *Drosophila melanogaster*. Implications for structure–function relationships, J. Biol. Chem. 269 (1994) 10370–10377.
[23] T. Janvilisri, H. Venter, S. Shahi, G. Reuter, L. Balakrishnan, H.W. van Veen, Sterol transport by the human breast cancer resistance protein (ABCG2) expressed in *Lactococcus lactis*, J. Biol. Chem. 278 (2003) 20645–20651.
[24] H. Woehlecke, A. Pohl, N. Alder-Baerens, H. Lage, A. Herrmann, Enhanced exposure of phosphatidylserine in human gastric carcinoma cells overexpressing the half-size ABC transporter BCRP (ABCG2), Biochem. J. 376 (2003) 489–495.
[25] M. Muller, E. Bakos, E. Welker, A. Varadi, U.A. Germann, M.M. Gottesman, B.S. Morse, I.B. Roninson, B. Sarkadi, Altered drug-stimulated ATPase activity in mutants of the human multidrug resistance protein, J. Biol. Chem. 271 (1996) 1877–1883.
[26] M. Yoshikawa, H. Yabuuchi, A. Kuroiwa, Y. Ikegami, Y. Sai, I. Tamai, A. Tsuji, Y. Matsuda, H. Yoshida, T. Ishikawa, Molecular and cytogenetic characterization of the mouse ATP-binding cassette transporter Abcg4, Gene 293 (2002) 67–75.
[27] S.M. Mackenzie, A.J. Howells, G.B. Cox, G.D. Ewart, Subcellular localisation of the white/scarlet ABC transporter to pigment granule membranes within the compound eye of *Drosophila melanogaster*, Genetica 108 (2000) 239–252.

9. sz. közlemény

dc_46_10

Biochimica et Biophysica Acta 1778 (2008) 2378–2387

Contents lists available at ScienceDirect

Biochimica et Biophysica Acta

journal homepage: www.elsevier.com/locate/bbamem

Functional ABCG1 expression induces apoptosis in macrophages and other cell types

László Seres [a], Judit Cserepes [a], N. Barry Elkind [a], Dániel Törőcsik [b], László Nagy [b], Balázs Sarkadi [a], László Homolya [a,*]

[a] Research Group for Membrane Biology, Semmelweis University, Hungarian Academy of Sciences, Diószegi u. 64, H-1113 Budapest, Hungary
[b] Department of Biochemistry and Molecular Biology, Medical and Health Science Center, University of Debrecen, Hungary

ARTICLE INFO

Article history:
Received 13 February 2008
Received in revised form 9 June 2008
Accepted 9 June 2008
Available online 19 June 2008

Keywords:
ABC transporter
Macrophage
LXR-ligand
Annexin V binding
Atherosclerosis

ABSTRACT

The expression of the ATP-binding cassette transporter ABCG1 is greatly increased in macrophages by cholesterol loading via the activation of the nuclear receptor LXR. Several recent studies demonstrated that ABCG1 expression is associated with increased cholesterol efflux from macrophages to high-density lipoprotein, suggesting an atheroprotective role for this protein. Our present study uncovers an as yet not described cellular function of ABCG1. Here we demonstrate that elevated expression of human ABCG1 is associated with apoptotic cell death in macrophages and also in other cell types. We found that overexpression of the wild type protein results in phosphatidyl serine (PS) translocation, caspase 3 activation, and subsequent cell death, whereas neither the inactive mutant variant of ABCG1 ($ABCG1_{K124M}$) nor the ABCG2 multidrug transporter had such effect. Induction of ABCG1 expression by LXR activation in Thp1 cells and in human monocyte-derived macrophages was accompanied by a significant increase in the number of apoptotic cells. Thyroxin and benzamil, previously identified inhibitors of ABCG1 function, selectively prevented ABCG1-promoted apoptosis in transfected cells as well as in LXR-induced macrophages. Collectively, our results suggest a causative relationship between ABCG1 function and apoptotic cell death, and may offer new insights into the role of ABCG1 in atherogenesis.

1. Introduction

Since the concept of apoptosis was introduced in the early 70s by Kerr et al. [1], considerable knowledge on the physiological relevance of this phenomenon has accumulated. In a number of physiological processes the proper balance between cell proliferation and controlled cell death regulates organ development. The progression of atherosclerotic lesions is also determined by the balance of a series of pro- and antiatherogenic events. In recent years, apoptosis has been implicated as one of the key factors influencing the cellularity, stability, and thrombogenicity of the atherosclerotic lesions (for reviews see [2–4]).

Apoptosis in the atherosclerotic plaque can be either beneficial or harmful, depending on the cell type, the stage of the lesion, and the context. Apoptosis of endothelial cells and smooth muscle cells favors plaque instability [3–7], whereas macrophage apoptosis seems to be a double edged sword. In the early lesions, decrease in the number of macrophages is antiatherogenic as macrophage apoptosis results in a lower level of metalloproteinase activity and reduction in collagen breakdown, thus, increases plaque stability [2,3,8,9]. In contrast, in advanced atherosclerotic lesions, where the clearance of apoptotic bodies by intimal phagocytes becomes limiting [2,10,11], macrophage apoptosis is believed to promote atherogenesis. Loss of macrophages leads to further reduction in phagocytic activity, and with a positive feed-back mechanism results in the accumulation of non-scavenged apoptotic bodies, which are potential sources of inflammatory cytokines and tissue factors [12,13]. Thus this process leads to necrotic core formation, complement and thrombin activation. In addition, increased activity of metalloproteinases secreted by residual surviving macrophages reduces the stability of the atherosclerotic lesion [2,8,9]. Inflammation, thrombogenicity and augmented vulnerability can finally lead to plaque rupture. The molecular machinery regulating macrophage apoptosis under these circumstances, however, is not well understood.

Here we present evidence for an unexpected link between macrophage apoptosis and the activity of an ATP-binding cassette (ABC) transporter protein, ABCG1, highly expressed in cholesterol-loaded macrophages. The ABCG1 membrane protein belongs to the G subfamily of ABC transporters, the members of which are termed 'reverse order' half transporters. Unlike canonical ABC transporters, ABCG proteins consist of only a single nucleotide binding domain and a single transmembrane domain, which is localized C-terminally to the former one. An active ABC transporter requires the presence of at least two nucleotide binding domains and two transmembrane domains, therefore, the half transporters have to dimerize to form a functional unit. The ABCG1 transporter typically forms homodimers

* Corresponding author. Fax: +36 1 372 4353.
E-mail address: homolya@biomembrane.hu (L. Homolya).

0005-2736/$ – see front matter © 2008 Elsevier B.V. All rights reserved.
doi:10.1016/j.bbamem.2008.06.010

[14], but heterodimerization with ABCG4, the most closely related member of the ABCG subfamily, has also been demonstrated in our previous study [15].

In contrast to full length ABC transporters, which normally reside in the plasma membrane, several ABC half transporters localize to the membranes of intracellular organelles. Not only regarding dimerization, but also in terms of subcellular localization, ABCG1 seems to be a Janus-faced protein because both cell surface and intracellular expression of this transporter has been demonstrated [14,16,17]. Wang et al. proposed that a translocation of ABCG1 from the internal membrane to the cell surface occurs in response to LXR activation [16], although this notion was questioned by others [18]. Like most ABC transporters, ABCG1 possesses ATPase activity, which can be stimulated by putatively transported substrates [15], although direct transport of any substrate has not been demonstrated as yet. Also, the physiological substrates of ABCG1 remain to be identified.

Despite the growing number of studies on ABCG1, its physiological function is still elusive. Based on its homology with the Drosophila *White* gene product, which regulates the tryptophan and guanine uptake in fruit flies, the first studies on the mammalian ABCG1 predicted its contribution to the cellular transport of tryptophan, which is a precursor for serotonin, and suggested that the mutations in the human *ABCG1* gene may be associated with neurological disorders [19,20]. Subsequent studies did not provide further support for this hypothesis [21]. Recently, the most commonly accepted concept on the ABCG1 function is that this protein plays a role in cholesterol efflux in macrophages.

The involvement of ABCG1 in lipid homeostasis has been implicated by several studies demonstrating that the expression of ABCG1 in macrophages was induced by cholesterol load [22–24]. The possible connection of ABCG1 with lipid metabolism was further supported by the finding that its expression is regulated by LXR/RXR and PPARγ [25–27], the nuclear receptor systems that typically regulate genes controlling lipid metabolism. Direct cholesterol efflux from ABCG1-overexpressing cells to HDL and other lipoprotein particles has also been demonstrated by several studies [16,17,28–31]. Abolition of ABCG1 expression either by RNAi knockdown or by generation of knockout animals resulted in reduced cholesterol efflux to HDL [16,29,31,32]. Surprisingly, ABCG1 was unable to induce cellular cholesterol efflux to lipid-free apoA-I, the major apolipoprotein of HDL, to which ABCA1, another member of the ABC protein family mediates cellular efflux of cholesterol [33–35]. Based on this, ABCA1 and ABCG1 have been proposed to co-operate in the cellular removal of cholesterol. According to this model, ABCA1 facilitates loading of lipid-poor apoA-I with cholesterol, thus forming “nascent” HDL, which is further lipidated by the ABCG1-dependent cholesterol efflux [30,36–38].

The present work provides new insight into the possible function of the ABCG1 transporter. Here we demonstrate a link between the activity of ABCG1 and apoptotic cell death in macrophages and other cell types. These observations may extend our understanding of the formation and progression of atherosclerotic lesions.

2. Materials and methods

2.1. Expression of ABCG1 in Sf9 insect and mammalian cells

For infection of Sf9 (*Spodoptera frugiperda*) cells, the cDNAs of human ABCG1 and its mutant variant ($ABCG1_{K124M}$) were cloned into recombinant baculovirus transfer vectors as described previously [15]. For transfection of mammalian cells, the entire open reading frame of ABCG1 variants were cloned into pEGFP-N1 vectors (Becton Dickinson Clontech) leaving a stop codon and a frame shift between ABCG1 and eGFP sequences. The insect cell culturing and infection were carried out as detailed in [39]. HEK293 and MDCK cells were maintained in D-MEM containing 10% FCS, whereas HepG2 cells were cultured in F12 and D-MEM (1:1) +10% FCS. For transfection, the cells were seeded onto eight-well Nunc Lab-Tek II Chambered Coverglass (Nalge Nunc) at $1–3\times10^4$ per well cell density, and grown for 24 h. The cells were transfected with the DNA constructs by using the FuGENE 6 (Roche) reagent according to the manufacturer's instruction. The medium was changed 24 h after transfection, immunofluorescence and apoptosis studies were performed 48 h post-transfection.

2.2. Isolation of monocytes and culturing macrophages

Thp-1 cells were maintained in RPMI+10% FCS medium, and pretreated with 2 nM PMA 24 h before the induction of ABCG1 expression. Human monocytes were obtained from peripheral blood of healthy subjects by Ficoll separation followed by CD14 immunoisolation. Positive selection method was applied using CD14 MicroBeads and MiniMACS Separator (Miltenyi Biotec). The monocyte-derived macrophages were cultured in D-MEM containing 10% FCS for 5 days. The ABCG1 expression was induced in both PMA-pretreated Thp-1 cells and monocyte-derived macrophages by the addition of a synthetic LXR agonist, T0901317 (1 μM, Alexis Biochemicals) 8 or 24 h prior to quantitative RT-PCR and cell biology studies, respectively.

2.3. RNA isolation and real time RT-PCR

To obtain total RNA, 1×10^6 cells were dissolved in 1 ml Trizol (Invitrogen), and RNA was extracted according to the manufacturer's instructions. The purity of the RNA preparation was checked by measuring the absorbance ratio at 260/280 nm. Samples containing 1 μg of RNA were used for reverse transcription, which was carried out at 42 °C for 2 h and 72 °C for 5 min using Superscript II reverse transcriptase and Random hexamers (both from Invitrogen) according to the recommendation of the manufacturer. cDNA obtained was used for real-time quantitative PCR (ABI PRISM 7900, Applied Biosystems), 40 cycles of 95 °C for 10 s and 60 °C for 1 min. The sequence of the primers and probes are: ABCG1 (208+) TCCTCTTCAAGAGGACCTTCCT (284−) CCCAATGTGCGAGGTGAT (1233+) FAM-CATCATGAGGGACTCGGTCCTGACAC, cyclophilin: (52+) ACGGCGAGCCCTTGG (117−) TTTCTGCTGTCTTTGGGACCT (69+) FAM-CGCGTCTCCTTTGAGCTGTTTGCA. The comparative Ct method was used to quantify transcript levels and to normalize for cyclophilin expression.

2.4. Generation of monoclonal antibodies and Western blot analysis

Mice previously immunized with a GST-fused N-terminal domain of ABCG1, and producing ABCG1-specific sera as demonstrated in [15], were sacrificed and hybridoma cells were generated at the EMBL Antibody Core Facility (Monterotondo, Italy). The ELISA-positive hybridoma cells were cloned by limiting dilution and their supernatants were tested by Western blot analysis using ABCG1-containing Sf9 membrane preparations. Immunoblotting was performed as previously described [39]. The clones producing high level of antibody were expanded and their supernatants were enriched in the antibodies by step-wise serum deprivation. The supernatants were further concentrated by centrifugal ultrafiltering and the monoclonal antibodies were isotyped. Their selectivity was tested by immunoblotting using Sf9 membranes containing ABCG1, ABCG4, ABCG2, ABCG5, or ABCG5. Subsequent Western blot analyses and immunofluorescence studies were performed by using 6G1/7, a highly sensitive and specific, IgG1 isotype anti-ABCG1 monoclonal antibody.

2.5. Immunofluorescence staining

For immunofluorescence studies, the cells were gently washed with Dulbecco's modified PBS (DPBS), and fixed with 4% paraformaldehyde in DPBS for 5 min at room temperature. After 5 washes with DPBS, the samples were further fixed and permeabilized in pre-chilled methanol for 5 min at −20 °C. The cells were then blocked for 1 h at

room temperature in DPBS containing 2 mg/ml bovine serum albumin, 1% fish gelatin, 0.1% Triton-X 100, and 5% goat serum (blocking buffer). The samples were then incubated for 1 h at room temperature with 6G1/7, anti-ABCG1 antibody, diluted 100x in blocking buffer. After washing with DPBS, the cells were incubated for 1 h at room temperature with Alexa Fluor 488-conjugated goat anti-mouse IgG (H+L) (Molecular Probes), diluted 250× in blocking buffer. For isotype control, mouse IgG1 (Sigma) and Alexa Fluor 488-conjugated goat anti-mouse IgG were used. The green fluorescence of stained samples was studied by an Olympus FV500-IX confocal laser scanning microscope using a UPLAPO 40× (0.85) dry or a PLAPO 60× (1.4) oil immersion objective (Olympus) at 488 nm excitation.

2.6. Cell death and apoptosis studies

For assessment of Sf9 cell death, the insect cells were infected with recombinant baculoviruses containing the sequences of the human ABCG1, ABCG1$_{KM}$, ABCG2, or β-galactosidase under identical circumstances (10^8 PFU virus per 10^7 cells) [15,39]. The fraction of living cells was determined 24, 36, 48, 72 and 96 h after infection by using Trypan-blue (Sigma) counterstaining.

To study apoptosis in mammalian cells, the cells were incubated with Alexa Fluor 488-conjugated Annexin V (Molecular Probes) in 1:20 dilution in Annexin binding buffer (10 mM Hepes, 140 mM NaCl, 2.5 mM $CaCl_2$, pH: 7.4) containing 2 μM propidium iodide for 3 min. When indicated, the cells were preincubated with 100 μM thyroxin or 50 μM benzamil 24 h before apoptosis studies. In control experiments, apoptosis was induced by the addition of 2 nM staurosporine 5 h prior to studies. For combined PS translocation and caspase 3 studies, the cells were first incubated with a fluorogenic caspase 3 substrate, 10 μM PhiPhiLuxG_2D_2 (Calbiochem)+10% FCS (final conc.: 9 μM) for 20 min, washed twice and labeled with Alexa Fluor 488-conjugated Annexin V as described above. For combined PS translocation and immunofluorescence studies, the cells were first labeled with Alexa Fluor 488-conjugated Annexin V, washed, fixed, and immunostained as described above using Alexa Fluor 647-conjugated secondary antibody. The stained samples were studied with the confocal microscope specified above. The green, red, and deep red fluorescence were acquired between 505–525, 560–600 nm and above 650 nm, using 488, 543, and 633 nm excitations, respectively.

For quantitative evaluation of Annexin V binding, the labeled cells were counted in the fluorescence image, whereas the total cell number was determined in the corresponding DIC image. The fraction of Annexin V-labeled cells (% of total) was determined in 6–8 fields of view in several independent experiments ($n>3$). For statistical analyses, unpaired, 2-tailed, Student's *t*-test was used. Results are expressed as mean±s.e.m.

3. Results

In our previous work, we have biochemically characterized the ABCG1 transporter by using a heterologous baculovirus Sf9 insect cell system. In this transient expression system, transfection of the insect cells with baculovirus ultimately results in cell death. However, we have observed that the fraction of living cells in cultures expressing the wild type ABCG1 (wtABCG1) was significantly lower than in control cultures transduced with either β-galactosidase (β-gal), ABCG2, or the inactive, catalytic site mutant variant of ABCG1 (ABCG1$_{KM}$), even though the infection procedure were carried out under identical circumstances (10^8 PFU virus per 10^7 Sf9 cells) (Fig. 1). The proteins were expressed at similar high levels 72 h after transduction as observed by Coomassie staining or by Western blotting for ABCG1 and ABCG1$_{KM}$ (data not shown). The half life times determined from the kinetic analysis shown in Fig. 1, were 40.5±1.2 h for cells transduced with the wild type ABCG1, and around 60 h for cells expressing ABCG1$_{KM}$, ABCG2, or β-gal. Accordingly, cells

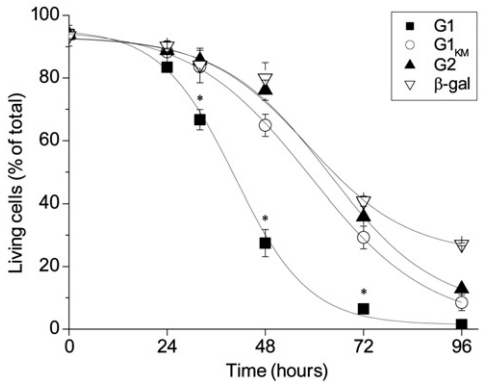

Fig. 1. Accelerated cell death caused by functional expression of ABCG1 in Sf9 cells. The wild type ABCG1 (filled square), its inactive mutant variant ABCG1$_{KM}$ (open circle), ABCG2 (filled up triangle), and β-galactosidase (open down triangle) were expressed in Sf9 heterologous expression system. The fraction of living cells was determined by Trypan-blue counterstaining at different time points after infection carried out under identical conditions (10^8 PFU virus per 10^7 Sf9 cells). Cells expressing the functional ABCG1 exhibited reduced viability as compared to cells expressing ABCG1$_{KM}$, ABCG2, or β-gal. Results are presented as mean±s.e.m. ($n=4$). Asterisks indicate significant difference between the viabilities of cells expressing wtABCG1 or ABCG1$_{KM}$ ($p<0.05$).

expressing wtABCG1 exhibited low accumulation of fluorescent viability markers, MitoTracker and calcein, as compared to their accumulation in cells expressing β-gal, ABCG2, or ABCG1$_{KM}$ (data not shown).

Previously, we demonstrated that the membrane cholesterol content substantially influences the activity of ABCG2 multidrug transporter [40]. Either cholesterol depletion or expression in cholesterol-poor Sf9 cell membrane results in reduced activity of ABCG2. Such a cholesterol-dependence has not been demonstrated for the activity of ABCG1. The significant difference seen between the viability of Sf9 cells expressing wtABCG1 or ABCG1$_{KM}$ indicates that ABCG1 remains active in the cholesterol-poor Sf9 membrane.

To explore whether the ABCG1-induced cell death can also be seen in mammalian cells, we expressed ABCG1 and its inactive variant (ABCG1$_{KM}$) in various cell lines (HEK-293, HepG2, COS-7, and MDCK cells). Mammalian cells transiently transfected with ABCG1 or ABCG1$_{KM}$ were immunostained with our monoclonal antibody specific for ABCG1 (6G1/7), and the morphology of the transfected cells was studied by confocal microscopy. As documented in Fig. 2, expression of wtABCG1 induced changes in cell shape with characteristic 'rounding up' and detachment, whereas cells expressing ABCG1$_{KM}$ exhibited normal cell morphology. In cultures transfected with wtABCG1, a substantial amount of cell debris, stained positively with the anti-ABCG1 monoclonal antibody, was also observed.

For subsequent functional studies we attempted to generate stable cell lines expressing the variants of ABCG1. Since the vectors used for transient transfection contained *neo*-resistance, the HEK-293 cells transfected with ABCG1 or ABCG1$_{KM}$ were subsequently selected with G418 for 10–14 days. Several attempts of generating a stable cell line expressing the wild type ABCG1 have failed, while we were able to obtain cells stably expressing the ABCG1$_{KM}$ mutant regularly. Furthermore, MDCK cells were transduced by retroviruses containing the ABCG1 and ABCG1$_{KM}$ sequences. The expression was frequently checked by Western blot analysis. After a short transient expression the cells lost the wild type protein, whereas cells transduced with the ABCG1$_{KM}$ variant stably expressed the protein (data not shown). These results are consistent with the observations of accelerated cell degradation seen in the ABCG1-transfected Sf9 cells, and implicated that the expression of the wtABCG1 also causes cell death in mammalian cells.

Since the morphological alterations observed in the ABCG1-expressing mammalian cells were indicative of apoptosis, next we examined several apoptotic markers in HEK-293 and HepG2 cells

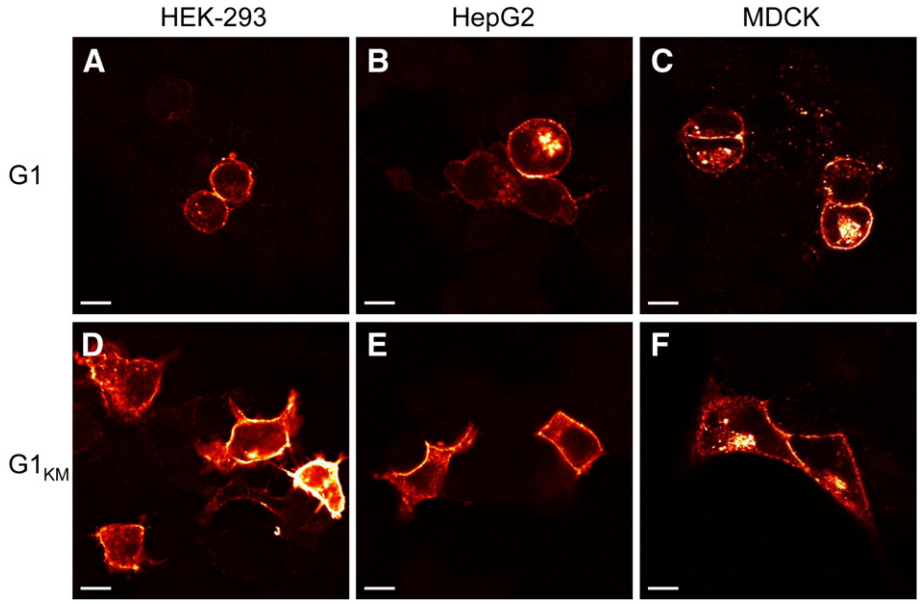

Fig. 2. Morphology changes associated with the functional expression of ABCG1 in various mammalian cells. HEK-293 (A, D), HepG2 (B, E) and MDCK (C, F) cells were transfected with the wild type ABCG1 (A–C) and the inactive mutant $ABCG1_{KM}$ (D–F). The cultures were immunostained with 6G1/7, an ABCG1-specific monoclonal antibody 48 h after transfection. Immunofluorescence was studied by confocal microscopy. Cells expressing the wild type ABCG1 protein were loosely attached and exhibited a 'rounded up' morphology, which is typical for apoptotic cells, whereas cells expressing $ABCG1_{KM}$ exhibited normal cell morphology. The white bars indicate 10 μm.

transiently transfected with wtABCG1 and $ABCG1_{KM}$. Annexin V binding was used to monitor the early apoptotic event of phosphatidyl serine (PS) translocation, while the activity of caspase 3, one of the key enzymes of apoptosis, was visualized by using the cell-permeable, fluorogenic caspase 3 substrate, $PhiPhiLuxG_2D_2$.

We found that the cultures transfected with wtABCG1 contained a large number of cells exhibiting Annexin V binding and elevated caspase 3 activity (Fig. 3A–C). The two apoptotic markers showed mostly overlapping patterns. In contrast, hardly any labeling for PS translocation and caspase 3 activity was seen in cultures transfected with $ABCG1_{KM}$ (Fig. 3D–G). The protein expression was verified by Western blotting in both cases (data not shown). It is important to note that despite caspase 3 and Annexin V positivity observed in the wtABCG1-expressing cells, membrane blebbing, another characteristic feature of apoptotic cells, or the condensation of the nuclei, as visualized by fluorescent nuclear staining, was not typically observed in these cells.

To investigate whether PS translocation is functionally associated with ABCG1 expression, Annexin V binding and ABCG1 expression were simultaneously investigated in HEK-293 and HepG2 cells transfected with wtABCG1 or $ABCG1_{KM}$. Close correlation between Annexin V binding and protein expression was observed in cultures transfected with the wild type protein (Fig. 4A–C). In contrast, no labeling with Annexin V was seen in cultures transfected with

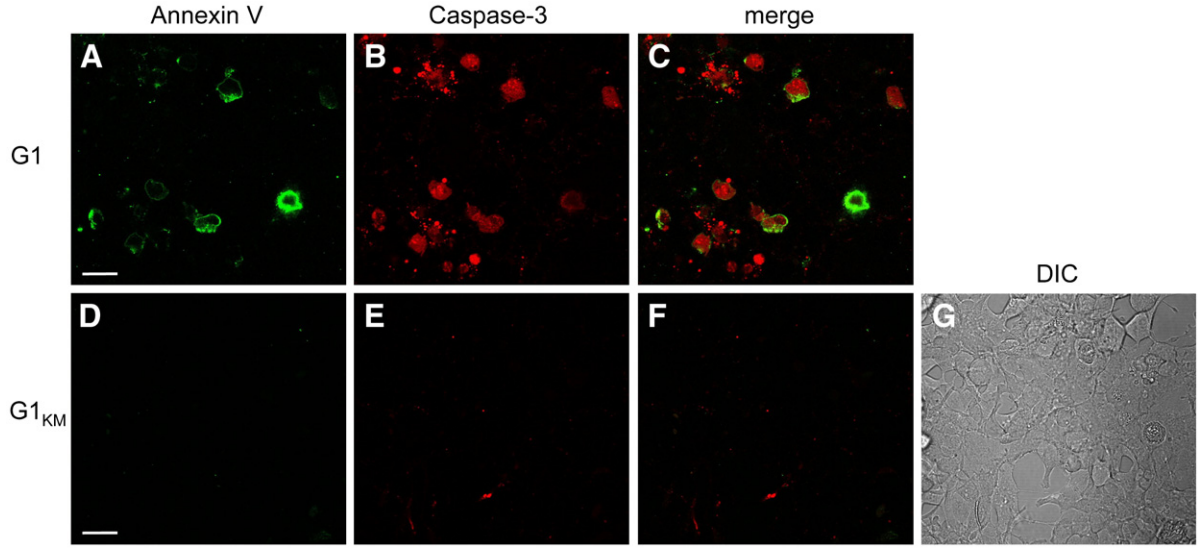

Fig. 3. Apoptotic markers in cell cultures transfected with ABCG1 or $ABCG_{KM}$. Phosphatidyl serine (PS) translocation and caspase 3 activity were assessed in HEK-293 and HepG2 cell transiently transfected with the wild type ABCG1 (A–C) or its inactive variant, $ABCG1_{KM}$ (D–G) 48 h after transfection. Representative experiments performed with HEK-293 cells are shown. PS exposure was visualized by the cell surface labeling of Annexin V conjugated with a green fluorophore (A, D), whereas the activity of caspase 3 was assessed by $PhiPhiLuxG_2D_2$, a cell-permeable caspase 3 substrate, which produces a red fluorescent product upon cleavage (B, E). Merged images are shown on the right (C, F). Substantial portion of cells were positively labeled for both PS translocation and caspase 3 activation in cultures transfected with the wild type protein, whereas hardly any staining was seen in $ABCG1_{KM}$-transfected cultures. The DIC image is to show the presence of the cells in the negatively stained sample. The white bars indicate 30 μm.

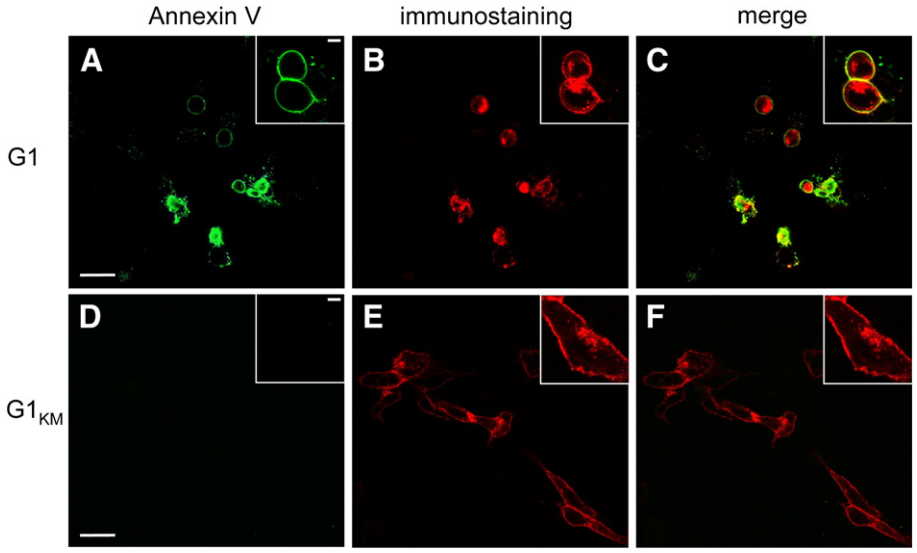

Fig. 4. Simultaneous assessment of phosphatidyl serine translocation and ABCG1 expression in cells cultures transfected with ABCG1 or $ABCG_{KM}$. HEK-293 and HepG2 cells transfected with ABCG1 (A–C) or $ABCG1_{KM}$ (D–F) were labeled with Alexa Fluor 488-conjugated Annexin V 48 h after transfection. The samples were subsequently fixed and immunostained with the ABCG1-specific monoclonal antibody, 6G1/7. Results obtained with HepG2 cells are shown. Annexin V binding (A, D) is depicted on the left, middle panels show the immunostaining (B, E), whereas merged images are shown on the right (C, F). In the ABCG1-transfected cultures, Annexin V binding was observed only in cells expressing ABCG1. In contrast, no labeling with Annexin V was seen in cultures transfected with $ABCG1_{KM}$, although the protein was expressed and localized normally. Similar results were obtained with HEK-293 cells. The white bars indicate 30 μm. Insets show a representative cell from the same field at higher magnification; bars: 5 μm.

$ABCG1_{KM}$ (Fig. 4D–F). The latter experiment also demonstrates that the mutant protein was expressed both on the cell surface and within intracellular compartments, similar to the wild type protein. It is important to note that apoptotic signs were only observed in cells expressing the ABCG1 protein (see Discussion).

The observation that the expression of the wild type ABCG1 resulted in morphological and functional alterations typical for apoptosis, whereas the inactive, catalytic site mutant variant exhibited no sign of apoptosis, suggested that the apoptotic events are related to the activity of the transporter. For exploring this question, in the subsequent experiments we employed thyroxin and benzamil, which were identified as efficient inhibitors of the ABCG1 ATPase activity in previous studies [15]. The quantitative analysis of Annexin V binding in ABCG1-transfected HEK-293 and HepG2 cells shown in Fig. 5 verified that the cultures transfected with the wild type ABCG1 contain significantly more Annexin V positive cells as compared to cultures transfected with the empty vector. However, preincubation of the cells either with thyroxin or benzamil completely blocked the ABCG1-induced apoptosis. Annexin V binding in $ABCG1_{KM}$-transfected cells was not different from the vector control, and was not affected by thyroxin or benzamil pretreatment.

For a comparison of the fraction of Annexin V positive cells in HEK-293 and HepG2 cell cultures, the values ought to be corrected by the transfection efficacy, which was about 30% in HEK-293 cells and 15% in

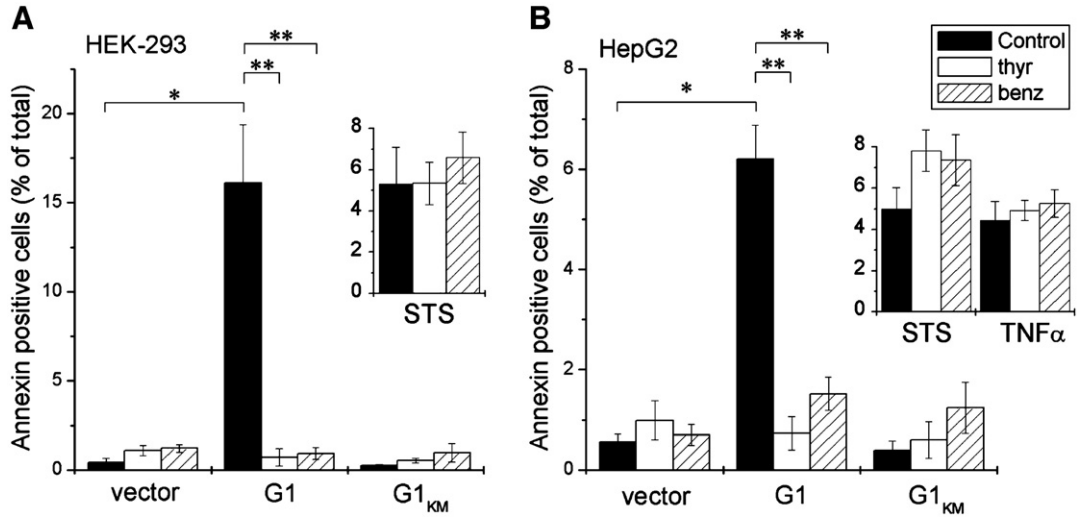

Fig. 5. Inhibition of phosphatidyl serine translocation in ABCG1-expressing cells with the inhibitors of ABCG1 function. The fraction of apoptotic cells was determined in HEK-293 (A) and HepG2 (B) cell cultures transfected with the empty vector, ABCG1 or $ABCG1_{KM}$. For quantitative analysis, the Annexin V-labeled cells were counted in the confocal fluorescence image, the total cell number was determined in the corresponding DIC image. Results are expressed as positively stained cells as percentage of total cell number. Between 1000 and 3000 cells were analyzed for each column in at least three independent experiments. Results are presented as mean ± s.e.m. The transfection efficiency for HEK-293 and HepG2 cells were 29.2 ± 3.5 and 12.1 ± 1.2, respectively. Significantly elevated number of apoptotic cells was seen in cultures transfected with wild type ABCG1 as compared to cultures transfected with the vector or $ABCG1_{KM}$ (black bars) (*, $p<0.001$ by Student's *t*-test). Preincubation with the previously identified inhibitors of ABCG1 function, thyroxin (thyr, white bars) and benzamil (benz, hatched bars), completely prevented PS translocation in the ABCG1-expressing cells (**, $p<0.001$ by Student's *t*-test). These compounds had no effect on Annexin V binding in cells transfected with the empty vector or $ABCG1_{KM}$, neither in cultures, in which apoptosis was induced by staurosporine (STS) or TNFα (see insets).

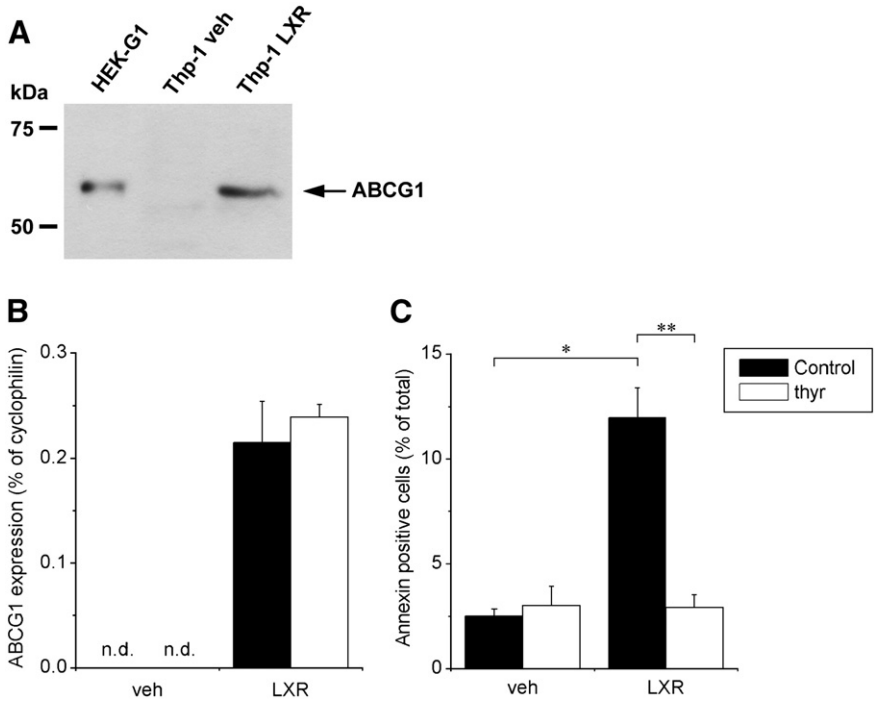

Fig. 6. Induction of ABCG1 expression in Thp-1 cells by LXR agonist; assessment of apoptosis in the LXR-induced Thp-1 cells. PMA-pretreated Thp-1 cells were subjected to 1 μM T0901317, an LXR agonist, and expression of endogenous ABCG1 expression was detected by Western blotting (A) and quantitative PCR (B). Western blot analysis was performed with total cell lysates (50 μg protein) using 6G1/7, ABCG1-specific antibody. As a positive control, HEK-293 cells transfected with ABCG1 (5 μg protein) was used. Considerable elevation in the ABCG1 expression was observed at both mRNA and protein levels in response to the LXR agonist. Quantitative Annexin V binding experiments were performed with PMA-pretreated Thp-1 cells (C) as described in detail in the legend of Fig. 5. In parallel with the induction of ABCG1 expression, T0901317 significantly increased the number of apoptotic cells (black bars). This elevation was completely inhibited by the pretreatment with 100 μM thyroxin (thyr), a blocker of ABCG1 function (C, white bars), without any effect on the expression level of the transporter (B, white bar). Results are expressed as mean ± s.e.m. Asterisks indicate significant differences: *, when compared with vehicle control; **, when compared with cells not-pretreated with thyroxin by Student's *t*-test ($p<0.005$). n.d.: not detected.

HepG2 cells, respectively. Thus, about 50% of the transfected cells exhibited Annexin V labeling at the examined time point, i.e., 48 h after transfection. In order to demonstrate the relative specificity of the effect of thyroxin and benzamil on ABCG1-induced apoptosis, in parallel experiments apoptosis was induced by staurosporine both in HEK-293 and HepG2 cells. As shown in Fig. 5, the fraction of Annexin positive cells in the staurosporine-treated cultures was not reduced by the ABCG1 inhibitors. Similarly, Annexin V binding in TNFα-induced HepG2 cells was not affected by the pretreatment with thyroxin or benzamil.

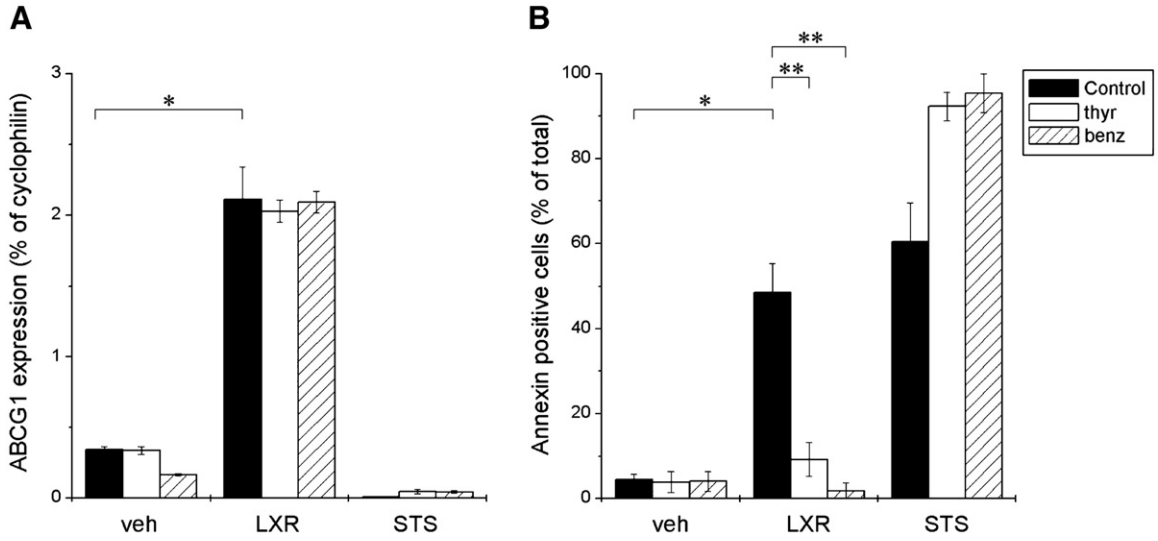

Fig. 7. Parallel induction of ABCG1 expression and apoptosis in human monocyte-derived macrophages and inhibition of apoptosis with the ABCG1 inhibitors. Human monocyte-derived macrophages were obtained from peripheral blood by CD14 immunoisolation. After 5 days of culturing, the cells were incubated with 1 μM T0901317, and the expression level of ABCG1 was measured by quantitative PCR (A). In parallel the fraction of apoptotic cells was determined by Annexin V binding (B). Both ABCG1 expression level and number of apoptotic cells were significantly increased in response to LXR activation (black bars). Preincubation with 100 μM thyroxin (thyr, white bars) or 50 μM benzamil (benz, hatched bars), prevented PS translocation in the LXR-ligand-induced cells, without any effect on ABCG1 expression. To exclude a non-specific effect of thyroxin and benzamil on the Annexin V binding, in control experiments apoptosis was induced in the monocyte-derived macrophages by staurosporine (STS) pretreatment. These compounds did not block Annexin V binding in the STS-induced apoptotic cells. ABCG1 expression was not induced by staurosporine (A). Results are expressed as mean ± s.e.m ($n=4$). Asterisks indicate significant differences: *, when compared with vehicle control; **, when compared with non-treated cells by Student's *t*-test ($p<0.001$).

In order to explore whether the ABCG1-induced apoptosis is solely a consequence of forced expression of the transporter, or the phenomenon also occurs in cell types that endogenously express ABCG1, we investigated Annexin V binding in PMA-pretreated human Thp-1 cells (a macrophage model system), and in isolated human monocyte-derived macrophages. The endogenous ABCG1 expression in these cell types was induced by T0901317, a known activator of LXR, the nuclear receptor that regulates *ABCG1* gene [26,27].

As shown in Fig. 6, in Thp-1 cells the expression level of ABCG1 was studied by both quantitative PCR and Western blotting and, in parallel, the fraction of apoptotic cells was determined by Annexin V binding. As expected, a marked induction in the ABCG1 expression was seen in response to LXR activation (Fig. 6A, B). In parallel, hardly any Annexin V positivity was seen in the control cells, which were treated with the vehicle only, whereas substantial Annexin V labeling was observed in the LXR-induced cultures (Fig. 6C). Similar to that seen in the ABCG1-transfected cell lines, preincubation with thyroxin prevented Annexin V labeling in the LXR-ligand-induced Thp-1 cells.

In similar experiments, carried out with monocyte-derived human macrophages, a substantial induction of ABCG1 expression and a subsequent elevation of the fraction of apoptotic cells were seen in response to LXR agonist (Fig. 7). Preincubation with thyroxin and benzamil completely blocked Annexin V labeling in the LXR-ligand-induced macrophages without affecting the ABCG1 expression. These observations indicate that the PS translocation in the LXR-induced macrophages depends on the functional presence of ABCG1 protein. To exclude a non-specific effect of thyroxin and benzamil on Annexin V binding, apoptosis was also induced by staurosporine in these cells. As shown in Fig. 7, the expression of ABCG1 was not elevated by staurosporine, and the marked Annexin V binding observed in the staurosporine-induced cells was not reduced by thyroxin or benzamil pretreatment (rather a small increase was detected).

4. Discussion

In order to explore the functional role of the human ABCG1 membrane transporter protein, in the present experiments we explored the effects of ABCG1 expression in numerous cell types, including human macrophages involved in atherosclerosis development. Previous studies suggested that overexpression of ABCG1 causes an increase in cholesterol efflux from cells to HDL and other lipid acceptors [16,17,28–31]. In addition to such a possible role, our present experiments suggest another cellular function for ABCG1, and may offer new insights into the function of this transporter protein.

Here we demonstrate that ABCG1 functionally contributes to apoptotic events in various cell types, the function of the over-expressed protein is closely connected to cell death, activation of caspase 3, and PS translocation. We show that physiological ABCG1 expression, induced by the addition of a synthetic LXR agonist in monocyte-derived macrophages or PMA-treated Thp-1 cells, also results in a substantial increase in phosphatidyl serine surface exposure. In all cases the function of ABCG1 is required to evoke these apoptotic signs.

Several previous studies demonstrated an induction of ABCG1 expression in macrophages in response to cholesterol loading [22,23,41], whereas other studies showed PS translocation in macrophages induced by cholesterol [42,43]. However, the causative connection between ABCG1 and apoptotic events was documented in our present study by the effects of ABCG1 inhibitors on PS exposure. In addition, the fact that the ABCG1-transfected cells exhibited PS surface exposure, whereas this was not observed in cells transfected with the inactive ABCG1 variant ($ABCG1_{KM}$), clearly indicates an association between the PS translocation and the transport activity of ABCG1.

A distant relative of ABCG1 in the ABC protein family, MDR3 (ABCB4) is known as a phosphatidyl choline (PC) floppase, translocating PC from the inner membrane leaflet to the outer leaflet. Based on this homology, we may hypothesize that ABCG1 acts as a PS translocator. However, PS surface exposure in the ABCG1-expressing cells is most likely not a consequence of direct floppase activity, but a component of a concerted apoptotic process, since caspase 3 activation as well as accelerated cell death were observed in cells expressing the wild type ABCG1. None of these apoptotic events was seen in cells expressing the inactive, catalytic site mutant variant of ABCG1 ($ABCG1_{KM}$), although the expression level and the subcellular localization of the mutant form was similar to those of the wild type protein. Therefore, our results imply a functional association between macrophage apoptosis and ABCG1 transport activity.

Numerous studies reported collateral sensitivity to certain compounds along with the overexpression of ABCB1 (MDR1/Pgp) or ABCC1 (MRP1). These drugs exemplified by gemcitabine, cytosine arabinoside, arsenic trioxide, and NSC73306 for ABCB1 [44–47], as well as verapamil, its derivative, $NMeOHI_2$, cytosine arabinoside, melphalan, apigenin, and buthionine sulphoximine for ABCC1 [48–51]. Although the mechanism behind this collateral sensitivity is still elusive, it has been suggested that at least in ABCC1-expressing cells the decreased glutathione level content and the subsequent oxidative stress account for the hypersensitivity to drugs causing further reduction in glutathione content. Since in our study no exogenous drug was added to the cells, some endogenous component(s) can be responsible for the ABCG1-promoted cell death.

There are several factors that are known to induce apoptosis in macrophages. These include ATP depletion, binding of death receptors ligands, growth factor withdrawal, high concentration of oxidized LDL, oxysterols, and intracellular accumulation of unesterified or “free” cholesterol [2,42,43,52]. In addition to their apoptotic effect, these agents are also known to induce ABCG1 expression in macrophages [22,23,27,41,53], which is in accordance with our present results.

Regarding the ABCG1-dependent apoptosis found in this study, several possibilities can be excluded from the list of the aforementioned pro-apoptotic factors. ATP depletion cannot account for the ABCG1-dependent apoptosis, since overexpression of a closely related ABC transporter, ABCG2, which possesses higher ATPase activity, does not result in PS translocation, caspase 3 activation, and subsequent cell death (see Fig. 1). The involvement of death receptors is also unlikely, since TNFα-induced apoptosis was not blocked by the inhibitors of ABCG1.

A possible explanation for the mechanism of ABCG1-dependent apoptosis could be that the transporter may act as an export pump, and mediate the excretion of certain cytotoxic compounds to the media, which cause apoptosis in the adjacent cells. Recently, it has been suggested that 7β-hydroxycholesterol or 7-ketocholesterol is expelled from cells by ABCG1 [54,55]. In order to explore this possibility, we examined whether the apoptotic effect of ABCG1 is restricted to the cell that expresses the transporter or a paracrin effect can be seen on the adjacent cells. As shown in Fig. 4B, PS translocation was observed solely in ABCG1-expressing cells, and no signs of apoptosis can be seen in the neighboring cells. In addition, we co-cultured GFP-expressing cells with ABCG1-transfected cells, but no apoptotic GFP-expressing cells adjacent to the ABCG1-expressing cells were seen (data not shown). Based on these experimental observations the paracrin model seems to be unlikely.

As mentioned above, intracellular accumulation of unesterified or free cholesterol is one of the apoptotic inducers in lesional macrophages. It has been demonstrated that free cholesterol-induced apoptosis is a multifactorial process, which involves ER stress caused by free cholesterol trafficking to ER, which, in turn, results in unfolded protein response (UPR), and activation of the C/EBP homologous protein (CHOP) [56–58]. Other cellular events that greatly influence free cholesterol-induced macrophage apoptosis include activation of c-Jun N-terminal kinase (JNK), biding of scavenger receptor A (SRA)

ligands, cellular calcium perturbation, and activation of group VIA phospholipase A_2 (iPLA$_2\beta$) [57–60]. The requirement of cholesterol trafficking to the ER is demonstrated by the inhibitory effect of selective blockers of cholesterol trafficking [56,61], and by the reduced macrophage apoptosis in advanced lesion in mice with a heterozygous mutation in the cholesterol-trafficking protein Niemann-Pick C1 [62]. Given that ABCG1 is likely involved in cholesterol transport and it exhibits both cell surface and intracellular expression [14,16,17,36,63], we can speculate that elevated expression of this transporter results in ER stress, which in turn, leads to apoptosis. This hypothesis presumes that the transport activity of ABCG1 surpasses the cholesterol esterification capacity of the cell, which results in accumulation of free cholesterol in the ER. However, this speculative model needs to be investigated and experimentally justified.

At present the most widely accepted concept for the physiological function of ABCG1 is that this transporter expels cholesterol from macrophages and other cell types to HDL. It is a plausible explanation for the ABCG1-induced apoptosis that the observed cell death is a consequence of the cholesterol efflux associated with the functional ABCG1, since neither the ABCG1$_{KM}$- nor the ABCG2-expressing cells exhibited this phenotype. Although it was previously suggested that ABCG2 stimulates cellular efflux of sterols including cholesterol [64], this hypothesis was based on the observation that sterols stimulate the ATPase activity of ABCG2 expressed in bacterial membrane lacking cholesterol. To our recent understanding ABCG2 does not expel cholesterol but its ATPase activity is allosterically stimulated by cholesterol [40]. Nevertheless, cholesterol depletion itself did not significantly increase the number of apoptotic cells in HEK-293 culture pretreatment with 4 mM cyclodextrin for 30 min, despite the fact that about 25% decrease in total cholesterol content was achieved with this treatment (data not shown).

The hypothesis that ABCG1 extrudes cellular cholesterol to HDL is based on numerous in vitro and in vivo studies demonstrating cellular cholesterol efflux in connection with ABCG1 expression [14,16,17,28–32,36,55]. However, the specificity of this transport process is questioned by the fact that similar ABCG1-mediated cholesterol efflux was seen to various lipid acceptors, such as LDL, PC vesicles, PC/ApoA-I discs, even BSA and cyclodextrin [14,16,31,36]. The observation that Ldr −/− mice transplanted with ABCG1 −/− bone marrow exhibited reduced cholesterol level in lipoproteins other than HDL [55], makes the specific role of HDL in ABCG-mediated cholesterol efflux even more tentative. Our recent finding, that ABCG1 promotes macrophage apoptosis, provides an alternative explanation for the non-specific cholesterol efflux in connection with ABCG1 expression. Our observation suggests that cholesterol efflux can be a consequence of cell death induced by ABCG1. This model is also consistent with the suggested protective role of ABCG1 in the atherogenesis [38,65].

Another concern that adds complexity to the issue of ABCG1-dependent apoptosis is that two recent studies suggested that ABCG1 diminishes the apoptotic effect of 7β-hydroxycholesterol or 7-ketocholesterol on macrophages [54,55]. This apparent contradiction can be resolved if we take into consideration that these studies demonstrated increased susceptibility to exogenously added cytotoxic compounds when ABCG1 was defective (either by using an inactive mutant form, or cells from ABCG1 knockout animals), whereas our study is based on endogenous transport activity of ABCG1. Since the externally added oxysterols at low concentrations can act as competitive inhibitors of the endogenous substrate(s), addition of these compounds can result in a decreased cell death in cells possessing active ABCG1. In accordance with this concept, only a slight and transient change in the dose–response relations was seen in connection with ABCG1 in the aforementioned studies [54,55]. An alternative explanation for the notion that ABCG1 can act both as an inducer and inhibitor of macrophage apoptosis is that the transporter may play different roles, depending on its subcellular localization. When the transporter is located in the plasma membrane, it can expel cytotoxic compounds from the cell, whereas it can stimulate apoptosis, when located in the internal membranes, e.g., can induce an ER stress.

Whether ABCG1-dependent apoptosis of macrophages has a physiological and clinical relevance, our findings should be evaluated in the context of studies in animal model systems of atherosclerosis. These studies demonstrated an inverse relationship between macrophage apoptosis and the early lesion area, and concluded that macrophage apoptosis is physiologically beneficial in the early atherosclerotic lesions [2,3,66–69]. In contrast, loss of macrophages becomes detrimental in the advanced lesions, where phagocytic activity becomes limiting [2,3,10,11]. With respect to the role of ABCG1 in atherogenesis, recent in vivo studies have led to contradicting results, demonstrating either an increase or a reduction in lesion size in mice transplanted with ABCG1-deficient bone marrow [70–75]. It has been hypothesized by L. K. Curtiss in an editorial [76] that the different degree of hyperlipidemia achieved in the recipient animals, and consequently the different progression rate of atherosclerosis can account for these conflicting results. Our recent finding, the phenomenon of ABCG1-promoted apoptosis, is in accordance with this hypothesis, and can reconcile the disparate results of ABCG1 transplantation studies. Since macrophage apoptosis can be both atherogenic and atheroprotective, ABCG1, which may be involved in the apoptotic processes, can also have a dual role in the pathogenesis of atherosclerosis, depending on the progression of atherosclerosis.

Although the above discussion focused on macrophage apoptosis, the ABCG1-promoted apoptosis described here might have a role in other cells types as well, in which this transporter is expressed in an inducible manner. These include vascular endothelial cells, astrocytes, microglia, and neuronal cells [28,63,77–81]. Given that apoptotic cell death has a crucial role in neuroprotection and normal vascular function, it is an intriguing possibility that ABCG1 expression and function contributes to apoptotic processes in these tissues.

Acknowledgements

This work was supported by the research grants from OTKA (K68936, F48986), ETT (557/2006), and NKFP (1A/005/2004). N. Barry Elkind was a recipient of a Young Investigator Fellowship from the Hungarian Academy of Sciences. László Homolya was an EMBO-HHMI Young Scientist. We appreciate the technical help of Gyöngyi Bézsenyi and Judit Kis. We are thankful for the valuable advice of Éva Karászi, András Váradi, and Gergely Szakács.

References

[1] J.F. Kerr, A.H. Wyllie, A.R. Currie, Apoptosis: a basic biological phenomenon with wide-ranging implications in tissue kinetics, Br. J. Cancer 26 (1972) 239–257.
[2] I. Tabas, Consequences and therapeutic implications of macrophage apoptosis in atherosclerosis: the importance of lesion stage and phagocytic efficiency, Arterioscler Thromb. Vasc. Biol. 25 (2005) 2255–2264.
[3] M.M. Kockx, A.G. Herman, Apoptosis in atherosclerosis: beneficial or detrimental? Cardiovasc. Res. 45 (2000) 736–746.
[4] Y.J. Geng, P. Libby, Progression of atheroma: a struggle between death and procreation, Arterioscler Thromb. Vasc. Biol. 22 (2002) 1370–1380.
[5] T. Bombeli, A. Karsan, J.F. Tait, J.M. Harlan, Apoptotic vascular endothelial cells become procoagulant, Blood 89 (1997) 2429–2442.
[6] P.D. Flynn, C.D. Byrne, T.P. Baglin, P.L. Weissberg, M.R. Bennett, Thrombin generation by apoptotic vascular smooth muscle cells, Blood 89 (1997) 4378–4384.
[7] M.M. Kockx, G.R. De Meyer, J. Muhring, W. Jacob, H. Bult, A.G. Herman, Apoptosis and related proteins in different stages of human atherosclerotic plaques, Circulation 97 (1998) 2307–2315.
[8] P. Libby, Y.J. Geng, M. Aikawa, U. Schoenbeck, F. Mach, S.K. Clinton, G.K. Sukhova, R.T. Lee, Macrophages and atherosclerotic plaque stability, Curr. Opin. Lipidol. 7 (1996) 330–335.
[9] Z.S. Galis, G.K. Sukhova, M.W. Lark, P. Libby, Increased expression of matrix metalloproteinases and matrix degrading activity in vulnerable regions of human atherosclerotic plaques, J. Clin. Invest. 94 (1994) 2493–2503.

[10] D.M. Schrijvers, G.R. De Meyer, M.M. Kockx, A.G. Herman, W. Martinet, Phagocytosis of apoptotic cells by macrophages is impaired in atherosclerosis, Arterioscler Thromb. Vasc. Biol. 25 (2005) 1256–1261.
[11] D.M. Schrijvers, G.R. De Meyer, A.G. Herman, W. Martinet, Phagocytosis in atherosclerosis: molecular mechanisms and implications for plaque progression and stability, Cardiovasc. Res. 73 (2007) 470–480.
[12] Z. Mallat, B. Hugel, J. Ohan, G. Leseche, J.M. Freyssinet, A. Tedgui, Shed membrane microparticles with procoagulant potential in human atherosclerotic plaques: a role for apoptosis in plaque thrombogenicity, Circulation 99 (1999) 348–353.
[13] E.W. Greeno, R.R. Bach, C.F. Moldow, Apoptosis is associated with increased cell surface tissue factor procoagulant activity, Lab. Invest. 75 (1996) 281–289.
[14] A. Kobayashi, Y. Takanezawa, T. Hirata, Y. Shimizu, K. Misasa, N. Kioka, H. Arai, K. Ueda, M. Matsuo, Efflux of sphingomyelin, cholesterol, and phosphatidylcholine by ABCG1, J. Lipid Res. 47 (2006) 1791–1802.
[15] J. Cserepes, Z. Szentpetery, L. Seres, C. Ozvegy-Laczka, T. Langmann, G. Schmitz, H. Glavinas, I. Klein, L. Homolya, A. Varadi, B. Sarkadi, N.B. Elkind, Functional expression and characterization of the human ABCG1 and ABCG4 proteins: indications for heterodimerization, Biochem. Biophys. Res. Commun. 320 (2004) 860–867.
[16] N. Wang, M. Ranalletta, F. Matsuura, F. Peng, A.R. Tall, LXR-induced redistribution of ABCG1 to plasma membrane in macrophages enhances cholesterol mass efflux to HDL, Arterioscler Thromb. Vasc. Biol. 26 (2006) 1310–1316.
[17] A.M. Vaughan, J.F. Oram, ABCG1 redistributes cell cholesterol to domains removable by high density lipoprotein but not by lipid-depleted apolipoproteins, J. Biol. Chem. 280 (2005) 30150–30157.
[18] Q. Xie, T. Engel, M. Schnoor, J. Niehaus, O. Hofnagel, I. Buers, P. Cullen, U. Seedorf, G. Assmann, S. Lorkowski, Cell surface localization of ABCG1 does not require LXR activation, Arterioscler. Thromb. Vasc. Biol. 26 (2006) e143–e144. author reply e145.
[19] M. Nakamura, S. Ueno, A. Sano, H. Tanabe, Polymorphisms of the human homologue of the Drosophila white gene are associated with mood and panic disorders, Mol. Psychiatry 4 (1999) 155–162.
[20] J.M. Croop, G.E. Tiller, J.A. Fletcher, M.L. Lux, E. Raab, D. Goldenson, D. Son, S. Arciniegas, R.L. Wu, Isolation and characterization of a mammalian homolog of the *Drosophila* white gene, Gene 185 (1997) 77–85.
[21] G. Kirov, C.A. Lowry, M. Stephens, S. Oldfield, M.C. O'Donovan, S.L. Lightman, M.J. Owen, Screening ABCG1, the human homologue of the *Drosophila* white gene, for polymorphisms and association with bipolar affective disorder, Mol. Psychiatry 6 (2001) 671–677.
[22] J. Klucken, C. Buchler, E. Orso, W.E. Kaminski, M. Porsch-Ozcurumez, G. Liebisch, M. Kapinsky, W. Diederich, W. Drobnik, M. Dean, R. Allikmets, G. Schmitz, ABCG1 (ABC8), the human homolog of the *Drosophila* white gene, is a regulator of macrophage cholesterol and phospholipid transport, Proc. Natl. Acad. Sci. U. S. A. 97 (2000) 817–822.
[23] A. Venkateswaran, J.J. Repa, J.M. Lobaccaro, A. Bronson, D.J. Mangelsdorf, P.A. Edwards, Human white/murine ABC8 mRNA levels are highly induced in lipid-loaded macrophages. A transcriptional role for specific oxysterols, J. Biol. Chem. 275 (2000) 14700–14707.
[24] A. Baldan, P. Tarr, R. Lee, P.A. Edwards, ATP-binding cassette transporter G1 and lipid homeostasis, Curr. Opin. Lipidol. 17 (2006) 227–232.
[25] A.C. Li, C.J. Binder, A. Gutierrez, K.K. Brown, C.R. Plotkin, J.W. Pattison, A.F. Valledor, R.A. Davis, T.M. Willson, J.L. Witztum, W. Palinski, C.K. Glass, Differential inhibition of macrophage foam-cell formation and atherosclerosis in mice by PPARalpha, beta/delta, and gamma, J. Clin. Invest. 114 (2004) 1564–1576.
[26] M.A. Kennedy, A. Venkateswaran, P.T. Tarr, I. Xenarios, J. Kudoh, N. Shimizu, P.A. Edwards, Characterization of the human ABCG1 gene: liver X receptor activates an internal promoter that produces a novel transcript encoding an alternative form of the protein, J. Biol. Chem. 276 (2001) 39438–39447.
[27] B.A. Laffitte, J.J. Repa, S.B. Joseph, D.C. Wilpitz, H.R. Kast, D.J. Mangelsdorf, P. Tontonoz, LXRs control lipid-inducible expression of the apolipoprotein E gene in macrophages and adipocytes, Proc. Natl. Acad. Sci. U. S. A. 98 (2001) 507–512.
[28] K. Nakamura, M.A. Kennedy, A. Baldan, D.D. Bojanic, K. Lyons, P.A. Edwards, Expression and regulation of multiple murine ATP-binding cassette transporter G1 mRNAs/isoforms that stimulate cellular cholesterol efflux to high density lipoprotein, J. Biol. Chem. 279 (2004) 45980–45989.
[29] M.A. Kennedy, G.C. Barrera, K. Nakamura, A. Baldan, P. Tarr, M.C. Fishbein, J. Frank, O.L. Francone, P.A. Edwards, ABCG1 has a critical role in mediating cholesterol efflux to HDL and preventing cellular lipid accumulation, Cell. Metab. 1 (2005) 121–131.
[30] A.M. Vaughan, J.F. Oram, ABCA1 and ABCG1 or ABCG4 act sequentially to remove cellular cholesterol and generate cholesterol-rich HDL, J. Lipid. Res. 47 (2006) 2433–2443.
[31] N. Wang, D. Lan, W. Chen, F. Matsuura, A.R. Tall, ATP-binding cassette transporters G1 and G4 mediate cellular cholesterol efflux to high-density lipoproteins, Proc. Natl. Acad. Sci. U. S. A. 101 (2004) 9774–9779.
[32] X. Wang, H.L. Collins, M. Ranalletta, I.V. Fuki, J.T. Billheimer, G.H. Rothblat, A.R. Tall, D.J. Rader, Macrophage ABCA1 and ABCG1, but not SR-BI, promote macrophage reverse cholesterol transport in vivo, J. Clin. Invest. 117 (2007) 2216–2224.
[33] J.F. Oram, A.M. Vaughan, ABCA1-mediated transport of cellular cholesterol and phospholipids to HDL apolipoproteins, Curr. Opin. Lipidol. 11 (2000) 253–260.
[34] R.M. Lawn, D.P. Wade, M.R. Garvin, X. Wang, K. Schwartz, J.G. Porter, J.J. Seilhamer, A.M. Vaughan, J.F. Oram, The Tangier disease gene product ABC1 controls the cellular apolipoprotein-mediated lipid removal pathway, J. Clin. Invest. 104 (1999) R25–R31.
[35] N. Wang, A.R. Tall, Regulation and mechanisms of ATP-binding cassette transporter A1-mediated cellular cholesterol efflux, Arterioscler. Thromb. Vasc. Biol. 23 (2003) 1178–1184.
[36] I.C. Gelissen, M. Harris, K.A. Rye, C. Quinn, A.J. Brown, M. Kockx, S. Cartland, M. Packianathan, L. Kritharides, W. Jessup, ABCA1 and ABCG1 synergize to mediate cholesterol export to apoA-I, Arterioscler. Thromb. Vasc. Biol. 26 (2006) 534–540.
[37] W. Jessup, I.C. Gelissen, K. Gaus, L. Kritharides, Roles of ATP binding cassette transporters A1 and G1, scavenger receptor BI and membrane lipid domains in cholesterol export from macrophages, Curr. Opin. Lipidol. 17 (2006) 247–257.
[38] J.F. Oram, A.M. Vaughan, ATP-binding cassette cholesterol transporters and cardiovascular disease, Circ. Res. 99 (2006) 1031–1043.
[39] B. Sarkadi, E.M. Price, R.C. Boucher, U.A. Germann, G.A. Scarborough, Expression of the human multidrug resistance cDNA in insect cells generates a high activity drug-stimulated membrane ATPase, J. Biol. Chem. 267 (1992) 4854–4858.
[40] A. Telbisz, M. Muller, C. Ozvegy-Laczka, L. Homolya, L. Szente, A. Varadi, B. Sarkadi, Membrane cholesterol selectively modulates the activity of the human ABCG2 multidrug transporter, Biochim. Biophys. Acta 1768 (2007) 2698–2713.
[41] X. Fu, J.G. Menke, Y. Chen, G. Zhou, K.L. MacNaul, S.D. Wright, C.P. Sparrow, E.G. Lund, 27-hydroxycholesterol is an endogenous ligand for liver X receptor in cholesterol-loaded cells, J. Biol. Chem. 276 (2001) 38378–38387.
[42] M.L. Liu, M.P. Reilly, P. Casasanto, S.E. McKenzie, K.J. Williams, Cholesterol enrichment of human monocyte/macrophages induces surface exposure of phosphatidylserine and the release of biologically-active tissue factor-positive microvesicles, Arterioscler. Thromb. Vasc. Biol. 27 (2007) 430–435.
[43] P.M. Yao, I. Tabas, Free cholesterol loading of macrophages induces apoptosis involving the fas pathway, J. Biol. Chem. 275 (2000) 23807–23813.
[44] G. Szakacs, J.P. Annereau, S. Lababidi, U. Shankavaram, A. Arciello, K.J. Bussey, W. Reinhold, Y. Guo, G.D. Kruh, M. Reimers, J.N. Weinstein, M.M. Gottesman, Predicting drug sensitivity and resistance: profiling ABC transporter genes in cancer cells, Cancer Cell. 6 (2004) 129–137.
[45] A.M. Bergman, B. Munch-Petersen, P.B. Jensen, M. Sehested, G. Veerman, D.A. Voorn, K. Smid, H.M. Pinedo, G.J. Peters, Collateral sensitivity to gemcitabine (2′,2′-difluorodeoxycytidine) and cytosine arabinoside of daunorubicin- and VM-26-resistant variants of human small cell lung cancer cell lines, Biochem. Pharmacol. 61 (2001) 1401–1408.
[46] S. Martin-Aragon, S.K. Mukherjee, B.J. Taylor, S.P. Ivy, C.H. Fu, V.C. Ardi, V.I. Avramis, Cytosine arabinoside (ara-C) resistance confers cross-resistance or collateral sensitivity to other classes of anti-leukemic drugs, Anticancer Res. 20 (2000) 139–150.
[47] T. Seo, Y. Urasaki, H. Takemura, T. Ueda, Arsenic trioxide circumvents multidrug resistance based on different mechanisms in human leukemia cell lines, Anticancer Res. 25 (2005) 991–998.
[48] D. Trompier, X.B. Chang, R. Barattin, A. du Moulinet D'Hardemare, A. Di Pietro, H. Baubichon-Cortay, Verapamil and its derivative trigger apoptosis through glutathione extrusion by multidrug resistance protein MRP1, Cancer Res. 64 (2004) 4950–4956.
[49] K. Jonsson-Videsater, G. Andersson, J. Bergh, C. Paul, Doxorubicin-resistant, MRP1-expressing U-1285 cells are sensitive to idarubicin, Ther. Drug Monit. 25 (2003) 331–339.
[50] A.M. Bergman, H.M. Pinedo, I. Talianidis, G. Veerman, W.J. Loves, C.L. van der Wilt, G.J. Peters, Increased sensitivity to gemcitabine of P-glycoprotein and multidrug resistance-associated protein-overexpressing human cancer cell lines, Br. J. Cancer 88 (2003) 1963–1970.
[51] R.M. Laberge, J. Karwatsky, M.C. Lincoln, M.L. Leimanis, E. Georges, Modulation of GSH levels in ABCC1 expressing tumor cells triggers apoptosis through oxidative stress, Biochem. Pharmacol. 73 (2007) 1727–1737.
[52] R. Salvayre, N. Auge, H. Benoist, A. Negre-Salvayre, Oxidized low-density lipoprotein-induced apoptosis, Biochim. Biophys. Acta 1585 (2002) 213–221.
[53] A. Venkateswaran, B.A. Laffitte, S.B. Joseph, P.A. Mak, D.C. Wilpitz, P.A. Edwards, P. Tontonoz, Control of cellular cholesterol efflux by the nuclear oxysterol receptor LXR alpha, Proc. Natl. Acad. Sci. U. S. A. 97 (2000) 12097–12102.
[54] T. Engel, F. Kannenberg, M. Fobker, J.R. Nofer, G. Bode, A. Lueken, G. Assmann, U. Seedorf, Expression of ATP binding cassette-transporter ABCG1 prevents cell death by transporting cytotoxic 7beta-hydroxycholesterol, FEBS Lett. 581 (2007) 1673–1680.
[55] N. Terasaka, N. Wang, L. Yvan-Charvet, A.R. Tall, High-density lipoprotein protects macrophages from oxidized low-density lipoprotein-induced apoptosis by promoting efflux of 7-ketocholesterol via ABCG1, Proc. Natl. Acad. Sci. U. S. A. 104 (2007) 15093–15098.
[56] B. Feng, P.M. Yao, Y. Li, C.M. Devlin, D. Zhang, H.P. Harding, M. Sweeney, J.X. Rong, G. Kuriakose, E.A. Fisher, A.R. Marks, D. Ron, I. Tabas, The endoplasmic reticulum is the site of cholesterol-induced cytotoxicity in macrophages, Nat. Cell Biol. 5 (2003) 781–792.
[57] T. Devries-Seimon, Y. Li, P.M. Yao, E. Stone, Y. Wang, R.J. Davis, R. Flavell, I. Tabas, Cholesterol-induced macrophage apoptosis requires ER stress pathways and engagement of the type A scavenger receptor, J. Cell Biol. 171 (2005) 61–73.
[58] T.A. Seimon, A. Obstfeld, K.J. Moore, D.T. Golenbock, I. Tabas, Combinatorial pattern recognition receptor signaling alters the balance of life and death in macrophages, Proc. Natl. Acad. Sci. U. S. A. 103 (2006) 19794–19799.
[59] S. Bao, Y. Li, X. Lei, M. Wohltmann, W. Jin, A. Bohrer, C.F. Semenkovich, S. Ramanadham, I. Tabas, J. Turk, Attenuated free cholesterol loading-induced apoptosis but preserved phospholipid composition of peritoneal macrophages from mice that do not express group VIA phospholipase A2, J. Biol. Chem. 282 (2007) 27100–27114.
[60] Y. Li, M. Ge, L. Ciani, G. Kuriakose, E.J. Westover, M. Dura, D.F. Covey, J.H. Freed, F.R. Maxfield, J. Lytton, I. Tabas, Enrichment of endoplasmic reticulum with cholesterol inhibits sarcoplasmic-endoplasmic reticulum calcium ATPase-2b activity in parallel with increased order of membrane lipids: implications for depletion of endoplasmic reticulum calcium stores and apoptosis in cholesterol-loaded macrophages, J. Biol. Chem. 279 (2004) 37030–37039.

[61] Y. Li, R.F. Schwabe, T. DeVries-Seimon, P.M. Yao, M.C. Gerbod-Giannone, A.R. Tall, R.J. Davis, R. Flavell, D.A. Brenner, I. Tabas, Free cholesterol-loaded macrophages are an abundant source of tumor necrosis factor-alpha and interleukin-6: model of NF-kappaB- and map kinase-dependent inflammation in advanced atherosclerosis, J. Biol. Chem. 280 (2005) 21763–21772.
[62] B. Feng, D. Zhang, G. Kuriakose, C.M. Devlin, M. Kockx, I. Tabas, Niemann-Pick C heterozygosity confers resistance to lesional necrosis and macrophage apoptosis in murine atherosclerosis, Proc. Natl. Acad. Sci. U. S. A. 100 (2003) 10423–10428.
[63] P.T. Tarr, P.A. Edwards, ABCG1 and ABCG4 are coexpressed in neurons and astrocytes of the CNS and regulate cholesterol homeostasis through SREBP-2, J. Lipid Res. 49 (2008) 169–182.
[64] T. Janvilisri, H. Venter, S. Shahi, G. Reuter, L. Balakrishnan, H.W. van Veen, Sterol transport by the human breast cancer resistance protein (ABCG2) expressed in *Lactococcus lactis*, J. Biol. Chem. 278 (2003) 20645–20651.
[65] G. Schmitz, T. Langmann, High-density lipoproteins and ATP-binding cassette transporters as targets for cardiovascular drug therapy, Curr. Opin. Investig. Drugs 6 (2005) 907–919.
[66] B.J. van Vlijmen, G. Gerritsen, A.L. Franken, L.S. Boesten, M.M. Kockx, M.J. Gijbels, M.P. Vierboom, M. van Eck, B. van De Water, T.J. van Berkel, L.M. Havekes, Macrophage p53 deficiency leads to enhanced atherosclerosis in APOE*3-Leiden transgenic mice, Circ. Res. 88 (2001) 780–786.
[67] J. Liu, D.P. Thewke, Y.R. Su, M.F. Linton, S. Fazio, M.S. Sinensky, Reduced macrophage apoptosis is associated with accelerated atherosclerosis in low-density lipoprotein receptor-null mice, Arterioscler. Thromb. Vasc. Biol. 25 (2005) 174–179.
[68] S. Arai, J.M. Shelton, M. Chen, M.N. Bradley, A. Castrillo, A.L. Bookout, P.A. Mak, P.A. Edwards, D.J. Mangelsdorf, P. Tontonoz, T. Miyazaki, A role for the apoptosis inhibitory factor AIM/Spalpha/Api6 in atherosclerosis development, Cell. Metab. 1 (2005) 201–213.
[69] J.L. Johnson, A.H. Baker, K. Oka, L. Chan, A.C. Newby, C.L. Jackson, S.J. George, Suppression of atherosclerotic plaque progression and instability by tissue inhibitor of metalloproteinase-2: involvement of macrophage migration and apoptosis, Circulation 113 (2006) 2435–2444.
[70] A. Baldan, L. Pei, R. Lee, P. Tarr, R.K. Tangirala, M.M. Weinstein, J. Frank, A.C. Li, P. Tontonoz, P.A. Edwards, Impaired development of atherosclerosis in hyperlipidemic Ldlr−/− and ApoE−/− mice transplanted with Abcg1−/− bone marrow, Arterioscler. Thromb. Vasc. Biol. 26 (2006) 2301–2307.
[71] M. Ranalletta, N. Wang, S. Han, L. Yvan-Charvet, C. Welch, A.R. Tall, Decreased atherosclerosis in low-density lipoprotein receptor knockout mice transplanted with Abcg1−/− bone marrow, Arterioscler. Thromb. Vasc. Biol. 26 (2006) 2308–2315.
[72] R. Out, M. Hoekstra, R.B. Hildebrand, J.K. Kruit, I. Meurs, Z. Li, F. Kuipers, T.J. Van Berkel, M. Van Eck, Macrophage ABCG1 deletion disrupts lipid homeostasis in alveolar macrophages and moderately influences atherosclerotic lesion development in LDL receptor-deficient mice, Arterioscler. Thromb. Vasc. Biol. 26 (2006) 2295–2300.
[73] R. Out, M. Hoekstra, I. Meurs, P. de Vos, J. Kuiper, M. Van Eck, T.J. Van Berkel, Total body ABCG1 expression protects against early atherosclerotic lesion development in mice, Arterioscler. Thromb. Vasc. Biol. 27 (2007) 594–599.
[74] L. Yvan-Charvet, M. Ranalletta, N. Wang, S. Han, N. Terasaka, R. Li, C. Welch, A.R. Tall, Combined deficiency of ABCA1 and ABCG1 promotes foam cell accumulation and accelerates atherosclerosis in mice, J. Clin. Invest. 117 (2007) 3900–3908.
[75] R. Out, M. Hoekstra, K. Habets, I. Meurs, V. de Waard, R.B. Hildebrand, Y. Wang, G. Chimini, J. Kuiper, T.J. Van Berkel, M. Van Eck, Combined deletion of macrophage ABCA1 and ABCG1 leads to massive lipid accumulation in tissue macrophages and distinct atherosclerosis at relatively low plasma cholesterol levels, Arterioscler. Thromb. Vasc. Biol. 28 (2008) 258–264.
[76] L.K. Curtiss, Is two out of three enough for ABCG1? Arterioscler. Thromb. Vasc. Biol. 26 (2006) 2175–2177.
[77] K. Abildayeva, P.J. Jansen, V. Hirsch-Reinshagen, V.W. Bloks, A.H. Bakker, F.C. Ramaekers, J. de Vente, A.K. Groen, C.L. Wellington, F. Kuipers, M. Mulder, 24(S)-hydroxycholesterol participates in a liver X receptor-controlled pathway in astrocytes that regulates apolipoprotein E-mediated cholesterol efflux, J. Biol. Chem. 281 (2006) 12799–12808.
[78] B. Karten, R.B. Campenot, D.E. Vance, J.E. Vance, Expression of ABCG1, but not ABCA1, correlates with cholesterol release by cerebellar astroglia, J. Biol. Chem. 281 (2006) 4049–4057.
[79] M. Hoekstra, J.K. Kruijt, M. Van Eck, T.J. Van Berkel, Specific gene expression of ATP-binding cassette transporters and nuclear hormone receptors in rat liver parenchymal, endothelial, and Kupffer cells, J. Biol. Chem. 278 (2003) 25448–25453.
[80] B.J. O'Connell, M. Denis, J. Genest, Cellular physiology of cholesterol efflux in vascular endothelial cells, Circulation 110 (2004) 2881–2888.
[81] N. Wang, L. Yvan-Charvet, D. Lutjohann, M. Mulder, T. Vanmierlo, T.W. Kim, A.R. Tall, ATP-binding cassette transporters G1 and G4 mediate cholesterol and desmosterol efflux to HDL and regulate sterol accumulation in the brain, FASEB J. 22 (2008) 1073–1082.

10. sz. közlemény

dc_46_10

BMC Cell Biology 2009, 10:93

BioMed Central

Methodology article

Open Access

Model system for the analysis of cell surface expression of human ABCA1

Ildikó Kasza†[1], Zoltán Hegyi†[1], Katalin Szabó[2], Hajnalka Andrikovics[3], Katalin Német[3], András Váradi[2], Balázs Sarkadi[1,3] and László Homolya*[1]

Address: [1]Membrane Biology Research Group, Hungarian Academy of Sciences, Department of Biophysics and Radiation Biology, Semmelweis University, Diószegi u 64, H-1113, Budapest, Hungary, [2]Institute of Enzymology, Hungarian Academy of Sciences, Karolina út 29-31, H-1113 Budapest, Hungary and [3]Department of Molecular Cell Biology, National Blood Center, Diószegi u 64, H-1113, Budapest, Hungary

Email: Ildikó Kasza - kasza@kkk.org.hu; Zoltán Hegyi - zoltan.hegyi@kkk.org.hu; Katalin Szabó - szkata@enzim.hu; Hajnalka Andrikovics - andrikovics@kkk.org.hu; Katalin Német - nemet@biomembrane.hu; András Váradi - varadi@enzim.hu; Balázs Sarkadi - sarkadi@biomembrane.hu; László Homolya* - homolya@biomembrane.hu

* Corresponding author †Equal contributors

Published: 21 December 2009

BMC Cell Biology 2009, **10**:93 doi:10.1186/1471-2121-10-93

Received: 16 June 2009
Accepted: 21 December 2009

This article is available from: http://www.biomedcentral.com/1471-2121/10/93

Abstract

Background: The ABCA1 protein plays a pivotal role in reverse cholesterol transport, by mediating the generation of HDL particles and removing cellular cholesterol. Both the proper expression of ABCA1 in the plasma membrane and the internalization along with apoA-I are required for function. Therefore, we developed a model system to investigate the effect of clinically relevant drugs on the cell surface appearance of ABCA1.

Results: By retroviral transduction system, we established stable mammalian cell lines expressing functional and non-functional ABCA1 variants, tagged with an extracellular hemagglutinin epitope. After characterization of the expression, proper localization and function of different ABCA1 variants, we followed quantitatively their cell surface expression by immunofluorescent staining, using flow cytometry. As expected, we found increased cell surface expression of ABCA1 after treatment with a calpain inhibitor, and observed a strong decrease in plasma membrane ABCA1 expression upon treatment with a trans-Golgi transport inhibitor, Brefeldin A. We tested cholesterol level lowering drugs and other potential inhibitors of ABCA1. Here we demonstrate that ezetimibe affects ABCA1 cell surface expression only in the case of a functional ABCA1.

Conclusions: Our model system allows a quantitative detection of cell surface expression of ABCA1, screening of substrates or specific inhibitors, and investigating transport regulation.

Background

Elevated low-density lipoprotein (LDL) cholesterol, reduced high-density lipoprotein (HDL) cholesterol, and increased triglyceride levels significantly contribute to the accumulation of lipids in atherosclerotic lesions. Reverse cholesterol transport is believed to be crucial for preventing atherogenesis and hence the development of cardiovascular diseases [1,2]. It is commonly accepted that the ATP-binding cassette protein, ABCA1 plays a pivotal role in the initial steps of the reverse cholesterol transport pathway by mediating the interactions of amphiphilic apolipoproteins (e.g., apoA-I) with cellular lipids to generate nascent HDL particles thus removing excess cellular cholesterol [3,4]. Mutations in ABCA1 cause Tangier dis-

ease, a disorder characterized by very low HDL levels, cholesterol deposition in macrophages, and premature atherosclerosis [5-7]. There is increasing evidence suggesting a role for ABCA1 not only in the hepatic but also in the intestinal HDL-production [8].

Therapeutic efforts to raise HDL levels with different drugs have been promising. Clinical trials tested various statins, niacin, and ezetimibe alone and in various combinations to raise plasma HDL- and to reduce the plasma LDL-cholesterol levels [9,10]. Niacin and ezetimibe together with statins were proven to be the most effective combination *in vivo* [11]. However, conflicting results were reported about the effects of statins on lipid efflux and the modulation of ABCA1 expression in *in vitro* experiments [12-16]. Recently, certain types of calcium channel blockers (CCBs), e.g., verapamil, nifedipine, have been found to be anti-atherogenic in clinical trials [17,18]. When their effects on ABCA1 expression were investigated, contradictory results were obtained. These agents either increased ABCA1 mRNA levels or elevated the protein expression without affecting the mRNA level, depending on the cellular test system used [19,20].

Similar to other plasma membrane proteins, the cell surface expression of ABCA1 is modulated by a complex process, which includes transcriptional and post-transcriptional regulation, as well as internalization, degradation, and recycling [21,22]. There is evidence that not only sufficient plasma membrane expression but internalization along with apoA-I is required for proper function of ABCA1 [23,24]. Thus, in the present study we aimed to develop a quantitative *in vitro* test system, which is suitable for monitoring the plasma membrane level of ABCA1, independently from direct transcriptional regulation. In order to generate such an experimental tool, we introduced a hemagglutinin (HA) epitope into the first extracellular loop of ABCA1, and stably expressed this tagged ABCA1 in various mammalian cell lines, using a constitutive promoter. In addition, to make our method suitable for studying trafficking processes of ABCA1 in conjunction with its function, we generated different loss-of-function mutant variants of the HA-tagged transporter. In the present study we demonstrate the applicability and reliability of the developed cellular test system, and report the effects of several pharmaceuticals, which are known to have cholesterol-lowering effects *in vivo*. When studying whether they act through modifying the cell surface expression of functional ABCA1, we found that among several drugs, ezetimibe lowers the plasma membrane level of a functional ABCA1.

Results

Stable expression of HA-tagged ABCA1 variants in mammalian cells

Since we aimed to generate different cell lines stably expressing ABCA1 at moderate levels, we used a bicistronic retroviral vector containing ABCA1 and a neoresistance gene (SsA1neoS) as described in [25]. In order to make our model system suitable for monitoring the cell surface appearance of ABCA1, we introduced an HA epitope into the first extracellular loop of ABCA1 [26]. In addition to the HA-tagged wild type (wt) ABCA1, we generated three mutant variants containing a methionine-lysine substitution in either one or both Walker A motifs (K939 M, K1952 M, and K939 M/K1952 M). These loss-of-function mutations were shown to impair cholesterol efflux and apoA-I binding without affecting protein folding and intracellular routing [27-29]. The assemblies of various retroviral constructs are shown in Figure 1. Retroviral particles were generated by using ecotropic Phoenix and PG13 packaging cells as described in the Materials and Methods section. Thereafter MDCKII and HEK293H cells were transduced and selected with G418 for stable expression of the transgenes [25,30].

It has been previously reported that ABCA1 expression rapidly declines in transfected cells after a few passages [31]. In order to obtain a model system with stable expression of each HA-tagged ABCA1 variant at comparable levels, we applied two strategies: i) four different clones with similar expression levels were combined; or ii) the cells, showing similar HA staining, were sorted by FACS. The former method (pooling) was used for the transduced MDCKII cells; whereas the latter (sorting) was used for HEK293H cells. The ABCA1 mRNA expression level of the established cell lines was determined by quantitative RT-PCR, and compared to that of HepG2 cells, macrophage model cells, i.e. PMA-pretreated Thp-1 cells, and human monocyte-derived macrophages (MDM). We found that ABCA1 was moderately over-expressed in our cell lines (app. 10-40-fold as compared to HepG2); nevertheless the expression levels were comparable with that of macrophages induced by the LXR agonist, T0901317 (Figure 2A). The protein expression level in the generated cell lines was also monitored through several passages by Western blot analysis (Figure 2B). Stable transgene expression was found up to 50 and 20 passages in MDCKII and HEK293H cells, respectively.

Cellular localization and functional characterization of HA-tagged ABCA1 variants

Besides analyzing the total expression levels, we also studied the cellular localization of ABCA1 variants in the established cell lines. In the first set of experiments indirect immunofluorescent labeling with anti-HA antibody was performed in intact cells, and cell surface staining was

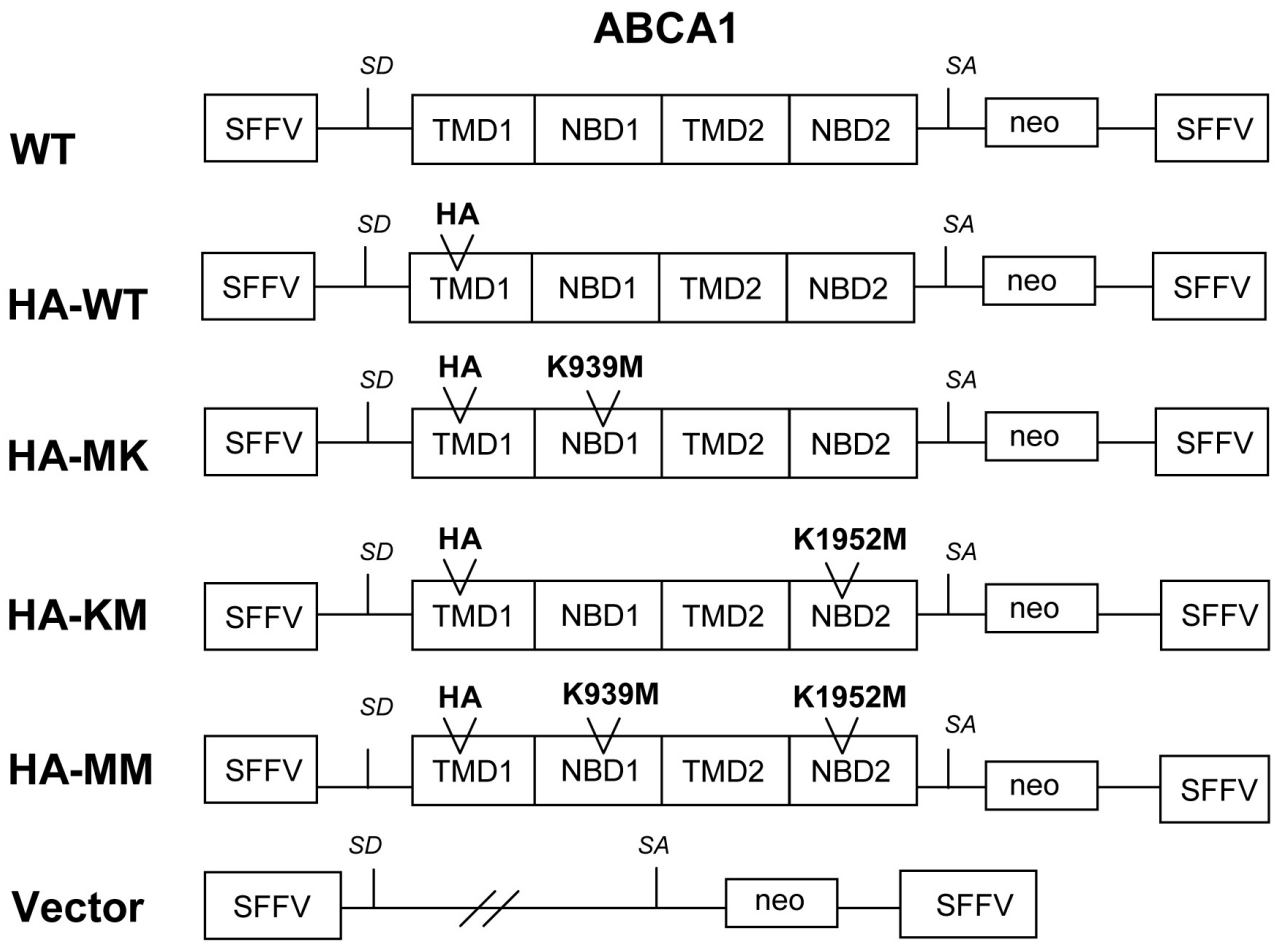

Figure 1

Schematic representation of bicistronic retroviral vectors. The ABCA1 cDNA was inserted behind a spleen focus-forming virus (SFFV) retroviral LTR following the splice donor (SD) site. The neomycin resistance (neo) cDNA was inserted after a splice acceptor (SA) site derived from the genome of the Moloney murine leukemia virus. Hemagglutinin (HA) epitope was introduced into the first extracellular loop of the N-terminal transmembrane domain (TMD) of ABCA1 (between residues 207 and 208). WT: wild type untagged ABCA1 construct; HA-WT: wild type HA-tagged ABCA1 construct; HA-MK: a variant with a methionine-lysine substitution (K939 M) in the Walker A motif of the N-terminal nucleotide-binding domain (NBD1); HA-KM: methionine-lysine substitution (K1952 M) in the C-terminal nucleotide-binding domain (NBD2); HA-MM: methionine-lysine substitution in both Walker A motifs (K939 M/K1952 M). A vector containing only the neo cDNA after the SA site was used as a negative control (vector).

detected by flow cytometry. We found comparable plasma membrane expression levels of all ABCA1 variants in both MDCKII and HEK293H cells (Figure 3). Similar to total expression levels of ABCA1 variants, the cell surface expression was also unaffected up to 50 and 20 passages in MDCKII and HEK293H cells, respectively.

The subcellular localization of HA-tagged ABCA1 variants was also studied by immunofluorescent staining followed by confocal microscopy. Detailed subcellular localization analysis performed with HEK293H cells clearly demonstrated that the HA-tagged ABCA1 is expressed predominantly in the plasma membrane (Figure 4E-F). A minor intracellular HA-ABCA1 expression was found in the Golgi-apparatus (Figure 4H-I), and some degree of colocalization was seen with an endosomal marker (Figure 4K-L). The subcellular localization of the HA-tagged ABCA1 variants was also studied in polarized MDCKII. Staining of Na^+/K^+ ATPase was used as a basolateral plasma membrane marker. Similar to previous reports on the untagged protein [32], the HA-tagged wt ABCA1 was also localized to the basolateral membrane compartment

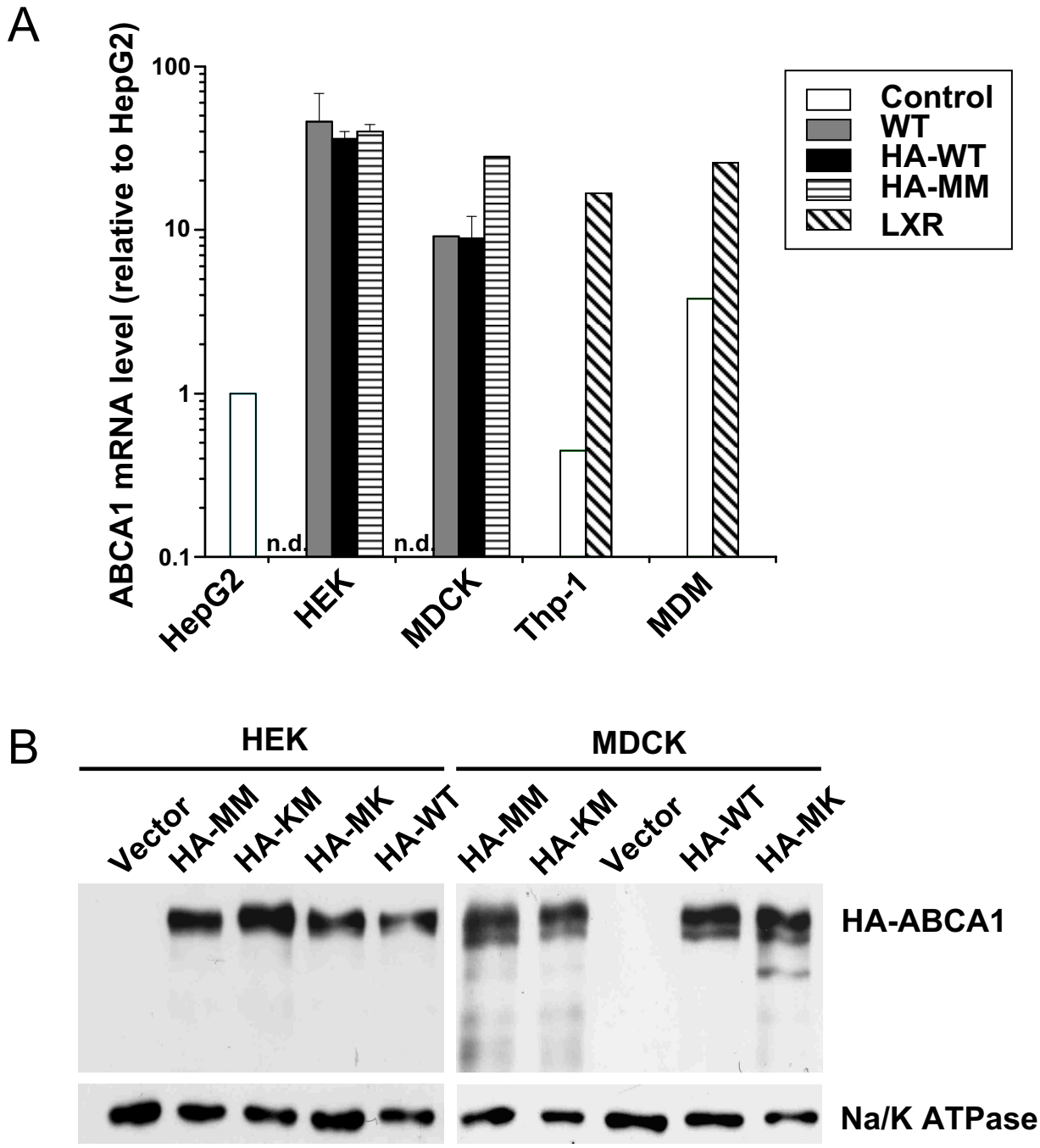

Figure 2 *(see legend on next page)*

Figure 2 *(see previous page)*
Expression of wild type and mutant HA-tagged ABCA1 variants in HEK293H and MDCKII cells. **A**. The mRNA expression level of ABCA1 was measured by real time RT-PCR in the parental HEK293H and MDCKII cells, as well as in cells expressing the ABCA1 variants. The ABCA1 expression of HepG2 cells were used as a reference for relative mRNA expression levels. For comparison, ABCA1 mRNA level was also determined in PMA-pretreated Thp-1 cells and in human monocyte-derived macrophages (MDM). To induce ABCA1 expression, the latter two cell types were treated with 1 μM T0901317, an LXR agonist (LXR). Control: original, parental, or non-treated cells; n.d. - not detected. The expression of ABCA1 variants were similar in the established cell lines and comparable with that seen in LXR-induced macrophages. **B**. The protein expression level of HA-tagged ABCA1 variants was determined using anti-HA antibody by Western blot analysis on whole cell lysates. Panels demonstrate representative blots for the variants of HEK293H and MDCKII cells at passage number 5. Each lane contains 15 μg and 40 μg of protein per well from HEK293H and MDCKII cells, respectively. Anti-Na/K ATPase antibody was used to control the sample loading. For further details see legend for Figure 1.

(Figure 5D-F), indicating that neither the modest overexpression nor HA-tagging affect proper localization. Similarly, all non-functional HA-tagged ABCA1 variants exhibited basolateral localization (Figure 5G-I, J-L, M-O).

To investigate the functional properties of our HA-tagged ABCA1 variants, we measured the apoA-I-dependent cholesterol efflux and apoA-I binding in the established model cells. In accordance with previous observations with the untagged protein [33,34], ABCA1 expression significantly elevated the apoA-I-specific cholesterol efflux in both HEK293H and MDCKII cells (Figure 6A). More importantly, no difference was observed between the untagged and the HA-tagged ABCA1 in this respect. It is noteworthy that the observed apoA-I-dependent cholesterol efflux was smaller in our case than in preceding reports, most likely due to the moderated ABCA1 expression in our cells versus the massive overexpresssion in the

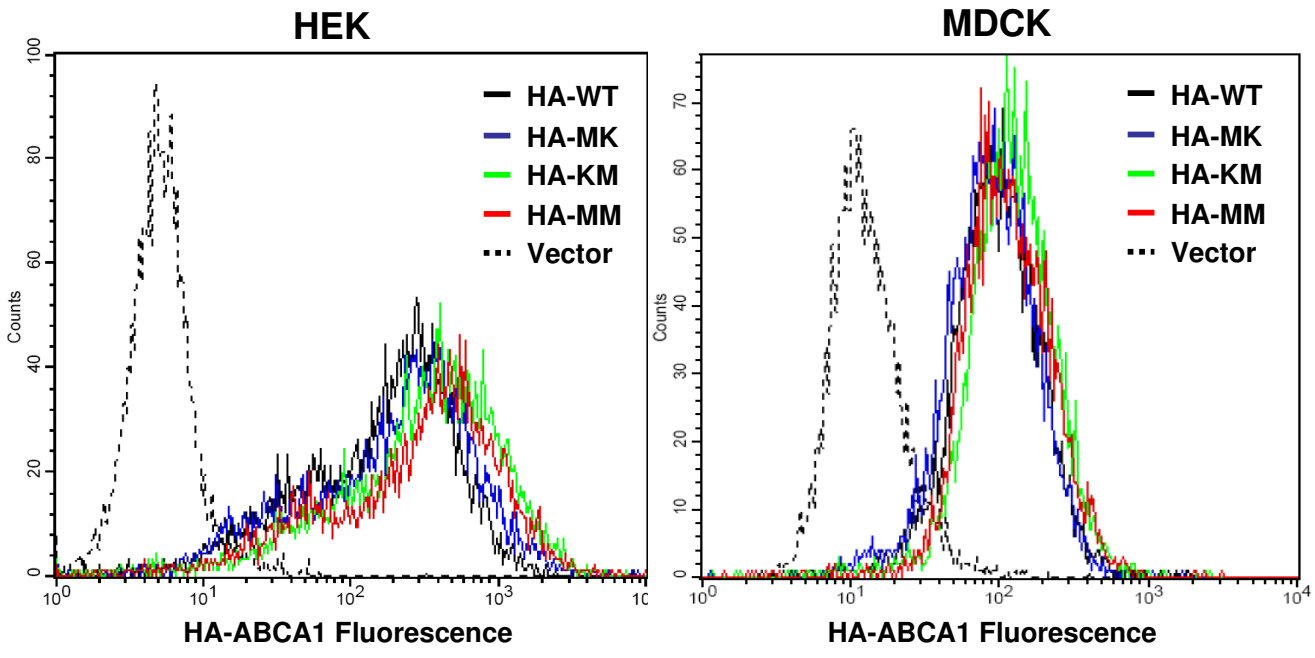

Figure 3
Flow cytometry analysis of cell surface expression of wild type and mutant HA-tagged ABCA1 variants. Indirect immunofluorescent labeling with anti-HA antibody and anti-mouse IgG antibody conjugated with Alexa 488 was performed with intact HEK293H and MDCKII cells expressing the different variants of HA-tagged ABCA1. Representative flow cytometry experiments demonstrate the cell surface expression of ABCA1 variants. HA-WT: (black line); HA-MK: (blue line); HA-KM: (green line); HA-MM (red line); vector (dotted line). HA-tagged ABCA1 variants showed comparable plasma membrane appearance in both MDCKII and HEK293H cells.

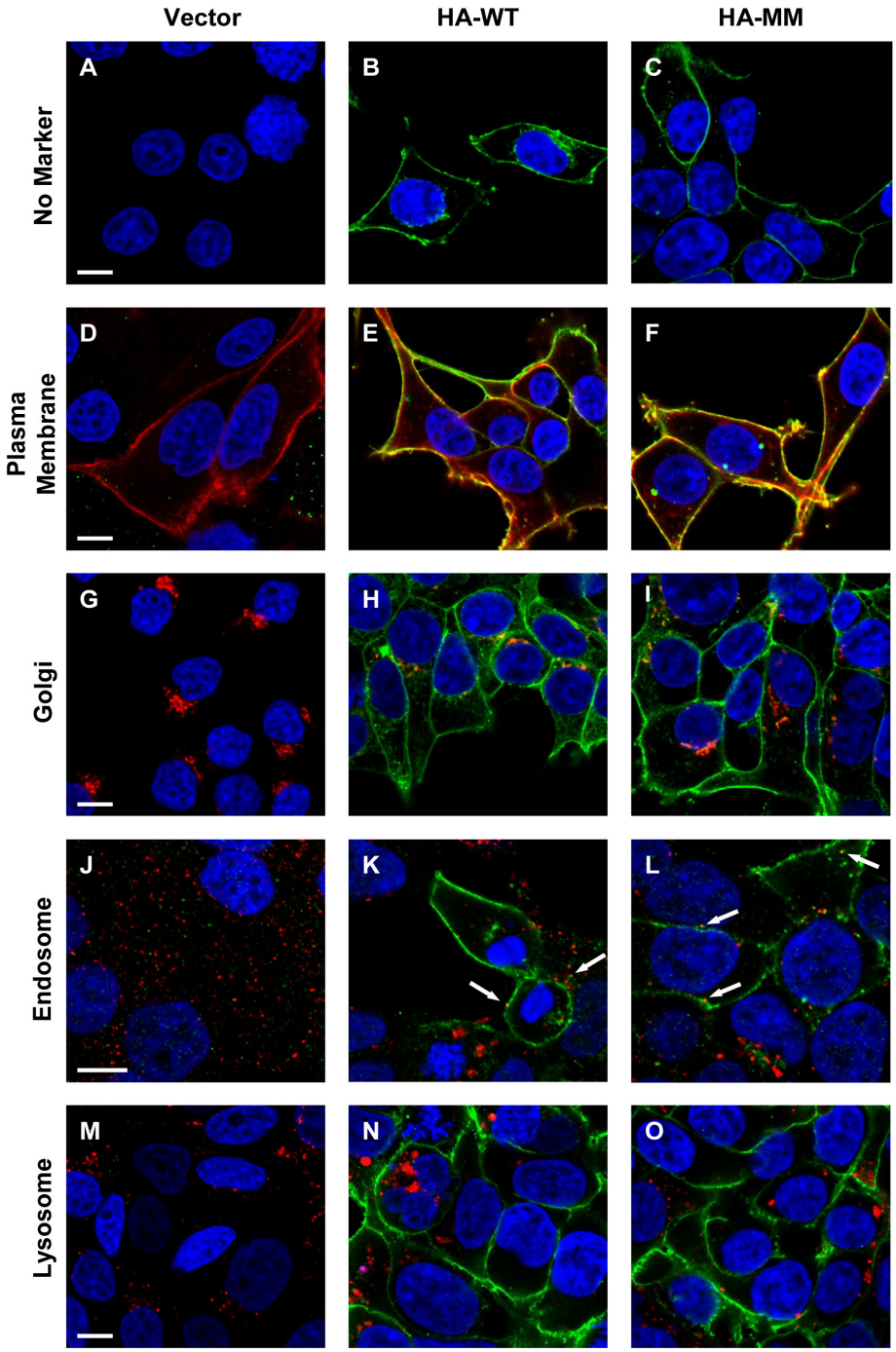

Figure 4
Subcellular localization of HA-tagged ABCA1 in HEK293H cells. HEK293H cells expressing the wild type (HA-WT) or double mutant variant (HA-MM) of HA-ABCA1 were immunostained with anti-HA antibody and visualized by confocal microscopy (green). As a negative control HEK293H cells transduced with the empty vector was used. Various cellular markers (wheat germ agglutinin, anti-Giantin and anti-EEA1 antibodies, as well as LysoTracker) were used to identify the different cell organelles (red), whereas DAPI staining was used to label the nuclei (blue). Both wild type and MM variant of HA-ABCA1 were localized predominantly in the plasma membrane. The minor intracellular staining colocalized primarily with the Golgi marker, and rarely with the endosomes (see white arrows). The scale bars indicate 10 μm.

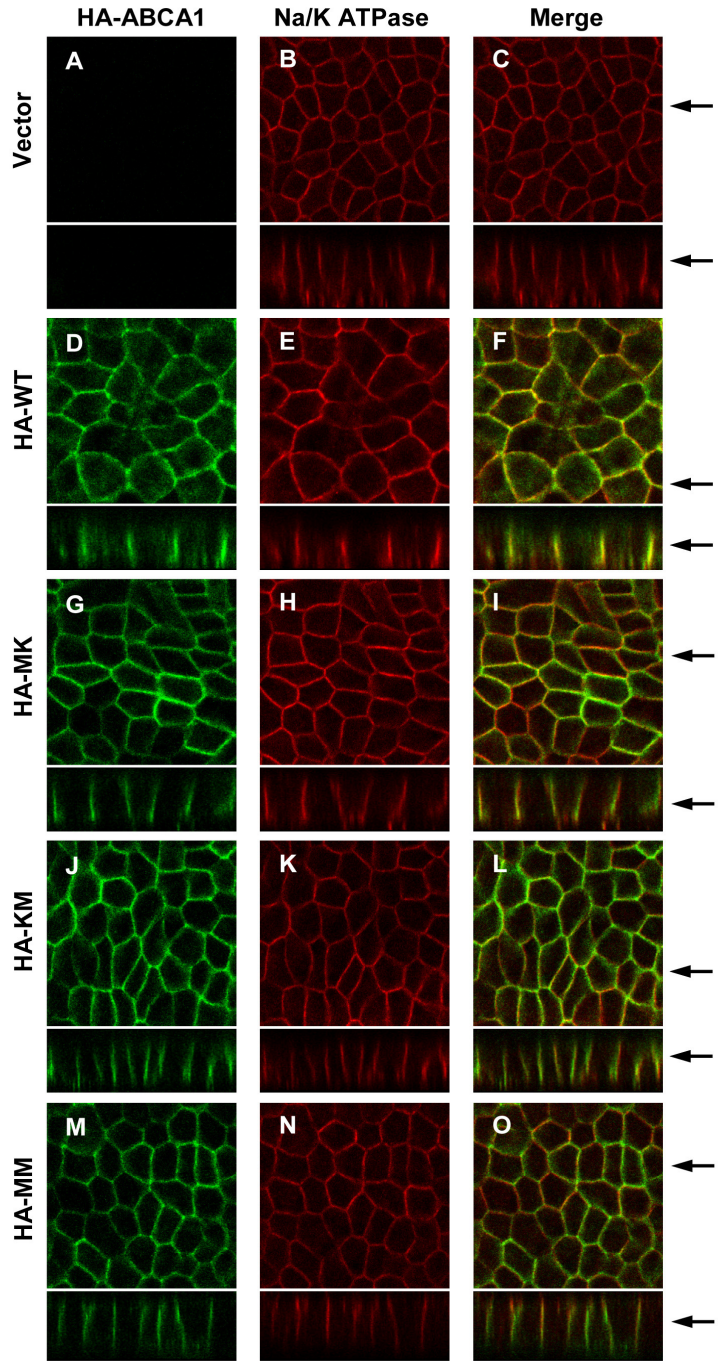

Figure 5
Subcellular localization of HA-tagged ABCA1 variants in polarized MDCKII cells. MDCKII cells expressing the wild type (D-F) or mutant variants (G-O) of HA-ABCA1 were grown on a permeable membrane support to form polarized cultures. As a negative control, cells transduced with the neo-containing vector (see Figure 1) were used (A-C). HA-ABCA1 variants were visualized by immunofluorescent staining of permeabilized cells, using confocal microscopy. ABCA1 protein detected by anti-HA antibody is shown in green; staining of Na^+/K^+ ATPase (red) served as a basolateral plasma membrane marker. Right panels depict the overlay. Cross sections are shown at the bottom of each panel; arrows at the side indicate the position of the presented xz and xy planes. All HA-tagged ABCA1 variants exhibited similar and clear basolateral plasma membrane localization, showing only a low level intracellular staining.

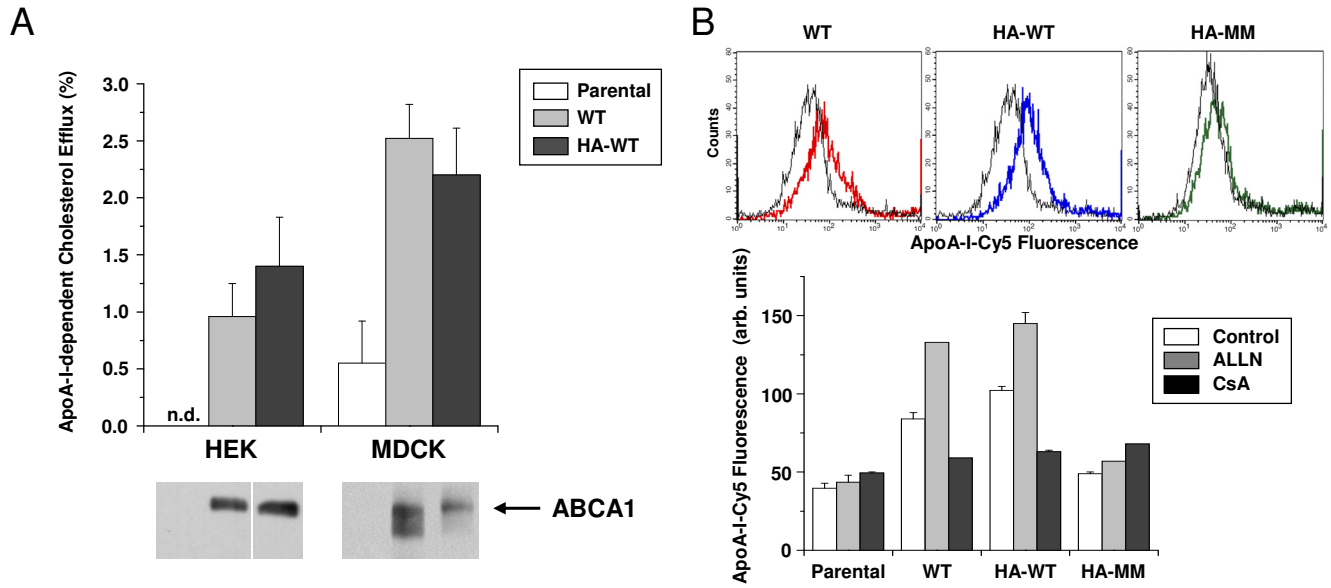

Figure 6

Functional characterization of the HA-tagged ABCA1. **A**. The apoA-I-dependent cholesterol efflux was measured in HEK293H and MDCKII cells expressing the untagged (WT) and HA-tagged (HA-WT) ABCA1. As a control the parental cell lines were used. Western blots at the bottom, developed with anti-ABCA1 antibody, indicate the expression levels in the studied cell lines. ABCA1 expression significantly elevated the apoA-I-specific cholesterol efflux in both cell types. HA-tagging did not alter the function of ABCA1. n.d. - not detected. **B**. Binding of Cy5-labeled apoA-I was determined in HEK293H cells expressing the untagged (WT), the HA-tagged wild type ABCA1 (HA-WT) and the mutant form of HA-ABCA1 (HA-MM). Substantial labeling was observed in cells expressing the untagged and the HA-tagged wild type ABCA1 (colored histograms) as compared to parental cells (grey histograms). No apoA-I binding was seen in cells expressing the mutant form of HA-ABCA1. 4 h pretreatment with the calpain inhibitor, ALLN (50 μM) significantly increased apoA-I-binding in both untagged and HA-tagged wt ABCA1-expressing cells, whereas 50 μM cylcosporin A (CsA) pretreatment slightly reduced the apoA-I-binding in these cells. ALLN and CSA had no effect on apoAI-binding of the parental and mutant HA-ABCA1 expressing cells. Control - cells treated with vehicle.

transient expression systems used in previous studies. The apoA-I-dependent cholesterol effluxes from cells expressing the KM, KM, or MM mutants were not significantly different from that seen in the parental cells.

Similar to apoA-I-dependent cholesterol efflux, apoA-I binding was found to be elevated in cells expressing either the untagged or HA-tagged ABCA1, whereas it was unaffected in cells expressing the mutant form of HA-ABCA1 (Figure 6B). Since the calpain inhibitor Acetyl-L-Leucyl-L-Leucyl-L-Norleucinal (ALLN) and cylcosporin A (CsA) were used in further experiments, we investigated the effect of these drugs on the apoA-I-binding in the established cell lines. We found that ALLN significantly increased apoA-I-binding in cells expressing either the untagged or HA-tagged wt ABCA1-expressing, whereas CsA pretreatment slightly reduced the apoA-I-binding in these cells. This observation is in good accordance with previous studies performed with untagged ABCA1 [35-38], and clearly indicates that HA-tagging did not alter the function of the protein. ALLN and CsA had no significant effect on apoAI-binding in the parental cell line and in cell expressing the mutant form of HA-ABCA1.

In summary, we demonstrated reasonable and stable expression, correct subcellular localization, as well as proper function for the HA-tagged ABCA1. Since all three HA-tagged ABCA1 mutants were proven to be non-functional with normal expression and localization, only the wild type HA-tagged and the double mutant variant (MM) were used in further experiments.

Effect of calpain inhibitor, BFA, and apoA-I on cell surface expression of ABCA1 variants

In order to demonstrate the applicability of the HA-tagged ABCA1 variants for monitoring cell surface expression, we studied the effect of different substances which are known to influence ABCA1 trafficking and degradation. Since calpain has been shown to participate in ABCA1 degradation [35-37], the HA-ABCA1-expressing cells were treated with the calpain inhibitor, ALLN. This drug was expected to elevate the cell surface expression of ABCA1 due to the inhi-

bition of the degradation pathway. To decrease the cell surface appearance of the protein, Brefeldin A (BFA), an inhibitor of trans-Golgi transport [39] was applied. Indirect immunofluorescent labeling with anti-HA antibody was performed with intact cells 4 h after the treatment with ALLN and BFA, then studied by flow cytometry. Figures 7A and 7B show representative experiments with HEK293H cells expressing wt and MM variant of the HA-tagged ABCA1. Quantitative results are depicted in Figures 7C and 7D. A substantial alteration in the cell surface expression of both variants was observed as compared to non-treated cells. ALLN caused about 1.6-fold increase, whereas BFA treatment resulted in 60% reduction in the plasma membrane level of wt HA-ABCA1 (Figure 7C). It is of note that the effects of drugs were slightly smaller in cells expressing the MM variant of HA-ABCA1 as compared to cells expressing the wt HA-ABCA1 (Figure 7D). Similar to BFA, a general protein synthesis blocker, cycloheximide also reduced the cell surface expression of both ABCA1 variants; however, this drug substantially affected cell viability (data not shown).

ApoA-I has also been demonstrated to increase ABCA1 expression by binding to the transporter and preventing it from degradation [36,37]. As expected, apoA-I significantly increased the cell surface expression of wt HA-tagged ABCA1 (Figure 7C). The MM mutant ABCA1, which was shown to be unable to bind apoA-I [29], exhibited no alteration of the cell surface expression levels when incubated with apoA-I (Figure 7D). These experiments clearly demonstrate that our model system is suitable to detect the effects of various substances on the cell surface expression of either the functional or non-functional variant of ABCA1.

In similar experiments, HA-ABCA1-expressing MDCKII cells were treated with ALLN or BFA. Even though a wide range of drug concentrations was tested, no marked changes in the ABCA1 cell surface expression were seen in these cells. Therefore, in further experiments HEK293H cells expressing the HA-tagged ABCA1 variants were used.

Effect of different drugs on cell surface expression of ABCA1 variants

By having a verified test system, we studied the effect of various drugs on the cell surface expression of ABCA1 variants. We primarily tested the effect of pharmaceuticals which are known to have cholesterol-lowering effects *in vivo*, to see whether they also act through modifying the cell surface appearance of ABCA1. These drugs included atorvastatin, ezetimibe, and niacin [9], 40-45, as well as calcium channel blockers, nifedipine and verapamil [19,20]. In addition, we investigated the effect of cyclosporin A and glyburide, which have previously been reported to influence the plasma membrane level or function of ABCA1 [29,38]. The studied drugs were applied in a wide concentration range with various incubation times. As positive controls, ALLN and BFA were used to elevate and reduce the ABCA1 cell surface expression, respectively. The results are summarized in Table 1.

We found that atorvastatin (10-50 μM), niacin (0.1-1 mM), verapamil (10-50 μM) and nifedipine (30-100 μM) had no significant effect on the plasma membrane level of ABCA1 even in a wide concentration range. However, CsA (10 μM) substantially elevated the cell surface expression of wt HA-ABCA1 (Figure 7C) in accordance with previous results indicating ABCA1 sequestration in the plasma membrane by CsA [38]. It has not been shown yet whether this effect of CsA is associated with the protein function, therefore we performed similar experiments with the non-functional mutant (MM) variant of ABCA1. We found that CsA equally increased the ABCA1 cell surface expression in wt and MM HA-ABCA1-expressing cells (Figure 7C-D), thus the trapping effect of CsA is independent from ABCA1 function. Unexpectedly, ezetimibe (EZ), a blocker of the intestinal cholesterol absorption, significantly (by 20%) reduced the cell surface expression of wt HA-ABCA1 (Figure 7C). Interestingly, this effect of EZ was found to be associated with ABCA1 function, since no reduction in the cell surface expression of the MM HA-ABCA1 was seen in response to EZ treatment (Figure 7D). Glyburide, which has previously been reported to inhibit ABCA1-mediated cholesterol efflux and apoA-I binding without altering the cell surface levels or total protein levels of ABCA1 [29,46], had no effect of the plasma membrane level of ABCA1 (see Table 1). However, at higher concentrations a slight reduction in the ABCA1 cell surface expression was observed in parallel with a substantial decline in the cell viability in both wt and MM HA-ABCA1-expressing cells. Treatment with 200-500 μM glyburide for 4 h resulted in 50% cell death in both cell types.

We also investigated the effect of plasma membrane cholesterol levels on the cell surface expression of ABCA1 variants. Treatment with 0.1-2.5 mM methyl-β-cyclodextrin (CD), which results in membrane cholesterol depletion [47], had no effect on the plasma membrane level of either wild type or MM variant of HA-ABCA1 even in a wide range of incubation time (20-240 min), although a substantial reduction in the cell viability was observed. Similarly, cholesterol overload by cholesterol-containing CD treatment (0.1-2.5 mM, 20-240 min) did not alter the cell surface expression of ABCA1 in either cell type.

Discussion

ABCA1 protein is involved in lipid metabolism in several regards. This protein promotes reverse cholesterol transport from the peripheral tissues. ABCA1, being located on the basolateral surface of hepatocytes and intestinal cells,

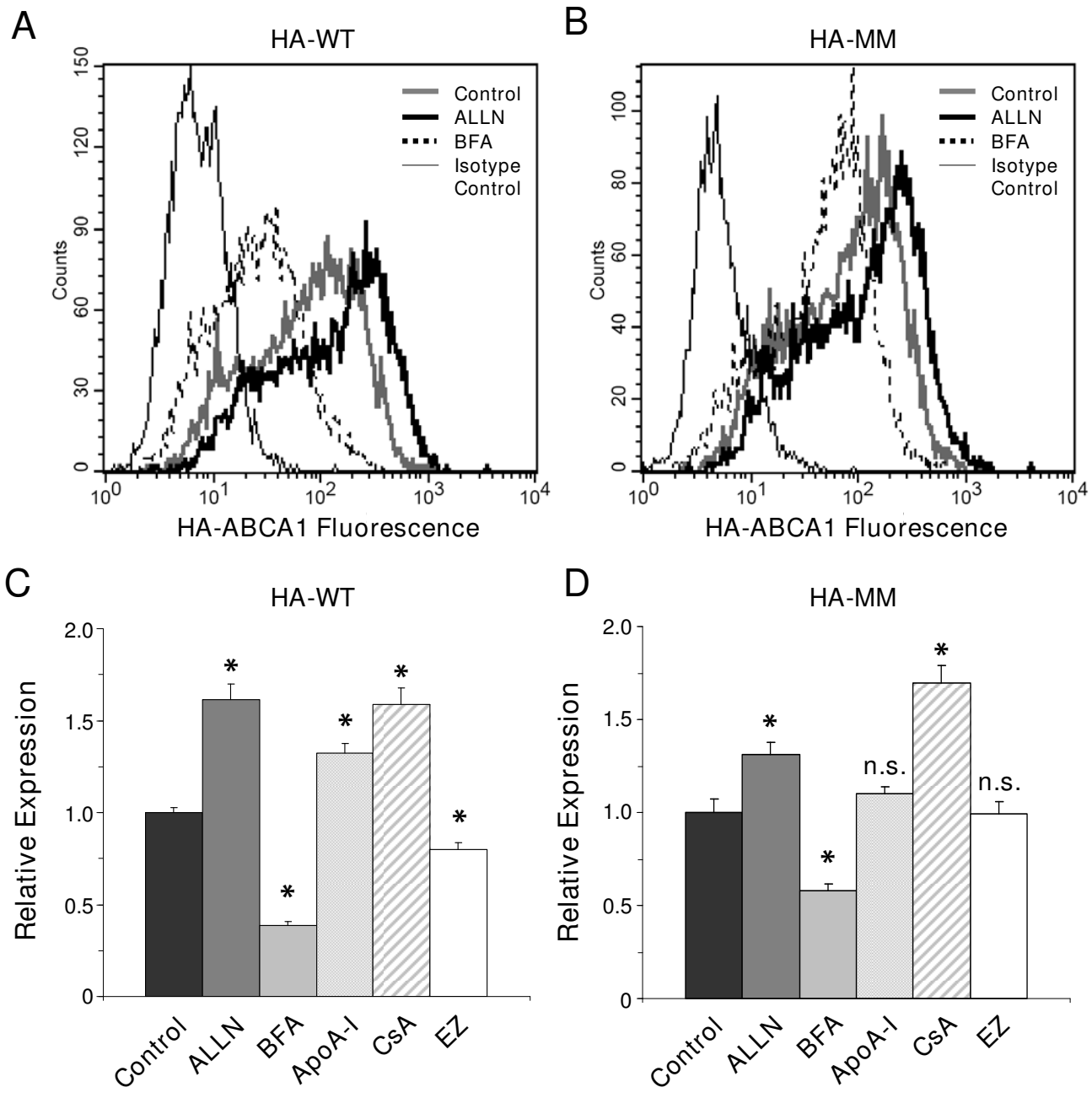

Figure 7

Effect of different drugs on the cell surface expression of HA-ABCA1 variants. Flow cytometry analysis of HEK293H cells expressing wild type or MM variant of HA-tagged ABCA1. (A, B) Representative histograms show indirect immunofluorescent staining of intact cells, using anti-HA antibody (thick lines) or mouse IgG1 (isotype control, thin black line). Treatment with 50 μM ALLN (thick black line) substantially increased, whereas 5 mg/ml BFA (dotted line) reduced the cell surface expression level of both wild type (HA-WT) and mutant (HA-MM) HA-ABCA1 variants, as compared to cells treated with vehicle only (control, grey line). (C, D) Cell surface expression of wild type and MM mutant HA-ABCA1 variants in HEK293H cells treated with 50 μM ALLN, 5 mg/ml BFA, 10 μg/ml apoA-I, 10 μM CsA, or 50 μM EZ for 4 h. Relative expression levels were expressed as the geometric mean fluorescence intensities of drug-treated cells normalized to that of vehicle-treated samples (control). Each column represents the mean ± S.E.M. of at least 3 independent experiments. (* $p < 0.005$; n.s.: non-significant)

Table 1: Effect of various substances on the cell surface expression of wild type (HA-WT) and mutant (HA-MM) HA-ABCA1 variants

Drug	Known effect	ABCA1 cell surface expression	
		HA-WT	HA-MM
ALLN	Calpain inhibitor	(+ 60%)	(+ 30%)
ApoA-I	cholesterol acceptor	(+ 30%)	no effect
Atorvastatin	cholesterol level lowering	no effect	no effect
Brefeldin A	trans-Golgi transport inhibitor	(- 60%)	(- 40%)
Cycloheximide	protein synthesis inhibitor	(- 30%) (viability)	(- 30%) (viability)
Cyclosporin A	immunosuppressor	(+ 60%)	(+ 60%)
Ezetimibe	inhibitor of intestinal cholesterol absorption	(- 20%)	no effect
Glyburide	ABCA1 inhibitor	no effect	no effect
Niacin	cholesterol level lowering	no effect	no effect
Nifedipine	Ca^{2+}-channel blocker	no effect	no effect
Methyl-β-cyclodextrin	cholesterol depletion	no effect (viability)	no effect (viability)
Cholesterol-methyl-β-cyclodextrin	cholesterol overloading	no effect (viability)	no effect (viability)
Verapamil	Ca^{2+}-channel blocker	no effect	no effect

has been shown to play a crucial role in the hepatic and intestinal secretion of HDL [48]. In the present study we generated and characterized a model system for the quantitative assessment of the plasma membrane level of ABCA1. Inclusion of an extracellular hemagglutinin epitope into ABCA1 enabled monitoring of its cell surface expression by flow cytometry and confocal microscopy. By using retroviral transduction we established mammalian cell lines stably expressing functional and non-functional HA-tagged ABCA1 variants. This experimental tool allowed us to investigate the effect of different drugs on cell surface expression of ABCA1.

In previous studies, the protein expression level and subcellular localization of wild type ABCA1 and non-functional mutant forms were found to be identical [27,31]. Similarly, in our model system, both the overall and the plasma membrane expression levels of each HA-tagged ABCA1 variant were comparable, as determined by Western blotting and cell surface labeling (Figures 2B, 3). ABCA1 has been reported to be localized to the basolateral membrane in polarized cells [32]. We found proper subcellular localization for each HA-tagged ABCA1 variant (Figures 4, 5) in accordance with previous reports on the untagged versions of the transporter [27].

Since the applicability and reproducibility of a cellular model system requires stable protein expression levels, we investigated the persistence of our transgene in various cell lines. We found that ABCA1 expression remains stable in MDCKII and HEK293H cells up to 50 and 20 passages, respectively. Thus, our experimental test system substantially surpasses previous attempts to generate cellular models with ABCA1, since in those cases protein expression rapidly declined after a few passages [31]. We demonstrated the applicability of our system to assess the cell surface appearance of ABCA1 by using BFA and ALLN, which have been reported to influence ABCA1 trafficking and degradation (Figure 7A, B).

In agreement with previous reports [35,36], we demonstrated the stabilizing effect of apoA-I on the HA-tagged ABCA1 at the cell surface (Figure 7C). Furthermore, we found that the cell surface levels of the Walker motif mutant ABCA1 (MM), which fails to bind apoA-I (Figure 6B) [28,29], was unaffected by apoA-I (Figure 7D). This observation is in line with previous findings demonstrating that binding of apoA-I is required for the apoA-I-mediated increase of ABCA1 expression [29,37].

In clinical trials, statins were highly effective in reducing LDL-cholesterol, but only moderate effects were seen on the HDL levels. Among a number of different statins, atorvastatin was the most effective and induced redistribution in HDL subpopulations by increasing the fraction of larger HDL particles [49]. Conflicting results were published on the effect of statins on ABCA1 expression and lipid efflux in various cellular systems. Wong et al. demonstrated down-regulation of ABCA1 mRNA and protein levels as well as reduction in the apoA-I-mediated cholesterol efflux in response to statin treatment of PMA-induced Thp-1 cells [14,15]. In contrast, another study found that atorvastatin increased mRNA expression of ABCA1 and promoted cholesterol efflux in the same cell type [12]. In hepatoma cells, statins induced ABCA1 expression resulting in cholesterol and phospholipid efflux to apoA-I [50]. These observations leave the question open, whether statins influence apoA-I-dependent cholesterol efflux solely by changing ABCA1 expression levels or by modifying its subcellular trafficking and cell surface appearance. Since our model system excludes transcriptional regulation, our results revealed that atorvastatin has no effect on the plasma membrane expression of ABCA1.

Niacin has been reported to be one of the most potent agents increasing HDL cholesterol levels [9], and to stimulate ABCA1 expression and function in monocytic cell lines via influencing the cAMP/PKA pathway [51]. By investigating the effect of niacin in our system, we observed no direct effect on cell surface appearance of ABCA1 in accordance with previous observations on the regulatory mechanism of niacin.

Calcium channel blockers have also been reported to influence ABCA1 expression. Hasegawa et al. demonstrated the role of different signaling pathways including PKA, tyrosine kinase, and Janus kinase in ABCA1 expression modulation in response to various CCBs. They found that some of the CCBs, e.g., aranidipine and efonidipine, increase ABCA1 protein expression without altering the mRNA level [20]. In contrast, Suzuki et al. demonstrated a dose-dependent stimulatory effect of other CCBs, such as verapamil, nifedipine, and nicardipine, on both the mRNA and protein expression levels of ABCA1, resulting in elevated cellular lipid release [19]. Our results do not support these findings, since we observed no significant effect on the plasma membrane level of ABCA1 in a wide concentration range of verapamil and nifedipine.

Membrane cholesterol has been implicated to regulate many membrane proteins, including several ABC transporters, e.g. ABCB1 and ABCG2 [47,52,53]. Membrane microdomains with high cholesterol content have been suggested to play a role in such regulation [47]. However, neither cholesterol overload nor depletion influenced ABCA1 cell surface expression in our model system. It is noteworthy that treatment with methyl-β-cyclodextrin (CD) reduced, whereas cholesterol-loaded CD significantly increased cell viability. The most plausible explanation for this observation is that CD treatment makes the cell membrane fragile and more sensitive to mechanical stress. This notion should be taken in account in future studies on ABCA1-expressing cells treated with CD.

We studied the effect of glyburide and CsA, which have previously been reported to influence the plasma membrane level or function of ABCA1 [29,38]. In accordance with previous observations, glyburide had no effect on ABCA1 plasma membrane appearance in our model system [29], whereas CsA greatly increased the cell surface level of ABCA1 (Figure 7C). ALLN elevated both ABCA1 cell surface expression and apoA-I binding, whereas CsA reduced apoA-I binding despite the increased plasma membrane level of ABCA1. This observation is line with a previous report suggesting that CsA sequesters ABCA1 in the plasma membrane [38]. The observation that cell surface expression of the non-functional ABCA1 mutant (MM) is also increased by CsA pretreatment clearly indicates that the trapping effect of this drug is independent from ABCA1 function.

Ezetimibe, a drug which is known to block the intestinal cholesterol absorption, has not only an inhibitory effect on several brush border membrane proteins, including Niemann-Pick C1-like 1, scavenger receptor B-I and CD36 [54], but has also been reported to lower the mRNA level of several other genes involved in lipid metabolism. The transcription of ABCA1 is also reduced by EZ [55], but no study has yet been reported on its effect on the cell surface expression of ABCA1. Our model system allows us to investigate the plasma membrane expression of ABCA1 independently from its transcriptional regulation. Strikingly, we found that EZ significantly lowers the cell surface expression of wt HA-ABCA1 (Figure 7C). Since no reduction in the cell surface expression of the MM HA-ABCA1 was seen in response to EZ treatment (Figure 7D), the effect of EZ occurs only with a functional ABCA1, thus, its effect is likely connected to a functional form of the protein.

There are several possibilities to explain the lack of effect of EZ on cell surface expression of the non-functional MM-ABCA1 variant. It is theoretically possible but very unlikely that EZ inhibits the trafficking of only the *de novo* synthesized functional proteins. It is more plausible that EZ influences the protein internalization and recycling to the plasma membrane, since ABCA1 has been shown to undergo a relatively rapid internalization and recycling to the plasma membrane, which process is widely accepted

to require protein function [39,56]. Therefore, if EZ either accelerates protein internalization or inhibits recycling, and in the meantime MM-ABCA1 has a lower internalization and recycling turnover compared to wild type, EZ causes a smaller effect on the cell surface appearance of the mutant transporter. This hypothesis is supported by the observation that the effects of ALLN were also smaller in HA-MM-ABCA1-expressing cells, as compared to wild type HA-ABCA1. It is also possible that EZ accelerates ABCA1 degradation, since the internalization itself is dependent on the transporter function. This idea is not supported by our recent observations using confocal microscopy, when we found that following EZ treatment the wt HA-ABCA1, but not the MM variant, accumulated intracellularly in vesicles but not in lysosomes (data not shown). Nevertheless, further studies are needed to reveal the mechanism of EZ effect on the cell surface expression of ABCA1.

Conclusions

In the current study, we have provided a model system suitable for the quantitative assessment of the plasma membrane level of ABCA1. We have shown that this test system can be reliably applied for studying the effect of various pharmaceuticals on the cell surface expression of the transporter. Therefore, our model system provides a new tool for acquiring more information on the post-translational regulation, internalization, degradation and recycling of the ABCA1 protein.

Methods

Plasmid constructs

For the generation of SsA1neoS vector, the full length wild type human ABCA1 cDNA [57] was cloned into a bicistronic retroviral SPsLdS vector [58], which was modified to contain the neomycin resistance cassette (neo) as previously described [25]. A cassette containing the coding sequence of an HA epitope (YPYDVPDY) was inserted into the full-length human ABCA1 cDNA, between residues 207 and 208 [26]. For control experiments, a vector containing only the neo cDNA was generated. The HA-ABCA1 K939 M, K1952 M mutants were constructed in the pBlscrSK- vector containing XhoI/NotI cassette from the SsHAA1neoS vector. HA-ABCA1 K939 M was constructed by the overlap extension PCR technique using the internal 5'-TGGCTGTGATCATCAAGGGC-3' and 5'-CCAGGACGTCCGCTTCATCCAT-3' and external 5'-ATTGACATGGTGGTCGTC**A**TCC-3' and 5'-GGA**T**GACGACCACCATGTCAAT-3' oligonucleotides. The external primer pair includes AAG (lysine) to ATG (methionine) single mutation and a new FokI restriction site (in bold). The HA-ABCA1 K1952 M mutant was generated by using 5'-AGCCAAAAGCTTAAAGAACAAGATCTGGGTG-3' and 5'-CTCCTGTTAACATCTTGAAAGTTGATGA**CA**TC-CCAGCC-3' oligonucleotides, which results in a lysine to methionine mutation (in bold) and contains a GC substitution (underlined) to create a new FokI restriction site. The mutant constructs were verified by FokI digestion. HA-ABCA1 variant containing double methionine substitution was created by cassette exchange in pBlscrSK- vector by using HindIII/HpaI digestion. After partial digestion of each mutant construct in pBlscrSK- vector by XhoI/BamHI enzymes the fragments were transferred into SsHAA1neoS vector and verified by sequencing.

Cell culturing

Phoenix-eco [59] was a gift from G. Nolan (Department of Pharmacology, Stanford University, Stanford, CA); PG13 retrovirus producing cells [60], HepG2, Thp-1, and MDCKII cells were obtained form the ATCC (Manassas, VA). HEK293H cells were purchased from Invitrogen. Most cell lines were grown in DMEM containing 10% FCS, whereas HepG2 were cultured in DMEM and F12 (1:1) + 10% FCS medium. Thp-1 cells were maintained in RPMI + 10% FCS medium, and pretreated with 2 nM PMA for 24 h. Human monocytes were isolated from peripheral blood of healthy subjects, as previously described [61], and cultured in DMEM containing 10% FCS for 5 days. ABCA1 expression was induced in both PMA-pretreated Thp-1 cells and monocyte-derived macrophages by the addition of a synthetic LXR agonist, T0901317 (1 μM, Alexis Biochemicals) 8 h prior to studies.

Generation of cell lines stably expressing ABCA1 variants

Retroviral particles and cell lines stably expressing the ABCA1 variants were generated as described previously [25,30] with some modifications. Briefly, the Phoenix-eco packaging cell line was transfected by calcium phosphate coprecipitation (Invitrogen). The cell-free viral supernatant was collected 24 and 48 hours after transfection and immediately used to transduce PG13 cells. The transduction of PG13 cells was repeated on the following day. HEK293H and MDCKII cells were transduced with viral supernatant collected from PG13 packaging cells 24 and 48 hours after transduction. The target cells were then selected with 0.5 mg/ml and 0.8 mg/ml G418 for HEK293H and MDCKII cells, respectively. Single-cell clones of transduced MDCKII cells were isolated by limiting dilutions on 96-well plates under continuous G418 selection. In contrast, HEK293H cells were labeled with direct anti-HA antibody and sorted by a FACSAria (Becton Dickinson) cell sorter. To reduce the heterogeneity, a subsequent cell sorting was performed.

RNA isolation and real time RT-PCR

Total RNA was isolated by a single-step method using Tri-Zol (Invitrogen). The purity of the RNA preparation was checked by measuring the absorbance ratio at 260/280 nm. For each reaction 1 μg total RNA was reverse-transcribed into cDNA according to the manufacturer's proto-

col (Promega) using random hexamer oligonucleotides. The resulting cDNA was then subjected to real-time quantitative PCR (Light Cycler 480 II, Roche), 45 cycles of 95°C for 30 s, 58°C for 1 s and 72°C for 1 s by using specific primers to detect human ABCA1 cDNA, but not the genomic *ABCA1* sequence. Oligonucleotides designed for PCR analysis of ABCA1 or housekeeping Glyceraldehyde 3-phosphate dehydrogenase (GAPDH) cDNAs were: 5-ACAAGATGCTGAGGGCTGAT-3 and 5-CCCAAGACTATGCAGCAATG-3 or 5-GAAGGTGAAGGTCGGAGTCA-3 and 5-GACAAGCTTCCCGTTCTCAG-3, respectively. PCRs contained 3 mM $MgCl_2$, 0.25 μM from ABCA1 and 0.5 μM from GAPDH forward and reverse primers, and 5 μl LightCycler DNA Master SYBR Green I (2×, Roche). Before amplification, a preincubation step (60 seconds at 95°C) was performed to activate FastStart DNA polymer and to ensure complete denaturation of the cDNA. Following the last cycle, melting curve analysis was carried out to specify the integrity and purity of the amplicons. Amplification profiles were analyzed using the Fit Points and 2nd Derivative Maximum calculation described in the LightCycler Relative Quantification Software. The comparative Ct method was used to quantify transcript levels and to normalize for GAPDH expression.

Western blot analysis

Preparation of whole cell lysates and immunoblotting were performed as described previously [62] with some modifications. Cell were suspended in 2× Laemmli buffer and sonicated for 5 seconds at 4°C. 15 μg and 40 μg of protein per well from HEK293H cells and MDCKII cells, respectively, were loaded onto a Laemmli-type 6% SDS-polyacrylamide gel, separated, and blotted onto PVDF membranes. Immunodetection was performed by using an anti-HA monoclonal (HA.11, BabCo, 1:3000) or rabbit polyclonal anti-ABCA1 (Abcam, 1:250) antibodies. A HRP-conjugated goat anti-mouse or anti-rabbit IgG secondary antibody (Jackson Immunoresearch, 1:10.000), and enhanced chemiluminescence (ECL) technique was applied. For loading control, a mouse anti-Na^+/K^+ ATPase antibody (BioMol, 1:1000) was used.

Confocal microscopy

For immunolocalization studies, HEK293H cells were seeded onto eight-well Lab-Tek II Chambered Coverglass (Nalge Nunc) at 5×10^4 per well cell density, and grown for 2 days. For plasma membrane staining, the cells were gently fixed with 1% paraformaldehyde (PFA) for 5 min at room temperature, and incubated with 5 μg/ml AlexaFluor633-conjugated wheat germ agglutinin (WGA, Invitrogen) for 10 min at room temperature. For lysosome staining, the living cells were subjected to LysoTracker Red (Invitrogen) in culturing medium for 30 min at 37°C. After marker staining the cells were fixed and permeabilized with 8% PFA for 15 min at room temperature, and labeled with anti-HA (HA.11, MMS-101R BabCo, 1:500) antibody. To label the Golgi-apparatus and endosomes, double-labeling was performed using rabbit anti-Giantin (Abcam, 1:500) and anti-EEA1 antibodies (1:250), respectively, as described previously [61]. For secondary antibodies AlexaFluor-488-conjugated anti-mouse IgG and AlexaFluor-594-conjugated anti-rabbit IgG antibodies (Invitrogen, 1:250) were used. After immunolabeling the samples were counterstained with 1 μM DAPI for 10 min at room temperature.

For subcellular localization studies in polarized cells, the MDCKII cells were seeded at 5×10^5 cells/cm^2 density on 6.5-mm Transwell Col filters (pore diameter 0.4, Corning Costar) previously coated with 0.03 mg/ml Vitrogen (Cohesion Technologies). The cultures were regularly washed with culturing medium to remove cell debris. Studies were carried out with confluent cultures 10 days after seeding. The cultures were permeabilized and labeled with anti-HA (HA.11, MMS-101R BabCo, 1:500) and anti-Na^+/K^+ ATPase (Abcam, 1:250) antibodies, as previously described [61]. AlexaFluor-488-conjugated anti-mouse IgG and AlexaFluor-647-conjugated anti-chicken IgG secondary antibodies (Invitrogen, 1:250) were used.

The blue, green, red and far red fluorescence of stained samples was studied by an Olympus FV500-IX confocal laser scanning microscope using a PLAPO 60× (1.4) oil immersion objective (Olympus) at 405, 488, 543, and 633 nm excitations.

Cholesterol efflux measurement

Cholesterol efflux measurement was performed as described previously [34]. Briefly, near confluent HEK293H and non-polarized MDCKII cultures grown on 6 well plates were labeled with 100 nM (4 μCi/ml) ^{3}H-cholesterol (PerkinElmer) at 37°C for 24 hours in serum-free DMEM containing 2 mg/ml fatty acid free BSA. The media were then replaced with fresh DMEM/BSA in the presence or absence of 15 μg/ml of apoA-I and incubated at 37°C for 24 hours. Supernatants were collected and spun down to remove cellular material. The pellets and the cell layers were lysed in 2% SDS and 1 M NaOH. The radioactivity of both samples was measured by liquid scintillation; the cholesterol efflux was expressed as the percentage of total (extruded plus cellular) ^{3}H-cholesterol. The apoA-I-dependent efflux was obtained from the difference of the effluxes measured in the presence and absence of apoA-I.

Cell surface expression studies

For cell surface expression studies, the cells were detached by trypsinization and after washing steps blocked for 10 min at room temperature in phosphate-buffered saline

containing 2 mg/ml bovine serum albumin (BSA/PBS). The samples were then incubated for 40 min at room temperature with anti-HA antibody (HA.11, MMS-101R BabCo, 1:250 in BSA/PBS). After subsequent washing steps AlexaFluor-488-conjugated anti-mouse IgG secondary antibody (Invitrogen, 1:500 in BSA/PBS) was applied for 40 min at room temperature. As an isotype control a mouse IgG1 (1:10) from Sigma-Aldrich was used. The cell surface expression of the HA-ABCA1 variants was detected by flow cytometry (Becton Dickinson FACS Calibur).

When the modifying effect of various drugs was studied, the cells in the culture dish were pretreated for 4 hours with the following substances: 50 μM ALLN, 10 μg/ml apoA-I (Calbiochem), 10-50 μM atorvastatin (Pfizer), 5 μg/ml BFA, 10-50 μM ezetimibe (Schering-Plough), 0.1-1 mM niacin, 10-50 μM verapamil, 30-100 μM nifedipine, 50-500 μM glyburide, 10-50 μM cyclosporin A, 100 μg/ml cycloheximide, 0.1-2.5 mM random methylated beta cyclodextrin (CD, CycloLab), or 0.1-2.5 mM CD preloaded with 4.4% cholesterol (CycloLab). The materials were obtained from Sigma-Aldrich if not indicated otherwise. After treatment, cells were trypsinized, prestained for 2 min with 10 mg/ml propidium-iodide, and gently fixed with PFA for 10 min. Immunofluorescent staining of drug-treated cells was performed at 4 C. Relative expression levels were expressed as the ratio of geometric mean fluorescence of drug-treated and the vehicle-treated samples. For statistical analysis Student's t test was used.

ApoA-I binding

ApoA-I conjugation and binding-experiments were performed as described previously [28] with minor modifications. Briefly, apoA-I was conjugated to the fluorochrome Cy5 (PA25001, Amersham Pharmacia Biotech) according to the recommendation of the manufacturer. For all experiments the labeled apoA-I (apoA-I-Cy5) was diluted in binding buffer (1.8 mM $CaCl_2$, 1 mM $MgCl_2$, 5 mM KCl, 150 mM NaCl, 10 mM HEPES, pH 7.4), and aggregates were removed by ultracentrifugation for 30 min at 100,000 g. Binding was performed in the presence of 20 μg/ml of apoA-I-Cy5 for 1 h at 4°C on 5×10^5 cells detached by trypsinization. After the incubation, cells were rapidly washed and not fixed with 1% PFA. For studying the effect of ALLN and CsA, the cells were pretreated with same concentrations of drugs as in the cell surface expression studies. After incubation for 4 hours cells were washed and apoA-I binding experiment was performed. The apoA-I binding was detected by flow cytometry (Becton Dickinson FACS Calibur) and analyzed by CellQuest Pro software. Binding data are calculated from the median of apoA-I-Cy5 fluorescence intensity.

Authors' contributions

IK participated in generation of HA-ABCA1 variant plasmid constructs and retroviral transduction processes of HEK293H cells; carried out characterization of cell lines and cell surface expression studies by flow cytometry; as well as contributed to manuscript preparation. ZH participated in generation of plasmid constructs; prepared MDCKII cell lines expressing HA-ABCA1 variants; carried out the Western blot analysis and cholesterol efflux measurements. KSZ coordinated the retroviral transduction process, immunofluorescent labeling, and flow cytometry studies; generated plasmids and performed cholesterol efflux measurements. HA participated in design of plasmid constructs, carried out plasmid sequencing. KN participated in design and coordination of the retroviral transduction work. AV and BS participated in design and coordination of the study and helped in manuscript preparation. LH contributed to the design and coordination of the study, coordinated immunofluorescent staining and carried out confocal microscopy studies, as well as participated in manuscript preparation.

Acknowledgements

The authors thank Dr. Olga Újhellyi, Dr. Attila Iliás, Dr János Éles, and Dr. György Váradi for their support and advices; Mónika Bátkai, Gyöngyi Bézsenyi, Judit Kiss, Zsuzsanna Andrási and Györgyi Vermes for the perfect technical assistance. This work was supported by research grants from the OTKA (K68936, T38337).

References

1. Boden WE: **High-density lipoprotein cholesterol as an independent risk factor in cardiovascular disease: assessing the data from Framingham to the Veterans Affairs High--Density Lipoprotein Intervention Trial.** *Am J Cardiol* 2000, **86:**19L-22L.
2. Fielding CJ, Fielding PE: **Molecular physiology of reverse cholesterol transport.** *J Lipid Res* 1995, **36:**211-228.
3. Oram JF, Lawn RM: **ABCA1. The gatekeeper for eliminating excess tissue cholesterol.** *J Lipid Res* 2001, **42:**1173-1179.
4. Srivastava N: **ATP binding cassette transporter A1--key roles in cellular lipid transport and atherosclerosis.** *Mol Cell Biochem* 2002, **237:**155-164.
5. Oram JF: **ATP-binding cassette transporter A1 and cholesterol trafficking.** *Curr Opin Lipidol* 2002, **13:**373-381.
6. Oram JF: **Molecular basis of cholesterol homeostasis: lessons from Tangier disease and ABCA1.** *Trends Mol Med* 2002, **8:**168-173.
7. Schmitz G, Langmann T: **Structure, function and regulation of the ABC1 gene product.** *Curr Opin Lipidol* 2001, **12:**129-140.
8. Brunham LR, Kruit JK, Iqbal J, Fievet C, Timmins JM, Pape TD, Coburn BA, Bissada N, Staels B, Groen AK, Hussain MM, Parks JS, Kuipers F, Hayden MR: **Intestinal ABCA1 directly contributes to HDL biogenesis in vivo.** *J Clin Invest* 2006, **116:**1052-1062.
9. Schachter M: **Strategies for modifying high-density lipoprotein cholesterol: a role for nicotinic acid.** *Cardiovasc Drugs Ther* 2005, **19:**415-422.
10. **Executive Summary of The Third Report of The National Cholesterol Education Program (NCEP) Expert Panel on Detection, Evaluation, And Treatment of High Blood Cholesterol In Adults (Adult Treatment Panel III).** *Jama* 2001, **285:**2486-2497.
11. Bays HE, Neff D, Tomassini JE, Tershakovec AM: **Ezetimibe: cholesterol lowering and beyond.** *Expert Rev Cardiovasc Ther* 2008, **6:**447-470.
12. Argmann CA, Edwards JY, Sawyez CG, O'Neil CH, Hegele RA, Pickering JG, Huff MW: **Regulation of macrophage cholesterol**

efflux through hydroxymethylglutaryl-CoA reductase inhibition: a role for RhoA in ABCA1-mediated cholesterol efflux. *J Biol Chem* 2005, **280:**22212-22221.
13. Sone H, Shimano H, Shu M, Nakakuki M, Takahashi A, Sakai M, Sakamoto Y, Yokoo T, Matsuzaka K, Okazaki H, Nakagawa Y, Iida KT, Suzuki H, Toyoshima H, Horiuchi S, Yamada N: **Statins downregulate ATP-binding-cassette transporter A1 gene expression in macrophages.** *Biochem Biophys Res Commun* 2004, **316:**790-794.
14. Wong J, Quinn CM, Brown AJ: **Statins inhibit synthesis of an oxysterol ligand for the liver x receptor in human macrophages with consequences for cholesterol flux.** *Arterioscler Thromb Vasc Biol* 2004, **24:**2365-2371.
15. Wong J, Quinn CM, Gelissen IC, Jessup W, Brown AJ: **The effect of statins on ABCA1 and ABCG1 expression in human macrophages is influenced by cellular cholesterol levels and extent of differentiation.** *Atherosclerosis* 2008, **196:**180-189.
16. Martin G, Duez H, Blanquart C, Berezowski V, Poulain P, Fruchart JC, Najib-Fruchart J, Glineur C, Staels B: **Statin-induced inhibition of the Rho-signaling pathway activates PPARalpha and induces HDL apoA-I.** *J Clin Invest* 2001, **107:**1423-1432.
17. Mancini GB: **Antiatherosclerotic effects of calcium channel blockers.** *Prog Cardiovasc Dis* 2002, **45:**1-20.
18. Waters D, Lesperance J: **Calcium channel blockers and coronary atherosclerosis: from the rabbit to the real world.** *Am Heart J* 1994, **128:**1309-1316.
19. Suzuki S, Nishimaki-Mogami T, Tamehiro N, Inoue K, Arakawa R, Abe-Dohmae S, Tanaka AR, Ueda K, Yokoyama S: **Verapamil increases the apolipoprotein-mediated release of cellular cholesterol by induction of ABCA1 expression via Liver X receptor-independent mechanism.** *Arterioscler Thromb Vasc Biol* 2004, **24:**519-525.
20. Hasegawa K, Wakino S, Kanda T, Yoshioka K, Tatematsu S, Homma K, Takamatsu I, Sugano N, Hayashi K: **Divergent action of calcium channel blockers on ATP-binding cassette protein expression.** *J Cardiovasc Pharmacol* 2005, **46:**787-793.
21. Kaminski WE, Piehler A, Wenzel JJ: **ABC A-subfamily transporters: structure, function and disease.** *Biochim Biophys Acta* 2006, **1762:**510-524.
22. Schmitz G, Liebisch G, Langmann T: **Lipidomic strategies to study structural and functional defects of ABC-transporters in cellular lipid trafficking.** *FEBS Lett* 2006, **580:**5597-5610.
23. Lorenzi I, von Eckardstein A, Cavelier C, Radosavljevic S, Rohrer L: **Apolipoprotein A-I but not high-density lipoproteins are internalised by RAW macrophages: roles of ATP-binding cassette transporter A1 and scavenger receptor BI.** *J Mol Med* 2008, **86:**171-183.
24. Smith JD, Le Goff W, Settle M, Brubaker G, Waelde C, Horwitz A, Oda MN: **ABCA1 mediates concurrent cholesterol and phospholipid efflux to apolipoprotein A-I.** *J Lipid Res* 2004, **45:**635-644.
25. Albrecht C, McVey JH, Elliott JI, Sardini A, Kasza I, Mumford AD, Naoumova RP, Tuddenham EG, Szabo K, Higgins CF: **A novel missense mutation in ABCA1 results in altered protein trafficking and reduced phosphatidylserine translocation in a patient with Scott syndrome.** *Blood* 2005, **106:**542-549.
26. Tanaka AR, Ikeda Y, Abe-Dohmae S, Arakawa R, Sadanami K, Kidera A, Nakagawa S, Nagase T, Aoki R, Kioka N, Amachi T, Yokoyama S, Ueda K: **Human ABCA1 contains a large amino-terminal extracellular domain homologous to an epitope of Sjogren's Syndrome.** *Biochem Biophys Res Commun* 2001, **283:**1019-1025.
27. Hamon Y, Broccardo C, Chambenoit O, Luciani MF, Toti F, Chaslin S, Freyssinet JM, Devaux PF, McNeish J, Marguet D, Chimini G: **ABC1 promotes engulfment of apoptotic cells and transbilayer redistribution of phosphatidylserine.** *Nat Cell Biol* 2000, **2:**399-406.
28. Chambenoit O, Hamon Y, Marguet D, Rigneault H, Rosseneu M, Chimini G: **Specific docking of apolipoprotein A-I at the cell surface requires a functional ABCA1 transporter.** *J Biol Chem* 2001, **276:**9955-9960.
29. Wang N, Silver DL, Thiele C, Tall AR: **ATP-binding cassette transporter A1 (ABCA1) functions as a cholesterol efflux regulatory protein.** *J Biol Chem* 2001, **276:**23742-23747.
30. Ujhelly O, Ozvegy C, Varady G, Cervenak J, Homolya L, Grez M, Scheffer G, Roos D, Bates SE, Varadi A, Sarkadi B, Nemet K: **Application of a human multidrug transporter (ABCG2) variant as selectable marker in gene transfer to progenitor cells.** *Hum Gene Ther* 2003, **14:**403-412.
31. Alder-Baerens N, Muller P, Pohl A, Korte T, Hamon Y, Chimini G, Pomorski T, Herrmann A: **Headgroup-specific exposure of phospholipids in ABCA1-expressing cells.** *J Biol Chem* 2005, **280:**26321-26329.
32. Ohama T, Hirano K, Zhang Z, Aoki R, Tsujii K, Nakagawa-Toyama Y, Tsukamoto K, Ikegami C, Matsuyama A, Ishigami M, Sakai N, Hiraoka H, Ueda K, Yamashita S, Matsuzawa Y: **Dominant expression of ATP-binding cassette transporter-1 on basolateral surface of Caco-2 cells stimulated by LXR/RXR ligands.** *Biochem Biophys Res Commun* 2002, **296:**625-630.
33. Bortnick AE, Rothblat GH, Stoudt G, Hoppe KL, Royer LJ, McNeish J, Francone OL: **The correlation of ATP-binding cassette 1 mRNA levels with cholesterol efflux from various cell lines.** *J Biol Chem* 2000, **275:**28634-28640.
34. Wang N, Silver DL, Costet P, Tall AR: **Specific binding of ApoA-I, enhanced cholesterol efflux, and altered plasma membrane morphology in cells expressing ABC1.** *J Biol Chem* 2000, **275:**33053-33058.
35. Martinez LO, Agerholm-Larsen B, Wang N, Chen W, Tall AR: **Phosphorylation of a pest sequence in ABCA1 promotes calpain degradation and is reversed by ApoA-I.** *J Biol Chem* 2003, **278:**37368-37374.
36. Arakawa R, Yokoyama S: **Helical apolipoproteins stabilize ATP-binding cassette transporter A1 by protecting it from thiol protease-mediated degradation.** *J Biol Chem* 2002, **277:**22426-22429.
37. Wang N, Chen W, Linsel-Nitschke P, Martinez LO, Agerholm-Larsen B, Silver DL, Tall AR: **A PEST sequence in ABCA1 regulates degradation by calpain protease and stabilization of ABCA1 by apoA-I.** *J Clin Invest* 2003, **111:**99-107.
38. Le Goff W, Peng DQ, Settle M, Brubaker G, Morton RE, Smith JD: **Cyclosporin A traps ABCA1 at the plasma membrane and inhibits ABCA1-mediated lipid efflux to apolipoprotein A-I.** *Arterioscler Thromb Vasc Biol* 2004, **24:**2155-2161.
39. Neufeld EB, Remaley AT, Demosky SJ, Stonik JA, Cooney AM, Comly M, Dwyer NK, Zhang M, Blanchette-Mackie J, Santamarina-Fojo S, Brewer HB Jr: **Cellular localization and trafficking of the human ABCA1 transporter.** *J Biol Chem* 2001, **276:**27584-27590.
40. Schwartz GG, Olsson AG, Ezekowitz MD, Ganz P, Oliver MF, Waters D, Zeiher A, Chaitman BR, Leslie S, Stern T: **Effects of atorvastatin on early recurrent ischemic events in acute coronary syndromes: the MIRACL study: a randomized controlled trial.** *Jama* 2001, **285:**1711-1718.
41. Pedersen TR, Faergeman O, Kastelein JJ, Olsson AG, Tikkanen MJ, Holme I, Larsen ML, Bendiksen FS, Lindahl C, Szarek M, Tsai J: **High-dose atorvastatin vs usual-dose simvastatin for secondary prevention after myocardial infarction: the IDEAL study: a randomized controlled trial.** *Jama* 2005, **294:**2437-2445.
42. Davidson MH, McGarry T, Bettis R, Melani L, Lipka LJ, LeBeaut AP, Suresh R, Sun S, Veltri EP: **Ezetimibe coadministered with simvastatin in patients with primary hypercholesterolemia.** *J Am Coll Cardiol* 2002, **40:**2125-2134.
43. Guyton JR, Brown BG, Fazio S, Polis A, Tomassini JE, Tershakovec AM: **Lipid-altering efficacy and safety of ezetimibe/simvastatin coadministered with extended-release niacin in patients with type IIa or type IIb hyperlipidemia.** *J Am Coll Cardiol* 2008, **51:**1564-1572.
44. Kerzner B, Corbelli J, Sharp S, Lipka LJ, Melani L, LeBeaut A, Suresh R, Mukhopadhyay P, Veltri EP: **Efficacy and safety of ezetimibe coadministered with lovastatin in primary hypercholesterolemia.** *Am J Cardiol* 2003, **91:**418-424.
45. Sudhop T, Lutjohann D, Kodal A, Igel M, Tribble DL, Shah S, Perevozskaya I, von Bergmann K: **Inhibition of intestinal cholesterol absorption by ezetimibe in humans.** *Circulation* 2002, **106:**1943-1948.
46. Nieland TJ, Chroni A, Fitzgerald ML, Maliga Z, Zannis VI, Kirchhausen T, Krieger M: **Cross-inhibition of SR-BI- and ABCA1-mediated cholesterol transport by the small molecules BLT-4 and glyburide.** *J Lipid Res* 2004, **45:**1256-1265.
47. Telbisz A, Muller M, Ozvegy-Laczka C, Homolya L, Szente L, Varadi A, Sarkadi B: **Membrane cholesterol selectively modulates the activity of the human ABCG2 multidrug transporter.** *Biochim Biophys Acta* 2007, **1768:**2698-2713.

48. Attie AD: **ABCA1: at the nexus of cholesterol, HDL and atherosclerosis.** *Trends Biochem Sci* 2007, **32:**172-179.
49. Asztalos BF, Horvath KV, McNamara JR, Roheim PS, Rubinstein JJ, Schaefer EJ: **Comparing the effects of five different statins on the HDL subpopulation profiles of coronary heart disease patients.** *Atherosclerosis* 2002, **164:**361-369.
50. Zanotti I, Favari E, Sposito AC, Rothblat GH, Bernini F: **Pitavastatin increases ABCA1-mediated lipid efflux from Fu5AH rat hepatoma cells.** *Biochem Biophys Res Commun* 2004, **321:**670-674.
51. Rubic T, Trottmann M, Lorenz RL: **Stimulation of CD36 and the key effector of reverse cholesterol transport ATP-binding cassette A1 in monocytoid cells by niacin.** *Biochem Pharmacol* 2004, **67:**411-419.
52. Bacso Z, Nagy H, Goda K, Bene L, Fenyvesi F, Matko J, Szabo G: **Raft and cytoskeleton associations of an ABC transporter: P-glycoprotein.** *Cytometry A* 2004, **61:**105-116.
53. Orlowski S, Martin S, Escargueil A: **P-glycoprotein and 'lipid rafts': some ambiguous mutual relationships (floating on them, building them or meeting them by chance?).** *Cell Mol Life Sci* 2006, **63:**1038-1059.
54. Hui DY, Labonte ED, Howles PN: **Development and physiological regulation of intestinal lipid absorption. III. Intestinal transporters and cholesterol absorption.** *Am J Physiol Gastrointest Liver Physiol* 2008, **294:**G839-843.
55. During A, Dawson HD, Harrison EH: **Carotenoid transport is decreased and expression of the lipid transporters SR-BI, NPC1L1, and ABCA1 is downregulated in Caco-2 cells treated with ezetimibe.** *J Nutr* 2005, **135:**2305-2312.
56. Neufeld EB, Stonik JA, Demosky SJ Jr, Knapper CL, Combs CA, Cooney A, Comly M, Dwyer N, Blanchette-Mackie J, Remaley AT, Santamarina-Fojo S, Brewer HB Jr: **The ABCA1 transporter modulates late endocytic trafficking: insights from the correction of the genetic defect in Tangier disease.** *J Biol Chem* 2004, **279:**15571-15578.
57. Szakacs G, Langmann T, Ozvegy C, Orso E, Schmitz G, Varadi A, Sarkadi B: **Characterization of the ATPase cycle of human ABCA1: implications for its function as a regulator rather than an active transporter.** *Biochem Biophys Res Commun* 2001, **288:**1258-1264.
58. Becker S, Wasser S, Hauses M, Hossle JP, Ott MG, Dinauer MC, Ganser A, Hoelzer D, Seger R, Grez M: **Correction of respiratory burst activity in X-linked chronic granulomatous cells to therapeutically relevant levels after gene transfer into bone marrow CD34+ cells.** *Hum Gene Ther* 1998, **9:**1561-1570.
59. Pear WS, Nolan GP, Scott ML, Baltimore D: **Production of high-titer helper-free retroviruses by transient transfection.** *Proc Natl Acad Sci USA* 1993, **90:**8392-8396.
60. Miller AD, Garcia JV, von Suhr N, Lynch CM, Wilson C, Eiden MV: **Construction and properties of retrovirus packaging cells based on gibbon ape leukemia virus.** *J Virol* 1991, **65:**2220-2224.
61. Seres L, Cserepes J, Elkind NB, Torocsik D, Nagy L, Sarkadi B, Homolya L: **Functional ABCG1 expression induces apoptosis in macrophages and other cell types.** *Biochim Biophys Acta* 2008, **1778:**2378-2387.
62. Sarkadi B, Price EM, Boucher RC, Germann UA, Scarborough GA: **Expression of the human multidrug resistance cDNA in insect cells generates a high activity drug-stimulated membrane ATPase.** *J Biol Chem* 1992, **267:**4854-4858.

dc_46_10

11. sz. közlemény

dc_46_10

Physiol Rev 86: 1179–1236, 2006;
doi:10.1152/physrev.00037.2005.

Human Multidrug Resistance ABCB and ABCG Transporters: Participation in a Chemoimmunity Defense System

BALÁZS SARKADI, LÁSZLÓ HOMOLYA, GERGELY SZAKÁCS, AND ANDRÁS VÁRADI

National Medical Center, Institute of Hematology and Immunology, Membrane Research Group, and Institute of Enzymology, Hungarian Academy of Sciences, Budapest, Hungary

Sarkadi, Balázs, László Homolya, Gergely Szakács, and András Váradi. Human Multidrug Resistance ABCB and ABCG Transporters: Participation in a Chemoimmunity Defense System. *Physiol Rev* 86: 1179–1236, 2006; doi:10.1152/physrev.00037.2005.—In this review we give an overview of the physiological functions of a group of ATP binding cassette (ABC) transporter proteins, which were discovered, and still referred to, as multidrug resistance (MDR) transporters. Although they indeed play an important role in cancer drug resistance, their major physiological function is to provide general protection against hydrophobic xenobiotics. With a highly conserved structure, membrane topology, and mechanism of action, these essential transporters are preserved throughout all living systems, from bacteria to human. We describe the general structural and mechanistic features of the human MDR-ABC transporters and introduce some of the basic methods that can be applied for the analysis of their expression, function, regulation, and modulation. We treat in detail the biochemistry, cell biology, and physiology of the ABCB1 (MDR1/P-glycoprotein) and the ABCG2 (MXR/BCRP) proteins and describe emerging information related to additional ABCB- and ABCG-type transporters with a potential role in drug and xenobiotic resistance. Throughout this review we demonstrate and emphasize the general network characteristics of the MDR-ABC transporters, functioning at the cellular and physiological tissue barriers. In

addition, we suggest that multidrug transporters are essential parts of an innate defense system, the "chemoimmunity" network, which has a number of features reminiscent of classical immunology.

I. INTRODUCTION: MULTIDRUG/XENOBIOTIC RESISTANCE AND ABC TRANSPORTERS

The so-called "multidrug resistance" proteins were discovered as membrane transporters producing chemotherapy resistance in cancer. In the mid to late 1970s, clinical oncologists realized that certain tumors show an inherent resistance pattern, while others develop resistance during the course of the treatment against a number of otherwise highly efficient chemotherapeutic compounds. Moreover, when tumor resistance developed against a single particular chemotherapeutic agent, in many cases the resulting phenotype involved a wide-range (or multi-)drug resistance pattern. Biochemists, molecular biologists, and cell biologists in the last 30 years clearly established that this phenomenon is due to the expression of plasma membrane "pumps," which actively extrude various cytotoxic agents from cancer cells. Upregulation of pump expression and/or selection of resistant cancer cells thus result in cancer multidrug resistance, which extends to the diverse substrates of these transporters (for the first description of cancer "drug pumps," see Refs. 71 and 164).

Multidrug resistance transporters belong to the evolutionarily conserved family of the ATP binding cassette (ABC) proteins, present in practically all living organisms from prokaryotes to mammals. ABC transporters are large, membrane-bound proteins, built from a combination of characteristic domains, including membrane-spanning regions and cytoplasmic ATP-binding domains (see sect. II).

In humans, the three major types of multidrug resistance (MDR) proteins include members of the ABCB (ABCB1/MDR1/P-glycoprotein), the ABCC (ABCC1/MRP1, ABCC2/MRP2, probably also ABCC3–6, and ABCC10–11), and the ABCG (ABCG2/MXR/BCRP) subfamily. On the basis of a great deal of clinical and experimental work, it has been established that these pumps recognize a very wide range of drug substrates. Although recognized substrates are mostly hydrophobic compounds, MDR pumps are also capable to extrude a variety of amphipathic anions and cations. As discussed in detail below, ABCB1 preferentially extrudes large hydrophobic molecules, while ABCC1 and ABCG2 can transport both hydrophobic drugs and large anionic compounds, e.g., drug conjugates (Fig. 1). This "promiscuous" character, and the additional overlapping substrate recognition by the three major classes of the MDR-ABC transporters, provide an amazing network of drug resistance capacity in cancer cells.

Of course, these multidrug transporters did not evolve to protect cancer cells from medical interventions. In contrast, they are only co-opted and "misused" by the rapidly dividing cancer cells, especially when a population of malignant cells overexpressing an MDR-ABC transporter is selected by drug treatment. With regard to their physiological role, MDR-ABC transporters most probably evolved as complex cellular defense systems, for the recognition and the energy-dependent removal of toxic agents entering the living cells or organisms from their environment. In this review we document the wide variety of cellular functions that involve multidrug transporters. In addition, we put forward a general concept to suggest that the key physiological task of the MDR-ABC transporter network is to provide general xenobiotic resistance.

We also describe the general structural and mechanistic features of the MDR-ABC transporters and introduce some of the basic methods that can be applied for the analysis of their expression, function, regulation, and modulation. We treat in detail the biochemistry, cell biology, and physiological aspects of the ABCB1 (MDR1/P-glycoprotein) and the ABCG2 (MXR/BCRP) proteins, while a detailed description of the ABCC (MRP) group of transporters is provided by the review of Deeley et al. (73). We also mention here emerging information related to additional ABC transporters with a potential role in drug and xenobiotic resistance and provide a general picture about key aspects of their cellular regulation.

Throughout this review, although biased in focusing on selected human ABC proteins, we demonstrate and emphasize the general network characteristics of the multidrug transporters, functioning at cellular and physiological tissue barriers. We try to provide a new framework for the appreciation of their role in physiological defense against chemicals, by suggesting that multidrug transporters are essential parts of an immune-like defense system. This cellular antitoxic network provides a "chemoimmunity," having a number of features reminiscent of innate immunology.

Thus physiology, biochemistry, pharmacology, and toxicology aspects inherently overlap in the present review. We certainly hope that, in addition to a detailed characterization of these transport systems, we will be able to convince the readers about the validity of a general concept that we hope will further our understanding of these multidrug transporter proteins of outstanding medical importance.

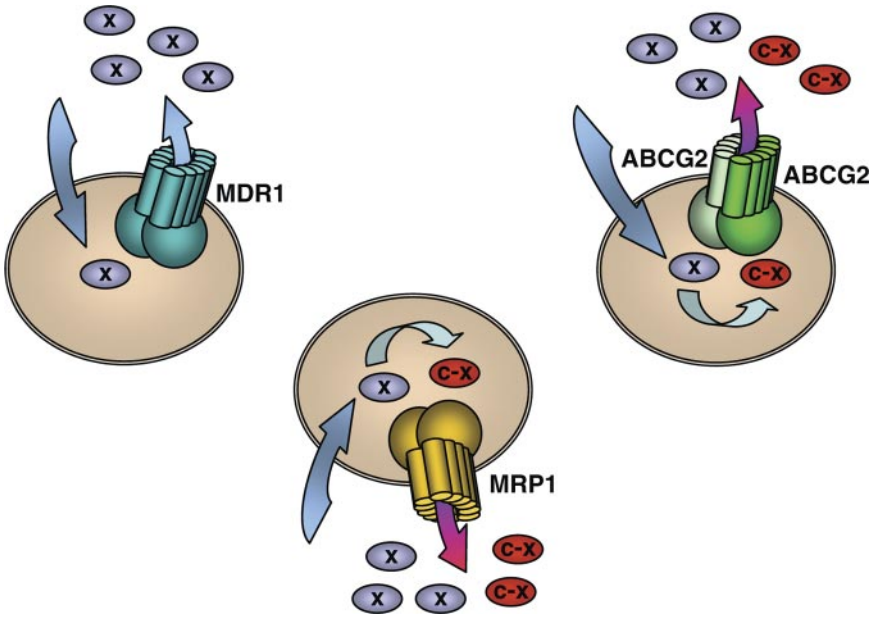

FIG. 1. Function of the multidrug/xenobiotic ABC transporters. Multidrug/xenobiotic ABC transporters reside in the plasma membrane and extrude various hydrophobic and/or amphipatic xenobiotics and metabolic products. MDR1/Pgp transports hydrophobic compounds (X), while MRP1 and ABCG2 can extrude both hydrophobic drugs and intracellularly formed metabolites, e.g., glutathione or glucuronide conjugates (C-X).

II. GENERAL STRUCTURE AND MECHANISM OF ACTION OF MDR-ABC TRANSPORTERS

A. Basic Features of the ABC Transporters

1. Conserved domains, structural motifs, and catalytic mechanism

ABC proteins have been identified in each genome sequenced, and they typically form large families with 30–100 members in various organisms. ABC proteins are named after a conserved, specific ABC domain (140), a 200- to 250-amino acid globular protein unit, which can bind and hydrolyze ATP. The ABC unit (also called nucleotide binding domain or NBD) harbors several conserved sequence motifs. From NH_2 to COOH terminal, these are the Walker A (P-loop), a glycine-rich sequence; a conserved glutamine (Q-loop), the family-specific ABC-signature (LSGGQ) motif (also called the C-loop), the Walker B motif, and a conserved His (His-switch). The ABC-signature motif is diagnostic for the family as it is present only in ABC proteins, while Walker A and B motifs are found in many other ATP-utilizing proteins (396).

ABC transporters also contain transmembrane domains (TMD), composed in most cases of six membrane-spanning helices. In archea and in prokaryotes, the ABC and the transmembrane domains are often encoded by separate genes within the same operon, while in some cases a single gene contains the TMD fused to an ABC unit. In bacteria these proteins either function as importers of essential compounds, or they export materials from the cell or lipids into the outer leaflet of the membrane. In eukaryotes, most active ABC transporters export compounds from the cytosol to the outside of the cell, or move molecules into intracellular organelles, like the endoplasmic reticulum, or the peroxisome. The human (mammalian) xenobiotic transporters discussed in this review are all export pumps, predominantly residing in the plasma membrane.

The multidrug/xenobiotic resistance (MDR) ABC proteins are primary active transporters, since they utilize the energy of cellular ATP for the promotion of vectorial, transmembrane movement of drugs or xenobiotics. These ATP hydrolytic enzymes (ATPases) interact with two different types of substrates. The energy donor substrate is the intracellular MgATP complex, and the chemical energy for the active transport of substrates is provided by binding and hydrolysis of ATP within the ABC units. In contrast to P-type ATPases, in MDR-ABC proteins ATP hydrolysis does not involve covalent phosphorylation. The end products of the hydrolysis are intracellular ADP and inorganic phosphate (for recent reviews, see Refs. 13, 34, 48, 102, 118, 123, 156, 210, 213, 300, 313, 322, 331, 389). Based on this molecular mechanism of action, the catalytic and transport properties of MDR-ABC transporters are significantly different from those of the P-type ATPases. Since these data are best provided for the MDR1/P-glycoprotein (Pgp) transporter, we discuss these issues in section IV.

In all MDR-ABC transporters, the sites interacting with the transported substrates are most probably located within the TMDs. It seems likely that a minimum of 12 membrane-spanning helices are required to ensure the complex reaction with the transported substrates. In a phenomenological sense, the transported substrates are bound to intracellular (or in some cases probably intramembrane), high-affinity "on" sites and are unloaded at extracellular, low-affinity "off" sites. However, all recent

structural studies indicate a relatively large drug binding pocket within the transmembrane regions of the MDR-ABC proteins (see Refs. 48, 50, 156, 213). The molecular link, transmitting intramolecular signals between the TMDs and the ABCs, that is the substrate binding area and the catalytic machinery, respectively, is still unidentified.

These basic catalytic and active transport features of MDR-ABC transporters have been documented in numerous expression and isolation/reconstitution systems, although the exact binding sites, as well as the energetics and thermodynamics ("uphill" or "downhill" nature) of the transport processes are difficult to estimate. As detailed in this review, many of the transported substrates are hydrophobic molecules, which are concentrated in the membranes, while they have only minimum solubility either in the cytoplasmic or extracellular water phase. Therefore, the classical solute concentration ratios or electrochemical potential gradients cannot be fully appreciated, and even the stoichiometry of the transport and ATP cleavage is difficult to determine. Moreover, it is often questionable if a given molecule is a transported substrate, an inhibitor, or a transport modulator (see sect. IV). In the respective sections we discuss some of the details of the energetics and substrate recognition of individual MDR-ABC transporters.

The main subjects of this review are the human ATP-driven ABC transporter proteins, which can act as xenobiotic exporters. However, there are several membrane-associated human ABC proteins with predominant channel- or even receptor-type functions, which share common structural and regulatory features with the active drug transporters. While active ABC transporters hydrolyze ATP in close coupling with the transmembrane movement of a substrate molecule, channels and receptors use the ATP binding domains mostly for the regulation of opening and/or closing pathways, allowing the passage of ions or conveying information through the membrane. Among the human ABC transporters, well-characterized proteins carrying out such functions are ABCC7/CFTR, ABCC8/SUR1, and ABCC9/SUR2.

The ABCC7/CFTR protein forms a chloride ion channel, in which opening and closing is regulated by the binding of ATP, and by a subsequent, relatively slow ATP hydrolysis. Here the driving force of the chloride ion movement is the electrochemical potential gradient, and the ion movement has no stoichiometric relationship with ATP hydrolysis by the CFTR (for recent reviews, see Refs. 99, 142, 286, 391). The sulfonylurea receptors (ABCC8 and -9 or SUR1 and SUR2, respectively) work as regulatory subunits of ATP-dependent potassium channels in the insulin-producing beta cells of the pancreas, and in the heart, respectively. The SUR/K_{ATP} channel tetramer, formed by ABCC protein/Kir6.x heterodimer units, is activated by ADP and inhibited by ATP; therefore, the SUR subunit serves as an ADP/ATP sensor that "translates" cellular metabolic changes into alterations of the membrane potential. Again, ATP hydrolysis is very slow in this protein complex (38, 233, 324).

2. Composition and membrane topology of human MDR-ABC transporters

According to a general consensus, all functionally active ABC transporters contain a minimum of two ABC units and two TMDs. These four elements in many cases are present in one single polypeptide chain, called "full transporters," like the MDR1/Pgp/ABCB1 protein. In contrast, "half-transporters," such as the members of the ABCG family, possess only a single ABC and a single TMD. Half-transporters must form homodimers or heterodimers to generate a functional ABC transporter.

The human genome encodes 48 (according to some databases, 49) ABC proteins. Their amino acid sequence alignments revealed that these proteins can be grouped into seven subfamilies, from A to G. The proteins relevant in multidrug transport are depicted in Figure 2A. With the comparison of the individual members, sequence identity/similarity of the ABC units is generally higher than that of the TMDs. However, each subfamily is characterized by typical and somewhat different membrane topology patterns. There are no high-resolution structural data available for any of the eukaryotic ABC transporters; therefore; combination of computer-assisted prediction methods, biochemical experimental data, and model building has been used to establish the position and orientation of the transmembrane segments within the polypeptide chain.

To elucidate the structural properties of ABC transporters, the biochemical arsenal includes epitope insertion, localization of *N*-glycosylation sites, generation of new *N*-glycosylation sites, limited proteolysis, and chemical cross-linking experiments. These experimental data are detailed in the relevant sections, discussing the human MDR-ABC transporters.

As a short summary, members of the ABCA subfamily are "full transporters" with the domain arrangement of TMD1-ABC1-TMD2-ABC2. The TMDs in this family contain very large extracellular loops with numerous glycosylation sites. The ABCB subfamily consists of three full transporters (including MDR1/Pgp/ABCB1) with the domain arrangement of TMD1-ABC1-TMD2-ABC2, and seven TMD-ABC type half-transporters. The membrane topology of the 12 members of the ABCC subfamily, containing an NH_2-terminal extension, is discussed in detail in the review by Deeley et al. (73). The ABCD subfamily includes four half-transporters, with a TMD-ABC type arrangement. Members of the ABCE and ABCF family are not involved in membrane transport processes and lack

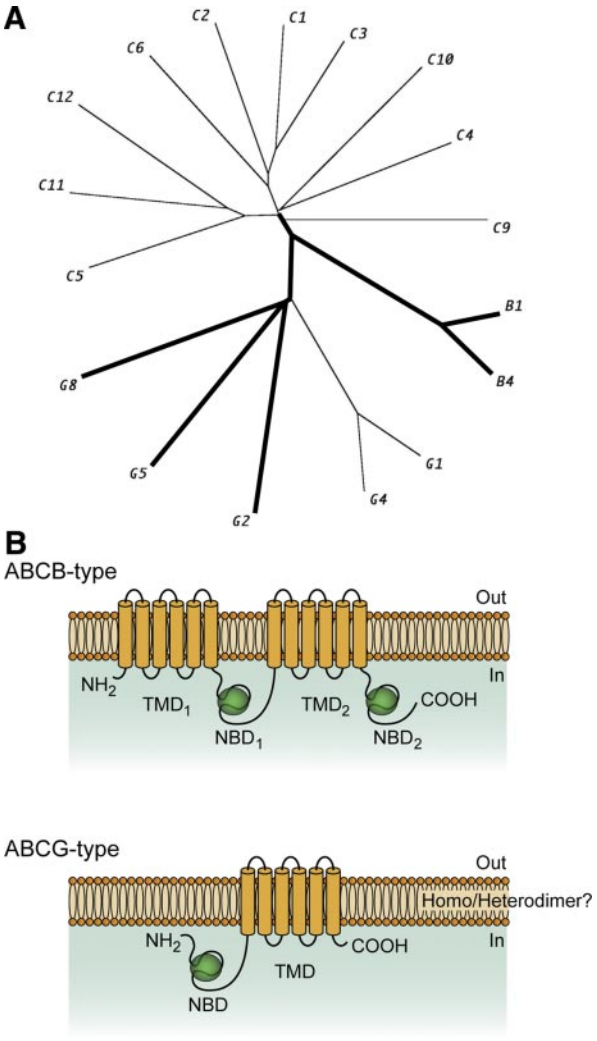

FIG. 2. Phylogenetic tree and domain arrangement of the human ABC transporter proteins. *A*: phylogenetic tree of selected human ABC transporters. In this figure, only a part of the human ABC transporter phylogenetic tree is presented, depicting members of the ABCB, ABCC, and ABCG family. The transporters discussed in this review are shown in boldface. *B*: membrane topology models of the ABCB1 (MDR1/Pgp) and the ABCG2 (MXR/BCRP) proteins. The models were constructed based on sequence analysis and the available experimental data (see text). The position of the conserved regions is indicated.

transmembrane domains. The five half-transporters in the ABCG subfamily show a reverse domain arrangement (ABC-TMD).

Of the 48 ABC transporters, MDR1/Pgp, several MRPs, and the ABCG2 protein certainly qualify for the MDR-ABC protein status. MDR3 (ABCB4), a closely related protein to MDR1/Pgp, and the relatives of ABCG2, the heterodimer ABCG5/ABCG8, are also ATP-dependent active transporters, and their involvement in drug and/or xenobiotic transport has also been documented. Figure 2*B* demonstrates the schematic membrane topology arrangements for the relevant ABCB and ABCG transporters.

Emerging information may suggest a similar, active drug transporter role for ABCG1 and/or ABCG4, as well as for ABCB5 and some ABCA type proteins, but we still have relatively little knowledge about these transporters. There are many other ABC transporters that most probably carry out substrate translocation by using the energy of cellular ATP [ABCB11 (BSEP/sister-Pgp), ABCB2/ABCB3 (TAP1/TAP2), ABCA4, members of the ABCD subfamily], but these have been not implicated in drug or xenobiotic transport and therefore are not discussed in this review.

B. Structural Basis of the Molecular Mechanism of Action in ABC Transporters

As of today, high-resolution structures are only available for bacterial ABC transporters. Therefore, for the discussion of human MDR-ABC proteins we have to rely on these data and models, which indicate a well-conserved structure and suggest a common basic mechanism of action. Unfortunately, the models reveal relatively little information about the substrate recognition or the intramolecular regulation of the individual mammalian homologs. In this section we discuss only general molecular aspects and provide further mechanistic details in the sections dealing with individual transporters.

1. The ABC fold

In several bacterial ABC proteins, the ABC units are expressed as separate proteins, and the first structural information was obtained in such systems. The first high-resolution structures of an ABC unit, that of RbsA (16) and HisP (139), were published in 1998. The HisP structure was solved with a resolution of 1.5 Å and represents an ABC monomer with the typical L-shaped (two lobe) ABC fold. Since then, the structure of several ABC units has been determined (see Fig. 3).

From these studies it became clear that the ABC domain has a unique fold, as the particular assembly of all the characteristic secondary structure elements is found only in ABC-ATPases. The ABC structure can be divided into three subdomains. The "F1-type ATP-binding core" is similar to the core of F1-ATPases and consists of six (5 parallel and 1 antiparallel) β-sheets. This subdomain contains the Walker A motif (P-loop), the Q-loop (γ-phosphate linker), the Walker B motif, and the "His-switch" (see Fig. 3*A*). The ABC-specific α-subdomain is built of four α-helices and contains the family-specific ABC signature (LSGGQ) motif, while the antiparallel β-subdomain contains elements responsible for the ribose/adenine orientation and interaction. The F1-type core and the ABC-specific β-subdomain form the larger lobe (the longer arm of the L-shaped structure), while the α-subdomain forms the smaller lobe (the shorter arm of the L).

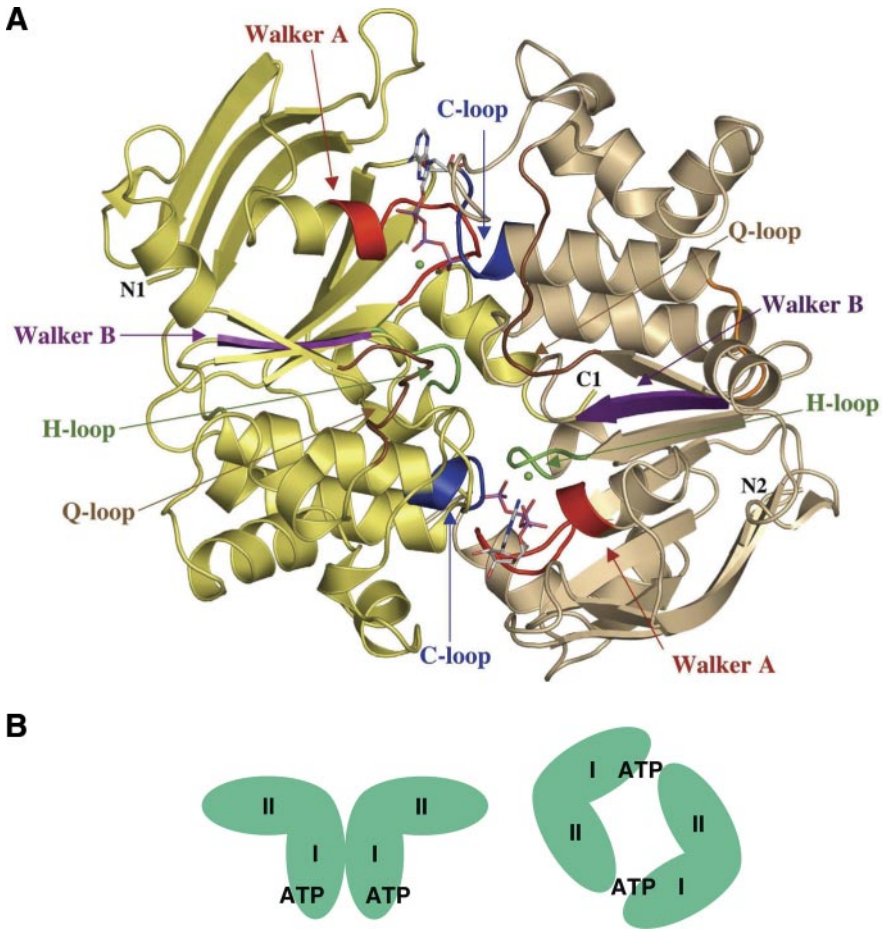

FIG. 3. *A*: crystal structure of the HlyB-NBD dimer with bound ATP/Mg^{2+} (417). ATP and Mg^{2+} (in stick representation and green spheres, respectively) are sandwiched at the interface of the two HlyB-NBD monomers (shown in light tan and light yellow). NH_2 and COOH termini of the individual monomers are labeled. Conserved motifs are colored in red (Walker A motif), brown (Q-loop), blue (C-loop or ABC signature motif), magenta (Walker B), and green (H-loop) and labeled accordingly. (Model is courtesy of L. Schmitt, Heinrich-Heine University, Düsseldorf, Germany.) *B*: model of different arrangements of ABC-ABC dimers. The originally proposed back-to-back arrangement is shown on the *left* with individual, surface-exposed catalytic sites indicated with "ATP." The head-to-tail orientation, which represents the widely accepted model, is shown on the *right*; the composite catalytic sites buried in the interdimer surface are indicated with "ATP." I: "F1-type ATP-binding core," containing the Walker A motif (P-loop), the Q-loop (γ-phosphate linker), the Walker B motif, and the "His-switch" (see text). II: α-subdomain, containing the family-specific ABC-signature (LSGGQ) motif.

In the first publications, the ABC structures were obtained for monomers, and the authors suggested a dimer, in which the two ABC units were positioned in a back-to-back orientation (139) (see Fig. 3*B*, *I*). However, this assembly represents an energetically unfavorable interaction of the two monomers and suggests two highly exposed nucleotide binding/catalytic sites, which is difficult to reconcile with the regulated function of the active sites. By now it has been convincingly documented that the two functionally interacting ABC subunits dimerize in a "head-to-tail" orientation. The two ABC domains complement each other's active sites, forming two composite catalytic centers. The Walker A sequence of one subunit and the ABC signature motif of the opposite subunit are involved in the formation of each of the two composite ATP-binding/catalytic sites (Fig. 3*B*, *II*). This orientation was first suggested in studies describing the Rad50cd structure (a nontransporter bacterial ABC-ATPase) (130) and in models built using the HisP monomers (160). Later, similar arrangements were found in the ABC domains of various bacterial transporters, including that of MJ0796 (348), HlyB (417), and MalK (54). The orientation of the two ABC units in the dimer and the positions of the conserved sequence motifs are illustrated in Figure 3*A*, based on the high-resolution structure of the HlyB ABC-ABC dimer. The regulated formation of these composite active sites is in harmony with many mechanistic studies, indicating the direct involvement of both the Walker A and the ABC signature regions in ATP binding and hydrolysis. Further analysis of Rad50cd crystal structures obtained in the presence or absence of nucleotide analogs revealed that during the catalytic cycle, the composite site is formed as a result of a major intramolecular rotation, which brings the contralateral Walker A/B and signature sequences within close proximity.

By now we also have detailed structural information regarding the amino acid residues involved in nucleotide binding and the possible catalytic steps of ATP hydrolysis within the ABC dimers. Figure 4 demonstrates the nucleotide contacts within the composite active site, based on a bacterial ABC structure (MJ0796 ABC; see Ref. 416) and sequence comparisons with human ABC transporters. Based on these structures, a detailed molecular mechanism of ATP hydrolysis by ABC transporters was suggested (see Refs. 171, 416). During ATP binding, the residues of the Walker A segment in ABC unit I coordinate the three phosphate groups of ATP, while the adenine ring is oriented by interactions with a neighboring bulky resi-

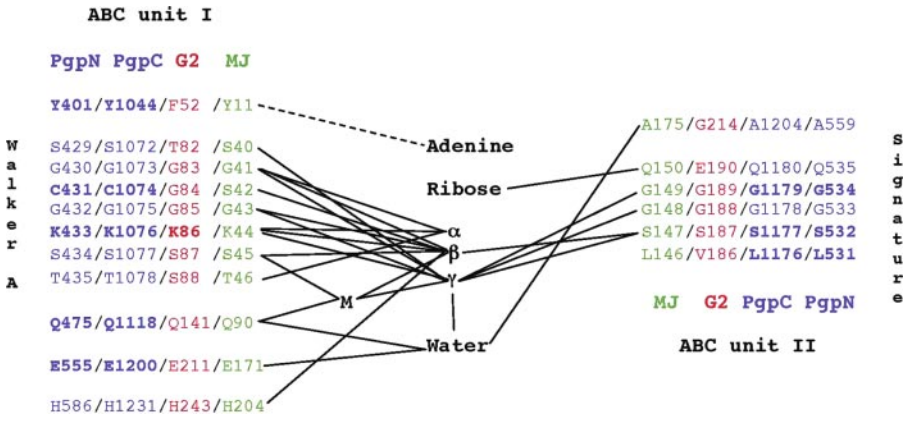

FIG. 4. Nucleotide contacts in the MJ0796 dimer and in the corresponding human transporters. Residues of the MJ0796 ABC ATPase involved in nucleotide contacts and catalysis are indicated in green in the MJ columns (348). Corresponding residues in the NH_2- and COOH-proximal ABC domains of human Pgp (PgpN and PgpC, respectively) are indicated in blue; corresponding residues of human ABCG2 (G2) are indicated in red. The interactions are represented with solid lines; stacking of the adenine ring by the hydrophobic sidechain (Y11) is indicated with a dashed line. Residues subjected to mutagenesis or chemical modification in Pgp or in ABCG2 and discussed in the text are boldface.

due. In the same ABC unit, the Q-loop and the Walker B glutamate alternately interact with a water molecule involved in ATP hydrolysis. From ABC unit II, residues of the signature region are also involved in the coordination of the phosphate groups and the ribose part of ATP, while an additional alanine interacts with the catalytic water molecule. During ATP hydrolysis, that is in a change from a "prehydrolytic" state to a Mg-ADP-bound, "posthydrolytic" structure, together with several minor intramolecular alterations, the Q-loop and the signature regions perform major movements. The movement of the signature (LSGGQ) segment is triggered by a rotation of the ABC-specific α-subdomain. Interactions between the signature motif and the γ-phosphate give additional cooperative stabilization to the nucleotide ("ATP-bound") sandwich dimer. ATP can be considered a "molecular glue" with the γ-phosphate coupling the Walker A and B motifs and the Q-loop of one of the ABCs with the LSGGQ signature motif of the opposite ABC unit. After hydrolysis, ADP remains bound to the Walker A motif, while the cleaved phosphate anion remains bound to the signature region.

2. *Communication between the ABC units and the membrane-bound domains*

The high-resolution structures of various ABC-ABC dimers do not answer several questions concerning the structural basis of the ABC-TMD interactions that ensure the transmission of signals from the substrate binding sites to the catalytic machinery. It is also unknown how ATP binding and hydrolysis serve as the "power stroke" of transmembrane transport. Furthermore, in the separate ABC-ABC dimers, the molecular interactions are not influenced by the presence of the TMDs, and thus the ABC units may enjoy more freedom than in the full transporter complexes. In the case of eukaryote ABC transporters, only low-resolution studies, e.g., electron microscopy (EM) of single particles combined with image analysis (289) and EM analysis of two-dimensional crystals of MDR1/Pgp (203, 291, 293), are available. Typically, the resolution of these structures is 12–25 Å, allowing only the detection of major conformational changes and the relative position of the major structural elements. These data are included in the presentation of the individual MDR-ABC transporters in the following sections.

At the time when this review was compiled, several structures of complete bacterial ABC transporters were already obtained at an atomic resolution. These include the dimeric forms of the homodimer BtuCD (213) and the MsbA "half-transporters," the latter being a close homolog of human MDR1/Pgp, for which crystal structures from various bacterial strains and in various catalytic states were solved with high resolution (49, 50, 285).

Importantly, the composite nature of the active/catalytic centers within the ABC domains, discussed above, is reflected in each of these structures. Another key piece of information provided by these structures seems to be trivial, that is, the transmembrane regions are indeed composed of α-helices, spanning the membranes with the predicted numbers. Although fully expected, this evidence settles the issue for a number of proposed alternative transmembrane domain arrangements (158, 159). Another major finding of these structures is that an intracellular domain (ICD) forms a bridge between the TMDs and the ABCs. The ICD is built up from three subdomains, formed from elements of the intracellular loops between transmembrane (TM) helices and between the TMD and ABC.

In the first published full MsbA structure (50), the TM helices form a cone-shaped chamber, with a wide opening from the intracellular side. In contrast, the structure of MsbA in the presence of ADP, vanadate, and a transported ligand (287) indicated a large rotation and translation of the TMDs, resulting in the opening and closure of the chamber to the periplasmic direction and the intracellular face, respectively. However, the question still remains open, are these major molecular movements indeed parts of the molecular mechanism, or do they just represent crystallization artifacts? A space-filling model of the hu-

man MDR1/Pgp is shown in Figure 5, constructed on the basis of the atomic resolution information obtained in bacterial transporters and low-resolution structures available for this human transporter. Some details of this model are further discussed in section IV.

III. METHODS FOR FUNCTIONAL INVESTIGATION OF HUMAN MDR-ABC TRANSPORTERS

A. Why Bother: Why So Special?

In addition to "curiosity-driven" basic research, the two major practical causes for measuring MDR-ABC transporter expression and function are related to cancer drug resistance and predicting/following the general fate and effect of pharmaceutical agents in our body. In both cases, the goal is to determine the actual drug transport capacity, that is, the functional expression level of the relevant transporter(s).

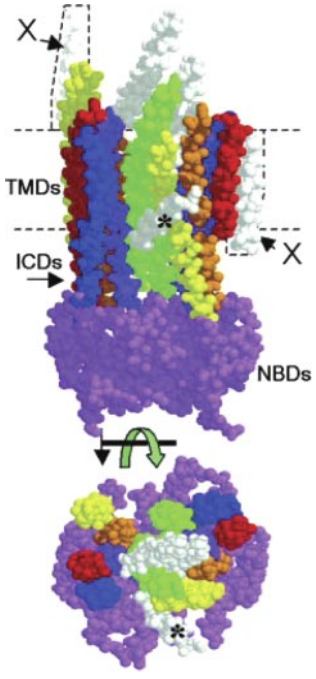

FIG. 5. Space-filling model of human MDR1/Pgp in the nucleotide-bound form. The interpretation is based on cryoelectron microscopy data and with all residues modeled as alanine (290). The figure shows a side view of the protein with the NBDs (violet) at the bottom with a top view below. The 12 putative membrane-spanning helices have been colored in pairs to indicate the two halves of the transporter. Four additional gray-colored helices do not show an obvious symmetry relationship: one helix labeled by an asterisk is intracellular, tilted, and too short to cross a membrane; another helix, which is shown in the side view by X, is ambiguous in its location; the other two helices are at the extracellular side of the protein. The dashed lines indicate the putative boundaries of the lipid bilayer. Scale bar = 5 nm. [Adapted from Rosenberg et al. (290).]

As described in the sections dealing with the individual transporters, this task is not easily achieved by the routinely available classical methods. MDR-ABC protein expression is often not correlated with mRNA levels, as translation, protein processing, localization, and degradation are all regulated processes. Moreover, the physiological or cancer cell expression level of an MDR-ABC transporter is often below the detection threshold, as relatively few active transporter molecules may cause major alterations in drug transport. Even if the overall determination of the transporter protein levels is successful, in many cases the variable, regulated localization of the protein may result in misleading conclusions. In addition, these proteins cannot be studied by the classical membrane transport methods, developed for, e.g., ion exchangers, P-type ATPases, or regulated channels. The major differences may lie in the hydrophobic or amphipathic nature of the transported substrates and the relatively loose coupling of transport and ATP hydrolysis in these proteins (see sect. II and below). Based on these problems, the quantitative, functional determination of MDR-ABC transporters gained a special emphasis in the research efforts.

Another major issue is the relevance of in vitro experiments to the in vivo role of MDR-ABC transporters. Although initial indications for the role of membrane transporters in cancer multidrug resistance originated from clinically oriented studies, it is important to emphasize that the role of these transporters in clinical anticancer drug resistance is still unsettled. According to our view, this is mostly due to the still underdeveloped methodological arsenal of the clinical laboratory studies, especially the lack of proper, quantitative assay methods directly applicable for studying the function of all relevant MDR-ABC proteins in human solid cancer tissues.

In the initial in vitro experiments, cellular multidrug resistance was modeled by the in vitro drug selection of the tumor cells. However, since the transported drugs/compounds are mostly hydrophobic, their cellular accumulation strongly depends on the availability of intracellular binding sites, sequestration, as well as the "passive" permeability of the cell membrane. Vesicular transport studies encountered similar problems; if there is no binding or sequestration, the "leakage" of the accumulated drug rapidly counteracts the accumulating transport process. This is the reason why many indirect methods (drug-stimulated ATPase activity, fluorescent dye transport, "nucleotide trapping," drug binding, etc.) were developed to appreciate the drug transport and related drug resistance functions, but a consensus in their application is still lacking.

While this wide array of methods to investigate the function and substrate interaction of MDR-ABC transporters has been developed by various research laboratories, the pharmacological industry became a major consumer

and contributor to these studies as well. This is partly due to the development of new anticancer agents, but even more to the interest in defining the role of ABC transporters in drug absorption, distribution, metabolism, excretion, and toxicology (ADME-Tox). As detailed in the relevant sections, MDR-ABC transporters are key determinants of drug permeation into different tissues, as these proteins are located in the absorption, secretion, and sanctuary barriers.

Based on the above-described questions, in section III we discuss the relevant in vitro systems, the various cellular and enzymatic/vesicular models applied for the studies of MDR-ABC transporters. We focus on in vitro functional assays, the analysis of cytotoxicity, translocation of substrates, and ATP hydrolysis and emphasize methods that can be used to quantitatively estimate transporter function. We refer to all in vivo investigations in the sections discussing the individual multidrug transporters.

B. Cellular Assay Systems

1. Drug resistance studies

Typically, in vitro studies use cell lines overexpressing a desired ABC transporter. Such cells may be readily engineered using routine molecular biology techniques. Alternatively, cell lines with pleiotropic drug resistance may be generated through exposure to increasing concentrations of antitumor drugs. Fulfilling their role in detoxification, several ABC transporters (such as ABCA2, ABCB1, ABCC1, ABCC2, ABCC4, and ABCG2) have been found to be overexpressed in cell lines cultured under selective pressure (367). For example, elevated levels of ABCB1 were found in cells selected with Vinca alkaloids, anthracyclines, and colchicine, among others. Similarly, ABCG2 was overexpressed in cells selected for resistance to topotecan and mitoxantrone. To some extent, in vitro selection of cells resembles the in vivo acquisition of the MDR phenotype. However, resistant cells have to be cultured under constant selective pressure to ensure a stable phenotype. Under these conditions, cells usually develop multiple mechanisms of resistance (15), involving the overexpression of further transporters. Discerning signal from noise in selected cells can be achieved by control experiments using parental cells, or cells treated with specific inhibitors. In general, availability of appropriate control cells is a limitation, since cells undergoing selection may have inherent differences that are not readily identified or controlled. Furthermore, inhibitors are rarely specific. Despite these constraints, selected cell lines overexpressing an ABC transporter are extensively used both in research and industrial settings.

Some of the ABC transporters implicated in MDR have never been found overexpressed in drug-selected cells. Still, these transporters (such as ABCB11, ABCC3, ABCC5, ABCC6, ABCC10, and ABCC11) could confer drug resistance when they were transfected into cells. Again, cell lines stably overexpressing these ABC transporters showed characteristic resistance to compounds that are substrates for transport. Thus cytotoxicity assay is a convenient tool that is often used to search for substrates and reversing agents. Cytotoxicity assays can be well quantitated, and "killing curves" provide proper IC_{50} values for the estimation of changes in cellular drug resistance. However, drug sensitivity may be entirely different in different immortalized or tumor-derived cell lines, and the complex cellular sensitivity and resistance mechanisms greatly modify the effects of such studies.

2. Transient expression systems

Studies using mammalian cells subjected to drug selection with or without the introduction of *MDR1* cDNA are subject to contention because of the pleiotropic effects of the drugs (12). To overcome this concern, ABC transporters may be expressed in transient expression systems. Gottesman and colleagues (283) adapted a vaccinia virus-T7 RNA polymerase hybrid transient expression system that does not involve selection for the functional expression of MDR1/Pgp. In this system, high levels of expression can be achieved within 48 h posttransfection, allowing the study of transport and drug-stimulated ATPase.

In the case of several ABC transporters, including MDR1/Pgp and its close relatives, expression of the gene products in insect (e.g., *Spodoptera frugiperda*, Sf9) cells, using recombinant baculoviruses, proved to be an efficient tool for analyzing various aspects of transporter function. This system allowed studying the protein interactions with substrates and also the substrate-stimulated ATPase activity (307). Although the baculovirus expression system ensures relatively high expression levels (4–5% of the total membrane protein), expression is transient, and the functional analysis of the expressed proteins in most cases has to be performed using microsomes prepared from the infected cells. Despite the lack of full glycosylation in insect cells (proteins are only core-glycosylated), we have successfully used this system for the expression and characterization of several ABC transporters (22, 260, 305, 307, 346). In case a mammalian protein has to be complemented by (an)other protein(s) for function, a heterologous system may not be suitable for functional analysis. Still, functional expression in insect cells can be used to characterize mammalian proteins outside the context of interacting networks. We have used this argument to show that ABCG2, an ABC half-transporter, functions as a homodimer (see sect. V). As mentioned below, transient expression systems are especially useful

for direct enzymatic or transport studies of MDR-ABC transporters.

3. *Whole cell transport studies: fluorescent dyes and the calcein assay*

The multidrug resistance phenotype suggests the overexpression of an MDR-ABC transporter and the decreased cellular accumulation of the toxic compounds. To verify this relation, experiments can be designed to follow the steady-state cellular accumulation of radioactively labeled or fluorescent compounds. In case a reduced accumulation or an increased extrusion is detected, experiments can be performed to define the kinetic parameters, energy dependence, and the specificity of the efflux. However, as mentioned above, intracellular binding, sequestration, and "membrane leakage" of the compounds are major difficulties in quantitating these studies. Therefore, a large number of indirect transport assays, where substrates and inhibitors are identified by following the transport of a reporter substrate, have been developed. Reporter substrates should be generally not toxic, their cellular fate should be well characterized, and an easily measurable fluorescence is a major advantage for such test compounds (Fig. 6).

The functions of MDR-ABC transporters have been characterized by measuring the cellular uptake, efflux, or steady-state distribution of a number of fluorescent substrates, including Hoechst dyes, fluorescent verapamil and prazosin derivatives, or various rhodamine derivatives. Several drawbacks have been noted relating to the sensitivity of most fluorophores because of protein binding, sequestration, or changes in the intracellular milieu (e.g., pH or free calcium) (124). Fluorescent indicators such as fura 2 are linked to an acetoxymethyl ester (AM) group to grant the access of the conjugates through the plasma membrane into the intracellular milieu. In an experiment in which our aim was to characterize the role of MDR1/Pgp in calcium homeostasis, we noticed that several fluorescent indicators used to measure intracellular calcium levels showed a decreased accumulation in MDR1/Pgp overexpressing cells (126). This observation prompted a search for a hydrophobic fluorescent indicator measuring the activity of MDR1/Pgp.

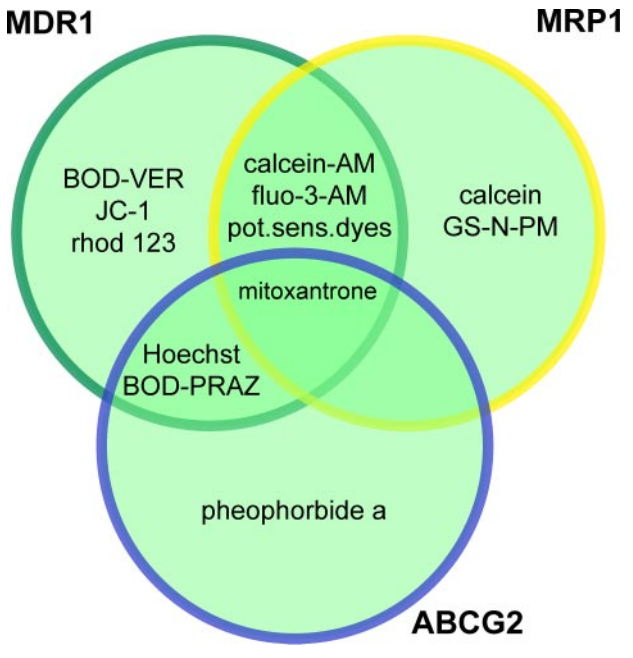

FIG. 6. Venn diagram of the fluorescent probes used for studying MDR-ABC transporter function. Several fluorescent substrates have been described for the respective multidrug transporters. Some of these are selective for one or two transporters, but most of the probes have overlapping specificities.

We found calcein-AM to be the dye of choice, because *1*) the hydrophobic, nonfluorescent AM form is an excellent substrate for MDR1/Pgp; *2*) the fluorescent, hydrophilic free acid is trapped inside the cells, does not bind to intracellular proteins, and is no longer a MDR1/Pgp substrate; and *3*) the fluorescence of free calcein is not sensitive to changes in pH and ion concentrations. Due to the enzymatic enhancement of the dye-trapping process, the sensitivity of an assay measuring calcein accumulation highly surpasses that of other functional assays (Fig. 7, Ref. 124). Based on these considerations, we developed a quantitative calcein transport assay, which correlated with functional MDR1/Pgp expression. The assay kit is suitable for flow cytometry-based clinical laboratory applications and was found applicable in predicting multidrug resistance in acute leukemia (170). The calcein assay can be used for the estimation of the transport properties of certain MRPs as well, while ABCG2 does not transport either calcein-AM or free calcein (see sect. V).

4. *Monolayer transport assays*

In vivo, drugs have to cross pharmacological barriers to get absorbed (intestinal epithelial cells), distributed (blood-brain barrier endothelial cells), or excreted (hepatocytes, proximal tubule epithelial cells). This transcellular movement is modeled by cellular monolayer efflux ("vectorial transport") assays. The cell lines used in these assays are polarized epithelial or endothelial cells, such as the human intestinal epithelial line Caco-2. Caco-2 cells have characteristics that resemble intestinal epithelial cells such as the formation of a polarized monolayer, with a well-defined brush border on the apical surface, and intercellular junctions. Measuring the rate of transport across the Caco-2 monolayer provides insight into absorption across the gut wall. Test drugs can be applied to either side of the cell layer, and the rate of transport across the monolayer is measured from the apical to basolateral (A-B) or from the basolateral to apical (B-A)

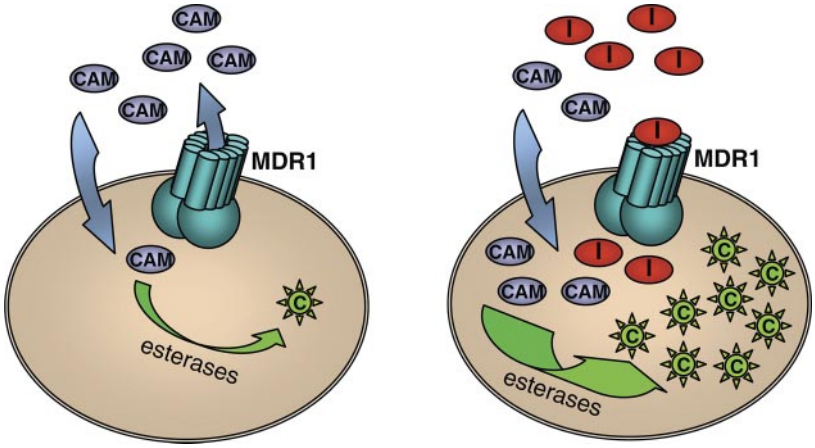

FIG. 7. The calcein assay for studying MDR1/Pgp expression and function. Calcein acetoxymethyl ester (AM), a nonfluorescent compound, rapidly traverses the cell membrane and is converted to a fluorescent form (calcein free acid) by cellular esterases. In multidrug resistant cells expressing MDR1/Pgp, calcein-AM is extruded by the multidrug transporter before its intracellular conversion. Since the amount of calcein-AM available for cellular esterases is reduced, the accumulation of calcein, which is not an MDR1/Pgp substrate, is also reduced in these cells. When calcein-AM extrusion is blocked by an agent that interferes with MDR1/Pgp (e.g., verapamil), fluorescent calcein free acid rapidly accumulates, providing a measure of MDR1/Pgp function (125).

direction. The bidirectional apparent "permeability" of the test compound reflects the complex transport processes across the cell membranes. Measuring transport in both directions across the cell monolayer provides an indicator of active transport, chiefly mediated in Caco-2 cells by MDR1/Pgp (see sect. IV).

To establish specific roles of different MDR-ABC transporters, transfected versions of the canine kidney cell lines MDCKI, MDCKII, or the porcine kidney epithelial cells LLC-PK_1 can be used. In these assays, polarized cells are grown on semipermeable filters, and the MDR-ABC transporters are localized to the proper apical or basolateral surfaces of the cells (for reviews, see Ref. 197). Fluorescent compounds can also be used in indirect transport assays in such polarized cells, e.g., the "vectorial calcein assay" can be applied for the estimation of drug interactions with various MDR-ABC proteins (33, 288). Especially in ADME-Tox drug research assays the application of cell lines with well-defined "efflux" and "influx" transporters can be an advantage. For such complex cellular or monolayer transport assays, the stable coexpression of various MDR-ABC transporters and a number of "influx" transporters are already available (70, 189, 206, 308, 309, 421).

5. *Pharmacogenomic approach to identify ABC substrates*

To determine substrate specificities of ABC transporters and their role in drug resistance of cancer cells, Szakacs et al. (363) have measured the expression profile of the 48 ABC transporters in the National Cancer Institute 60 (NCI-60) cancer cell panel. The NCI-60 cell panel was set up by the Developmental Therapeutics Program (DTP) of the National Cancer Institute (NCI), which has screened the cytotoxicity profiles of more than 100,000 chemical compounds in the 60 cell lines (97). Through the measurement of ABC transporter expression levels, it was possible to link ABC transporter function to a variety of already determined molecular, physiological, and pharmacological features of the cells. Analysis of the correlations between ABC transporter expression and known patterns of drug activity for 1,429 compounds across the 60 cancer cell lines yielded strongly inverse-correlated pairs, where the expression of an ABC transporter was strongly correlated with decreased sensitivity to a drug. As expected, good agreement was found between the mRNA expression of MDR1/Pgp and the reduced cellular sensitivity to anticancer drugs that are known to be substrates of this transporter. Furthermore, the method also allowed the identification of previously unknown MDR1/Pgp substrates (363). Interestingly, the same approach indicated that ABC transporters other than the well-characterized MDR proteins can provide resistance in naive (unselected) cancer cell lines. Follow-up experiments, using cells transfected with ABCC2, ABCC11, or ABCC4 (401), validated the predictions. These results suggested that this pharmacogenomic approach provides an unbiased method for discovering the substrate specificities of known, as well as yet uncharacterized members of the ABC superfamily.

C. MDR-ABC Enzymatic or Transport Assays

1. *ATPase assay, detection of the catalytic cycle steps*

As discussed in section II, MDR-ABC transporters exhibit a catalytic activity that is coupled to drug transport. Indeed, crude and purified preparations of various MDR-ABC transporters exhibit substrate-induced, vanadate-sensitive ATPase activities. The rate of ATP hydrolysis is easily determined by measuring the liberation of inorganic phosphate, using membrane vesicles prepared, e.g., from MDR-ABC expressing insect or mammalian cells. Isolated and reconstituted MDR-ABC transporters have also been successfully applied in this regard (10, 14, 81, 114, 219, 307, 329, 336).

The profile of the drug-stimulated ATPase reflects the nature of interaction: compounds may be substrates or inhibitors or may have no effect on the transporter. In the presence of transported substrates, the ATPase activity of the transporter increases (activation protocol). Noncompetitive inhibitors, or compounds transported at a lower rate, inhibit the ATPase activity of the stimulated transporter (inhibition protocol). In general, most of the efficiently transported compounds stimulate the ATPase. In the case of MDR1/Pgp, exceptions were noted, and some substrates were shown to stimulate activity at lower, and inhibit the ATPase at higher, concentrations. Further complicating the issues, the ATPase activity in most cases has a basal rate, probably related to an endogenous stimulation and/or a partial uncoupling (see below) and may also be affected by the lipid environment and the experimental conditions (9, 248, 330, 332). However, because of its simplicity and reproducibility, the ATPase assay is one of the most widely used assays to search for compounds that interact with various ABC transporters.

The application of the vanadate-sensitive membrane ATPase assay for drug interaction studies circumvents the problems of measuring the transport of hydrophobic substrate compounds, if indeed MDR-ABC ATPase is closely coupled to transport activity. While most studies agree that in general this is the case, a certain "slippage" between ATP hydrolysis and drug transport by the MDR-ABC transporters may be a basic feature of the catalytic mechanism (see sect. II). Studies on the wild-type and mutant variants of the major multidrug transporters may answer this basic question.

As described in more detail in the relevant sections, several methods have been developed for the analysis of the catalytic steps of the ATPase/transport reaction of MDR-ABC transporters. These include the determination of the modulation of the vanadate-dependent adenine nucleotide "trapping" (26, 362), and the vanadate-induced cleavage of the transporter protein (134), induced by transported substrates or modulators. Often applied methods are following the interaction of membrane-bound or isolated MDR-ABC proteins with labeled photoaffinity analogs of ATP or the transported substrates. The conformation-sensitive binding of specific monoclonal antibodies both in the case of MDR1/Pgp (267a) and ABCG2 (265) has been successfully applied to study substrate interactions and models of the catalytic cycle. While these methods may yield valuable information about the mechanism and transport properties of the given ABC protein, they are usually expensive with a low throughput; thus they may not be efficiently applied in cancer drug detection or drug research.

2. Vesicular transport

A more direct measurement of substrate translocation and its modulation can be achieved by the quantitation of the intravesicularly trapped substrates in vesicular transport assays. However, as noted above, this assay has major limitations when using hydrophobic substrates, due to significant nonspecific binding and rapid leakage of the compounds from the vesicles.

Successful vesicular transport studies using membranes from various sources (insect cells, transformed and selected cell lines, artificial membrane vesicles) have been reported by several laboratories (337, 422). Given the orientation of ABC transporters in cells (where the NBDs are in the intracellular compartment), in inside-out vesicles, the NBDs face the incubation media (accessible to ATP and other chemicals), and substrates are actively transported into the vesicles. Rapid filtration, using glass fiber filters or nitrocellulose membranes, is used to separate the vesicles from the incubation solution, and the test compound, trapped inside the vesicles, is retained on the filter. The quantity of the transported unlabeled molecules can be determined by high-resolution, high-sensitivity analytical methods. Alternatively, the compounds are radiolabeled or a fluorescent tag is attached, and the radioactivity or fluorescence retained on the filter is quantified.

In the case of MDR1/Pgp, which recognizes mostly hydrophobic compounds, a vesicular transport assay for most of the relevant substrates could not be established, due to the high nonspecific binding and passive diffusion of compounds. For some less hydrophobic, relatively low-affinity substrates, such an assay is available. Transport of hydrophilic quaternary drugs (such as *N*-methylated derivatives of quinidine) was demonstrated into vesicles isolated from MDR1/Pgp overexpressing insect cells (129). In another experiment, using rat hepatocye canalicular membrane preparations, ATP-dependent uptake of radioactively labeled doxorubicin and *N*-pentylquinidium could be measured by centrifugation of the vesicles through a gel matrix (397). It has to be noted that vesicles prepared from hepatocytes contain additional ABC transporters, such as ABCB11 (BSEP, or "sister-of-Pgp") and ABCC2/MRP2. For these other ABC transporters, including members of the ABCC and the ABCG subfamilies, a number of transported substrates are less hydrophobic and therefore are trapped inside the vesicle compartment. Vesicular transport can also be performed in an "indirect" setup, where interacting test drugs modulate the transport rate of a labeled reporter compound.

As a general conclusion, a great variety of assays have been developed for functional studies on MDR-ABC transporters, but none of these methods can be singularly applied to answer all questions of functional expression, substrate handling, and regulation. The adaptation and/or the proper combination of these assays for detection of

MDR-ABC effects in cancer cells, or predicting their role in the ADME-Tox properties for a given compound, is still more an art than an established procedure. Another key question is the simple, reliable, if possible high-throughput application of the most informative methods in generally available laboratory settings. International method selection and standardization efforts may soon improve this situation both for the clinic and the pharmacological industry.

IV. ABCB1 (P-GLYCOPROTEIN, MDR1): THE CLASSICAL HUMAN MDR-ABC TRANSPORTER

A. Biochemistry and Cell Biology of MDR1/Pgp

Human ABCB1 (MDR1/Pgp) is the archetypal ABC transporter and has earned its reputation by being the first discovered, the most important medically, the most studied, and the one with the broadest substrate specificity (156). Models describing the function of MDR1/Pgp rely on biochemical experiments, mutagenesis studies, low-resolution structures, and the atomic level structures of various other ABC proteins.

ABCB1 is a member of the ABCB subfamily, which in humans has 11 transporters. The *ABCB1 (MDR1)* gene is located on chromosome 7q21. It consists of 28 exons, which encode a 1,280 amino acid glycoprotein (MDR1/Pgp). Analysis of the primary sequence delineates a tandem repeat of transmembrane domains and ATP-binding cassettes and a linker region connecting the two homologous halves of the protein. The two halves form a single transporter with a pseudo-twofold symmetry, in which the transmembrane helices define a "pore" for substrate translocation, and the nucleotide binding cassettes harvest the energy of ATP binding and hydrolysis.

The membrane topology of MDR1/Pgp has been elucidated by epitope insertion experiments (172, 173), fully supporting the original topology model of six TM helices in both TMDs of the protein (52). The linker region connecting the two halves of the protein plays a critical role in ensuring proper interaction of two subunits. The overall shape of the molecule has been revealed by low-resolution techniques. Cryoelectron microscopy images (at a resolution of ~8 Å) suggest that the transmembrane domains form a funnel-shaped aqueous chamber in the plane of the membrane (290). The chamber opens towards the extracellular compartment and seems to be closed at the intracellular end. The two NBDs are located intracellularly, in close proximity that allows extensive interactions between the two catalytic sites (Fig. 5).

ATP hydrolysis and drug transport are promoted by different segments of the protein, and the collaboration of these modules ensures that *1*) ATP is hydrolyzed when a substrate is presented for transport, *2*) the substrate is translocated as the energy of ATP is released, and *3*) the two ABC units act in a concerted fashion (see sect. II). While a large body of biochemical experiments, coupled with mutagenesis studies summarized below, have elucidated some key features, in the absence of structural evidence the exact mechanism of how conformational signals are transmitted within the protein, resulting in coupling of ATPase and transport cycles, awaits more relevant and/or higher resolution structural data. In particular, there is much controversy regarding the mechanism by which transported substrates promote ATP hydrolysis (substrates may affect ATP binding, ATP hydrolysis, or both), and the details of how the energy of ATP hydrolysis is harnessed for transport.

MDR1/Pgp recognizes substrates that belong to very diverse chemical classes. Several investigators have attempted to catalog the chemical fingerprint of a "model substrate." The consensus that has emerged from these studies is that MDR1/Pgp substrates are amphipatic, with a molecular mass of 300–2,000 Da. Despite the wealth of mutagenesis and photolabeling studies (reviewed in Ref. 13), the structural basis of the transporter's promiscuity remains unknown. Mutations affecting substrate specificity are clustered predominantly in transmembrane domains 5, 6 and 11, 12, but they are also found throughout the rest of the molecule, including the intracellular loops and the ATP binding domains (12). In a series of experiments, Loo and Clarke (217) have used cysteine scanning mutagenesis to assess the relative position of moieties involved in drug binding within the transmembrane regions. Models based on disulfide cross-linking experiments place transmembrane helices 6 and 12 in close proximity. Similarly, TM helices 5 and 8, as well as TM2/TM11, are close to each other, in agreement with the proposed funnel shape of the channel (214). During transport, drugs are translocated from a high-affinity "loading" site located in the intracellular or inner leaflet compartments to a low-affinity, outward-facing "unloading" site. This energy-dependent translocation event involves the repacking of the membrane-spanning α-helices (291, 293).

Crude membranes purified from insect cells expressing MDR1/Pgp show ATPase activity that is stimulated by transported substrates (307). Similarly, purified MDR1/Pgp reconstituted in proteoliposomes exhibit substantial drug-stimulated ATPase activity (14). The MDR1/Pgp ATPase has a low affinity and low specificity for nucleotides with a single apparent K_m for MgATP of 0.5–1 mM that is not affected by the transported substrates. The turnover of the maximal, drug-stimulated ATPase is 10–20/s, the activity ranges between 5 and 22 μmol $\cdot$ min^{-1} $\cdot$ mg MDR1/Pgp^{-1}, and the degree of drug stimulus is 2- to 11-fold. It is generally agreed that the stoichiometry of ATP hydrolysis to drug transport is in the range of 1–3 (14).

ATP binding and cleavage occur at the ABC units, and the close interaction of two ABC units results in the formation of a fully competent ATP-hydrolytic site (see sect. II). MDR1/Pgp (as all ABC transporters) differs from P-type ATPases in that it does not show a high-affinity ATP binding and does not utilize a covalently phosphorylated protein intermediate. Theoretically, the ATPase cycle can be described as containing the following basic steps: ATP binding, cleavage of the terminal phosphate bond, and release of the catalytic products (P_i and ADP). Practically, these steps are empirically defined and characterized in experiments described below (for a summary, see Fig. 8).

To study ATP binding, researchers have used various ATP analogs that are either nonhydrolyzable (230), emit fluorescence (212, 334, 335), or covalently label nucleotide binding sites (252, 303). Under conditions preventing ATP hydrolysis (such as low temperature), two ATP molecules are seen bound to MDR1/Pgp. Compared with most ATPases, the affinity of MDR1/Pgp for ATP is low, with a K_m of 0.3–1 mM. Binding curves can be described by a single K_d, indicating lack of cooperativity of the two

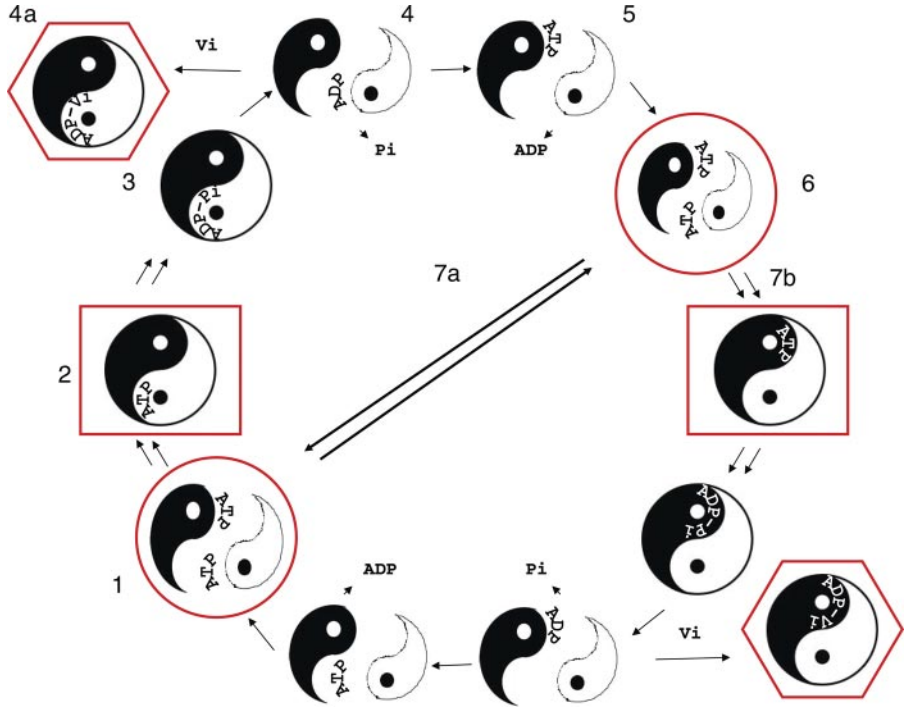

FIG. 8. ATP hydrolytic cycle of MDR1/Pgp. The ying and yang represent the two composite nucleotide binding folds. *Step 1*: ATP binding. Two ATP molecules are loosely bound to MDR1/Pgp (red circles). This is consistent with experimental data showing 2 ATP molecules bound to MDR1/Pgp with a low affinity. *Step 2*: ATP occlusion ("high-affinity binding"). ATP binding brings about a tighter interaction of the two NBDs, which results in the formation of the composite catalytic sites (dimerization). Although in the wild-type MDR1/Pgp ATP binding (*step 1*) is rapidly followed by ATP hydrolysis (*step 3*), mutational studies (312, 380, 381) strongly indicated the presence of such an ATP occlusion step. This prehydrolytic conformation is probably evoked by the binding of nonhydrolyzable ATP analogs. Experimental evidence suggests that in the "occluded state" only 1 ATP is bound tightly to MDR1/Pgp, consistent with the observation that only one catalytic site is committed to hydrolysis in the subsequent steps (red squares) (375). At present, it is not clear if the noncommitted site is unoccupied (as shown in this figure) or loosely binds a nucleotide. *Step 3*: ATP hydrolysis. This is probably a multistep process with minor conformational changes within the composite active center(s). *Step 4*: the cleaved terminal phosphate is released, and ADP still remains occluded. At this step, vanadate (and other phosphate mimicking transition state analogs) can replace the phosphate, thus stabilizing a complex containing ADP:V_i:Pgp ("trap," *step 4a*). Ample experimental evidence suggests that only 1 ADP is trapped at a time (red hexagon). Moreover, in the trapped stage, the affinity of MDR1/Pgp for the nucleotide is drastically reduced (310), suggesting that no nucleotide is bound to the noncommitted (idle) site. *Step 5*: release of ADP. In the absence of vanadate, ADP dissociates. *Step 6*: ATP binding. With the renewed accessibility of the NBDs, 2 ATP molecules loosely bind to MDR1/Pgp. At this point, there are two possibilities. *Step 7a*: since *steps 6* and *1* are identical, the cycle continues with the random recruitment of one of the composite catalytic sites. *Step 7a* would allow repeated hydrolysis at the same composite site. *Step 7b*: according to the widely accepted model proposed by Senior et al. (328), the two sites alternate in catalysis. Thus, in a "full cycle," 2 ATP molecules are hydrolyzed in identical steps, alternating between the two sites (*steps 7b–1*). The original model suggested that 2 nucleotides may be bound to MDR1/Pgp at a time, and ATP binding at one site was proposed to promote hydrolysis at the other. Although this may indeed be the case, at present, there exists no experimental evidence to ultimately prove this interaction. Except for the initial loose binding of 2 ATP molecules (red circles, *steps 1* and *6*), consistently with experimental evidence, the model shown here involves steps where only one nucleotide is bound to MDR1/Pgp. This model is compatible with alternating catalysis (*step 7b*), if it is assumed that *steps 6* and *1* are different, and in *step 6*, MDR1/Pgp "remembers" at which site hydrolysis has occurred in *step 3* (this may be ensured, e.g., by the preferential binding of ATP to the previously idle site in *step 5*). At present, several contrasting views exist regarding the coupling of the ATPase to drug transport (see text). ATPase activity is clearly required for transport, and transported substrates typically increase the rate of ATP hydrolysis (steps that may be accelerated by transported substrate are shown by double arrows). It is not clear, however, which steps are associated with the binding, transport, and release of the transported drug (not shown, but see Ref. 310).

NBDs (205). The prevailing view in the literature is that transported substrates do not have any effect on ATP binding (205, 252), although this is still an unsettled dispute (see below).

The transport and ATPase cycle of MDR1/Pgp is blocked by phosphate-mimicking anions, such as orthovanadate. Being similar in size and charge, vanadate replaces the cleaved gamma phosphate and locks the complex consisting of MDR1/Pgp and ADP (Pgp-ADP-V_i). This complex is formed under conditions allowing hydrolysis of at least one ATP molecule, and it is generally accepted to closely mimic the conformation of a transition state. The trapped nucleotide can be visualized by covalent photoaffinity-labeling of the NBDs by α-^{32}P-8-azido-ATP, which is an efficient energy donor substrate of MDR1/Pgp. In contrast to ATP binding, "ADP trapping" is accelerated by the transported drug substrates (176, 362). In the presence of drug substrates, a strong correlation exists between the increase in the rate of trapping and the steady-state fold stimulation of ATPase activity, indicating that they provide a measure of the same catalytic step (362).

Vanadate trapping has proven to be a very useful tool to dissect the catalytic cycle. The first model of the ATPase cycle, proposed by Senior et al. (328) in a seminal paper, suggested that both ABC domains bind and hydrolyze ATP in an alternating fashion. According to this model, ATP binding at one NBD promotes hydrolysis at the other, and parallel hydrolysis at the two NBDs is inhibited. This hydrolytic step leads to a high chemical potential conformation, the relaxation of which is coupled to drug transport. The basic paradigm of the Senior model has survived the test of time and has served as the framework for later refinements (157; Fig. 8).

The formation of the transition state clearly manifests in extensive conformational changes, which were detected by proteolysis experiments (165) and structural studies (293). Several authors agree that the decrease in drug binding affinity ("unloading") is associated with this step of the catalytic cycle. Indeed, monitoring the binding of the substrate analog ^{125}I-iodoarylazidoprazosine (IIAP), Sauna and Ambudkar (311) found that the vanadate-trapped transition state complex exhibited a reduced affinity to drugs and nucleotides. The reduced drug binding affinity persisted as the transition state collapsed (release of V_i and ADP), and only through the hydrolysis of a second ATP molecule did MDR1/Pgp regain its high-affinity binding site (282, 311). Thus a model was proposed in which a second ATP has to be hydrolyzed to reset the protein to the initial conformation with a high-affinity drug binding site. According to the Sauna model, release of the substrate occurs following hydrolysis of the first ATP molecule, and the resetting of the transporter requires the hydrolysis of a second ATP (13).

This model has been challenged by Sharom et al. (333), who used various fluorescent spectroscopic approaches to follow the catalytic cycle. They found that the stably trapped Pgp-ADP-V_i complex does not exhibit reduced drug binding affinity and that the affinity of NBDs for nucleotides does not change during conversion from the resting state (where 2 ATP molecules are bound) to the transition state (279). In addition, the same authors found a modest stimulation of ATP binding in the presence of transported substrates. Taken together, they interpret their data as signifying that the transported substrates are released before the formation of the transition state (ATP cleavage), suggesting a mechanism involving concerted conformational changes rather than a multistep process (279, 333).

Higgins and Linton (120) also observed an increase in ATP binding affinity of MDR1/Pgp in the presence of vinblastine. Furthermore, in experiments using nonhydrolyzable ATP analogs, the Higgins group found that ATP binding results in extensive conformational changes affecting the TMDs that eventually decrease the affinity of MDR1/Pgp to vinblastine (229, 230, 292, 349). These observations led to a model in which it is the binding, rather than the hydrolysis, of ATP that provides the "power stroke" for transport (120). According to the ATP switch model, in a "resting state," the two NBDs are far from each other ("open conformation"). Substrate binding facilitates ATP binding, which in turn results in the dimerization of the two NBDs (closed formation). The extensive conformational changes prompted by ATP binding mediate signals to the drug binding domains and ultimately translate into the translocation of the drug substrate. Importantly, this model assumes that the conformational changes facilitating the translocation of the transported substrates are brought about by ATP binding, resulting in the switch between the closed and open states of the NBD interface. In this interpretation, hydrolysis of 2 ATP molecules (and the release of P_i and ADP) is triggered by the dissociation of the transported substrate, the result of which is the opening of the NBD dimer interface that resets the transporter to the starting conformation.

Concerning the mechanistic details of the communication between the NBDs and the drug-translocating domains and the role of ATP binding/hydrolysis in promoting drug translocation, the above-described models are clearly at odds with each other. The ultimate transport scheme will be based on detailed thermodynamic studies and crystal structures representing snapshots of MDR1/Pgp as it cycles through its physiological conformations. In the meantime, apparent discrepancies may be discussed in the context of the different experimental strategies used to define the catalytic steps. For example, advocates of the fluorescent nucleotide analogs argue that photolabeling techniques are subject to artifacts, and

reflect the variable efficiency of photoprobe cross-linking rather than the true binding affinities (279). On the other hand, it can be argued that fluorescent techniques (using fluorescent ATP analogs along with a quenching agent associated to the NBDs) provide but an indirect measure of ATP binding, especially as most of these analogs have clearly different affinities than ATP. In addition to specific artifacts related to these experimental protocols, another reason behind these contrasting views may be that these experimental techniques capture different steps of the catalytic cycle. At low temperatures, α-^{32}P-8-azido-ATP labeling of MDR1/Pgp is thought to represent ATP binding. As mentioned earlier, nonhydrolyzable ATP analogs are also used to study the same catalytic step. However, while neither condition is expected to allow ATP cleavage, nonhydrolyzable ATP analogs may nevertheless permit the formation of a prehydrolytic state (following binding but preceding hydrolysis) in which ATP is occluded (Fig. 8). Due to the high turnover of ATP hydrolysis, this state is difficult to capture in the wild-type protein. Interestingly, MDR1/Pgp variants containing combined mutations at the "catalytic carboxylate" and the contralateral signature region (E552A/S1173A) show vanadate-independent retention of ATP, suggesting that a closed formation of the dimer interface (with an occluded ATP) can indeed occur without ATP hydrolysis (374).

Most models agree that in MDR1/Pgp the two nucleotide binding domains are functionally equivalent and the integrity of both is needed for transport. Several lines of evidence prove the close interaction of the NBDs. Whereas (in saturating conditions) MDR1/Pgp may bind two ATP molecules, only one ADP is trapped at a time, suggesting that ATP hydrolysis at one site prevents ATP binding or hydrolysis at the other NBD (134). Also, the inactivation of one NBD (by mutations, chemical modifications, or ADP trapping) blocks catalysis at the other site. The structural basis for this interaction of the two NBDs is best explained by a model where the two NBDs form common ATP binding sites. This formation, with the ATP sandwiched between residues provided by both nucleotide binding domains, was predicted by Jones and George (160) and confirmed in several ABC crystals (see sect. II; Figs. 3 and 4). The "open conformation" seen in crystals (in which the two NBDs are far apart) is in agreement with experimental evidence showing that α-^{32}P-8-azido-ATP binds to MDR1/Pgp with a low affinity and is readily exchangeable with unlabeled ATP (252). In the closed conformation, the bound ATP forms contacts with amino acids from both NBDs, which suggests that closing of the dimer interface precedes hydrolysis. Cross-linking studies (215, 218) have shown that at 37°C, cysteines located in the two NBDs can be within 1 Å from each other and that the "LSGGQ" motif in each nucleotide-binding domain is adjacent to the opposing Walker A sequence.

The very strong conservation of the ABC signature sequence implies an important role in catalysis. Mutational studies have confirmed that the conserved serine residues ("LSGGQ") cooperatively accelerate ATP hydrolysis (374). Our own results showed that mutation of the conserved glycine residue ("LSGGQ") in either NBD results in the loss of MDR1 ATPase. At the same time, ATP binding remained intact, and the formation of an AlF_4^- dependent transition state suggested that the mutants can promote the hydrolysis of at least one ATP molecule (365). Similarly, mutating the key Walker A lysine to methionine at either NBD inactivates the transporter but nevertheless remains compatible with ATP binding (252) and the hydrolysis of at least one ATP (366). Thus the inactivation of a single NBD does not prevent ATP binding or the dimerization of the NBDs. However, when the conserved amino acids were changed in both NBDs, despite intact ATP binding, the mutants fell into a complete catalytic silence, suggesting that the inactivation of both ATP binding sites prevents the formation of the integrated catalytic site.

The ATPase activity of MDR1/Pgp is stimulated by the transported substrates. As demonstrated above, it has been difficult to assess whether it is the ATP binding, hydrolysis, or the release of the hydrolytic products that is facilitated by the transported substrates. It can be argued that, to increase the overall rate of the ATPase cycle, substrate stimulation has to increase the rate of the limiting step. Our own results (in agreement with other reports using α-^{32}P-8-azido-ATP-labeling under nonhydrolytic conditions as a measure of ATP binding) indicate that ATP binding is not affected by the presence of substrates even when the substrates are present at saturating concentrations (252, 366). In contrast, the formation of the Pgp-ADP-V_i complex is accelerated by the transported drug substrates. Thus, with the assumption that the vanadate-trapped state reflects a physiological state in the catalytic cycle, the rate-limiting step has to precede the formation of the transition state. Therefore, it is unlikely that the release of ADP or P_i could be the rate-limiting steps of the cycle (176), especially considering that these steps are not dependent on transported substrates (9). If we assume that in the presence of vanadate the catalytic cycle is arrested after the first turnover, this result implies that drugs exert their stimulatory effect at steps that follow ATP binding but precede the formation of the transition state. Such a state may involve the "occlusion" of the ATP, where the nucleotide is not yet hydrolyzed, but has already evoked a closer association of the dimer interface (Fig. 8).

One of the outstanding issues remaining to be clarified is the elucidation of the intramolecular network that propagates signals from the transmembrane domains involved in drug binding to the ATP-binding domains, fueling the transport. Insight into the TMD-NBD communica-

tion may be gained from the analysis of mutant MDR1/Pgp variants. A spontaneous glycine to valine mutation in the intracellular end of the third transmembrane helix of MDR1/Pgp (G185V) was shown to confer increased colchicine resistance to cells. Interestingly, improved resistance to colchicine is not accompanied by changes in apparent drug binding affinity or the velocity of the ATPase (9). Al-Shawi et al. (9) suggest that, rather, the activation energy of the coupled transition state is reduced, indicating that G185 has a pivotal role in transmitting signals from the drug binding to the catalytic domains. In structural models of MDR1/Pgp, the intracellular loop containing G185 interacts with the Q-loop of the NH_2-terminal catalytic site. The conserved glutamines of the Q-loop have been shown to play a role in interdomain communication (381). Interestingly, in MDR1/Pgp variants harboring mutations in the ABC-signature region in either one of the catalytic sites, the presence of the transported substrate strongly inhibited (rather than stimulated) the formation of the transition state, indicating that the conserved glycine residue in the signature region may be involved in the intramolecular signal transduction that carries information from the TMD to the NBDs. Based on these observations, we suggested a model where ATP hydrolysis is initiated by drug-induced conformational changes, in the course of which the ABC-signature region is juxtaposed to the ATP bound in the contralateral NBD, facilitating the formation of the ultimate dimer interface, and the hydrolysis of the ATP (see Fig. 8) (365, 368). Only one ATP is hydrolyzed at a time. Based on molecular modeling, Jones and George (157) speculate that, while an ATP is hydrolyzed at one NBD, the helical region of this NBD is "retracted" from the contralateral ATP to prevent parallel ATP hydrolysis at the other site (157).

B. Transported Substrates of MDR1/Pgp

MDR1/Pgp is an omnivore; it confers resistance to a vast array of clinically and toxicologically relevant compounds, including (but certainly not limited to) anticancer drugs, human immunodeficiency virus (HIV)-protease inhibitors, antibiotics, antidepressants, antiepileptics, and analgesics (Table 1).

Bacterial multidrug-binding proteins (such as the transcription regulator BmrR from *Bacillus subtilis*) may provide model systems for the analysis of these wide-range drug interactions. Crystal structures of these proteins indicate that they interact with drugs through van der Waals interactions and hydrophobic stacking (426). However, models based on chemical cross-linking studies, photolabeling experiments, homology modeling, and pharmacophore patterns (266) suggest that MDR1/Pgp makes different interactions with different drugs, implying the involvement of several, partially overlapping residues. Thus each substrate appears to define a unique niche in the complex binding pocket through an "induced-fit" mechanism (216, 272).

TABLE 1. *Substrates of MDR1/Pgp*

Anticancer drugs
Anthracyclines
Daunorubicin
Doxorubicin
Epirubicon
Anthracenes
Bisantrene
Mitoxantrone
Vinca alkaloids
Vinblastine
Vincristine
Vinorelbine
Vindesine
Tubulin polymerizing drugs
Colchicine
Paclitaxel
Docetaxel
HIV protease inhibitors
Ritonavir
Indinavir
Saquinavir
Other compounds
Hoechst 33342
Rhodamine 123
Calcein-AM

AM, acetoxymethyl ester. [Data are from Ambudkar et al. (12) and Litman et al. (210).]

MDR1/Pgp substrates are expected to freely diffuse into the cells, and MDR1/Pgp may recognize them in the context of the plasma membrane (268). Studies using fluorescent substrates and FRET have confirmed that the drug binding sites are located within the membrane plane (225). There are strong indications that this type of recognition makes the MDR1 protein a highly effective multidrug resistance pump, preventing the cellular entry of toxic compounds. Theoretical models (353) and in vitro experiments (211) indicated that MDR1/Pgp may recognize its substrates before they reach the cytoplasm ("preemptive pumping"). This is in accordance with our observation that calcein-AM and other fluorescent methyl esters are extruded from the cell membrane, before the cleavage of the AM group occurs in the cytoplasm (126). The finding that the binding site of MDR1/Pgp for the transported substrate Hoechst 33342 is localized in the cytoplasmic leaflet of the bilayer (333) is in keeping with this proposal.

If MDR1/Pgp reacts with its substrates within the membrane lipid phase, it is still a question if drug removal occurs to the external water phase ("hydrophobic vacuum cleaner" model, Refs. 32, 268) or the drugs are only flipped from the internal membrane leaflet to the external leaflet, which promotes their overall removal from the cell (drug flippase model, Ref. 119). Most probably both mechanisms may occur, differently for different substrates of

variable size and hydrophobicity. In fact, it has been proposed that MDR1/Pgp evolved through mutations that expanded its substrate specificity from lipids to lipid-soluble toxic chemicals (194). Flippase activity has been attributed to other related transporters (see sect. VI), indicating a possible conservation of function between ABC proteins.

Besides the broad substrate specificity, MDR1/Pgp's unique feature is its basal ATPase activity. Basal ATPase activity is usually attributed to the transport of an "endogenous" substrate, present in the membrane or the lipid environment. However, purified MDR1/Pgp shows ATPase activity even in the absence of added lipids (205). A detailed analysis of purified MDR1/Pgp indicated that the drug-induced and basal ATPase activities are influenced by a single overall rate-limiting step that shows significantly different thermodynamic properties depending on the presence of a transported substrate (9). To avoid futile cycles, ABC transport engines should harvest the energy of ATP only in the presence of transported substrates. However, the distinct thermodynamic profile of the basal ATPase activity indicated that it is not linked to the transport (or flipping) of an endogenous substrate. Why is MDR1/Pgp "wasting" ATP molecules in uncoupled cycles? To maximize the chance of successful transport, MDR1/Pgp has to remain in a "transport-competent" conformation even in the absence of transported substrates. Al-Shawi et al. (9) speculate that this conformation has only one bound ATP (9). Therefore, in the event another ATP binds to MDR1/Pgp in the absence of the transported drug, MDR1/Pgp "resets" the transport-competent conformation by "wasting" an ATP. In the presence of saturating drug concentrations, the transporter follows the coupled pathway, where ATP is utilized exclusively for transport.

A partially uncoupled power source may be ideally suited for a transporter whose task is to handle compounds newly presented to the organism (194). As a prominent multidrug transporter, MDR1/Pgp has to retain a very low selectivity to substrates. Low selectivity comes at a price; in the absence of specific interactions, the transport process cannot benefit from the energy of drug binding. Therefore, the energy-dependent reorientation of the binding sites (the conformational changes necessary for transport) should also occur in the absence of transported substrates in an autonomous, although in a slow manner (uncoupled activity), during which a high-affinity loading site for drug binding is exposed. Thus, for the sake of broad substrate specificity, coupling efficiency is sacrificed and the need for specific substrate interactions is reduced.

Several groups have attempted to define the common pharmacophore of MDR1/Pgp substrates and inhibitors. One approach is based on the systematic modification of known inhibitors and substrates, such as chloroquine (420), vinblastine (3), reserpine (273), colchicines (372), verapamil (373), as well as of several peptides (337) (for review, see Ref. 12). No clear consensus has emerged, except for the finding that substrates are hydrophobic and tend to have planar aromatic domains and tertiary amino groups (326). The analysis of three-dimensional structures revealed that substrates typically contain hydrogen bond acceptor (or electron donor) groups with defined spatial separations. Modeling indicates that the rate-limiting step for the interaction of a substrate with MDR1/Pgp is the partitioning of the compound into the lipid membrane. Conversely, dissociation of the Pgp-substrate complex is determined by the number and strength of the hydrogen bonds formed between the substrate and the transporter. Thus a compound with a higher potential to form hydrogen bonds with MDR1/Pgp generally acts as an inhibitor (326).

A variety of in vitro assays have been used to classify compounds as substrates, nonsubstrates, or inhibitors (see also sect. III). Each approach has strengths and limitations, depending on the research setting and the questions asked. Monolayer efflux ("vectorial transport") systems are regarded as standard, because they measure efflux in the most direct manner, and they closely model pharmacological barriers. Indirect tests, such as the ATPase and calcein assays, are readily automated and offer higher throughput, but if used alone, they are less reliable in classifying compounds. Classification of compounds depends on the assay types. Admittedly, there is confusion. For example, verapamil is not predicted to be a substrate in the monolayer system (270), whereas, ironically, it was one of the first compounds to be identified as a stimulator of the MDR1/Pgp ATPase (307). Further complicating issues, above a certain concentration, verapamil inhibits the basal ATPase activity (see preceding section). From a cancer drug resistance viewpoint, verapamil is one of the most potent in vitro MDR1/Pgp inhibitors, tested even in clinical trials (27).

Using a systematic and uniform approach, Polli et al. (278) compared these methods using a set of structurally diverse compounds. Of the 66 compounds studied, the 3 assays (i.e., the monolayer efflux, ATPase, and calcein-AM assays) showed concordant results with only 35 drugs. Differences in predictions in the remaining set related to the apparent permeability [P(app)] of the compounds. Detection of Pgp-mediated efflux was associated with compounds having low/moderate P(app) values, whereas inability to detect Pgp-mediated efflux was associated with compounds having high P(app) values. Interestingly, the calcein-AM and ATPase assays revealed Pgp interactions for highly permeable compounds but were less responsive than monolayer efflux for low/moderate P(app) compounds. All assays detected substrates across a broad range of P(app), but the efflux assay was more prone to fail at high P(app), whereas the calcein-AM and ATPase assays were more prone to fail at low P(app). These

results indicate that when the apparent permeability of a compound is relatively low, efflux is a greater factor in the disposition of Pgp substrates (278).

It should be noted that transcellular flux assays are carried out under nonsink conditions, that is, in the absence of physiological binding proteins or hydrophobic components, usually examining the transport of only one compound at a time. As a consequence, efflux assays are more reliable at low/moderate *P*(app) and can be the method of choice for evaluating the absorption and distribution of such drug candidates. However, they may provide false-negative results in the case of compounds with high *P*(app), when MDR1/Pgp interaction is masked by a rapid back-leakage of the compound. Still, this interaction may significantly modulate in vivo drug absorption where acceptor molecules are present, or strongly modulate the transport of other transporter-interacting compounds. We certainly suggest that a proper combination of direct transporter interaction and flux assays should be applied to model any pharmacological relevance of the MDR-ABC proteins.

C. MDR1/Pgp in Cancer Multidrug Resistance

Despite recent developments, effectiveness of chemotherapy is still rather limited for most types of cancer, including tumors of the colon, lung, kidney, pancreas, and liver. Why some cancers respond better than others may be explained by factors relating to the anatomy and physiology of the cancer-ridden organ or the pharmacokinetics of the drugs used to combat the disease. In addition, tumors may resort to cellular mechanisms, which may prevent the accumulation of cytotoxic drugs in the cancer cells. Whereas the plasma membrane efficiently prevents the entry of hydrophilic drugs, the free diffusion of hydrophobic compounds is limited by active transport mechanisms.

With the discovery of MDR1/Pgp, it became evident that even a single protein can be responsible for the increased efflux of structurally unrelated compounds. As we have seen, MDR1/Pgp can export most neutral and cationic hydrophobic compounds, and cancer cells readily co-opt this mechanism as a primary shield against chemotherapy. This "first-line" defense is reasonably successful, as most of the routinely used agents of the current chemotherapy regimens are MDR1/Pgp substrates (see Table 1).

Certain tumors (including hepatomas and lung or colon carcinomas) often show intrinsic resistance to cancer chemotherapy. However, tumors may also develop resistance over the course of the disease progression and the treatment. Cancer cells, often heterogeneous with respect to initial MDR1/Pgp expression, are constantly selected for increased survival and proliferation. In line of the general protective function of ABC transporters, cells with higher levels of MDR1/Pgp have a selective advantage during adaptation to the hostile environment (such as hypoxia or inflammation). Thus, at the time of diagnosis, tumors may be prepared to cope with the additional stress of chemotherapy. Cytotoxic agents may eliminate most of the tumor mass, but the surviving cells usually give rise to clones that are resistant to repeated treatment efforts (Fig. 9).

Although in vitro models clearly show that MDR1/Pgp can protect tumor cells, the relevance of MDR1/Pgp function in clinical oncology remains controversial. To date, clinical researchers have failed to embrace universally accepted guidelines to standardize methods for the measurement and evaluation of the impact of MDR1/Pgp in therapy. There are several challenges pertinent to the estimation of expression levels, acquisition of tumor cells, and the evaluation of the results (an important pitfall is that MDR1/Pgp may be present in stroma). There are at least three different approaches to detect clinical MDR at the mRNA, protein, or functional level. Assays measuring mRNA levels benefit from the specificity and sensitivity of the available technologies that are, however, too expensive and time consuming for the routine clinical practice. Measuring protein levels seems to be a more relevant

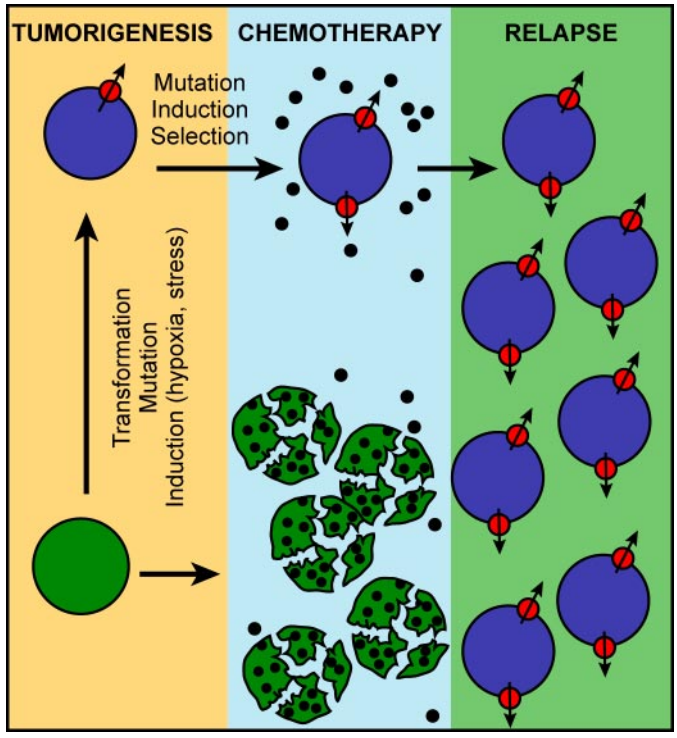

FIG. 9. Evolution of MDR1/Pgp positive cancer. Tumor cells arise by a complex mutation and induction pathway. Cells that do not express multidrug transporters are sensitive to chemotherapy and are eliminated. In the course of chemotherapy, further mutations and selection may greatly increase the expression of multidrug transporters, which protect the tumor cells against chemotherapy.

option, although it has proven difficult if not impossible to standardize procedures and evaluation criteria. Finally, tests measuring the capacity of cells to extrude drugs (daunorubicin, doxorubicin) or fluorescent dyes (rhodamine-123, calcein, $DiOC_2$) (95, 232, 240, 364) estimate the functional impact of transporters, which is arguably most relevant to clinical MDR. Our laboratory has pioneered the application of calcein-AM as a functional marker of the drug resistance phenotype. We have established a simple assay and demonstrated its applicability and predictive power in adult acute myelocytic leukemia (170). The development of this assay for solid tumors is in progress.

It is generally agreed that proper evaluation of clinical MDR should lead to a more efficient treatment of malignant diseases. Furthermore, chemotherapy-containing drug resistance-modulating agents should be planned and performed on the basis of a proper diagnosis of the actual presence and relevance of MDR (367). Because ABC transporters mediate resistance to a whole array of drugs, they should be an attractive target for the improvement of anticancer therapy. In theory, coadministration of MDR1/Pgp inhibitors with cytotoxic agents could reverse MDR and improve treatment outcome. There is no lack of compounds that have the capacity to inhibit MDR1/Pgp function. Nevertheless, despite promising in vitro results, successful modulation of clinical MDR through the chemical blockade of drug efflux from cancer cells remains elusive. Over the years, several generations of MDR1 modulators have raised hopes only to fail in clinical trials. The negative results may be explained by several factors, such as the intrinsic toxicity of the modulators and the unwelcome inhibition of MDR1/Pgp residing in pharmacological barriers, resulting in the altered distribution of the simultaneously administered chemotherapy. In our view, the lack of a serious effort to connect proper MDR-ABC transporter diagnostics, involving all major multidrug transporters, in the clinical trials of MDR modulators is another major factor in the current failure of such attempts.

D. Physiological and Pharmacological Functions of MDR1/Pgp

MDR1/Pgp shows high expression in the apical (luminal) membranes of epithelial cells lining the lower gastrointestinal tract, in the apical surface of proximal tubule cells of the kidney, in the canalicular membranes of hepatocytes, and in the capillary endothelial cells in the brain and testes. Lower levels are expressed in the placenta, the adrenal cortex, and CD34+ hematopoetic stem cells. Crucial data regarding the physiological relevance of MDR1/Pgp in these locations came from knockout mice studies. Mice have two *Mdr*1 genes (*Mdr*1a and *Mdr*1b), both of which were inactivated by insertional mutagenesis (321). Surprisingly, loss of either or both genes did not result in an obvious phenotype: the knockout mice were viable and fertile, almost indistinguishable from their wild-type littermates. These results were interpreted to suggest that pharmacological modulation of human MDR1/Pgp is a feasible strategy to treat multidrug-resistant cancer.

It is important to note that laboratory mice are raised in a well-controlled environment, where the function of the ABC transporter-based "chemoimmunity network" may be less relevant. This was proven in a legendary (and unplanned) experiment, in which the caretakers of the Netherlands Cancer Institute's animal department took center stage. Without prior notice, they sprayed the animal cages with ivermectin, a potent GABA receptor agonist of natural origin, routinely used to treat mite infestation. Ivermectin was supposed to kill only nematodes and arthropods, since mammalian neurons were expected to be protected by the blood-brain barrier. However, the treatment left all the knockout mice dead. When the scientists reproduced the experiment, the detailed toxicity assays showed that the Mdr1a (−/−) mice were 50- to 100-fold more sensitive to orally administered ivermectin, due to an increased accumulation in the brain (319, 321). These results were consistent with the high MDR1/Pgp expression in brain capillary cells and suggested that MDR1/Pgp plays a predominant role in the blood-brain barrier of mice. Interestingly, the well-known sensitivity of inbred dogs, such as collies and Australian shepherds, to ivermectin was also linked to a 4-bp deletion mutation resulting in a frame-shift and a lack of canine MDR1/Pgp expression (296). On the other hand, ivermectin is widely used to treat river blindness (onchocerciasis) in Africa. Interestingly, more than 20 million patients have been treated with ivermectin without any documented central side effects (208).

MDR1/Pgp is expressed in the apical (luminal) membranes of epithelial cells, lining organs regulating drug distribution. The expression pattern and the hypersensitivity of the knockout mice to xenobiotic toxins suggest a major physiological role of this protein in the protection of the organism against orally ingested natural toxins. MDR1/Pgp influences drug distribution in three ways: it limits drug absorption in the gastrointestinal tract; it promotes drug elimination in the liver, kidney, and intestine; and it regulates drug uptake into cells, tissues, or pharmacological compartments. The gastrointestinal tract, which represents the first line of defense against orally ingested toxins and drugs, is well equipped with a range of ABC transporters (see sects. VI and VIII). The AUC (area under the plasma concentration vs. time curve) of orally administered taxol is significantly higher in the knockout mice, suggesting that intestinal MDR1/Pgp is a major determinant of the reduced uptake of orally administered drugs (319).

Clinical studies indicate that the inhibition of intestinal MDR1/Pgp increases the oral bioavailability of substrate drugs, such as cyclosporin A (CsA). CsA is a critical immunosuppressive drug with a narrow therapeutic range and wide interindividual variation in its pharmacokinetics. Amlodipine, which is a substrate of MDR1/Pgp, significantly increases CsA absorption (198). As oral bioavailability is an important parameter in the development of drug candidates, the role of MDR1/Pgp-mediated transport in the gastrointestinal tract bears significant consequences in the design and formulation of pharmacological agents. To account for MDR1/Pgp-mediated restriction of oral absorption, in vitro models are used to follow the transcellular transport of drugs through the MDR1/Pgp-expressing intestinal cell line Caco-2 (see sect. III). Interestingly, intestinal MDR1/Pgp is also responsible for the excretory function of the gut wall mucosa (155, 234).

Exquisitely sensitive compartments, such as the testes and the brain, are protected by a second line of defense presented by the blood-tissue barriers. The central nervous system is shielded from the circulating blood by a complex physiological interface. In addition to the barrier formed by the tightly adjoined capillary endothelial cells (blood-brain barrier), the brain is further protected by the selective permeability of the epithelial cells in the choroid plexus (blood-cerebrospinal fluid barrier). At both locations, ABC transporters play a prominent role in restricting the passage of hydrophobic compounds that would otherwise cross these barriers by passive diffusion. The role of MDR1/Pgp was discerned in studies examining the brain accumulation of compounds in the knockout mice. Compared with wild-type mice, MDR1/Pgp substrates (such as ivermectin and vinblastine) show one to two orders of magnitude higher accumulation in the brain of the knockout animals (319).

This is relevant to human pharmacology, as illustrated by an experiment where the effect of loperamide on the central nervous system was followed. Although the antidiarrheal loperamide is a potent opiate, it does not produce opioid central nervous system effects at usual doses in patients. However, when loperamide was coadministered with the MDR1/Pgp-inhibitor quinidine, central opioid effects, such as respiratory depression, became prominent (299). The pharmacological relevance of MDR1/Pgp expands beyond the protection of the brain from ingested toxins and drugs of serious abuse potential. MDR1/Pgp represents an obstacle to the brain penetration of agents targeted to the central nervous system (CNS) to treat epilepsy, central infections (such as HIV), or brain tumors. Thus there is a pharmacological need to overcome barriers maintained by MDR1/Pgp in tissue-blood and tumor-blood interfaces. Because selective modulation of MDR1/Pgp in cancer cells is difficult to achieve, attempts to circumvent MDR will have to face the profound effects of MDR1/Pgp inhibition on the distribution of concomitantly administered drugs.

In addition to pharmacological barriers, expression of MDR1/Pgp can be detected in the adrenal gland, the pregnant uterus, the placental trophoblasts, and hematopoetic stem cells. Perhaps MDR1/Pgp has a specific role in these locations (such as the excretion of steroid hormones). Alternatively, it may just stand guard to protect valuable physiological sanctuaries (see sect. VII).

As we have seen, the majority of experimental data support that MDR1/Pgp is an active transporter and that the energy of ATP hydrolysis is used for the removal of cytotoxic compounds from the cells. However, it is particularly tempting to speculate that MDR1/Pgp (or other ABC transporters) regulate important physiological mechanisms, such as the self-renewal of stem cells. Recent observations support the possibility that MDR1/Pgp can regulate cell fate. In these experiments, MDR1/Pgp was found to confer drug resistance to cancer cells through the inhibition of caspase-dependent apoptosis (155). In fact, this antiapoptotic effect persisted even when MDR1/Pgp was rendered inactive by mutation of key lysine residues of the Walker A region. Intriguingly, these data suggest a dual activity model for MDR1/Pgp-induced MDR, involving both ATPase-dependent drug efflux and ATPase-independent inhibition of apoptosis (369). Although direct interaction between MDR1/Pgp and apoptotic enzymes has not been documented, it has also been hypothesized that MDR1/Pgp acts as a primary antiapoptotic regulator by reducing ceramide levels either through the reduction of inner leaflet sphingomyelin pools or through the modulation of the glyco-sphingomyelin pathway (222, 377). The validity of these interesting conjectures awaits further confirmation and back up by experiments using, e.g., knockout models.

It has been advocated that in mammalian cell membranes most of MDR1/Pgp is localized in "raft" domains, that is, in cholesterol-rich, relatively detergent-insensitive, light membrane fractions, and this localization and/or the level of lipids, especially cholesterol, drastically modulate MDR1/Pgp transport activity (see Refs. 19, 101, 226). However, functional reconstitution studies of purified MDR1/Pgp into different lipid mixtures argued against a profound effect of specific lipids or cholesterol on MDR1/Pgp function (248). A number of studies still suggest that a rather complex effect of the membrane environment, including the possible "flipping" of some membrane lipids, may modify the transport capacity or the substrate affinity of MDR1/Pgp (see Refs. 88, 335).

E. Regulation of MDR1/Pgp Expression and Function

1. Transcriptional regulation

Undoubtedly, MDR1/Pgp-mediated resistance of in vitro engineered cells is due to the wide substrate recognition and the high efficiency of the pump. In addition, the predominant clinical (in vivo) role of MDR1/Pgp in multidrug resistance is ensured by mechanisms regulating its expression. In that setting, regulatory mechanisms enable adaptation of cancer cells, and also orchestrate the detoxification machinery that involves drug metabolism and the efflux systems (see sect. VII).

Data from the literature suggest a coordinated regulation of MDR1 promoter activity, with several overlapping binding sites for many different transcription factors. It is likely that through the competition for binding sites, transcription factors regulate transcription in a highly complex and interactive manner, where the combination, rather than the individual elements of the myriads of factors shape the ultimate response and provide specificity. In this review, we only provide a brief description of the structure of the promoter, in addition to the list of cellular factors and mechanisms that are involved in the transcriptional regulation of human *ABCB1*. For more details, we refer the reader to an excellent recent review (325).

The MDR1 gene, as is true for all of the human multidrug transporters examined to date, has a "TATA-less" promoter, where, instead of a TATA box, the transcription complex is controlled by an initiator (Inr) element. The transcriptional factors acting on the MDR1 promoter can be classified into several major groups, which include the inverted CCAAT-box (Y-box) binding proteins (NF-Y, YB-1), the CAAT-box interacting proteins (c-*fos*, NFκB), and the GC-box interacting proteins (Sp1–3, EGR1, WT1). The requirement of each element in the constitutive expression of ABCB1 has been demonstrated in several cell lines.

The high-level expression of MDR1/Pgp in tumors raised the possibility that oncogenes or tumor suppressor genes may regulate constitutive *ABCB1* expression. p53 plays a complex role in the regulation of *ABCB1*, which may depend on the cellular environment, the cytotoxic drug used during selection or treatment, and mutations in p53 (43). The negative regulatory role (i.e., suppression) of wild-type p53 was published more than a decade ago (59), but the interacting site (a novel head-to-tail site, HT-site) in the *ABCB1* proximal promoter region was identified much later (153). Surprisingly, several common p53 mutants activate, rather than suppress, the *ABCB1* promoter (302). The effect of two members of the p53 family (p63 and p73) on *ABCB1* transcription has been discovered recently. Overexpression of p63 and/or p73 in certain types of tumors may facilitate *ABCB1* expression, thus influencing multidrug resistance in cancer. Both p63 and p73 activate, rather than repress, the *ABCB1* promoter (154). The activation is independent of the p53-interacting ("repressor") site or the "activator" site involved in the effect of the mutant p53.

Overexpression of MDR1/Pgp (or other multidrug transporters) in drug-resistant cells is either due to gene amplification or to elevated level of transcription. As mentioned above, a multiple start site element is present in the *ABCB1* promoter, which was found to be functional in the activation of the gene in drug-resistant cell lines (228). In a recent report, this site (invMED1) was precisely localized between −105 and −100 bp, and the LRP130 protein was identified as a component of the nuclear factor that binds to the invMED1 site (199). It was also demonstrated that the invMED1/LRP130 complex formation increased with the chemoresistance level. The presence of another regulatory site between −118 and −111 bp was identified, binding a 130-kDa nuclear protein, named MDR1 promoter-enhancing factor (MEF1) (258). This interaction results in the upregulation of the *ABCB1* gene. Recently, it was reported that RNA helicase A (RHA) is a component of the multiprotein complex that interacts with the −118 to −111 site in the *ABCB1* promoter of a drug-resistant cell line (427). It was also shown that RHA is involved in upregulation of the *ABCB1* expression in drug-resistant but not in drug-sensitive cells.

Permanent genomic alterations, like translocations or mutations in regulatory sequences, provide a possible mechanism for transcriptional alterations. Fojo and colleagues have used fluorescence in situ hybridization (FISH) to reveal breakpoints between MDR1 and sequences 500–1,000 kb telomeric to it. The rearrangements resulted in the capture of MDR1 by constitutively expressed genes, suggesting that random chromosomal rearrangement is a mechanism for activation of MDR1 in drug-selected cell lines and patient samples acquiring anticancer drug resistance (182, 238, 352).

The dynamic changes in the structure of chromatin can fundamentally influence gene expression. Chromatin-modifying enzymes, like histone acetylases (HATs) and histone deacetylases (HDACs), were found to be involved in the regulation of the *ABCB1* gene. It was observed that upon treating the cells with specific HDAC inhibitors, the endogenous *ABCB1* promoter as well as *ABCB1* promoter/reporter constructs were activated (152). It was also shown that this activation is dependent on both an intact inverted CCAAT box and the transcription factor NF-Y.

Several studies have shown that the transcription of *ABCB1* is regulated by DNA methylation. One consequence of CpG methylation is the silencing of *ABCB1*, which correlates with binding of methyl-CpG binding protein 2 (MeCP2) to the promoter, as was demonstrated by

chromatin immunoprecipitation (94). According to the suggested model, inhibition of HDAC activity results in hyperacetylated core histones, but this does not activate transcription unless chromatin is demethylated and MeCP2 is released. This means that the transcriptional control is managed by two epigenetic events; when densely methylated, *ABCB1* is transcriptionally silent, and upon demethylation, activation of *ABCB1* is mediated by HATs. There is a large body of evidence supporting the notion that methylation is a central mechanism by which *ABCB1* is silenced in tumor cells. However, the epigenetic events during tumorigenesis are not well understood, and the role of this mechanism in various tumor types can be fundamentally different. A recent review discusses how new developments of the expanding epigenetics field contributes to understanding *ABCB1* transcriptional regulation (21).

MDR1/Pgp levels respond to stress signals, like heat shock, inflammation, hypoxia, exposure to xenobiotics, toxic metabolites, or ultraviolet (UV) irradiation. A heat shock element (HSE) is localized in the −152 to −178 bp region, and interaction of heat shock transcription factor 1 (HSF-1) with this element results in activation of *ABCB1* (58, 392). Clearly, activation by chemical stress agents, cell differentiating agents, and UV radiation occur independently of this site and involve another promoter region called "MDR1 enhancer" or "MDR1 enhansome" (325). This region harbors sites for transcription factors of the Sp family with GC-binding activity and NF-Y. These factors, upon DNA-binding, recruit histone acetyltransferase to the *ABCB1* promoter, which triggers histone acetylation and transcriptional activation.

Expression of multidrug transporters is often induced transiently in response to chemotherapeutic compounds. In contrast to the original hypothesis stating that only drugs that are transported substrates of MDR1/Pgp induce expression, it was found that non-MDR drugs can also trigger *ABCB1* transcription. In such cases, the induction was associated with cellular damage, raising the possibility that induction of *ABCB1* transcription is an element of the general cellular response to toxic effects (51).

Several nuclear receptors (like the retinoic acid receptor, RAR; the steroid-activate receptor, SXR; the constitutive androstane receptor, CAR; and the farnesoid receptor, FXR) were found to be involved in regulating the expression of various human ABC transporters. The *ABCB1* promoter is activated by all-*trans*-retinoic acids in neuroblastoma cell lines, but the pathway is independent of RAR/RXR-binding (which is the general mechanism in regulation of other ABC transporters). Rather, it is mediated by Sp family member transcription factors interacting with the GC site of the MDR1 enhansome (325).

Hypoxia causes genomic instability and is linked to metastasis and tumor growth and the induction of stress-associated genes. It is not unexpected that MDR1/Pgp expression increases under hypoxic conditions. The hypoxia-inducible factor 1 (HIF-1) binds to a site in the *ABCB1* promoter, which overlaps with the GC site playing a role in constitutive and in inducible expression, and activates the promoter (325).

Under acute phase conditions (i.e., in response to inflammation), when inflammatory cytokines act on the gene expression profile of the liver, *ABCB1* is also induced in this organ (256). The interleukin-6-induced CAAT enhancer-binding protein (C/EBPβ) activates human *ABCB1* via interaction with the −147 to −139 bp region of the promoter (63). In rodents, a homologous site is present that is involved in the glucocorticoid receptor-mediated activation of the hamster *Mdr1* gene (325). This may suggest that in hamster, inflammatory and anti-inflammatory signals act in a concerted manner on the *Abcb1* promoter. It was also shown that both mouse *Mdrl* and *Mdr3* and human *ABCB1* can be activated in hepatoma cells exposed to dexamethasone (a synthetic glucocorticoid), demonstrating that the expression of these genes can be modulated by glucocorticoids. Glucocorticoids are used in chemotherapy of cancer, and better understanding of their regulatory role in *ABCB1* transcription would be important (425).

2. Posttranscriptional regulation of MDR1/Pgp

Increased mRNA stability was identified as the basis of MDR1/Pgp overexpression in certain drug-selected cell lines (405). On the other hand, several studies indicate that the correlation between the level of mRNA and functional MDR1/Pgp expression is relatively poor, and highly variable under different in vitro and in vivo conditions. This discrepancy may be one of the causes why the role of MDR1/Pgp in cancer resistance is still debated.

As mentioned above, MDR1/Pgp is extensively glycosylated, but this glycosylation is clearly not a major factor either in the localization or the transport activity of the protein. According to recent information, MDR1/Pgp localization and stability may be more efficiently regulated by ubiquitination (424). MDR1/Pgp has also been shown to be phosphorylated at numerous sites, especially in the cytoplasmic linker region, connecting the two homologous halves (2, 103, 105). In early experiments the potential role of protein kinase C (PKC)-dependent phosphorylation (2, 410) in the function of MDR1/Pgp was advocated, especially because several PKC inhibitors also inhibited MDR1/Pgp function (see Refs. 23, 109). However, these results may have reflected a direct interaction of PKC inhibitors with MDR1/Pgp, and not a regulation through protein phosphorylation (135, 347). In detailed experiments, involving mutagenesis of the potential phosphorylation sites and direct measurement of MDR1/Pgp function, it became clear that phosphorylation has no essential role in the transport capacity of this protein,

while a slight modulation of substrate affinity or selectivity may involve such a covalent modification (46, 103, 106, 347, 361).

V. THE ABCG2 (MXR/BCRP) PROTEIN

A. Biochemistry and Cell Biology of ABCG2

The ABCG2 protein is a member of the ABCG subfamily, which in humans contains five homologous half-transporters, with the ABC domains located toward the NH_2 terminus of the polypeptide chain (see sect. II). Within this group we have no detailed knowledge about the physiological function of ABCG1 and G4, while ABCG5 and G8 are known to work as heterodimers, transporting various cholesterol-related molecules and providing resistance to plant-derived sterols (see sect. VI). As far as we currently appreciate, the only bona fide plasma membrane multidrug transporter in this group is ABCG2.

1. Structure and cellular localization

ABCG2, a 655-amino acid glycoprotein, was cloned independently from two drug-selected cell lines and a human cDNA library and was given three different names. ABCG2 cloned from a heavily drug-selected breast cancer cell line was named breast cancer resistance protein (BCRP; Ref. 83). The cDNA obtained from cells selected by mitoxantrone in the presence of verapamil (to block MDR1 function) codes for a protein denoted as mitoxantrone resistance protein (MXR) (245). The putative protein product of the cDNA obtained from a human cDNA library and showing enrichment in the placenta was named ABCP (8). Interestingly, the only cDNA coding for the wild-type protein was this latter one, while both cDNAs obtained from drug-selected cells contained a single nucleotide mutation, coding for altered amino acids at position 482 (R in the wild-type protein, T in BCRP, and G in MXR). These cloning differences produced a lot of controversy in the literature related to the substrate recognition and transport properties of ABCG2 (see below).

The suggested membrane insertion pattern and topology of ABCG2 have been already shown in Figure 2, with six TM helices and a conserved ABC domain, although in a reverse arrangement compared with the ABCB or ABCC groups of transporters. It should be mentioned that membrane topology predictions for the ABCG group indicate a major difference in the interhelical loop arrangements compared with those in other subfamilies. Namely, the members of the ABCG family contain a relatively large extracellular loop between TM5 and TM6, and this arrangement prevents proper homology modeling for ABCG2, based on related ABC structures.

ABCG2 is physiologically expressed in a variety of tissues, most abundantly in the liver and intestinal epithelia, the placenta, the blood-brain barrier, and various stem cells. ABCG2 is a plasma membrane glycoprotein, in polarized cell types localizing to the apical regions (161, 227). ABCG2 is extensively glycosylated (from among the three predicted *N*-glycosylation sites) on asparagine-596, which is located within the third extracellular loop of the polypeptide (78, 250, 370). The extent of glycosylation of ABCG2 is variable in different tissues, but it has been clearly established that ABCG2 glycosylation, similarly to that found for MDR1 or MRPs, is not required either for the proper expression, function, or routing of this protein. Despite the lack of glycosylation, ABCG2 could be functionally expressed both in insect cells (260, 261) and in *Lactococcus* bacteria (151), and the removal of the predicted glycosylation sites did not modify either the membrane localization or the transport function of the protein in mammalian cells (78, 370). Moreover, in glycosylation-deficient mutants, both the steady-state expression and the half-life of the protein were unchanged (78).

An interesting feature of the ABCG2 protein that its structure and/or dimer form is stabilized by S-S bridges within the third extracellular loop of its transmembrane domain (see below). Recent biochemical studies established that alterations or removal of the NH_2-terminal 5–10 amino acid regions are not harmful for ABCG2 localization or function, while the COOH terminus (which, according to the membrane topology model has only a few amino acids outside the transmembrane region) is highly sensitive. Decoration of this area by conventional tags (e.g., 10-His or GFP) drastically reduces transport function and in most cases alters the membrane localization of ABCG2 (370 and C. Özvegy-Laczka and B. Sarkadi, unpublished experiments).

2. Transport properties

ABCG2 is an active transporter for many different drugs and metabolites, by extruding these compounds from the cells through a process energized by ATP hydrolysis. As discussed in detail below, the transported substrates of ABCG2 include many cytotoxic drugs, their partially detoxified metabolites, toxins, and carcinogens found in food products, as well as endogenous compounds. Similarly to all ABC multidrug transporters, drug extrusion by ABCG2 is closely coupled to a drug-stimulated, vanadate-sensitive ATPase activity, which requires the presence of Mg^{2+} (260). The direct, ATP-dependent transport of several less-hydrophobic substrates of ABCG2, e.g., methotrexate (264, 394), glucuronidated methotrexate, or sulfated estrogens and xenobiotics (56, 143, 359, 394) has been directly demonstrated in inside-out membrane vesicles. In polarized cell lines, obtained from MDR/MRP knock-out mice and transfected with human ABCG2, the transepithelial transport of a dietary

carcinogen and an H2 receptor antagonist, cimetidine, was demonstrated (271).

The substrate transport and ATP cleavage cycle of ABCG2 has not been investigated as yet in such detail as for MDR1 or MRP1, but we suspect no major differences in the basic steps. Mutation of the key lysine residue within the Walker A domain (K86) to methionine (similarly to that found for MDR1 or MRP1) abolishes both transport and ATPase activity of ABCG2. ATP binding and the formation of a reaction cycle intermediate, occluded ADP, stabilized (trapped) by vanadate in this protein have also been documented (261). Recently, we found that the binding of the anti-ABCG2 monoclonal antibody 5D3, recognizing an extracellular epitope of this protein, can be applied to investigate the catalytic cycle-dependent conformational changes of ABCG2. The ATP-bound or nucleotide-trapped forms of ABCG2 show low-affinity antibody binding, while the ADP-bound and substrate-inhibited forms show maximum antibody-binding (265). These binding differences suggest major conformational movements within ABCG2, which have also been suggested by the molecular models for various ABC transporters detailed in section II.

In the case of ABCG2 we have the advantage of having a specific, high-affinity inhibitor molecule. Rabindran and co-workers (280, 281) first observed that a micotoxin, Fumitremorgin C, was a strong inhibitor of drug resistance in ABCG2-expressing tumor cells, and Koomen and co-workers (386) developed derivatives of this molecule with potent and selective inhibitory action on ABCG2. One of these molecules, Ko143 (7), inhibits ABCG2 in nanomolar concentrations, whereas it has practically no effect on other multidrug transporters or on cellular functions up to micromolar levels. As shown in several studies, Ko143 blocks both the transport and the ATPase activity of ABCG2 at the same low concentrations. According to our unpublished studies, Ko143 is a high-affinity competitive-type inhibitor, probably interacting with the "off-site" of drug binding in the ABCG2 protein (Özvegy-Laczka, Glavinas, and Sarkadi, unpublished data).

ATP cleavage and the transport cycle, as in all ABC multidrug transporters, seem to be coupled to events in the ABCG2 protein. However, when the ATPase activity of the human ABCG2 protein was examined in isolated Sf9 cell membranes, we found that the ATPase activity of the wild-type protein was high and could be hardly stimulated by substrates of the transporter (260, 261). In contrast, in membranes isolated from ABCG2-overexpressing mammalian cells, the ABCG2-ATPase activity was significantly stimulated by many transported substrates (67, 247). The lack of glycosylation of ABCG2 in Sf9 membranes cannot be responsible for this effect (370), and we suspect that the lipid composition of the insect cell membrane results in an endogenous modulation of the ABCG2 ATPase activity (see below). As judged from expression levels and transport/ATPase measurements in isolated cell membranes, human ABCG2 has a similar, or even higher turnover than the MDR1 protein (260).

3. Dimer formation

As detailed in section II, according to our current knowledge the minimum requirement for a functional ABC transporter is the cooperation of two ABC and two transmembrane domains; thus the functional form of ABCG2 must be at least a dimer. Most experimental data indicate that in the case of ABCG2, the prevalent form is a homodimer; at least a homodimer can carry out all the relevant transport functions. In drug-selected cell lines, the upregulation of the *ABCG2* gene expression alone was sufficient to cause drug resistance (183, 245), and transfection by the ABCG2 cDNA alone produced massive drug resistance in various mammalian cells (82). When human ABCG2 was expressed in heterologous Sf9 cells (260), or even in *Lactococcus* (151), the protein was fully functional, although unlikely to find any endogenous dimerization partners in the insect cells or bacteria, respectively. A dominant negative effect of a nonfunctional ABCG2 mutant on drug resistance and transport function (93, 166) is also indicative of protein homodimerization.

Homodimerization of the ABCG2 protein was directly demonstrated by using nonreducing SDS gels, where a disulfide-bridged dimer of ABCG2 was found to occur (166, 277, 370). Due to the reducing intracellular environment, such a physiological disulfide link can only be formed between SH groups present on the extracellular loops of the protein. Indeed, three cysteines, conserved in most mammalian ortholog ABCG2 sequences in the third extracellular loop, were found to play a key role in the dimerization, expression, and localization of this protein (117, 370). According to our unpublished studies (Özvegy-Laczka and Sarkadi, unpublished data), chemical cross-linking of ABCG2 dimers may still preserve transport function, while various modifications of the cell surface S-S bridges may result in the loss of ABCG2 transport activity. Several sequence motifs within ABCG2 have been suggested to influence ABCG2 function and dimerization (277), but a clear-cut picture has not yet been established in this regard. As suggested by one experimental study, higher order oligomerization of ABCG2 may be involved in the function of this protein (404).

B. Transported Substrates of ABCG2 and Its Mutants/Variants

ABCG2 is a drug transporter with a wide substrate specificity, that includes large molecules, both positively and negatively charged, with amphiphilic character. The reported cytotoxic drugs extruded by the wild-type hu-

man ABCG2 are mitoxantrone, topotecan, the active metabolite (SN-38) of irinotecan, camptothecin, flavopiridol, and methotrexate. The transported substrates of this protein also include sulfated hormone metabolites, antibiotics such as nitrofurantoin, antihelmintic benzimidazoles, various flavonoids, the food carcinogen PhIP, the chlorophyll metabolite pheophorbide a, fluorescent dyes such as Hoechst 33342 and BODIPY-prazosin, or the H2 receptor antagonist cimetidine (24, 146, 161, 162, 210, 235, 254, 271, 287, 384, 393). The pharmacological and possible physiological substrates are discussed in detail in the relevant following sections.

There is little information on the structural elements responsible for the substrate recognition and transport by ABCG2. In the case of MDR1 and MRP1 (see above). The transmembrane domains were found to be responsible for the recognition of transported substrates. In the case of ABCG2, the artificial R482 mutants and the naturally found polymorphic variants of this protein might give a lead to study these recognition sites and patterns.

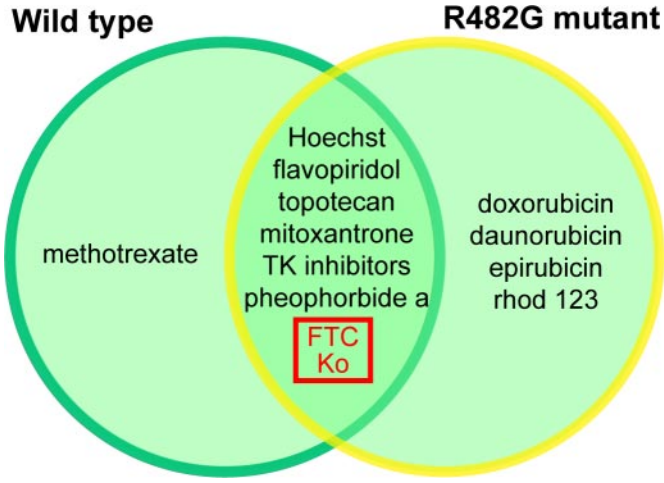

FIG. 10. Transported substrates and inhibitors of the wild-type and R482G ABCG2 protein. The Venn diagram depicts some of the transported substrates and inhibitors (in a square) for the wild-type and the R482G mutant variant of ABCG2. The major differences in this selectivity are discussed in the text.

1. Mutant variants of ABCG2

The cloning variants first characterized in drug-selected mammalian cells (R482G and R482T) caused a lot of uncertainty regarding the substrate profile of ABCG2, but became also educative regarding the substrate handling of this protein. ABCG2 variants containing either R482G or R482T conferred increased mitoxantrone resistance to transfected cells; moreover, they introduced anthracyclin (doxorubicin) resistance and rhodamine-123 extrusion capacity, which were not found in the case of the wild-type protein (see Fig. 10, Refs. 127, 261). In contrast, the R482G and R482T mutants were not able to extrude methotrexate, which is a transported substrate of the wild-type ABCG2 (56, 242, 393). Interestingly, the same phenomenon was observed in the case of the mouse Abcg2 protein; drug selection induced a mutation exactly at the same position (R482M or R482S in the mouse Abcg2), similarly altering the substrate handling of this ortholog (5). Numerous groups carried out human population studies to find the occurrence of 482 variants, but none of the amino acid 482 mutants was found in human SNP screening studies, meaning that this alteration cannot be causative of different drug extrusion patterns found in normal human populations (5, 128, 148, 185, 247).

Still, the role of this mutation in ABCG2 may give important information on the structure-function aspects. Recently two detailed studies (244, 264), examining the effects of artificial amino acid 482 mutations in ABCG2 by using various cellular expression and transport systems, have clearly demonstrated a key role of this site in the ABCG2 transport function. In intact, transfected cells, these mutants showed significantly different drug resistance patterns, some with a gain-of-function while several others with a loss-of-function character (244). When expressing nine Arg-482 mutants of ABCG2 in Sf9 cells (264), we found that none of these changes was detrimental for the correct folding, cell surface expression, or ABCG2-specific ATPase activity (inhibited by Ko143). Mitoxantrone was transported by all ABCG2 variants, except by R482K. Rhodamine-123 was extruded by most of the mutants, except by R482K, R482Y, and the wild-type ABCG2. Interestingly, the R482K variant had relatively low activity in all assays, although this mutation (Arg to Lys) represents only a minor change without charge alteration. In contrast, the removal of the positive charge or even the introduction of a negative charge at this site, in several cases greatly increased or in other cases did not alter the transport activity. While no detailed structural data for ABCG2 are currently available, according to the topology models amino acid 482 is localized within, or near to, the cytoplasmic end of the third transmembrane helix of the protein. The above functional data may become even more valuable when the substrate recognition site of ABCG2 can be properly modeled.

A key observation in these studies was that methotrexate transport was singularly supported by the wild-type ABCG2. This finding suggests that, although the natural R482-ABCG2 protein has a lower turnover and narrow substrate recognition, a group of transported molecules, including folates, methotrexate, and its conjugated variants, may be preferential substrates of ABCG2 under in vivo conditions. This special recognition might give a strong selective force in evolution to keep this variant uniformly present in the population. No apparent mutation hot spots such as CpG islands can be identified in this particular region, and these mutations were probably generated as a combined result of the mutagenic

effect of the cytotoxic drugs and a long-term in vitro drug selection. As mentioned later, these variants with a selected transport profile may be helpful for various cell protection applications.

It is worth noting that in addition to the amino acid 482 *ABCG2* mutations, several other variants, A149P, T153M, R163K, and P269S, were identified in different cell lines that were also not detected in healthy individuals (188, 247) (Fig. 11). In the case of in vitro expression, the above ABCG2 variants did not show any difference from the wild-type ABCG2 protein, neither in their subcellular localization in LLC-PK_1 polarized cells, nor in their estrone sulfate, dehydroepiandrosterone sulfate (DHEAS), methotrexate, or *p*-aminohippurate (PAH) transport. Therefore, it is not clear why these variants appeared in drug-selected cell lines (188), although it is interesting that three out of four mutations identified to date affect nonconserved amino acids of the ATP binding domain. In the first cloning of the *ABCG2* cDNA from human placenta (8), several sequence alterations causing amino acid changes, including A24V, Q166E, and F208S, were recorded, compared with the database reference sequence. In subsequent studies, these nucleotide substitutions were not detected in healthy individuals or patients (see Ref. 418), and we are unaware of any functional consequences of these alterations. In contrast, the polymorphic variants of the ABCG2 protein, appearing in >1% in the human populations, have attracted a lot of attention in the past few years. We discuss these variants in section V, *C* and *D*.

C. ABCG2 in Cancer Multidrug Resistance

1. Anticancer agents and ABCG2

As mentioned above, ABCG2 transports a wide variety of anticancer agents. A key group in this regard includes topoisomerase I inhibitors, e.g., topotecan, irinotecan, and its active metabolite SN-38 (255, 317). From the discovery of the protein we know that ABCG2 extrudes the important anticancer agents mitoxantrone, camptothecin and its analogs (e.g., diflomotecan, a synthetic derivative of camptothecin), as well as flavopiridol, a promising drug under clinical development (96). As described in section IV, the MDR1 protein has an overlapping transport profile with ABCG2, and the relative role of the different MDR-ABC transporters in the extrusion of a given compound is difficult to assess.

A potentially clinically important role of ABCG2 is to transport methotrexate (MTX) and its polyglutamated forms, thus greatly modifying both short-term and long-term methotrexate resistance in various cancer cells. Among the MDR-ABC transporters, several MRPs can also transport methotrexate, but these pumps are usually unable to extrude the intracellularly glutamated forms of folates or folate antagonists, while ABCG2 is a highly active pump for all glutamated folates. Moreover, ABCG2 has a relatively high capacity and affinity in transporting newly developed antifolate agents and folate derivatives (399) as well. The in vivo relevance of MTX transport is suggested by the finding that in cancer patients the coad-

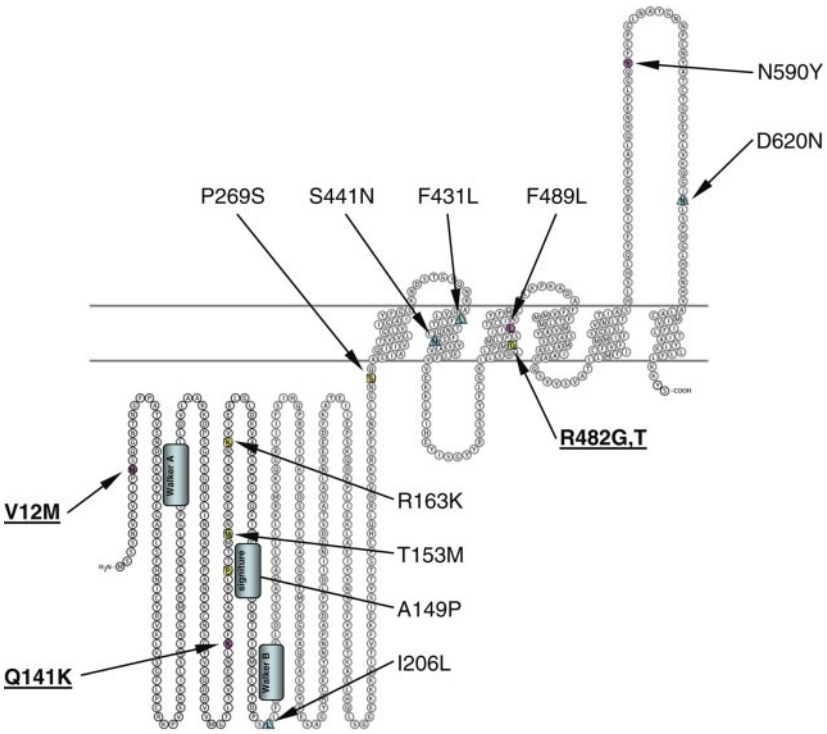

FIG. 11. Mutations and polymorphisms in the ABCG2 protein, demonstrated in a membrane topology model. The key mutations and polymorphic variants described in ABCG2 are demonstrated in the membrane topology model of this protein (for details, see text).

ministration of benzimidazoles and MTX can result in severe toxicity, with an increase in the serum concentrations of MTX. Competition of MTX and the ABCG2 substrate benzimidazol on this transporter may explain this pharmacological interaction (37).

The chemically heterogeneous group of anticancer agents interacting with ABCG2 includes a variety of tyrosine kinase inhibitors (TKIs). In current antitumor drug research, TKIs are highly promising agents for specific inhibition of malignant cell growth and metastasis formation. However, their therapeutic potential also depends on access to intracellular targets, which may be significantly modulated by ABC membrane transporters. Several research groups have recently shown that the human ABCG2 multidrug transporter interacts with a number of anticancer TKIs, including Imatinib (STI-571) and Iressa (ZD 1839).

According to our in vitro experiments (263), both Iressa and Imatinib inhibit the transport function and cell protecting activity of ABCG2 in submicromolar concentrations. Because low Iressa concentrations stimulated the ABCG2-ATPase activity, we suggested that Iressa may be a transported substrate. Stewart et al. (355) examined the effect of Iressa in tumor xenografts and Saos2 cells and found that this TKI reversed ABCG2-mediated resistance to irinotecan and SN-38. Still, their experiments indicated that Iressa is not a transported substrate for ABCG2.

To answer the question if Iressa is extruded by ABCG2, two recent studies examined a pharmacologically relevant model system, that is the growth of A431 tumor cells, depending on epidermal growth factor (EGF) receptor signaling. Yanase et al. (406) reported that in transfected A431 cells, ABCG2 provided a significant resistance against Iressa. In our experiments (93), the retroviral expression of ABCG2 protected A431 cells from Iressa, while this protection was absent in the presence of the selective ABCG2 inhibitor Ko143 or in cells expressing an inactive ABCG2 mutant. ABCG2 function also prevented EGF receptor dephosphorylation and the extracellular appearance of phosphatidylserine, a marker for early apoptosis (93).

When studying the action of Imatinib in Saos2 osteosarcoma cells expressing ABCG2, Houghton et al. (133) found that this TKI reversed SN-38 and topotecan resistance in submicromolar concentrations. However, the sensitivity to Imatinib, or the accumulation and efflux of labeled Imatinib, was not modulated by ABCG2 expression; therefore, these authors concluded that Imatinib is a high-affinity inhibitor, and not a transported substrate of ABCG2. In contrast, by using labeled Imatinib and ABCG2-expressing MCF-7 or HEK cell lines, Burger et al. (40) showed that the accumulation of Imatinib was significantly lower in ABCG2-expressing cell lines than in the parental cells. Moreover, when the specific ABCG2 inhibitor Ko143 was added, Imatinib accumulation in ABCG2-expressing cell lines reached the same high level as in parental cells. Breedveld et al. (36) found an active, vectorial transport of Imatinib in an epithelial cell monolayer, transfected with the mouse Abcg2. Moreover, according to their results, ABCG2 function limits the penetration of Imatinib through the blood-brain barrier (see below).

These experimental data suggest that both Iressa and Imatinib interact with ABCG2 at low, pharmacologically relevant concentrations and while they inhibit the transport of other substrates, these TKIs are also transported by ABCG2. These data also indicate that the expression and function of ABCG2 may significantly alter the absorption, metabolism, and toxicity of TKIs (262).

Some of the above discussed results suggest that there may be a narrow concentration range in which multidrug resistance proteins can transport the TKIs, while above these concentrations TKIs inhibit the function of these proteins (93, 262). Therefore, it is possible that ABCG2 may not influence the intestinal absorption of, e.g., Iressa, present at this site in high concentrations, but may play a role in cellular extrusion of this compound where its local concentration is lower.

2. ABCG2 expression in tumors

Although experimental data for cytotoxic drug transport by ABCG2 are convincing, a key question for the in vivo relevance is the functional expression of ABCG2 in various human tumors. Overexpression of ABCG2 was first documented in drug-selected cell lines from ovary, lung, breast, colon, and gastric cancer, mediating in vitro resistance against various cytotoxic compounds (6). According to the analysis of ABCG2 mRNA and protein levels in blast cells from acute leukemia patients, ~30% of the patient samples were identified with relatively high expression of ABCG2 (295, 304). In acute lymphoblastic leukemia (ALL), ABCG2 expression was more abundant in B-cell lineage ALL, with a function to produce significant drug resistance (275). More and more data indicate that individuals with higher ABCG2 expression in their leukemic blast cells have a higher probability of poor response to chemotherapy (28, 354, 358, 378).

Immunohistochemical studies in human tumors revealed frequent expression of ABCG2, especially in adenocarcinomas of the digestive tract, lung, and endometrium (76). However, both intracellular and plasma membrane staining was observed; thus the drug extrusion relevance of this protein expression may be questionable. In non-small cell lung cancer (NSCLC) tissue extracts, the expression and function of ABCG2 were analyzed in parallel experiments (174), and the authors concluded that these tumors expressed sufficient functional ABCG2 to confer drug resistance. In a retrospective study in NSCLC, the chemotherapy response rate in patients was found to

be correlated with ABCG2 expression (while not with MDR1, MRP1, or MRP3 expression), suggesting that the inhibition of ABCG2 function may help overcome drug resistance in such patients (408).

ABCG2 expression was greatly increased in irinotecan- and SN 38-resistant colon cancer cell lines, and the in vivo overexpression of ABCG2 in the metastases of irinotecan treated patients was also detected (44). Still, the controversy about the actual role of ABCG2 in cancer multidrug resistance is unresolved, and the major hope in this regard is the introduction of proper, quantitative laboratory diagnostic methods for the detection of ABCG2 in tumor samples.

3. Diagnostics of ABCG2 expression and function

On the basis of the above-described role of ABCG2 in tumor drug resistance, the selective and sensitive detection of the ABCG2 protein may have a major importance in cancer diagnostics and treatment. Determination of RNA or total protein levels in the case of MDR-ABC transporters may lead to seriously misleading results, as the active form of these transporters is only the protein properly localized on the cell surface and in polarized cells in the right membrane compartment. One possible way is thus to determine the cell surface expression level by using monoclonal antibodies, while the other approach is to directly measure the transport function of the protein in intact tumor cells.

As to the determination of ABCG2 cell surface expression, a group of monoclonal antibodies have been developed that specifically recognize this protein on extracellular epitopes in intact cells (430). Interestingly, the antibody, named 5D3, inhibits the transport and ATPase function of ABCG2 in intact cells (265, 430), and both antibody binding and the inhibition of ABCG2 function depend on the actual conformation of the transporter (265). Thus the proper detection of quantitative ABCG2 expression by this antibody requires fixation of the protein in a high-affinity conformation, either by chemical cross-linking or by stabilization of a specific step within the transport cycle. The increasing knowledge on the antibody-reactive conformations of ABCG2 should improve the use of this important diagnostic tool.

The other major way to characterize the relevant multidrug transporter activity of ABCG2 is to measure the active extrusion of a labeled or fluorescent compound. In practical laboratory diagnostics, the use of a nontoxic fluorescent dye, with a unique interaction with ABCG2, and providing high level fluorescence in a convenient wavelength area, would be most advantageous both in flow cytometry and fluorescence microscopy studies. The most often applied method in this regard is the measurement of the fluorescent dye Hoechst 33342 by flow cytometry (430). Several other fluorescent substrates of ABCG2 (e.g., topotecan, flavopiridol, BODIPY-prazosin, or mitoxantrone) have also been applied in this regard. However, these dye transport assays are not specific for ABCG2, and the combined use of ABCG2-specific inhibitors is advocated in these methods. A recent report suggests that the chlorophyll derivative pheophorbide a is a selective ABCG2 substrate that can be used for flow cytometry analysis of this protein (287).

As a summary, the laboratory detection of functionally relevant ABCG2 expression in cancer cells has several encouraging options, but a highly sensitive and selective morphological and/or functional recognition of this transporter is still to be introduced.

D. Physiological and Pharmacological Functions of ABCG2: Drugs, Sex, and Survival

Both the transport properties and the tissue distribution of ABCG2 indicate a key role of this protein in the protection of our body against xenobiotics (227, 316). Since ABCG2 transports a variety of amphipathic molecules, we can expect that both natural and artificial toxins can be eliminated by its function. Moreover, ABCG2 is physiologically expressed in relatively high levels in the canalicular membrane of the liver, in the epithelia of small intestine, colon, lung, kidney, adrenal, and sweat glands, as well as in the endothelia of veins and capillaries, including the capillary endothelial cells of the blood-brain barrier, and in stem cells (66, 227, 430).

The apical membrane expression of ABCG2 in epithelial cells along the gastrointestinal track suggests a major role of this protein in the first line of defense against xenobiotics. This protection is further extended by the function of ABCG2 in the biliary and renal luminal epithelia, responsible for toxin clearance. Interestingly, issues related to drugs, sex differences, hormonal regulation, and protection of the fetus and stem cells all seem to be connected to ABCG2 function.

Again, it is important to note that ABCG2 has an overlapping transported substrate profile and localization with other major multidrug transporters, especially that of MDR1 and MRP2. Therefore, the appreciation of the physiological and pharmacological role of ABCG2 requires special experimental approaches, that is, the use of inhibitors or various transporter knock-out conditions.

1. First line defense and secretion: general xenobiotic resistance

As to the role of Abcg2/ABCG2 in xenobiotic (toxin and drug) absorption and bioavailability, the first important information was provided by investigations carried out in *Mdr1a* knock-out mice. When topotecan (an ABCG2 substrate) and GF120918, an inhibitor of ABCG2, were coadministered orally to these animals, the bioavail-

ability of topotecan in the blood plasma was drastically increased. The hepatobiliary excretion of intravenously administered topotecan was decreased by oral GF120918, consistent with an excretory role of canalicular Abcg2 into the bile (163). Based on these experiments, similar studies were carried out in human patients treated with topotecan. The oral administration of the ABCG2/MDR1 inhibitor GF120918 significantly increased the oral absorption and systemic bioavailability of topotecan (192). These data indicate that ABCG2 function limits the uptake of topotecan from the intestinal lumen, while it increases the hepatobiliary excretion of this compound.

To appreciate this physiological role, the development of the Abcg2 knock-out mice was initiated (161, 429). The nonessential nature of Abcg2 in these knock-out animals, that is, the lack of any phenotype in a controlled environment, was the first key observation. However, under various environmental or pharmacological challenges, several alterations have been observed connected to the lack of functional Abcg2.

The Dutch group first reported that in the Abcg2 knock-out mice the combination of exposure to UV light and an alfalfa diet, rich in chlorophyll, led to serious phototoxic skin lesions (161). These lesions were caused by the accumulation of a chlorophyll degradation product, pheophorbide a, found in various plant-derived nutrients and food supplements. Normally, Abcg2 actively transports pheophorbide a, efficiently limiting the uptake of this compound from ingested food, while in the knock-outs there was an increased intestinal absorption and decreased biliary secretion of this toxin. Based on these studies, it has been suggested that the malfunctioning of ABCG2 may cause an increased risk for developing protoporphyria and diet-dependent phototoxicity. This finding is a striking illustration of the importance of drug transporters in protection from toxicity of normal food constituents (161). Indeed, van Herwaarden et al. (384) demonstrated that Abcg2 knock-out mice have elevated plasma levels and decreased intestinal, fecal, and hepatobiliary excretion of the food carcinogen 2-amino-1-methyl-6-phenylimidazo[4,5-b]pyridine (PhIP). A recent study of Adachi et al. (1), using either MRP2-deficient or Abcg2 knock-out animals, demonstrated that ABCG2 has a key role in extruding glucuronide and sulfate conjugates of drugs and hormones, formed in the enterocytes, into the intestinal lumen.

There are numerous ABCG2 substrate compounds that could compete with each other during absorption or secretion, and this competition may involve various food constituents. Flavonoids are important modifiers of several physiological processes (see the "French paradox," probably caused by flavonoids in red wine), and they also interact with ABCG2. As shown by Imai et al. (146), several flavonoids, including genistein and naringenin, increased the cellular accumulation of topotecan in ABCG2-expressing cells. A direct transport of labeled, unmetabolized genistein has also been documented. Thus flavonoid consumption may significantly alter the pharmacokinetics, increasing the toxicity or the antitumor action of ABCG2 substrate compounds. In summary, all these data suggest that ABCG2 has a major role in the modulation of the absorption of toxic materials from food, as well as of their excretion mostly through the biliary pathway (77).

2. Prevention of endogenous toxin accumulation

The Abcg2 knock-out mouse study, carried out in the United States, revealed a hypersensitivity of the tissues in these animals to hypoxic challenges (191). Progenitor cells obtained from Abcg2 knock-out mice showed a reduced ability to form colonies under hypoxia. Moreover, blocking of Abcg2 function in normal progenitor cells reduced survival under hypoxic conditions. As it turned out, the primary cause of this hypoxic susceptibility was the accumulation of cellular heme and/or porphyrins. The blockade of heme/porphyrin synthesis reversed this condition, while cells overexpressing ABCG2 accumulated lower amounts of porphyrin. Heme was shown to be specifically bound by ABCG2, and drug transport by ABCG2 was significantly modulated by heme.

These studies suggest that ABCG2 permits enhanced cell survival in oxygen-poor environments by reducing the accumulation of toxic heme metabolites; thus ABCG2 expression provides an important cell survival advantage under hypoxic conditions. Of course, the chemical similarity of pheophorbide and porphyrin is evident and should direct our interest to possible ABCG2-dependent transport of various related compounds.

3. ABCG2 in the placenta

The wild-type human ABCG2 was first cloned from a placenta library (8), and the protein is abundantly expressed in chorion epithelial cells. The maternal-fetal barrier in the placenta, protecting the fetus from drugs and environmental toxins, has been indicated to involve the function of MDR1/Pgp. Further studies in Mdr1 knock-out mice indicated an important role of ABCG2 in this tissue. In pregnant, Mdr1-deficient mice, when topotecan was coadministered with the inhibitor GF120918, the fetal penetration of topotecan was significantly higher than without this inhibitor (163). In the Abcg2 knock-out mice, the fetal exposure to topotecan and dietary toxins greatly increased, compared with normal mice (320). The selective inhibition of Abcg2 by fumitremorgin C also produced a large increase of the topotecan and mitoxantrone levels in the fetus (187). All these data indicate that ABCG2 plays a major role in protecting the fetus against toxic compounds ingested by the mother (Fig. 12).

4. ABCG2 in the blood-brain barrier

The presence of ABCG2 in the brain endothelia was indicated by RNA expression measurements (90, 423), and the expression of the ABCG2 protein was directly demonstrated in the luminal surface of brain microvessels, forming the blood-brain barrier (BBB), by immunofluorescence confocal microscopy (66). The vectorial drug transport by ABCG2 overexpressed in immortalized endothelial cells indicated a functional role of this protein, limiting the brain penetration of hydrophobic compounds (115). By using in situ brain perfusion techniques, in Mdr1 knockout mice an efficient extrusion of prazosin and mitoxantrone by Abcg2 in the BBB was clearly demonstrated (62). Interestingly, flavonoid transport through the BBB was also modified by the function of ABCG2 (409). In a rat BBB model, the expression and function of rABCG2 was upregulated by astrocyte-derived soluble factors (132), and the application of an siRNA reduced both the expression and the transport function of endogenous rABCG2 in capillary endothelial cells (131). Recently, Breedveld et al. (36) have shown that the brain penetration of intravenously administered Imatinib was significantly increased in Abcg2 knockout mice. All these data strongly indicate an important function of ABCG2 in the BBB, protecting the brain from potentially toxic agents (Fig. 12).

5. ABCG2 in stem cells

A fascinating development in the field of stem cell research was the finding that a high-level expression of the ABCG2 protein and its fluorescent dye extrusion function could identify hemopoietic stem cells (177, 314, 430). The so-called "side population (SP)" of progenitor cells, actively extruding the fluorescent Hoechst 33342 dye, seems to represent pluripotent stem cells in a variety of tissues (177, 201, 314, 357, 430) (Fig. 12). Although we do not know as yet why ABCG2 expression is high in these cells, it seems likely that it is required for the metabolic protection of stem cells. ABCG2 expression decreases during stem cell differentiation. Still, both the knock-out mouse studies and recent transplantation experiments suggest that the lack of ABCG2 expression or ABCG2 overexpression do not directly influence stem cell function and differentiation (249, 429) (O. Ujhelly, unpublished data). As mentioned above, ABCG2 function may protect against local hypoxia; thus its presence may be a survival factor for stem cells under unfavorable conditions. This role may have important implications for increasing medical activities connected to stem cell transplantation.

6. Sex differences in ABCG2 expression and function

Recent studies demonstrated a sex-dependent expression and function of ABCG2 in various organs. In mice a significant difference was observed in the pharmacokinetic behavior of ABCG2 substrate drugs between male and female animals, leading to much higher plasma levels in female mice after a similar drug exposure (237). The main cause of this difference was the higher liver expression and biliary clearance function of Abcg2 in male mice, while this pharmacokinetic sex difference was absent in Abcg2 knockout animals. The authors also found a much higher hepatic expression of ABCG2 in men than in women (237). Imai et al. (144) reported that estrogens, like 17β-estradiol, downregulate ABCG2 expression through an estrogen receptor α-interaction pathway in various cell lines (see below). Another recent study (371) has found a much higher ABCG2 expression in the intestine and kidney of male rats compared with females, and a male-dominant expression was observed in the mouse liver. Moreover, when following ABCG2 expression, a suppressive effect of estradiol and an induction by testosterone (371) were observed. These data may have a major importance in characterizing the often ob-

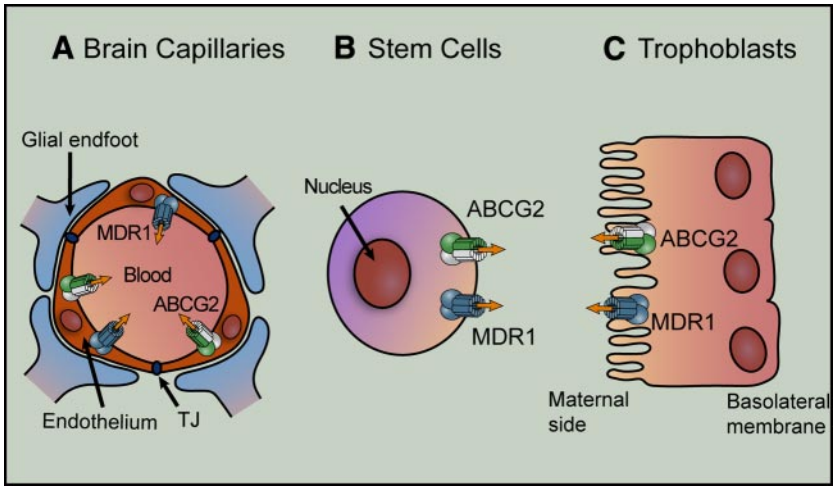

FIG. 12. Physiological role of the MDR1 and ABCG2 multidrug/xenobiotic ABC transporters in the blood-brain barrier (*A*), in stem cells (*B*), and in placenta (*C*). The endothelial cells of the blood-brain barrier are connected with tight junctions and provide a barrier against the entrance of hydrophilic compounds into the brain area. Hydrophobic drugs or toxins penetrate the cell membranes and may enter the brain compartment. Multidrug transporters, especially MDR1/Pgp and ABCG2, are expressed in the apical membrane (facing the blood compartment) of the endothelial cells and extrude a variety of hydrophobic drugs and toxins. ABCG2 is abundantly expressed in various stem cells, with as yet unknown function. Hemopoietic stem cells can be separated by their low-level Hoechst dye staining (side population, SP), due to active dye extrusion by ABCG2. ABCG2 and MDR1/Pgp are highly expressed in the maternal side of the chorion epithelial cells in the placenta. These transporters prevent the entrance of a variety of toxins and drugs into the fetal compartment.

served sex differences in drug effectiveness and toxicity. Importantly, the sex hormone-dependent regulation of ABCG2 expression may be connected to its role in the transport of various hormone metabolites, e.g., estrone sulfate.

In connection with sex-related differences, ABCG2 was shown to have an important role in drug and toxin secretion into milk. As reported recently by Jonker et al. (162), ABCG2 expression (as examined in mice, cows, and humans) is greatly increased in the mammary gland during lactation, and the ABCG2 protein actively secretes various drug and toxin substrates into the milk. The secretion of the antibiotic nitrofurantoin into milk has been reported to be 80 times higher in wild-type mice compared with the Abcg2 knock-out animals (236). Thus the regulation and function of ABCG2 may significantly modulate contamination of milk with drugs and xenobiotics, leading to toxin exposures in infants or consumers of dairy products.

E. Polymorphisms and Regulation of ABCG2

Both the pharmacological and physiological functions of the ABCG2 protein have been indicated to be significantly influenced by interindividual variations and regulatory responses. In this section we discuss the two main apparent sources of these variations: a widespread genetic polymorphism, probably affecting both protein expression and function, and the response to toxin exposure, stress, or hormonal changes by a variable expression and processing of ABCG2.

1. SNPs in ABCG2

Analysis of the ABCG2 sequences in the human population identified several single nucleotide polymorphisms (SNPs), and their effects on protein expression and function have been the subject of numerous recent studies. Earlier reports indicated considerable interindividual variations in the oral bioavailability and clearance of drugs that are ABCG2 substrates, such as topotecan (163, 419), which may reflect such a polymorphism.

The *ABCG2* gene is located on chromosome 4q22, spans over 66 kb, and consists of 16 exons, ranging from 60 to 532 bp in length (20). In healthy individuals or patients, altogether eight nonsynonymous (V12M, Q141K, I206L, F431L, S441N, F489L, N590Y, D620N), five synonymous (silent) (c. 114T>C, c. 369C>T, c. 474C>T, c. 1098G>A, c. 1425A>G) mutations, one nonsense (Q126X, c. 376C>T), and one frameshift (c. 1515delC) mutation were identified in the coding region of *ABCG2*. The sequence variant Q126X, leading to premature termination of protein synthesis, was consistently observed in certain Japanese cohorts, while absent in different Caucasian and African American groups (145, 148, 185). From these numerous reported alterations, two protein variants, V12M, and Q141K, were found in relatively high frequencies, with significant differences in allele frequencies in different areas of the world (Fig. 11).

The V12M polymorphism affects the NH_2-terminal intracellular region of the protein. Both the wild-type (valine) and the variant (methionine) amino acids have uncharged, hydrophobic side chains. The V12M polymorphism was found in all ethnic groups tested, with the highest allele frequency in Mexican-Indians (90%), while only 2% in a Swedish population (18, 418), and also with a significant difference in allele frequencies in Caucasian and Japanese populations.

The Q141K polymorphism leads to the replacement of the uncharged glutamine residue with a positively charged lysine within the ATP-binding domain, between the Walker A motif (amino acids 83–89) and the signature region (amino acids 186–189). The Q141K variant was also detected in all ethnic groups tested: the allele frequency ranged between 1 and 35% (the African and African-American subjects with low, while the Japanese and Chinese populations with high allele frequencies; see Refs. 45, 74, 185).

To clarify the possible physiological or pathological relevance of the ABCG2 polymorphisms, several studies attempting the functional characterization of the variants were performed. Interestingly, the results of the different research groups, regarding expression levels, localization, and functionality, are quite contradictory. Imai et al. (145) and Morisaki et al. (251), by using stable mammalian expression systems, found that in PA317 or HEK-293 cells the expressed Q141K ABCG2 protein had a lower expression level than the wild-type ABCG2, or the V12M variant. Morisaki et al. (251) demonstrated that both the V12M and Q141K ABCG2 could reach the plasma membrane in the HEK-293 cells, while a significant portion of Q141K remained intracellular. Other studies found a 30–40% reduction in cell surface expression of the Q141K variant, despite a similar mRNA level than the wild-type ABCG2 (145, 188).

Recent investigation of 99 Japanese placenta samples revealed that individuals homozygous for the Q141K variant showed significantly lower expression levels of this transporter protein, while the heterozygous samples displayed an intermediate expression level (185). In contrast, another study, investigating the expression of natural allelic variants of ABCG2 in the human intestine, demonstrated no significant differences in mRNA and protein levels between subjects expressing the K141 allele in heterozygous form, or the Q141 (wild-type) allelic variant (418).

Mizuarai et al. (247) expressed ABCG2 in polarized LLC-PK_1 cells, and by using confocal microscopy, the authors observed that the wild-type ABCG2 and Q141K showed mainly apical staining, while the V12M variant

showed mostly intracellular localization. In a recent study, Kondo et al. (188) also used LLC-PK_1 cells to express the V12M and Q141K variants and found that all polymorphisms, including V12M and Q141K, had an apical localization. These contradictory expression and localization data for the ABCG2 variants, even when similar cell lines were applied, indicate that differences in culture conditions or other cellular determinants may variably affect the cellular processing of these proteins.

When the functions of the ABCG2 variants were examined in cytotoxicity assays, a 10-fold decrease in drug resistance, compared with the wild-type ABCG2, was reported by Mizuarai et al. (247), when the V12M or Q141K-transfected LLC-PK_1 cells were challenged by mitoxantrone, topotecan, or an indolocarbazole topoisomerase I inhibitor. In contrast, Morisaki et al. (251) found that only the Q141K variant had a moderately lower level resistance against mitoxantrone, topotecan, or SN-38, compared with the wild-type ABCG2-transfected cells. Moreover, in experiments comparing the transport activities of the wild-type protein and its variants for estrone 3-sulfate, dehydroepiandrosterone sulfate, methotrexate, or PAH, no significant differences were reported, when the transport activities were normalized for the expression levels of ABCG2 proteins (188).

Q141K is mapped to a functionally important ABC region of ABCG2; therefore, it is possible that the ATPase activity of this variant is altered. Two studies compared the vanadate-sensitive ATPase activity of ABCG2 V12M and Q141K variants, using Sf9 (*Spodoptera frugiperda*) cell membranes (247, 251). A reduced basal ATPase activity was observed by both groups for the Q141K variant. On the other hand, the V12M ABCG2 showed a similar ATPase activity as the wild-type protein.

All these transport, ATPase, and cell survival data suggested that the investigated SNPs may not substantially alter the substrate specificity of ABCG2. On the other hand, if their expression level is indeed lower, or their membrane localization is impaired, these alterations may modify ABCG2-dependent drug transport. Clearly, more detailed studies are required to clarify the mechanism of a reduced protein expression for Q141K, and the altered cellular localization found for the V12M and Q141K variants under certain conditions. It is important to note that in heterozygous individuals, different ratios of the ABCG2 dimers may be present. The above in vitro experiments investigated homodimers of the variants, which is a model applicable only for the rare cases of homozygotes.

In addition to the above-described in vitro investigations, several pharmacokinetic studies are in progress to evaluate the potential functional differences of various ABCG2 genotypes. De Jong et al. (74) investigated patients with solid malignant tumors receiving irinotecan treatment. In 84 European Caucasian patients, the frequency of the K141 allele was 10.7%, with 14 patients carrying heterozygous alleles and 2 patients homozygous for the variant. According to this study, the pharmacokinetic parameters of irinotecan and SN-38 were not significantly different between patients carrying the wild-type ABCG2 or at least one polymorphic allele. However, one of the two homozygous individuals showed increased accumulation of SN-38 and SN-38 glucuronide, indicating that the K141 homodimer may have an impaired function.

A recent investigation performed an exploratory, retrospective evaluation of the functional consequence of the ABCG2 Q141K variant in 20 adult patients, treated with diflomotecan, a synthetic derivative of camptothecin (350). In five patients carrying one K141 variant allele, after oral administration of diflomotecan, no difference was found in serum levels compared with individuals with the wild-type genotype. However, after intravenous administration of the drug, the plasma concentration in the heterozygous patients was markedly increased compared with the individuals with the wild-type genotype. This observation is in harmony with studies indicating a reduced protein expression and function for the Q141K variant, while it seems to contradict the results of De Jong et al. (74).

As mentioned above, the allele frequency of Q141K varies in diverse populations, and in Japan and China, this polymorphism appears to be common, with an overall allele frequency of ~30%. The resulting frequent occurrence of the wild-type/K141 heterodimer and even the K141 homodimer ABCG2 transporters in this population, as well as the appearance of other mutations, leading to a reduced ABCG2 protein level, may strongly modify the ADME-Tox properties of many different drugs. Since the recently introduced anticancer tyrosine kinase inhibitor Iressa (Gefitinib) is a transported substrate of ABCG2 (93, 406), polymorphisms in this protein may be involved in the different effectiveness and toxicity of this drug in distinct populations. Moreover, because ABCG2 was demonstrated to have a protective role against food toxins, especially plant metabolites, a lower expression or impaired function of ABCG2 variants may affect the diet-related health conditions in a huge human population (161).

2. Regulation of ABCG2

A) TRANSCRIPTIONAL REGULATION. Relatively little is known as yet about the transcriptional regulation and promoter structure of ABCG2. In their pioneering work, Bailey-Dell et al. (20) have analyzed the 5′-upstream ~2-kb region of the human ABCG2 by bioinformatic tools and localized positive and negative regulatory elements by a luciferase reporter assay. They showed that, similar to other ABC protein coding genes, the *ABCG2* gene lacks the canonical TATA box within the region 100 bp up-

stream to the transcriptional start site. Several Sp1 sites were found within the corresponding −222 to −49 bp region (relative to the transcriptional start site). The presence of Sp1 sites is a common feature of genes without TATA box, and *ABCB1* and *ABCC1*, both lacking TATA boxes, possess several SP1 binding sites. A CCAAT-box is present in the −274 bp position, and CpG islands are found in its downstream proximity. These elements predict a putative promoter/enhancer in the −266 to −36 bp region. The reporter assays identified potential positive regulatory elements between −1285 and −62 bp, and potential negative regulatory elements between −628 and −31 bp. Removal of the CCAAT box and part of the predicted region reduced and further truncation of this region further decreased transcription activity.

A novel estrogen response element has been identified in the −188 to −172 bp segment of the gene (89), and it has been demonstrated that the 17β-estradiol-liganded estrogene receptor (E_2/ER) binds directly to this element and, by interacting with components of the RNA polymerase II transcriptional machinery, triggers an enhanced transcription of human ABCG2 in ER-positive T47D: A18 cells (89). The same element has been found by a systematic genome-wide bioinformatic study by analyzing promoter elements for transcription factor binding sites with the aim of identifying estrogen-responsive genes (169). However, the regulation of *ABCG2* seems to be cell line specific, because it is actually downregulated following estrogen treatment in ER-positive MCF7 cells (169). Moreover, as mentioned below, estrogen regulation of ABCG2 may be mostly of posttranslational nature.

ABCG2 is probably also regulated by drug treatment and cellular stress, but this phenomenon has not yet been explored as critically as in the case of MDR1 or MRPs. Benzopyrene conjugates were reported to induce ABCG2 expression in the Caco-2 intestinal cells (87). Burger et al. (41) demonstrated that in the same cell type, the addition of Imatinib, an ABCG2-substrate TKI, upregulates the transporter expression through an SXR-dependent mechanism.

As mentioned above, ABCG2 may have a key role in protecting the cells against porphyrin metabolites during hypoxia, and this coincides with an upregulation of this transport protein (191). ABCG2 expression was found to be upregulated through an interaction of the hypoxia-inducible transcription factor complex HIF-1 with the ABCG2 promoter region. Because MDR1/Pgp is also upregulated during hypoxia by HIF-1 through the activation of a stress-activated kinase pathway (64, 65), this could be a general type of stress response also involving the ABCG2 protein.

Interestingly, the lack of Mdr1 expression in knockout mice greatly upregulates Abcg2 expression in a functionally important area, the BBB (62). This excessive overproduction of a related transporter in a given tissue and its role in a defense network is discussed in detail in section VII.

B) POSTTRANSLATIONAL REGULATION. One possibility for a posttranslational regulation stems from the dimerization properties of this ABC half-transporter. In heterozygotes, dimerization of polymorphic variants in fact results in functional heterodimer formation, and thus may alter the localization and/or function of the protein (see above). Clearly, a nonfunctional mutant (K86M) ABCG2 variant induces a dominant negative effect, that is, a nonfunctional dimer formation suppresses the activity of the wild-type protein (93, 166). Such a dominant negative effect may be a rare case in vivo, but the polymorphic heterodimerization may be pharmacologically relevant.

Similarly to that found for MDR1/Pgp (see sect. IV), the transport function or localization of ABCG2 is not significantly modulated by protein glycosylation (78, 250, 370). There are no published experimental data as yet on the possible phosphorylation-dependent regulation of ABCG2. Based on earlier observations when ABCG2 was expressed in Sf9 cells (260, 261) and in *Lactococcus* (151), as well as on our recent experiments (Sarkadi, unpublished data), membrane lipid composition, especially the local concentration of cholesterol, has a key regulatory effect on ABCG2 transport activity. This may be most relevant in transport function, when ABCG2 is retained in the cholesterol-poor endoplasmic reticulum membrane, or transferred to the cholesterol-rich plasma membrane.

As mentioned above, sex hormones have a regulatory effect on ABCG2, that is, estrogen in general downregulates ABCG2 protein expression and function (144). This regulation involves estrogen receptor alpha and is reversed by the antiestrogen tamoxifen. Interestingly, according to this study, estrogen does not affect the level of ABCG2 mRNA, but the regulation is posttranscriptional, by decreasing ABCG2 protein biosynthesis and maturation. According to Tanaka et al. (371), based on gonadectomy and hypophysectomy experiments, the lower level ABCG2 expression in female rat kidney is probably caused by estradiol suppression, while higher ABCG2 expression in male mouse liver is induced by testosterone.

These data raise the possibility that ABCG2 is under a complex posttranslational regulation, which involves the interaction of this protein with cytoskeletal and other intracellular elements that may significantly influence the cell surface exposure, that is, the drug extrusion function of this protein.

F. ABCG2 in Medical Applications: Drug Development and Gene Therapy

1. ABCG2 in drug screening and development

Based on the above-described drug interactions, ABCG2 plays a major role in tumor drug resistance, as

well as in the absorption, metabolism, excretion, and toxicity (ADME-Tox) of various pharmacological compounds. Therefore, an in vitro prescreening of new therapeutic compounds and their metabolites may provide a great advantage; all these parameters could be predicted without tiresome and expensive in vivo screening, costing a lot of animal lives.

As described in section III, the major MDR-ABC transporter screening methods include direct enzymatic (ATPase, nucleotide trapping, fluorescence-based enzyme activity measurements, etc.) and vesicular transport assays, by using isolated membrane vesicles exclusively or predominantly expressing the desired transport protein in a functional form. The overexpression of the ABCG2 protein in the heterologous insect cell/baculovirus system is a well-established possibility for such screenings, and isolated membranes of mammalian cells could also be used for this purpose (see Ref. 104). Another type of basic drug screening can be performed by using cultured mammalian cell lines, specifically engineered to express the given transporter. In this case both the direct transport measurements for labeled compounds and indirect assays by using fluorescent or otherwise labeled reporter compounds are available. Without detailing these assays here (see sect. III), we feel that these methods should be rapidly optimized and standardized by the research and development community, to provide the drug development industry with a well-established toolkit for prescreening new drugs in their pipelines. Since, as demonstrated above, ABCG2 is a "transporter for all seasons" (306), performing numerous tasks in a number of organs, screens for ABCG2 should be in the first line of such development strategies. The excessive polymorphisms and the sex-dependent distribution of this transporter add an extra task to design such a meaningful in vitro screening panel, but may also lead to a major increase in the cost-to-benefit ratio of drug development.

2. ABCG2 in gene therapy

The physiological presence of ABCG2 in stem cells provides the basis for a gene therapy application of this transport protein. The introduction of a selectable marker in ex vivo stem cell gene modification provides a selective advantage of the modified cells after transplantation. The coexpression of a drug-resistance protein with a therapeutic gene product should allow both an enrichment of the corrected cells and an in vivo drug selection during clinical gene therapy. The use of the MDR1-Pgp as such a selectable marker has been widely investigated and advocated, while other studies reported major problems with this approach (39, 113, 318). Recent studies in our laboratory suggest that a mutant ABCG2 protein is an ideal candidate for human stem cell protection and for use as a selectable marker in gene therapy. The cDNA encoding this protein is relatively small (~2 kb), and the active dimer is spontaneously formed in the overexpressing cells (379). Because the substrate specificity of the R482G variant of ABCG2 differs from that of the wild-type protein, this mutant has a special advantage in gene therapy applications.

We have documented that when the mutant ABCG2 was coexpressed with a therapeutic gene, the expression of the therapeutic gene in hematopoietic progenitor cells corrected the loss-of-function mutation responsible for human chronic granulomatous disease (379). At the same time, the mutant ABCG2 protein selectively protected the transduced cells against clinically applicable cytotoxic agents. Overexpression of ABCG2 did not affect in vitro hematopoietic cell maturation or the restoration of granulocyte function by the therapeutic gene. The first in vivo mouse studies (Ujhelly et al., unpublished data) have demonstrated that the ABCG2 expressing bone marrow stem cells can be used for efficient transplantation, the production of all blood cells remains normal, and there is no change in cell repopulation or differentiation patterns.

VI. ADDITIONAL TRANSPORTERS IN CANCER DRUG/XENOBIOTIC RESISTANCE

Up to now only three human ABC transporters, MDR1/Pgp (ABCB1), MRP1 (ABCC1), and ABCG2, have unambiguously been shown to contribute to cancer multidrug resistance. However, as mentioned earlier, there are several other ABC proteins that were implicated in cancer drug resistance and xenobiotic transport. In this section we give an overview of selected ABC transporters that are major candidates for participating in drug and xenobiotic resistance.

A. The MDR3 (ABCB4) Protein

P-glycoproteins (Pgps) form a small subfamily within the superfamily of ABC transporter proteins. In mice, there are three genes that encode for Pgps, *Mdr1a*, *Mdr1b*, and *Mdr2*. In humans, in addition to *MDR1*, only one other Pgp gene has been identified: *MDR3* (also known as MDR2, PGY3, ABC21, or PFIC-3). According to the classification of ABC transporters, MDR3 belongs to the ABCB subfamily and is called ABCB4. Shortly after the identification of MDR1, the human *MDR3* gene product was cloned from a liver cDNA library (382). The protein encoded by the *MDR3* gene consists of 1,279 amino acids and has a deduced M_r of 140,000, which is increased by glycosylation. The MDR3 protein is a prototypical ABC transporter, consisting of two cytosolic nucleotide-binding domains (ABC units) and two large transmembrane domains, each composed of six transmembrane helices. It shows a high, 77% amino acid sim-

ilarity with the product of the *MDR1* gene (52). The level of sequence conservation is the highest in the ABC units and in the transmembrane domains and the lowest at the NH_2 terminus and in the 60-amino acid linker region connecting the two halves of the protein.

The *MDR3* gene covers 78.74 kb and maps to chromosome 7, at 7q21.1, in the proximity of the *MDR1* gene (209). The two genes are separated by a 34-kb intergenic region. It has been postulated that the *MDR3* gene evolved from the *MDR1* sequence by gene duplication. This hypothesis is supported by the observation that the exon/intron structure of these genes is almost identical, each containing 28 exons, of which 27 encode the functional protein (209).

1. *Tissue distribution and cellular localization of MDR3*

The *MDR1* and *MDR3* gene products have different tissue distributions. In contrast to the wide-range expression of MDR1 in a number of organs (see sect. IV), the expression of MDR3 protein is constrained predominantly to the canalicular membrane of hepatocytes. Low levels of MDR3 RNA have been found in some tissues other than liver, namely, in the heart, skeletal muscle, and spleen, although the MDR3 protein was not detected by Western analysis (341). A high-affinity antibody, however, was able to demonstrate MDR3 protein expression in the glomeruli of the kidney (315). The regulation of expression of MDR3 is not clarified. It has recently been reported that the MDR3 protein, along with other major canalicular transporters, is expressed at midgestational stage during human fetal development. However, the level of MDR3 expression was found to be much lower in fetal liver than in the adult tissue (53).

The sequences and protein-protein interactions that are responsible for proper maturation and accurate targeting of MDR3 to the canalicular membrane are also yet to be discovered. Epitope insertion studies have revealed that intracellular loops between transmembrane helices 3 and 4 as well as between 4 and 5 are crucial for proper targeting (172). Mutation in the ABC unit of MDR3 also prevents correct trafficking and results in the loss of function of the protein (79). The MDR3 protein colocalizes with MDR1 and with the bile salt transporter (BSEP/ABCB11) in the apical compartment of hepatocytes. Binding of these ABC transporters to regulatory proteins such as HAX-1 and myosin II regulatory light chain (Mlc2) has also been demonstrated (47, 259). These observations suggest that HAX-1, Mlc2, and possibly cortactin are involved in the trafficking of these ABC transporters. It has been proposed that canalicular ABC transporters, like several canalicular ectoenzymes and cell adhesion molecules, transcytose from the basolateral plasma membrane to the apical surface. However, evidence has been provided for the fact that newly synthesized MDR1 and MDR2 are directly targeted from the Golgi apparatus to the canalicular membrane without entering the basolateral compartment (179).

2. *Transport properties and the physiological function of MDR3*

Since the MDR3 protein was found to be sequentially similar to MDR1, MDR3 was also predicted to be an efflux pump, possibly a drug transporter with broad substrate specificity. However, this Pgp, in contrast to MDR1, was proven to be a highly specialized transporter which translocates solely phospholipids with a choline head group (297, 298, 345). The restricted tissue distribution, particular cellular localization, and specialized transport properties suggest a key physiological function for MDR3 in the bile formation. The generation and phenotyping of the Mdr2 −/− mouse unambiguously demonstrated that this transporter is essential for biliary phosphatidylcholine extrusion (342), since the bile of Mdr2-deficient mice is devoid of phosphatidylcholine. MDR3 is a selective transporter regarding the fatty acid moieties of the transported lipid. Lipid analogs with C_6 and C_{16} fatty acids as well as with a ceramide backbone are transported by MDR3, whereas a phosphatidylcholine analog with two C_8 fatty acids is not recognized (383). This substrate selectivity of MDR3 is assumed to be responsible for the particular fatty acid composition of the phosphatidylcholine pool in the bile, which differs from that in the liver tissue.

A suggested model for MDR1 transport mechanisms is that this protein acts as a flippase, i.e., it translocates amphipathic molecules from the inner leaflet of the plasma membrane to the outer leaflet (119). Based on the homology between MDR1 and MDR3 proteins, the latter one was also predicted to function as a flippase, specialized for phosphatidylcholine (PC) (see Fig. 13). This hypothesis was supported by detailed transport studies demonstrating an ATP-dependent translocation of fluorescent PC analogs from the outer to the inner leaflet of yeast secretory vesicles containing Mdr2 (298). This model system was used in a subsequent study to reveal that the flippase activity of Mdr2 was stimulated by the bile salt taurocholate but not by the nonmicelle-forming counterpart taurodehydrocholate (297). Asymmetric translocation of PC analogs was also demonstrated by Nies et al. (257) using rat canalicular membrane vesicles. This transport was also increased by taurocholate but not by taurodehydrocholate. The flippase model for MDR3 transport mechanism was also supported by studies by Smith et al. (345) using fibroblasts from transgenic mice. In these experiments mouse fibroblasts were labeled with [^{14}C]PC, and the efflux of the labeled substrate from the cells was monitored by adding purified PC transfer protein and acceptor liposomes into the bath. Compared with

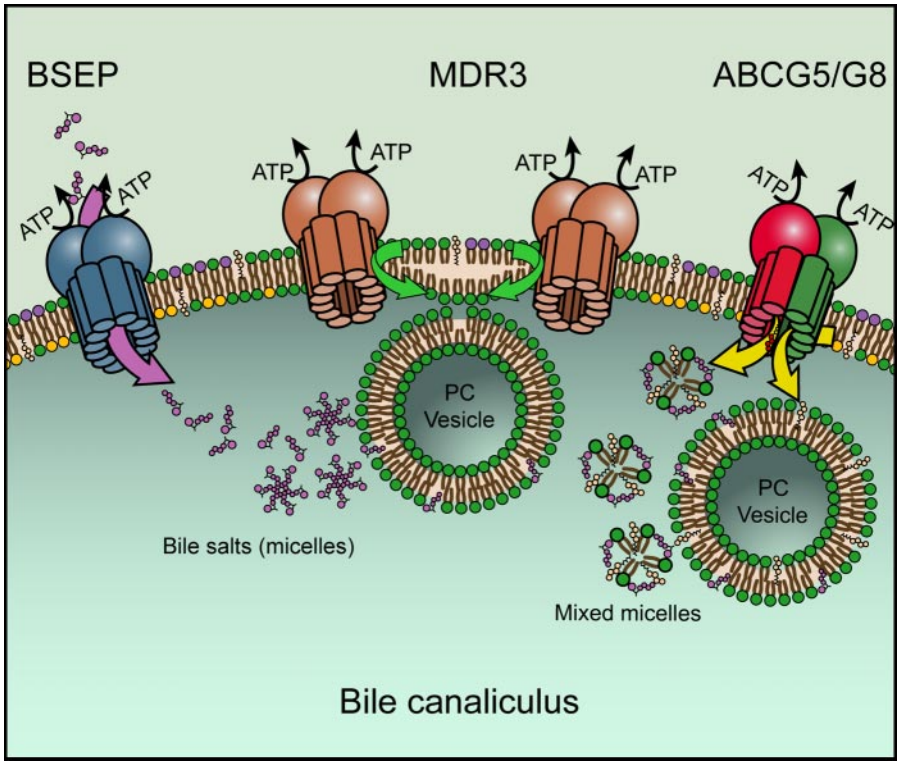

FIG. 13. Physiological localization and role of ABC transporters in the bile formation of the liver. The ABC transporters, which play a crucial role in the bile formation, include BSEP (bile salt export pump, sister Pgp, ABCB11), MDR3 (ABCB4), and the ABCG5/ABCG8 heterodimer. These transporters reside in the canalicular membrane of hepatocytes and perform active transport of various bile constituents. BSEP extrudes bile salts into the canaliculus, where bile salt micelles are formed. MDR3, the phosphatidylcholine (PC) flippase, translocates PC from the inner hemileaflet of the membrane into the outer hemileaflet. Bile salts promote destabilization of the PC-containing microdomains, which ultimately develop into phospholipid vesicles rich in PC. These biliary vesicles and mixed micelles are loaded with cholesterol by the transport activity of the ABCG5/ABCG8 heterodimer, which makes cholesterol accessible for the acceptors.

normal mouse fibroblasts, which do not express Mdr2, cells expressing the human MDR3 exhibited a threefold increase in the rate of translocation of PC. All these data support the concept that MDR3 is an ATP-dependent PC flippase, which translocates its substrate from the inner to the outer leaflet of the canalicular membrane of hepatocytes.

Smith et al. (344) generated a transgenic mouse deficient in murine Mdr2, but expressing the human MDR3 protein under the control of an albumin promoter. The expression of the transgene restored PC excretion in the transgenic animals. The lack of other defects in these mice raises doubt about the significance of low level Mdr2/MDR3 expression in extrahepatic tissues. Moreover, these studies have clearly demonstrated that PC secretion depends both on Mdr2/MDR3 expression and the availability of bile salts. The current understanding of biliary PC excretion can be summarized as follows (35, 92). The Mdr2/MDR3 protein, residing in the canalicular membrane of hepatocytes, flips PC into the outer hemileaflet. Bile salts destabilize the PC-containing microdomains, which grow into a vesicular structure by the ongoing translocation of PC, driven by Mdr2/MDR3. Finally, the biliary vesicle pinches off the canalicular membrane. This hypothesis was supported by the observations that vesiculation of the canalicular membrane is dependent both on bile salt secretion (69) and Mdr2 expression (68). It should be noted that, in addition to PC deficiency, Mdr2 −/− mice also exhibited reduced biliary cholesterol excretion. However, the role of Mdr2 was proven to be secondary in this effect.

3. Clinical relevance of MDR3

Lack of PC in the bile of the Mdr2-deficient mice results in a mild liver disease. Since bile salt secretion is normal in these animals, the high bile salt concentration causes damage in the hepatocytes and the small bile ducts, resulting in extensive proliferation of bile duct epithelium, portal inflammation, and fibrosis (92). Because human bile salts are more hydrophobic than their murine counterparts, lack of MDR3 expression results in a more severe liver disease in humans. It was first shown by de Vree et al. (75) that mutations in the *MDR3* gene are the primary cause of type 3 progressive familial intrahepatic cholestasis (PFIC). This autosomal recessive liver disease is characterized by an early onset of cholestasis that progresses to cirrhosis and liver failure before adulthood. Patients with type 3 PFIC are distinguished from the other two types of PFIC by high γ-glutamyltransferase activity and a bile that lacks phospholipids but has a normal bile acid concentration. These patients exhibit portal duct inflammation and ductular proliferation, reminiscent of the phenotype exhibited by the Mdr2 −/− mice. Several MDR3 mutations have been identified in type 3 PFIC patients (150). Most of these mutations result in truncated proteins, which do not reach their destination in the canalicular membrane. However, a recent

study reported that MDR3 protein expression was detectable in the canalicular membrane of a few patients with type 3 PFIC (175).

Two other diseases are associated with mutations in the *MDR3* gene, namely, intrahepatic cholestasis of pregnancy (ICP) and low phospholipid-associated cholelithiasis. ICP is a liver disorder characterized by cholestasis during pregnancy in women with otherwise normal medical history and by the occurrence of generalized pruritus mostly in the third trimester. ICP is frequently associated with fetal distress, spontaneous immature delivery, and idiopathic intrauterine fetal death in the third trimester. Heterozygotes for either nonsense or missense mutations in the MDR3 gene are susceptible to develop intrahepatic cholestasis of pregnancy (79, 149, 223). Recently, a detailed study has demonstrated the close correlation between the genetic variations in *MDR3* gene and the pathophysiology of pregnancy-associated cholestasis (269).

Mutations in the *MDR3* gene lead to the absence or low level of phospholipids in the bile. The elevated cholesterol-to-phospholipids ratio promotes lithogenicity of the bile with crystallization of cholesterol. Therefore, mutations in the *MDR3* gene represent a risk factor for symptomatic cholelithiasis (294). Recently, a novel phenotype has been described in the Mdr2 −/− mice. By the end of the 15th week of age, half of the animals kept on chow diet develop gallstones with cholesterol crystals (200). Thus these mice can serve as an animal model for low phospholipid-associated cholelithiasis.

4. MDR3 and drug resistance

Since the *MDR3* gene most likely evolved from the gene encoding for the drug-transporting MDR1, it has been postulated that MDR3 also possesses drug-pumping activity. However, initial studies using cells transfected either with the murine Mdr2 or the human MDR3 failed to confirm this hypothesis. It has been shown that Mdr2 exhibits reduced drug binding capacity compared with that of Mdr1 (42). Surprisingly, Ruetz and Gros (298) found that the PC translocation in yeast secretory vesicles containing Mdr2 was inhibited by verapamil, a known competitive inhibitor of the drug-pumping activity of MDR1.

The first study, demonstrating MDR3-dependent drug resistance, was provided by Kino et al. (178). Yeast cells, transfected either with the human MDR1 or with the human MDR3, acquired resistance against Aureobasidin A, an antifungal antibiotic. By using polarized cultures of pig kidney epithelial cells transfected with MDR3, Smith et al. (346) have shown MDR3-dependent vectorial transport of digoxin, paclitaxel, and vinblastine. The transport of digoxin was inhibited by verapamil, cyclosporin A, and PSC833, compounds that are known MDR1 inhibitors. The interaction between MDR3 and these drugs was also supported by the observation that nucleotide trapping in MDR3 is reduced by paclitaxel, vinblastine, verapamil, cyclosporin A, and PSC833 (346). However, no ATPase activity of MDR3 was detected in the same experimental setup. The most plausible explanation for these observations is that MDR3 has a relatively high affinity for drugs but shows a low transport rate, which is not sufficient for conferring drug resistance to the cells. In contrast, MDR1 possesses high transport activity, which allows effective extrusion of hydrophobic drugs from the cells. This concept is supported by the recent finding that targeting of MDR3 RNA with siRNA results in a minor decrease of paclitaxel resistance in human ovarian cell lines, whereas MDR1 siRNA strongly reduced drug resistance in these cells (86).

These findings raise the question whether the observed affinity for drugs and the poor drug pumping activity of MDR3 is only an evolutionary relict or it has a relevant physiological role. It has been suggested that MDR3 serves as a "dual-function protein," which transports PC and also some toxins that are especially threatening to the liver (35). However, these two types of transport activities of MDR3 can be combined in a single function, if we consider PC translocation as a protective mechanism against toxic compounds. MDR3 plays a key role in bile formation, which represents a central component of detoxification processes. The protective role of MDR3 becomes evident from the phenotype of the Mdr2-deficient mice and the human diseases associated with MDR3 dysfunction. In these cases, the toxic bile acids are not sequestered in mixed micelles by phospholipids, and this causes extensive damage to hepatocytes and bile duct epithelial cells. The composition and cytotoxicity of bile salts greatly varies from species to species. The lack of phospholipids in the Mdr2 −/− mice results in a mild liver disease, whereas in humans it leads to complete loss of liver function. Interestingly, no biliary lipid excretion was found in the little skate *Raja erinacea*, implying that these primitive animals possess no functional ortholog of MDR3 (91). The bile salt excreted by the little skate was still found to be as cytotoxic as taurocholate, and in experiments it stimulated phospholipid and cholesterol secretion in isolated mouse liver. It has been proposed that cell membranes in little skate are protected against bile salt mainly by their high sphingomyelin content, and Mdr2/MDR3-like protective mechanism evolved later in evolution.

In addition, it has been postulated that phospholipid vesicles and mixed micelles contribute to the biliary excretion of organic anions and serve as a "micellar sink" (Fig. 13). It has been reported that the biliary excretion of protoporphyrin and indocyanine green is almost abolished in the Mdr2-deficient mouse, whereas estradiol-17β-D-glucuronide and glutathione excretion were reduced to a lesser extent (31, 136). The decrease in the number of

phospholipid vesicles in the canalicular lumen of these animals was found to be similar to the reduction in biliary excretion of protoporphyrin and indocyanine green. These observations strongly support the hypothesis that phospholipid vesicles participate in biliary excretion of certain organic anions.

Collectively, MDR3 either directly or indirectly contributes to the elimination of a number of toxic compounds from the body; therefore, this transporter should be considered as an important component of xenobiotic resistance and the proposed chemoimmunity network.

B. The ABCG5 and ABCG8 Proteins

The ABCG subfamily of ABC transporters consists of five members. All of them are half-transporters, i.e., they are composed of only one NBD and a single TMD. In addition to ABCG2, discussed in section v, two other members of the ABCG subfamily, ABCG5 and ABCG8, may contribute to the chemoimmunity network by controlling the selective absorption and excretion of important dietary components.

The ABCG5 and ABCG8 transporters were identified by Berge et al. (29), based on a disease condition: mutations in either the *ABCG5* or *ABCG8* genes were found to cause sitosterolemia, an autosomal recessive disorder. This serious disease is characterized by the accumulation of plant-derived toxic sterols (phytosterols) and cholesterol in a large variety of tissues. As documented below, the active phytosterol and cholesterol extrusion by a heterodimer of ABCG5 and ABCG8 proteins is the protective mechanism in our body to prevent such a disease condition.

The deduced 651- and 673-amino acid sequences for ABCG5 and ABCG8 share 28% identity, and both show a "reverse order half-transporter" structure, like other members of the ABCG subfamily (see Fig. 2). Both genes map to chromosome 2, at 2p21, and are tandemly arranged in a head-to-head orientation, separated only by 374 bp. The genomic organization of *ABCG5* and *ABCG8* genes are similar; they both contain 13 exons and span ~28 kb each. The murine orthologs of ABCG5 and ABCG8 exhibiting ~80% identity with the corresponding human proteins were identified by Lu et al. (221).

It has been reported that cholesterol feeding induces a coordinate increase in ABCG5 and ABCG8 expression, suggesting the possible involvement of liver X receptor (LXR) in the regulation of these genes (29). Direct evidence for LXR regulation of *ABCG5* and *ABCG8* genes was provided by several studies (193, 284). It has been demonstrated that cholesterol, LXR agonists as well as retinoid X receptor (RXR) agonists upregulate ABCG5 and ABCG8 expression in mice, whereas these changes were not observed in LXRα-deficient mice (284). These studies also pointed toward the possible involvement of the bile acid receptor (FXR) in the *ABCG5* and *ABCG8* gene regulation. This hypothesis was justified by a recent study demonstrating FXR-dependent increase in ABCG5 and ABCG8 mRNA in response to cholate feeding (411). In contrast, diosgenin, a plant sterol that activates pregnane X receptor (PXR), failed to increase ABCG5 and ABCG8 expression levels (190, 411).

Although no obvious LXR response element was identified in the sequence (29, 284), a binding site for orphan nuclear hormone receptor homolog 1 (LHR-1) has been identified in the intergenic region of *ABCG5* and *ABCG8* genes (98). It has been shown that mutation in this binding site greatly reduced the promoter activity, whereas LHR-1 overexpression increased the expression of ABCG5 and ABCG8, unambiguously demonstrating that LHR-1 is a positive transcription factor for these genes.

1. *Tissue distribution and cellular localization of ABCG5 and ABCG8*

Initial studies demonstrated that ABCG5 and ABCG8 exhibit a contiguous and restricted tissue distribution. These transporters are expressed congruently in the liver and the intestine, since the mRNA of both ABCG5 and ABCG8 was found to be abundant in these tissues (29, 204, 220). However, the tissue- and cell-specific distribution of these proteins exhibits a more complex pattern. A detailed analysis revealed that the mRNA expression profiles are not uniform along the intestinal tract (253). Although the results of microarray and RT-PCR techniques did not correlate closely, the trend indicated low expression levels in the colon and elevated levels in the jejunum, when compared with duodenal expression. Additionally, a physiological study demonstrated that the functional presence of ABCG5 and ABCG8 can be detected in the jejunum and the ileum rather than in the duodenum (85). A low-level expression for both ABCG5 and ABCG8 has also been detected in the choroid plexus (61).

For studying the expression pattern of ABCG5 and ABCG8, in situ localization studies were performed with liver and intestinal sections from mice (284). In the liver, both proteins were uniformly distributed along the hepatic lobule, indicating expression in the hepatocytes, whereas in the intestine, ABCG5 and ABCG8 were found in the enterocytes lining the villi. To circumvent the unavailability of good antibodies for these proteins, the subcellular localization of ABCG5 and ABCG8 has been studied with epitope-tagged proteins in cultured hepatocyte models (111). The coexpressed ABCG5 and ABCG8 proteins were localized to the apical (canalicular) membrane of hepatocytes. This finding was further supported by subsequent in vivo experiments, when antibodies for these proteins became available. In these studies, Abcg5/

Abcg8-deficient (G5G8 −/−) double-knockout mice were infected with adenovirus constructs for the human ABCG5 and ABCG8 (112). The human ABCG8 and an apical marker exhibited a similar distribution pattern in plasma membrane sheets isolated from the liver of the transgenic mice.

A more straightforward and detailed biochemical and immunolocalization analysis was performed by Klett et al. (180) by using human liver, gallbladder, and intestine samples. They raised peptide antibodies against ABCG5 and ABCG8 and demonstrated that these proteins are mostly cofractionated and colocalized to the apical surface in the liver and the intestine. Nevertheless, the distribution of the two proteins was not completely contiguous: ABCG5 was found primarily in the canalicular cells, whereas ABCG8 was more readily detectable in the bile duct cells. In addition, ABCG5 was seen in the canalicular membrane, whereas ABCG8 in hepatocytes was expressed in a more diffuse pattern. Conversely, in the intestine, ABCG8 was found in the apical membrane of enterocytes, whereas the expression of ABCG5 was found to be more diffuse. An interesting addition to the list of diverse expression pattern of ABCG5 and ABCG8 was also provided by Klett et al. (181), demonstrating that both hepatic and intestinal expression of Abcg5 remained apical in the Abcg8-deficient mice.

2. Dimer formation

As discussed earlier, it is commonly accepted that ABC half-transporters must homo- or heterodimerize to yield a functioning unit. The genomic arrangement of *ABCG5* and *ABCG8* genes, which is typical for coordinately regulated genes that encode for subunits of functional complexes, suggests that these proteins may form heterodimers. The similar tissue distribution and cell-specific expression of these proteins is also indicative for heterodimerization. In addition, mutations in either *ABCG5* or *ABCG8* genes cause a disease of a clinically identical phenotype (29, 204, 220). By using epitope-tagged versions of ABCG5 or ABCG8 proteins, Graf et al. (111) have demonstrated that proper targeting of these transporters to the apical plasma membrane requires coexpression of both proteins, as single expression of either of the proteins resulted in retention in the endoplasmic reticulum. Further support for heterodimerization came from colocalization and coimmunoprecipitation of these tagged proteins and from the observations that they undergo posttranslational modification only when coexpressed (111).

Even more compelling confirmation of heterodimerization was provided by Graf et al. (112) in a subsequent study, showing the requirement of coexpression of ABCG5 and ABCG8 for function. They introduced either the human ABCG5 and ABCG8 alone or both proteins into the liver of G5G8 −/− mice. The phenotype of markedly reduced biliary cholesterol secretion in the G5G8 −/− mice was restored only when both ABCG5 and ABCG8 proteins were expressed. In contrast to coexpression of ABCG5 and ABCG8, the coexpression of ABCG2 either with ABCG5 or ABCG8 in the G5G8 −/− mice failed to promote sterol excretion into the bile, indicating that ABCG5 and ABCG8 are obligate heterodimers.

3. Physiological function and clinical relevance of ABCG5/ABCG8

The cholesterol homeostasis in our body is determined by three processes: de novo synthesis, intestinal absorption, and biliary excretion. Under normal circumstances, our diet contains about equal amounts of animal-derived sterol, mostly cholesterol, and plant-derived sterols, that is, sitoserol, campesterol, or stigmasterol. These phytosterols are selectively eliminated from our body, and only regulated amounts of cholesterol are retained.

Mutations in either *ABCG5* or *ABCG8* genes are associated with sitosterolemia (29), a rare autosomal recessive disorder characterized by accumulation of both plant-derived sterols and cholesterol in the blood and different tissues. Due to sterol deposition in various tissues, patients with sitosterolemia frequently develop tendon and tuberous xanthomas, as well as premature coronary atherosclerosis. The accumulation of sterols in the blood is a consequence of both intestinal hyperabsorption and reduced biliary excretion (239). Hitherto, six mutations in *ABCG5* and nine mutations in *ABCG8* genes have been identified in patents with sitosterolemia (29, 204, 220, 398). Graf et al. (110) have demonstrated that most disease-causing missense mutations prevent the formation of stable ABCG5/ABCG8 heterodimers and result in impaired trafficking from the endoplasmic reticulum to the cell surface.

Six missense polymorphisms, one in the *ABCG5* gene and five in the *ABCG8* gene, have been identified, four of which were proven to be associated with changes in plasma sterol levels, either in sitosterol, campesterol, or cholesterol concentration (30, 137, 243). Two of these polymorphisms have been recently demonstrated to be responsible for the gender-specific response of plasma cholesterol levels after changes in dietary composition (138). A third one, which was previously shown to be linked to altered plasma campesterol and sitosterol levels (137), has been found to be associated with a more profound response to statin therapy, i.e., atorvastatin treatment, in patients with hypercholesterolemia (167).

Direct evidence for the involvement of ABCG5/ABCG8 in fractional sterol absorption was provided by Yu et al. (412) by generating and phenotyping G5G8 −/− mice. These mice exhibited a 3-fold increase in intestinal absorption of plant sterols and a 30-fold increase in the

plasma sitosterol level. Interestingly, the accumulation of plant sterols in these animals was associated with a compensatory decrease in plasma cholesterol levels (by ~50%); thus the total sterol content of the blood was not significantly altered (415). However, the knockout mice were found to be extremely sensitive to changes in dietary sterol content. When they were challenged with a 2% cholesterol diet, the plasma cholesterol increased 2.4-fold in the G5G8 −/− animals but not in controls.

According to our current understanding, the intestinal uptake of sterols is primarily controlled by the Niemann-Pick C1 Like 1 protein (NPC1L1) (11, 72), a transporter residing in the apical membrane of the jejunal enterocytes, whereas the ABCG5/ABCG8 heterodimer is responsible for selective extrusion of plant sterols and resecretion of cholesterol into the gut lumen. Exclusion of plant-derived sterols from the body seems to be crucial, since accumulation of these sterols profoundly perturbs cholesterol homeostasis not only in the blood and the liver but also in the adrenal gland (407), a tissue/organ in which sterols have a very special role.

The net luminal absorption of cholesterol in enterocytes is primarily determined by the steady state of fluxes driven by the NPC1L1 protein and the ABCG5/ABCG8 heterodimer, both transporters residing in the brush-border membranes. This scenario is supported by several experimental observations. Overexpression of ABCG5 and ABCG8 results in about a 40% reduction in fractional cholesterol absorption (413). Conversely, impaired function of ABCG5/ABCG8 leads to hypercholesterolemia and hyperabsorption of plant sterols in patients with sitosterolemia (239), as well as increased plasma levels of plant sterols in the G5G8 −/− mice (412). Despite the fact that ezetimibe, a known inhibitor of intestinal absorption of both animal- and plant-derived sterols, selectively blocks NPC1L1 (100), this drug also corrects the impaired fractional absorption and plasma levels of sterols in patients with sitosterolemia (301) and in the G5G8 −/− mice (414), demonstrating the importance of balance between uptake and resecretion processes. It should be noted, however, that the total intestinal absorption of sterols in enterocytes is influenced by several other factors, i.e., the activity of carriers from and to the brush border membrane, the esterification of cholesterol in the endoplasmic reticulum, as well as the serosal transport processes, probably involving another ABC transporter, ABCA1.

In addition to their role in the intestinal absorption, the involvement of ABCG5 and ABCG8 in biliary excretion of sterols is also supported by a growing body of evidence. In the G5G8 −/− mice, secretion of sterols into the bile was markedly reduced (by 91%) (412). Transgenic mice overexpressing human ABCG5 and ABCG8 show increased biliary cholesterol levels (5-fold) and a reduced intestinal absorption of sterols (413). Selective hepatic overexpression of human ABCG5 and ABCG8 in mice results in elevated biliary excretion of cholesterol and plant-derived sterols without affecting their intestinal absorption (402). In addition, overexpression of ABCG5 and ABCG8 in the livers of G5G8 −/− mice restores biliary cholesterol levels (112). Moreover, hepatic mRNA levels and biliary cholesterol concentrations were shown to be directly proportional in genetically modified mice containing different copy numbers of the *ABCG5* and *ABCG8* genes (411). All these observations imply that the ABCG5/ABCG8 heterodimer plays a crucial role in the biliary excretion of sterols.

It should be noted, however, that although Abcg8-deficient, single-knockout mice also exhibited impaired biliary cholesterol excretion, sitosterol secretion into the bile was still maintained (181). Additionally, biliary cholesterol excretion in Abcg5-deficient mice remained inducible by LXR activation (276). These data can be explained either by independent function of these proteins or by the existence of an alternative sterol excretion pathway. The latter hypothesis is consistent with the finding that at least two loci distinct from the ABCG5/ABCG8 locus in mice are associated with plant-derived sterol levels (327).

4. *Substrates and transport mechanism of ABCG5/ABCG8*

The key substrates of the ABCG5/ABCG8 heterodimer are sterols and possibly sterol derivatives. These transporters are clearly responsible for the vitally important exclusion of plant-derived sterols from our body; thus they must selectively recognize and remove phytosterols even in the presence of high concentrations of cholesterol. At the same time, ABCG5/ABCG8 also seem to participate in cholesterol transport at various sites, including the gut and the bile canaliculi. How important this latter function is in humans has not yet been clearly established. Interestingly, our recent, unpublished data indicate that the ABCG5/ABCG8 heterodimer may also be involved in the transport of sterol derivative sex hormones.

Two distinct transport models for the operation of ABCG5/ABCG8 heterodimer have been suggested. In analogy with the transport mechanism of MDR1 and MDR3, Wittenburg and Carey (400) proposed a flippase model for ABCG5/ABCG8. Cholesterol is equally distributed in both hemileaflets of the membrane. According to the flippase model, the ABCG5/ABCG8 heterodimer generates an uneven distribution of cholesterol by facilitating its translocation from the inner to the outer hemileaflet, from which cholesterol is extracted by acceptors. Based on energetic considerations and experimental observations, Small (340) favored another, so-called "activation-collision" model for the operation of ABCG5/ABCG8. In this model, the energy of ATP hydrolysis is used by the transporters

to partially push cholesterol from the inner leaflet to the lumen (activation). If this occurs without flipping the molecule, the isooctyl tail of cholesterol is presented for the acceptors. Thus cholesterol can be readily transferred to small mixed micelles and phospholipid vesicles in the lumen.

In summary, ABCG5 and ABCG8 proteins form functional heterodimers in the brush-border membrane of enterocytes, and in the canalicular membrane of hepatocytes. They extrude sterols from these epithelia to the lumen (gut or bile canaliculus). These transporters are responsible for the exclusion of plant-derived sterols from the body. This physiological role seems to be vital, since the accumulation of these sterols is toxic and profoundly perturbs cholesterol homeostasis.

VII. ROLE OF ABC TRANSPORTERS IN XENOBIOTIC METABOLISM: THE CONCEPT OF A "CHEMOIMMUNITY" DEFENSE SYSTEM

In this review we suggest that the ABC multidrug transporters are essential parts of an immune-like defense system, and their network is a major contributor to "chemoimmunity" in living organisms. It has been documented in detail in the preceding sections that substrate recognition and ATP-dependent toxin extrusion by the MDR-ABC transporters are directly relevant to xenobiotic resistance. How are these resistance proteins organized in our body to become part of a coordinated defense system against toxic compounds? In the following passages we describe this concept, currently with a lot of uncertainties and without a quantitative model. Still, we feel that this may stimulate further work in establishing a quantitative systems biology approach and detailed modeling.

Classical immunology is concerned with the response of the organism to an environmental challenge by mostly water-soluble toxic compounds, microorganisms, or other living agents, e.g., cancer cells. The ultimate function of the immune system is to seek and destroy foreign agents and substances in our body. The classical immune system, however, is practically ineffective in the case of hydrophobic toxic invader molecules, which rapidly cross cell membrane-based tissue barriers. The lipid core structure of the biological membranes makes these barriers essentially freely permeable for hydrophobic compounds, and it is only the cellular toxin transport and metabolism that can protect our body against such chemicals.

The essential basis of the classical immune defense is the discrimination of the self from the nonself, followed by an immediate response to the acute challenge of any possible invaders by the apparatus of the innate immune system. If this response is weak or not fully successful, it is followed by an adaptive, amplified response, more specific for the intruders that could not be eliminated by the first line of defense. The adaptive form of the immune system shows memory for invader recognition and a complex regulation of the interacting elimination pathways. An overreactive response by the adaptive system causes hypersensitivity or allergy to certain immune challenges. We try to demonstrate below that the proposed chemoimmunity system has many similar features to these classical pathways.

A. Chemoimmunity and Toxin Metabolism

Chemoimmunity, as appreciated here, is based on the coordinated action of specific transport systems and cellular xenobiotic metabolism in a defense against hydrophobic or amphipathic compounds. In textbooks, toxin metabolism is usually divided into two major steps. Phase I metabolism is characterized by the oxidation of the toxic compounds, essentially based on the function of cytochrome *P*-450 (CYP) enzymes. This phase may also include the reduction or chemical cleavage of certain toxic compounds. Phase II metabolism involves conjugation, mostly of the already oxidized chemicals, with cellular glutathione, glucuronide, or other small hydrophilic molecules. The abundance and variety of CYP superfamily enzymes in our tissues makes xenobiotic oxidation an effective means of detoxification. The large conjugation capacity of phase II enzymes, especially in the liver cells, provides the following step for the elimination of these toxins.

In this review we do not detail these cellular toxin metabolizing systems but concentrate on the role of MDR-ABC membrane transporters. These proteins are involved in two additional, essential steps of the xenobiotic defense mechanisms that may be called phase zero and phase III.

1. Toxin extrusion at the gates

Phase zero has been described as the cellular uptake step of the toxic compounds (see Refs. 356, 387). In this phase, the above-described MDR-ABC proteins pump out several hydrophobic compounds before they would reach the intracellular compartments and consequently the "milieu interieur" of our body ("preemptive pumping"). These transporters extrude xenobiotics directly from the plasma membrane bilayer or from the vicinity of this lipid bilayer, in cells predominantly located in tissue barriers.

As discussed above, multidrug transporters preferentially interact with substrate molecules concentrating in the hydrophobic membrane environment of the lipid bilayer. The pumps remove the accumulated hydrophobic compounds from the inner membrane leaflet and either pump these compounds into the external leaflet or di-

rectly into the extracellular water-phase. We have no means as yet to distinguish these particular pathways, but this is the mechanism after which the multidrug transporters have been named "hydrophobic vacuum cleaners" (see Refs. 107, 108, 119). It is clear though that their function in phase zero is a most effective way to keep chemoinvaders out of our cells or entirely out of our body, without allowing toxin interaction with intracellular enzymes or compartments.

2. Extrusion of modified toxins

The need for a phase III of toxin metabolism, an additional key step in the xenobiotic defense, was first emphasized by Ishikawa (147). He predicted that during toxin metabolism the efficient elimination of the intracellular, already detoxified (oxidized and/or conjugated) molecules requires an active, ATP-dependent transport mechanism. This active extrusion has to help these metabolites to enter the extracellular fluids and eventually the bile or urine, and thus reduce their accumulation in the key detoxifying cell types. Indeed, with the discovery of the ABCC-type and the ABCG2 multidrug transporters, the identity of these efflux pumps was revealed, and it has become clear that these proteins perform a crucial task in eliminating conjugated toxins.

In this review we do not detail the information related to the transport function of the key conjugate export transporters, the MRPs, as this is extensively provided by the review of Deeley et al. (73). We only emphasize here that the transport features of MRPs are most adapted to this type of phase III metabolic function. Although the relative transport capacity (turnover) of the MRP pumps is much lower than that of MDR1/Pgp, their combined action allows the rapid transport of conjugated metabolites in the required direction with a flexible metabolic control; that is, MRPs are variably located in the apical or basolateral membranes of the cells, their transport is allosterically regulated by cellular metabolites through multiple binding and transport sites, and their expression is also strongly modified depending on the actual metabolic conditions within the cell. As described in the relevant section, ABCG2 may be an important additional player in phase III reactions.

As a conclusion, phase zero and phase III, and the multidrug transporters involved in these reactions, seem to be just as important in xenobiotic elimination as the generally acknowledged phase I and phase II metabolic reactions. In a composite toxicology approach, all these pathways should be included and their interactions analyzed. In addition, both MRPs and ABCG2 have a major role in the elimination of the endogenous toxic metabolic products, also using the phase III pathway (see Ref. 73).

Of course, in xenobiotic transport processes, the "passive" permeability of the respective cell membranes for xenobiotics, based on physical solubility and diffusion criteria, as well as the possible involvement of other transporters should also be considered. Many pharmaceutical agents and toxins are transported by multispecific solute carrier (SLC) transporters for organic anions (e.g., OATP-SLCO/SLC21 and OAT-SLC22A1–3) and organic cations (OCT-SLC 22A4–5). These solute carriers, often called "uptake transporters," include a large variety of related membrane proteins, and in many cases possess overlapping substrate profiles with the MDR-ABC proteins (for recent reviews, see Refs. 196, 231, 246, 360). Some of these transporters perform obligatory exchange of organic compounds (e.g., OAT3), while in others transport is modulated and/or driven by monovalent ions and the membrane potential (e.g., OCTN). Moreover, there is a coordinated expression pattern for various SLC and ABC transporters in the liver, kidney, and BBB, which may govern the overall vectorial transport of many compounds that are mutual substrates of MDR-ABC and SLC proteins (see Ref. 196).

At the time of writing this review there is an accelerating accumulation of permeability and membrane-mediated transport data that may elucidate the complex pattern of drug absorption and distribution. Moreover, expression systems with coordinated expression of MDR-ABC and SLC transporters are becoming available (70) for such detailed studies. We are aware of several consortial efforts in this regard; major international groups are set to perform this enormous task, by using a variety of screening methods, establishing standard, comparative protocols and joint computer bases. A systems biology approach, based on the above experimental work, should soon allow a better understanding of this drug metabolism and transport network.

B. Innate Chemoimmunity

In the complex functioning of this xenobiotic defense mechanism, the analogy to the classical immune system is rather compelling. Similarly to the immune system, the transport and metabolic machineries have to react with an enormous number of compounds, previously not met by the organism. During this step, the immediate recognition of the nonself invader and an innate type of acute defense reaction are both essential.

The first major question is how this selective, still wide-range recognition of the toxic, nonself molecules by the transporters and metabolic enzymes occurs. In the case of the CYP system, the solution is basically similar to that of any metabolic pathways. There are numerous forms of these enzymes; in seven subfamilies a large number of related proteins carry out somewhat different tasks and recognize different substrate molecules (for reviews, see Refs. 60, 207, 376, 403). Still, the CYP pro-

teins are relatively nonspecific enzymes and recognize a variety of substrate molecules. This is further emphasized by the fact that, e.g., in humans, most of the oxidative drug metabolism is carried out by only a limited number of the members of the CYP1, CYP2, and CYP3 families, and a few key enzymes (like CYP1A2, CYP2A6, CYP2C9, and CYP3A4) perform most of the metabolic tasks. Thus selectivity and overlap in drug recognition are both important features in this case.

As far as the functioning of the intracellular conjugation systems is understood, these enzymes preferentially recognize molecules already "decorated" by phase I metabolism, while they also conjugate a large variety of molecules that have available valences with little specificity.

In the case of the multidrug transporters, especially when extruding foreign chemicals (in the phase zero reaction) at the initial tissue barriers, e.g., in the intestine and the fetomaternal or blood-brain barrier, the recognition of the foreign molecules is still a puzzling process. MDR1/Pgp, MRP1, and ABCG2 are the key transporters involved, and there is only one gene in the human genome for each of these transporters. There are no known isoforms produced, e.g., by alternative splicing or other mechanisms; thus one single protein, such as MDR1/Pgp, has to recognize and eliminate thousands of different hydrophobic agents. In addition, a major task is the recognition of the "self" molecules to prevent the removal of essential elements.

As described in the sections dealing with the individual transporters, the molecular mechanism of the discrimination between the self and nonself compounds by the MDR-ABC transporters is still far from being resolved, and we have no definite clue as yet how the "receptor" and "effector" functions, that is, the recognition and elimination of the foreign materials, respectively, are engineered into one single machinery within these proteins. In a phenomenological approach, however, we can state that the function of MDR-ABC proteins in xenobiotic metabolism is based on an extremely wide-range recognition and extrusion of any possible foreign hydrophobic compounds.

From an evolutionary viewpoint, there are indications that MDR-ABC transporters have evolved from early bacterial transporters devoted to specific solute transport, initially using the energy of the protonmotive force (see Ref. 390). In the continuous fight for survival, both attacking and protecting armors have developed, and microorganisms possessing efficient toxins and antitoxin defense systems (at least protecting themselves from these toxins) had a selective advantage. A possible way of producing a promiscuous "defense" mechanism was to decrease the selectivity of a transporter by making the substrate recognition site larger, more complex, and able to accommodate a variety of toxic compounds. This might have led to a loss of efficiency in transport, but provided survival. The forthcoming acquisition of the ATP-binding and hydrolytic domains as energy providers for this transport may have led to less dependence on the actual membrane potential and allowed the eukaryotic cells to use this invention in their plasma membrane.

Regarding the physiological role of the mammalian/human ABC-MDR transporters, we have to deal with the following two important issues.

1) Knockout animals lacking MDR1/Pgp, ABCC1, or ABCG2 (including a variety of combined MDR1/Pgp and ABCC1 knockouts) are practically healthy and have no pathological alterations in the controlled environment of an animal house. These knockout animals are sensitive to various toxins that are normally harmless to the same species, but there are no major physiological alterations even after long-term observations (see above). Another example is the occurrence of homozygous MDR1/Pgp loss of function in the collie dogs, which are healthy, but very sensitive to certain drugs, e.g., ivermectin (298).

2) There are no data in the literature describing human diseases based on a nonfunctional MDR1/Pgp protein, or disease conditions caused by any MDR1/Pgp mutation. An extensive search for null alleles of *MDR1* has also remained negative. Thus the lack of MDR1/Pgp in humans may be either early lethal (very unlikely) or harmless. In the case of ABCG2, individuals with genes coding for a nonfunctional ABCG2 (a truncated form of the protein) have been found in a low percentage (141, 428), with no apparent disease condition. However, it has been suggested that drug hypersensitivity (188, 242, 251) and even alfalfa hypersensitivity (see Refs. 271, 385) in some Japanese cohorts may be due to the absence or the polymorphisms of ABCG2.

These data may suggest that, in a general sense, MDR-ABC transporters are not essential for the basic physiological processes in mammalian life. Nevertheless, it is quite clear that they are key players in the "chemodefense" mechanisms.

C. Adaptive Chemoimmunity Response, Memory, and Hypersensitivity

Similarly to that seen in the classical immune system, there is a possibility that xenobiotic resistance based on transporters may show an adaptive phase, with increasing specificity and efficiency. In this review we have already described the regulation of the individual MDR-ABC proteins, and in this context we only emphasize a few key points, concerning the adaptive nature of this network.

Several data indicate that the expression of the MDR-ABC transporters in tumors is characteristically induced by cytotoxic agents. This finding is not directly relevant to physiology, but the same may be true in normal tissues

exposed to xenobiotics, and there are indications that several tissues react to a toxin exposure by a rapid overexpression of the relevant multidrug transporter. In bacteria, most multidrug transport systems are under the tight control of specific regulatory elements, composed of toxin-recognition and DNA-binding domains and (usually located within the same operon) that significantly modulate the expression of the relevant transporter protein(s) (see Refs. 323, 388, 426). Toxin recognition by these regulatory proteins is just as promiscuous and/or specific as that by the regulated transporter, providing a very efficient way to increase or decrease the defense capabilities of the microorganism. In eukaryotes, exemplified, e.g., by yeast, these regulatory and multidrug transport systems are combined into a complex network, containing a number of overlapping elements.

With regard to the human MDR-ABC transporters, transcriptional and posttranscriptional regulatory mechanisms have been already detailed in the respective sections. Here we just mention again that many stress factors, including steroid hormones, heat shock, or hypoxia (for MDR1/Pgp, see Refs. 64, 65; for ABCG2, see Ref. 191), upregulate these transporters, which may thus be considered as parts of a general cellular stress response. It is assumed that cellular toxin activated receptors, including the PXR-SXR (pregnane X receptor) and the CAR (constitutive androstane receptor), play a major role in this response (see Refs. 195, 351, 403), which is an integrated phenomenon including the regulation of metabolic enzymes as well (25, 55, 195). A general and coordinated upregulation of the multidrug transporters and CYP enzymes may significantly alter several drug effects. This seems to be the case, e.g., during the application of a widely used herbal extract from Saint John's wort (SJW), a holistic medicine to accelerate wound healing, treat nerve pain, or depression. Chronic exposure by SJW reduces the bioavailability for a number of drugs because of the induction of both CYP3 and MDR1/Pgp expression and activity (274).

Interestingly, under conditions resulting in major cell damage and increased endotoxin exposure (55, 168), or in various forms of inflammatory bowel disease (IBD) (267), the expression of several MDR-ABC transporters is downregulated, which makes the affected tissues even more defenseless. The stress responsiveness of MDR1 expression is interestingly exemplified by the observation that this protein is measurably upregulated in nerve cells (normally hardly expressing MDR1) after limbic seizures (395).

In connection to the general stress responsiveness, the classical immune system also has a strong influence on the chemoimmunity transporters, as several immune mediators directly influence MDR-ABC transporter expression. As examples, transforming growth factor-β upregulates MDR1/Pgp in the BBB (80), the cytokines interleukin (IL)-1β, IL-6, and tumor necrosis factor-α reduce MDR1/Pgp expression in HepG2 cells (202) and in Caco2 cells (26), while MDR1/Pgp expression is upregulated again by interferon-γ (26). Inflammatory cytokines, including IL-1β, inhibit MRP2 expression in the liver (122), while IL-6 transcriptionally upregulates various MRPs in normal epidermal fibroblasts (84), through the activation of the STAT1, STAT3, and MAPK pathways. Lipopolysaccharide exposure regulates the expression of several hepatic MDR-ABC proteins, including MDR1/Pgp and MRP2 (57).

It has been established that hormones and mediators also have important regulatory effects on MDR-ABC transporters. Thyroid hormones upregulate the expression of MDR1/Pgp (241) in several tissues, while in the BBB MDR1 expression and related transport is reduced by endothelin through endothelin B receptors (116). Interestingly, sex hormones have major regulatory effects on ABCG2 expression, that is, testosterone increases while estradiol decreases ABCG2 expression in various animal models (144, 371). As mentioned above, pathological activation of brain tissues increases MDR1/Pgp expression, and this regulation may occur through glutamate release. This mediator was shown to upregulate MDR1/Pgp expression through an *N*-methyl-D-aspartate receptor mechanism (431). Increasing glutamate release during ischemic, anoxic brain injury may thus increase the level of MDR-ABC transporters and provide a defense mechanism against accumulating toxins. Interestingly, serotonin may have an opposite effect: in the small intestine serotonin depletion induced an increased MDR1/Pgp expression (121).

As a summary, the expression and function of MDR-ABC transporters are subject to complex regulation, which differently modifies their presence and efficiency in different tissues. Moreover, this regulation is in close coupling with that of the metabolic enzymes and other membrane transporters. It seems to be a general rule that MDR-ABC transporters are regulated in a positive correlation with the key metabolic enzymes of antitoxin defense, while uptake (SLC) transporters, which in most cases accelerate cellular toxin exposure, are coordinately downregulated (4).

Interestingly, the MDR-ABC transporters seem to "feel" the presence of their transporter network partners, and the reduction of one transporter modifies the expression of a related other pump protein. This seems to be the case in the Dubin-Johnson disease, or other alterations of conjugate transport by MRP2, when conjugate export into the bile is insufficient. In this case, several studies observed an upregulation of other MRP proteins, especially MRP3, transporting conjugates into the bloodstream. Although this does not help the biliary clearance of conjugated toxins, it at least protects the hepatocytes from a harmful accumulation of these metabolites. Another interesting example of this adaptive cross-regulation may be the large increase of MDR1

protein expression in ABCG2 knockout animals, especially observed in the BBB (62).

The above-described, sometimes long-term modulation by hormones, mediators, immune-components or even by the altered expression of corresponding transporters causes an adaptive memory in the chemoimmunity transporter network. We still have only very limited information about the molecular details of this adaptation. At the cellular level, gene amplification, epigenetic, or other transcriptional modulation of gene expression, posttranscriptional, and even posttranslational modulation of various MDR-ABC transporters have already been described (see above). On the basis of environmental toxicology studies and clinical experience, it is quite compelling that long-time exposure to toxic compounds results in a new steady-state, with higher metabolic enzyme and MDR-ABC transporter expression levels all over our body. Although with little evidence as yet for humans, this may be an important mechanism for survival in a polluted environment, or for tolerating medical or nonmedical drug abuse.

At the same time, a hypersensitivity of our tissues to certain chemicals may occur under conditions when elevated levels of the MDR-ABC transporters ensure the adaptation to a toxic environment. In the continuous presence of various MDR-ABC transporter substrate toxins, the upregulation of the transporters provides a new steady-state, in which an increased toxin and toxin metabolite extrusion allows proper adaptation. However, cells may become "addicted," and the appearance of a new toxic compound, which inhibits the function of a given ABC transporter, may disturb the balance in this environment and cause an apparent hypersensitivity to a large number of chemicals well tolerated before. Such a phenomenon has already been explored in several animal species (see Refs. 224, 339). Although with little evidence as yet in humans, this chemosensitization effect may be an increasing danger in our over-polluted world. The complex, harmful effects of MDR-ABC transporter inhibitor toxins can only be investigated in the presence of other, unrelated toxic compounds (see Refs. 17, 224, 339, 343). The clinical consequences of this phenomenon, often denoted as "collateral sensitivity," have just begun to be appreciated. With as yet unknown mechanisms, a similar hypersensitivity was observed in several MDR1/Pgp-expressing tumor cell lines against completely unrelated chemicals, which are not MDR1/Pgp substrates but cause cell destruction in close correlation with the MDR1/Pgp expression (363).

D. Chemoimmunity Transporters: Why the MDR-ABC Proteins?

As already mentioned above, defense against internal and external toxins is very old and efficient. Over 60% of the current anticancer drugs are derived from natural sources. These chemicals have evolved to provide an evolutionary preference for their hosts, which also had to develop self-protecting mechanisms. Natural products are "privileged structures" selected by evolutionary pressure to interact with a wide array of biological targets (186). Perhaps not surprisingly, evolution produced equally effective countermeasures against these noxious chemicals. MDR-ABC transporters are present from bacteria to human; thus their structure and function survived all pressures during evolution. This requires a very efficient and adaptable mechanism of action. In fact, according to a whole-genome analysis, in *Caenorhabditis elegans*, the 60 ABC transporters evolved with higher than expected rates of duplication (338), suggesting that ABC transporters are particularly adaptable evolutionary modules, used for variable functions. How do we think MDR-ABC transporters could cope with all these requirements?

The trick of this efficiency could have been to couple ATP hydrolysis to substrate binding and export within one protein complex, or later during the evolution within one protein. In bacteria and lower eukaryotes, many ABC transporters are formed from independent polypeptides representing the transmembrane domains or the ABC units. In higher eukaryotes, these are combined into major units, containing at least one transmembrane and one ABC domain, but in most cases the two TM and two ABC domains are within one polypeptide chain.

In section II we provided a description of our current knowledge about the molecular mechanism of MDR-ABC transporters. Although we are far from understanding all details, some principles of this mechanism of action can be appreciated. These suggest that ATP hydrolysis is coupled to drug substrate transport in a relatively loose fashion, that is, the ATPase machinery has a low basic activity even in the absence of transported drug substrates. This may be ensured by a relatively low rate of lipid flippase activity or by interactions with endogenous substrates. In accordance with this notion, the drug binding region in the MDR-ABC transporters is a relatively large cavity with multiple binding sites of variable polarity. According to recent models, this is the way substrate recognition may be very wide and still efficient.

For the construction of efficient target/receptor interactions, nature has many different solutions. In the classical immune system, foreign agent recognition is ensured by a huge repertoire of antibody proteins, formed by millions of variants from relatively few genes through gene rearrangement. Thus there is a good chance for every single intruder "epitope" to find a recognition partner, which then can be selected and expressed in large quantities.

In the case of the chemoimmunity transporter network, the relatively few MDR-ABC proteins involved share a wide substrate recognition; thus only a few genes

are required to handle the huge number of possible toxins. One trick for this "promiscuity" or multispecificity might be the composition of the substrate binding site (see above), and also, that this drug binding site is buried in the plasma membrane (see the "hydrophobic vacuum cleaner" model). In the case of the transport of amphipathic, and even more of hydrophobic toxic agents, this results in a relatively high local concentration of the substrates at the binding site. Thus even a relatively low-affinity binding allows the recognition of the transported molecules.

In the years to come we expect to learn a lot more about the structure and molecular mechanism of action of the human MDR-ABC transporters, which will solidify or discard some of the speculations presented here. Still, we believe that the concepts described above may stimulate the analysis of these systems as interacting members of a general physiological defense network.

ACKNOWLEDGMENTS

We appreciate the critical reading, useful suggestions and corrections of this manuscript by Prof. G. Gardos.

Address for reprint requests and other correspondence: B. Sarkadi, National Medical Center, Institute of Haematology and Immunology, 1113 Budapest, Diószegi u. 64, Hungary (e-mail: sarkadi@biomembrane.hu).

GRANTS

We appreciate the support of research grants (OTKA AT48986, PF60435, AT48729, ETT, and NKFP, Hungary) that allowed us to compile this review article. B. Sarkadi is a recipient of a Howard Hughes International Scholarship. L. Homolya is an EMBO-HHMI Young Investigator. G. Szakács is the recipient of a Special Fellow Award from the Leukemia and Lymphoma Society.

REFERENCES

1. **Adachi Y, Suzuki H, Schinkel AH, and Sugiyama Y.** Role of breast cancer resistance protein (Bcrp1/Abcg2) in the extrusion of glucuronide and sulfate conjugates from enterocytes to intestinal lumen. *Mol Pharmacol* 67: 923–928, 2005.
2. **Ahmad S, Safa AR, and Glazer RI.** Modulation of P-glycoprotein by protein kinase C alpha in a baculovirus expression system. *Biochemistry* 33: 10313–10318, 1994.
3. **Akiyama S, Cornwell MM, Kuwano M, Pastan I, and Gottesman MM.** Most drugs that reverse multidrug resistance also inhibit photoaffinity labeling of P-glycoprotein by a vinblastine analog. *Mol Pharmacol* 33: 144–147, 1988.
4. **Aleksunes LM, Slitt AM, Cherrington NJ, Thibodeau MS, Klaassen CD, and Manautou JE.** Differential expression of mouse hepatic transporter genes in response to acetaminophen and carbon tetrachloride. *Toxicol Sci* 83: 44–52, 2005.
5. **Allen JD, Jackson SC, and Schinkel AH.** A mutation hot spot in the Bcrp1 (Abcg2) multidrug transporter in mouse cell lines selected for Doxorubicin resistance. *Cancer Res* 62: 2294–2299, 2002.
6. **Allen JD and Schinkel AH.** Multidrug resistance and pharmacological protection mediated by the breast cancer resistance protein (BCRP/ABCG2). *Mol Cancer Ther* 1: 427–434, 2002.
7. **Allen JD, van Loevezijn A, Lakhai JM, van der Valk M, van Tellingen O, Reid G, Schellens JH, Koomen GJ, and Schinkel AH.** Potent and specific inhibition of the breast cancer resistance protein multidrug transporter in vitro and in mouse intestine by a novel analogue of fumitremorgin C. *Mol Cancer Ther* 1: 417–425, 2002.
8. **Allikmets R, Schriml LM, Hutchinson A, Romano-Spica V, and Dean M.** A human placenta-specific ATP-binding cassette gene (ABCP) on chromosome 4q22 that is involved in multidrug resistance. *Cancer Res* 58: 5337–5339, 1998.
9. **Al-Shawi MK, Polar MK, Omote H, and Figler RA.** Transition state analysis of the coupling of drug transport to ATP hydrolysis by P-glycoprotein. *J Biol Chem* 278: 52629–52640, 2003.
10. **Al-Shawi MK and Senior AE.** Characterization of the adenosine triphosphatase activity of Chinese hamster P-glycoprotein. *J Biol Chem* 268: 4197–4206, 1993.
11. **Altmann SW, Davis HR Jr, Zhu LJ, Yao X, Hoos LM, Tetzloff G, Iyer SP, Maguire M, Golovko A, Zeng M, Wang L, Murgolo N, and Graziano MP.** Niemann-Pick C1 Like 1 protein is critical for intestinal cholesterol absorption. *Science* 303: 1201–1204, 2004.
12. **Ambudkar SV, Dey S, Hrycyna CA, Ramachandra M, Pastan I, and Gottesman MM.** Biochemical, cellular, and pharmacological aspects of the multidrug transporter. *Annu Rev Pharmacol Toxicol* 39: 361–398, 1999.
13. **Ambudkar SV, Kimchi-Sarfaty C, Sauna ZE, and Gottesman MM.** P-glycoprotein: from genomics to mechanism. *Oncogene* 22: 7468–7485, 2003.
14. **Ambudkar SV, Lelong IH, Zhang J, Cardarelli CO, Gottesman MM, and Pastan I.** Partial purification and reconstitution of the human multidrug-resistance pump: characterization of the drug-stimulatable ATP hydrolysis. *Proc Natl Acad Sci USA* 89: 8472–8476, 1992.
15. **Annereau JP, Szakacs G, Tucker CJ, Arciello A, Cardarelli C, Collins J, Grissom S, Zeeberg BR, Reinhold W, Weinstein JN, Pommier Y, Paules RS, and Gottesman MM.** Analysis of ATP-binding cassette transporter expression in drug-selected cell lines by a microarray dedicated to multidrug resistance. *Mol Pharmacol* 66: 1397–1405, 2004.
16. **Armstrong S, Tabernero L, Zhang H, Hermodsen M, and Stauffacher P.** Powering the ABC transporters: the 2.5 Å crystal structure of the ABC domain of RBSA. *Pediatr Pulmonol* 17: 91–92, 1998.
17. **Backhaus T, Arrhenius A, and Blanck H.** Toxicity of a mixture of dissimilarly acting substances to natural algal communities: predictive power and limitations of independent action and concentration addition. *Environ Sci Technol* 38: 6363–6370, 2004.
18. **Backstrom G, Taipalensuu J, Melhus H, Brandstrom H, Svensson AC, Artursson P, and Kindmark A.** Genetic variation in the ATP-binding cassette transporter gene ABCG2 (BCRP) in a Swedish population. *Eur J Pharm Sci* 18: 359–364, 2003.
19. **Bacso Z, Nagy H, Goda K, Bene L, Fenyvesi F, Matko J, and Szabo G.** Raft and cytoskeleton associations of an ABC transporter: P-glycoprotein. *Cytometry* 61: 105–116, 2004.
20. **Bailey-Dell KJ, Hassel B, Doyle LA, and Ross DD.** Promoter characterization and genomic organization of the human breast cancer resistance protein (ATP-binding cassette transporter G2) gene. *Biochim Biophys Acta* 1520: 234–241, 2001.
21. **Baker EK and El-Osta A.** MDR1, chemotherapy and chromatin remodeling. *Cancer Biol Ther* 3: 819–824, 2004.
22. **Bakos E, Evers R, Szakacs G, Tusnady GE, Welker E, Szabo K, de Haas M, van Deemter L, Borst P, Varadi A, and Sarkadi B.** Functional multidrug resistance protein (MRP1) lacking the N-terminal transmembrane domain. *J Biol Chem* 273: 32167–32175, 1998.
23. **Bates SE, Lee JS, Dickstein B, Spolyar M, and Fojo AT.** Differential modulation of P-glycoprotein transport by protein kinase inhibition. *Biochemistry* 32: 9156–9164, 1993.
24. **Bates SE, Medina-Perez WY, Kohlhagen G, Antony S, Nadjem T, Robey RW, and Pommier Y.** ABCG2 mediates differential resistance to SN-38 (7-ethyl-10-hydroxycamptothecin) and homocamptothecins. *J Pharmacol Exp Ther* 310: 836–842, 2004.
25. **Bauer D, Wolfram N, Kahl GF, and Hirsch-Ernst KI.** Transcriptional regulation of CYP2B1 induction in primary rat hepatocyte cultures: repression by epidermal growth factor is mediated via a distal enhancer region. *Mol Pharmacol* 65: 172–180, 2004.

26. **Belliard AM, Lacour B, Farinotti R, and Leroy C.** Effect of tumor necrosis factor-alpha and interferon-gamma on intestinal P-glycoprotein expression, activity, and localization in Caco-2 cells. *J Pharm Sci* 93: 1524–1536, 2004.
27. **Belpomme D, Gauthier S, Pujade-Lauraine E, Facchini T, Goudier MJ, Krakowski I, Netter-Pinon G, Frenay M, Gousset C, Marie FN, Benmiloud M, and Sturtz F.** Verapamil increases the survival of patients with anthracycline-resistant metastatic breast carcinoma. *Ann Oncol* 11: 1471–1476, 2000.
28. **Benderra Z, Faussat AM, Sayada L, Perrot JY, Chaoui D, Marie JP, and Legrand O.** Breast cancer resistance protein and P-glycoprotein in 149 adult acute myeloid leukemias. *Clin Cancer Res* 10: 7896–7902, 2004.
29. **Berge KE, Tian H, Graf GA, Yu L, Grishin NV, Schultz J, Kwiterovich P, Shan B, Barnes R, and Hobbs HH.** Accumulation of dietary cholesterol in sitosterolemia caused by mutations in adjacent ABC transporters. *Science* 290: 1771–1775, 2000.
30. **Berge KE, von Bergmann K, Lutjohann D, Guerra R, Grundy SM, Hobbs HH, and Cohen JC.** Heritability of plasma noncholesterol sterols and relationship to DNA sequence polymorphism in ABCG5 and ABCG8. *J Lipid Res* 43: 486–494, 2002.
31. **Beukeveld GJ, In 't Veld G, Havinga R, Groen AK, Wolthers BG, and Kuipers F.** Relationship between biliary lipid and protoporphyrin secretion: potential role of mdr2 P-glycoprotein in hepatobiliary organic anion transport. *J Hepatol* 24: 343–352, 1996.
32. **Bolhuis H, van Veen HW, Molenaar D, Poolman B, Driessen AJ, and Konings WN.** Multidrug resistance in *Lactococcus lactis*: evidence for ATP-dependent drug extrusion from the inner leaflet of the cytoplasmic membrane. *EMBO J* 15: 4239–4245, 1996.
33. **Boraldi F, Quaglino D, Croce MA, Garcia Fernandez MI, Tiozzo R, Gheduzzi D, Bacchelli B, and Pasquali Ronchetti I.** Multidrug resistance protein-6 (MRP6) in human dermal fibroblasts. Comparison between cells from normal subjects and from Pseudoxanthoma elasticum patients. *Matrix Biol* 22: 491–500, 2003.
34. **Borges-Walmsley MI, McKeegan KS, and Walmsley AR.** Structure and function of efflux pumps that confer resistance to drugs. *Biochem J* 376: 313–338, 2003.
35. **Borst P, Zelcer N, and van Helvoort A.** ABC transporters in lipid transport. *Biochim Biophys Acta* 1486: 128–144, 2000.
36. **Breedveld P, Pluim D, Cipriani G, Wielinga P, van Tellingen O, Schinkel AH, and Schellens JH.** The effect of Bcrp1 (Abcg2) on the in vivo pharmacokinetics and brain penetration of imatinib mesylate (Gleevec): implications for the use of breast cancer resistance protein and P-glycoprotein inhibitors to enable the brain penetration of imatinib in patients. *Cancer Res* 65: 2577–2582, 2005.
37. **Breedveld P, Zelcer N, Pluim D, Sonmezer O, Tibben MM, Beijnen JH, Schinkel AH, van Tellingen O, Borst P, and Schellens JH.** Mechanism of the pharmacokinetic interaction between methotrexate and benzimidazoles: potential role for breast cancer resistance protein in clinical drug-drug interactions. *Cancer Res* 64: 5804–5811, 2004.
38. **Bryan J, Vila-Carriles WH, Zhao G, Babenko AP, and Aguilar-Bryan L.** Toward linking structure with function in ATP-sensitive K^+ channels. *Diabetes* 53 *Suppl* 3: S104–S112, 2004.
39. **Bunting KD, Lu T, Kelly PF, and Sorrentino BP.** Self-selection by genetically modified committed lymphocyte precursors reverses the phenotype of JAK3-deficient mice without myeloablation. *Hum Gene Ther* 11: 2353–2364, 2000.
40. **Burger H, van Tol H, Boersma AW, Brok M, Wiemer EA, Stoter G, and Nooter K.** Imatinib mesylate (STI571) is a substrate for the breast cancer resistance protein (BCRP)/ABCG2 drug pump. *Blood* 104: 2940–2942, 2004.
41. **Burger H, van Tol H, Brok M, Wiemer EA, de Bruijn EA, Guetens G, de Boeck G, Sparreboom A, Verweij J, and Nooter K.** Chronic imatinib mesylate exposure leads to reduced intracellular drug accumulation by induction of the ABCG2 (BCRP) and ABCB1 (MDR1) drug transport pumps. *Cancer Biol Ther* 4: 742–752, 2005.
42. **Buschman E and Gros P.** The inability of the mouse mdr2 gene to confer multidrug resistance is linked to reduced drug binding to the protein. *Cancer Res* 54: 4892–4898, 1994.
43. **Bush JA and Li G.** Cancer chemoresistance: the relationship between p53 and multidrug transporters. *Int J Cancer* 98: 323–330, 2002.
44. **Candeil L, Gourdier I, Peyron D, Vezzio N, Copois V, Bibeau F, Orsetti B, Scheffer GL, Ychou M, Khan QA, Pommier Y, Pau B, Martineau P, and Del Rio M.** ABCG2 overexpression in colon cancer cells resistant to SN38 and in irinotecan-treated metastases. *Int J Cancer* 109: 848–854, 2004.
45. **Cervenak J, Andrikovics H, Ozvegy-Laczka C, Tordai A, Nemet K, Varadi A, and Sarkadi B.** The role of the human ABCG2 multidrug transporter and its variants in cancer therapy and toxicology. *Cancer Lett* 234: 62–72, 2005.
46. **Chambers TC, Germann UA, Gottesman MM, Pastan I, Kuo JF, and Ambudkar SV.** Bacterial expression of the linker region of human MDR1 P-glycoprotein and mutational analysis of phosphorylation sites. *Biochemistry* 34: 14156–14162, 1995.
47. **Chan W, Calderon G, Swift AL, Moseley J, Li S, Hosoya H, Arias IM, and Ortiz DF.** Myosin II regulatory light chain is required for trafficking of bile salt export protein (BSEP) to the apical membrane in MDCK cells. *J Biol Chem*: 280: 23741–23747, 2005.
48. **Chang G.** Multidrug resistance ABC transporters. *FEBS Lett* 555: 102–105, 2003.
49. **Chang G.** Structure of MsbA from *Vibrio cholera*: a multidrug resistance ABC transporter homolog in a closed conformation. *J Mol Biol* 330: 419–430, 2003.
50. **Chang G and Roth CB.** Structure of MsbA from *E. coli:* a homolog of the multidrug resistance ATP binding cassette (ABC) transporters. *Science* 293: 1793–1800, 2001.
51. **Chaudhary PM and Roninson IB.** Induction of multidrug resistance in human cells by transient exposure to different chemotherapeutic drugs. *J Natl Cancer Inst* 85: 632–639, 1993.
52. **Chen CJ, Chin JE, Ueda K, Clark DP, Pastan I, Gottesman MM, and Roninson IB.** Internal duplication and homology with bacterial transport proteins in the mdr1 (P-glycoprotein) gene from multidrug-resistant human cells. *Cell* 47: 381–389, 1986.
53. **Chen HL, Liu YJ, Feng CH, Wu CY, Shyu MK, Yuan RH, and Chang MH.** Developmental expression of canalicular transporter genes in human liver. *J Hepatol* 43: 742–747, 2005.
54. **Chen J, Lu G, Lin J, Davidson AL, and Quiocho FA.** A tweezers-like motion of the ATP-binding cassette dimer in an ABC transport cycle. *Mol Cell* 12: 651–661, 2003.
55. **Chen YH, Wang JP, Wang H, Sun MF, Wei LZ, Wei W, and Xu DX.** Lipopolysaccharide treatment downregulates the expression of the pregnane X receptor, cyp3a11 and mdr1a genes in mouse placenta. *Toxicology* 211: 242–252, 2005.
56. **Chen ZS, Robey RW, Belinsky MG, Shchaveleva I, Ren XQ, Sugimoto Y, Ross DD, Bates SE, and Kruh GD.** Transport of methotrexate, methotrexate polyglutamates, and 17beta-estradiol 17-(beta-D-glucuronide) by ABCG2: effects of acquired mutations at R482 on methotrexate transport. *Cancer Res* 63: 4048–4054, 2003.
57. **Cherrington NJ, Slitt AL, Li N, and Klaassen CD.** Lipopolysaccharide-mediated regulation of hepatic transporter mRNA levels in rats. *Drug Metab Dispos* 32: 734–741, 2004.
58. **Chin KV, Tanaka S, Darlington G, Pastan I, and Gottesman MM.** Heat shock and arsenite increase expression of the multidrug resistance (MDR1) gene in human renal carcinoma cells. *J Biol Chem* 265: 221–226, 1990.
59. **Chin KV, Ueda K, Pastan I, and Gottesman MM.** Modulation of activity of the promoter of the human MDR1 gene by Ras and p53. *Science* 255: 459–462, 1992.
60. **Choudhary D, Jansson I, Sarfarazi M, and Schenkman JB.** Xenobiotic-metabolizing cytochromes *P*450 in ontogeny: evolving perspective. *Drug Metab Rev* 36: 549–568, 2004.
61. **Choudhuri S, Cherrington NJ, Li N, and Klaassen CD.** Constitutive expression of various xenobiotic and endobiotic transporter mRNAs in the choroid plexus of rats. *Drug Metab Dispos* 31: 1337–1345, 2003.
62. **Cisternino S, Mercier C, Bourasset F, Roux F, and Scherrmann JM.** Expression, up-regulation, and transport activity of the multidrug-resistance protein Abcg2 at the mouse blood-brain barrier. *Cancer Res* 64: 3296–3301, 2004.
63. **Combates NJ, Rzepka RW, Chen YN, and Cohen D.** NF-IL6, a member of the C/EBP family of transcription factors, binds and

trans-activates the human MDR1 gene promoter. *J Biol Chem* 269: 29715–29719, 1994.
64. **Comerford KM and Colgan SP.** Assessing oxygen sensitivity of the multidrug resistance (MDR) gene. *Methods Enzymol* 381: 376–387, 2004.
65. **Comerford KM, Cummins EP, and Taylor CT.** c-Jun NH_2-terminal kinase activation contributes to hypoxia-inducible factor 1 alpha-dependent P-glycoprotein expression in hypoxia. *Cancer Res* 64: 9057–9061, 2004.
66. **Cooray HC, Blackmore CG, Maskell L, and Barrand MA.** Localisation of breast cancer resistance protein in microvessel endothelium of human brain. *Neuroreport* 13: 2059–2063, 2002.
67. **Cooray HC, Janvilisri T, van Veen HW, Hladky SB, and Barrand MA.** Interaction of the breast cancer resistance protein with plant polyphenols. *Biochem Biophys Res Commun* 317: 269–275, 2004.
68. **Crawford AR, Smith AJ, Hatch VC, Oude Elferink RP, Borst P, and Crawford JM.** Hepatic secretion of phospholipid vesicles in the mouse critically depends on mdr2 or MDR3 P-glycoprotein expression. Visualization by electron microscopy. *J Clin Invest* 100: 2562–2567, 1997.
69. **Crawford JM, Mockel GM, Crawford AR, Hagen SJ, Hatch VC, Barnes S, Godleski JJ, and Carey MC.** Imaging biliary lipid secretion in the rat: ultrastructural evidence for vesiculation of the hepatocyte canalicular membrane. *J Lipid Res* 36: 2147–2163, 1995.
70. **Cui Y, Konig J, and Keppler D.** Vectorial transport by double-transfected cells expressing the human uptake transporter SLC21A8 and the apical export pump ABCC2. *Mol Pharmacol* 60: 934–943, 2001.
71. **Dano K.** Active outward transport of daunomycin in resistant Ehrlich ascites tumor cells. *Biochim Biophys Acta* 323: 466–483, 1973.
72. **Davis HR Jr, Zhu LJ, Hoos LM, Tetzloff G, Maguire M, Liu J, Yao X, Iyer SP, Lam MH, Lund EG, Detmers PA, Graziano MP, and Altmann SW.** Niemann-Pick C1 Like 1 (NPC1L1) is the intestinal phytosterol and cholesterol transporter and a key modulator of whole-body cholesterol homeostasis. *J Biol Chem* 279: 33586–33592, 2004.
73. **Deeley RG, Westlake C, and Cole SPC.** Transmembrane transport of endo- and xenobiotics by the ATP binding cassette multidrug resistance proteins (MRPs). *Physiol Rev* 86: 849–899, 2006.
74. **De Jong FA, Marsh S, Mathijssen RH, King C, Verweij J, Sparreboom A, and McLeod HL.** ABCG2 pharmacogenetics: ethnic differences in allele frequency and assessment of influence on irinotecan disposition. *Clin Cancer Res* 10: 5889–5894, 2004.
75. **De Vree JM, Jacquemin E, Sturm E, Cresteil D, Bosma PJ, Aten J, Deleuze JF, Desrochers M, Burdelski M, Bernard O, Oude Elferink RP, and Hadchouel M.** Mutations in the MDR3 gene cause progressive familial intrahepatic cholestasis. *Proc Natl Acad Sci USA* 95: 282–287, 1998.
76. **Diestra JE, Scheffer GL, Catala I, Maliepaard M, Schellens JH, Scheper RJ, Germa-Lluch JR, and Izquierdo MA.** Frequent expression of the multi-drug resistance-associated protein BCRP/MXR/ABCP/ABCG2 in human tumours detected by the BXP-21 monoclonal antibody in paraffin-embedded material. *J Pathol* 198: 213–219, 2002.
77. **Dietrich CG, Geier A, and Oude Elferink RP.** ABC of oral bioavailability: transporters as gatekeepers in the gut. *Gut* 52: 1788–1795, 2003.
78. **Diop NK and Hrycyna CA.** *N*-linked glycosylation of the human ABC transporter ABCG2 on asparagine 596 is not essential for expression, transport activity, or trafficking to the plasma membrane. *Biochemistry* 44: 5420–5429, 2005.
79. **Dixon PH, Weerasekera N, Linton KJ, Donaldson O, Chambers J, Egginton E, Weaver J, Nelson-Piercy C, de Swiet M, Warnes G, Elias E, Higgins CF, Johnston DG, McCarthy MI, and Williamson C.** Heterozygous MDR3 missense mutation associated with intrahepatic cholestasis of pregnancy: evidence for a defect in protein trafficking. *Hum Mol Genet* 9: 1209–1217, 2000.
80. **Dohgu S, Yamauchi A, Takata F, Naito M, Tsuruo T, Higuchi S, Sawada Y, and Kataoka Y.** Transforming growth factor-beta1 upregulates the tight junction and P-glycoprotein of brain microvascular endothelial cells. *Cell Mol Neurobiol* 24: 491–497, 2004.
81. **Doige CA, Yu X, and Sharom FJ.** The effects of lipids and detergents on ATPase-active P-glycoprotein. *Biochim Biophys Acta* 1146: 65–72, 1993.
82. **Doyle LA and Ross DD.** Multidrug resistance mediated by the breast cancer resistance protein BCRP (ABCG2). *Oncogene* 22: 7340–7358, 2003.
83. **Doyle LA, Yang W, Abruzzo LV, Krogmann T, Gao Y, Rishi AK, and Ross DD.** A multidrug resistance transporter from human MCF-7 breast cancer cells. *Proc Natl Acad Sci USA* 95: 15665–15670, 1998.
84. **Dreuw A, Hermanns HM, Heise R, Joussen S, Rodriguez F, Marquardt Y, Jugert F, Merk HF, Heinrich PC, and Baron JM.** Interleukin-6-type cytokines upregulate expression of multidrug resistance-associated proteins in NHEK and dermal fibroblasts. *J Invest Dermatol* 124: 28–37, 2005.
85. **Duan LP, Wang HH, and Wang DQ.** Cholesterol absorption is mainly regulated by the jejunal and ileal ATP-binding cassette sterol efflux transporters Abcg5 and Abcg8 in mice. *J Lipid Res* 45: 1312–1323, 2004.
86. **Duan Z, Brakora KA, and Seiden MV.** Inhibition of ABCB1 (MDR1) and ABCB4 (MDR3) expression by small interfering RNA and reversal of paclitaxel resistance in human ovarian cancer cells. *Mol Cancer Ther* 3: 833–838, 2004.
87. **Ebert B, Seidel A, and Lampen A.** Identification of BCRP as transporter of benzo[a]pyrene conjugates metabolically formed in Caco-2 cells and its induction by Ah-receptor agonists. *Carcinogenesis* 26: 1754–1763, 2005.
88. **Eckford PD and Sharom FJ.** The reconstituted P-glycoprotein multidrug transporter is a flippase for glucosylceramide and other simple glycosphingolipids. *Biochem J* 389: 517–526, 2005.
89. **Ee PL, Kamalakaran S, Tonetti D, He X, Ross DD, and Beck WT.** Identification of a novel estrogen response element in the breast cancer resistance protein (ABCG2) gene. *Cancer Res* 64: 1247–1251, 2004.
90. **Eisenblatter T, Huwel S, and Galla HJ.** Characterisation of the brain multidrug resistance protein (BMDP/ABCG2/BCRP) expressed at the blood-brain barrier. *Brain Res* 971: 221–231, 2003.
91. **Elferink RP, Ottenhoff R, Fricker G, Seward DJ, Ballatori N, and Boyer J.** Lack of biliary lipid excretion in the little skate, *Raja erinacea*, indicates the absence of functional Mdr2, Abcg5, and Abcg8 transporters. *Am J Physiol Gastrointest Liver Physiol* 286: G762–G768, 2004.
92. **Elferink RP, Tytgat GN, and Groen AK.** Hepatic canalicular membrane 1: the role of mdr2 P-glycoprotein in hepatobiliary lipid transport. *FASEB J* 11: 19–28, 1997.
93. **Elkind NB, Szentpetery Z, Apati A, Ozvegy-Laczka C, Varady G, Ujhelly O, Szabo K, Homolya L, Varadi A, Buday L, Keri G, Nemet K, and Sarkadi B.** Multidrug transporter ABCG2 prevents tumor cell death induced by the epidermal growth factor receptor inhibitor Iressa (ZD1839, Gefitinib). *Cancer Res* 65: 1770–1777, 2005.
94. **El-Osta A, Kantharidis P, Zalcberg JR, and Wolffe AP.** Precipitous release of methyl-CpG binding protein 2 and histone deacetylase 1 from the methylated human multidrug resistance gene (MDR1) on activation. *Mol Cell Biol* 22: 1844–1857, 2002.
95. **Feller N, Broxterman HJ, Wahrer DC, and Pinedo HM.** ATP-dependent efflux of calcein by the multidrug resistance protein (MRP): no inhibition by intracellular glutathione depletion. *FEBS Lett* 368: 385–388, 1995.
96. **Fischer PM and Gianella-Borradori A.** Recent progress in the discovery and development of cyclin-dependent kinase inhibitors. *Exp Opin Invest Drugs* 14: 457–477, 2005.
97. **Fojo T, Farrell N, Ortuzar W, Tanimura H, Weinstein J, and Myers TG.** Identification of non-cross-resistant platinum compounds with novel cytotoxicity profiles using the NCI anticancer drug screen and clustered image map visualizations. *Crit Rev Oncol Hematol* 53: 25–34, 2005.
98. **Freeman LA, Kennedy A, Wu J, Bark S, Remaley AT, Santamarina-Fojo S, and Brewer HB Jr.** The orphan nuclear receptor LRH-1 activates the ABCG5/ABCG8 intergenic promoter. *J Lipid Res* 45: 1197–1206, 2004.

99. **Gadsby DC and Nairn AC.** Control of CFTR channel gating by phosphorylation and nucleotide hydrolysis. *Physiol Rev* 79 *Suppl*: S77–S107, 1999.
100. **Garcia-Calvo M, Lisnock J, Bull HG, Hawes BE, Burnett DA, Braun MP, Crona JH, Davis HR Jr, Dean DC, Detmers PA, Graziano MP, Hughes M, Macintyre DE, Ogawa A, O'Neill K A, Iyer SP, Shevell DE, Smith MM, Tang YS, Makarewicz AM, Ujjainwalla F, Altmann SW, Chapman KT, and Thornberry NA.** The target of ezetimibe is Niemann-Pick C1-Like 1 (NPC1L1). *Proc Natl Acad Sci USA* 102: 8132–8137, 2005.
101. **Garrigues A, Escargueil AE, and Orlowski S.** The multidrug transporter, P-glycoprotein, actively mediates cholesterol redistribution in the cell membrane. *Proc Natl Acad Sci USA* 99: 10347–10352, 2002.
102. **Geourjon C, Orelle C, Steinfels E, Blanchet C, Deleage G, Di Pietro A, and Jault JM.** A common mechanism for ATP hydrolysis in ABC transporter and helicase superfamilies. *Trends Biochem Sci* 26: 539–544, 2001.
103. **Germann UA, Chambers TC, Ambudkar SV, Licht T, Cardarelli CO, Pastan I, and Gottesman MM.** Characterization of phosphorylation-defective mutants of human P-glycoprotein expressed in mammalian cells. *J Biol Chem* 271: 1708–1716, 1996.
104. **Glavinas H, Krajcsi P, Cserepes J, and Sarkadi B.** The role of ABC transporters in drug resistance, metabolism, and toxicity. *Curr Drug Delivery* 1: 27–42, 2004.
105. **Glavy JS, Horwitz SB, and Orr GA.** Identification of the in vivo phosphorylation sites for acidic-directed kinases in murine mdr1b P-glycoprotein. *J Biol Chem* 272: 5909–5914, 1997.
106. **Goodfellow HR, Sardini A, Ruetz S, Callaghan R, Gros P, McNaughton PA, and Higgins CF.** Protein kinase C-mediated phosphorylation does not regulate drug transport by the human multidrug resistance P-glycoprotein. *J Biol Chem* 271: 13668–13674, 1996.
107. **Gottesman MM and Pastan I.** Biochemistry of multidrug resistance mediated by the multidrug transporter. *Annu Rev Biochem* 62: 385–427, 1993.
108. **Gottesman MM and Pastan I.** The multidrug transporter, a double-edged sword. *J Biol Chem* 263: 12163–12166, 1988.
109. **Gottesman MM, Pastan I, and Ambudkar SV.** P-glycoprotein and multidrug resistance. *Curr Opin Genet Dev* 6: 610–617, 1996.
110. **Graf GA, Cohen JC, and Hobbs HH.** Missense mutations in ABCG5 and ABCG8 disrupt heterodimerization and trafficking. *J Biol Chem* 279: 24881–24888, 2004.
111. **Graf GA, Li WP, Gerard RD, Gelissen I, White A, Cohen JC, and Hobbs HH.** Coexpression of ATP-binding cassette proteins ABCG5 and ABCG8 permits their transport to the apical surface. *J Clin Invest* 110: 659–669, 2002.
112. **Graf GA, Yu L, Li WP, Gerard R, Tuma PL, Cohen JC, and Hobbs HH.** ABCG5 and ABCG8 are obligate heterodimers for protein trafficking and biliary cholesterol excretion. *J Biol Chem* 278: 48275–48282, 2003.
113. **Hafkemeyer P, Licht T, Pastan I, and Gottesman MM.** Chemoprotection of hematopoietic cells by a mutant P-glycoprotein resistant to a potent chemosensitizer of multidrug-resistant cancers. *Hum Gene Ther* 11: 555–565, 2000.
114. **Hamada H and Tsuruo T.** Purification of the 170- to 180-kilodalton membrane glycoprotein associated with multidrug resistance. 170- to 180-kilodalton membrane glycoprotein is an ATPase. *J Biol Chem* 263: 1454–1458, 1988.
115. **Han B and Zhang JT.** Multidrug resistance in cancer chemotherapy and xenobiotic protection mediated by the half ATP-binding cassette transporter ABCG2. *Curr Med Chem Anti-Canc Agents* 4: 31–42, 2004.
116. **Hartz AM, Bauer B, Fricker G, and Miller DS.** Rapid regulation of P-glycoprotein at the blood-brain barrier by endothelin-1. *Mol Pharmacol* 66: 387–394, 2004.
117. **Henriksen U, Fog JU, Litman T, and Gether U.** Identification of intra- and intermolecular disulfide bridges in the multidrug resistance transporter ABCG2. *J Biol Chem* 280: 36926–36934, 2005.
118. **Higgins CF.** ABC transporters: physiology, structure and mechanism—an overview. *Res Microbiol* 152: 205–210, 2001.
119. **Higgins CF and Gottesman MM.** Is the multidrug transporter a flippase? *Trends Biochem Sci* 17: 18–21, 1992.
120. **Higgins CF and Linton KJ.** The ATP switch model for ABC transporters. *Nat Struct Mol Biol* 11: 918–926, 2004.
121. **Hiraoka H, Kimura N, Furukawa Y, Ogawara K, Kimura T, and Higaki K.** Up-regulation of P-glycoprotein expression in small intestine under chronic serotonin-depleted conditions in rats. *J Pharmacol Exp Ther* 312: 248–255, 2005.
122. **Hisaeda K, Inokuchi A, Nakamura T, Iwamoto Y, Kohno K, Kuwano M, and Uchiumi T.** Interleukin-1beta represses MRP2 gene expression through inactivation of interferon regulatory factor 3 in HepG2 cells. *Hepatology* 39: 1574–1582, 2004.
123. **Holland IB and Blight MA.** ABC-ATPases, adaptable energy generators fuelling transmembrane movement of a variety of molecules in organisms from bacteria to humans. *J Mol Biol* 293: 381–399, 1999.
124. **Hollo Z, Homolya L, Davis CW, and Sarkadi B.** Calcein accumulation as a fluorometric functional assay of the multidrug transporter. *Biochim Biophys Acta* 1191: 384–388, 1994.
125. **Homolya L, Hollo M, Muller M, Mechetner EB, and Sarkadi B.** A new method for a quantitative assessment of P-glycoprotein-related multidrug resistance in tumour cells. *Br J Cancer* 73: 849–855, 1996.
126. **Homolya L, Hollo Z, Germann UA, Pastan I, Gottesman MM, and Sarkadi B.** Fluorescent cellular indicators are extruded by the multidrug resistance protein. *J Biol Chem* 268: 21493–21496, 1993.
127. **Honjo Y, Hrycyna CA, Yan QW, Medina-Perez WY, Robey RW, van de Laar A, Litman T, Dean M, and Bates SE.** Acquired mutations in the MXR/BCRP/ABCP gene alter substrate specificity in MXR/BCRP/ABCP-overexpressing cells. *Cancer Res* 61: 6635–6639, 2001.
128. **Honjo Y, Morisaki K, Huff LM, Robey RW, Hung J, Dean M, and Bates SE.** Single-nucleotide polymorphism (SNP) analysis in the ABC half-transporter ABCG2 (MXR/BCRP/ABCP1). *Cancer Biol Ther* 1: 696–702, 2002.
129. **Hooiveld GJ, Heegsma J, van Montfoort JE, Jansen PL, Meijer DK, and Muller M.** Stereoselective transport of hydrophilic quaternary drugs by human MDR1 and rat Mdr1b P-glycoproteins. *Br J Pharmacol* 135: 1685–1694, 2002.
130. **Hopfner KP, Karcher A, Shin DS, Craig L, Arthur LM, Carney JP, and Tainer JA.** Structural biology of Rad50 ATPase: ATP-driven conformational control in DNA double-strand break repair and the ABC-ATPase superfamily. *Cell* 101: 789–800, 2000.
131. **Hori S, Ohtsuki S, Ichinowatari M, Yokota T, Kanda T, and Terasaki T.** Selective gene silencing of rat ATP-binding cassette G2 transporter in an in vitro blood-brain barrier model by short interfering RNA. *J Neurochem* 93: 63–71, 2005.
132. **Hori S, Ohtsuki S, Tachikawa M, Kimura N, Kondo T, Watanabe M, Nakashima E, and Terasaki T.** Functional expression of rat ABCG2 on the luminal side of brain capillaries and its enhancement by astrocyte-derived soluble factor(s). *J Neurochem* 90: 526–536, 2004.
133. **Houghton PJ, Germain GS, Harwood FC, Schuetz JD, Stewart CF, Buchdunger E, and Traxler P.** Imatinib mesylate is a potent inhibitor of the ABCG2 (BCRP) transporter and reverses resistance to topotecan and SN-38 in vitro. *Cancer Res* 64: 2333–2337, 2004.
134. **Hrycyna CA, Ramachandra M, Ambudkar SV, Ko YH, Pedersen PL, Pastan I, and Gottesman MM.** Mechanism of action of human P-glycoprotein ATPase activity. Photochemical cleavage during a catalytic transition state using orthovanadate reveals cross-talk between the two ATP sites. *J Biol Chem* 273: 16631–16634, 1998.
135. **Hu YP and Robert J.** Inhibition of protein kinase C in multidrug-resistant cells by modulators of multidrug resistance. *J Cancer Res Clin Oncol* 123: 201–210, 1997.
136. **Huang L and Vore M.** Multidrug resistance P-glycoprotein 2 is essential for the biliary excretion of indocyanine green. *Drug Metab Dispos* 29: 634–637, 2001.
137. **Hubacek JA, Berge KE, Cohen JC, and Hobbs HH.** Mutations in ATP-cassette binding proteins G5 (ABCG5) and G8 (ABCG8) causing sitosterolemia. *Hum Mutat* 18: 359–360, 2001.
138. **Hubacek JA, Berge KE, Stefkova J, Pitha J, Skodova Z, Lanska V, and Poledne R.** Polymorphisms in ABCG5 and ABCG8 transporters and plasma cholesterol levels. *Physiol Res* 53: 395–401, 2004.

139. **Hung LW, Wang IX, Nikaido K, Liu PQ, Ames GF, and Kim SH.** Crystal structure of the ATP-binding subunit of an ABC transporter. *Nature* 396: 703–707, 1998.
140. **Hyde SC, Emsley P, Hartshorn MJ, Mimmack MM, Gileadi U, Pearce SR, Gallagher MP, Gill DR, Hubbard RE, and Higgins CF.** Structural model of ATP-binding proteins associated with cystic fibrosis, multidrug resistance and bacterial transport. *Nature* 346: 362–365, 1990.
141. **Iida A, Saito S, Sekine A, Mishima C, Kitamura Y, Kondo K, Harigae S, Osawa S, and Nakamura Y.** Catalog of 605 single-nucleotide polymorphisms (SNPs) among 13 genes encoding human ATP-binding cassette transporters: ABCA4, ABCA7, ABCA8, ABCD1, ABCD3, ABCD4, ABCE1, ABCF1, ABCG1, ABCG2, ABCG4, ABCG5, and ABCG8. *J Hum Genet* 47: 285–310, 2002.
142. **Ikuma M and Welsh MJ.** Regulation of CFTR Cl^- channel gating by ATP binding and hydrolysis. *Proc Natl Acad Sci USA* 97: 8675–8680, 2000.
143. **Imai Y, Asada S, Tsukahara S, Ishikawa E, Tsuruo T, and Sugimoto Y.** Breast cancer resistance protein exports sulfated estrogens but not free estrogens. *Mol Pharmacol* 64: 610–618, 2003.
144. **Imai Y, Ishikawa E, Asada S, and Sugimoto Y.** Estrogen-mediated post transcriptional down-regulation of breast cancer resistance protein/ABCG2. *Cancer Res* 65: 596–604, 2005.
145. **Imai Y, Nakane M, Kage K, Tsukahara S, Ishikawa E, Tsuruo T, Miki Y, and Sugimoto Y.** C421A polymorphism in the human breast cancer resistance protein gene is associated with low expression of Q141K protein and low-level drug resistance. *Mol Cancer Ther* 1: 611–616, 2002.
146. **Imai Y, Tsukahara S, Asada S, and Sugimoto Y.** Phytoestrogens/flavonoids reverse breast cancer resistance protein/ABCG2-mediated multidrug resistance. *Cancer Res* 64: 4346–4352, 2004.
147. **Ishikawa T.** Is the glutathione *S*-conjugate carrier an mdr1 gene product? *Trends Biochem Sci* 15: 219–220, 1990.
148. **Itoda M, Saito Y, Shirao K, Minami H, Ohtsu A, Yoshida T, Saijo N, Suzuki H, Sugiyama Y, Ozawa S, and Sawada J.** Eight novel single nucleotide polymorphisms in ABCG2/BCRP in Japanese cancer patients administered irinotacan. *Drug Metab Pharmacokinet* 18: 212–217, 2003.
149. **Jacquemin E, Cresteil D, Manouvrier S, Boute O, and Hadchouel M.** Heterozygous non-sense mutation of the MDR3 gene in familial intrahepatic cholestasis of pregnancy. *Lancet* 353: 210–211, 1999.
150. **Jacquemin E, De Vree JM, Cresteil D, Sokal EM, Sturm E, Dumont M, Scheffer GL, Paul M, Burdelski M, Bosma PJ, Bernard O, Hadchouel M, and Elferink RP.** The wide spectrum of multidrug resistance 3 deficiency: from neonatal cholestasis to cirrhosis of adulthood. *Gastroenterology* 120: 1448–1458, 2001.
151. **Janvilisri T, Venter H, Shahi S, Reuter G, Balakrishnan L, and van Veen HW.** Sterol transport by the human breast cancer resistance protein (ABCG2) expressed in *Lactococcus lactis*. *J Biol Chem* 278: 20645–20651, 2003.
152. **Jin S and Scotto KW.** Transcriptional regulation of the MDR1 gene by histone acetyltransferase and deacetylase is mediated by NF-Y. *Mol Cell Biol* 18: 4377–4384, 1998.
153. **Johnson RA, Ince TA, and Scotto KW.** Transcriptional repression by p53 through direct binding to a novel DNA element. *J Biol Chem* 276: 27716–27720, 2001.
154. **Johnson RA, Shepard EM, and Scotto KW.** Differential regulation of MDR1 transcription by the p53 family members. Role of the DNA binding domain. *J Biol Chem* 280: 13213–13219, 2005.
155. **Johnstone RW, Ruefli AA, and Smyth MJ.** Multiple physiological functions for multidrug transporter P-glycoprotein? *Trends Biochem Sci* 25: 1–6, 2000.
156. **Jones PM and George AM.** The ABC transporter structure and mechanism: perspectives on recent research. *Cell Mol Life Sci* 61: 682–699, 2004.
157. **Jones PM and George AM.** Mechanism of ABC transporters: a molecular dynamics simulation of a well characterized nucleotide-binding subunit. *Proc Natl Acad Sci USA* 99: 12639–12644, 2002.
158. **Jones PM and George AM.** Multidrug resistance in parasites: ABC transporters, P-glycoproteins and molecular modelling. *Int J Parasitol* 35: 555–566, 2005.
159. **Jones PM and George AM.** A new structural model for P-glycoprotein. *J Membr Biol* 166: 133–147, 1998.
160. **Jones PM and George AM.** Subunit interactions in ABC transporters: towards a functional architecture. *FEMS Microbiol Lett* 179: 187–202, 1999.
161. **Jonker JW, Buitelaar M, Wagenaar E, Van Der Valk MA, Scheffer GL, Scheper RJ, Plosch T, Kuipers F, Elferink RP, Rosing H, Beijnen JH, and Schinkel AH.** The breast cancer resistance protein protects against a major chlorophyll-derived dietary phototoxin and protoporphyria. *Proc Natl Acad Sci USA* 99: 15649–15654, 2002.
162. **Jonker JW, Merino G, Musters S, van Herwaarden AE, Bolscher E, Wagenaar E, Mesman E, Dale TC, and Schinkel AH.** The breast cancer resistance protein BCRP (ABCG2) concentrates drugs and carcinogenic xenotoxins into milk. *Nat Med* 11: 127–129, 2005.
163. **Jonker JW, Smit JW, Brinkhuis RF, Maliepaard M, Beijnen JH, Schellens JH, and Schinkel AH.** Role of breast cancer resistance protein in the bioavailability and fetal penetration of topotecan. *J Natl Cancer Inst* 92: 1651–1656, 2000.
164. **Juliano RL and Ling V.** A surface glycoprotein modulating drug permeability in Chinese hamster ovary cell mutants. *Biochim Biophys Acta* 455: 152–162, 1976.
165. **Julien M and Gros P.** Nucleotide-induced conformational changes in P-glycoprotein and in nucleotide binding site mutants monitored by trypsin sensitivity. *Biochemistry* 39: 4559–4568, 2000.
166. **Kage K, Tsukahara S, Sugiyama T, Asada S, Ishikawa E, Tsuruo T, and Sugimoto Y.** Dominant-negative inhibition of breast cancer resistance protein as drug efflux pump through the inhibition of S-S dependent homodimerization. *Int J Cancer* 97: 626–630, 2002.
167. **Kajinami K, Brousseau ME, Ordovas JM, and Schaefer EJ.** Interactions between common genetic polymorphisms in ABCG5/G8 and CYP7A1 on LDL cholesterol-lowering response to atorvastatin. *Atherosclerosis* 175: 287–293, 2004.
168. **Kalitsky-Szirtes J, Shayeganpour A, Brocks DR, and Piquette-Miller M.** Suppression of drug-metabolizing enzymes and efflux transporters in the intestine of endotoxin-treated rats. *Drug Metab Dispos* 32: 20–27, 2004.
169. **Kamalakaran S, Radhakrishnan SK, and Beck WT.** Identification of estrogen-responsive genes using a genome-wide analysis of promoter elements for transcription factor binding sites. *J Biol Chem* 280: 21491–21497, 2005.
170. **Karaszi E, Jakab K, Homolya L, Szakacs G, Hollo Z, Telek B, Kiss A, Rejto L, Nahajevszky S, Sarkadi B, and Kappelmayer J.** Calcein assay for multidrug resistance reliably predicts therapy response and survival rate in acute myeloid leukaemia. *Br J Haematol* 112: 308–314, 2001.
171. **Karpowich N, Martsinkevich O, Millen L, Yuan YR, Dai PL, MacVey K, Thomas PJ, and Hunt JF.** Crystal structures of the MJ1267 ATP binding cassette reveal an induced-fit effect at the ATPase active site of an ABC transporter. *Structure* 9: 571–586, 2001.
172. **Kast C, Canfield V, Levenson R, and Gros P.** Membrane topology of P-glycoprotein as determined by epitope insertion: transmembrane organization of the N-terminal domain of mdr3. *Biochemistry* 34: 4402–4411, 1995.
173. **Kast C, Canfield V, Levenson R, and Gros P.** Transmembrane organization of mouse P-glycoprotein determined by epitope insertion and immunofluorescence. *J Biol Chem* 271: 9240–9248, 1996.
174. **Kawabata S, Oka M, Soda H, Shiozawa K, Nakatomi K, Tsurutani J, Nakamura Y, Doi S, Kitazaki T, Sugahara K, Yamada Y, Kamihira S, and Kohno S.** Expression and functional analyses of breast cancer resistance protein in lung cancer. *Clin Cancer Res* 9: 3052–3057, 2003.
175. **Keitel V, Burdelski M, Warskulat U, Kuhlkamp T, Keppler D, Haussinger D, and Kubitz R.** Expression and localization of hepatobiliary transport proteins in progressive familial intrahepatic cholestasis. *Hepatology* 41: 1160–1172, 2005.
176. **Kerr KM, Sauna ZE, and Ambudkar SV.** Correlation between steady-state ATP hydrolysis and vanadate-induced ADP trapping in human P-glycoprotein. Evidence for ADP release as the rate-limit-

ing step in the catalytic cycle and its modulation by substrates. *J Biol Chem* 276: 8657–8664, 2001.
177. **Kim M, Turnquist H, Jackson J, Sgagias M, Yan Y, Gong M, Dean M, Sharp JG, and Cowan K.** The multidrug resistance transporter ABCG2 (breast cancer resistance protein 1) effluxes Hoechst 33342 and is overexpressed in hematopoietic stem cells. *Clin Cancer Res* 8: 22–28, 2002.
178. **Kino K, Taguchi Y, Yamada K, Komano T, and Ueda K.** Aureobasidin A, an antifungal cyclic depsipeptide antibiotic, is a substrate for both human MDR1 and MDR2/P-glycoproteins. *FEBS Lett* 399: 29–32, 1996.
179. **Kipp H and Arias IM.** Newly synthesized canalicular ABC transporters are directly targeted from the Golgi to the hepatocyte apical domain in rat liver. *J Biol Chem* 275: 15917–15925, 2000.
180. **Klett EL, Lee MH, Adams DB, Chavin KD, and Patel SB.** Localization of ABCG5 and ABCG8 proteins in human liver, gall bladder and intestine. *BMC Gastroenterol* 4: 21, 2004.
181. **Klett EL, Lu K, Kosters A, Vink E, Lee MH, Altenburg M, Shefer S, Batta AK, Yu H, Chen J, Klein R, Looije N, Oude-Elferink R, Groen AK, Maeda N, Salen G, and Patel SB.** A mouse model of sitosterolemia: absence of Abcg8/sterolin-2 results in failure to secrete biliary cholesterol. *BMC Med* 2: 5, 2004.
182. **Knutsen T, Mickley LA, Ried T, Green ED, du Manoir S, Schrock E, Macville M, Ning Y, Robey R, Polymeropoulos M, Torres R, and Fojo T.** Cytogenetic and molecular characterization of random chromosomal rearrangements activating the drug resistance gene, MDR1/P-glycoprotein, in drug-selected cell lines and patients with drug refractory ALL. *Genes Chromosomes Cancer* 23: 44–54, 1998.
183. **Knutsen T, Rao VK, Ried T, Mickley L, Schneider E, Miyake K, Ghadimi BM, Padilla-Nash H, Pack S, Greenberger L, Cowan K, Dean M, Fojo T, and Bates S.** Amplification of 4q21-q22 and the MXR gene in independently derived mitoxantrone-resistant cell lines. *Genes Chromosomes Cancer* 27: 110–116, 2000.
185. **Kobayashi D, Ieiri I, Hirota T, Takane H, Maegawa S, Kigawa J, Suzuki H, Nanba E, Oshimura M, Terakawa N, Otsubo K, Mine K, and Sugiyama Y.** Functional assessment of ABCG2 (BCRP) gene polymorphisms to protein expression in human placenta. *Drug Metab Dispos* 33: 94–101, 2005.
186. **Koehn FE and Carter GT.** The evolving role of natural products in drug discovery. *Nat Rev Drug Discov* 4: 206–220, 2005.
187. **Kolwankar D, Glover DD, Ware JA, and Tracy TS.** Expression and function of ABCB1 and ABCG2 in human placental tissue. *Drug Metab Dispos* 33: 524–529, 2005.
188. **Kondo C, Suzuki H, Itoda M, Ozawa S, Sawada J, Kobayashi D, Ieiri I, Mine K, Ohtsubo K, and Sugiyama Y.** Functional analysis of SNPs variants of BCRP/ABCG2. *Pharm Res* 21: 1895–1903, 2004.
189. **Kopplow K, Letschert K, Konig J, Walter B, and Keppler D.** Human hepatobiliary transport of organic anions analyzed by quadruple-transfected cells. *Mol Pharmacol* 68: 1031–1038, 2005.
190. **Kosters A, Frijters RJ, Schaap FG, Vink E, Plosch T, Ottenhoff R, Jirsa M, De Cuyper IM, Kuipers F, and Groen AK.** Relation between hepatic expression of ATP-binding cassette transporters G5 and G8 and biliary cholesterol secretion in mice. *J Hepatol* 38: 710–716, 2003.
191. **Krishnamurthy P, Ross DD, Nakanishi T, Bailey-Dell K, Zhou S, Mercer KE, Sarkadi B, Sorrentino BP, and Schuetz JD.** The stem cell marker Bcrp/ABCG2 enhances hypoxic cell survival through interactions with heme. *J Biol Chem* 279: 24218–24225, 2004.
192. **Kruijtzer CM, Beijnen JH, Rosing H, ten Bokkel Huinink WW, Schot M, Jewell RC, Paul EM, and Schellens JH.** Increased oral bioavailability of topotecan in combination with the breast cancer resistance protein and P-glycoprotein inhibitor GF120918. *J Clin Oncol* 20: 2943–2950, 2002.
193. **Kruit JK, Plosch T, Havinga R, Boverhof R, Groot PH, Groen AK, and Kuipers F.** Increased fecal neutral sterol loss upon liver X receptor activation is independent of biliary sterol secretion in mice. *Gastroenterology* 128: 147–156, 2005.
194. **Krupka RM.** Uncoupled active transport mechanisms accounting for low selectivity in multidrug carriers: P-glycoprotein and SMR antiporters. *J Membr Biol* 172: 129–143, 1999.
195. **Kullak-Ublick GA and Becker MB.** Regulation of drug and bile salt transporters in liver and intestine. *Drug Metab Rev* 35: 305–317, 2003.
196. **Kusuhara H and Sugiyama Y.** Active efflux across the blood-brain barrier: role of the solute carrier family. *NeuroRx* 2: 73–85, 2005.
197. **Kusuhara H and Sugiyama Y.** Efflux transport systems for organic anions and cations at the blood-CSF barrier. *Adv Drug Deliv Rev* 56: 1741–1763, 2004.
198. **Kuzuya T, Kobayashi T, Moriyama N, Nagasaka T, Yokoyama I, Uchida K, Nakao A, and Nabeshima T.** Amlodipine, but not MDR1 polymorphisms, alters the pharmacokinetics of cyclosporine A in Japanese kidney transplant recipients. *Transplantation* 76: 865–868, 2003.
199. **Labialle S, Dayan G, Gayet L, Rigal D, Gambrelle J, and Baggetto LG.** New invMED1 element *cis*-activates human multidrug-related MDR1 and MVP genes, involving the LRP130 protein. *Nucleic Acids Res* 32: 3864–3876, 2004.
200. **Lammert F, Wang DQ, Hillebrandt S, Geier A, Fickert P, Trauner M, Matern S, Paigen B, and Carey MC.** Spontaneous cholecysto- and hepatolithiasis in Mdr2−/− mice: a model for low phospholipid-associated cholelithiasis. *Hepatology* 39: 117–128, 2004.
201. **Lechner A, Leech CA, Abraham EJ, Nolan AL, and Habener JF.** Nestin-positive progenitor cells derived from adult human pancreatic islets of Langerhans contain side population (SP) cells defined by expression of the ABCG2 (BCRP1) ATP-binding cassette transporter. *Biochem Biophys Res Commun* 293: 670–674, 2002.
202. **Lee G and Piquette-Miller M.** Cytokines alter the expression and activity of the multidrug resistance transporters in human hepatoma cell lines; analysis using RT-PCR and cDNA microarrays. *J Pharm Sci* 92: 2152–2163, 2003.
203. **Lee JY, Urbatsch IL, Senior AE, and Wilkens S.** Projection structure of P-glycoprotein by electron microscopy. Evidence for a closed conformation of the nucleotide binding domains. *J Biol Chem* 277: 40125–40131, 2002.
204. **Lee MH, Lu K, Hazard S, Yu H, Shulenin S, Hidaka H, Kojima H, Allikmets R, Sakuma N, Pegoraro R, Srivastava AK, Salen G, Dean M, and Patel SB.** Identification of a gene, ABCG5, important in the regulation of dietary cholesterol absorption. *Nat Genet* 27: 79–83, 2001.
205. **Lerner-Marmarosh N, Gimi K, Urbatsch IL, Gros P, and Senior AE.** Large scale purification of detergent-soluble P-glycoprotein from *Pichia pastoris* cells and characterization of nucleotide binding properties of wild-type, Walker A, and Walker B mutant proteins. *J Biol Chem* 274: 34711–34718, 1999.
206. **Letschert K, Komatsu M, Hummel-Eisenbeiss J, and Keppler D.** Vectorial transport of the peptide CCK-8 by double-transfected MDCKII cells stably expressing the organic anion transporter OATP1B3 (OATP8) and the export pump ABCC2. *J Pharmacol Exp Ther* 313: 549–556, 2005.
207. **Lewis DF.** 57 varieties: the human cytochromes *P*450. *Pharmacogenomics* 5: 305–318, 2004.
208. **Lin JH and Yamazaki M.** Clinical relevance of P-glycoprotein in drug therapy. *Drug Metab Rev* 35: 417–454, 2003.
209. **Lincke CR, Smit JJ, van der Velde-Koerts T, and Borst P.** Structure of the human MDR3 gene and physical mapping of the human MDR locus. *J Biol Chem* 266: 5303–5310, 1991.
210. **Litman T, Druley TE, Stein WD, and Bates SE.** From MDR to MXR: new understanding of multidrug resistance systems, their properties and clinical significance. *Cell Mol Life Sci* 58: 931–959, 2001.
211. **Litman T, Skovsgaard T, and Stein WD.** Pumping of drugs by P-glycoprotein: a two-step process? *J Pharmacol Exp Ther* 307: 846–853, 2003.
212. **Liu R, Siemiarczuk A, and Sharom FJ.** Intrinsic fluorescence of the P-glycoprotein multidrug transporter: sensitivity of tryptophan residues to binding of drugs and nucleotides. *Biochemistry* 39: 14927–14938, 2000.
213. **Locher KP.** Structure and mechanism of ABC transporters. *Curr Opin Struct Biol* 14: 426–431, 2004.
214. **Loo TW, Bartlett MC, and Clarke DM.** Disulfide cross-linking analysis shows that transmembrane segments 5 and 8 of human

P-glycoprotein are close together on the cytoplasmic side of the membrane. *J Biol Chem* 279: 7692–7697, 2004.
215. **Loo TW, Bartlett MC, and Clarke DM.** The "LSGGQ" motif in each nucleotide-binding domain of human P-glycoprotein is adjacent to the opposing walker A sequence. *J Biol Chem* 277: 41303–41306, 2002.
216. **Loo TW, Bartlett MC, and Clarke DM.** Substrate-induced conformational changes in the transmembrane segments of human P-glycoprotein. Direct evidence for the substrate-induced fit mechanism for drug binding. *J Biol Chem* 278: 13603–13606, 2003.
217. **Loo TW and Clarke DM.** Determining the structure and mechanism of the human multidrug resistance P-glycoprotein using cysteine-scanning mutagenesis and thiol-modification techniques. *Biochim Biophys Acta* 1461: 315–325, 1999.
218. **Loo TW and Clarke DM.** Drug-stimulated ATPase activity of human P-glycoprotein is blocked by disulfide cross-linking between the nucleotide-binding sites. *J Biol Chem* 275: 19435–19438, 2000.
219. **Loo TW and Clarke DM.** Reconstitution of drug-stimulated ATPase activity following co-expression of each half of human P-glycoprotein as separate polypeptides. *J Biol Chem* 269: 7750–7755, 1994.
220. **Lu K, Lee MH, Hazard S, Brooks-Wilson A, Hidaka H, Kojima H, Ose L, Stalenhoef AF, Mietinnen T, Bjorkhem I, Bruckert E, Pandya A, Brewer HB Jr, Salen G, Dean M, Srivastava A, and Patel SB.** Two genes that map to the STSL locus cause sitosterolemia: genomic structure and spectrum of mutations involving sterolin-1 and sterolin-2, encoded by ABCG5 and ABCG8, respectively. *Am J Hum Genet* 69: 278–290, 2001.
221. **Lu K, Lee MH, Yu H, Zhou Y, Sandell SA, Salen G, and Patel SB.** Molecular cloning, genomic organization, genetic variations, and characterization of murine sterolin genes Abcg5 and Abcg8. *J Lipid Res* 43: 565–578, 2002.
222. **Lucci A, Han TY, Liu YY, Giuliano AE, and Cabot MC.** Multidrug resistance modulators and doxorubicin synergize to elevate ceramide levels and elicit apoptosis in drug-resistant cancer cells. *Cancer* 86: 300–311, 1999.
223. **Lucena JF, Herrero JI, Quiroga J, Sangro B, Garcia-Foncillas J, Zabalegui N, Sola J, Herraiz M, Medina JF, and Prieto J.** A multidrug resistance 3 gene mutation causing cholelithiasis, cholestasis of pregnancy, and adulthood biliary cirrhosis. *Gastroenterology* 124: 1037–1042, 2003.
224. **Luckenbach T, Corsi I, and Epel D.** Fatal attraction: synthetic musk fragrances compromise multixenobiotic defense systems in mussels. *Mar Environ Res* 58: 215–219, 2004.
225. **Lugo MR and Sharom FJ.** Interaction of LDS-751 with P-glycoprotein and mapping of the location of the R drug binding site. *Biochemistry* 44: 643–655, 2005.
226. **Luker GD, Pica CM, Kumar AS, Covey DF, and Piwnica-Worms D.** Effects of cholesterol and enantiomeric cholesterol on P-glycoprotein localization and function in low-density membrane domains. *Biochemistry* 39: 7651–7661, 2000.
227. **Maliepaard M, Scheffer GL, Faneyte IF, van Gastelen MA, Pijnenborg AC, Schinkel AH, van De Vijver MJ, Scheper RJ, and Schellens JH.** Subcellular localization and distribution of the breast cancer resistance protein transporter in normal human tissues. *Cancer Res* 61: 3458–3464, 2001.
228. **Marthinet E, Divita G, Bernaud J, Rigal D, and Baggetto LG.** Modulation of the typical multidrug resistance phenotype by targeting the MED-1 region of human MDR1 promoter. *Gene Ther* 7: 1224–1233, 2000.
229. **Martin C, Berridge G, Higgins CF, Mistry P, Charlton P, and Callaghan R.** Communication between multiple drug binding sites on P-glycoprotein. *Mol Pharmacol* 58: 624–632, 2000.
230. **Martin C, Higgins CF, and Callaghan R.** The vinblastine binding site adopts high- and low-affinity conformations during a transport cycle of P-glycoprotein. *Biochemistry* 40: 15733–15742, 2001.
231. **Marzolini C, Tirona RG, and Kim RB.** Pharmacogenomics of the OATP and OAT families. *Pharmacogenomics* 5: 273–282, 2004.
232. **Maslak P, Hegewisch-Becker S, Godfrey L, and Andreeff M.** Flow cytometric determination of the multidrug-resistant phenotype in acute leukemia. *Cytometry* 17: 84–93, 1994.
233. **Matsuo M, Kimura Y, and Ueda K.** K_{ATP} channel interaction with adenine nucleotides. *J Mol Cell Cardiol* 38: 907–916, 2005.
234. **Mayer U, Wagenaar E, Beijnen JH, Smit JW, Meijer DK, van Asperen J, Borst P, and Schinkel AH.** Substantial excretion of digoxin via the intestinal mucosa and prevention of long-term digoxin accumulation in the brain by the mdr 1a P-glycoprotein. *Br J Pharmacol* 119: 1038–1044, 1996.
235. **Merino G, Jonker JW, Wagenaar E, Pulido MM, Molina AJ, Alvarez AI, and Schinkel AH.** Transport of anthelmintic benzimidazole drugs by breast cancer resistance protein (BCRP/ABCG2). *Drug Metab Dispos* 33: 614–618, 2005.
236. **Merino G, Jonker JW, Wagenaar E, van Herwaarden AE, and Schinkel AH.** The breast cancer resistance protein (BCRP/ABCG2) affects pharmacokinetics, hepatobiliary excretion, and milk secretion of the antibiotic nitrofurantoin. *Mol Pharmacol* 67: 1758–1764, 2005.
237. **Merino G, van Herwaarden AE, Wagenaar E, Jonker JW, and Schinkel AH.** Sex-dependent expression and activity of the ATP-binding cassette transporter breast cancer resistance protein (BCRP/ABCG2) in liver. *Mol Pharmacol* 67: 1765–1771, 2005.
238. **Mickley LA, Spengler BA, Knutsen TA, Biedler JL, and Fojo T.** Gene rearrangement: a novel mechanism for MDR-1 gene activation. *J Clin Invest* 99: 1947–1957, 1997.
239. **Miettinen TA.** Phytosterolaemia, xanthomatosis and premature atherosclerotic arterial disease: a case with high plant sterol absorption, impaired sterol elimination and low cholesterol synthesis. *Eur J Clin Invest* 10: 27–35, 1980.
240. **Minderman H, Vanhoefer U, Toth K, Yin MB, Minderman MD, Wrzosek C, Slovak ML, and Rustum YM.** DiOC2(3) is not a substrate for multidrug resistance protein (MRP)-mediated drug efflux. *Cytometry* 25: 14–20, 1996.
241. **Mitin T, Von Moltke LL, Court MH, and Greenblatt DJ.** Levothyroxine up-regulates P-glycoprotein independent of the pregnane X receptor. *Drug Metab Dispos* 32: 779–782, 2004.
242. **Mitomo H, Kato R, Ito A, Kasamatsu S, Ikegami Y, Kii I, Kudo A, Kobatake E, Sumino Y, and Ishikawa T.** A functional study on polymorphism of the ATP-binding cassette transporter ABCG2: critical role of arginine-482 in methotrexate transport. *Biochem J* 373: 767–774, 2003.
243. **Miwa K, Inazu A, Kobayashi J, Higashikata T, Nohara A, Kawashiri M, Katsuda S, Takata M, Koizumi J, and Mabuchi H.** ATP-binding cassette transporter G8 M429V polymorphism as a novel genetic marker of higher cholesterol absorption in hypercholesterolemic Japanese subjects. *Clin Sci* 109: 183–188, 2005.
244. **Miwa M, Tsukahara S, Ishikawa E, Asada S, Imai Y, and Sugimoto Y.** Single amino acid substitutions in the transmembrane domains of breast cancer resistance protein (BCRP) alter cross resistance patterns in transfectants. *Int J Cancer* 107: 757–763, 2003.
245. **Miyake K, Mickley L, Litman T, Zhan Z, Robey R, Cristensen B, Brangi M, Greenberger L, Dean M, Fojo T, and Bates SE.** Molecular cloning of cDNAs which are highly overexpressed in mitoxantrone-resistant cells: demonstration of homology to ABC transport genes. *Cancer Res* 59: 8–13, 1999.
246. **Miyazaki H, Sekine T, and Endou H.** The multispecific organic anion transporter family: properties and pharmacological significance. *Trends Pharmacol Sci* 25: 654–662, 2004.
247. **Mizuarai S, Aozasa N, and Kotani H.** Single nucleotide polymorphisms result in impaired membrane localization and reduced ATPase activity in multidrug transporter ABCG2. *Int J Cancer* 109: 238–246, 2004.
248. **Modok S, Heyward C, and Callaghan R.** P-glycoprotein retains function when reconstituted into a sphingolipid- and cholesterol-rich environment. *J Lipid Res* 45: 1910–1918, 2004.
249. **Mogi M, Yang J, Lambert JF, Colvin GA, Shiojima I, Skurk C, Summer R, Fine A, Quesenberry PJ, and Walsh K.** Akt signaling regulates side population cell phenotype via Bcrp1 translocation. *J Biol Chem* 278: 39068–39075, 2003.
250. **Mohrmann K, van Eijndhoven MA, Schinkel AH, and Schellens JH.** Absence of *N*-linked glycosylation does not affect plasma membrane localization of breast cancer resistance protein (BCRP/ABCG2). *Cancer Chemother Pharmacol* 56: 344–350, 2005.

251. **Morisaki K, Robey RW, Ozvegy-Laczka C, Honjo Y, Polgar O, Steadman K, Sarkadi B, and Bates SE.** Single nucleotide polymorphisms modify the transporter activity of ABCG2. *Cancer Chemother Pharmacol* 56: 161–172, 2005.
252. **Muller M, Bakos E, Welker E, Varadi A, Germann UA, Gottesman MM, Morse BS, Roninson IB, and Sarkadi B.** Altered drug-stimulated ATPase activity in mutants of the human multidrug resistance protein. *J Biol Chem* 271: 1877–1883, 1996.
253. **Mutch DM, Anderle P, Fiaux M, Mansourian R, Vidal K, Wahli W, Williamson G, and Roberts MA.** Regional variations in ABC transporter expression along the mouse intestinal tract. *Physiol Gen* 17: 11–20, 2004.
254. **Nakagawa R, Hara Y, Arakawa H, Nishimura S, and Komatani H.** ABCG2 confers resistance to indolocarbazole compounds by ATP-dependent transport. *Biochem Biophys Res Commun* 299: 669–675, 2002.
255. **Nakatomi K, Yoshikawa M, Oka M, Ikegami Y, Hayasaka S, Sano K, Shiozawa K, Kawabata S, Soda H, Ishikawa T, Tanabe S, and Kohno S.** Transport of 7-ethyl-10-hydroxycamptothecin (SN-38) by breast cancer resistance protein ABCG2 in human lung cancer cells. *Biochem Biophys Res Commun* 288: 827–832, 2001.
256. **Nakatsukasa H, Silverman JA, Gant TW, Evarts RP, and Thorgeirsson SS.** Expression of multidrug resistance genes in rat liver during regeneration and after carbon tetrachloride intoxication. *Hepatology* 18: 1202–1207, 1993.
257. **Nies AT, Gatmaitan Z, and Arias IM.** ATP-dependent phosphatidylcholine translocation in rat liver canalicular plasma membrane vesicles. *J Lipid Res* 37: 1125–1136, 1996.
258. **Ogretmen B and Safa AR.** Identification and characterization of the MDR1 promoter-enhancing factor 1 (MEF1) in the multidrug resistant HL60/VCR human acute myeloid leukemia cell line. *Biochemistry* 39: 194–204, 2000.
259. **Ortiz DF, Moseley J, Calderon G, Swift AL, Li S, and Arias IM.** Identification of HAX-1 as a protein that binds bile salt export protein and regulates its abundance in the apical membrane of Madin-Darby canine kidney cells. *J Biol Chem* 279: 32761–32770, 2004.
260. **Ozvegy C, Litman T, Szakacs G, Nagy Z, Bates S, Varadi A, and Sarkadi B.** Functional characterization of the human multidrug transporter, ABCG2, expressed in insect cells. *Biochem Biophys Res Commun* 285: 111–117, 2001.
261. **Ozvegy C, Varadi A, and Sarkadi B.** Characterization of drug transport, ATP hydrolysis, and nucleotide trapping by the human ABCG2 multidrug transporter. Modulation of substrate specificity by a point mutation. *J Biol Chem* 277: 47980–47990, 2002.
262. **Ozvegy-Laczka C, Cserepes J, Elkind NB, and Sarkadi B.** Tyrosine kinase inhibitor resistance in cancer: role of ABC multidrug transporters. *Drug Resist Updat* 8: 15–26, 2005.
263. **Ozvegy-Laczka C, Hegedus T, Varady G, Ujhelly O, Schuetz JD, Varadi A, Keri G, Orfi L, Nemet K, and Sarkadi B.** High-affinity interaction of tyrosine kinase inhibitors with the ABCG2 multidrug transporter. *Mol Pharmacol* 65: 1485–1495, 2004.
264. **Ozvegy-Laczka C, Koblos G, Sarkadi B, and Varadi A.** Single amino acid (482) variants of the ABCG2 multidrug transporter: major differences in transport capacity and substrate recognition. *Biochim Biophys Acta* 1668: 53–63, 2005.
265. **Ozvegy-Laczka C, Varady G, Koblos G, Ujhelly O, Cervenak J, Schuetz JD, Sorrentino BP, Koomen GJ, Varadi A, Nemet K, and Sarkadi B.** Function-dependent conformational changes of the ABCG2 multidrug transporter modify its interaction with a monoclonal antibody on the cell surface. *J Biol Chem* 280: 4219–4227, 2005.
266. **Pajeva IK, Globisch C, and Wiese M.** Structure-function relationships of multidrug resistance P-glycoprotein. *J Med Chem* 47: 2523–2533, 2004.
267. **Panwala CM, Jones JC, and Viney JL.** A novel model of inflammatory bowel disease: mice deficient for the multiple drug resistance gene, mdr1a, spontaneously develop colitis. *J Immunol* 161: 5733–5744, 1998.
267a. **Park SW, Lomri N, Simeoni LA, Fruehauf JP, and Mechetner F.** Analysis of P-glycoprotein-mediated membrane transport in human peripheral blood lymphocytes using the UIC2 shift. *Cytometry A* 53: 67–78, 2003.
268. **Pastan I and Gottesman MM.** Multidrug resistance. *Annu Rev Med* 42: 277–286, 1991.
269. **Pauli-Magnus C, Lang T, Meier Y, Zodan-Marin T, Jung D, Breymann C, Zimmermann R, Kenngott S, Beuers U, Reichel C, Kerb R, Penger A, Meier PJ, and Kullak-Ublick GA.** Sequence analysis of bile salt export pump (ABCB11) and multidrug resistance p-glycoprotein 3 (ABCB4, MDR3) in patients with intrahepatic cholestasis of pregnancy. *Pharmacogenetics* 14: 91–102, 2004.
270. **Pauli-Magnus C, von Richter O, Burk O, Ziegler A, Mettang T, Eichelbaum M, and Fromm MF.** Characterization of the major metabolites of verapamil as substrates and inhibitors of P-glycoprotein. *J Pharmacol Exp Ther* 293: 376–382, 2000.
271. **Pavek P, Merino G, Wagenaar E, Bolscher E, Novotna M, Jonker JW, and Schinkel AH.** Human breast cancer resistance protein: interactions with steroid drugs, hormones, the dietary carcinogen 2-amino-1-methyl-6-phenylimidazo(4,5-b)pyridine, and transport of cimetidine. *J Pharmacol Exp Ther* 312: 144–152, 2005.
272. **Pawagi AB, Wang J, Silverman M, Reithmeier RA, and Deber CM.** Transmembrane aromatic amino acid distribution in P-glycoprotein. A functional role in broad substrate specificity. *J Mol Biol* 235: 554–564, 1994.
273. **Pearce HL, Safa AR, Bach NJ, Winter MA, Cirtain MC, and Beck WT.** Essential features of the P-glycoprotein pharmacophore as defined by a series of reserpine analogs that modulate multidrug resistance. *Proc Natl Acad Sci USA* 86: 5128–5132, 1989.
274. **Perloff MD, von Moltke LL, Stormer E, Shader RI, and Greenblatt DJ.** Saint John's wort: an in vitro analysis of P-glycoprotein induction due to extended exposure. *Br J Pharmacol* 134: 1601–1608, 2001.
275. **Plasschaert SL, van der Kolk DM, de Bont ES, Kamps WA, Morisaki K, Bates SE, Scheffer GL, Scheper RJ, Vellenga E, and de Vries EG.** The role of breast cancer resistance protein in acute lymphoblastic leukemia. *Clin Cancer Res* 9: 5171–5177, 2003.
276. **Plosch T, Bloks VW, Terasawa Y, Berdy S, Siegler K, Van Der Sluijs F, Kema IP, Groen AK, Shan B, Kuipers F, and Schwarz M.** Sitosterolemia in ABC-transporter G5-deficient mice is aggravated on activation of the liver-X receptor. *Gastroenterology* 126: 290–300, 2004.
277. **Polgar O, Robey RW, Morisaki K, Dean M, Michejda C, Sauna ZE, Ambudkar SV, Tarasova N, and Bates SE.** Mutational analysis of ABCG2: role of the GXXXG motif. *Biochemistry* 43: 9448–9456, 2004.
278. **Polli JW, Wring SA, Humphreys JE, Huang L, Morgan JB, Webster LO, and Serabjit-Singh CS.** Rational use of in vitro P-glycoprotein assays in drug discovery. *J Pharmacol Exp Ther* 299: 620–628, 2001.
279. **Qu Q, Chu JW, and Sharom FJ.** Transition state P-glycoprotein binds drugs and modulators with unchanged affinity, suggesting a concerted transport mechanism. *Biochemistry* 42: 1345–1353, 2003.
280. **Rabindran SK, He H, Singh M, Brown E, Collins KI, Annable T, and Greenberger LM.** Reversal of a novel multidrug resistance mechanism in human colon carcinoma cells by fumitremorgin C. *Cancer Res* 58: 5850–5858, 1998.
281. **Rabindran SK, Ross DD, Doyle LA, Yang W, and Greenberger LM.** Fumitremorgin C reverses multidrug resistance in cells transfected with the breast cancer resistance protein. *Cancer Res* 60: 47–50, 2000.
282. **Ramachandra M, Ambudkar SV, Chen D, Hrycyna CA, Dey S, Gottesman MM, and Pastan I.** Human P-glycoprotein exhibits reduced affinity for substrates during a catalytic transition state. *Biochemistry* 37: 5010–5019, 1998.
283. **Ramachandra M, Gottesman MM, and Pastan I.** Recombinant vaccinia virus vectors for functional expression of P-glycoprotein in mammalian cells. *Methods Enzymol* 292: 441–455, 1998.
284. **Repa JJ, Berge KE, Pomajzl C, Richardson JA, Hobbs H, and Mangelsdorf DJ.** Regulation of ATP-binding cassette sterol transporters ABCG5 and ABCG8 by the liver X receptors alpha and beta. *J Biol Chem* 277: 18793–18800, 2002.
285. **Reyes CL and Chang G.** Structure of the ABC transporter MsbA in complex with ADP, vanadate and lipopolysaccharide. *Science* 308: 1028–1031, 2005.

286. **Riordan JR.** Assembly of functional CFTR chloride channels. *Annu Rev Physiol* 67: 701–718, 2005.
287. **Robey RW, Steadman K, Polgar O, Morisaki K, Blayney M, Mistry P, and Bates SE.** Pheophorbide A is a specific probe for ABCG2 function and inhibition. *Cancer Res* 64: 1242–1246, 2004.
288. **Romiti N, Tramonti G, Donati A, and Chieli E.** Effects of grapefruit juice on the multidrug transporter P-glycoprotein in the human proximal tubular cell line HK-2. *Life Sci* 76: 293–302, 2004.
289. **Rosenberg MF, Callaghan R, Ford RC, and Higgins CF.** Structure of the multidrug resistance P-glycoprotein to 2.5 nm resolution determined by electron microscopy and image analysis. *J Biol Chem* 272: 10685–10694, 1997.
290. **Rosenberg MF, Callaghan R, Modok S, Higgins CF, and Ford RC.** Three-dimensional structure of P-glycoprotein: the transmembrane regions adopt an asymmetric configuration in the nucleotide-bound state. *J Biol Chem* 280: 2857–2862, 2005.
291. **Rosenberg MF, Kamis AB, Callaghan R, Higgins CF, and Ford RC.** Three-dimensional structures of the mammalian multidrug resistance P-glycoprotein demonstrate major conformational changes in the transmembrane domains upon nucleotide binding. *J Biol Chem* 278: 8294–8299, 2003.
292. **Rosenberg MF, Mao Q, Holzenburg A, Ford RC, Deeley RG, and Cole SP.** The structure of the multidrug resistance protein 1 (MRP1/ABCC1). Crystallization and single-particle analysis. *J Biol Chem* 276: 16076–16082, 2001.
293. **Rosenberg MF, Velarde G, Ford RC, Martin C, Berridge G, Kerr ID, Callaghan R, Schmidlin A, Wooding C, Linton KJ, and Higgins CF.** Repacking of the transmembrane domains of P-glycoprotein during the transport ATPase cycle. *EMBO J* 20: 5615–5625, 2001.
294. **Rosmorduc O, Hermelin B, Boelle PY, Parc R, Taboury J, and Poupon R.** ABCB4 gene mutation-associated cholelithiasis in adults. *Gastroenterology* 125: 452–459, 2003.
295. **Ross DD, Karp JE, Chen TT, and Doyle LA.** Expression of breast cancer resistance protein in blast cells from patients with acute leukemia. *Blood* 96: 365–368, 2000.
296. **Roulet A, Puel O, Gesta S, Lepage JF, Drag M, Soll M, Alvinerie M, and Pineau T.** MDR1-deficient genotype in Collie dogs hypersensitive to the P-glycoprotein substrate ivermectin. *Eur J Pharmacol* 460: 85–91, 2003.
297. **Ruetz S and Gros P.** Enhancement of Mdr2-mediated phosphatidylcholine translocation by the bile salt taurocholate. Implications for hepatic bile formation. *J Biol Chem* 270: 25388–25395, 1995.
298. **Ruetz S and Gros P.** Phosphatidylcholine translocase: a physiological role for the mdr2 gene. *Cell* 77: 1071–1081, 1994.
299. **Sadeque AJ, Wandel C, He H, Shah S, and Wood AJ.** Increased drug delivery to the brain by P-glycoprotein inhibition. *Clin Pharmacol Ther* 68: 231–237, 2000.
300. **Safa AR.** Identification and characterization of the binding sites of P-glycoprotein for multidrug resistance-related drugs and modulators. *Curr Med Chem Anti-Canc Agents* 4: 1–17, 2004.
301. **Salen G, von Bergmann K, Lutjohann D, Kwiterovich P, Kane J, Patel SB, Musliner T, Stein P, and Musser B.** Ezetimibe effectively reduces plasma plant sterols in patients with sitosterolemia. *Circulation* 109: 966–971, 2004.
302. **Sampath J, Sun D, Kidd VJ, Grenet J, Gandhi A, Shapiro LH, Wang Q, Zambetti GP, and Schuetz JD.** Mutant p53 cooperates with ETS and selectively upregulates human MDR1 not MRP1. *J Biol Chem* 276: 39359–39367, 2001.
303. **Sankaran B, Bhagat S, and Senior AE.** Photoaffinity labelling of P-glycoprotein catalytic sites. *FEBS Lett* 417: 119–122, 1997.
304. **Sargent JM, Williamson CJ, Maliepaard M, Elgie AW, Scheper RJ, and Taylor CG.** Breast cancer resistance protein expression and resistance to daunorubicin in blast cells from patients with acute myeloid leukaemia. *Br J Haematol* 115: 257–262, 2001.
305. **Sarkadi B, Bauzon D, Huckle WR, Earp HS, Berry A, Suchindran H, Price EM, Olson JC, Boucher RC, and Scarborough GA.** Biochemical characterization of the cystic fibrosis transmembrane conductance regulator in normal and cystic fibrosis epithelial cells. *J Biol Chem* 267: 2087–2095, 1992.
306. **Sarkadi B, Ozvegy-Laczka C, Nemet K, and Varadi A.** ABCG2—a transporter for all seasons. *FEBS Lett* 567: 116–120, 2004.
307. **Sarkadi B, Price EM, Boucher RC, Germann UA, and Scarborough GA.** Expression of the human multidrug resistance cDNA in insect cells generates a high activity drug-stimulated membrane ATPase. *J Biol Chem* 267: 4854–4858, 1992.
308. **Sasaki M, Suzuki H, Aoki J, Ito K, Meier PJ, and Sugiyama Y.** Prediction of in vivo biliary clearance from the in vitro transcellular transport of organic anions across a double-transfected Madin-Darby canine kidney II monolayer expressing both rat organic anion transporting polypeptide 4 and multidrug resistance associated protein 2. *Mol Pharmacol* 66: 450–459, 2004.
309. **Sasaki M, Suzuki H, Ito K, Abe T, and Sugiyama Y.** Transcellular transport of organic anions across a double-transfected Madin-Darby canine kidney II cell monolayer expressing both human organic anion-transporting polypeptide (OATP2/SLC21A6) and multidrug resistance-associated protein 2 (MRP2/ABCC2). *J Biol Chem* 277: 6497–6503, 2002.
310. **Sauna ZE and Ambudkar SV.** Characterization of the catalytic cycle of ATP hydrolysis by human P-glycoprotein. The two ATP hydrolysis events in a single catalytic cycle are kinetically similar but affect different functional outcomes. *J Biol Chem* 276: 11653–11661, 2001.
311. **Sauna ZE and Ambudkar SV.** Evidence for a requirement for ATP hydrolysis at two distinct steps during a single turnover of the catalytic cycle of human P-glycoprotein. *Proc Natl Acad Sci USA* 97: 2515–2520, 2000.
312. **Sauna ZE, Muller M, Peng XH, and Ambudkar SV.** Importance of the conserved Walker B glutamate residues, 556 and 1201, for the completion of the catalytic cycle of ATP hydrolysis by human P-glycoprotein (ABCB1). *Biochemistry* 41: 13989–14000, 2002.
313. **Sauna ZE, Smith MM, Muller M, Kerr KM, and Ambudkar SV.** The mechanism of action of multidrug-resistance-linked P-glycoprotein. *J Bioenerg Biomembr* 33: 481–491, 2001.
314. **Scharenberg CW, Harkey MA, and Torok-Storb B.** The ABCG2 transporter is an efficient Hoechst 33342 efflux pump and is preferentially expressed by immature human hematopoietic progenitors. *Blood* 99: 507–512, 2002.
315. **Scheffer GL, Kool M, Heijn M, de Haas M, Pijnenborg AC, Wijnholds J, van Helvoort A, de Jong MC, Hooijberg JH, Mol CA, van der Linden M, de Vree JM, van der Valk P, Elferink RP, Borst P, and Scheper RJ.** Specific detection of multidrug resistance proteins MRP1, MRP2, MRP3, MRP5, and MDR3 P-glycoprotein with a panel of monoclonal antibodies. *Cancer Res* 60: 5269–5277, 2000.
316. **Scheffer GL, Maliepaard M, Pijnenborg AC, van Gastelen MA, de Jong MC, Schroeijers AB, van der Kolk DM, Allen JD, Ross DD, van der Valk P, Dalton WS, Schellens JH, and Scheper RJ.** Breast cancer resistance protein is localized at the plasma membrane in mitoxantrone- and topotecan-resistant cell lines. *Cancer Res* 60: 2589–2593, 2000.
317. **Schellens JH, Maliepaard M, Scheper RJ, Scheffer GL, Jonker JW, Smit JW, Beijnen JH, and Schinkel AH.** Transport of topoisomerase I inhibitors by the breast cancer resistance protein. Potential clinical implications. *Ann NY Acad Sci* 922: 188–194, 2000.
318. **Schiedlmeier B, Schilz AJ, Kuhlcke K, Laufs S, Baum C, Zeller WJ, Eckert HG, and Fruehauf S.** Multidrug resistance 1 gene transfer can confer chemoprotection to human peripheral blood progenitor cells engrafted in immunodeficient mice. *Hum Gene Ther* 13: 233–242, 2002.
319. **Schinkel AH.** The physiological function of drug-transporting P-glycoproteins. *Semin Cancer Biol* 8: 161–170, 1997.
320. **Schinkel AH and Jonker JW.** Mammalian drug efflux transporters of the ATP binding cassette (ABC) family: an overview. *Adv Drug Deliv Rev* 55: 3–29, 2003.
321. **Schinkel AH, Mayer U, Wagenaar E, Mol CA, van Deemter L, Smit JJ, van der Valk MA, Voordouw AC, Spits H, van Tellingen O, Zijlmans JM, Fibbe WE, and Borst P.** Normal viability and altered pharmacokinetics in mice lacking mdr1-type (drug-transporting) P-glycoproteins. *Proc Natl Acad Sci USA* 94: 4028–4033, 1997.
322. **Schmitt L and Tampe R.** Structure and mechanism of ABC transporters. *Curr Opin Struct Biol* 12: 754–760, 2002.

323. **Schumacher MA and Brennan RG.** Structural mechanisms of multidrug recognition and regulation by bacterial multidrug transcription factors. *Mol Microbiol* 45: 885–893, 2002.
324. **Schwanstecher M, Sieverding C, Dorschner H, Gross I, Aguilar-Bryan L, Schwanstecher C, and Bryan J.** Potassium channel openers require ATP to bind to and act through sulfonylurea receptors. *EMBO J* 17: 5529–5535, 1998.
325. **Scotto KW.** Transcriptional regulation of ABC drug transporters. *Oncogene* 22: 7496–7511, 2003.
326. **Seelig A and Landwojtowicz E.** Structure-activity relationship of P-glycoprotein substrates and modifiers. *Eur J Pharm Sci* 12: 31–40, 2000.
327. **Sehayek E, Duncan EM, Lutjohann D, Von Bergmann K, Ono JG, Batta AK, Salen G, and Breslow JL.** Loci on chromosomes 14 and 2, distinct from ABCG5/ABCG8, regulate plasma plant sterol levels in a C57BL/6J × CASA/Rk intercross. *Proc Natl Acad Sci USA* 99: 16215–16219, 2002.
328. **Senior AE, al-Shawi MK, and Urbatsch IL.** The catalytic cycle of P-glycoprotein. *FEBS Lett* 377: 285–289, 1995.
329. **Shapiro AB and Ling V.** ATPase activity of purified and reconstituted P-glycoprotein from Chinese hamster ovary cells. *J Biol Chem* 269: 3745–3754, 1994.
330. **Shapiro AB and Ling V.** Reconstitution of drug transport by purified P-glycoprotein. *J Biol Chem* 270: 16167–16175, 1995.
331. **Sharma R, Awasthi YC, Yang Y, Sharma A, Singhal SS, and Awasthi S.** Energy dependent transport of xenobiotics and its relevance to multidrug resistance. *Curr Cancer Drug Targets* 3: 89–107, 2003.
332. **Sharom FJ.** The P-glycoprotein multidrug transporter: interactions with membrane lipids, and their modulation of activity. *Biochem Soc Trans* 25: 1088–1096, 1997.
333. **Sharom FJ, Liu R, Qu Q, and Romsicki Y.** Exploring the structure and function of the P-glycoprotein multidrug transporter using fluorescence spectroscopic tools. *Semin Cell Dev Biol* 12: 257–265, 2001.
334. **Sharom FJ, Liu R, and Romsicki Y.** Spectroscopic and biophysical approaches for studying the structure and function of the P-glycoprotein multidrug transporter. *Biochem Cell Biol* 76: 695–708, 1998.
335. **Sharom FJ, Liu R, Romsicki Y, and Lu P.** Insights into the structure and substrate interactions of the P-glycoprotein multidrug transporter from spectroscopic studies. *Biochim Biophys Acta* 1461: 327–345, 1999.
336. **Sharom FJ, Yu X, and Doige CA.** Functional reconstitution of drug transport and ATPase activity in proteoliposomes containing partially purified P-glycoprotein. *J Biol Chem* 268: 24197–24202, 1993.
337. **Sharom FJ, Yu X, Lu P, Liu R, Chu JW, Szabo K, Muller M, Hose CD, Monks A, Varadi A, Seprodi J, and Sarkadi B.** Interaction of the P-glycoprotein multidrug transporter (MDR1) with high affinity peptide chemosensitizers in isolated membranes, reconstituted systems, and intact cells. *Biochem Pharmacol* 58: 571–586, 1999.
338. **Sheps JA, Ralph S, Zhao Z, Baillie DL, and Ling V.** The ABC transporter gene family of *Caenorhabditis elegans* has implications for the evolutionary dynamics of multidrug resistance in eukaryotes. *Genome Biol* 5: R15, 2004.
339. **Shuilleabhain SN, Davoren M, Mothersill C, Sheehan D, Hartl MG, Kilemade M, O'Brien NM, O'Halloran J, Van Pelt FN, and Lyng FM.** Identification of a multixenobiotic resistance mechanism in primary cultured epidermal cells from *Oncorhynchus mykiss* and the effects of environmental complex mixtures on its activity. *Aquat Toxicol* 73: 115–127, 2005.
340. **Small DM.** Role of ABC transporters in secretion of cholesterol from liver into bile. *Proc Natl Acad Sci USA* 100: 4–6, 2003.
341. **Smit JJ, Schinkel AH, Mol CA, Majoor D, Mooi WJ, Jongsma AP, Lincke CR, and Borst P.** Tissue distribution of the human MDR3 P-glycoprotein. *Lab Invest* 71: 638–649, 1994.
342. **Smit JJ, Schinkel AH, Oude Elferink RP, Groen AK, Wagenaar E, van Deemter L, Mol CA, Ottenhoff R, van der Lugt NM, van Roon MA, van der Valk MA, Offerhaus GJA, Berns AJM, and Borst P.** Homozygous disruption of the murine mdr2 P-glycoprotein gene leads to a complete absence of phospholipid from bile and to liver disease *Cell* 75: 451–462, 1993.
343. **Smital T, Luckenbach T, Sauerborn R, Hamdoun AM, Vega RL, and Epel D.** Emerging contaminants—pesticides, PPCPs, microbial degradation products and natural substances as inhibitors of multixenobiotic defense in aquatic organisms. *Mutat Res* 552: 101–117, 2004.
344. **Smith AJ, de Vree JM, Ottenhoff R, Oude Elferink RP, Schinkel AH, and Borst P.** Hepatocyte-specific expression of the human MDR3 P-glycoprotein gene restores the biliary phosphatidylcholine excretion absent in Mdr2 (−/−) mice. *Hepatology* 28: 530–536, 1998.
345. **Smith AJ, Timmermans-Hereijgers JL, Roelofsen B, Wirtz KW, van Blitterswijk WJ, Smit JJ, Schinkel AH, and Borst P.** The human MDR3 P-glycoprotein promotes translocation of phosphatidylcholine through the plasma membrane of fibroblasts from transgenic mice. *FEBS Lett* 354: 263–266, 1994.
346. **Smith AJ, van Helvoort A, van Meer G, Szabo K, Welker E, Szakacs G, Varadi A, Sarkadi B, and Borst P.** MDR3 P-glycoprotein, a phosphatidylcholine translocase, transports several cytotoxic drugs and directly interacts with drugs as judged by interference with nucleotide trapping. *J Biol Chem* 275: 23530–23539, 2000.
347. **Smith CD and Zilfou JT.** Circumvention of P-glycoprotein-mediated multiple drug resistance by phosphorylation modulators is independent of protein kinases. *J Biol Chem* 270: 28145–28152, 1995.
348. **Smith PC, Karpowich N, Millen L, Moody JE, Rosen J, Thomas PJ, and Hunt JF.** ATP binding to the motor domain from an ABC transporter drives formation of a nucleotide sandwich dimer. *Mol Cell* 10: 139–149, 2002.
349. **Sonveaux N, Vigano C, Shapiro AB, Ling V, and Ruysschaert JM.** Ligand-mediated tertiary structure changes of reconstituted P-glycoprotein. A tryptophan fluorescence quenching analysis. *J Biol Chem* 274: 17649–17654, 1999.
350. **Sparreboom A, Gelderblom H, Marsh S, Ahluwalia R, Obach R, Principe P, Twelves C, Verweij J, and McLeod HL.** Diflomotecan pharmacokinetics in relation to ABCG2 421C > A genotype. *Clin Pharmacol Ther* 76: 38–44, 2004.
351. **Staudinger JL, Madan A, Carol KM, and Parkinson A.** Regulation of drug transporter gene expression by nuclear receptors. *Drug Metab Dispos* 31: 523–527, 2003.
352. **Stein U, Walther W, and Wunderlich V.** Point mutations in the mdr1 promoter of human osteosarcomas are associated with in vitro responsiveness to multidrug resistance relevant drugs. *Eur J Cancer* 30A: 1541–1545, 1994.
353. **Stein WD.** Kinetics of the multidrug transporter (P-glycoprotein) and its reversal. *Physiol Rev* 77: 545–590, 1997.
354. **Steinbach D, Sell W, Voigt A, Hermann J, Zintl F, and Sauerbrey A.** BCRP gene expression is associated with a poor response to remission induction therapy in childhood acute myeloid leukemia. *Leukemia* 16: 1443–1447, 2002.
355. **Stewart CF, Leggas M, Schuetz JD, Panetta JC, Cheshire PJ, Peterson J, Daw N, Jenkins JJ, 3rd Gilbertson R, Germain GS, Harwood FC, and Houghton PJ.** Gefitinib enhances the antitumor activity and oral bioavailability of irinotecan in mice. *Cancer Res* 64: 7491–7499, 2004.
356. **Stieger B and Meier PJ.** Bile acid and xenobiotic transporters in liver. *Curr Opin Cell Biol* 10: 462–467, 1998.
357. **Summer R, Kotton DN, Sun X, Ma B, Fitzsimmons K, and Fine A.** Side population cells and Bcrp1 expression in lung. *Am J Physiol Lung Cell Mol Physiol* 285: L97–L104, 2003.
358. **Suvannasankha A, Minderman H, O'Loughlin KL, Nakanishi T, Ford LA, Greco WR, Wetzler M, Ross DD, and Baer MR.** Breast cancer resistance protein (BCRP/MXR/ABCG2) in adult acute lymphoblastic leukaemia: frequent expression and possible correlation with shorter disease-free survival. *Br J Haematol* 127: 392–398, 2004.
359. **Suzuki M, Suzuki H, Sugimoto Y, and Sugiyama Y.** ABCG2 transports sulfated conjugates of steroids and xenobiotics. *J Biol Chem* 278: 22644–22649, 2003.
360. **Sweet DH.** Organic anion transporter (Slc22a) family members as mediators of toxicity. *Toxicol Appl Pharmacol* 204: 198–215, 2005.

361. **Szabo K, Bakos E, Welker E, Muller M, Goodfellow HR, Higgins CF, Varadi A, and Sarkadi B.** Phosphorylation site mutations in the human multidrug transporter modulate its drug-stimulated ATPase activity. *J Biol Chem* 272: 23165–23171, 1997.
362. **Szabo K, Welker E, Bakos Muller M, Roninson I, Varadi A, and Sarkadi B.** Drug-stimulated nucleotide trapping in the human multidrug transporter MDR1. Cooperation of the nucleotide binding domains. *J Biol Chem* 273: 10132–10138, 1998.
363. **Szakacs G, Annereau JP, Lababidi S, Shankavaram U, Arciello A, Bussey KJ, Reinhold W, Guo Y, Kruh GD, Reimers M, Weinstein JN, and Gottesman MM.** Predicting drug sensitivity and resistance: profiling ABC transporter genes in cancer cells. *Cancer Cell* 6: 129–137, 2004.
364. **Szakacs G, Jakab K, Antal F, and Sarkadi B.** Diagnostics of multidrug resistance in cancer. *Pathol Oncol Res* 4: 251–257, 1998.
365. **Szakacs G, Ozvegy C, Bakos E, Sarkadi B, and Varadi A.** Role of glycine-534 and glycine-1179 of human multidrug resistance protein (MDR1) in drug-mediated control of ATP hydrolysis. *Biochem J* 356: 71–75, 2001.
366. **Szakacs G, Ozvegy C, Bakos E, Sarkadi B, and Varadi A.** Transition-state formation in ATPase-negative mutants of human MDR1 protein. *Biochem Biophys Res Commun* 276: 1314–1319, 2000.
367. **Szakacs G, Paterson J, Ludwig J, Booth-Genthe C, and Gottesman MM.** Targeting multidrug resistance in cancer. *Nat Rev Drug Discov* 5: 219–234, 2006.
368. **Szentpetery Z, Kern A, Liliom K, Sarkadi B, Varadi A, and Bakos E.** The role of the conserved glycines of ATP-binding cassette signature motifs of MRP1 in the communication between the substrate-binding site and the catalytic centers. *J Biol Chem* 279: 41670–41678, 2004.
369. **Tainton KM, Smyth MJ, Jackson JT, Tanner JE, Cerruti L, Jane SM, Darcy PK, and Johnstone RW.** Mutational analysis of P-glycoprotein: suppression of caspase activation in the absence of ATP-dependent drug efflux. *Cell Death Differ* 11: 1028–1037, 2004.
370. **Takada T, Suzuki H, and Sugiyama Y.** Characterization of polarized expression of point- or deletion-mutated human BCRP/ABCG2 in LLC-PK_1 cells. *Pharm Res* 22: 458–464, 2005.
371. **Tanaka Y, Slitt AL, Leazer TM, Maher JM, and Klaassen CD.** Tissue distribution and hormonal regulation of the breast cancer resistance protein (Bcrp/Abcg2) in rats and mice. *Biochem Biophys Res Commun* 326: 181–187, 2005.
372. **Tang-Wai DF, Brossi A, Arnold LD, and Gros P.** The nitrogen of the acetamido group of colchicine modulates P-glycoprotein-mediated multidrug resistance. *Biochemistry* 32: 6470–6476, 1993.
373. **Toffoli G, Simone F, Corona G, Raschack M, Cappelletto B, Gigante M, and Boiocchi M.** Structure-activity relationship of verapamil analogs and reversal of multidrug resistance. *Biochem Pharmacol* 50: 1245–1255, 1995.
374. **Tombline G, Bartholomew LA, Tyndall GA, Gimi K, Urbatsch IL, and Senior AE.** Properties of P-glycoprotein with mutations in the "catalytic carboxylate" glutamate residues. *J Biol Chem* 279: 46518–46526, 2004.
375. **Tombline G, Muharemagic A, White LB, and Senior AE.** Involvement of the "occluded nucleotide conformation" of p-glycoprotein in the catalytic pathway. *Biochemistry* 44: 12879–12886, 2005.
376. **Totah RA and Rettie AE.** Cytochrome *P*450 2C8: substrates, inhibitors, pharmacogenetics, and clinical relevance. *Clin Pharmacol Ther* 77: 341–352, 2005.
377. **Turzanski J, Grundy M, Shang S, Russell N, and Pallis M.** P-glycoprotein is implicated in the inhibition of ceramide-induced apoptosis in TF-1 acute myeloid leukemia cells by modulation of the glucosylceramide synthase pathway. *Exp Hematol* 33: 62–72, 2005.
378. **Uggla B, Stahl E, Wagsater D, Paul C, Karlsson MG, Sirsjo A, and Tidefelt U.** BCRP mRNA expression v. clinical outcome in 40 adult AML patients. *Leuk Res* 29: 141–146, 2005.
379. **Ujhelly O, Ozvegy C, Varady G, Cervenak J, Homolya L, Grez M, Scheffer G, Roos D, Bates SE, Varadi A, Sarkadi B, and Nemet K.** Application of a human multidrug transporter (ABCG2) variant as selectable marker in gene transfer to progenitor cells. *Hum Gene Ther* 14: 403–412, 2003.
380. **Urbatsch IL, Beaudet L, Carrier I, and Gros P.** Mutations in either nucleotide-binding site of P-glycoprotein (Mdr3) prevent vanadate trapping of nucleotide at both sites. *Biochemistry* 37: 4592–4602, 1998.
381. **Urbatsch IL, Gimi K, Wilke-Mounts S, and Senior AE.** Investigation of the role of glutamine-471 and glutamine-1114 in the two catalytic sites of P-glycoprotein. *Biochemistry* 39: 11921–11927, 2000.
382. **Van der Bliek AM, Baas F, Ten Houte de Lange T, Kooiman PM, Van der Velde-Koerts T, and Borst P.** The human mdr3 gene encodes a novel P-glycoprotein homologue and gives rise to alternatively spliced mRNAs in liver. *EMBO J* 6: 3325–3331, 1987.
383. **Van Helvoort A, Smith AJ, Sprong H, Fritzsche I, Schinkel AH, Borst P, and van Meer G.** MDR1 P-glycoprotein is a lipid translocase of broad specificity, while MDR3 P-glycoprotein specifically translocates phosphatidylcholine. *Cell* 87: 507–517, 1996.
384. **Van Herwaarden AE, Jonker JW, Wagenaar E, Brinkhuis RF, Schellens JH, Beijnen JH, and Schinkel AH.** The breast cancer resistance protein (Bcrp1/Abcg2) restricts exposure to the dietary carcinogen 2-amino-1-methyl-6-phenylimidazo[4,5-b]pyridine. *Cancer Res* 63: 6447–6452, 2003.
385. **Van Herwaarden AE and Schinkel AH.** The function of breast cancer resistance protein in epithelial barriers, stem cells and milk secretion of drugs and xenotoxins. *Trends Pharmacol Sci* 27: 10–16, 2006.
386. **Van Loevezijn A, Allen JD, Schinkel AH, and Koomen GJ.** Inhibition of BCRP-mediated drug efflux by fumitremorgin-type indolyl diketopiperazines. *Bioorg Med Chem Lett* 11: 29–32, 2001.
387. **Van Montfoort JE, Hagenbuch B, Groothuis GM, Koepsell H, Meier PJ, and Meijer DK.** Drug uptake systems in liver and kidney. *Curr Drug Metab* 4: 185–211, 2003.
388. **Van Veen HW and Konings WN.** Drug efflux proteins in multidrug resistant bacteria. *Biol Chem* 378: 769–777, 1997.
389. **Varadi A, Szakacs G, Bakos E, and Sarkadi B.** P glycoprotein and the mechanism of multidrug resistance. *Novartis Found Symp* 243: 54–65, 2002.
390. **Venter H, Shilling RA, Velamakanni S, Balakrishnan L, and Van Veen HW.** An ABC transporter with a secondary-active multidrug translocator domain. *Nature* 426: 866–870, 2003.
391. **Vergani P, Nairn AC, and Gadsby DC.** On the mechanism of MgATP-dependent gating of CFTR Cl^- channels. *J Gen Physiol* 121: 17–36, 2003.
392. **Vilaboa NE, Galan A, Troyano A, de Blas E, and Aller P.** Regulation of multidrug resistance 1 (MDR1)/P-glycoprotein gene expression and activity by heat-shock transcription factor 1 (HSF1). *J Biol Chem* 275: 24970–24976, 2000.
393. **Volk EL, Farley KM, Wu Y, Li F, Robey RW, and Schneider E.** Overexpression of wild-type breast cancer resistance protein mediates methotrexate resistance. *Cancer Res* 62: 5035–5040, 2002.
394. **Volk EL and Schneider E.** Wild-type breast cancer resistance protein (BCRP/ABCG2) is a methotrexate polyglutamate transporter. *Cancer Res* 63: 5538–5543, 2003.
395. **Volk HA, Potschka H, and Loscher W.** Increased expression of the multidrug transporter P-glycoprotein in limbic brain regions after amygdala-kindled seizures in rats. *Epilepsy Res* 58: 67–79, 2004.
396. **Walker JE, Saraste M, Runswick MJ, and Gay NJ.** Distantly related sequences in the alpha- and beta-subunits of ATP synthase, myosin, kinases and other ATP-requiring enzymes and a common nucleotide binding fold. *EMBO J* 1: 945–951, 1982.
397. **Wallstab A, Koester M, Bohme M, and Keppler D.** Selective inhibition of MDR1 P-glycoprotein-mediated transport by the acridone carboxamide derivative GG918. *Br J Cancer* 79: 1053–1060, 1999.
398. **Wang J, Joy T, Mymin D, Frohlich J, and Hegele RA.** Phenotypic heterogeneity of sitosterolemia. *J Lipid Res* 45: 2361–2367, 2004.
399. **Wielinga P, Hooijberg JH, Gunnarsdottir S, Kathmann I, Reid G, Zelcer N, van der Born K, de Haas M, van der Heijden I, Kaspers G, Wijnholds J, Jansen G, Peters G, and Borst P.** The human multidrug resistance protein MRP5 transports folates and can mediate cellular resistance against antifolates. *Cancer Res* 65: 4425–4430, 2005.

400. **Wittenburg H and Carey MC.** Biliary cholesterol secretion by the twinned sterol half-transporters ABCG5 and ABCG8. *J Clin Invest* 110: 605–609, 2002.
401. **Wu CP, Klokouzas A, Hladky SB, Ambudkar SV, and Barrand MA.** Interactions of mefloquine with ABC proteins, MRP1 (ABCC1) and MRP4 (ABCC4) that are present in human red cell membranes. *Biochem Pharmacol* 70: 500–510, 2005.
402. **Wu JE, Basso F, Shamburek RD, Amar MJ, Vaisman B, Szakacs G, Joyce C, Tansey T, Freeman L, Paigen BJ, Thomas F, Brewer HB Jr, and Santamarina-Fojo S.** Hepatic ABCG5 and ABCG8 overexpression increases hepatobiliary sterol transport but does not alter aortic atherosclerosis in transgenic mice. *J Biol Chem* 279: 22913–22925, 2004.
403. **Xu C, Li CY, and Kong AN.** Induction of phase I, II and III drug metabolism/transport by xenobiotics. *Arch Pharm Res* 28: 249–268, 2005.
404. **Xu J, Liu Y, Yang Y, Bates S, and Zhang JT.** Characterization of oligomeric human half-ABC transporter ATP-binding cassette G2. *J Biol Chem* 279: 19781–19789, 2004.
405. **Yague E, Armesilla AL, Harrison G, Elliott J, Sardini A, Higgins CF, and Raguz S.** P-glycoprotein (MDR1) expression in leukemic cells is regulated at two distinct steps, mRNA stabilization and translational initiation. *J Biol Chem* 278: 10344–10352, 2003.
406. **Yanase K, Tsukahara S, Asada S, Ishikawa E, Imai Y, and Sugimoto Y.** Gefitinib reverses breast cancer resistance protein-mediated drug resistance. *Mol Cancer Ther* 3: 1119–1125, 2004.
407. **Yang C, Yu L, Li W, Xu F, Cohen JC, and Hobbs HH.** Disruption of cholesterol homeostasis by plant sterols. *J Clin Invest* 114: 813–822, 2004.
408. **Yoh K, Ishii G, Yokose T, Minegishi Y, Tsuta K, Goto K, Nishiwaki Y, Kodama T, Suga M, and Ochiai A.** Breast cancer resistance protein impacts clinical outcome in platinum-based chemotherapy for advanced non-small cell lung cancer. *Clin Cancer Res* 10: 1691–1697, 2004.
409. **Youdim KA, Qaiser MZ, Begley DJ, Rice-Evans CA, and Abbott NJ.** Flavonoid permeability across an in situ model of the blood-brain barrier. *Free Radic Biol Med* 36: 592–604, 2004.
410. **Yu G, Ahmad S, Aquino A, Fairchild CR, Trepel JB, Ohno S, Suzuki K, Tsuruo T, Cowan KH, and Glazer RI.** Transfection with protein kinase C alpha confers increased multidrug resistance to MCF-7 cells expressing P-glycoprotein. *Cancer Commun* 3: 181–189, 1991.
411. **Yu L, Gupta S, Xu F, Liverman AD, Moschetta A, Mangelsdorf DJ, Repa JJ, Hobbs HH, and Cohen JC.** Expression of ABCG5 and ABCG8 is required for regulation of biliary cholesterol secretion. *J Biol Chem* 280: 8742–8747, 2005.
412. **Yu L, Hammer RE, Li-Hawkins J, Von Bergmann K, Lutjohann D, Cohen JC, and Hobbs HH.** Disruption of Abcg5 and Abcg8 in mice reveals their crucial role in biliary cholesterol secretion. *Proc Natl Acad Sci USA* 99: 16237–16242, 2002.
413. **Yu L, Li-Hawkins J, Hammer RE, Berge KE, Horton JD, Cohen JC, and Hobbs HH.** Overexpression of ABCG5 and ABCG8 promotes biliary cholesterol secretion and reduces fractional absorption of dietary cholesterol. *J Clin Invest* 110: 671–680, 2002.
414. **Yu L, von Bergmann K, Lutjohann D, Hobbs HH, and Cohen JC.** Ezetimibe normalizes metabolic defects in mice lacking ABCG5 and ABCG8. *J Lipid Res* 46: 1739–1744, 2005.
415. **Yu L, von Bergmann K, Lutjohann D, Hobbs HH, and Cohen JC.** Selective sterol accumulation in ABCG5/ABCG8-deficient mice. *J Lipid Res* 45: 301–307, 2004.
416. **Yuan YR, Blecker S, Martsinkevich O, Millen L, Thomas PJ, and Hunt JF.** The crystal structure of the MJ0796 ATP-binding cassette. Implications for the structural consequences of ATP hydrolysis in the active site of an ABC transporter. *J Biol Chem* 276: 32313–32321, 2001.
417. **Zaitseva J, Jenewein S, Jumpertz T, Holland IB, and Schmitt L.** H662 is the linchpin of ATP hydrolysis in the nucleotide-binding domain of the ABC transporter HlyB. *EMBO J* 24: 1901–1910, 2005.
418. **Zamber CP, Lamba JK, Yasuda K, Farnum J, Thummel K, Schuetz JD, and Schuetz EG.** Natural allelic variants of breast cancer resistance protein (BCRP) and their relationship to BCRP expression in human intestine. *Pharmacogenetics* 13: 19–28, 2003.
419. **Zamboni WC, Bowman LC, Tan M, Santana VM, Houghton PJ, Meyer WH, Pratt CB, Heideman RL, Gajjar AJ, Pappo AS, and Stewart CF.** Interpatient variability in bioavailability of the intravenous formulation of topotecan given orally to children with recurrent solid tumors. *Cancer Chemother Pharmacol* 43: 454–460, 1999.
420. **Zamora JM, Pearce HL, and Beck WT.** Physical-chemical properties shared by compounds that modulate multidrug resistance in human leukemic cells. *Mol Pharmacol* 33: 454–462, 1988.
421. **Zelcer N, Saeki T, Bot I, Kuil A, and Borst P.** Transport of bile acids in multidrug-resistance-protein 3-overexpressing cells cotransfected with the ileal Na^+-dependent bile-acid transporter. *Biochem J* 369: 23–30, 2003.
422. **Zeng H, Liu G, Rea PA, and Kruh GD.** Transport of amphipathic anions by human multidrug resistance protein 3. *Cancer Res* 60: 4779–4784, 2000.
423. **Zhang W, Mojsilovic-Petrovic J, Andrade MF, Zhang H, Ball M, and Stanimirovic DB.** The expression and functional characterization of ABCG2 in brain endothelial cells and vessels. *FASEB J* 17: 2085–2087, 2003.
424. **Zhang Z, Wu JY, Hait WN, and Yang JM.** Regulation of the stability of P-glycoprotein by ubiquitination. *Mol Pharmacol* 66: 395–403, 2004.
425. **Zhao JY, Ikeguchi M, Eckersberg T, and Kuo MT.** Modulation of multidrug resistance gene expression by dexamethasone in cultured hepatoma cells. *Endocrinology* 133: 521–528, 1993.
426. **Zheleznova EE, Markham P, Edgar R, Bibi E, Neyfakh AA, and Brennan RG.** A structure-based mechanism for drug binding by multidrug transporters. *Trends Biochem Sci* 25: 39–43, 2000.
427. **Zhong X and Safa AR.** RNA helicase A in the MEF1 transcription factor complex up-regulates the MDR1 gene in multidrug-resistant cancer cells. *J Biol Chem* 279: 17134–17141, 2004.
428. **Zhou Q, Sparreboom A, Tan EH, Cheung YB, Lee A, Poon D, Lee EJ, and Chowbay B.** Pharmacogenetic profiling across the irinotecan pathway in Asian patients with cancer. *Br J Clin Pharmacol* 59: 415–424, 2005.
429. **Zhou S, Morris JJ, Barnes Y, Lan L, Schuetz JD, and Sorrentino BP.** Bcrp1 gene expression is required for normal numbers of side population stem cells in mice, and confers relative protection to mitoxantrone in hematopoietic cells in vivo. *Proc Natl Acad Sci USA* 99: 12339–12344, 2002.
430. **Zhou S, Schuetz JD, Bunting KD, Colapietro AM, Sampath J, Morris JJ, Lagutina I, Grosveld GC, Osawa M, Nakauchi H, and Sorrentino BP.** The ABC transporter Bcrp1/ABCG2 is expressed in a wide variety of stem cells and is a molecular determinant of the side-population phenotype. *Nat Med* 7: 1028–1034, 2001.
431. **Zhu HJ and Liu GQ.** Glutamate up-regulates P-glycoprotein expression in rat brain microvessel endothelial cells by an NMDA receptor-mediated mechanism. *Life Sci* 75: 1313–1322, 2004.

12. sz. közlemény

dc_46_10

BioFactors 17 (2003) 103–114
IOS Press

Multidrug resistance-associated proteins: Export pumps for conjugates with glutathione, glucuronate or sulfate[1]

László Homolya[a], András Váradi[b] and Balázs Sarkadi[a,c]
[a]*Membrane Research Group, Hungarian Academy of Sciences, Budapest, Hungary*
[b]*Institute of Enzymology, Hungarian Academy of Sciences, Budapest, Hungary*
[c]*Institute of Haematology, National Medical Center, Budapest, Hungary*

Abstract. Many endogenous or xenobiotic lipophilic substances are eliminated from the cells by the sequence of oxidation, conjugation to an anionic group (glutathione, glucuronate or sulfate) and transport across the plasma membrane into the extracellular space. The latter step is mediated by integral membrane glycoproteins belonging to the superfamily of ATP-Binding Cassette (ABC) transporters. A subfamily, referred as ABCC, includes the famous/infamous cystic fibrosis transmembrane regulator (CFTR), the sulfonylurea receptors (SUR 1 and 2), and the multidrug resistance-associated proteins (MRPs). The name of the MRPs refers to their potential role in clinical multidrug resistance, a phenomenon that hinders the effective chemotherapy of tumors. The MRPs that have been functionally characterized so far share the property of ATP-dependent export pumps for conjugates with glutathione (GSH), glucuronate or sulfate. MRP1 and MRP2 are also mediating the cotransport of unconjugated amphiphilic compounds together with free GSH. MRP3 preferentially transports glucuronides but not glutathione S-conjugates or free GSH. MRP1 and MRP2 also contribute to the control of the intracellular glutathione disulfide (GSSG) level. Although these proteins are low affinity GSSG transporters, they can play essential role in response to oxidative stress when the activity of GSSG reductase becomes rate limiting. The human MRP4, MRP5 and MRP6 have only partially been characterized. However, it has been revealed that MRP4 can function as an efflux pump for cyclic nucleotides and nucleoside analogues, used as anti-HIV drugs. MRP5 also transports GSH conjugates, nucleoside analogues, and possibly heavy metal complexes. Transport of glutathione S-conjugates mediated by MRP6, the mutation of which causes pseudoxantoma elasticum, has recently been shown. In summary, numerous members of the multidrug resistance-associated protein family serve as export pumps that prevent the accumulation of anionic conjugates and GSSG in the cytoplasm, and play, therefore, an essential role in detoxification and defense against oxidative stress.

1. Superfamily of ABC transporters

The ATP-Binding Cassette (ABC) transporters form one of the largest protein families; the members of the superfamily can be found in most living organisms from bacteria to man. These proteins are defined by the presence of an ABC unit (or NBD; Nucleotide-Binding Domain), which harbors two short ATP-binding motifs (Walker A and Walker B), and another conserved sequence, the so-called ABC signature motif, which is a hallmark for all ABC transporters. In addition to the sequence homology, these proteins also share distinguishing structural characteristics. They are built from cytosolic nucleotide-binding

[1]This article also appeared in *Thiol Metabolism and Redox Regulation of Cellular Functions,* A. Pompella, G. Bánhegyi and M. Wellman-Rousseau, eds, IOS Press, Amsterdam.

domains and large transmembrane domains, in most cases composed of 6 transmembrane helices. To our recent knowledge, a functioning ABC transporter consists of at least two transmembrane and two nucleotide-binding units. Some ABC transporters consist of one polypeptide chain (Pgp/MDR1), others form dimers from half transporters (TAP1/TAP2) or are composed from smaller associated subunits [for more information see: ref [1] and [2]]. The three-dimensional structure of the mammalian ABC transporters is currently unknown. A low-resolution structure of the MDR1 [3] indicates that the protein is embedded into the membrane as a cylinder with a large central pore and with an opening to the lipid phase. Recent structural studies on a bacterial ABC-transporter [4] first demonstrated the presence of transmembrane helices.

After a long period of confusion in naming and numbering of the newly identified ABC transporters, a consistent nomenclature based on sequence homology has been introduced. The approximately 50 human ABC proteins were classified into seven subfamilies, ranging from ABCA to ABCG [see: http://nutrigene.4t.com/humanabc.htm]. Figure 1 depicts the phylogenetic tree of the ABC transporter superfamily. The subfamily ABCA includes ABCA1, the protein that has been proposed as a key component of the reverse cholesterol transport. One of the first identified human ABC transporters, the P-glycoprotein (Pgp or MDR1) belongs to the ABCB subfamily. The Pgp-mediated drug extrusion is still the most widely observed mechanism in clinical multidrug resistance (see below). The ABCC subfamily includes numerous multidrug resistance-associated proteins (MRPs), ABC transporters, which play key role in the cellular elimination of endogenous and xenobiotic lipophilic compounds. In addition, the cystic fibrosis transmembrane conductance regulator (CFTR, or ABCC7), the mutation of which is responsible for the frequent, fatal, inherited disease, the cystic fibrosis, also belongs to this subfamily.

Members of the ABC transporters superfamily are associated with a broad spectrum of physiological functions including detoxification (MDR1, MRP1), defense against xenobiotics and oxidative stress (MRPs), absorption and secretion processes (MDRs, MRPs), lipid metabolism (ABCA1, MDR3), antigen presentation (TAP1/TAP2), cell to cell communication (STE6), etc. Most of the ABC proteins are active transporters, mediate uphill transport of substances across the plasma membrane into the extracellular space, or across internal membranes into cellular compartments. This transport activity is driven by the energy of ATP hydrolysis accomplished by the nucleotide-binding domains. Despite the relatively high sequence homology and structural similarity, some ABC transporters possess very different characteristics in terms of their function. In contrast to other ABC transporters, the sulfonylurea receptors (SUR1 and SUR2) modulate the permeability of specific potassium channels. Similarly, CFTR is not an active transport pump, but it forms a chloride channel. According to our current understanding, the major function of CFTR is not its chloride channel activity but it plays a regulatory role in controlling the function of other membrane transport proteins [5].

2. ABC transporters in multidrug resistance

The most intriguing members of ABC transporters are the so-called multidrug resistance (MDR) proteins, which are associated with the clinical multidrug resistance. These transporters exhibit an unusual broad substrate specificity to a series of hydrophobic compounds used in chemotherapy of cancer. The generally accepted basic mechanism of multidrug resistance is that the MDR proteins actively expel the cytotoxic agents from the cells, maintaining the drug level below a cell-killing threshold. Unlike other, selective (classical) transport proteins, multidrug transporters recognize and handle a wide range of substrates. This wide substrate specificity explains the cross-resistance to several chemically unrelated compounds, the characteristic feature found in the multidrug resistance phenotype [6–8]. Up to now,

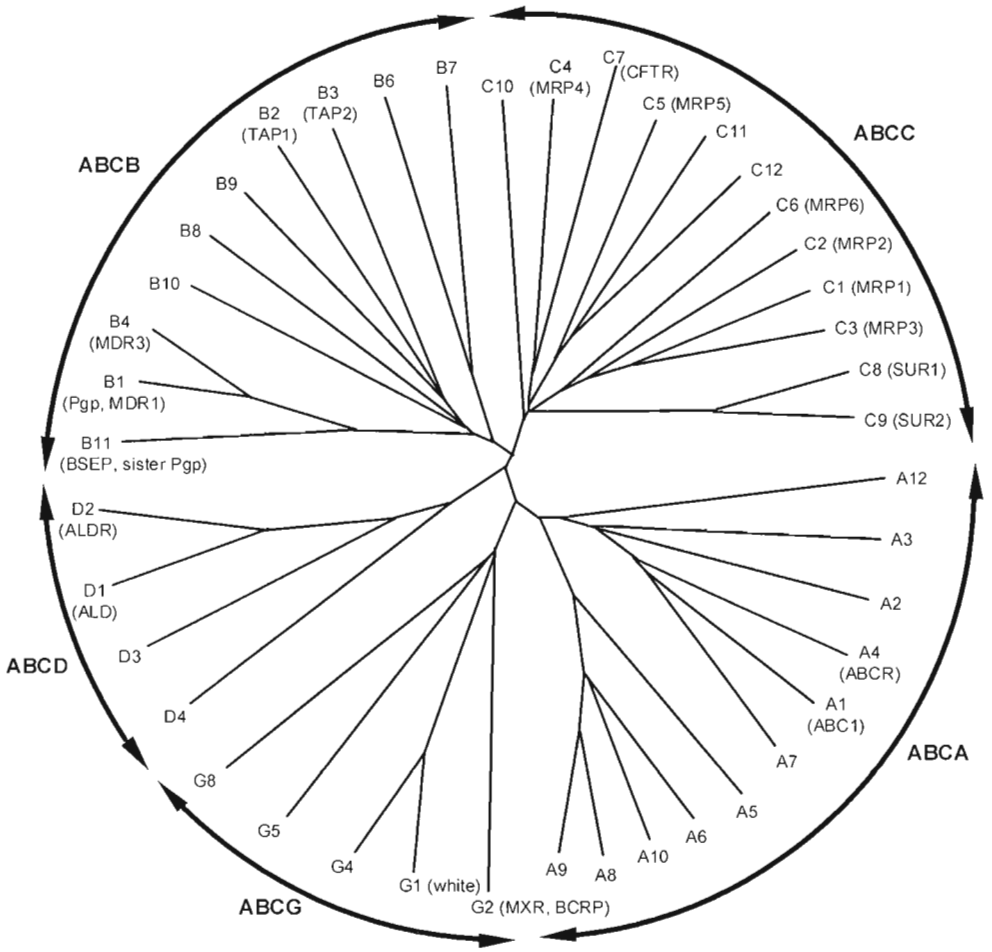

Fig. 1. Phylogenetic tree of the human ATP-Binding Cassette (ABC) transporter proteins. On the basis of sequence homology, ABC proteins are classified into seven subfamilies, among which ABCA, ABCB, ABCC, ABCD and ABCG contain the transporter proteins.

there are three ABC transporters, which have definitely been demonstrated to participate in the multidrug resistance of tumors: the P-glycoprotein (MDR1, ABCB1), the multidrug resistance-associated protein 1 (MRP1, ABCC1), and the recently identified, mitoxantrone resistance protein (MXR/BCRP, ABCG2) [9, 10]. In addition, some other human ABC proteins are able to transport a wide variety of therapeutic agents, they may participate in selected cases of multidrug resistance. These include MDR3 (ABCB4) and sister Pgp or BSEP (ABCB11), and several other members of the MRP subfamily (e.g. MRP2 or ABCC2). These transporters are the prime suspects in unexplained cases of multidrug resistance, although proof of their contribution to clinical drug resistance is still missing [for review see [11]].

3. Overview of the members of the MRP family

ABC transporters, belonging to the multidrug resistance-associated protein (MRP) family, have been identified in various species including man, nematodes, yeast, and plants. The human MRP family

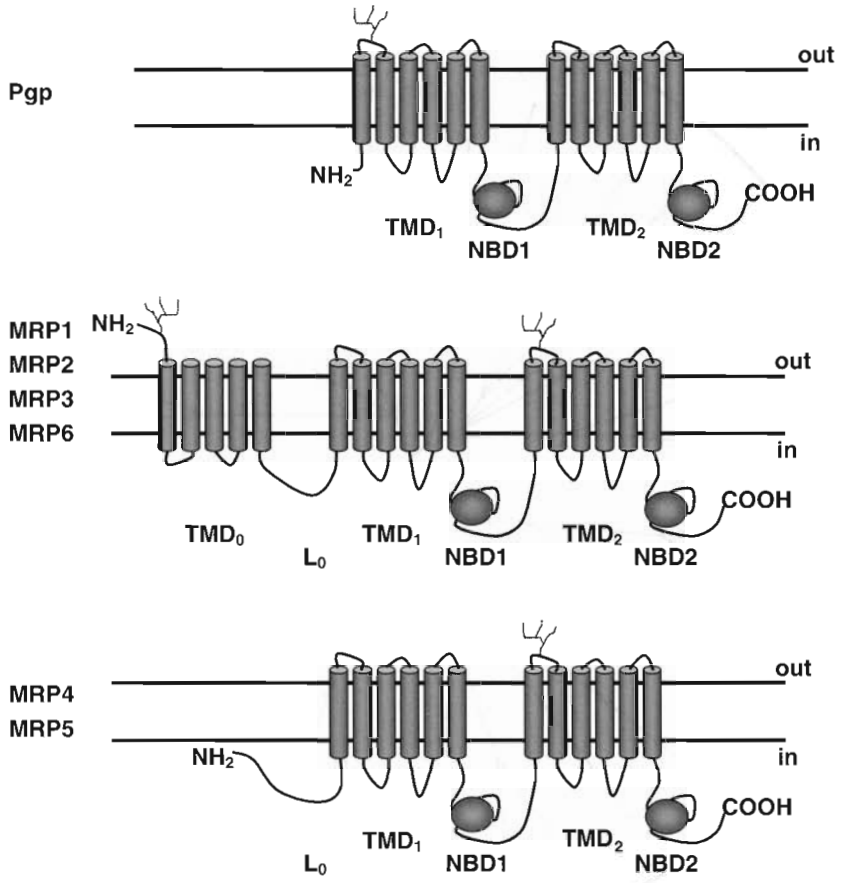

Fig. 2. Comparison of the two-dimensional membrane topology models for P-glycoprotein (Pgp) and various multidrug resistance-associated proteins (MRPs). In addition to the Pgp-like core structure, most MRPs have an extra N-terminal 5-spanner transmembrane domain (TMD_0) linked by a cytoplasmic loop (L_0). TMD_0 is absent in MRP4 and MRP5.

consists of nine members (ABCC1-6, ABCC10-12). The deduced amino acid sequence lengths range from 1325 amino acids for MRP4 to 1545 amino acids for MRP2. As a hallmark for the ABCC subfamily, MRP family members contains a 13 amino acid long 'deletion' between the Walker A and Walker B motifs of the N-terminal nucleotide binding domain, in comparison to the NBDs of most other ABC transporters.

Although the drug-profiles of multidrug resistance caused by MRP1 and P-glycoprotein (MDR1) seem to be similar, suggesting comparable substrate specificity, these two transport proteins share only 15 % amino acid identity. In addition to the typical, MDR-like core structure consisting of two six-spanner transmembrane units and two cytosolic nucleotide-binding domains, MRP1 has an extra N-terminal transmembrane domain containing 5 membrane-spanning helices (TMD_0) (see Fig. 2). The core region and TMD_0 domain are linked by a shorter cytoplasmic loop (L_0) [12]. It has been shown that TMD_0 part of MRP1 is not required for transport activity, but the L_0 linker region is essential for the function of the protein [13]. With regard to membrane topology, MRP2, MRP3, MRP6 and MRP7 are predicted to be similar to MRP1. In contrast, MRP4 and MRP5 are somewhat smaller, they appear to lack the TMD_0, and the identity of these proteins with MRP1 is below 40 %. Nevertheless, MRP4 and MRP5 are more homologous to the other MRPs than to MDR1 or other classes of ABC-transporters. MRP4 and MRP5

Table 1
Tissue distribution and cellular localization of the human multidrug resistance-associated proteins (MRPs)

	tissue distribution	cellular localization in polarized cells
MRP1	ubiquitous (high in lung and testis, low in liver)	basolateral membrane
MRP2	liver, kidney, and gut	apical membrane
MRP3	liver, adrenals, pancreas, kidney, and gut	basolateral membrane
MRP4	prostate, lung, kidney, muscle, pancreas, testis, ovary, bladder, and gall bladder	
MRP5	ubiquitous	
MRP6	liver and kidney	basolateral membrane
MRP7	ubiquitous	
MRP8	ubiquitous	

possess a long cytoplasmic N-terminus that is homologous to the L_0 linker region of MRP1.

Four members of the family: MRP1, MRP5, MRP7 and MRP8 are expressed ubiquitously, although MRP1 expression is elevated in the lung and the testes, and reduced in the liver, whereas a higher expression of MRP5 can be found in the liver. MRP2 (cMOAT) is predominantly expressed in the canalicular membrane of hepatocytes, and the apical membrane of kidney proximal tubule epithelia. MRP3 can be found in the kidney and the intestine, MRP4 is expressed in several tissues including prostate, lung, kidney, muscle, pancreas, testis, ovary, bladder, and gall bladder, whereas MRP6 expression can be predominantly seen in hepatocytes and the kidney. In contrast to Pgp, in polarized cells MRP1 is localized solely in the basolateral membrane domain. It has also been demonstrated that MRP3 and MRP6 exhibit basolateral expression. However, the expression of MRP2 is limited to the apical membrane of polarized cells.

4. MRP family of ATP-dependent conjugate export pumps

MRP1, the first member of the MRP family, has been demonstrated to function as a pump for cytostatic agents (e.g. vincristine, vinblastine, doxorubicin, daunorubicine) with a substrate specificity similar to that seen in the case of P-glycoprotein. However, further functional characterization of the multidrug resistance transporters revealed that the preferred substrates for MRP1 are organic anions, including drugs conjugated to glutathione (GSH), glucoronate, or sulfate, whereas P-glycoprotein favors uncharged or positively charged, hydrophobic compounds. Subsequent studies showed that MRP1 is one of the mysterious glutathione S-conjugate pumps transporting endogenous toxic compounds and xenobiotic agents conjugated to GSH out of the cells [14,15]. Typical high-affinity substrates include leukotriene C_4 (LTC_4), bisglucuronosyl bilirubin and 17β-glucuronosyl estradiol. Several other members of the MRP family that have functionally been characterized so far share the property of ATP-dependent export pumps for anionic conjugates and lipophilic anions. Human ABC transporters for which the conjugate transport function has directly been shown include MRP1, MRP2, MRP3, MRP5, and MRP6 [16–19]. Function of MRP-related proteins has been intensively studied in several other species. The non-human transporters for those the ATP-dependent conjugate export pump activity has unambiguously been shown include the murine MRP1 and MRP5, the rat and rabbit MRP2, the yeast cadmium factor 1 (YCF1), and more recently several MRP orthologs in *Arabidopsis* [20]. Studies on *Caenorhabditis elegans* provided indirect evidence for that four MRP-related transporters mediate ATP-dependent glutathione S-conjugate transport in this soil nematode [21].

5. Substrate specificity of conjugate export pumps belonging to the MRP family

The substrate specificity of multidrug resistance-associated proteins has been intensively studied by using inside-out membrane vesicles from cells expressing the recombinant protein at a high level. The detailed functional characterization of the human MRP1, MRP2 and MRP3 revealed that these transporters possess overlapping substrate specificity, but with marked differences in transport kinetics and affinities for various substrates [for review see refs. [16] and [22]]. According to the V_{max}/K_m ratios, the rank order of the most important substrates of the human MRP1 is as follows: $LTC_4 > LTD_4 >$ S-(2,4,-dinitrophenyl) glutathione $> 17\beta$-glucuronyosyl estradiol > monoglucuronosyl bilirubin $> 3\alpha$-sulfatolithocholyl taurine > glutathione disulfide (GSSG). This spectrum of substrates is very similar to that can be found in the case of MRP2 (cMOAT), the ATP-dependent hepatocyte canalicular conjugate export pump. However, MRP1 exhibits a 10-fold higher affinity to leukotriene C_4 (K_m value 0.1 μM), and a 10-fold higher affinity to 17β-glucuronyosyl estradiol (K_m value 1.5 μM) in comparison to MRP2, whereas bilirubin glucuronides are preferably transported by the latter. Since a similar range of conjugates is transported by MRP1 and MRP2, it was expected that MRP2 would also be able to mediate the transport of cytostatic agents that are MRP1 substrates. Studies on transfected cells overexpressing MRP2 provided evidence for the ability of this transporter to expell several anti-cancer drugs including methotrexate, vinblastine, etoposide and cisplatine. However, no connection between the expression of MRP2 and clinical multidrug resistance has ever been demonstrated. Despite the overlapping substrate specificity of MRP1 and MRP2, the differences in transport kinetic properties, tissue distribution and cellular localization confer distinctive functions for them.

Studies have shown that MRP3, which exhibits a similar tissue distribution as MRP2, but differs in cellular localization (i.e. MRP3 resides in the basolateral membrane of polarized cells) also functions as an ATP-dependent conjugate export pump [23]. In contrast to MRP1 and MRP2, this transporter prefers glucuronate conjugates over glutathione conjugates, which are relatively poor substrates. However, the K_m value for 17β-glucuronyosyl estradiol was found to be around 70 μM, that is, almost 10-fold higher than in the case of MRP2. This observation suggests that MRP3 serves as a basolateral overflow system in hepatocytes for the elimination of toxic agents when the MRP2-mediated canalicular secretion is impaired. A detailed analysis using recombinant human MRP3 in membrane vesicles is in progress. The results obtained from this study will make possible a more specific comparison between the substrate specificity of different MRPs.

The human MRP4, MRP5 and MRP6 have only partially been characterized. An interesting finding revealed, however, that MRP4 can function as an efflux pump for several nucleoside analogues, including drugs that are used against the human immunodeficiency virus such as 9-(2-phosphonylmethoxyethyl) adenine (PMEA) and azidothymidine monophosphate (AZTMP). 9-(2-phosphonylmethoxyethyl) guanine (PMEG), a compound with some neoplastic activity has also been proposed as substrate for this transport protein [24]. A recent study has also demonstrated MRP4-mediated transport of cyclic nucleotides (cAMP, cGMP), methotrexate and 17β-glucuronyosyl estradiol [25]. It has been suggested that MRP4 residing in the apical membrane of the kidney proximal tubules is responsible for the urinary efflux of cAMP and cGMP. Similar to MRP4, MRP5 also appears to be a nucleoside analogue pump, conferring drug resistance to PMEA and thiopurines such as 6-mercaptopurine and thioguanine, drugs that are used in the treatment of acute lymphoblastic leukemia (ALL) and acute myeloid leukemia (AML) [17]. However, glutathione conjugate transport mediated by MRP5 has been demonstrated. There has been a controversy in the literature over whether MRP5 can confer drug-resistance to heavy metals.

Recently, functional studies on the MRP6, the mutation of which causes pseudoxanthoma elasticum (PXE), a rare heritable disorder resulting in the calcification of elastic fibers, has been published. It has

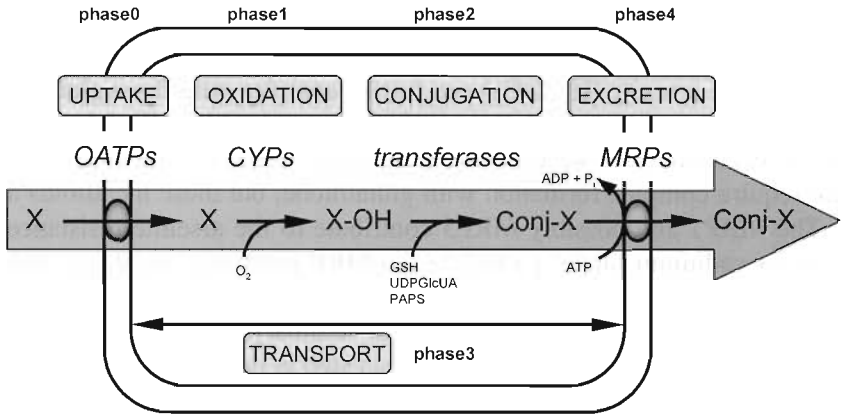

Fig. 3. Detoxification of endogenous substances and xenobiotics. Conjugates with glutathione, glucuronate, or sulfate are expelled by ATP-dependent transport mediated by members of the MRP family.

been demonstrated that MRP6 can also mediate the transport of glutathione conjugates, i.e. LTC_4, and N-ethylmaleimide S-glutathione [18,19].

6. Role of MRP isoforms in detoxification

In addition to the contribution of MRP1 (and possibly MRP2) to the clinical multidrug resistance, members of the MRP family have an important physiological role in detoxification. Elimination of endogenous and exogenous lipophilic toxic substances takes place by a multi-step process. The sequence of detoxification comprises the cellular uptake of these compounds (phase 0), followed by an oxidation step (phase 1), conjugation with an anionic group, i.e. glutathione, glucuronate or sulfate (phase 2), transcellular transport (phase3), and ATP-dependent cellular extrusion of the conjugates (phase 4) [26]. It has been demonstrated that numerous transport proteins belonging to the MRP-family are able to mediate the sequestration of S-conjugates, and contribute to the terminal excretion of lipophilic toxic compounds.

The importance of MRP isoforms in the process of detoxification becomes apparent in the mild liver disease, Dubin-Johnson syndrome, an autosomal recessively inherited disorder characterized by conjugated hyperbilirubinemia and pigment deposition in the liver. Several mutations in the *MRP2* gene have been shown to associate with the absence of the MRP2 protein in the canalicular membrane of the hepatocytes. The lack of MRP2 results in deficient transport of monoglucuronosyl and bisglucuronosyl bilirubin, as well as other anionic conjugates from hepatocytes into bile [27]. The vital importance of MRPs in detoxification and cellular homeostasis is also exemplified by studies in two rat strains, which have been considered as animal models of the human Dubin-Johnson syndrome, the GY/TR- mutant and the Eisai hyperbilirubinemic rat (EHBR). These mutant animals, which lack MRP2 in the hepatocyte canalicular membrane, are unable to sequestrate endogenous metabolites into bile [28–30]. This dysfunction results in the cellular accumulation of the conjugates in the hepatocytes, and a subsequent overflow across the basolateral membrane into the blood. The latter transport step is most probably mediated by MRP3 [31]. Finally, these animals eliminate the LTC_4 metabolites via renal excretion. Since several members of the MRP family are redundantly present in most cells, in addition to the specialized role of MRP2 in the hepatic function, these proteins seem to prevent the intracellular accumulation of conjugates, contributing to the defense mechanism against lipophilic toxic compounds.

Several members of the MRP family may participate in the detoxification of heavy metals, e.g. arsenite, antimony, and cadmium. The proposed mechanism for the cellular removal of these heavy metals also involves glutathione. Since arsenite (H_3AsO_3) can form a complex with three glutathione molecules, it has earlier been proposed that the glutathione complex of arsenite [$As(SG)_3$] is sequestrated by these transport proteins. A recent study, however, demonstrated that MRP1-mediated transport of arsenic and antimony does not require complex formation with glutathione, but these metalloids are cotransported with GSH [32]. The MRP1 and possibly MRP5 contribute to the arsenite resistance in humans [33, 34], whereas the yeast cadmium factor 1 (YCF1), an MRP orthologs in yeast, confers resistance to cadmium [35]. The MRP-related transporters of the soil nematode, *Caenorhabditis elegans* participate in the detoxification of cadmium and arsenite [21]. In summary, the ATP-dependent MRP-mediated export of conjugates represents an indispensable terminal step in detoxification.

6.1. Role of MRP family members in cellular GSH release

Overexpression of MRP1 or MRP2 in cells confers resistance to Vinca alkaloids and anthracyclines. These molecules are weak organic bases, and are not known to be conjugated to acidic ligands in human cells. However, the MRP1-mediated drug resistance was proven to be dependent on cellular GSH level. In addition, vesicular transport measurements have demonstrated that transport of vincristine, vinblastine, and daunorubicine requires the presence of reduced GSH. The most plausible explanation for these findings is that GSH serves as a co-substrate, and the drugs are co-transported with reduced glutathione [11]. This hypothesis is further supported by the observation that elevated MRP1 expression in tumors is often accompanied by increased expression of γ-glutamylcysteine syntetase [36]. Similar mechanism was proposed for the MRP-dependent transport of aflatoxin B1 [37].

ATP-dependent low affinity transport of GSH has also been demonstrated in yeast. This release of GSH involves the MRP-like transporter, YCF1 [38]. Similarly, the human MRP2 has been proposed to act as a low affinity export pump for the release of GSH across the canalicular membrane into the bile [39]. However, it is not possible to discriminate between the transport of GSH from an MRP2-mediated cotransport of GSH together with an unidentified endogenous substrate. Interestingly, reduced GSH transport mediated by MRP3 has not been observed [40]. It should be noted that additional, non-MRP-like transport proteins involved in cellular GSH release are present in both canalicular and sinusoidal membranes of the hepatocytes. An interesting member of this group is the organic anion transporter OATP1, an antiporter, which resides in the sinusoidal membrane of hepatocytes, and mediates simultanous release of GSH and uptake of hydrophobic S-conjugates such as leukotriene C_4 from the blood into cells [41].

6.2. Defense against oxidative stress

The defense machinery that abolishes the elevated level of hydroperoxides under condition of oxidative stress includes GSH peroxidase, producing glutathione disulfide (GSSG), and GSSG reductase, eliminating the increased level of GSSG (see Fig. 4) [42]. Release of GSSG can also be observed in several cell types and tissues in response to external addition of hydroperoxides or other conditions causing oxidative stress. This finding suggest the existence of an overflow mechanism for the elimination of elevated GSSG level [43]. Since MRP1 and MRP2 are able to transport GSSG with low-affinity, these transporters appear to play crucial role in the control of the intracellular GSSG level, when the activity of GSSG reductase becomes rate limiting. This hypothesis is further supported by the observation that oxidative stress induces elevation in the MRP1 expression in cultured cells [44].

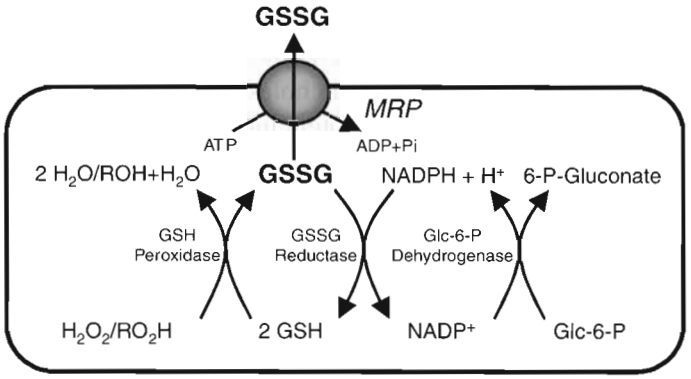

Fig. 4. Contribution of members of the MRP-family to the defense mechanism against oxidative stress. MRP1 and MRP2 are low affinity transporters for glutathione disulfide (GSSG). Under condition of oxidative stress, when the activity GSSG reductase becomes rate-limiting, MRPs expel GSSG from the cells, compensating the oxidative burden.

6.3. Outlook

Detailed characterization of the transport properties of MRP1 has established the link between membrane transport proteins and the GSH system, previously associated with the clinical resistance to a wide range of anticancer drugs. However, it still remains to be answered whether other members of the MRP family with similar substrate specificity, e.g. MRP2 and MRP3, actually contribute to the clinical multidrug resistance of cancer.

The human MRP4, MRP5 and MRP6 have only partially been characterized. A detailed analysis, using inside-out membrane vesicles from cells expressing the recombinant proteins at a high level, can provide further information on substrate specificity and transport kinetics of these transporters. The characterization of the new additions of the MRP family, MRP7, MRP8 and MRP9 is in progress. Further studies are also needed on non-human MRP orthologs and their role in drug resistance and detoxification of xenobiotics.

Numerous controversial issues with regard to transport processes mediated by the members of the MRP family remain to be answered. These include the contribution of MRPs to clinical methotrexate resistance, the cisplatine [$(NH_3)_2PtCl_2$] resistance associated with increased MRP2 level [45], the mechanism of MRP2-mediated reduced GSH release from the hepatocytes into bile [40], and the role of MRP5 in heavy metal resistance [34]. One of the greatest challenges for future research is elucidating the physiological function of several partially characterized members of the MRP family, such as MRP4, MRP5, and MRP6. Finding the link between the mutations in the genes encoding MRPs and the impaired physiological functions associated with these mutations represents an especially intriguing scientific problem with relevant clinical aspects.

Regulation processes of MRP family members are also subject of ongoing research. It has been demonstrated that p53 suppresses the transcription of MRP1 by diminishing the effect of the transcription activator SP1 [46]. This finding can elucidate the MRP1 upregulation by the loss of p53, as it often occurs in tumors. Further studies are required, however, to identify the regulatory sequences of MRP1 gene involved in this process as well as in the upregulation of MRP1 expression in response to oxidative stress [44]. Similarly, the mechanism of transcriptional upregulation of MRP3 in the MRP2-deficient rat strain (EHBR) and in patients with Dubin-Johnson syndrome still remains to be disclosed [27,47].

The protein sorting to the plasma membrane (routing process) represents an important component of the regulation of MRP expression, and has become an intensively studied issue of this research field.

The cellular localization of various MRP isoforms greatly influences their function. This is exemplified by the intracellular retention of MRP2 observed in certain cases of Dubin-Johnson syndrome and by the endocytic retrieveal of MRP2 in endotoxin-induced cholestasis [27,48]. Since it has been postulated the regulatory function of CFTR involves protein protein interactions [49,50], the potential involvement of such interactions in the function and posttranslational regulation of MRP family members is another intriguing issue.

In conclusion, despite the fact that considerable knowledge on the MRPs has accumulated since 1992, when MRP1 was identified, the growing number of the MRP family members and non-human MRP orthologs, as well as the complexity of the transport mediated by these proteins represent a great challenge for future research.

References

[1] I. Klein, B. Sarkadi and A. Varadi, An inventory of the human ABC proteins, *Biochim. Biophys. Acta* **1461** (1999), 237–262.

[2] M. Dean, Y. Hamon and G. Chimini, The human ATP-binding cassette (ABC) transporter superfamily, *J Lipid Res.* **42** (2001), 1007–1017.

[3] M.F. Rosenberg, R. Callaghan, R.C. Ford and C.F. Higgins, Structure of the multidrug resistance P-glycoprotein to 2.5 nm resolution determined by electron microscopy and image analysis, *J. Biol. Chem.* **272** (1997), 10685–10694.

[4] G. Chang and C.B. Roth, Structure of MsbA from E. coli: a homolog of the multidrug resistance ATP binding cassette (ABC) transporters, *Science* **293** (2001), 1793–1800.

[5] K. Kunzelmann and R. Schreiber, CFTR, a regulator of channels, *J. Membr. Biol.* **168** (1999), 1–8.

[6] C.F. Higgins, ABC transporters: from microorganisms to man, *Ann. Rev. Cell Biol.* **8** (1992), 67–113.

[7] M.M. Gottesman and I. Pastan, Biochemistry of multidrug resistance mediated by the multidrug transporter, *Annu. Rev. Biochem.* **62** (1993), 385–427.

[8] M.M. Gottesman, T. Fojo and S.E. Bates, Multidrug resistance in cancer: role of ATP-dependent transporters, *Nat. Rev. Cancer* **2** (2002), 48–58.

[9] S.E. Bates, R. Robey, K. Miyake, K. Rao, D.D. Ross and T. Litman, The role of half-transporters in multidrug resistance, *J. Bioenerg. Biomembr.* **33** (2001), 503–511.

[10] T. Litman, T.E. Druley, W.D. Stein, S.E. Bates, From MDR to MXR: new understanding of multidrug resistance systems, their properties and clinical significance, *Cell. Mol. Life. Sci.* **58** (2001), 931–959.

[11] P. Borst, R. Evers, M. Kool and J. Wijnholds, A family of drug transporters: the multidrug resistance-associated proteins, *J. Natl. Cancer Inst.* **92**(16) (2000), 1295–1302.

[12] E. Bakos, R. Evers, G. Calenda, G.E. Tusnady, G. Szakacs, A. Varadi and B. Sarkadi, Characterization of the amino-terminal regions in the human multidrug resistance protein (MRP1), *J. Cell Sci.* **113** (2000), 4451–4461.

[13] E. Bakos, T. Hegedus, Zs. Hollo, E. Welker, G.E. Tusnady, G.J. Zaman, M.J. Flens, A. Varadi and B. Sarkadi, Membrane topology and glycosylation of the human multidrug resistance-associated protein, *J. Biol. Chem.* **271**(21) (1996), 12322–12326.

[14] M. Müller, C. Meijer, G.J. Zaman, P. Borst, R.J. Scheper, N.H. Mulder, E.G. de Vries and P.L. Jansen, Overexpression of the gene encoding the multidrug resistance-associated protein results in increased ATP-dependent glutathione S-conjugate transport, *Proc. Natl. Acad. Sci.* USA, **91**(26) (1994), 13033–13037.

[15] G. Jedlitschky, I. Leier, U. Buchholz, K. Barnouin, G. Kurz and D. Keppler, Transport of glutathione, glucuronate, and sulfate conjugates by the MRP gene-encoded conjugate export pump, *Cancer Res.* **56**(5) (1996), 988–994.

[16] D. Keppler, Export pumps for glutathione S-conjugates, *Free Radic. Biol. Med.* **27** (9–10) (1999), 985–991.

[17] J. Wijnholds, C.A. Mol, L. van Deemter, M. de Haas, G.L. Scheffer, F. Baas, J.H. Beijnen, R.J. Scheper, S. Hatse, E. De Clercq, J. Balzarini and P. Borst, Multidrug-resistance protein 5 is a multispecific organic anion transporter able to transport nucleotide analogs, *Proc. Natl. Acad. Sci.* USA, **97**(13) (2000), 7476–7481.

[18] A. Ilias, Z. Urban, T.L. Seidl, O. Le Saux, E. Sinko, C.D. Boyd, B. Sarkadi and A. Varadi, Loss of ATP-dependent transport activity in pseudoxanthoma elasticum-associated mutants of human ABCC6(MRP6), *J. Biol. Chem.* **277** (2002), 16860–16867.

[19] M.G. Belinsky, Z-S. Chen, I. Shchaveleva, H. Zeng and G.D. Kruh, Characterization of the drug resistance and transport properties of multidrug resistance protein 6 (MRP6, ABCC6), *Cancer Research* **62** (2002), 6172–6177.

[20] P.A. Rea, Z.-S. Li, Y.-P. Lu, Y.M. Drozdowicz and E. Martinoia, From vaculoar GS-X pumps to multispecific ABC-transporters, *Annu. Rev. Plant Physiol. Plant Mol. Biol.* **49** (1998), 727–760.

[21] A. Broeks, B. Gerrard, R. Allikmets, M. Dean and R.H. Plasterk, Homologues of the human multidrug resistance genes MRP and MDR contribute to heavy metal resistance in the soil nematode Caenorhabditis elegans, *EMBO J.* **15**(22) (1996), 6132–6143.
[22] J. König, A.T. Nies, Y. Cui, I. Leier and D. Keppler, Conjugate export pumps of the multidrug resistance protein (MRP) family: localization, substrate specificity, and MRP2-mediated drug resistance, *Biochim. Biophys. Acta.* **1461**(2) (1999), 377–394.
[23] T. Hirohashi, H. Suzuki and Y. Sugiyama, Characterization of the transport properties of cloned rat multidrug resistance-associated protein 3 (MRP3), *J. Biol. Chem.* **274**(21) (1999), 15181–15185.
[24] J.D. Schuetz, M.C. Connelly, D. Sun, S.G. Paibir, P.M. Flynn, R.V. Srinivas, A. Kumar and A. Fridland, MRP4: A previously unidentified factor in resistance to nucleoside-based antiviral drugs, *Nat. Med.* **5**(9) (1999), 1048–1051.
[25] R.A. van Aubel, P.H. Smeets, J.G. Peters, R.J. Bindels and F.G. Russel, The MRP4/ABCC4 gene encodes a novel apical organic anion transporter in human kidney proximal tubules: putative efflux pump for urinary cAMP and cGMP, *J. Am. Soc. Nephrol.* **13**(3) (2002), 595–603.
[26] T. Ishikawa, The ATP-dependent glutathione S-conjugate export pump, *Trends. Biochem. Sci.* **17**(11) (1992), 463–468.
[27] C.C. Paulusma, M. Kool, P.J. Bosma, G.L. Scheffer, F. ter Borg, R.J. Scheper, G.N. Tytgat, P. Borst, F. Baas and R.P. Oude Elferink, A mutation in the human canalicular multispecific organic anion transporter gene causes the Dubin-Johnson syndrome, *Hepatology* **25**(6) (1997), 1539–1542.
[28] C.C. Paulusma, P.J. Bosma, G.J. Zaman, C.T. Bakker, M. Otter, G.L. Scheffer, R.J. Scheper, P. Borst and R.P. Oude Elferink, Congenital jaundice in rats with a mutation in a multidrug resistance-associated protein gene, *Science* **271**(5252) (1996), 1126–1128.
[29] M. Büchler, J. König, M. Brom, J. Kartenbeck, H. Spring, T. Horie and D. Keppler, cDNA cloning of the hepatocyte canalicular isoform of the multidrug resistance protein, cMrp, reveals a novel conjugate export pump deficient in hyperbilirubinemic mutant rats, *J. Biol. Chem.* **271**(25) (1996), 15091–15098.
[30] K. Ito, H. Suzuki, T. Hirohashi, K. Kume, T. Shimizu and Y. Sugiyama, Molecular cloning of canalicular multispecific organic anion transporter defective in EHBR, *Am. J. Physiol.* **272** (1997), G16–22.
[31] J. König, D. Rost, Y. Cui and D. Keppler, Characterization of the human multidrug resistance protein isoform MRP3 localized to the basolateral hepatocyte membrane, *Hepatology* **29**(4) (1999), 1156–1163.
[32] M. Salerno, M. Petroutsa and A. Garnier-Suillerot, The MRP1-mediated effluxes of arsenic and antimony do not require arsenic-glutathione and antimony-glutathione complex formation, *J. Bioenerg. Biomembr.* **34**(2) (2002), 135–145.
[33] G.J. Zaman, J. Lankelma, O. van Tellingen, J. Beijnen, H. Dekker, C. Paulusma, R.P. Oude Elferink, F. Baas and P. Borst, Role of glutathione in the export of compounds from cells by the multidrug-resistance-associated protein, *Proc. Natl. Acad. Sci.* USA, **92**(17) (1995), 7690–7694.
[34] M.A. McAleer, M.A. Breen, N.L. White and N. Matthews, pABC11 (also known as MOAT-C and MRP5), a member of the ABC family of proteins, has anion transporter activity but does not confer multidrug resistance when overexpressed in human embryonic kidney 293 cells, *J. Biol. Chem.* **274**(33) (1999), 23541–23548.
[35] Z.S. Li, M. Szczypka, Y.P. Lu, D.J. Thiele and P.A. Rea, The yeast cadmium factor protein (YCF1) is a vacuolar glutathione S-conjugate pump, *J. Biol. Chem.* **271**(11) (1996), 6509–6517.
[36] M.T. Kuo, S. Sen, W.N. Hittelman and T.C. Hsu, Chromosomal fragile sites and DNA amplification in drug-resistant cells, *Biochem. Pharmacol.* **56**(1) (1998), 7–13.
[37] D.W. Loe, R.K. Stewart, T.E. Massey, R.G. Deeley and S.P. Cole, ATP-dependent transport of aflatoxin B1 and its glutathione conjugates by the product of the multidrug resistance protein (MRP) gene, *Mol. Pharmacol.* **51**(6) (1997), 1034–1041.
[38] J.F. Rebbeor, G.C. Connolly, M.E. Dumont and N. Ballatori, ATP-dependent transport of reduced glutathione on YCF1, the yeast orthologue of mammalian multidrug resistance associated proteins, *J. Biol. Chem.* **273**(50) (1998), 33449–33454.
[39] C.C. Paulusma, M.A. van Geer, R. Evers, M. Heijn, R. Ottenhoff, P. Borst and R.P. Oude Elferink, Canalicular multispecific organic anion transporter/multidrug resistance protein 2 mediates low-affinity transport of reduced glutathione, *Biochem. J.* **338**(Pt 2) (1999), 393–401.
[40] M. Kool, M. van der Linden, M. de Haas, G.L. Scheffer, J.M. de Vree, A.J. Smith, G. Jansen, G.J. Peters, N. Ponne, R.J. Scheper, R.P. Elferink, F. Baas and P. Borst, MRP3, an organic anion transporter able to transport anti-cancer drugs, *Proc. Natl. Acad. Sci.* USA, **96**(12) (1999), 6914–6919.
[41] L. Li, T.K. Lee, P.J. Meier and N. Ballatori, Identification of glutathione as a driving force and leukotriene C4 as a substrate for oatp1, the hepatic sinusoidal organic solute transporter, *J. Biol. Chem.* **273**(26) (1998), 16184–16191.
[42] H. Sies, Intracellular effect of glutathione conjugates and their transport from cells, in: *Glutathione conjugation: mechanisms and biological significance*, H. Sies and B. Ketterer eds, Academic Press, London, 1988, pp. 175–192.
[43] T.P. Akerboom, M. Bilzer and H. Sies, The relationship of biliary glutathione disulfide efflux and intracellular glutathione disulfide content in perfused rat liver, *J. Biol. Chem.* **257**(8) (1982), 4248–4252.

[44] Y. Yamane, M. Furuichi, R. Song, N.T. Van, R.T. Mulcahy, T. Ishikawa and M.T. Kuo, Expression of multidrug resistance protein/GS-X pump and gamma-glutamylcysteine synthetase genes is regulated by oxidative stress, *J. Biol. Chem.* **273**(47) (1998), 31075–31085.

[45] T. Ishikawa, C.D. Wright and H. Ishizuka, GS-X pump is functionally overexpressed in cis-diamminedichloroplatinum (II)-resistant human leukemia HL-60 cells and down-regulated by cell differentiation, *J. Biol. Chem.* **269**(46) (1994), 29085–29093.

[46] Q. Wang and W.T. Beck, Transcriptional suppression of multidrug resistance-associated protein (MRP) gene expression by wild-type p53, *Cancer Res.* **58**(24) (1998), 5762–5769.

[47] T. Hirohashi, H. Suzuki, K. Ito, K. Ogawa, K. Kume, T. Shimizu and Y. Sugiyama, Hepatic expression of multidrug resistance-associated protein-like proteins maintained in eisai hyperbilirubinemic rats, *Mol. Pharmacol.* **53**(6) (1998), 1068–1075.

[48] M. Trauner, M. Arrese, C.J. Soroka, M. Ananthanarayanan, T.A. Koeppel, S.F. Schlosser, F.J. Suchy, D. Keppler and J.L. Boyer, The rat canalicular conjugate export pump (Mrp2) is down-regulated in intrahepatic and obstructive cholestasis, *Gastroenterology* **113**(1) (1997), 255–264.

[49] R. Schreiber, A. Hopf, M. Mall, R. Greger and K. Kunzelmann, The first-nucleotide binding domain of the cystic-fibrosis transmembrane conductance regulator is important for inhibition of the epithelial Na+ channel, *Proc. Natl. Acad. Sci. USA.* **96**(9) (1999), 5310–5315.

[50] D.B. Short, K.W. Trotter, D. Reczek, S.M. Kreda, A. Bretscher, R.C. Boucher, M.J. Stutts and S.L. Milgram, An apical PDZ protein anchors the cystic fibrosis transmembrane conductance regulator to the cytoskeleton, *J. Biol. Chem.* **273**(31) (1998), 19797–19801.

13. sz. közlemény

dc_46_10

Pflugers Arch - Eur J Physiol (2007) 453:621–641
DOI 10.1007/s00424-006-0160-8
dc_46_10

INVITED REVIEW

Portrait of multifaceted transporter, the multidrug resistance-associated protein 1 (MRP1/ABCC1)

Éva Bakos · László Homolya

Received: 2 January 2006 / Revised: 10 May 2006 / Accepted: 24 May 2006 / Published online: 23 December 2006

Abstract MRP1 (ABCC1) is a peculiar member of the ABC transporter superfamily for several aspects. This protein has an unusually broad substrate specificity and is capable of transporting not only a wide variety of neutral hydrophobic compounds, like the MDR1/P-glycoprotein, but also facilitating the extrusion of numerous glutathione, glucuronate, and sulfate conjugates. The transport mechanism of MRP1 is also complex; a composite substrate-binding site permits both cooperativity and competition between various substrates. This versatility and the ubiquitous tissue distribution make this transporter suitable for contributing to various physiological functions, including defense against xenobiotics and endogenous toxic metabolites, leukotriene-mediated inflammatory responses, as well as protection from the toxic effect of oxidative stress. In this paper, we give an overview of the considerable amount of knowledge which has accumulated since the discovery of MRP1 in 1992. We place special emphasis on the structural features essential for function, our recent understanding of the transport mechanism, and the numerous assignments of this transporter.

É. Bakos
Institute of Enzymology, Hungarian Academy of Sciences,
Karolina út 29-31,
1113 Budapest, Hungary

L. Homolya (✉)
Membrane Research Group for Membrane
Biology and Immunopathology,
Hungarian Academy of Sciences, National Medical Center,
Diószegi u. 64,
1113 Budapest, Hungary
e-mail: homolya@biomembrane.hu

Keywords ABC transporter · Xenobiotic transport · Multispecific organic anion transporter · Multidrug resistance · Cancer drug resistance · Glutathione conjugates · Detoxification

Abbreviations

ABC	ATP-binding cassette transporters
MDR	multidrug resistance
MRP1	multidrug resistance-associated protein 1 (ABCC1), ABCC-type protein
ABCC	C subfamily of ATP-binding cassette transporters
MDR1	multidrug resistance protein 1 (P-glycoprotein, ABCB1), ABCB-type protein
MDR3	multidrug resistance protein 3 (ABCB4), ABCB-type protein
MRP2	multidrug resistance-associated protein 2 (cMOAT, ABCC2), ABCC-type protein
sPgp	sister-P-glycoprotein (BSEP, ABCB11), ABCB-type protein
CFTR	cystic fibrosis transmembrane conductance regulator (ABCC7), ABCC-type protein
SUR	sulfonylurea receptor (ABCC8 and ABCC9), ABCC-type protein
ABCG2	multidrug transporter (breast cancer resistance protein, MXR/BCRP/ABCP)
NBD	nucleotide-binding domain, ABC domain
TMD	transmembrane domain
TMH	transmembrane helix
MOAT	multispecific organic anion transporter
LTA_4-D_4	leukotriene A_4-D_4
GSH	reduced glutathione
GSSG	glutathione disulfide
GS-X	glutathione conjugate

$E_2$17βG	estradiol-17-β-D-glucuronide
NNAL	4-(methylnitrosamino)-1-(3-pyridyl)-1-butanol
ALLN	*N*-acetyl-leucinyl-leucinyl-norleucinal
VP-16	etoposide
AML	acute myeloblastic leukemia
ALL	acute lymphoblastic leukemia
CLL	chronic lymphoblastic leukemia
SCLC	small-cell lung cancer
NSCLC	nonsmall-cell lung cancer
LRP/MVP	lung resistance-related protein, major vault protein
CYP	cytochrome P450
AM	acetoxy methyl ester
MK571	inhibitor of MRP1, MRP2, MRP4, and MRP7; LTD_4 receptor antagonist
Nrf2	nuclear factor-E2 p45-related factor
Ycf1	yeast cadmium factor-1
Kir6.2	inwardly rectifying K^+ channel
MJ0796	*Methanococcus jannaschii* hypothetical ABC transporter
HlyB	*Escherichia coli* hemolysin transporter
MalK	ATP-hydrolyzing subunit of the *Escherichia coli* maltose transporter
Rad50	*Pyrococcus furiosus* DNA repair ABC ATPase
BtuCD	*Escherichia coli* vitamin B_{12} importer
MsbA	*Salmonella typhimurium* lipid A transporter
PKC	protein kinase C
ROS	reactive oxygen species
γ-GCSh	γ-glutamylcysteine synthetase heavy subunit

Introduction

Multidrug resistance (MDR) is a major impediment to successful chemotherapy of cancer. The MDR phenotype is frequently associated with the overexpression of the MDR1/P-glycoprotein, which was identified as an active drug-extruding transporter with a broad substrate specificity. This distinctive feature of this drug pump explained the cross-resistance to a series of structurally and functionally unrelated anticancer agents. However, numerous unexplained cases of MDR phenotype implicated the existence of other mechanisms for MDR. Identification of the multidrug resistance protein 1 (MRP1, also denoted as ABCC1) in 1992 [24], and its initial characterization, elucidated that this protein indeed represents an alternative drug pump. The *MRP1* gene maps to chromosome 16p13.1 and encodes for a protein of 1,531 amino acids. Sequence analysis identified MRP1 as a member of the ATP-binding cassette (ABC) superfamily, to which the MDR1/P-glycoprotein also belongs. MRP1 is an integral membrane glycophosphoprotein with an apparent molecular weight of 190 kDa [3, 41] and functions as a primary active transporter utilizing the energy of ATP binding/hydrolysis [25, 181]. The transport activity of MRP1, similar to that of other ABC transporters, is characterized by vanadate sensitivity and lack of a phosphorylated intermediate. Like MDR1/P-glycoprotein, MRP1 also possesses a broad substrate specificity and can confer resistance to a wide variety of anticancer agents in tumor cell lines [25, 45, 181].

Subsequent analysis of MRP1 revealed that, in contrast to MDR1/P-glycoprotein, MRP1 also transports organic anions such as compounds conjugated to glutathione, glucuronate, or sulfate [60, 80, 102]. Following this perception, MRP1 has been identified as one of the elusive multispecific organic anion transporters (MOATs) or glutathione-conjugate (GS-X) pumps, which were described well before the discovery of MRP1. Since the cellular release of the inflammatory cytokine LTC_4 was attributed to the activity of MOATs, the MRP1 transporter has been proposed to play a role in leukotriene-mediated inflammatory responses [80]. Similarly, efflux of oxidized glutathione (GSSG) from cells during oxidative stress was reported years before the cloning of MRP1. The ability of MRP1 to transport GSSG [79] made this transporter the number one candidate for the GSSG overflow system.

Collectively, with the detailed investigation of MRP1, several previously discovered phenomena, such as non-P-glycoprotein-mediated drug resistance, transport of conjugates, and cellular release of LTC_4 and GSSG, converged and became explainable by the function of a single transporter. Due to its extraordinary transport properties, MRP1 contributes to several physiological functions and pathophysiological incidents.

Structure of MRP1 and the role of the amino-terminal regions

The cDNA encoding MRP1 was first cloned from a doxorubicin-selected, multidrug resistant human lung cancer cell line (H69R) by differential cDNA screening [24]. As mentioned above, on the basis of its primary sequence, MRP1 has been classified into the superfamily of ABC transporters. Thus, it contains characteristic short ATP-binding motifs (Walker A and Walker B) and in-between an additional conserved sequence (ABC signature motif). In addition to sequence homology, ABC proteins share a common molecular architecture: they are composed of the combinations of nucleotide-binding domains (NBDs), which harbor conserved peptide motifs, and transmembrane domains (TMDs), which generally consist of six transmembrane helices (TMHs).

Subsequent to the cloning of MRP1, several MRP-related proteins have been identified and classified into a subfamily. By the systematic classification of the human ABC transporters, the nine human MRPs, together with the cystic fibrosis transmembrane conductance regulator (CFTR) and two sulfonylurea receptors (SURs), form the ABCC subgroup. Accordingly, a systematic name, ABCC1, has been assigned to MRP1. In contrast to other ABC transporters, which exhibit a high similarity between the two NBDs, members of the ABCC subfamily share the peculiarity of "NBD asymmetry", that is, the two NBDs are fairly dissimilar in these proteins. The main difference comes from a small 13-amino-acid-long sequence between the Walker A and the ABC signature motifs, which is present only in the C-terminal NBDs (NBD2) of ABCC proteins. Other ABC proteins contain this "insert" in both NBDs. Other dissimilarities between the two NBDs of the ABCC subfamily members are found in sequences within the ABC signature regions and around the Walker B motifs.

The first sequence analysis of MRP1 indicated that this protein is not a canonical ABC transporter because the predicted membrane topology of the TMDs was peculiar. Although a common TMD1–NBD1–TMD2–NBD2 domain arrangement has been proposed, the N- and C-terminal membrane-bound regions have been described as domains consisting of eight and four TMHs, respectively [24]. This topology model was challenged by limited proteolysis experiments and hydrophobicity analysis; consequently, a revised secondary structure for MRP1 has been proposed independently by two research groups [7, 149]. According to this new topology model, MRP1 has a domain arrangement of TMD0–L0–TMD1–NBD1–TMD2–NBD2, i.e., the ABC transporter "core region" is extended with an N-terminal transmembrane domain (TMD0), which is connected to the core region with a characteristic intracellular linker region (L0). The three membrane-bound regions, TMD0, TMD1, and TMD2, consist of five, six, and another six TMHs, respectively (Fig. 1). Subsequent investigations introducing mutations to the glycosylation sites [49] and inserting hemagglutinin epitopes [67, 68] fully supported the latter membrane topology model. Furthermore, studies using an antibody against the N-terminal 1–18 amino acids also confirmed the extracellular localization of the amino terminus of MRP1 [14].

The first but very limited set of structural data for MRP1 was obtained at 22 Å resolution by electron microscopy of single particles of the purified protein [137]. The MRP1 monomer showed a pentagonal ring around a large pore. This ring exhibits a twofold pseudosymmetry, which may correspond to the core structure consisting of two TMDs and two NBDs. One of the two small dense regions, seen on the external side of the ring, might represent the TMD0 domain.

Although the TMD0 region is characteristic of several members of ABCC family, this domain was found to be dispensable for the function of MRP1. A truncated mutant, which lacks this domain, was functional with respect to transport activity, and similarly to the wild-type protein, localized to the basolateral membrane in polarized cells [6]. On the other hand, certain mutations in TMD0 resulted in significant conformational changes and reduced transport activity [59, 180]. Based on these observations, it has been suggested that certain residues in TMD0 contribute to the maintenance of the correct structure of the protein. Recently, a detailed study investigating the influence of TMD0 on the subcellular localization of MRP1 revealed that, although TMD0 is not essential for basolateral trafficking of MRP1, deletion of the TMD0 region affects the subcellular distribution of the protein [169]. About 50% of truncated protein was found in the recycling endosomes, whereas this was only 20% in the case of the intact MRP1. This finding suggests that TMD0 domain is important for the retention or the recycling of MRP1 to the plasma membrane. It has also been shown that both TMD0 and the remainder of the protein contain routing signals, and TMD0 becomes essential in trafficking when the COOH-terminal region of MRP1 is mutated or truncated [169].

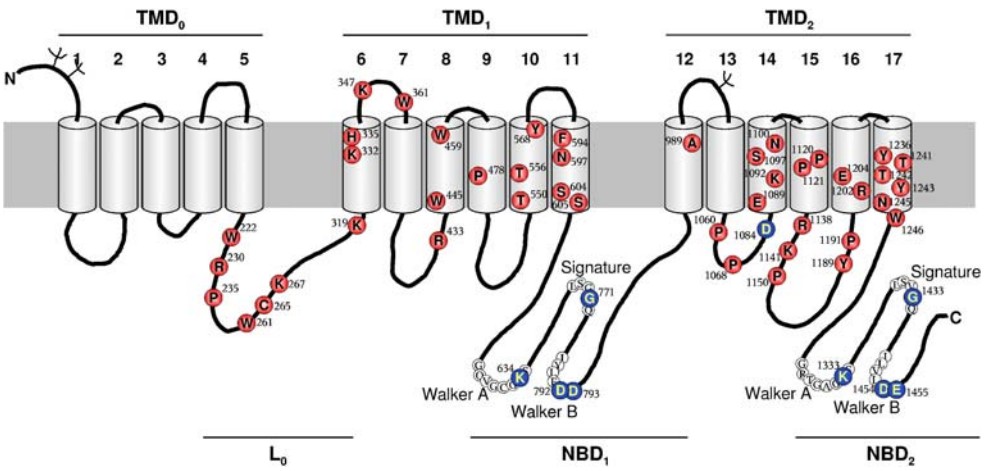

Fig. 1 Membrane topology model of MRP1. The depicted model was constructed on the basis of sequence analysis and the available experimental data (see text for details). *TMD* Transmembrane domain, *NBD* nucleotide-binding domain, *L0* linker region between TMD0 and TMD1. Mutations affecting substrate specificity and catalytic activity are indicated with *red and blue marks*, respectively

It is important to note that the TMD0 domains in other MRP1-related proteins, including the human MRP2 and yeast cadmium factor-1 (Ycf1), are required for correct apical targeting and for proper vacuolar localization, respectively [37, 98]. The TMD0 region of the human SUR1 anchors the protein to Kir6.2 potassium channel subunit. This interaction enhances their trafficking to the cell surface and supports the nucleotide-dependent gating of the channel [22].

In MRP1, the deletion of TMD0, together with the L0 linker region, abrogates the activity of the pump and causes its accumulation in intracellular membranes, indicating that the L0 domain is essential for function and proper trafficking [6]. Coexpression of the L0 peptide with the inactive core region results in restored activity and basolateral targeting of the transporter, suggesting that L0 forms a distinct domain that works in specific interaction with the core region of MRP1 [4]. The region in L0 responsible for the proper basolateral trafficking was mapped between amino acids 208 and 270, whereas the region of L0 required for transport activity falls between amino acids 208 and 260 [170]. Photoaffinity labeling and mutational studies implicated contribution of the L0 region to the formation of substrate-binding site because the L0 region was required for the binding of photoreactive analogs of certain characteristic substrates (see below) [126, 130, 170].

Surprisingly, the isolated L0 peptide, which was predicted to localize in the cytoplasm, was found to be attached to membranes [4]. Despite the relatively low sequence similarity, the proposed secondary structure of the L0 regions seems to be conserved in all members of the ABCC family. In accordance with the secondary structure predictions, the L0 region contains two helices, one of which is a characteristic amphipathic helix. This helix in MRP1 (amino acids 221–233) is responsible for the interaction with cell membranes because elimination of this helix abolishes membrane attachment of L0 [4]. In CFTR, an acidic cluster in the second helix of L0 was shown to interact with the R (regulatory) domain, which controls the channel activity [106]. In the case of MRP1, the nature of the interaction between the L0 linker region and the core structure is yet to be clarified.

Handling of substrates

The substrates of MRP1, identified indirectly by cytotoxicity assays and substrate-stimulated ATPase measurements, as well as directly by cellular and vesicular transport studies, comprise a vast variety of hydrophobic compounds, organic anion conjugates, and anionic nonconjugated substances. Table 1 summarizes the most characteristic substrates of MRP1. The typical conjugate substrates include glutathione, glucuronate, and sulfate conjugates, such as the cysteinyl leukotriene LTC_4 [80, 102], estradiol-17-β-D-glucuronide ($E_2$17βG) [60, 85], estrone 3-sulfate [127], and sulfated bile acids [60]. The ability of MRP1 to transport glutathione conjugates and the expression of this protein in numerous tissues make MRP1 a ubiquitous glutathione-conjugate pump.

MRP1 can confer resistance not only to many commonly used neutral natural product chemotherapeutic agents [25, 45], like MDR1/P-glycoprotein, but also to various anionic compounds, such as the folic acid antimetabolite, methotrexate [52], certain heavy metal oxyanions (arsenical,

Table 1 Selected substrates of human MRP1

Substrates	References
Conjugates	
Endobiotic conjugates	
GSH conjugates	
Leukotriene C_4, leukotriene D_4, leukotriene E_4	[60, 80, 102]
Prostaglandin A_2-SG	[35]
Hydroxynonenal-SG	[132]
Glucuronide conjugates	
Estradiol-17-β-D-glucuronide	[60, 85]
Glucuronosylbilirubin	[61]
Sulfate conjugates	
Estrone 3-sulfate,	[127]
Dehydroepiandrosterone 3-sulfate	[60]
Sulfatolithocholyl taurine	[60]
Xenobiotic conjugates	
GSH conjugates	
Aflatoxin B_1-epoxide-SG	[89]
Chlorambucil-SG, melphalan-SG	[9]
Glucuronide conjugates	
4-(Methylnitrosamino)-1-(3-pyridyl)-1-butanol (NNAL)-*O*-glucuronide	[84]
Therapeutic agents	
Anticancer drugs	
Anthracyclines	
Daunorubicin, doxorubicin	[25, 45, 133]
Plant alkaloids	
Vinblastine, vincristine, SN-38, etoposide	[25, 45, 87]
Others	
Methotrexate	[52]
Antiandrogens (flutamide)	[46]
HIV protease inhibitors	
Saquinavir, ritonavir	[115]
Other compounds	
Metalloids	
Sodium arsenite, potassium antimonite	[25, 58]
Peptides	
GSH, GSSG	[79, 87]
N-acetyl-Leu-Leu-norleucinal (ALLN)	[31]
Fluorescent probes	
Calcein-AM, calcein	[51]
BCECF	[33]

antimonial) [25, 58], and antiandrogens (flutamide) [46]. Contrary to the MDR1/P-glycoprotein, the MRP1-mediated active transport of unmodified chemotherapeutic drugs, as well as that of certain anionic conjugates, requires the presence of glutathione (GSH). The mechanism by which GSH participates in MRP1-mediated efflux is rather complex. The transport of some hydrophobic agents, such as vincristine, is stimulated by GSH, and conversely, these compounds stimulate GSH transport [87]. This cross-stimulation was originally explained by the cotransport of the two compounds, although a recent review by Borst et al. [15] suggests a mechanism of mutual heterotropic cooperativity of substrate-binding sites. On the other hand, glutathione stimulates the transport of certain substrates, but these compounds have no effect on GSH transport. These are exemplified by estrone 3-sulfate, 4-(methylnitrosamino)-1-(3-pyridyl)-1-butanol-*O*-glucuronide (NNAL-*O*-glucuronide), or daunorubicin [84, 127, 133]. In contrast to these substrates, certain compounds, such as verapamil and bioflavonoids, are not transported by MRP1 but they enhance the MRP1-mediated transport of GSH [82, 88].

To identify the regions of MRP1, which are directly involved in substrate binding, photoaffinity labeling studies and mutational analyses have been performed. The GSH-dependent azidoagosterol A labeling of the protein was detected only in TMD2 [130], whereas the azido analogs of GSH and unconjugated drugs, such as rhodamine123, or quinoline, labeled both halves of MRP1, reacting with TMHs 10–11 in TMD1 and TMHs 16–17 in TMD2 [29, 65, 126]. The iodoarylazido analog of LTC_4 labeled the above two regions as well as TMH 12 [66], while the labeling with unmodified LTC_4 showed that the TMHs 6, 7, 10, and 17 are parts of the LTC_4 binding site [176].

As mentioned earlier, the L0 region has also been shown to participate in substrate binding. Removal of the L0 region, together with TMD0, abolished the binding of LTC_4 or a photoaffinity analog of glutathione (azidophenacyl-GSH). The GSH-dependent binding of azidoagosterol A was also eliminated, although direct labeling of the L0 peptide with these compounds could not be demonstrated [126, 130, 170]. In contrast, the binding of azidoaryl derivative of glutathione to the L0 linker region has been detected [65]. Typical substrates, which are transported as glutathione or glucuronide conjugates, e.g., LTC_4 or $E_2$17βG, are not transported by an MRP1 variant mutated in the L0 region (W222L, W223L, R231A, W261A, K267M). In contrast, the transport of an unconjugated substrate (SN38) was not affected in this variant [108]. These observations suggest that L0 participates in the formation of the site interacting with glutathione or glucuronide moieties. A photoaffinity analog of LTC_4 also labeled the TMD0 domain; however, considering the fact that MRP1 lacking TMD0 is fully functional, it is more likely that TMD0 region does not directly contribute to the binding site of LTC_4, and this region was labeled due to its close proximity to the photoreactive group [66].

A molecular model of MRP1 indicated that five residues of TMHs 10, 11, 16, and 17 form an "aromatic basket", lining the putative substrate translocation pathway [20]. Mutational analyses demonstrated that amino acid changes affecting substrate specificity are found in almost all TMHs of TMD1, TMD2, as well as in the L0 region (for a review, see the work of Haimeur et al. [47]). However, these mutations are located predominantly in TMHs 11 and 17 and in the cytoplasmic loop connecting TMH 15 and TMH 16 (see Fig. 1).

Many substrates cross-inhibit the transport of one another, whereas several mutations inhibiting the transport of certain substrates have no effect on the transport of other substrates. These data indicate that these substrates bind to a common substrate-binding pocket and make contacts with overlapping but nonidentical sets of residues. In addition to the GSH-dependent transport, in some other cases, substrate-stimulated transports have also been observed. These include the cross-stimulation of the transport of LTC_4 and estrone 3-sulfate at low concentrations [127], the acceleration of LTC_4 transport by NNAL-*O*-glucuronide [84], and the stimulation of *N*-ethylmaleimide glutathione transport by indomethacin at low concentrations [5]. These observations suggest the existence of more than one allosterically cooperative, nonoverlapping substrate-binding sites within the large substrate-binding pocket. At low concentration, various substrates can bind to distinct substrate-binding sites, facilitating the binding and transport of one another, whereas at higher concentrations, they saturate all the available binding sites and, thus, cross-inhibit the transport of one another.

Catalytic cycle of MRP1

As mentioned above, the transport of MRP1, similar to that of most ABC transporters, is driven by ATP binding/hydrolysis. Unlike P-type ATPases, ABC transporters do not form phosphorylated intermediates during their transport cycle. To characterize the individual steps of the catalytic cycle, such as ATP binding, formation of the transition state, cleavage of the terminal phosphate bond (ATP hydrolysis), and release of ADP and phosphate, various experimental approaches are used. ATP binding is often examined by photoaffinity labeling under nonhydrolytic conditions by using azido-ATP. The transition-state complex formation can be followed by the so-called "nucleotide trapping" measurement. This also means photoaffinity labeling with azido-ATP but under hydrolytic conditions in the presence of a phosphate-mimicking anion,

e.g., vanadate [43, 53, 105]. This anion stabilizes the transition-state complex (MRP1·Mg·ADP·P_i) by replacing the gamma phosphate and arrests the transporter in this state. Another approach to characterize the individual steps of the ATPase cycle is the vanadate-catalyzed photooxidative cleavage reaction [69]. This method is based on the observation that the cleavage of the polypeptide chain upon UV irradiation in the presence of vanadate depends on the conformation of the protein. Thus, the ATP binding and the transition-state complex formation can be assessed by the accumulation of various cleavage products generated under nonhydrolytic and hydrolytic conditions, respectively. The full catalytic cycle, which also includes ATP hydrolysis and ADP/phosphate release, can be followed by ATPase measurements, determining the rate of phosphate liberation [5].

The scheme of the catalytic cycle of the ABC transporters is further complicated by the fact that these proteins contain two cooperating NBDs. In a number of bacterial ABC proteins, the NBDs and TMDs are expressed as separate proteins, which associate to form a functional unit. The analysis of the solved structures of dimeric NBDs of MJ0796, HlyB, MalK, and Rad50, as well as the studies on the structures of "complete" ABC transporters, which also contain the TMDs (BtuCD and MsbA), demonstrated that the two NDBs dimerize in a head-to-tail orientation and form two composite ATP-binding sites/catalytic sites [118]. In these dimeric arrangements, the Walker A of one NBD and the ABC signature motif of the other NBD are involved in the formation of an ATP-binding site. For simplicity, we subsequently refer to an active site in NDB1 or NBD2, which includes Walker A and Walker B of the respective NBD.

Both vanadate-induced cleavage reactions and azido-ATP labeling experiments resulted in the conclusion that both NBDs bind ATP, although NBD1 has higher affinity for ATP than NBD2 [43, 53, 69, 178]. Nucleotide trapping has also been shown in both catalytic sites, but the rate of the transition-state complex formation was greater in NBD2 than in NBD1 [43, 53, 105]. These observations imply that both sites are catalytically active, but the hydrolytic activity of NBD2 is higher than that of NBD1.

The two NBDs of MDR1/P-glycoprotein are functionally equivalent, and the integrity of both NBDs is needed for transport. Inactivation of any one of the two ATP-binding sites results in the complete loss of trapping activity of the protein [101]. In contrast, chemical modifications or mutations of the consensus motifs in the two NBDs of MRP1 have different effects on the transport [43, 53, 121, 178]. Mutations of key residues in the Walker A or Walker B of NBD1 decreased LTC_4 transport activity to 30–50% of the wild-type protein, whereas the corresponding mutations in NBD2 essentially inactivated the protein [43, 53, 121]. On the other hand, substitution of the conserved Gly in the ABC signature sequence of NBD1 for Ala completely inactivates the protein, while this mutation in NDB2 causes only a partial inactivation [121].

Unambiguous evidence for allosteric interactions between NBD1 and NBD2 has been provided by azido-ATP labeling experiments, demonstrating that binding of ATP at NBD1 increases the affinity for ATP and ADP trapping at NBD2 [54]. Conversely, the trapping of ADP at NBD2 has also been shown to enhance the ATP binding at NBD1 in one report [53], while other studies indicated that mutations affecting nucleotide binding and trapping at NDB2 had no effect on ATP binding at NBD1 [43, 121].

Collectively, the different properties of nucleotide binding and transition-state complex formation of the individual NBDs, the diverse consequences of mutations in these domains, as well as their different allosteric regulation implicate distinguishable activities and functions for the two NBDs of MRP1. The data detailed above suggest that ATP binding to both NBDs and the hydrolysis at the NBD2 are the key steps for MRP1-mediated transport. Although ATP is also hydrolyzed at NBD1, the significance of this hydrolysis in the transport is unknown. It is interesting to note that Yang et al. [179] and Zhao and Chang [184] found that certain mutations in the NBD1 decreased the affinity for ATP but increased the transport activity. They interpreted their data in a way that the dissociation rate of nucleotide from the mutated variants of NBD1 is higher than that of wild type, and they concluded that the transport is promoted by the release of the bound nucleotide from NBD1 regardless of ATP hydrolysis. Similar functional asymmetry of NBDs has been shown in CFTR, where ATP binding to both NBDs is required for channel opening, while hydrolysis at NBD2 is necessary for the channel closing [12].

From among the several sequence differences between the NBDs of MRP1, the only one which was established to contribute to the observed functional differences is the putative catalytic base following the Walker B motifs [122]. This residue is Asp in NBD1 and Glu in NBD2. An Asp to Glu mutation in NBD1 enhanced the hydrolytic activity of NBD1, whereas the corresponding mutation of Glu to Asp decreased the rate of hydrolysis at NBD2 and the rate of ADP release. These observations suggest that the presence of Asp in this position is partially responsible for the low hydrolytic activity of NBD1.

It has been documented that purified MRP1 reconstituted in proteoliposomes as well as MRP1 in isolated insect cell membranes shows ATPase activity, which is stimulated by certain transported substrates of MRP1 [5, 97]. However, the mechanism by which transported substrates promote ATP hydrolysis is controversial. Gao et al. [43] found that LTC_4 increased the binding of azido-ATP to NBD1 several

folds, whereas it had little effect on nucleotide binding to NBD2. In contrast, others have found that LTC_4 enhanced ATP binding to NBD2 but not to NBD1 [131]. These data differ from those obtained previously from nucleotide trapping studies on MDR1/P-glycoprotein [154] and recently from vanadate cleavage experiments with MRP1 [69]. These studies demonstrated that the transported substrates have no effect on nucleotide binding but accelerate the formation of the transition-state complex in both catalytic sites, suggesting that substrates stimulate a reaction step of the hydrolytic cycle after ATP binding but precede the formation of the transition-state complex. In accordance with this observation, the trapping of azido-ADP was found to be enhanced by LTC_4 at both NBDs [43]. The discrepancy considering the effect of substrates on ATP binding may be due to the fact that the experiments were performed in two different systems: azido-ATP labeling was done with coexpressed N-half and C-half of MRP1, while vanadate cleavage was done with the full-length wild-type protein.

It has been commonly accepted that during the transport cycle of ABC transporters, the substrate binds to a high-affinity binding site, which is subsequently reoriented, and its substrate binding affinity becomes reduced, facilitating the release of the substrate. High- and low-affinity drug binding states of MRP1 were also distinguished. Either ATP with or without vanadate, or the poorly hydrolyzable ATP analog, ATPγS, can result in the transition from a high- to a low-affinity state [121]. Prolonged binding of either ATP or ADP in NBD2 effectively locked the protein in a low-affinity substrate binding state, while increased ADP trapping in NBD1 prevented this transition [122]. Based on these observations, it has been proposed that occupancy of both NBDs with ATP results in the formation of a low-affinity drug binding state, which persists until NDB2 is occupied with ADP. Manciu et al. [96] have characterized the structural changes of MRP1 during transport by using protease accessibility and infrared spectroscopy. They have demonstrated that ATP binding induces conformational changes in TMDs and increases the accessibility of the protein toward the aqueous medium, while no additional change in the conformational state of TMHs takes place upon ATP hydrolysis. These findings indicate that ATP binding rather than the hydrolysis drives the major structural reorganization in MRP1. However, in the case of a bacterial ABC transporter, the MsbA, a recent electron paramagnetic resonance spectroscopic study has shown that the accessibility of the protein further increases at the external side upon the formation of the high-energy ADP-bound intermediate [32].

Taking together the structural and biochemical data discussed above, as well as the observed conformational changes during the catalytic cycle, the following transport model can be proposed. First, the substrate binds to its high-affinity binding site and MgATP binds to NBD1. Binding of ATP at NBD1 promotes the ATP binding to NBD2. ATP binding results in the formation of a closed dimer NBD conformation, and the subsequent conformational changes cause reconfiguration of the TMDs, resulting in lowering the affinity of the substrate binding site. A closed dimerization of NBDs allows the transition-state complex formation at NDB2. This causes a further conformational change, which results in getting the low-affinity substrate-binding site even more exposed to the extracellular medium, and the substrate becomes released. The step which follows the ATP binding and leads to the transition-state complex formation is accelerated by the presence of substrates. After ATP hydrolysis, the terminal phosphate and subsequently ADP are released from NBD2. There are three options at this point to restart the transport cycle: (1) the protein returns to the high-affinity substrate-binding state after ATP hydrolysis at NBD1 and ADP release, (2) the recovery takes place subsequent to the release of nonhydrolyzed ATP from NBD1, or (3) the protein is capable of binding of another substrate molecule without releasing the ATP from NBD1.

Substrate binding and ATP hydrolysis are promoted by different segments of the protein. However, the substrate-stimulated ATP hydrolysis and the ATP-energized substrate translocation require intramolecular interactions between the two halves of the protein. Studies on the structure of the MsbA transporter [134] revealed that the intracellular loop between TMH 2 and TMH 3 of this protein (ICD1), which consists of three helices in a U-like configuration, establishes contacts between the TMD and the NBD. The position of ICD1 makes feasible that this region is part of the pathway transmitting the conformational changes between the NBDs and the substrate-binding pocket. The corresponding first cytoplasmic loops in TMD1 and TMD2 of MRP1 have the same predicted architecture as the ICD1 in MsbA. Mutation of Asp 1084 in one of these loops in MRP1 drastically decreased nucleotide trapping at NBD2 and prevented the transition from high- to low-affinity state of protein, whereas ATP binding was unaffected [182]. These findings suggest that this intracellular region contributes to the transduction of conformational changes in MRP1, triggered by nucleotide binding and hydrolysis. However, the structural changes introduced into this loop by replacement of two prolines with alanines had no effect on the overall transport activity of the protein [71].

A recent study from our laboratory suggests that the ABC signature motif is a candidate for intramolecular communication [157]. The structures of ATP-bound NBD dimers show that the conserved second Gly residue in the ABC signature motif interacts with the oxygen of the gamma-phosphate of the ATP, bound to the Walker motif of

the opposite subunit [118]. Substitution of these glycines for aspartic acids in either NBDs of MRP1 eliminates transport activity, but the mutants are still capable of forming the transition-state complex [157]. It is interesting to note that in these mutants, the formation of the intermediate complex is inhibited by substrates, whereas it is accelerated in the wild-type protein. Based on these results, we suggested that substrate binding facilitates the signature region to turn toward the ATP molecule bound to the opposing NDB. This movement allows the formation of the proper dimer interface for ATP hydrolysis. When a critical residue is mutated in this region, the characteristic substrate-induced conformational change is altered, implicating that the movement of the signature region is at the endpoint of the substrate-induced allosteric changes, and this region is a key component of the coupling of substrate binding and ATP hydrolysis. Similar observations have been made with the MDR1/P-glycoprotein [156].

Regulation of MRP1 expression and function

MRP1 expression is a subject of multiple regulatory mechanisms. In some multidrug resistant cell lines that overexpress MRP1, the *MRP1* gene is amplified, while in others, an increased transcription occurs without gene amplification. The 5′-end region of *MRP1* gene was cloned, and the analysis of this region showed that, similar to other human multidrug transporters, *MRP1* has a TATA-less promoter [186]. The basal promoter activity was localized to nucleotides −91 to +103 in a GC-rich region of the *MRP1* gene. There are putative Sp1 binding sites in the GC elements, and it was demonstrated that Sp1 in fact interacts with these binding sites, which were proven to be essential for optimal MRP1 transcriptional activity [187].

High-level MRP1 expression was observed even in tumors originating from tissues, which originally exhibit little MRP1 expression. This elevation in MRP1 expression is likely due to the upregulation by components that are involved in malignant transformation, such as oncogenes and tumor suppressor proteins. The wild-type p53 tumor suppressor protein has been shown to repress the transcription of *MRP1* partially by deactivation of promoter-bound Sp1, whereas mutant p53 abrogates the repression of MRP1 [168]. Therefore, a loss of p53 function and/or an increase in Sp1 activity in tumor cells could contribute to an upregulation of the *MRP1* gene, as demonstrated in various tumor types including prostate [153] and nonsmall-cell lung cancer (NSCLC) [117]. The *MRP1* promoter contains a putative AP-1 site (−498 through −492), which interacts with a complex, containing c-*jun* and *jun*D oncogenes [75]. Accordingly, downregulation of MRP1 expression has been found in cells transfected with mutant c-*jun* [27].

Numerous chemotherapeutic agents, including doxorubicin [144] and vinblastine [141], as well as heavy metals such as arsenite, cadmium, and mercury [58, 70], have been reported to induce MRP1 expression. In addition, reactive oxygen species (ROS) have been found to regulate the expression of MRP1. High intracellular ROS levels induce MRP1 expression, whereas the elevation in GSH concentration lowers the ROS levels and consequently results in downregulation of MRP1 [177]. Prooxidants, such as menadione, *tert*-butylhydroquinone, 2,3-dimethoxy-1,4-naphthoquinone [177], and sulindac [161], which produce ROS and generate oxidative stress, have been shown to induce the expression of MRP1. It has been clearly demonstrated that the nuclear factor-E2 p45-related factor 2 (Nrf_2), the key transcriptional factor of antioxidant responsive element-driven genes [48], is involved in the regulation of MRP1 expression.

Similar to MRP1, another oxidative stress-sensitive gene product, the heavy subunit of γ-glutamylcysteine synthetase (γ-GCSh), which is the rate-limiting enzyme in glutathione biosynthesis, frequently shows elevated expression in many drug-resistant cell lines. Expressions of MRP1 and γ-GCSh are coinduced by many cytotoxic and redox active agents [58, 161]. Coordinated elevation in GSH production and in MRP1 pump activity ensures the effective extrusion of these toxic compounds by an MRP1-mediated, GSH-dependent transport mechanism. In addition, the expression of *MRP1* and *γ-GCSh* genes can also be upregulated by interleukin-1β through generation of nitric oxide, which is easily converted to reactive nitrogen species, reminiscent of ROS [56].

The mechanism underlying the concerted regulation of the *MRP1* and *γ-GCSh* genes is unknown. Several oxidative stress-responsive elements, located upstream from the promoter of the *MRP1* and the *γ-GCSh* genes, have been identified [186]. One possibility is that these putative *cis*-acting elements mediate the oxidative stress-induced expression by interacting with redox-sensitive transcription factors. On the other hand, it has recently been demonstrated that doxorubicin upregulates the transcription of *MRP1* gene via doxorubicin-activated c-*jun* N-terminal kinase (JNK), which enhances the association of the activated form of c-*jun* with the AP-1 site in the *MRP1* promoter [144]. Moreover, stimulation of JNK activity has been observed upon depletion of intracellular GSH. These results, together with the finding that *γ-GCSh* gene also contains an AP-1 binding site, implicate that c-*jun*/AP-1 may play a role in the coregulated expression of MRP1 and γ-GCSh.

Very little is known about the posttranslational regulations of MRP1. This transporter is extensively glycosylated, but either the transport function or the localization is not significantly modulated by protein glycosylation

[7, 103]. MRP1 has been shown to be phosphorylated primarily on serine residues. Initially, it has been proposed that phosphorylation by protein kinase C (PKC) plays a role in the regulation of transport function of MRP1 because PKC inhibitors blocked MRP1-mediated transport [93]. However, this result might reflect a direct interaction of PKC inhibitors with MRP1 instead of a regulation through protein phosphorylation.

Tissue distribution and subcellular localization

In contrast to MRP2 and MRP3, which exhibit a rather constrained tissue distribution, MRP1 is ubiquitously expressed in the body. The tissues showing the highest level of MRP1 expression include the lung, testis, kidney, heart, and placenta, whereas a moderate MRP1 expression was found in the small intestine, colon, brain, and peripheral blood mononuclear cells [24, 42, 116, 123]. Because most of these tissues belong to the defense lines of the body, it is somewhat unexpected that MRP1 is expressed at a very low level in the liver, the major organ of xenobiotic metabolism and detoxification. It is interesting to note that MRP1 expression is elevated in the regenerating regions of the liver after tissue damage [136]. Because animal models are often used for pharmacokinetic studies, it is noteworthy that certain differences in tissue distribution of MRP1 can be seen among various species, e.g., the canine liver shows a relatively high expression of MRP1, whereas, as mentioned earlier, in the normal human liver, MRP1 expression is hardly detectable [26, 42]. Gender differences in MRP1 expression in the kidney and liver have also been reported, i.e., higher MRP1 expressions were found in female mice [94].

In tissues where MRP1 is expressed at a relatively high level, the transporter is not distributed uniformly but primarily expressed in special cell types. Table 2 summarizes the cell-type-specific expression pattern of MRP1 in various tissues. In general, cells with a specialized barrier function or cells at a high proliferative status exhibit higher expression of MRP1 than the surrounding cell types. The former is exemplified by the choroid cells in the blood cerebrospinal fluid barrier [129], or the syncytiotrophoblasts and fetal blood-vessel endothelial cells in the placenta [147], whereas the latter notion is demonstrated by the reactive type II pneumocytes in hyperplastic alveoli of the lung [17], or the crypt Paneth cells in the small intestine [123]. The increased level of MRP1 expression in the reactive ductules of the damaged liver is explained by the activation of hepatic progenitor cells [136], which also represent a rapidly multiplying cell type. Similarly, the increase in MRP1 expression during culturing of brain microvessel isolates can be a consequence of the presence of a cell subpopulation with higher proliferative potential [143].

With respect to subcellular localization, MRP1 is primarily expressed in the plasma membrane [41, 181]. Immunocytochemical studies demonstrated basolateral lo-

Table 2 Cell type-specific distributions of MRP1

Tissues	High MRP1 expression	No/low MRP1 expression	References
Lung	Bronchial epithelial cells, bronchiolar epithelial cells, seromucinous glands, reactive type II pneumocytes, alveolar macrophages	Normal type I and II alveolar pneumocytes	[17, 42, 140, 175]
Testis	Sertoli cells in the seminiferous tubules, Leydig cells, testosterone-producing interstitial cells outside the seminiferous tubules		[42, 163, 173]
Kidney	Glomeruli, ascending limb cells, epithelial cells of the loop of Henle, distal and collecting duct cells	Proximal tubule cells	[123, 173]
Placenta	Fetal blood vessels of the terminal and intermediate villi, syncytiotrophoblasts, epithelial cells of the endoplacental yolk sac		[104, 146, 147]
Small intestine	Crypt cells (Paneth cells)	Enterocytes	[123]
Colon	Entire crypt–villous axis		[123]
Brain	Brain capillary endothelial cell		[107, 143, 151, 183]
	Choroidal and ependymal cells, tanycytes in the choroid plexus		[129, 171]
	Glial cells, parenchyma astrocytes		[28, 44]
Blood	Erythrocytes, T-cells, mast cells		[10, 111, 116, 125, 172]

calization for MRP1 in various polarized cell types, including drug-selected and transfected cells as well as epithelial and endothelial cells of normal tissues [17, 36, 83, 123, 140, 175]. In contrast, other ABC transporters which are thought to be crucial in tissue defense, such as MDR1/P-glycoprotein, MRP2, and ABCG2, reside in the apical membrane of polarized cells [19, 95, 162]. The relative position of MRP1 and these transporters in selected tissues is depicted in Fig. 2. Surprisingly, MRP1 was found to localize to the apical surface of the brain capillary endothelial cells [107, 151, 183]. Thus, the ipsilateral distribution of MRP1 with MDR1/P-glycoprotein, MRP2, and ABCG2 in the brain vessels represents an exception. Contradicting data have been published on the subcellular localization of MRP1 in the placental trophoblasts. Initial reports suggested apical localization [146]; however, more recent studies revealed that this transporter localizes to the basolateral membrane of syncytiotrophoblasts [104, 147].

In addition to the plasma membrane localization, intracellular expression of MRP1 has been found in various cell lines [3, 24, 44, 128, 167] and normal tissue samples [42, 174]. The subcellular organelles where MRP1 accumulation was seen include endocytic vesicles [3], perinuclearly located lysosomes [128], and trans-Golgi vesicles [44, 167]. The role of intracellular MRP1 is yet to be clarified. Because MRP1-dependent accumulation of fluorescent drugs into these organelles was also demonstrated [128, 167], it has been proposed that, in addition to extruding drugs through the plasma membrane, MRP1 can confer drug-resistant phenotype to cells by sequestering the drugs into the intracellular compartments. This suggestion would resolve the contradiction how a drug-resistant cell line expressing MRP1 may exhibit the same level of intracellular drug accumulation as its drug-sensitive counterpart [24]. Because these studies were performed with cells overexpressing the transporter and/or with MRP1 tagged with fluorescent proteins, for the evaluation of the physiological relevance of these observations, it should be considered that either overexpression or tagging may greatly influence the subcellular localization pattern. However, the predominant cytoplasmic expression of MRP1 seen in several normal tissues [42, 174] indicates that the intracellular localization of the transporter might have a physiological role. The interesting finding that MRP1 rapidly translocates from the Golgi to the plasma membrane in response to unconjugated bilirubin exposure [44] suggests that intracellularly expressed MRP1 serves as a cellular reservoir, which can be easily mobilized and targeted to the site of action. The particular trafficking signals directing MRP1 to the plasma membrane, as well as the retention and recycling mechanisms determining the further cellular routing of the transporter, are not known yet. However, certain regions such as the L0 domain [4, 6, 170], and the C-terminus in cooperation with the TMD0 [169], were found to be crucial for proper targeting.

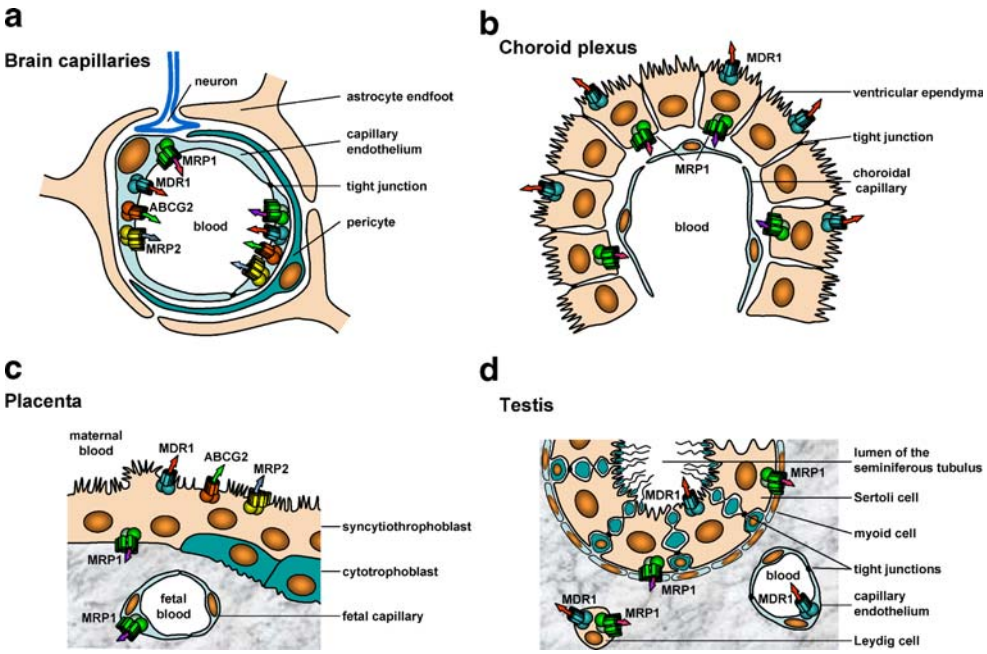

Fig. 2 Cell-type-specific expression and subcellular localization of MRP1 in various physiological barriers. The figure illustrates the relative position of MRP1 and other selected ABC transporters (MDR1/P-glycoprotein, ABCG2, and MRP2) at the blood–brain barrier (**a**), the blood–cerebrospinal fluid barrier (**b**), the placenta (**c**), and the blood–testis barrier (**d**). MRP1 is expressed in the basolateral membrane of the ventricular epithelial cells in the choroid plexus, the syncytiotrophoblasts in the placenta, and the Sertoli cells in the seminiferous tubules. In contrast, MRP1 is localized to the apical membrane of the brain capillary endothelial cells, ipsilaterally to MDR1/P-glycoprotein, ABCG2, and MRP2. MRP1 is also expressed in the fetal blood vessels in the placenta and in the testosterone-producing Leydig cells in the testis

Dual role of MRP1 in the physiological barriers

The substrate specificity of MRP1, together with its distribution in tissues which are considered as the major defense lines of the body, implies a physiological role for MRP1 in protection against xenobiotics and endogenous toxic metabolites (endobiotics). The cellular detoxification process comprises four stages: the uptake of the toxic compounds (phase 0), followed by oxidation (phase I) and conjugation with an anionic group (phase II), and finally, the conjugates are extruded from the cells in an ATP-dependent manner (phase III). MRP1 and related proteins were suggested to play a role in this terminal step of detoxification [57].

Unambiguous verification for this function of MRP1 has emerged from studies using knockout animals. Mice deficient in mrp1 (mrp1 (−/−)) were independently generated by two groups and found to be viable, healthy, and fertile with normal histological and hematological parameters [92, 172]. Challenging the knockout animals with etoposide (VP-16), however, revealed that the mrp1 (−/−) mice are hypersensitive to this cytotoxic drug. The affected tissues include bone marrow, oropharyngeal mucosa, Sertoli cells in the seminiferous tubules of the testis, and urinary collecting tubules in the kidney [92, 173]. Similarly, developing spermatocytes and spermatids were damaged in the testis of mrp1 (−/−) mice after a treatment with the pesticide methoxychlor [163].

Although numerous in vitro studies clearly demonstrated the MRP1-mediated transport of various xeno- and endobiotics, several attempts failed to prove this protective role of MRP1 in vivo. Constitutive expression of MRP1 failed to protect mice from the toxic effect of arsenical and antimonial compounds [90]. The carcinogenicity of aflatoxin B1 in the mrp1 (−/−) mice was not different from that seen in wild-type animals [91]. Similarly, the permeation of several drugs and conjugates across the blood–brain barrier and the blood–cerebrospinal fluid barrier was unaffected in the mrp1-deficient mice [23, 76]. These data were explained by the presence of other transporters which also contribute to these defense mechanisms and can compensate for the lack of MRP1. This explanation is rather plausible because numerous transmembrane export pumps with partially overlapping substrate specificities are present and highly expressed in the physiological barriers. The ABC transporters which are thought to play a crucial role in detoxification and tissue defense include MDR1/P-glycoprotein, MRP1, MRP2, and ABCG2 (for recent review, see the paper of Leslie et al. [83]).

More compelling results were obtained from studies combining different single knockouts and/or using multiple knockout animals. In mice deficient in mdr1a, mdr1b, and mrp1, vincristine and etoposide were found to be toxic to the bone marrow and the gastrointestinal mucosa [62], indicating their compensatory role in protection against these drugs. By using different knockout animals, the role of mrp1 in the tissue distribution and excretion of grepafloxacin, a new quinolone antibiotic, has also been demonstrated [139]. Contribution of MRP1 to blood–cerebrospinal fluid barrier was unambiguously shown by comparing the etoposide levels in the blood–cerebrospinal fluid in mdr1a/mdr1b double and mdr1a/mdr1b/mrp1 triple knockout mice after intravenous administration of this compound [171]. Similarly, the protective function of mrp1 in the blood–brain barrier was demonstrated by the decreased elimination rate of estradiol-17-β-D-glucuronide from the brain of the triple knockout mice [151].

With the exception of brain capillary endothelial cells, in most physiological barriers, MRP1 is expressed in the basolateral membrane of polarized cells, contralaterally to MDR1/P-glycoprotein, MRP2, and ABCG2 (see Fig. 2). This subcellular distribution confers a function for MRP1 distinct from that of the other efflux pumps. In the first line defense fronts of the body, in the lung and the gut, the primary task of the protective efflux system is the removal of toxic compounds back to the lumen. In the airway and intestinal epithelial cells, however, the transport of MRP1 is contrary to the luminal extrusion [123, 140]. Similarly, in the kidney and the liver, which are the major sites of elimination of xeno- and endobiotics, MRP1, when expressed, is facing the serosal side, opposite to the direction of excretion [123, 136]. Thus, it has been proposed that the role of MRP1 in these tissues is protecting the special, sensitive cell types from toxic effects of xeno- and endobiotics rather than the elimination of these compounds from the body [83]. This concept is supported by the note that a high level of MRP1 expression was observed in cells at a high proliferative status, such as hyperplastic reactive type II pneumocytes in the lung [17], Paneth cells in the small intestine [123], and hepatic progenitor cells in the damaged liver [136] (see above).

On the other hand, the role of MRP1 in the blood–tissue barriers seems to be different. As verified by the studies using mrp1-deficient mice, this transporter greatly contributes to the barrier function, protecting the various sanctuary sites of the body. Both in the blood–brain barrier and the choroid plexus, MRP1 is expressed at the serosal side, i.e., the apical surface of brain capillary [107, 151, 183], and the basolateral membrane of the ventricular epithelial (choroidal and ependymal) cells [129, 171], respectively. Thus, transport activity of MRP1 prevents the accumulation of toxins in the brain and cerebrospinal fluid by extruding these compounds into the blood. In the placenta, MRP1 is primarily expressed in the abluminal (basolateral) side of fetal vessel endothelial cells [104, 146] and in the epithelial cells of the endoplacental yolk sac [147]. This localization

brings about the protection of the fetus by limiting the entry and "quarantining" the toxic compounds. In contrast, the low-level expression of MRP1 found in the basolateral membrane of syncytiotrophoblasts rather serves as a defense system for the trophoblast itself or possibly mediates the transport of important metabolites across the maternal–fetal interface [83, 104]. In accordance with this notion, an increase in MRP1 expression can be observed with placental maturation [120, 147]. In the testis, MRP1 most probably plays a role in the local defense, protecting the special cell types such as the Sertoli cells and the developing spermatocytes in the seminiferous tubules. This suggestion has emerged from the observation that etoposide or methoxychlor exposure damaged primarily these cells in the testes of mrp1 −/− mice [163, 173]. A special role for MRP1 has been proposed in the testosterone-producing Leydig cells, where the transporter is expressed at a high level [42, 173]. Because this cell type is the major site of estrogen conjugation in the testis, and estrogen conjugates are known as high-affinity MRP1 substrates, it is not implausible to assume that MRP1 plays a role in protecting the testis from the feminizing effect of estrogens [127].

The role of MRP1 in leukotriene metabolism and oxidative stress defense

In addition to exogenous and endogenous toxic compounds, the inflammatory cytokine LTC_4 and its metabolites LTD_4 and LTE_4 were also identified as MRP1 substrates [80, 86]. These cysteinyl leukotrienes are known to increase vascular permeability and smooth-muscle contraction at the site of inflammation. LTC_4 is synthesized from LTA_4 by conjugation with GSH in leukotriene-generating cells such as mast cells, macrophages, basophilic and eosinophilic granulocytes, dendritic cells, and platelets. LTC_4 is released from these cells in an ATP-dependent manner and rapidly converted extracellularly to LTD_4 and LTE_4 by γ-glutamyltranspeptidase and dipeptidase, respectively. Because numerous photoaffinity labeling and vesicular transport studies have demonstrated that LTC_4 is one of the highest affinity MRP1 substrates [60, 80, 86, 102], it has been postulated that this transporter is responsible for the cellular release of LTC_4 from the leukotriene-producing cells. This hypothesis attributes an additional physiological function to MRP1, which greatly differs from its role in protecting special, sensitive cell types and sanctuary sites of the body.

Unambiguous evidence for the role of MRP1 in the leukotriene-mediated inflammatory responses was provided by studies with the mrp1 (−/−) mice. Bone marrow-derived mast cells isolated from the knockout animals exhibited only a minor residual LTC_4 release, which was accompanied by an intracellular accumulation of this cytokine [172]. This observation clearly demonstrated MRP1 as the major efflux pump for LTC_4 in mast cells. Even more compelling are the observations showing impaired immune reactions in the mrp1 (−/−) mice. The response to arachidonic acid, a leukotriene-inducing inflammatory stimulus, was greatly reduced in the mrp1-deficient mice as measured by decreased ear edema and vascular permeability, whereas the responses to topical application of phorbol ester (prostaglandin-induced inflammatory stimulus) or to intradermal injection of LTC_4 were unaffected [172].

The mobilization of dendritic cells from the skin to the lymph nodes was also found to be greatly reduced in the mrp1 knockout animals, whereas this defect was overcome by the exogenous administration of cysteinyl leukotrienes (LTC_4 and LTD_4), demonstrating the crucial role of MRP1 in the LTC_4 release [135]. Surprisingly, mrp1 (−/−) mice were found to be more resistant to *Streptococcus pneumoniae*-induced pneumonia than wild-type animals [142]. This observation also connects MRP1 with leukotriene metabolism. As a consequence of the lack of mrp1, intracellular LTC_4 is accumulated in the leukotriene-producing cells, which results in the accumulation of LTA_4, a common precursor for LTC_4 and LTB_4. Thus, LTA_4 becomes more available for conversion to LTB_4. This suggestion is supported by the observations that (1) LTB_4 concentration was elevated in the bronchoalveolar lavage fluid of the mrp1 (−/−) mice; (2) LTB_4-dimethyl amide, an LTB_4 antagonist, abolished the survival advantage of knockout animals; (3) peritoneal macrophages of mrp1 (−/−) mice produce more LTB_4 than macrophages from wild-type mice in response to arachidonic acid or heat-killed *S. pneumoniae*. Collectively, these studies with mrp1 (−/−) mice firmly established the intimate involvement of MRP1 in the leukotriene metabolism.

Several elements of the transcriptional regulation of *MRP1* gene, such as oxidative stress-responsive elements of its promoter region [186] and regulation of expression by Nrf2 [48] and by ROS [161, 177], implicate a connection between this transporter and the redox state of the cell. At a high oxidative state, the cell abolishes the toxic effect of peroxides by their reduction using glutathione (GSH) as an electron donor, producing glutathione disulfide (GSSG). GSH is normally recycled by GSSG reductase enzyme, but during oxidative stress, GSSG is also released from several cell types via an overflow system. Implicating an involvement of MRP1 in the GSH/GSSG metabolism, in the mrp1 (−/−) mice, increased accumulation of GSH was found in tissues which normally express MRP1, whereas GSH concentration was unchanged in tissues known to express little MRP1 [92].

Reduced glutathione was proven to be a poor substrate of MRP1 [79, 87], but its transport is stimulated by

bioflavonoids and verapamil by increasing the apparent affinity of the transporter for GSH [82, 88]. In contrast, GSSG by itself was found to be a substrate with an apparent K_m value of around 100 μM [79]. This affinity makes MRP1 capable of extruding GSSG from cell during oxidative stress when the activity of GSSG reductase becomes rate limiting. Although overexpression of MRP1 failed to increase resistance against oxidative stress in transfected cell lines [8], endogenously expressed MRP1 was shown to mediate cellular GSSG release in response to oxidative stress in astrocytes and endothelial cells [50, 100]. The specificity in these studies was demonstrated by blocking the GSSG efflux by the MRP1 inhibitor MK571 or by MRP1 siRNA. Further support was provided by the findings that the elevated endothelial GSSG efflux observed in the aorta of hypertensive mice was blocked by MK571 and was absent in hypertensive mrp1 (−/−) mice [100]. In addition to its role in the GSSG efflux, MRP1 also contributes to defense against oxidative stress by removal of GS conjugates formed in the cells at a high oxidative state. This is most well exemplified by 4-hydroxynonenal, the predominant toxic lipid peroxidation product, which was found to be bound to and transported by MRP1 [132]. In summary, MRP1 seems to be a multifunctional efflux pump, which not only functions as a part of a defense system against xenobiotics and toxic metabolites but also contributes to immunological responses and to the elimination of toxic effects caused by oxidative stress.

The pathophysiological aspect of MRP1

In addition to its diverse physiological functions, there is a significant body of evidence that MRP1 also contributes to the clinical MDR of several hematological and solid tumors. The MDR phenotype was described in drug-selected tumor cell lines, which exhibited cross-resistance to a wide range of structurally and functionally unrelated anticancer agents. With regard to the mechanism, it has been generally accepted that MDR is a consequence of the presence and activity of export pumps with broad substrate specificity. These transporters extrude cytotoxic agents from the cells, maintaining the drug level below a cell-killing threshold. Several ABC transporters, including MDR1/P-glycoprotein, MRP1-6, ABCG2, MRP7-8, MDR3 (ABCB4), sPgp (ABCB11), and ABCA2, have been shown to confer drug resistance for cell lines in vitro; however, their involvement in the clinical MDR has been established only for MDR1/P-glycoprotein, MRP1, and ABCG2.

As mentioned earlier, MRP1 was originally cloned from a doxorubicin-selected lung cancer cell line, which exhibited resistance to a range of cytotoxic agents without increased expression of MDR1/P-glycoprotein [24]. The substrate specificity of MRP1, as assessed in initial transport measurements with inside-out vesicles, did not correlate with the drug resistance profile found in cell lines. Most of these discrepancies were resolved by the findings that several drugs are transported by MRP1 as glutathione or glucuronide conjugates or require GSH for their transport. The former is exemplified by chlorambucil-GS, melphalan-GS, or etoposide-glucuronide [9, 60], while the latter is represented by vincristine and daunorubicin [86, 87, 133]. Overexpression of MRP1 has been found in numerous drug-selected cell lines derived from various tumors, including lung cancers, breast cancer, gastric and colon carcinomas, prostate cancer, melanoma, neuroblastoma and glioma, fibrosarcoma and epidermoid carcinoma, as well as diverse types of leukemias. Unlike MRP1-enriched inside-out vesicles, these cellular model systems most likely possess all the features, such as glutathione or the drug-conjugating apparatus, which are conceivably needed for effective transport. However, the MRP1-conferred drug resistance profiles found in these cell lines were still dissimilar. This variability was observed not only in cell lines with different origin but also in cells derived from the same parental cell line [30, 145], implicating that the MDR phenotype is multifactorial and possibly involves other resistance factors such as DNA-topoisomerases, cytochrome P450 enzymes, and other ABC transporters capable of conferring drug resistance. Consistent with this idea, several reports indicated that overexpression of MDR1/P-glycoprotein followed MRP1 overexpression in sequential selection procedures [18, 145, 185]. Thus, for a better evaluation of drug resistance in cell lines, a more complex approach is required. Recently, a novel pharmacogenomic method was introduced by Szakacs et al. [155], determining expression profiles for the entire human ABC transporter panel in 60 various cancer cell lines (NCI-60) and correlating them with the growth inhibitory profile of about 1,500 potential anticancer drugs.

To circumvent the problems deriving from multifactorial cellular responses to selective pressure of drug exposure, cell lines transfected with MRP1 cDNA have been generated to investigate MRP1-conferred MDR [3, 25, 45, 181]. These studies revealed similar drug resistance profiles in transfected cells of various origins, although minor differences still existed. In general, the transfectants exhibited increased resistance to doxorubicin, daunorubicin, epirubicine, vincristine, and etoposide (VP-16) but not to cisplatin, taxol, and mitoxantrone. Colchicine and vinblastine resistance conferred by MRP1 slightly varied from cell line to cell line. In addition to these "classical" anticancer agents, resistance to methotrexate [52], ethacrynic acid [99], arsenical and antimonial oxyanions [25], as well as to cytotoxic peptides such as ALLN and 4A6

[31] was observed in MRP1-transfected cells. Not only the drug resistance of these cells but also reduced intracellular accumulation and increased efflux of cytotoxic agents have been shown [25, 36, 52, 181]. After cloning the murine and rat orthologs of human MRP1, some remarkable species differences have been revealed. Cells transfected with mouse or rat mrp1 did not exhibit resistance to anthracyclines; furthermore, rat mrp1-transfected cells also remained sensitive to vinca alkaloids [148, 159]. These species differences call our attention to a careful interpretation of pharmacological studies using these animal models.

Although the cellular model systems are powerful tools to investigate the MDR phenotype conferred by MRP1, the clinical relevance of MRP1 in human malignancies was established by studies investigating the expression and/or function of MRP1 in clinical samples. Increased level of MRP1 expression has been found in a wide range of hematological and solid tumors (for references, see Table 3). Some of them, such as nonsmall-cell lung cancer (NSCLC) [13, 109, 150, 175] or chronic lymphoblastic leukemia [63, 111], generally exhibit high level of MRP1 expression and these tumors are intrinsically multidrug resistant, whereas others such as small-cell lung cancer (SCLC) [175], gastric carcinoma [2, 34], neuroblastoma [114], and retinoblastoma [21] exhibit high MRP1 expression with a lower frequency. A correlation between the MRP1 expression and the stage of the tumor has been reported in certain tumor types, such as acute myeloblastic leukemia (AML) [165], myelodysplastic syndromes (MDS) [124], and prostate cancer [153]. On the other hand, in lung adenocarcinomas, a reverse correlation was seen with tumor grading [13]. High MRP1 expression was also found to be associated with higher grade of tumor differentiation in digestive tract carcinomas [160], endometrial carcinomas [72], and various subtypes of NSCLC, such as lung adenocarcinoma and squamous cell carcinoma [109, 150].

In numerous cases, elevated MRP1 expression was found to be associated with transcriptional regulation events. Because p53 is a suppressor of MRP1 transcription [168], it is not surprising that a strong correlation between mutant p53 status and MRP1 expression was found in prostate cancer [153] and NSCLC [117]. Similarly, an association between the expression of MRP1 and the N-myc oncogen has been firmly established in neuroblastoma [114, 119]. Increased MRP1 expression was observed after chemotherapy in relapsed SCLC [73], bladder carcinomas [158], and acute lymphoblastic leukemia (ALL) [11]. Whether this is a consequence of repopulation of drug-resistant cells (selection) or upregulation of expression in response to drug exposure (induction) remains to be established.

Various clinical parameters, e.g., overall survival, event-free survival, responsiveness to chemotherapy, etc., were correlated with MRP1 expression to explore its contribution to clinical drug resistance. Many of these studies failed to establish a causative role for MRP1 in the negative disease outcome, whose failure is mainly attributable to the impediments hindering this kind of investigations. One of these difficulties is the fact that MRP1 is expressed in almost all normal tissues, and contamination of tumor samples with variable amounts of normal tissues can lead to ambiguous results. Another factor, which can also complicate the interpretation of the results of such studies, is the possible presence of other drug resistance-associated proteins, e.g., LRP/MVP or MDR1/P-glycoprotein. Moreover, the drug extrusion activity of the transporter is not necessarily proportional to the amount of mRNA or protein, especially at high levels of expression. Therefore, definitive conclusions can be obtained only from carefully designed and performed multiparametric studies, which include the identification of the tumor cells, detection of alternative resistance-associated proteins, and use of a specific functional assay, whenever possible.

The significance of this issue is clearly demonstrated by the example of acute myeloblastic leukemia (AML). Several independent studies indicated that MRP1 expression is not predictive of negative therapy outcome in AML [39, 81, 124]. However, when MDR1/P-glycoprotein and MRP1 were assessed together by an appropriate functional assay, the activity of the multidrug transporters was proven to be a negative prognostic factor for achievement of complete remission [64, 77, 78, 166]. Despite all these difficulties discussed above, MRP1 expression has been found to be predictive of poor response to chemotherapy in NSCLC [13, 117] and SCLC

Table 3 Tumor types with elevated MRP1 expression

Tumor types	References
Acute myeloblastic leukemia (AML)	[77, 78, 124, 165]
Acute lymphoblastic leukemia (ALL)	[11]
Chronic lymphoblastic leukemia (CLL)	[63, 111]
Nonsmall-cell lung cancer (NSCLC)	[13, 73, 109, 150, 175]
Small-cell lung cancers (SCLC)	[13, 73, 175]
Breast cancer	[38, 110, 138]
Prostate cancer	[152, 164]
Gastric carcinoma	[2, 34]
Esophageal squamous cell carcinoma (ESCC)	[112, 160]
Colorectal cancer	[40, 160]
Endometrial carcinoma	[72]
Glioma	[1]
Neuroblastoma	[113, 114]
Retinoblastoma	[21]

[55, 74]. Similarly, MRP1 positivity was strongly associated with reduction in both overall survival and event-free survival in breast cancer [38, 110] and neuroblastoma [113, 114, 119]. In addition, a strong correlation between MRP1 expression and shorter times to relapse has been found in breast cancer [38, 110, 138].

Because MDR represents a major obstacle to cancer treatment, the observations discussed above emphasize the significance of MRP1 with respect to clinical practice. Enormous efforts have been made to develop chemotherapeutics and modulators (reversing agents) to prevent MDR (for recent review, see the work of Boumendjel et al. [16]). However, application of modulators is a double-edged sword because these agents may abolish the physiological barriers or result in inhibition of other essential physiological functions of these transporters. Consequently, a more complex approach for better therapy achievements should include a proper, multiparametric diagnosis comprising the selective detection of all possible drug-resistance proteins, as well as a personalized therapeutic intervention that takes into consideration of the results of such diagnosis.

Conclusions

Since the identification of MRP1, considerable amount of experimental data accumulated on the structure, transport function, substrates, cosubstrates, and inhibitors of this transporter. Still, “we see in a mirror dimly” regarding the transport mechanism due to the complexity and the puzzling details of the transport cycle. Although MRP1 has been originally identified as an alternative multidrug transporter in drug-selected cell lines, it turned out to be a protein with multiple physiological functions. Generation and detailed investigation of knockout animals brought a breakthrough in understanding of the diverse physiological roles of MRP1, although these studies were also hampered by the compensatory effects of other ABC transporters with a substrate specificity partially overlapping that of MRP1. Collectively, according to our current understanding, this transporter (1) protects special cell types from the toxic effects of xeno- and endobiotics; (2) contributes to the barrier function of the defense lines of certain sanctuary sites of the body; (3) participates in leukotriene-mediated inflammatory responses through LTC_4 transport; and (4) contributes to defense against oxidative stress by providing an overflow system for GSSG. In addition to these numerous beneficial functions, there is also a vicious aspect of this transporter. Namely, MRP1 has been proven to be responsible for clinical MDR in several human malignancies such as lung, breast, prostate cancer, pediatric tumors, and various forms of leukemia.

Acknowledgments The authors apologize from those whose valuable work was not cited in this review article for space limitations. We are grateful to Dr. Balázs Sarkadi and Dr. András Váradi for their advice and comments. Dr. George Gárdos and Dr. Tamás Orbán are acknowledged for their critical reading and corrections of this manuscript. We appreciate the support of research grants (OTKA AT 048729, NF 61822), which allowed us to compile this review. László Homolya is an EMBO-HHMI Young Scientist.

References

1. Abe T, Mori T, Wakabayashi Y, Nakagawa M, Cole SP, Koike K, Kuwano M, Hori S (1998) Expression of multidrug resistance protein gene in patients with glioma after chemotherapy. J Neurooncol 40:11–18
2. Alexander D, Yamamoto T, Kato S, Kasai S (1999) Histopathological assessment of multidrug resistance in gastric cancer: expression of P-glycoprotein, multidrug resistance-associated protein, and lung-resistance protein. Surg Today 29:401–406
3. Almquist KC, Loe DW, Hipfner DR, Mackie JE, Cole SP, Deeley RG (1995) Characterization of the M(r) 190,000 multidrug resistance protein (MRP) in drug-selected and transfected human tumor cell. Cancer Res 55:102–110
4. Bakos E, Hegedus T, Hollo Z, Welker E, Tusnady GE, Zaman GJ, Flens MJ, Varadi A, Sarkadi B (1996) Membrane topology and glycosylation of the human multidrug resistance-associated protein. J Biol Chem 271:12322–12326
5. Bakos E, Evers R, Szakacs G, Tusnady GE, Welker E, Szabo K, de Haas M, van Deemter L, Borst P, Varadi A, Sarkadi B (1998) Functional multidrug resistance protein (MRP1) lacking the N-terminal transmembrane domain. J Biol Chem 273:32167–32175
6. Bakos E, Evers R, Calenda G, Tusnady GE, Szakacs G, Varadi A, Sarkadi B (2000) Characterization of the amino-terminal regions in the human multidrug resistance protein (MRP1). J Cell Sci 113(Pt 24):4451–4461
7. Bakos E, Evers R, Sinko E, Varadi A, Borst P, Sarkadi B (2000) Interactions of the human multidrug resistance proteins MRP1 and MRP2 with organic anions. Mol Pharmacol 57:760–768
8. Balcerczyk A, Rychlik B, Kruszewski M, Burchell B, Bartosz G (2003) MRP1-transfected cells do not show increased resistance against oxidative stress. Free Radic Res 37:189–195
9. Barnouin K, Leier I, Jedlitschky G, Pourtier-Manzanedo A, Konig J, Lehmann WD, Keppler D (1998) Multidrug resistance protein-mediated transport of chlorambucil and melphalan conjugated to glutathione. Br J Cancer 77:201–209
10. Bartosz G, Konig J, Keppler D, Hagmann W (1998) Human mast cells secreting leukotriene C4 express the MRP1 gene-encoded conjugate export pump. Biol Chem 379:1121–1126
11. Beck JF, Brugger D, Brischwein K, Liu C, Bader P, Niethammer D, Gekeler V (2001) Anticancer drug-mediated induction of multidrug resistance-associated genes and protein kinase C isozymes in the T-lymphoblastoid cell line CCRF-CEM and in blasts from patients with acute lymphoblastic leukemias. Jpn J Cancer Res 92:896–903
12. Berger AL, Ikuma M, Welsh MJ (2005) Normal gating of CFTR requires ATP binding to both nucleotide-binding domains and hydrolysis at the second nucleotide-binding domain. Proc Natl Acad Sci USA 102:455–460
13. Berger W, Setinek U, Hollaus P, Zidek T, Steiner E, Elbling L, Cantonati H, Attems J, Gsur A, Micksche M (2005) Multidrug resistance markers P-glycoprotein, multidrug resistance protein 1, and lung resistance protein in non-small cell lung cancer: prognostic implications. J Cancer Res Clin Oncol 131:355–363

14. Binyamin L, Assaraf YG, Haus-Cohen M, Stark M, Reiter Y (2004) Targeting an extracellular epitope of the human multidrug resistance protein 1 (MRP1) in malignant cells with a novel recombinant single chain Fv antibody. Int J Cancer 110:882–890
15. Borst P, Zelcer N, van de Wetering K, Poolman B (2006) On the putative co-transport of drugs by multidrug resistance proteins. FEBS Lett 580:1085–1093
16. Boumendjel A, Baubichon-Cortay H, Trompier D, Perrotton T, Di Pietro A (2005) Anticancer multidrug resistance mediated by MRP1: recent advances in the discovery of reversal agents. Med Res Rev 25:453–472
17. Brechot JM, Hurbain I, Fajac A, Daty N, Bernaudin JF (1998) Different pattern of MRP localization in ciliated and basal cells from human bronchial epithelium. J Histochem Cytochem 46:513–517
18. Brock I, Hipfner DR, Nielsen BS, Jensen PB, Deeley RG, Cole SP, Sehested M (1995) Sequential coexpression of the multidrug resistance genes MRP and mdr1 and their products in VP-16 (etoposide)-selected H69 small cell lung cancer cells. Cancer Res 55:459–462
19. Buchler M, Konig J, Brom M, Kartenbeck J, Spring H, Horie T, Keppler D (1996) cDNA cloning of the hepatocyte canalicular isoform of the multidrug resistance protein, cMrp, reveals a novel conjugate export pump deficient in hyperbilirubinemic mutant rats. J Biol Chem 271:15091–15098
20. Campbell JD, Koike K, Moreau C, Sansom MS, Deeley RG, Cole SP (2004) Molecular modeling correctly predicts the functional importance of Phe594 in transmembrane helix 11 of the multidrug resistance protein, MRP1 (ABCC1). J Biol Chem 279:463–468
21. Chan HS, Lu Y, Grogan TM, Haddad G, Hipfner DR, Cole SP, Deeley RG, Ling V, Gallie BL (1997) Multidrug resistance protein (MRP) expression in retinoblastoma correlates with the rare failure of chemotherapy despite cyclosporine for reversal of P-glycoprotein. Cancer Res 57:2325–2330
22. Chan KW, Zhang H, Logothetis DE (2003) N-terminal transmembrane domain of the SUR controls trafficking and gating of Kir6 channel subunits. EMBO J 22:3833–3843
23. Cisternino S, Rousselle C, Lorico A, Rappa G, Scherrmann JM (2003) Apparent lack of Mrp1-mediated efflux at the luminal side of mouse blood-brain barrier endothelial cells. Pharm Res 20:904–909
24. Cole SP, Bhardwaj G, Gerlach JH, Mackie JE, Grant CE, Almquist KC, Stewart AJ, Kurz EU, Duncan AM, Deeley RG (1992) Overexpression of a transporter gene in a multidrug-resistant human lung cancer cell line. Science 258: 1650–1654
25. Cole SP, Sparks KE, Fraser K, Loe DW, Grant CE, Wilson GM, Deeley RG (1994) Pharmacological characterization of multidrug resistant MRP-transfected human tumor cells. Cancer Res 54:5902–5910
26. Conrad S, Viertelhaus A, Orzechowski A, Hoogstraate J, Gjellan K, Schrenk D, Kauffmann HM (2001) Sequencing and tissue distribution of the canine MRP2 gene compared with MRP1 and MDR1. Toxicology 156:81–91
27. Cripe LD, Gelfanov VM, Smith EA, Spigel DR, Phillips CA, Gabig TG, Jung SH, Fyffe J, Hartman AD, Kneebone P, Mercola D, Burgess GS, Boswell HS (2002) Role for c-jun N-terminal kinase in treatment-refractory acute myeloid leukemia (AML): signaling to multidrug-efflux and hyperproliferation. Leukemia 16:799–812
28. Dallas S, Zhu X, Baruchel S, Schlichter L, Bendayan R (2003) Functional expression of the multidrug resistance protein 1 in microglia. J Pharmacol Exp Ther 307:282–290
29. Daoud R, Julien M, Gros P, Georges E (2001) Major photoaffinity drug binding sites in multidrug resistance protein 1 (MRP1) are within transmembrane domains 10–11 and 16–17. J Biol Chem 276:12324–12330
30. David-Beabes GL, Overman MJ, Petrofski JA, Campbell PA, de Marzo AM, Nelson WG (2000) Doxorubicin-resistant variants of human prostate cancer cell lines DU 145, PC-3, PPC-1, and TSU-PR1: characterization of biochemical determinants of antineoplastic drug sensitivity. Int J Oncol 17:1077–1086
31. de Jong MC, Slootstra JW, Scheffer GL, Schroeijers AB, Puijk WC, Dinkelberg R, Kool M, Broxterman HJ, Meloen RH, Scheper RJ (2001) Peptide transport by the multidrug resistance protein MRP1. Cancer Res 61:2552–2557
32. Dong J, Yang G, McHaourab HS (2005) Structural basis of energy transduction in the transport cycle of MsbA. Science 308:1023–1028
33. Draper MP, Martell RL, Levy SB (1997) Active efflux of the free acid form of the fluorescent dye 2′,7′-bis(2-carboxyethyl)-5(6)-carboxyfluorescein in multidrug-resistance-protein-overexpressing murine and human leukemia cells. Eur J Biochem 243:219–224
34. Endo K, Maehara Y, Ichiyoshi Y, Kusumoto T, Sakaguchi Y, Ohno S, Sugimachi K (1996) Multidrug resistance-associated protein expression in clinical gastric carcinoma. Cancer 77:1681–1687
35. Evers R, Cnubben NH, Wijnholds J, van Deemter L, van Bladeren PJ, Borst P (1997) Transport of glutathione prostaglandin A conjugates by the multidrug resistance protein 1. FEBS Lett 419:112–116
36. Evers R, Zaman GJ, van Deemter L, Jansen H, Calafat J, Oomen LC, Oude Elferink RP, Borst P, Schinkel AH (1996) Basolateral localization and export activity of the human multidrug resistance-associated protein in polarized pig kidney cells. J Clin Invest 97:1211–1218
37. Fernandez SB, Hollo Z, Kern A, Bakos E, Fischer PA, Borst P, Evers R (2002) Role of the N-terminal transmembrane region of the multidrug resistance protein MRP2 in routing to the apical membrane in MDCKII cells. J Biol Chem 277:31048–31055
38. Filipits M, Pohl G, Rudas M, Dietze O, Lax S, Grill R, Pirker R, Zielinski CC, Hausmaninger H, Kubista E, Samonigg H, Jakesz R (2005) Clinical role of multidrug resistance protein 1 expression in chemotherapy resistance in early-stage breast cancer: the Austrian Breast and Colorectal Cancer Study Group. J Clin Oncol 23:1161–1168
39. Filipits M, Suchomel RW, Zochbauer S, Brunner R, Lechner K, Pirker R (1997) Multidrug resistance-associated protein in acute myeloid leukemia: no impact on treatment outcome. Clin Cancer Res 3:1419–1425
40. Fillpits M, Suchomel RW, Dekan G, Stiglbauer W, Haider K, Depisch D, Pirker R (1997) Expression of the multidrug resistance-associated protein (MRP) gene in colorectal carcinomas. Br J Cancer 75:208–212
41. Flens MJ, Izquierdo MA, Scheffer GL, Fritz JM, Meijer CJ, Scheper RJ, Zaman GJ (1994) Immunochemical detection of the multidrug resistance-associated protein MRP in human multidrug-resistant tumor cells by monoclonal antibodies. Cancer Res 54: 4557–4563
42. Flens MJ, Zaman GJ, van der Valk P, Izquierdo MA, Schroeijers AB, Scheffer GL, van der Groep P, de Haas M, Meijer CJ, Scheper RJ (1996) Tissue distribution of the multidrug resistance protein. Am J Pathol 148:1237–1247
43. Gao M, Cui HR, Loe DW, Grant CE, Almquist KC, Cole SP, Deeley RG (2000) Comparison of the functional characteristics of the nucleotide binding domains of multidrug resistance protein 1. J Biol Chem 275:13098–13108

44. Gennuso F, Fernetti C, Tirolo C, Testa N, L'Episcopo F, Caniglia S, Morale MC, Ostrow JD, Pascolo L, Tiribelli C, Marchetti B (2004) Bilirubin protects astrocytes from its own toxicity by inducing up-regulation and translocation of multidrug resistance-associated protein 1 (Mrp1). Proc Natl Acad Sci USA 101: 2470–2475
45. Grant CE, Valdimarsson G, Hipfner DR, Almquist KC, Cole SP, Deeley RG (1994) Overexpression of multidrug resistance-associated protein (MRP) increases resistance to natural product drugs. Cancer Res 54:357–361
46. Grzywacz MJ, Yang JM, Hait WN (2003) Effect of the multidrug resistance protein on the transport of the antiandrogen flutamide. Cancer Res 63:2492–2498
47. Haimeur A, Conseil G, Deeley RG, Cole SP (2004) The MRP-related and BCRP/ABCG2 multidrug resistance proteins: biology, substrate specificity and regulation. Curr Drug Metab 5:21–53
48. Hayashi A, Suzuki H, Itoh K, Yamamoto M, Sugiyama Y (2003) Transcription factor Nrf2 is required for the constitutive and inducible expression of multidrug resistance-associated protein 1 in mouse embryo fibroblasts. Biochem Biophys Res Commun 310:824–829
49. Hipfner DR, Almquist KC, Leslie EM, Gerlach JH, Grant CE, Deeley RG, Cole SP (1997) Membrane topology of the multidrug resistance protein (MRP). A study of glycosylation-site mutants reveals an extracytosolic NH2 terminus. J Biol Chem 272:23623–23630
50. Hirrlinger J, Konig J, Keppler D, Lindenau J, Schulz JB, Dringen R (2001) The multidrug resistance protein MRP1 mediates the release of glutathione disulfide from rat astrocytes during oxidative stress. J Neurochem 76:627–636
51. Hollo Z, Homolya L, Hegedus T, Sarkadi B (1996) Transport properties of the multidrug resistance-associated protein (MRP) in human tumour cells. FEBS Lett 383:99–104
52. Hooijberg JH, Broxterman HJ, Kool M, Assaraf YG, Peters GJ, Noordhuis P, Scheper RJ, Borst P, Pinedo HM, Jansen G (1999) Antifolate resistance mediated by the multidrug resistance proteins MRP1 and MRP2. Cancer Res 59:2532–2535
53. Hou Y, Cui L, Riordan JR, Chang X (2000) Allosteric interactions between the two non-equivalent nucleotide binding domains of multidrug resistance protein MRP1. J Biol Chem 275:20280–20287
54. Hou YX, Riordan JR, Chang XB (2003) ATP binding, not hydrolysis, at the first nucleotide-binding domain of multidrug resistance-associated protein MRP1 enhances ADP.Vi trapping at the second domain. J Biol Chem 278:3599–3605
55. Hsia TC, Lin CC, Wang JJ, Ho ST, Kao A (2002) Relationship between chemotherapy response of small cell lung cancer and P-glycoprotein or multidrug resistance-related protein expression. Lung 180:173–179
56. Ikegami Y, Tatebe S, Lin-Lee YC, Xie QW, Ishikawa T, Kuo MT (2000) Induction of MRP1 and gamma-glutamylcysteine synthetase gene expression by interleukin 1beta is mediated by nitric oxide-related signalings in human colorectal cancer cells. J Cell Physiol 185:293–301
57. Ishikawa T (1992) The ATP-dependent glutathione S-conjugate export pump. Trends Biochem Sci 17:463–468
58. Ishikawa T, Bao JJ, Yamane Y, Akimaru K, Frindrich K, Wright CD, Kuo MT (1996) Coordinated induction of MRP/GS-X pump and gamma-glutamylcysteine synthetase by heavy metals in human leukemia cells. J Biol Chem 271: 14981–14988
59. Ito K, Weigl KE, Deeley RG, Cole SP (2003) Mutation of proline residues in the NH(2)-terminal region of the multidrug resistance protein, MRP1 (ABCC1): effects on protein expression, membrane localization, and transport function. Biochim Biophys Acta 1615:103–114
60. Jedlitschky G, Leier I, Buchholz U, Barnouin K, Kurz G, Keppler D (1996) Transport of glutathione, glucuronate, and sulfate conjugates by the MRP gene-encoded conjugate export pump. Cancer Res 56:988–994
61. Jedlitschky G, Leier I, Buchholz U, Hummel-Eisenbeiss J, Burchell B, Keppler D (1997) ATP-dependent transport of bilirubin glucuronides by the multidrug resistance protein MRP1 and its hepatocyte canalicular isoform MRP2. Biochem J 327(Pt 1):305–310
62. Johnson DR, Finch RA, Lin ZP, Zeiss CJ, Sartorelli AC (2001) The pharmacological phenotype of combined multidrug-resistance mdr1a/1b- and mrp1-deficient mice. Cancer Res 61: 1469–1476
63. Juszczynski P, Niewiarowski W, Krykowski E, Robak T, Warzocha K (2002) Expression of the multidrug resistance-associated protein (mrp) gene in chronic lymphocytic leukemia. Leuk Lymphoma 43:153–158
64. Karaszi E, Jakab K, Homolya L, Szakacs G, Hollo Z, Telek B, Kiss A, Rejto L, Nahajevszky S, Sarkadi B, Kappelmayer J (2001) Calcein assay for multidrug resistance reliably predicts therapy response and survival rate in acute myeloid leukaemia. Br J Haematol 112:308–314
65. Karwatsky J, Daoud R, Cai J, Gros P, Georges E (2003) Binding of a photoaffinity analogue of glutathione to MRP1 (ABCC1) within two cytoplasmic regions (L0 and L1) as well as transmembrane domains 10–11 and 16–17. Biochemistry 42: 3286–3294
66. Karwatsky J, Leimanis M, Cai J, Gros P, Georges E (2005) The leucotriene C4 binding sites in multidrug resistance protein 1 (ABCC1) include the first membrane multiple spanning domain. Biochemistry 44:340–351
67. Kast C, Gros P (1998) Epitope insertion favors a six transmembrane domain model for the carboxy-terminal portion of the multidrug resistance-associated protein. Biochemistry 37: 2305–2313
68. Kast C, Gros P (1997) Topology mapping of the amino-terminal half of multidrug resistance-associated protein by epitope insertion and immunofluorescence. J Biol Chem 272:26479–26487
69. Kern A, Szentpetery Z, Liliom K, Bakos E, Sarkadi B, Varadi A (2004) Nucleotides and transported substrates modulate different steps of the ATPase catalytic cycle of MRP1 multidrug transporter. Biochem J 380:549–560
70. Kim SH, Bark H, Choi CH (2005) Mercury induces multidrug resistance-associated protein gene through p38 mitogen-activated protein kinase. Toxicol Lett 155:143–150
71. Koike K, Conseil G, Leslie EM, Deeley RG, Cole SP (2004) Identification of proline residues in the core cytoplasmic and transmembrane regions of multidrug resistance protein 1 (MRP1/ABCC1) important for transport function, substrate specificity, and nucleotide interactions. J Biol Chem 279: 12325–12336
72. Koshiyama M, Yoshida M, Fujii H, Konishi M, Nanno H, Hayashi M, Tauchi K (1999) Expression of multidrug resistance-associated protein in endometrial carcinomas: correlation with clinicopathology and prognosis. Ann Diagn Pathol 3:81–87
73. Kreisholt J, Sorensen M, Jensen PB, Nielsen BS, Andersen CB, Sehested M (1998) Immunohistochemical detection of DNA topoisomerase IIalpha, P-glycoprotein and multidrug resistance protein (MRP) in small-cell and non-small-cell lung cancer. Br J Cancer 77:1469–1473
74. Kuo TH, Liu FY, Chuang CY, Wu HS, Wang JJ, Kao A (2003) To predict response chemotherapy using technetium-99m tetrofosmin chest images in patients with untreated small cell lung cancer and compare with p-glycoprotein, multidrug resistance

related protein-1, and lung resistance-related protein expression. Nucl Med Biol 30:627–632
75. Kurz EU, Cole SP, Deeley RG (2001) Identification of DNA-protein interactions in the 5′ flanking and 5′ untranslated regions of the human multidrug resistance protein (MRP1) gene: evaluation of a putative antioxidant response element/AP-1 binding site. Biochem Biophys Res Commun 285:981–990
76. Lee YJ, Kusuhara H, Sugiyama Y (2004) Do multidrug resistance-associated protein-1 and -2 play any role in the elimination of estradiol-17 beta-glucuronide and 2,4-dinitrophenyl-S-glutathione across the blood-cerebrospinal fluid barrier? J Pharm Sci 93:99–107
77. Legrand O, Simonin G, Beauchamp-Nicoud A, Zittoun R, Marie JP (1999) Simultaneous activity of MRP1 and Pgp is correlated with in vitro resistance to daunorubicin and with in vivo resistance in adult acute myeloid leukemia. Blood 94:1046–1056
78. Legrand O, Zompi S, Perrot JY, Faussat AM, Benderra Z, Chaoui D, Marie JP (2004) P-glycoprotein and multidrug resistance associated protein-1 activity in 132 acute myeloid leukemias according to FAB subtypes and cytogenetics risk groups. Haematologica 89:34–41
79. Leier I, Jedlitschky G, Buchholz U, Center M, Cole SP, Deeley RG, Keppler D (1996) ATP-dependent glutathione disulphide transport mediated by the MRP gene-encoded conjugate export pump. Biochem J 314(Pt 2):433–437
80. Leier I, Jedlitschky G, Buchholz U, Cole SP, Deeley RG, Keppler D (1994) The MRP gene encodes an ATP-dependent export pump for leukotriene C4 and structurally related conjugates. J Biol Chem 269:27807–27810
81. Leith CP, Kopecky KJ, Chen IM, Eijdems L, Slovak ML, McConnell TS, Head DR, Weick J, Grever MR, Appelbaum FR, Willman CL (1999) Frequency and clinical significance of the expression of the multidrug resistance proteins MDR1/P-glycoprotein, MRP1, and LRP in acute myeloid leukemia: a Southwest Oncology Group Study. Blood 94:1086–1099
82. Leslie EM, Deeley RG, Cole SP (2003) Bioflavonoid stimulation of glutathione transport by the 190-kDa multidrug resistance protein 1 (MRP1). Drug Metab Dispos 31:11–15
83. Leslie EM, Deeley RG, Cole SP (2005) Multidrug resistance proteins: role of P-glycoprotein, MRP1, MRP2, and BCRP (ABCG2) in tissue defense. Toxicol Appl Pharmacol 204:216–237
84. Leslie EM, Ito K, Upadhyaya P, Hecht SS, Deeley RG, Cole SP (2001) Transport of the beta-O-glucuronide conjugate of the tobacco-specific carcinogen 4-(methylnitrosamino)-1-(3-pyridyl)-1-butanol (NNAL) by the multidrug resistance protein 1 (MRP1). Requirement for glutathione or a non-sulfur-containing analog. J Biol Chem 276:27846–27854
85. Loe DW, Almquist KC, Cole SP, Deeley RG (1996) ATP-dependent 17 beta-estradiol 17-(beta-D-glucuronide) transport by multidrug resistance protein (MRP). Inhibition by cholestatic steroids. J Biol Chem 271:9683–9689
86. Loe DW, Almquist KC, Deeley RG, Cole SP (1996) Multidrug resistance protein (MRP)-mediated transport of leukotriene C4 and chemotherapeutic agents in membrane vesicles. Demonstration of glutathione-dependent vincristine transport. J Biol Chem 271:9675–9682
87. Loe DW, Deeley RG, Cole SP (1998) Characterization of vincristine transport by the M(r) 190,000 multidrug resistance protein (MRP): evidence for cotransport with reduced glutathione. Cancer Res 58:5130–5136
88. Loe DW, Deeley RG, Cole SP (2000) Verapamil stimulates glutathione transport by the 190-kDa multidrug resistance protein 1 (MRP1). J Pharmacol Exp Ther 293:530–538
89. Loe DW, Stewart RK, Massey TE, Deeley RG, Cole SP (1997) ATP-dependent transport of aflatoxin B1 and its glutathione conjugates by the product of the multidrug resistance protein (MRP) gene. Mol Pharmacol 51:1034–1041
90. Lorico A, Bertola A, Baum C, Fodstad O, Rappa G (2002) Role of the Multidrug Resistance Protein 1 in protection from heavy metal oxyanions: investigations in vitro and in MRP1-deficient mice. Biochem Biophys Res Commun 291:617–622
91. Lorico A, Nesland J, Emilsen E, Fodstad O, Rappa G (2002) Role of the multidrug resistance protein 1 gene in the carcinogenicity of aflatoxin B1: investigations using mrp1-null mice. Toxicology 171:201–205
92. Lorico A, Rappa G, Finch RA, Yang D, Flavell RA, Sartorelli AC (1997) Disruption of the murine MRP (multidrug resistance protein) gene leads to increased sensitivity to etoposide (VP-16) and increased levels of glutathione. Cancer Res 57:5238–5242
93. Ma L, Krishnamachary N, Center MS (1995) Phosphorylation of the multidrug resistance associated protein gene encoded protein P190. Biochemistry 34:3338–3343
94. Maher JM, Slitt AL, Cherrington NJ, Cheng X, Klaassen CD (2005) Tissue distribution and hepatic and renal ontogeny of the multidrug resistance-associated protein (Mrp) family in mice. Drug Metab Dispos 33:947–955
95. Maliepaard M, Scheffer GL, Faneyte IF, van Gastelen MA, Pijnenborg AC, Schinkel AH, van De Vijver MJ, Scheper RJ, Schellens JH (2001) Subcellular localization and distribution of the breast cancer resistance protein transporter in normal human tissues. Cancer Res 61:3458–3464
96. Manciu L, Chang XB, Buyse F, Hou YX, Gustot A, Riordan JR, Ruysschaert JM (2003) Intermediate structural states involved in MRP1-mediated drug transport. Role of glutathione. J Biol Chem 278:3347–3356
97. Mao Q, Leslie EM, Deeley RG, Cole SP (1999) ATPase activity of purified and reconstituted multidrug resistance protein MRP1 from drug-selected H69AR cells. Biochim Biophys Acta 1461:69–82
98. Mason DL, Michaelis S (2002) Requirement of the N-terminal extension for vacuolar trafficking and transport activity of yeast Ycf1p, an ATP-binding cassette transporter. Mol Biol Cell 13:4443–4455
99. Morrow CS, Smitherman PK, Townsend AJ (1998) Combined expression of multidrug resistance protein (MRP) and glutathione S-transferase P1-1 (GSTP1-1) in MCF7 cells and high level resistance to the cytotoxicities of ethacrynic acid but not oxazaphosphorines or cisplatin. Biochem Pharmacol 56:1013–1021
100. Mueller CF, Widder JD, McNally JS, McCann L, Jones DP, Harrison DG (2005) The role of the multidrug resistance protein-1 in modulation of endothelial cell oxidative stress. Circ Res 97:637–644
101. Muller M, Bakos E, Welker E, Varadi A, Germann UA, Gottesman MM, Morse BS, Roninson IB, Sarkadi B (1996) Altered drug-stimulated ATPase activity in mutants of the human multidrug resistance protein. J Biol Chem 271:1877–1883
102. Muller M, Meijer C, Zaman GJ, Borst P, Scheper RJ, Mulder NH, de Vries EG, Jansen PL (1994) Overexpression of the gene encoding the multidrug resistance-associated protein results in increased ATP-dependent glutathione S-conjugate transport. Proc Natl Acad Sci USA 91:13033–13037
103. Muller M, Yong M, Peng XH, Petre B, Arora S, Ambudkar SV (2002) Evidence for the role of glycosylation in accessibility of the extracellular domains of human MRP1 (ABCC1). Biochemistry 41:10123–10132
104. Nagashige M, Ushigome F, Koyabu N, Hirata K, Kawabuchi M, Hirakawa T, Satoh S, Tsukimori K, Nakano H, Uchiumi T, Kuwano M, Ohtani H, Sawada Y (2003) Basal membrane

localization of MRP1 in human placental trophoblast. Placenta 24:951–958
105. Nagata K, Nishitani M, Matsuo M, Kioka N, Amachi T, Ueda K (2000) Nonequivalent nucleotide trapping in the two nucleotide binding folds of the human multidrug resistance protein MRP1. J Biol Chem 275:17626–17630
106. Naren AP, Cormet-Boyaka E, Fu J, Villain M, Blalock JE, Quick MW, Kirk KL (1999) CFTR chloride channel regulation by an interdomain interaction. Science 286:544–548
107. Nies AT, Jedlitschky G, Konig J, Herold-Mende C, Steiner HH, Schmitt HP, Keppler D (2004) Expression and immunolocalization of the multidrug resistance proteins, MRP1-MRP6 (ABCC1-ABCC6), in human brain. Neuroscience 129:349–360
108. Noguchi T, Ren XQ, Aoki S, Igarashi Y, Che XF, Nakajima Y, Takahashi H, Mitsuo R, Tsujikawa K, Sumizawa T, Haraguchi M, Kobayashi M, Goto S, Kanehisa M, Aikou T, Akiyama S, Furukawa T (2005) MRP1 mutated in the L0 region transports SN-38 but not leukotriene C4 or estradiol-17 (beta-D-glucuronate). Biochem Pharmacol 70:1056–1065
109. Nooter K, Bosman FT, Burger H, van Wingerden KE, Flens MJ, Scheper RJ, Oostrum RG, Boersma AW, van der Gaast A, Stoter G (1996) Expression of the multidrug resistance-associated protein (MRP) gene in primary non-small-cell lung cancer. Ann Oncol 7:75–81
110. Nooter K, Brutel de la Riviere G, Look MP, van Wingerden KE, Henzen-Logmans SC, Scheper RJ, Flens MJ, Klijn JG, Stoter G, Foekens JA (1997) The prognostic significance of expression of the multidrug resistance-associated protein (MRP) in primary breast cancer. Br J Cancer 76:486–493
111. Nooter K, Burger H, Stoter G (1996) Multidrug resistance-associated protein (MRP) in haematological malignancies. Leuk Lymphoma 20:381–387
112. Nooter K, Kok T, Bosman FT, van Wingerden KE, Stoter G (1998) Expression of the multidrug resistance protein (MRP) in squamous cell carcinoma of the oesophagus and response to preoperative chemotherapy. Eur J Cancer 34:81–86
113. Norris MD, Bordow SB, Haber PS, Marshall GM, Kavallaris M, Madafiglio J, Cohn SL, Salwen H, Schmidt ML, Hipfner DR, Cole SP, Deeley RG, Haber M (1997) Evidence that the MYCN oncogene regulates MRP gene expression in neuroblastoma. Eur J Cancer 33:1911–1916
114. Norris MD, Bordow SB, Marshall GM, Haber PS, Cohn SL, Haber M (1996) Expression of the gene for multidrug-resistance-associated protein and outcome in patients with neuroblastoma. N Engl J Med 334:231–238
115. Olson DP, Scadden DT, D'Aquila RT, De Pasquale MP (2002) The protease inhibitor ritonavir inhibits the functional activity of the multidrug resistance related-protein 1 (MRP-1). Aids 16: 1743–1747
116. Oselin K, Mrozikiewicz PM, Pahkla R, Roots I (2003) Quantitative determination of the human MRP1 and MRP2 mRNA expression in FACS-sorted peripheral blood CD4+, CD8+, CD19+, and CD56+ cells. Eur J Haematol 71:119–123
117. Oshika Y, Nakamura M, Tokunaga T, Fukushima Y, Abe Y, Ozeki Y, Yamazaki H, Tamaoki N, Ueyama Y (1998) Multidrug resistance-associated protein and mutant p53 protein expression in non-small cell lung cancer. Mod Pathol 11: 1059–1063
118. Oswald C, Holland IB, Schmitt L (2006) The motor domains of ABC-transporters/What can structures tell us? Naunyn Schmiedebergs Arch Pharmacol 372:385–399
119. Pajic M, Norris MD, Cohn SL, Haber M (2005) The role of the multidrug resistance-associated protein 1 gene in neuroblastoma biology and clinical outcome. Cancer Lett 228:241–246
120. Pascolo L, Fernetti C, Pirulli D, Crovella S, Amoroso A, Tiribelli C (2003) Effects of maturation on RNA transcription and protein expression of four MRP genes in human placenta and in BeWo cells. Biochem Biophys Res Commun 303:259–265
121. Payen L, Gao M, Westlake C, Theis A, Cole SP, Deeley RG (2005) Functional interactions between nucleotide binding domains and leukotriene C4 binding sites of multidrug resistance protein 1 (ABCC1). Mol Pharmacol 67:1944–1953
122. Payen LF, Gao M, Westlake CJ, Cole SP, Deeley RG (2003) Role of carboxylate residues adjacent to the conserved core Walker B motifs in the catalytic cycle of multidrug resistance protein 1 (ABCC1). J Biol Chem 278:38537–38547
123. Peng KC, Cluzeaud F, Bens M, Van Huyen JP, Wioland MA, Lacave R, Vandewalle A (1999) Tissue and cell distribution of the multidrug resistance-associated protein (MRP) in mouse intestine and kidney. J Histochem Cytochem 47:757–768
124. Poulain S, Lepelley P, Preudhomme C, Cambier N, Cornillon J, Wattel E, Cosson A, Fenaux P (2000) Expression of the multidrug resistance-associated protein in myelodysplastic syndromes. Br J Haematol 110:591–598
125. Pulaski L, Jedlitschky G, Leier I, Buchholz U, Keppler D (1996) Identification of the multidrug-resistance protein (MRP) as the glutathione-S-conjugate export pump of erythrocytes. Eur J Biochem 241:644–648
126. Qian YM, Grant CE, Westlake CJ, Zhang DW, Lander PA, Shepard RL, Dantzig AH, Cole SP, Deeley RG (2002) Photolabeling of human and murine multidrug resistance protein 1 with the high affinity inhibitor [125I]LY475776 and azidophenacyl-[35S]glutathione. J Biol Chem 277: 35225–35231
127. Qian YM, Song WC, Cui H, Cole SP, Deeley RG (2001) Glutathione stimulates sulfated estrogen transport by multidrug resistance protein 1. J Biol Chem 276:6404–6411
128. Rajagopal A, Simon SM (2003) Subcellular localization and activity of multidrug resistance proteins. Mol Biol Cell 14: 3389–3399
129. Rao VV, Dahlheimer JL, Bardgett ME, Snyder AZ, Finch RA, Sartorelli AC, Piwnica-Worms D (1999) Choroid plexus epithelial expression of MDR1 P glycoprotein and multidrug resistance-associated protein contribute to the blood-cerebrospinal-fluid drug-permeability barrier. Proc Natl Acad Sci USA 96:3900–3905
130. Ren XQ, Furukawa T, Aoki S, Nakajima T, Sumizawa T, Haraguchi M, Chen ZS, Kobayashi M, Akiyama S (2001) Glutathione-dependent binding of a photoaffinity analog of agosterol A to the C-terminal half of human multidrug resistance protein. J Biol Chem 276:23197–23206
131. Ren XQ, Furukawa T, Haraguchi M, Sumizawa T, Aoki S, Kobayashi M, Akiyama S (2004) Function of the ABC signature sequences in the human multidrug resistance protein 1. Mol Pharmacol 65:1536–1542
132. Renes J, de Vries EE, Hooiveld GJ, Krikken I, Jansen PL, Muller M (2000) Multidrug resistance protein MRP1 protects against the toxicity of the major lipid peroxidation product 4-hydroxynonenal. Biochem J 350(Pt 2):555–561
133. Renes J, de Vries EG, Nienhuis EF, Jansen PL, Muller M (1999) ATP- and glutathione-dependent transport of chemotherapeutic drugs by the multidrug resistance protein MRP1. Br J Pharmacol 126:681–688
134. Reyes CL, Chang G (2005) Structure of the ABC transporter MsbA in complex with ADP.vanadate and lipopolysaccharide. Science 308:1028–1031
135. Robbiani DF, Finch RA, Jager D, Muller WA, Sartorelli AC, Randolph GJ (2000) The leukotriene C(4) transporter MRP1 regulates CCL19 (MIP-3beta, ELC)-dependent mobilization of dendritic cells to lymph nodes. Cell 103:757–768
136. Ros JE, Libbrecht L, Geuken M, Jansen PL, Roskams TA (2003) High expression of MDR1, MRP1, and MRP3 in the hepatic

progenitor cell compartment and hepatocytes in severe human liver disease. J Pathol 200:553–560
137. Rosenberg MF, Mao Q, Holzenburg A, Ford RC, Deeley RG, Cole SP (2001) The structure of the multidrug resistance protein 1 (MRP1/ABCC1). crystallization and single-particle analysis. J Biol Chem 276:16076–16082
138. Rudas M, Filipits M, Taucher S, Stranzl T, Steger GG, Jakesz R, Pirker R, Pohl G (2003) Expression of MRP1, LRP and Pgp in breast carcinoma patients treated with preoperative chemotherapy. Breast Cancer Res Treat 81:149–157
139. Sasabe H, Kato Y, Suzuki T, Itose M, Miyamoto G, Sugiyama Y (2004) Differential involvement of multidrug resistance-associated protein 1 and P-glycoprotein in tissue distribution and excretion of grepafloxacin in mice. J Pharmacol Exp Ther 310:648–655
140. Scheffer GL, Pijnenborg AC, Smit EF, Muller M, Postma DS, Timens W, van der Valk P, de Vries EG, Scheper RJ (2002) Multidrug resistance related molecules in human and murine lung. J Clin Pathol 55:332–339
141. Schrenk D, Baus PR, Ermel N, Klein C, Vorderstemann B, Kauffmann HM (2001) Up-regulation of transporters of the MRP family by drugs and toxins. Toxicol Lett 120:51–57
142. Schultz MJ, Wijnholds J, Peppelenbosch MP, Vervoordeldonk MJ, Speelman P, van Deventer SJ, Borst P, van der Poll T (2001) Mice lacking the multidrug resistance protein 1 are resistant to Streptococcus pneumoniae-induced pneumonia. J Immunol 166:4059–4064
143. Seetharaman S, Barrand MA, Maskell L, Scheper RJ (1998) Multidrug resistance-related transport proteins in isolated human brain microvessels and in cells cultured from these isolates. J Neurochem 70:1151–1159
144. Shinoda C, Maruyama M, Fujishita T, Dohkan J, Oda H, Shinoda K, Yamada T, Miyabayashi K, Hayashi R, Kawagishi Y, Fujita T, Matsui S, Sugiyama E, Muraguchi A, Kobayashi M (2005) Doxorubicin induces expression of multidrug resistance-associated protein 1 in human small cell lung cancer cell lines by the c-jun N-terminal kinase pathway. Int J Cancer 117:21–31
145. Slapak CA, Mizunuma N, Kufe DW (1994) Expression of the multidrug resistance associated protein and P-glycoprotein in doxorubicin-selected human myeloid leukemia cells. Blood 84:3113–3121
146. St-Pierre MV, Serrano MA, Macias RI, Dubs U, Hoechli M, Lauper U, Meier PJ, Marin JJ (2000) Expression of members of the multidrug resistance protein family in human term placenta. Am J Physiol Regul Integr Comp Physiol 279:R1495–R1503
147. St-Pierre MV, Stallmach T, Freimoser Grundschober A, Dufour JF, Serrano MA, Marin JJ, Sugiyama Y, Meier PJ (2004) Temporal expression profiles of organic anion transport proteins in placenta and fetal liver of the rat. Am J Physiol Regul Integr Comp Physiol 287:R1505–R1516
148. Stride BD, Grant CE, Loe DW, Hipfner DR, Cole SP, Deeley RG (1997) Pharmacological characterization of the murine and human orthologs of multidrug-resistance protein in transfected human embryonic kidney cells. Mol Pharmacol 52:344–353
149. Stride BD, Valdimarsson G, Gerlach JH, Wilson GM, Cole SP, Deeley RG (1996) Structure and expression of the messenger RNA encoding the murine multidrug resistance protein, an ATP-binding cassette transporter. Mol Pharmacol 49:962–971
150. Sugawara I, Yamada H, Nakamura H, Sumizawa T, Akiyama S, Masunaga A, Itoyama S (1995) Preferential expression of the multidrug-resistance-associated protein (MRP) in adenocarcinoma of the lung. Int J Cancer 64:322–325
151. Sugiyama D, Kusuhara H, Lee YJ, Sugiyama Y (2003) Involvement of multidrug resistance associated protein 1 (Mrp1) in the efflux transport of 17beta estradiol-D-17beta-glucuronide (E217betaG) across the blood-brain barrier. Pharm Res 20:1394–1400
152. Sullivan GF, Amenta PS, Villanueva JD, Alvarez CJ, Yang JM, Hait WN (1998) The expression of drug resistance gene products during the progression of human prostate cancer. Clin Cancer Res 4:1393–1403
153. Sullivan GF, Yang JM, Vassil A, Yang J, Bash-Babula J, Hait WN (2000) Regulation of expression of the multidrug resistance protein MRP1 by p53 in human prostate cancer cells. J Clin Invest 105:1261–1267
154. Szabo K, Welker E, Bakos, Muller M, Roninson I, Varadi A, Sarkadi B (1998) Drug-stimulated nucleotide trapping in the human multidrug transporter MDR1. Cooperation of the nucleotide binding domains. J Biol Chem 273:10132–10138
155. Szakacs G, Annereau JP, Lababidi S, Shankavaram U, Arciello A, Bussey KJ, Reinhold W, Guo Y, Kruh GD, Reimers M, Weinstein JN, Gottesman MM (2004) Predicting drug sensitivity and resistance: profiling ABC transporter genes in cancer cells. Cancer Cell 6:129–137
156. Szakacs G, Ozvegy C, Bakos E, Sarkadi B, Varadi A (2001) Role of glycine-534 and glycine-1179 of human multidrug resistance protein (MDR1) in drug-mediated control of ATP hydrolysis. Biochem J 356:71–75
157. Szentpetery Z, Kern A, Liliom K, Sarkadi B, Varadi A, Bakos E (2004) The role of the conserved glycines of ATP-binding cassette signature motifs of MRP1 in the communication between the substrate-binding site and the catalytic centers. J Biol Chem 279:41670–41678
158. Tada Y, Wada M, Migita T, Nagayama J, Hinoshita E, Mochida Y, Maehara Y, Tsuneyoshi M, Kuwano M, Naito S (2002) Increased expression of multidrug resistance-associated proteins in bladder cancer during clinical course and drug resistance to doxorubicin. Int J Cancer 98:630–635
159. Takayanagi S, Ishikawa T (2003) Molecular identification and characterization of rat Abcc1 cDNA: existence of two splicing variants and species difference in drug-resistance profile. J Exp Ther Oncol 3:136–146
160. Takebayashi Y, Akiyama S, Natsugoe S, Hokita S, Niwa K, Kitazono M, Sumizawa T, Tani A, Furukawa T, Aikou T (1998) The expression of multidrug resistance protein in human gastrointestinal tract carcinomas. Cancer 82:661–666
161. Tatebe S, Sinicrope FA, Kuo MT (2002) Induction of multidrug resistance proteins MRP1 and MRP3 and gamma-glutamylcysteine synthetase gene expression by nonsteroidal anti-inflammatory drugs in human colon cancer cells. Biochem Biophys Res Commun 290:1427–1433
162. Thiebaut F, Tsuruo T, Hamada H, Gottesman MM, Pastan I, Willingham MC (1987) Cellular localization of the multidrug-resistance gene product P-glycoprotein in normal human tissues. Proc Natl Acad Sci USA 84:7735–7738
163. Tribull TE, Bruner RH, Bain LJ (2003) The multidrug resistance-associated protein 1 transports methoxychlor and protects the seminiferous epithelium from injury. Toxicol Lett 142:61–70
164. van Brussel JP, Mickisch GH (2003) Multidrug resistance in prostate cancer. Onkologie 26:175–181
165. van der Kolk DM, de Vries EG, Noordhoek L, van den Berg E, van der Pol MA, Muller M, Vellenga E (2001) Activity and expression of the multidrug resistance proteins P-glycoprotein, MRP1, MRP2, MRP3 and MRP5 in de novo and relapsed acute myeloid leukemia. Leukemia 15:1544–1553
166. van der Kolk DM, de Vries EG, van Putten WJ, Verdonck LF, Ossenkoppele GJ, Verhoef GE, Vellenga E (2000) P-glycoprotein and multidrug resistance protein activities in relation to treatment outcome in acute myeloid leukemia. Clin Cancer Res 6:3205–3214

167. Van Luyn MJ, Muller M, Renes J, Meijer C, Scheper RJ, Nienhuis EF, Mulder NH, Jansen PL, De Vries EG (1998) Transport of glutathione conjugates into secretory vesicles is mediated by the multidrug-resistance protein 1. Int J Cancer 76:55–62
168. Wang Q, Beck WT (1998) Transcriptional suppression of multidrug resistance-associated protein (MRP) gene expression by wild-type p53. Cancer Res 58:5762–5769
169. Westlake CJ, Cole SP, Deeley RG (2005) Role of the NH2-terminal membrane spanning domain of multidrug resistance protein 1/ABCC1 in protein processing and trafficking. Mol Biol Cell 16:2483–2492
170. Westlake CJ, Qian YM, Gao M, Vasa M, Cole SP, Deeley RG (2003) Identification of the structural and functional boundaries of the multidrug resistance protein 1 cytoplasmic loop 3. Biochemistry 42:14099–14113
171. Wijnholds J, deLange EC, Scheffer GL, van den Berg DJ, Mol CA, van der Valk M, Schinkel AH, Scheper RJ, Breimer DD, Borst P (2000) Multidrug resistance protein 1 protects the choroid plexus epithelium and contributes to the blood-cerebrospinal fluid barrier. J Clin Invest 105:279–285
172. Wijnholds J, Evers R, van Leusden MR, Mol CA, Zaman GJ, Mayer U, Beijnen JH, van der Valk M, Krimpenfort P, Borst P (1997) Increased sensitivity to anticancer drugs and decreased inflammatory response in mice lacking the multidrug resistance-associated protein. Nat Med 3:1275–1279
173. Wijnholds J, Scheffer GL, van der Valk M, van der Valk P, Beijnen JH, Scheper RJ, Borst P (1998) Multidrug resistance protein 1 protects the oropharyngeal mucosal layer and the testicular tubules against drug-induced damage. J Exp Med 188:797–808
174. Wioland MA, Fleury-Feith J, Corlieu P, Commo F, Monceaux G, Lacau-St-Guily J, Bernaudin JF (2000) CFTR, MDR1, and MRP1 immunolocalization in normal human nasal respiratory mucosa. J Histochem Cytochem 48:1215–1222
175. Wright SR, Boag AH, Valdimarsson G, Hipfner DR, Campling BG, Cole SP, Deeley RG (1998) Immunohistochemical detection of multidrug resistance protein in human lung cancer and normal lung. Clin Cancer Res 4:2279–2289
176. Wu P, Oleschuk CJ, Mao Q, Keller BO, Deeley RG, Cole SP (2005) Analysis of human multidrug resistance protein 1 (ABCC1) by MALDI-TOF mass spectrometry: toward identification of leukotriene c4 binding sites. Mol Pharmacol 68: 1455–1465
177. Yamane Y, Furuichi M, Song R, Van NT, Mulcahy RT, Ishikawa T, Kuo MT (1998) Expression of multidrug resistance protein/GS-X pump and gamma-glutamylcysteine synthetase genes is regulated by oxidative stress. J Biol Chem 273:31075–31085
178. Yang R, Cui L, Hou YX, Riordan JR, Chang XB (2003) ATP binding to the first nucleotide binding domain of multidrug resistance-associated protein plays a regulatory role at low nucleotide concentration, whereas ATP hydrolysis at the second plays a dominant role in ATP-dependent leukotriene C4 transport. J Biol Chem 278:30764–30771
179. Yang R, McBride A, Hou YX, Goldberg A, Chang XB (2005) Nucleotide dissociation from NBD1 promotes solute transport by MRP1. Biochim Biophys Acta 1668:248–261
180. Yang Y, Chen Q, Zhang JT (2002) Structural and functional consequences of mutating cysteine residues in the amino terminus of human multidrug resistance-associated protein 1. J Biol Chem 277:44268–44277
181. Zaman GJ, Flens MJ, van Leusden MR, de Haas M, Mulder HS, Lankelma J, Pinedo HM, Scheper RJ, Baas F, Broxterman HJ et al (1994) The human multidrug resistance-associated protein MRP is a plasma membrane drug-efflux pump. Proc Natl Acad Sci USA 91:8822–8826
182. Zhang DW, Gu HM, Situ D, Haimeur A, Cole SP, Deeley RG (2003) Functional importance of polar and charged amino acid residues in transmembrane helix 14 of multidrug resistance protein 1 (MRP1/ABCC1): identification of an aspartate residue critical for conversion from a high to low affinity substrate binding state. J Biol Chem 278:46052–46063
183. Zhang Y, Schuetz JD, Elmquist WF, Miller DW (2004) Plasma membrane localization of multidrug resistance-associated protein homologs in brain capillary endothelial cells. J Pharmacol Exp Ther 311:449–455
184. Zhao Q, Chang XB (2004) Mutation of the aromatic amino acid interacting with adenine moiety of ATP to a polar residue alters the properties of multidrug resistance protein 1. J Biol Chem 279:48505–48512
185. Zhou DC, Ramond S, Viguie F, Faussat AM, Zittoun R, Marie JP (1996) Sequential emergence of MRP- and MDR1-gene overexpression as well as MDR1-gene translocation in homoharringtonine-selected K562 human leukemia cell lines. Int J Cancer 65:365–371
186. Zhu Q, Center MS (1994) Cloning and sequence analysis of the promoter region of the MRP gene of HL60 cells isolated for resistance to adriamycin. Cancer Res 54:4488–4492
187. Zhu Q, Center MS (1996) Evidence that SP1 modulates transcriptional activity of the multidrug resistance-associated protein gene. DNA Cell Biol 15:105–111